Author:
Taylor, Damian Russell

Title:
An analysis of sea level change in the Severn Estuary.

AN ANALYSIS OF SEA LEVEL CHANGE IN THE SEVERN ESTUARY

BY

DAMIAN RUSSELL TAYLOR

THESIS SUBMITTED FOR THE
DEGREE OF DOCTOR OF PHILOSOPHY

UNIVERSITY OF BRISTOL

SEPTEMBER 1995

MEMORANDUM

This thesis is the result of independent research at the Department of Geology, University of Bristol, between October 1990 and September 1993, under the supervision of Dr A.B. Hawkins. The research was carried out under a SERC CASE (with Parkman Limited) studentship. All other work than my own is fully acknowledged.

Damian Tayler

ABSTRACT

The Severn Estuary in Southwest Britain has undergone major changes to its sedimentary environments during the Quaternary, culminating in the accretion of extensive deposits of estuarine alluvium during the Flandrian. The transgression of the Flandrian seas is shown to have deposited variable thicknesses of silt and sand in the Bristol Channel and Lower Severn Estuary during an initial period of fast sea level rise, followed by estuary-wide deposits of mud over seven metres deep as the rate of sea level rise abated.

It is suggested that the relatively persistent organic sediments at about Ordnance Datum in the Lower Estuary represents a period of peat growth due to static sea levels about 6000 years ago. As the Estuary moved up the Severn Valley, considerable sand and mud deposits formed in the Upper Estuary due to the interaction of the river and estuary systems. Freshwater peats seem to have formed in response to rising groundwater levels away from the margin at a lower altitude than the near channel deposits. Recent studies of the rates of accretion on the saltmarshes of the Severn implies that sea level is rising and may be accelerating. In light of current predictions of eustatic sea level rise and the potential 'greenhouse effect' a computer model was derived to assess the future tidal regime of the Severn.

The simulation of the tidal regime was undertaken by deriving a mathematical model of flow, based upon the work of De St Venant. The flow equations were solved by an implicit finite difference method using Preissman's four point scheme. The model results show favourable correlation with known tidal events observed in the Severn and it was deemed that the model could be used as a predictive tool.

The model has been used to demonstrate the tidal heights, flows and velocities on spring, neap, surge , future and abnormal tides which may occur in the Severn. It is shown that the defences of the Severn are presently in need of raising and would require radical rethinking if there were to be significant rises sea level . The worst case prediction of sea level rise which is used in this work shows that the spring tide would breach parts of the tidal defences by 2100 AD. Model studies of historic tides show that the tidal extent of the Severn Estuary was up to 10km downstream than at present on a spring tide in 150 AD.

The morphology of the saltmarshes bounding the Estuary are described with reference to their positions in the tidal frame. It is suggested that two distinct morphologies exist which depend on the influence of prevailing currents. In areas where there is active erosion at the toe of the saltmarshes, a step like morphology of alluvial surfaces lower and young towards the main channel, falling as a small cliff to the intertidal mudflats. Marshes upstream tend to be higher and more mature than the younger marshes and have not been able to accrete in front due to the currents and extent of the channel. The position of present and buried cliffs in the saltmarshes suggests that the position of the erosive currents shaping these marshes are relatively unchanged over the last 2000 years. It is suggested that the accretion and erosion of these marshes is not due to apparently cyclic fluctuations in the climate or tidal regime, but has occurred under essentially the same conditions throughout history. The morphology is defined by the interaction of the currents, the marshes and the building up of the mudflats in front.

If sea levels are to rise as predicted in the near future, the Estuary would be vulnerable to greater erosion, especially in the Middle Estuary. Super high flood flows on the outsides of the meanders may pose a considerable threat to the tidal walls. It is seen in areas of the Estuary that the tidal walls are eroding or about to erode as the coast retreats. It is concluded that an alternative form of floodbank management should be considered where new embankments should be set back from the existing ones where possible. Areas of the Estuary should be allowed to occasionally flood, perhaps by neglecting some of the seawalls, to mitigate the effects of extreme tides or floods in other areas of the system.

ACKNOWLEDGEMENTS

I would like to thank Dr. Brian Hawkins for his supervision and encouragement throughout the period of this research.

The assistance and friendship afforded by the staff of the Department of Geology are gratefully acknowledged, in particular the use of the computer facilities and the help given by Paul Browning and John Healey. I also acknowledge the help and encouragement given by Prof. Peregrine of the Department of Mathematics during the early stages of this research.

I would like to thank the NRA in particular for providing valuable information and an insight in their work on the Severn Estuary. I would also like to thank Parkman Environment for their support and supply of information.

Personal thanks are extended to all my colleagues in the Geology Department, especially Brian McConnell, Chris McDonald, Dave Lloyd, Rob Narbett, Jo Fortune, Jo Collins, Emma Ludford, Craig Brown, Steve Hawkins, Sinan Al Jassar, Simon Davidson, Adam Fisher, Mike Higgins, Pete Forrest, Justin Wilson, Mike Overs, Wayne Bowery, the cricket team and any others who I have no doubt forgotten to mention, for their advice, support and friendship.

Finally I would like to thank my parents for their support for the financial and moral support over the years, and Andy and Liz Bonner, Jo Hudson, Helen Turley and Sue Heatherley without whom this would not have been possible.

This research was carried out under a SERC CASE (with Parkman Limited) studentship which is gratefully acknowledged.

TABLE OF CONTENTS

CHAPTER 2

SEA LEVEL CHANGE AND SEDIMENTATION

LIST OF FIGURES

LIST OF TABLES

LIST OF PLATES

CHAPTER 1

INTRODUCTION

1.1 Preamble.

"An estuary is a semi-enclosed coastal body of water which has a free connection with the open sea and within which sea water is measurably diluted with fresh water of river origin." (Cameron and Pritchard, 1963; Pritchard, 1967).

Estuaries are most frequently developed on passive (Atlantic type) continental margins, bounded by low coastal plains of estuarine deposits. Nearly two-thirds of the British Coast or 3% of the total British landmass consists of alluvial lowlands flanking estuarine waters. The location and extensive flat topography provides important sites for urban and industrial development.

By definition the past and future characteristics of an estuary are governed by changes in mean sea level. Past sea level changes have defined the morphological development of estuarine wetlands and the sedimentological history, thus ultimately the present geotechnical properties. Future sea level changes are of interest because of the effect they may have on man's utilisation of the coastal lowlands. Most modern research predicts global sea level change of about 0.3 to 0.9 m by the end of the next century which may endanger human populations, commercial maritime development and low lying wetlands, through inundation, salinization and changes in the sedimentary environment.

This thesis begins by discussing previous work on Quaternary sea level changes and their influence on the Severn Estuary, which provides the basis of a simple model of sea level change and sedimentation in the Estuary. This initial work concluded that a computer model was required to justify some of the findings which could also be used as a predictive tool to analyse the potential effects of global sea level rise. The thesis continues by discussing the equations of flow which have been derived for the model and their mathematical solution, before assessing the needs of the model in terms of real data from the Severn. The computer model and verification is subsequently described before the results of the model simulations are

discussed in detail. This work concludes by discussing applications of the model relevant to the salt marshes and their sedimentology.

1.2 Severn Estuary Study Area.

The Severn Estuary is located in the Southwest of Great Britain (Figure 1.1). The Severn is a remarkable estuary with one of the largest semi-diurnal tidal ranges in the world. The tidal sensitivity of the Estuary combined with the broad data available on the extensive bounding lowlands makes this a desirable area to study. The research in this thesis examines the tidal regime and estuarine sediments of the area, with emphasis on the effects of sea-level change on agriculture, erosion and inundation.

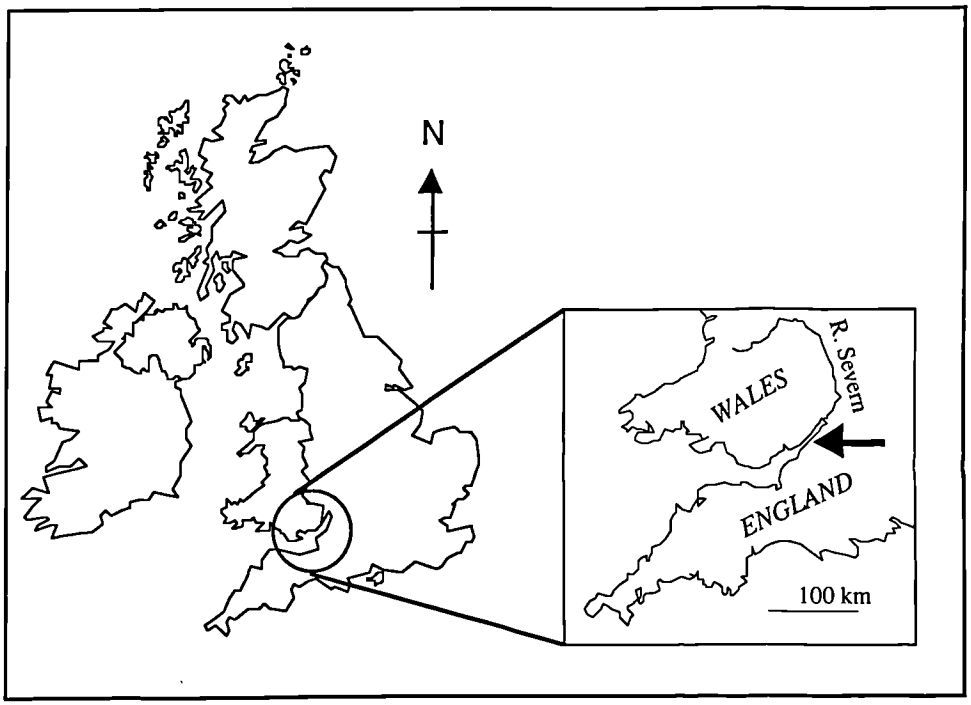

Fig 1.1. Location of the Severn Estuary, Southwest United Kingdom.

Typical of north-west European estuaries, the Severn Estuary is a funnel shaped coastal inlet, extending from Upton-on-Severn to Flat Holme and the Bristol Channel, a distance of over 150 km. The coastline of the Severn Estuary has a north-east to south-west trend and runs nearly continuously, broken only by the mouths of the rivers Usk, Bristol

Avon and Wye. The relevant geological maps of the region show that about one third of this coastline is represented by rocks and cliff, the remainder of the Estuary is bounded by reclaimed tidal marshes forming broad alluvial flood plains, known as the Severn Levels. From this evidence the Estuary is considered to be a region of net sediment accumulation rather than an eroding bedrock coast.

Maximum tidal heights in the Severn Estuary are amplified upstream due to the length and shape of the Estuary. The mean spring tidal range reaches a maximum of 12.4 m at Beachley (Hydrographer of the Navy). This range is thought to be the second largest in the world after the similarly shaped Bay of Fundy, Nova Scotia, although Ungava Bay in Northeast Canada is rumoured to have a tidal range which also exceeds that of the Severn Estuary.

The waters of the Seven Estuary are deemed to be well mixed due to turbulent mixing processes which dominate the area because of the high tidal velocities generated and their turbulent interaction with the floor and sides of the Estuary. Salinity in the Estuary generally increases seawards and tends to be uniform throughout the vertical column at a given position because of the dominant mixing forces.

1.3 Geographic Setting.

1.3.1 Severn River.

The catchment area of the Severn River system (Figure 1.2) is the largest in England and Wales, measured as 11,422 km^2 by the Severn River Authority in 1974. Rising at 610 mAOD on the slopes of Plynlimon, the River Severn flows some 350 km to the Bristol Channel. The Severn catchment system forms a 'Y' shape meeting at the southern apex of the Midland Triangle, with arms pointing towards the Bristol Channel, North Wales and Nottinghamshire. The main tributaries of the river system are the Teme, joining from the west at Worcester and the 'Warwick' Avon, joining from the east at Tewkesbury. The Severn River flows through four counties and drains eleven others.

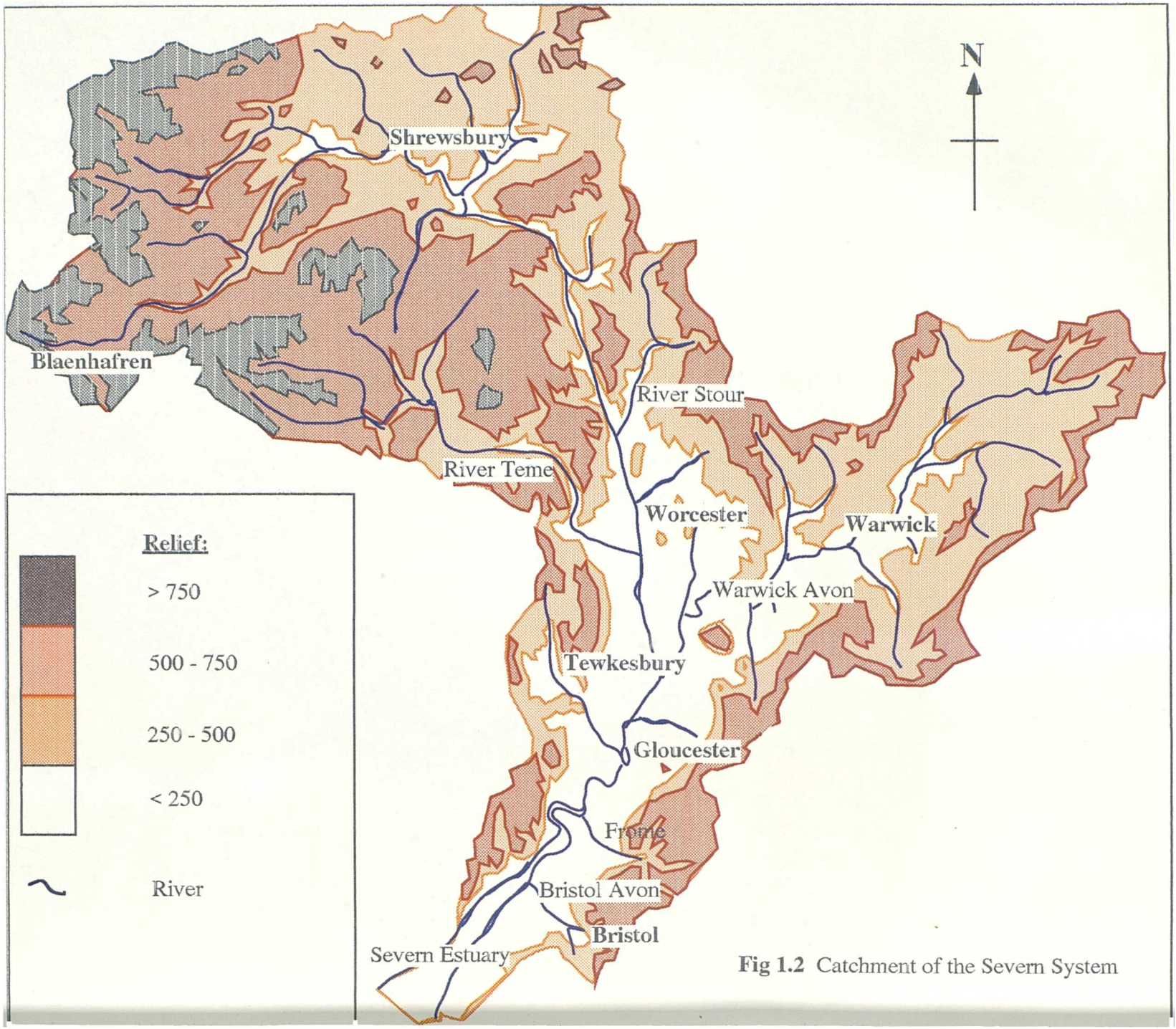

Fig 1.2 Catchment of the Severn System

The Severn rises in the Welsh Hills, where the catchment area reaches a maximum height of 827 mAOD with an average yearly rainfall in excess of 2500 mm/year. The Severn flows northwards from Blaenhafren until joining the Afron Vyrnwy where it turns east towards Shrewsbury, beyond which the river flows southwards until Worcester. The 'Warwick' Avon rises at a more modest height of about 150 m above sea level near the Northamptonshire and Leicestershire border where the annual rainfall averages 700 mm.

The maximum discharge at Diglis Weir just south of Worcester was estimated to be 650 m^3/s in 1947. South of Diglis Weir the Teme joins the Severn River and is estimated to have a maximum discharge of 450 m^3/s. The surface width of the Severn below this confluence is approximately 60m and possesses a capacity for a bank-full discharge in the region of 350m^3/s, highlighting the extent of flood water that needs to be taken by the 1km wide flood plain through which the River Severn meanders, if the maximum discharge is neared further upstream. After flowing southwards through Upton on Severn, the River Severn approaches Longdon Marsh on the right bank which is an area deemed important for the storage of flood waters by the local water authorities. The river proceeds downstream to Tewkesbury and then Gloucester, where it can be considered to comprise part of the tidal Severn Estuary. The flood plain extends to about a 1.5km width between Gloucester and Tewkesbury, although it narrows to a matter of a few hundred metres over a 3.5km reach between Ashleworth and Upper Parting. In general the channel capacity is estimated to be 500 m^3/s in this region.

Land use in the Severn Plain consists mainly of arable farming in bands reaching along the Severn River Valley from Gloucester toward Worcester and toward Leamington along the Warwick Avon. In the west, forest covers most of the Welsh Hills and the Forest of Dean. The east is bounded by the Cotswolds escarpment.

Whilst it is not intended to dwell in too much detail over the Upper Severn Region as it extends beyond the area of interest of this study, the two towns of Upton-on-Severn and Tewkesbury are critically positioned when considering flood alleviation problems. Upton is prone to flooding during high river flow. It lies on high ground on the right bank of the Severn although flood flow may occur either side of the town, often flooding south of the town first. Tewkesbury again lies on a high point at the confluence of the Warwick Avon and

Severn. It too can be flooded about either side so it is vital that any flood alleviation in the Lower Severn must not be allowed to cause a greater threat of flooding to these two areas.

1.3.2 Severn Estuary.

The division of the Severn Estuary and Bristol Channel is uncertain. Bassindale (1943) suggests that the Bristol Channel extends 112 km from Morte Point to King Road, offshore from Portishead Point and that the Severn Estuary extends 106 km from King Road to the upper tidal limit at Upton-on-Severn.

Although the Estuary can be considered to extend as far as Upton-on-Severn because a tidal effect may extend this far, tides are not often observed apart from on very high spring tides, being impeded by the navigational weirs at Tewkesbury, Maisemore and Llananthony. Maisemore weir at Gloucester has a sill level of 6.246 mAOD. For the purpose of this study the Severn Estuary is deemed to terminate at Maisemore and Llananthony weir at Gloucester.

The Severn River divides just upstream of Gloucester City at Upper Parting with the East and West Channels circumventing Alney Island. These channels reconverge about a kilometre south at Lower Parting and are now considered to be part of the Upper Estuary. As mentioned previously all but the highest tides are prevented from passing beyond the navigational weirs at Maisemore (West Channel) and Llananthony (East Channel). During river flood conditions the West Channel contains about three quarters of the tidal flow, but in very low flow conditions the East Channel carries nearly all the river flow.

South of Gloucester the Severn loops around small bends at Elmore and Minsterworth, before meandering around the 'great' bends at Epney and Arlingham. In this region the Severn resembles a large sinuous river, although the steep sided mud banks which are up to 5m high indicate the daily tidal nature of this area. Surface breadths vary little, widening slightly seawards below Lower Parting to Waterend, with the exception of narrowing for the rocky outcrops at Epney. Within the tidal region of the Severn it is difficult to accurately estimate the channel capacity.

The main channel leaves the final bend and expands at Frampton to form 'The Noose' becoming 2km wide, downstream of which the river assumes a typical funnel shaped

morphology with a south-westerly aspect. The river progresses south past the Slimbridge Wildfowl Trust before narrowing further south at Sharpness to a width of 0.8km, with both sides being bounded by a wide rural floodplain. South of Sharpness the western side begins to rise towards the Forest of Dean, whilst the eastern side remains flat and rural, punctuated by local higher ground near Berkeley and Oldbury nuclear power stations. The Estuary gradually expands in width downstream, up to a width of 3.6km at Oldbury, although the tidal reservoir here is only flooded at high water, where an artificial bund has been constructed to provide coolant for the power station during lower tidal levels.

Further south the Estuary reconverges to a width of 1.2km, bounded on either side of the channel by Aust Cliff and Beachley and is traversed by the Severn Road Bridge, the lowest bridging point of the Severn at present. South of the higher ground at Aust Cliff, the rural plains on the English side give way to the conurbation of Avonmouth and Bristol. The west side is met by the River Wye at Beachley. South of Beachley, until Newport, the western side consists of extensive plains of reclaimed saltmarshes protected by seawalls. In the area of Severn Beach and Sudbrook, the location of the Severn Rail Tunnel, flat rocky platforms such as the English Stones, have provided a convenient location for the Second Severn Road Crossing which is due for completion in 1996. These rocky outcrops have resulted in the tidal flow being relatively confined, especially on low tides to a narrow channel, where the water flows at such a rate that it has been named "The Shoots". At low spring tides the water flow is limited to a 750m wide channel, although the high tidal breadth is approximately 3.5km.

To the south of Sudbrook the Estuary again widens to a breadth of 8.6 km at Avonmouth, 13.4 km at Newport and 14.7 km at Cardiff, before meeting the east-west trending Bristol Channel at a discordant angle.

The Bristol conurbation on the east side subsides soon after Avonmouth, the area becoming more rural. The Estuary is now bounded by large reclamations, especially the Somerset Levels, with occasional coastal resorts, such as Weston Super Mare and Burnham. The topography is punctuated by the Mendip Hills and a series of rock shore outcrops such as Woreberry Hill, Brean Down and Black Nore Point which protect isolated bays. The Welsh side seawards of Cardiff and Barry is rural, fronted by cliffs, although the land use here will

undoubtedly change in the near future after the construction of the Cardiff Bay Barrage Scheme.

1.4 Geological Setting.

The area is geologically complex with most formations from the Pre-Cambrian in the Malvern Hills to the Cretaceous in the Wiltshire Downs being exposed with the exception of the Permian. The orientation of the Estuary has been influenced by structural trends associated with the Variscan Orogeny of Permo-Carboniferous age, the resilience of the Carboniferous strata to erosion and the denuded system that developed in the Permo-Trias. Post-Glacial sea level rise has caused the deposition of extensive tidal marshes which dominate the modern coastal zone. Only a third of the Severn Estuary coastline is represented by solid strata, with limited rock ledges exposed within the channel at low tide. The remaining coast comprises soft alluvial deposits of Quaternary age.

1.4.1 Solid Geology.

The floor of the Severn Estuary and the Bristol Channel is dominated by Triassic (mudstones and sandstones) and Liassic sediments (mudstones and limestones), all of which are relatively weak and have been exploited by later glaciation. The geological evolution of the area can be summarised by the four stages of the Precambrian, Caledonian, Variscan and Post-Variscan phases which are categories based upon major periods of deformation.

- Precambrian

Although only exposed in the Malvern Hills, a 12km north-south trending ridge of moderately high relief along the former border of Hereford and Worcester, this is one of the most extensive exposures of Precambrian and Cambrian strata in England. The Malverns comprise a Precambrian metamorphic and volcanic series, overlain to the west by Lower Palaeozoic rocks of moderate undulatory relief and by Triassic-Liassic and Quaternary deposits of low

relief to the east in the Severn Vale. The Precambrian at Malvern consists of two groups representing a meta basement of predominantly igneous origin and closely related volcanics.

- Caledonian

The oldest rocks immediately adjacent to the Severn Estuary are found in the Tortworth Inlier. This structurally complex area north of Bristol possesses Tremadocian marine shales unconformably overlain by shallow shelf deposits of Silurian Age. The Ordovician is not obvious and is believed to be missing as a result of tectonic upheaval. Lavas and ashes within the Silurian sediments indicate contemporaneous volcanic activity. Towards the end of the Silurian (Ludlow), upheaval of the area caused a marine regression and predominantly terrestrial deposits were laid down during the Lower and Upper Devonian derived from the Caledonian Mountains of Central and North Wales. Mid Devonian sediments are not present as this age was another period of great uplift and deformation. Consulting the relevant geological maps shows that the Ordovician, which is often accredited a Cambrian age, and Silurian deposits are mainly seen to extend in a narrow band approximately northwards from the region around Whitfield, NGR ST (675 910) to Sharpness on the east side of the Estuary. These outcrop northwards beyond the west bank to form the foot of the Forest of Dean uplands. Upper Old Red Sandstone (ORS) deposits are dispersed in patchy ribbons between Clevedon and north Bristol to the west of the Lower ORS deposits.

- Variscan

A marine transgression occurred at the end of the Devonian. The Lower Carboniferous is represented by shallow marine deposits and volcanics. As a result of uplift, deltaic conditions prevailed during the later Carboniferous with the resultant Westphalian Coal Measure sediments being lain. As the Variscan Orogeny reached its climax, sedimentation becomes sporadic with no sediments being present for the latest Carboniferous and entire Permian. The Carboniferous can be seen extensively in the Bristol and Mendip regions and is folded and thrust faulted to a large degree. Coal measure deposits are prevalent to the east of Bristol and in the Forest of Dean.

- Post Variscan

Mesozoic sedimentation began in the Estuary region during the late Triassic as continental deposits infilled the eroded tracts of the Variscan highlands. Deposition persisted in extensional grabens until the end of the Triassic when another marine transgression occurred with the deposition of marginal marine deposits for the entire Jurassic. Cretaceous sediments are not represented next to the Estuary, but are found inland to the east in the Marlborough and Wiltshire Downs. Sedimentation in the Severn Estuary region did not restart until the late Quaternary.

The shape of the Severn Estuary is dominated by the structures developed during the Variscan Orogeny, resulting in a north-south alignment in the Bristol Coalfield and the Forest of Dean, and the east-west trending periclines forming the Mendip Hills. These major orogenic elements meet at the northeast to southwest trending Vale of Gordano and Westbury on Trym structures. The Severn Estuary Fault Zone runs in an arcuate fashion approximately northeast to southwest from the Bristol Channel, nearly through the main estuary axis, before passing inland at Lydney. This fault zone has be identified to have been primarily active during the early Carboniferous (Wilson, Davies, Smith & Walters, 1988).

This section has only given a brief introduction to the geology of the Severn Estuary; readers are directed towards the relevant British Geological Society Memoirs for the area and other publications.

1.4.1 Quaternary Geology.

The deposits of the Severn Estuary marked as alluvium on the relevant geological maps have been formed within the last 8500 years. The morphology of the Estuary has been developed as a result of Pleistocene glacial and interglacial interactions with the underlying bedrock and the subsequent deposition of alluvium during the Flandrian.

There are approximately four river terraces bordering the Severn, the Kidderminster, Main, Worcester and Power House, (Wills, 1938; Mitchell, Penny, Shotton and West, 1973) which have been attributed a Devensian age by Mitchell *et al.* Precise stratigraphical

correlation of these deposits is difficult, but in lower parts of the Estuary when they are present have a close stratigraphic relation to the post glacial (Holocene or Flandrian) sediments.

Periods of low sea level up to 110m below the present level led to the incision of narrow river gorges into the essentially broad Severn Valley. The most prominent instant of which is the Shoots, where the side slopes are known to be extremely steep. These valleys have subsequently been infilled by alluvium of a generally fining upwards sequence of gravels, sands, silts, peats and clays up to 15m thick or more during the marine transgression of the warmer postglacial period. The sea-level changes identified in the Severn, the palaeoclimate and the effect on sedimentation during the Quaternary are described in more detail in Chapter 2.

1.5 Severn Estuary Classification.

Several estuarine classification systems have been suggested by various authors. These encompass criteria including topography, salinity, tidal action, river flow and mixing. An estuary will posses a unique combination of all these properties, so that a single unifying classification system would be unable to account for all the effects.

Leeder (1982) points out that the definition of an estuary given by Pritchard (1967) restricts the term 'estuary' to the region of dynamic interference between sea and river water which suggests that parts of the large funnel shaped inlets of the Severn and Bay of Fundy are not necessarily estuarine.

1.5.1 Classification by Salinity.

The Severn Estuary can be called a 'positive' estuary, using the system suggested by Pritchard (1955). This term implies that the rate of river inflow exceeds evaporation in the system, thus dilution of sea water occurs in the estuary. This classification is very basic giving little indication of the differences between estuaries, especially as very few 'negative' estuaries exist where hypersaline conditions prevail (e.g. Laguna Madre, Texas, U.S.A.). The author deems that it is not necessary to justify this estuarine classification by comparing river inflow with (calculated) evaporation rates.

1.5.2 Classification by Topography.

Pritchard (1955) presented three topographical categories: coastal plain, fjords and bar-built estuaries. The Severn Estuary is a coastal plain, or drowned river valley type. Typically these can be found on low coastal plains where flooding of pre-Flandrian river valleys has occurred. In these types of estuaries the topography resembles a large river system because sedimentation rates struggle to match the rate of inundation, forming wide shallow cross-sections. The central channel is often sinuous, bounded by extensive mudflats and saltmarshes and the geographical position of the main channel may have varied substantially with time. River flow is often small compared to the salt-water volume entering and evacuating the system over a tidal cycle. Coastal plain estuaries are most common in temperate latitudes especially in North America and North-west Europe. Other British examples include the Thames and Mersey.

Elsewhere in tropical or equatorial regions the river flow and sediment discharge are usually so high that delta type formation overrides what would otherwise be an estuarine type development.

1.5.3 Classification by Salinity Structure.

Water circulation and sediment dynamics are mainly dependant on the interaction of tidal, river and wave processes. Pritchard (1955), Cameron and Pritchard (1963), Pritchard and Carter (1971) and Schubel (1971) define four estuary types by salinity stratification and distribution. These are salt wedge (type A), highly stratified (fjord), partially mixed (type B) and homogenous or well mixed (types C and D). It is not intended to describe all these categories, but to mention the features salient to the Severn.

The Severn Estuary is best categorised as a well mixed or homogenous estuary. Such estuaries show little or no vertical salinity structure at a given cross section, but with a general increase in salinity towards the sea. Stratification is destroyed because tidal flow is much greater than riverine flow with the resultant bottom shear causing mixing throughout the vertical column.

Vertical salinity profiles measured during neap tides by Griffiths (1974) in Spring 1972 at stations near Charston Sands, Slime Road and Beacon Sand show that although there is no substantial salinity change over depth, there seems to be a small degree of stratification. This is indicated by a near surface salinity reduction during the later stages of the ebb tide and an increase during flood. At Charston Sands the reduction seems to be due to over-riding fresher water from the River Wye, the other two stations are effected by the diversion of the main ebb channel from Oldbury Reservoir. The well mixed classification can be further sub-divided to include the lateral salinity structure of a given cross section. The Severn Estuary shows characteristics of both the type C and type D categories.

- Type C, Laterally inhomogenous:

In a wide estuary the Coriolis effect may establish a horizontal separation of flow. In the Northern Hemisphere an object's motion is deflected to the right as a consequence of this effect. In the Lower Severn Estuary flood flow dominates the west side and the ebb dominates the east. However, this should be attribted to diversions by rock headlands and indeed is reversed in the Middle Estuary. Salinity data cannot conclusively define the Estuary as a type C as there is insufficient data available.

- Type D - Laterally homogenous:

In an estuary where lateral shear forces are sufficient, often in a narrow or irregularly shaped estuary where turbulent effects are caused by the irregular sides of the estuary, the salinity across a cross-section will not vary at a given time. The salinity increases evenly towards the mouth. Tidally averaged flow is seaward causing a downstream driving off of salt which is counteracted by a turbulent upstream exchange due to the reaction of tidal flow with topographic irregularities and bottom friction. Typically these estuaries show maximum flood current speeds near high water and maximum ebb near low water. At high water the estuary volume is considerably greater than at low water, thus the large mass salt transport inland on the flood helps to counteract the flushing from the mean seaward flow throughout the cycle.

Further classifications by salinity are given by Ippen and Harleman (1961) and Hansen and Rattray (1966) which form a more complete and numerically justified expansion of the

salinity categorisation system. These methods do have a degree of shortcomings associated with the quality of data used and assumptions made about channel morphology.

1.6 Tides.

Tides are caused by the difference in gravitational pull of the moon and the sun on particles at the earth's surface. Newton originally formulated his Equilibrium Tide Theory assuming that the earth is totally covered with water and not rotating. He showed that in the open sea the moon could cause a maximum rise of 0.36m and fall of 0.18m, with the sun causing a superimposed effect of approximately half that amount.

Laplace described both the theoretical and mathematical relationships between periodic forces and tidal phenomenon in the late Eighteenth to early Nineteenth Century. Accounting for actual particle motion and inertia, neglected by both Bernoulli and Newton, Laplace's works became the basis of the modern harmonic method of tidal prediction. Thomson in the late Nineteenth Century further developed the harmonic theory to include individual tidal constituents, the sum of which adding up to the full tide. The magnitude and phase of each of the periodic terms were evaluated from actual observations.

The harmonic theory was subsequently refined by Darwin, Harris , Borgen in the late Nineteenth Century, and especially Doodson who developed the "Admiralty Method of Analysis of Tides" a simple calculation based on a small (monthly) period of observation. Harmonic methods of tidal analysis were improved by the introduction of the digital computer.

As a tide comprises a number of components which drive it, Admiralty prediction methods can use a complex Fourier series of analysis for every component which effect the tide based on a cycle of 18.6 years. However, there are only four principle components which account for over 75% of the tide which are used in the simplified method of tidal prediction (simple harmonic method).

The principle constituents of a tide are given in Table 1.1. The M2 semi-diurnal tide is the principle individual component of the tide.

Name	Type	Period	Notes
M1	Moon diurnal	Daily	
M2	Moon semi-diurnal	12.42 hours	Principle component
M4	Moon quarter diurnal	4 times daily	
S2	Solar semi-diurnal	12.00 hours	Principle solar

Table 1.1 Principle tidal constituents.

1.6.1 Tidal Behaviour in Estuaries

Tidal motion in estuaries and rivers can be described as shallow water motion where propagation is influenced by depth and frictional effects. Airy (1842) showed that as a tide progresses into shallow water the original sinusoidal wave is increasingly distorted with higher harmonics being added to explain the non-linear nature of propagation.

The degree of amplification of a tide or long wave is related to the closeness of the natural period of resonance of the coastal inlet to the period of the wave or tide. The distance from the continental shelf to the estuary head and geometry in both the Severn and Bay of Fundy results in a natural period of resonance close to that of the driving tide (Equation 1.1).

$$T = \frac{2L}{(g\,h)^{0.5}} \qquad (1.1)$$

Where T = natural period of resonance.

L = length of estuary.

h = mean water depth.

g = acceleration due to gravity.

Arbitary figures of L = 250 km and h = 13m give a period of resonance of 12.3 hours.

1.7 Tidal Behaviour in the Severn Estuary.

The macrotidal Severn Estuary is extremely dynamic, it is almost impossible to summarise every phenomenon that occurs within the system without writing an entire thesis on it's own. The next sections describe the relevant terms which will be commonly used in the thesis. The following sections intend to describe the heights and times of tidal levels occurring along the Estuary on an average spring and neap tide, the highest astronomical tide, mean levels and the Severn Bore. Data for these descriptions was collated in the main from the Admiralty Tide Tables (1990-1994) which use a simplified harmonic system of tidal prediction. The methodology of analysis is contained in the relevant Admiralty publications and is also available as a simple computer package published by the Hydrographer of the Navy.

1.7.1 Tidal Datums.

The Admiralty Tide Tables quote tidal levels relative to a spatially variable datum called the *Chart Datum* (CD). The Chart Datum has been agreed internationally to be a level so low that the tide will not frequently drop below that value. In the UK *the Chart Datum is set to* correspond approximately to the value of the Lowest Astronomical Tide. Tidal datums therefore can vary considerably with a small region of an estuary

1.7.2 The Astronomical Tide.

The *Highest Astronomical Tide* (HAT) and *Lowest Astronomical Tide* (LAT) represent the maximum and minimum levels which may occur under average meteorological conditions using any combination of the astronomical arguments used in the harmonic method of tidal predictions. These levels may not be reached every year and do not take into account storm surges which may cause appreciably higher and lower levels to occur.

The Astronomical Levels are given in the Admiralty Tables for the Standard Ports only, which is Avonmouth in the Severn Estuary. The intermediate values of HAT and LAT have to

be derived for the secondary ports of the Estuary from a linear interpolation method using the height differences given in the charts for spring and neap levels. This means that the astronomical levels have a direct mathematical relationship to the lower levels, rather than being an average of observed values. Consultation with the NRA and Hydrographer of the Navy affirmed that the mathematically derived values bore a close relationship to the naturally occurring levels. The values of HAT and LAT for a standard port are determined by inspection over a number of years.

1.7.3 Spring Tides.

The terms *Mean High Water Spring* (MHWS) and *Mean Low Water Spring* (MLWS) are used to describe the mean levels throughout the year of two consecutive high or low water heights during a twenty four hour period, when the average maximum declination of the moon is 23.5 degrees. In a simplified way, spring tides occur in the Severn two days after the Full and New Moon, approximately once a fortnight, when the tidal range is the greatest. The average of the two highest and lowest consecutive tides is taken and these bi-monthly values are then averaged over a year or longer to give the mean spring levels.

The values of the mean spring tide levels and mean neap tide levels vary from year to year over a period of approximately 18.6 years. The levels are generally computed from at least one year's predictions and then adjusted for the long period variations.

1.7.4 Neap Tides.

The *Mean High Water Neap* (MHWN) and *Mean Low Water Neap* (MLWN) describe the average minimum tidal range at a location and are determined in the same manner as the spring tides, only at the time when the tidal range is at its least.

1.7.5 Mean Levels.

The *Mean Level* (ML) is the level that would exist if there was an absence of tides or is the average level of the sea surface over a long time, preferably the 18.6 year long period variation. An approximation to the Mean Level used in this thesis can be made by the *Mean Tide Level* (MTL) which is calculated from averaging the heights of the mean spring and neap maxima and minima.

1.7.6 Tidal Surges and Storms.

The meteorological effects on tides come into two categories, barometric conditions and wind.

Barometric effects tend to affect the tidal levels by no more than 0.3m, raising the levels if there is low pressure and lowering at high pressure. Although it can be computed that an average of 34 millibars can cause such a height difference, the adjustment is not immediate and varies is relation to a change in pressure averaged over a substantial area.

Wind effects can be much more important on a variety of scales and vary considerably with the topography of the affected area. Generally wind will cause a rise in the mean level in the direction in which it is blowing. A wind blowing onshore will 'pile' the water up against the shore also raising the levels through wave run-up. An even more important effect is the storm surge which occurs when a wind blows parallel to the coastline, raising the tidal crest and lowering the trough.

The Severn is sensitive to a depression moving slowly down the Irish Sea and St George's Channel. This can cause a rise in sea-levels due to the low pressure which compounds the tidal heights. Additionally the wind direction which tends to be south-westerly will blow directly up the mouth of the Severn causing a storm surge. If one of these surges occurs at the time of the highest tides, which tend to have the highest range near to the Spring and Autumn Equinoxes, then the Estuary is prone to flood. Storm Surges are hard to predict, but their effect can be considerable, for instance a storm in January 1953 caused a rise in

excess of 3.0m on the Netherlands coast resulting in large scale flooding and considerable loss of life.

1.8 Tides in the Severn Estuary.

The Astronomical, Mean Spring and Mean Neap Tide Levels are compared graphically in Figure 1.3.

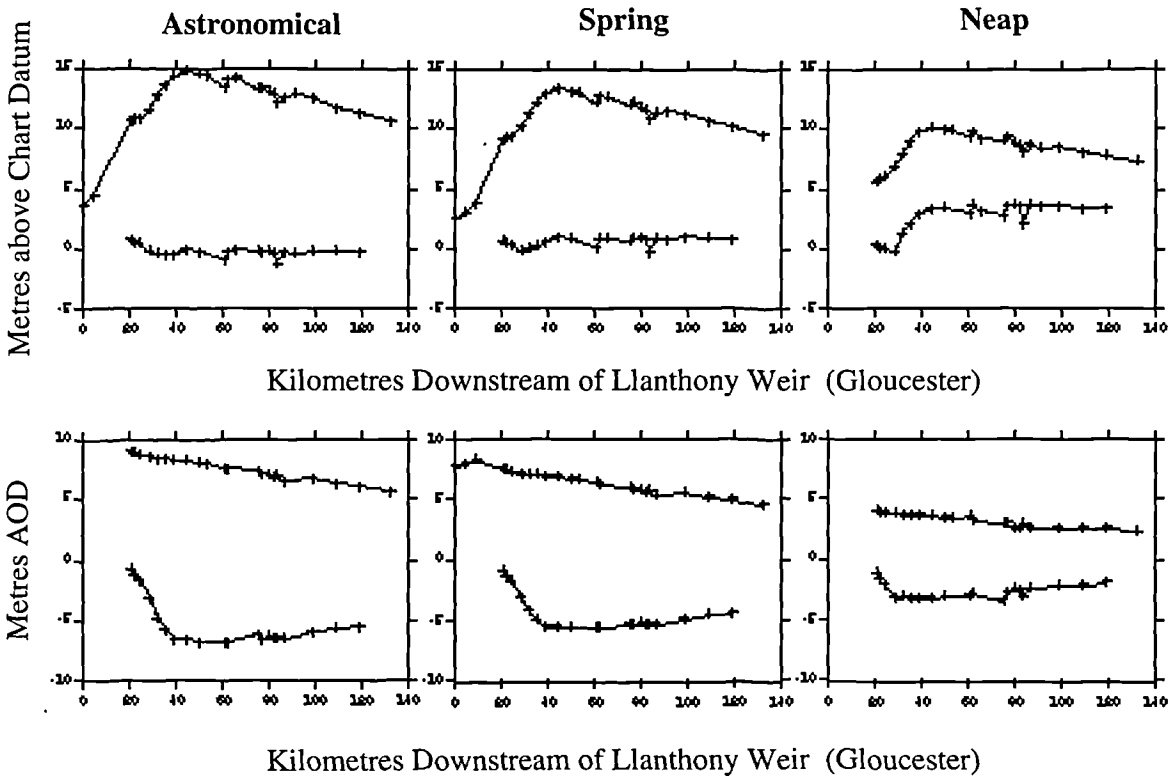

Fig 1.3 Tidal levels in the Severn Estuary in relation to Chart and Ordnance Datum.

In this thesis tidal height is described in relation to Ordnance Datum, rather than Chart Datum, because of the simplicity in comparison and the use of a single unchanging datum in the later computer modelling.

The maximum (astronomical) range is 14.86 metres at Sudbrook, which is the site of the Severn Road Bridge. At this point the highest tidal velocities and turbulence are also generated. Other selected tidal ranges are displayed in Table 1.2 and shown graphically in Figure 1.4. The tides of the Severn are macrotidal, as a result of which tidal currents (non

wind generated) are fast and turbulence is high, resulting in the well mixed muddy waters in the Estuary. Immediately downstream of Aust at the Shoots there is little or no slack water during a tidal cycle, due to the large tidal range and the narrow low water channel carved during the glacial periods. Turbidity is at a maximum at Aust to the first great bend at Frampton due to the high tidal range and the interaction of the channel bottom with the generated currents. The tidal range decreases upstream of Aust because the river rises abruptly to delineate the level of tidal minima.

Place	Distance (km)	Tidal Range			Notes
		Astronomical	Spring	Neap	
Porlock Bay	119.4	11.55	9.40	4.40	
Watchet	98.7	12.63	10.30	4.90	
Cardiff	76.5	13.67	11.30	5.80	
Sudbrook	43.6	14.86	12.40	6.70	Maximum
Berkeley	23.5	10.31	9.00	6.00	
Wellhouse	20.3	9.80	8.40	5.20	

Table 1.2. Tidal ranges on Astronomical, Spring and Neap Tides. Distance is in Km downstream of Llanthony Weir at Gloucester.

Low tidal heights above Inward Rocks are affected by the river flow of the Severn and its tributaries, thus the tidal ranges shown in Figure 1.4 are for a low rate of flow, with the figures being derived from Admiralty tide tables. Riverine flood water can increase the height of the free surface at low tide at this point and upstream by 0.6 to 1.0m. The height of high water is rarely affected except when extreme river flows are occurring which is less than once per annum.

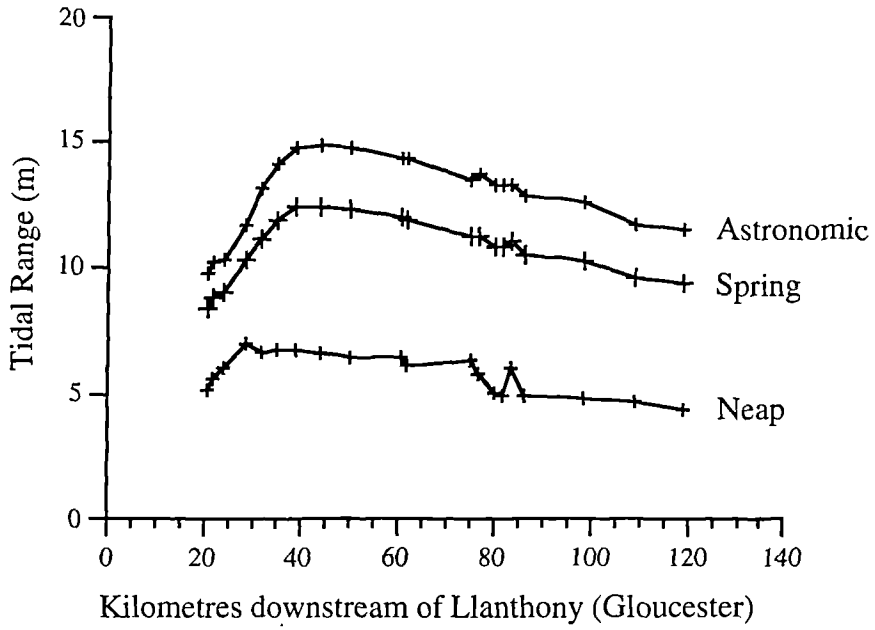

Fig 1.4 Tidal ranges in the Severn Estuary.

Upstream of the Framilode and Epney area, the Severn is generally considered to be non-tidal during neap tides. The spring high water is generally considered only as far as the weir at Maisemore, however, extreme tides have been known to overtop this weir and extend as far as the weir at Tewkesbury, 15km upstream. The original tidal limit of the Severn was considered to have been Upton-on-Severn, 25 km north of Gloucester before the weirs were constructed.

The distortion and amplification of tides in an estuary were first described by Airy (1842) who demonstrated that high tide levels are increasingly amplified up an estuary due to its funnel shaped nature, until the bottom slope or friction effects reduce the peak height. In the Severn the tides are close to an harmonic resonance proportional to the length of the Estuary system, measured from the head to the continental shelf, to the period of the tides forming the large tidal ranges. The tidal distortion in an estuary is related to this increased amplification of an incoming tide. As waves travel faster in deeper water, the tidal peak accelerates upslope at a greater rate than the trough assuming there is little frictional resistance. The Severn Bore occurs when the peak of the incoming tide effectively catches up the low water trough and the tidal front becomes vertical. The highest tides occur in the Spring and Autumn and produce spectacular tidal bores at the Equinox period. The height and speed of

the bore also depend on the level of the freshwater flow, being higher and slower during drier periods. At Longney, 10 km downstream from Gloucester, the upstream surge of the bore reaches heights of between 1 and 1.5 m; the speed increasing upstream from 8 km/h at Sharpness to approximately 18 km/h between Minsterworth and Gloucester. The bore usually reaches Minsterworth 45 minutes after the high tide at Avonmouth and after an hour at Stonebench. From a spectator's point of view, the Severn Bore is a relatively rare occurrence to catch, however, it occurs much more frequently than assumed, albeit less spectacularly, when a tide in excess of 13.5m at Avonmouth occurs.

An interesting feature of the upstream tides within the Severn Estuary is that the low tidal level of the spring tide upstream of Oldbury is higher than the low tidal level of the neap tide (Fig. 1.3). This can be explained by the storage of water on the high tides. During a high spring tide, such an amount of water enters the Upper Estuary that the low tide is unable to flush this volume back at a sufficient speed. Some of the high tide water is effectively stored in tidal pills and upon the salt marshes.

1.9 Flooding in the Severn Estuary.

The Bristol Channel and Severn Estuary are bounded by nearly 80,000 ha of low lying land. The risk of inundation in these areas has been greatly reduced by the building of sea defence banks. The age of these banks varies greatly from Roman Times to the present day.

Crest levels of the banks generally rise in an upstream direction, although they are often raised in areas of industrial and urban importance. Reaches prone to severe wave attack and high winds, from the south and south-west, are also locally higher than the general levels. There are local low points in the banks where old banks have been maintained inadequately or settlement has occurred.

The defence heights downstream from Portbury have been set on the calculated 100 years sea level, with some allowance for wave run-up. Bank heights vary greatly as exposure along the coast is highly variable. Upstream of Avonmouth there are considerable reaches of old banks in need of raising. The need for immediate review of these walls was highlighted during the storms in the Winter and Spring of 1989-1990.

There have been a number of flooding events within the Severn Estuary; Plate 1 shows a woodcutting depicting the area around Peterstone Wentlooge which gives a somewhat over emphasised visual appraisal of this flood. Local records do, however, give an account of the severity of the flooding during this time. Archive searches of the records and newspapers in Gloucester City & County Library and Records Offices provided numerous other events often caused by a combination of high river flow, especially from the Frome and high tides in the Frampton, Framilode and Epney areas. During the Autumn and Spring of 1989 and 1990, two further events highlighted the vulnerability of the Estuary to inundation.

1.10 Conclusion.

Having introduced the Severn Estuary area and it's tides this thesis will continue in the following manner;

- Chapter 2

Sea level changes in the Severn Estuary, including global climate and sea level change during the Quaternary and postulated sea level changes.

- Chapter 3

The hydraulic theory behind the computer model developed because of the shortcomings highlighted in Chapter 2.

- Chapter 4

The mathematical method of solving the hydraulic equations derived in Chapter 3.

- Chapter 5

The data needs and how an ideal model is adjusted to allow for flow in a natural river or estuary.

- Chapter 6

Model results and verification, which describes the computer model derived, it's execution and the verfication process.

- Chapter 7

This Chapter presents the results of the model simulations to various aspects of the present, past and future Estuary conditions.

- Chapter 8

Describes the morphology of saltmarshes and their sedimentological response to different tidal regimes

- Chapter 9

The final chapter concludes and summarises the findings of this thesis and how future work may be beneficial to the study of the Severn Estuary.

There are a number of appendices which accompany the main body of text, Appendix A contains location plans of many of the sites described in this work.

The thesis is presented as a double spaced text to facilitate accurate representation of equations in the later chapters which could not be achieved with different layouts.

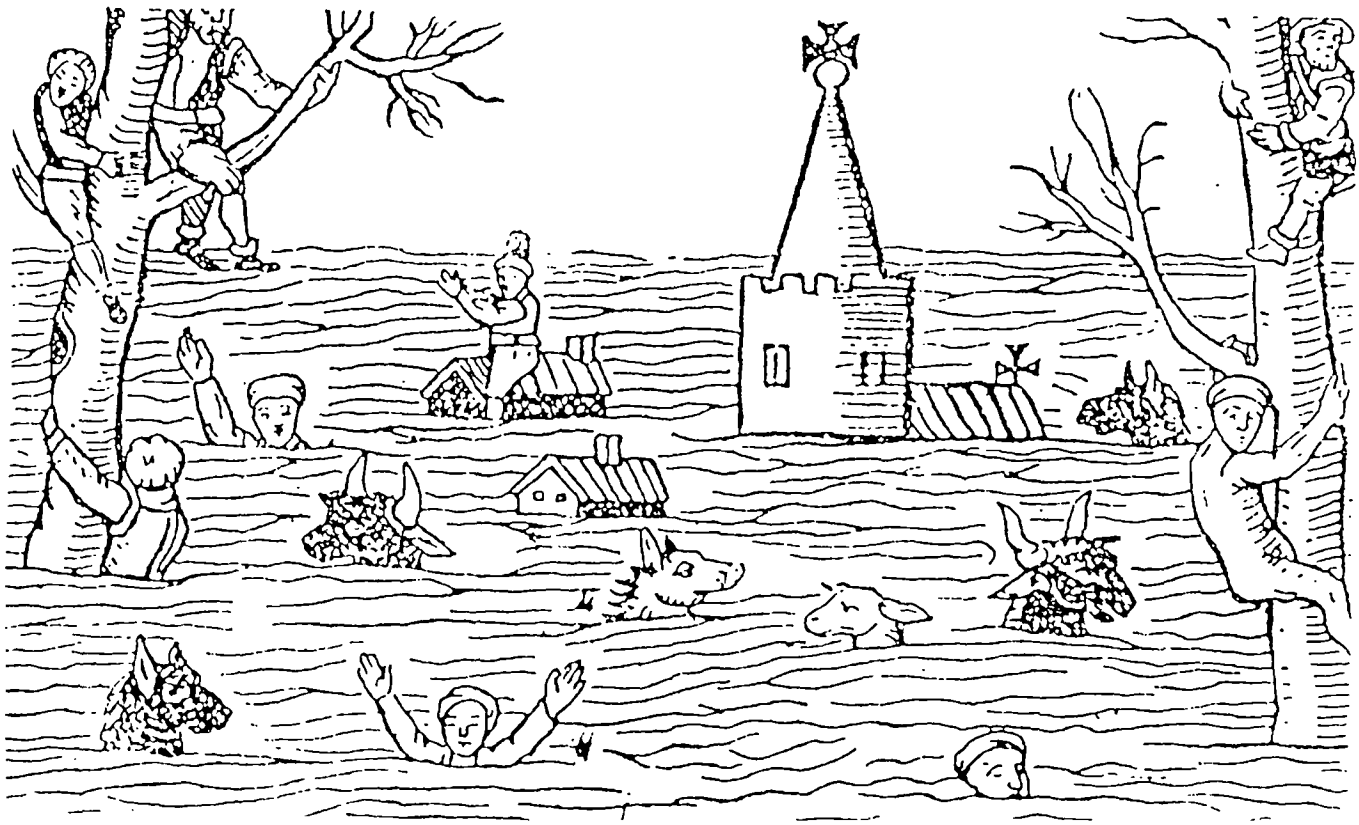

Plate 1. Flooding of the Wentlooge levels, 1607, wood carving from Peterstone Church.

CHAPTER 2.

SEA LEVEL CHANGE AND SEDIMENTATION.

2.1 Introduction.

The theory of glacio-eustatic sea level change is over one hundred years old. However, it is only since the 1960's after advances in radio-carbon dating, geophysics, climate modelling and Quaternary stratigraphy that there has been any significant interest in late Quaternary sea levels.

The glacio-eustatic theory is based upon the relationship of global temperature and the entrapment of water in massive ice sheets. It is the wax and wane of these ice sheets which have affected the global sea level and hence influenced much of the modern day coastline.

This chapter presents a broad overview of some of the global Quaternary sea level changes and the development of the Severn Estuary. The variations in global mean temperature during these periods led to sea-level changes as water was retained at, or melted from the higher latitudes of the Northern and Southern Hemispheres. The chapter describes the geological development of the Severn Estuary in response to sea level changes, particularly the Flandrian (Holocene) Transgression which is responsible for the present morphology of the Estuary and how future sea levels may change the Estuary environment.

The chapter is structured to give a brief overview of global sea level changes during the Pleistocene, and then more detailed sea level changes during the Flandrian. Afterwards the nature of the Quaternary sediments of the Severn Estuary is briefly described, before the subject of the estuarine retreat and sedimentation in response to sea level rise is described by a simplistic model. The existing tidal regime is described and then analysed in terms of the potential rise in levels in response to a global climate change.

2.2 Quaternary Stratigraphy.

The Quaternary is divided into a number of stratigraphic units. These stratigraphic terms are man's attempts at terminology to represent the climatic fluctuations which cause the ice advances and recessions.

2.2.1 Origin of Terms.

The term Quaternary was introduced by Desnoyers in 1829 for deposits within the Paris Basin. Reboull (1833) defined the Quaternary as representing the Ice Age which included flora and fauna still living. Lyell (1839) used the term Pleistocene (most recent) for all rocks and sediments in which over 70% of the molluscan species are still living. These terms have been subsequently reviewed in relation to the ice movements, Agassiz (1840, 1847) first presented a coherent theory of the ice ages world-wide, but it was Forbes (1846) who proposed the term 'Recent' to represent the Post Glacial Epoch and thus the Pleistocene as the Glacial Epoch.

Maclaren (1841) first related changes in relative sea level with the glacial events of the Pleistocene calculating that at the maximum extent of the ice masses sea levels would have stood at about 110m below present levels. Jamieson (1865) identified that raised beaches and flat platforms represented former periods of high sea level stands related to glacial isostacy. Towards the end of the Nineteenth Century it had become clear that there had been at least 4 glacial episodes in the USA, East Anglia (Geikie, 1894) and the Alps (Penck and Bruckner, 1909) which were attributed to climatic fluctuations. Study of clays in Scandinavia identified the presence of varved sequences representing annual layering and hence De Greer (1940) was able to date the sediments present by counting the varves present.

It was not until the 1950's and especially the 1960's that radio carbon dating (^{14}C) oxygen isotope, K-Ar methods, dendrochronology and palaeomagnetic methods provided a much more detailed insight into the Quaternary. Amino acid analyses which were popularised in the 1970's were a further development, especially in the dating of shells.

2.2.2 The Pleistocene and Flandrian (Holocene).

In 1948 a meeting at the International Geological Congress suggested the base of the Pleistocene should be placed at the base of the Calabrian in Southern Italy, based on Mollusc and Foramnifera extinctions. This boundary had already been dated by relative stratigraphy as being at the end of the Astian or Pliocene Period marked by the colonisation by Elephant and Horse species. The Upper Villafranchian was identified as containing the same fauna as the Calabrian, leading to the stratigraphic divisions shown in Table 2.1.

Villafranchian	Upper	Calabrian	Lower Pleistocene
	Middle	Astian	Pliocene
	Lower		

Table 2.1. Early Quaternary Stratigraphy.

In literature the term 'Ice Age' is confusing and must be treated with care as different authors consider an Ice Age to be either a glacial epoch, glacial stage or cycle. The Pleistocene Epoch is the first stratigraphic part of the Quaternary and consisted of several glacial and interglacial periods, the number of which depends on the geographic position and personal interpretations. The INQUA meeting in Paris (1967) decided that the boundary between the Pleistocene and the Flandrian should be set at 10000 years BP and we are now in the Holocene Epoch which started at the end of the last (Devensian) cold period. This separation was decided as a point of convenience rather than fact as in some parts of the world Devensian conditions prevailed, as they still do on land in Greenland for instance. It is not totally clear why the Quaternary is divided by some into the Pleistocene and Holocene as in reality it seems that the Holocene is just another interglacial warm period and should be a sub-division of the Pleistocene. Whilst the distinction between the two is based upon a period of predominantly mammalian extinctions it is clearly to assist academics in creating a convenient boundary to describe the period in which the modern landscape and mankind's development has been of prime importance.

In the terms of this thesis the Quaternary will consider the Pleistocene to be followed by the Holocene (or Flandrian) for simplicity without arguing the stratigraphic merits of such a division. The Severn system as recognised today has developed over the period of the Pleistocene, although the data to construct the full history is sparse. Following the denudation of the area during the Devensian, the Flandrian infilling of the Estuary and sea-level change is much easier to interpret.

2.2.3 Methods of Study.

- $^{40}K/^{40}Ar$ Dating.

This method of dating, largely restricted to volcanic rocks is most useful for dating rocks greater than 100000 years old through the measurement of the ratio of Argon which has developed by natural decay. Measurement of younger rocks generally tends to be prone to a large standard error in the data, thus limiting its usage. K-Ar dating was used to great effect on the lava flows in sediments in East Africa which are interbedded with igneous sequences. The sedimentary rocks in this area contain some of the earliest hominid remains and were found to contain Upper Villafranchian fauna found to have a base of about 1.7-1.9 million years BP.

- Palaeomagnetism.

The magnetic field of the earth undergoes sudden changes over periods of milliseconds to millions of years. Sediments and igneous rocks may be magnetised during formation to leave a natural remnant magnetism (NRM) which reflects the magnetic field within which they accumulated. The long term field reversals have particularly been identified in marine sediments and igneous rocks, which can be K-Ar dated to derive a magnetostratigraphic time series (Table 2.2), based upon periods of a predominant magnetic field polarity. During each of the Epochs there have been a number of minor and relatively short lived polar reversals, in some cases there has been times where these reversals have been of a sufficient duration to be called 'events', the most important of which is the Olduvai Event which has been identified at between 1.72 to 1.8 million years ago. As the Olduvai Event occurred at a similar age to the base of the Lower Pleistocene it can be used as a stratigraphic marker.

Magnetostratigraphic Epoch	Age to base (millions of years)
Brunhes	0.73
Matuyama	2.47
Gauss	3.4
Gilbert	5.26
Epoch 5	N/A

Table 2.2. Magnetostratigraphic Epochs (Berggren et al . 1980)

- Oxygen Isotopes.

Oxygen isotope analysis was pioneered by Emiliani in 1955 who found that analysis of the two common stablest isotopes of oxygen, ^{18}O and ^{16}O, allows a correlation between the variation in proportion of the isotopes and the prevailing climate, with the proportion of ^{18}O reducing with higher temperatures. The variation in oxygen isotope concentrations of oceanic water will be recorded in the shells and skeletons which lived within the seas, especially planktonic and benthonic foramnifera, which where subsequently preserved in the marine sediments. There are a number of inherent problems in the analysis of this kind and the assumptions made upon the prevailing conditions at the time, however, the correlation of oxygen isotope ratios with palaeomagnetic events has allowed the dating of ice cores to be undertaken.

- Ice Cores.

The annual accumulation and snow melts can be determined from ice cores and the relative concentrations of oxygen isotopes related to the prevailing climate. Patterson *et al.* (1977) showed that there was a significant correlation of datable temperature trends between cores taken from Camp Century (Greenland) and Devon Island in Canada. Both temperature curves showed that until 65000 BP the proportion of ^{16}O was greater, indicating generally warmer conditions which were attributed to represent an interglacial warm period. The Ipswichian Interglacial is now considered to have ended at 75000 BP. Patterson also identified a period of extreme cold of around 7°C cooler than today at about 20000 BP followed by a

relatively fast rate of climatic warming. Patterson's analyses also indicate that the Ipswichian Interglacial was some 2 to 3° C warmer that at present, whilst the temperature in the two study areas appears to have cooled by about 1°C in the last 5000 years.

- Palaeobotony.

Floral remains, especially pollen, can also give indications of the prevailing climatic conditions at the time of growth. The onset or end of a glacial period will be accompanied by a change in flora type, forming belts of similar floral assemblages which migrate up and down latitudes as the temperature cools or warms. Four early pollen zones have been proposed representing different predominant climatic conditions (Table 2.3 and Figure 2.1).

Pollen Zone	Predominant Flora	Environment
IV	Boreal genera, Pinus, Hertula and herbaceous types	Thinning of forests and development of heath land
III	Trees, Abies, Quercus, Corpinus	Forest expansion at the expense of oak forest genera.
II	Temperate trees, mixed oak, Quercus, Ulnus, Alnus, Frascinus and Carylus	Stable forest.
I	Boreal genera, Hertula, Pinus and herbaceous types	Heath land

Table 2.3. Pollen Zone assemblages.

- Insects.

Coleopteran remains tend to be well preserved in Quaternary sediments as the chitinous exoskeletons are robust and resistant to degradation. The ample variation in identifiable species types makes them desirable for study, with over 3800 species being identified within the UK. Different species tend to favour different environments, especially organic wetlands, hence

providing a good record of the climatic conditions. Coope's 1977 study of beetle remains found that there appeared to have been a relatively warm period about 11000 to 14000 BP where average July temperatures were in the order of 17°C before the onset of the Loch Lomond (or Highland) Readvance when average temperatures dropped to around 10°C (Figure 2.1).

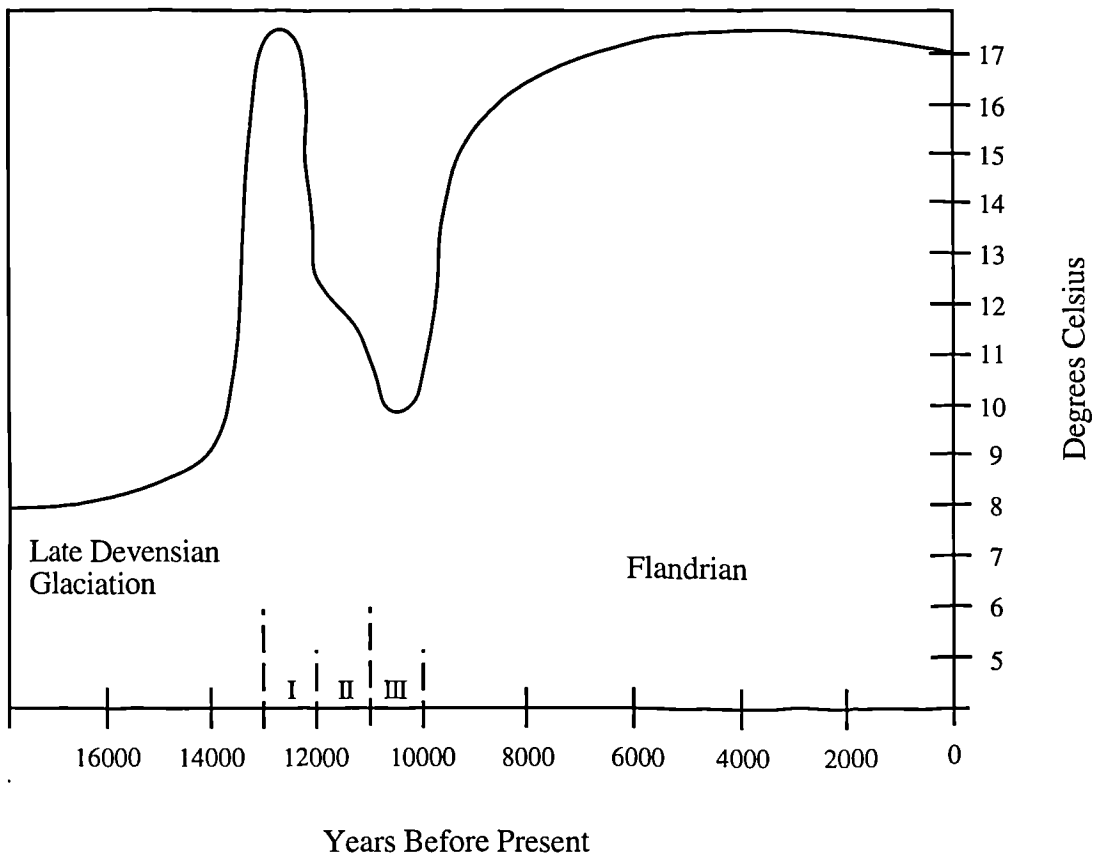

Fig. 2.1 Late and Post-Devensian temperature change. Average July temperatures (after Coope, 1977). I, II and III represent pollen zones for middle England.

- Radiocarbon Dating.

When radiocarbon dating was popularised by Libby in the mid 1950's it produced a revolution in chronological studies of the Quaternary. Nuclear reactions within the upper atmosphere cause the displacement of protons from nitrogen atoms to produce carbon atoms (^{14}C isotope). This isotope is unstable and gradually decays to form the stable ^{14}N isotope. Carbon-14 readily oxidises to carbon dioxide and is mixed in the atmosphere with carbon

dioxide containing Carbon-12 isotopes, as a result ^{14}C becomes adsorbed by the oceans and living organisms. Radiocarbon dating assumes that the rate of production of ^{14}C is constant with time and that the ratio of ^{14}C and ^{12}C adsorbed in the biosphere and hydrosphere accurately reflects the atmospheric ratio. Assuming that the decay rate of ^{14}C is known then the age of organic tissue can be dated from the time of its death, until there is a natural replenishment of decaying ^{14}C by new ^{14}C. Carbon-14 decays at a rate of 15 disintegrations per minute (dpm), with an activity half-life of 5730±40 years. This period of the half-life was calculated by Libby (1955) as being 5568±30 years, resulting in a discrepancy in the calculations of age using the old half life value and the newer one. There are, however, a number additional factors which reduce the reliability of radio carbon dating. Vries (1958) found that the calculated dates of wood samples from the 17th Century were 2% in error and suggested that there were long term variations in the production of carbon isotopes. This was confirmed by the study of tree rings. Industrial activity by man has led to the liberation of more carbon-12 to the atmosphere from the burning of organic fuels, offset to some extent by nuclear detonations, leaving modern samples as an unsatisfactory benchmark, hence the carbon contents are back calculated to give an 1890 carbon-14 value (representable pre-industrial value) and then corrected to 1950 which is taken to represent day 1 in the radiocarbon calendar. A lack of correlation can also occur from preferences for the adsorption of different isotopes; sea water tends to preferentially absorb ^{14}C and plants ^{12}C. The adsorption of carbon isotopes by the sea gives it an apparent age and deeper marine samples tend to show ages considerably greater than those of shallow ones.

2.2.4 Summary of Stratigraphic Terms

Lowe and Walker (1987) correlated the various terms for the Quaternary events (Table 2.4) based upon the findings and cross correlation of studies using all the methods described in the previous section. This table of terms cannot be considered to encompass all the events or history of the Quaternary, indeed some of the periods may not have occurred, or cannot be established through a lack of preserved information, similarly the events cannot be seen as synchronous worldwide.

BRITAIN	NORTHERN EUROPE	EUROPEAN ALPS	CENTRAL NORTH AMERICA
Flandrian	Holocene	Post glacial	Holocene
Devensian	**Weichselian**	**Wurm**	**Wisconsian**
Ipswichian	Ermian	Riss-Wurm	Sangamon
Wolstonian	**Saalian**	**Riss**	**Illinoian**
Hoxnian	Holsteinian	Mindel-Riss	Yarmouthian
Anglian	**Elsterian**	**Mindel**	**Kansan**
Cromerian	Cromerian	Gunz-Mindel	Aftonian
Beestonian	**Menapian**	**Gunz**	**Nebraskan**
Pastonian	Waalian		

Table 2.4. Quaternary Stratigraphy in Europe and Northern America (after Lowe and Walker, 1987). Cold periods in bold type.

2.3 Sea Level Changes during the Pleistocene Epoch.

Global sea level changes during the Pleistocene are based on the observations of raised and submerged coastlines in geologically stable areas so that they can be considered to represent eustatic sea level change. Platform areas around and above the coast have long been interpreted as old marine platforms and physical geologists and geomorphologists in particular have studied these phenomena. For instance the flat coastal regions of Southwest England and South Wales have been studied by such as Bowen (1978) who criticised the previous dating that had previously been given to these 'flats' by earlier authors.

Most recent studies have considered that the maximum Hoxnian sea level to have been 5 to 15m above the present high water spring tide level (Gilbertson and Hawkins, 1977), with Ipswichian levels being similar to those of today. Cooper (1948) drew attention to the submerged cliff line off the coast near Plymouth indicating periods of lower sea level, work which was advanced by Donovan and Stride and brought together by Hawkins (1972). It must

be noted, however, that the derivation of the age of the Pleistocene events before the Ipswichian is beyond the range of most reliable dating methods, so interpretation of these sea level stands is often of ancient shore lines which may have been considerably effected by tectonism and erosion. Several authors have placed the maximum Hoxnian sea levels in regions far removed from the United Kingdom as being 20 to 30m above today's levels (Stephens and Synge 1966, West 1972, Mitchell 1977). However, this period is believed by Coope (1977) as being cooler than both the Ipswichian and Cromerian interglacials based on fossil insect assemblages. In contrast to Gilbertson and Hawkins, Stearns (1971 & 1978) puts the high Ipswichian sea level at 10 to 30 m above the present levels and Fairbridge (1961) places the levels considerably higher although it must be remembered that glacio-isostatic events can cause significant local variations.

The late Ipswichian and early Devensian sea levels have been determined by Uranium series disequilibrium dating and other isotopes (Bowen 1977, 1978) on fossil corals and less reliably, fossil shells. Much of the recent work on coasts of these periods has been undertaken on tectonically unstable regions because the sea level history of a stable coast is vertically compressed with respect to one which is moving. One of the best examples of this phenomenon is the terraced Huon Peninsula in Papua New Guinea where over 20 reef features can be found up to 600m above present sea level. Chappell (1974 & 1983) devised a method of separating eustatic and tectonic movement to give curves similar to other authors (e.g. Broecker *et al.*, 1968) in Barbados. In Europe, Morner (1969, 1971) studied unstable areas which had been loaded by glacial ice masses in Scandinavia and Scotland from which he was able to describe glacio-eustatic relationships. However, the more recent tectonic activity in the active neo-tectonic regions of the Mediterranean Sea has left remains of submerged coastal features many metres above sea level, leaving a false impression of previous levels. The complexity of volcanic areas, such as near Vesuvius, is in some cases shown by marine features upon old Roman columns, representing colonisation on ground levels which have been raised by stress bulging and have subsequently subsided following eruption.

In view of the many problems associated with the analysis of Pleistocene sea levels, it seems clear that a simplified altitude correlation of sea levels is difficult. This is exacerbated by the effect of the tidal range at the point of interest, if modern tidal regimes can be considered to

mimic past ones, where the height of the high water spring tide can vary from in excess of 8mAOD in the Severn Estuary and Bay of Fundy, to as little as 0.5m in Sicily. Some postulated global sea levels which are generally in non-UK areas are tabulated in table 2.5 which shows some major discrepancies in global sea levels analysed by differing authors at different locations.

Period	Age (Ka BP)	Level (m AOD)	Location	Author
	570	High stand	Curacao	Schubert 1978.
	400	High stand	Atauro	Ward 1971, 1973
	325	Ca. 0m	New Guinea	Bender *et al* 1973, 1979
	220	-20m -32m Ca. 0m	Bermuda Barbados Atauro	Labeyrie *et al* 1969 Cronin *et al* 1981 Chappell 1978
	200 180	+ 2m -20m to -30m	Bermuda	Harmon *et al* 1983
Hoxnian		+20 to +30m +10 to +30m	UK general	Stephens 1966 Mitchell 1977 Land *et al* 1967 Stearns 1971 & 1978 Fairbridge 1961
Ipswichian	120	+3 to +10 m	Pacific Ocean Bahamas	Chappell 1974 Veeh 1966 Broecker 1965 & 1968
Ipswichian	82 & 103	0 m to -13m	general	Broecker 1968 Stearns 1976

Table 2.5. Pleistocene sea levels.

2.4 Sea level Changes of the Flandrian.

2.4.1 Climatic events of the Flandrian which have affected sea levels.

Coope (1977) presented a simplified graph of the average July temperature for the last 18000 years (Figure 2.1) which shows a much greater range than the seasonally dampened

global temperature estimates of Imbrie and Imbrie (1979). Coope's graph also shows the pollen zones adopted by Godwin 1940, used as stratigraphic markers for the late Devensian. Pollen zones I and II represent a period of warmth (The Late Devensian Interstadial) and pollen zone III the Younger Dryas event (Highland Readvance). The curve also shows the ensuing Holocene climatic amelioration, signifying the onset of the Flandrian Transgression which is the last great marine transgression and hence has the most visible effect upon the modern coastline. Unfortunately there is no substantial proof of the Late Devensian Interstadial in the Severn, although ApSimon, Donovon and Taylor (1961) have identified faunal remains of the temporary colder phase of the Highland Readvance on Brean Down in the south east of the Severn Estuary.

2.4.2 Flandrian Sea Level Changes.

Since the introduction of radiocarbon dating in the late 1950's there has been a considerable input into the construction of post glacial sea level curves and it seems that authors fall into three groups of thought;

- Sea level rose at a quick rate before slowing down to reach its present position in an asymptotic nature
- Sea level reached its present position about 4 Ka BP and has remained stable
- Sea level reached its present position about 4 Ka BP and has since fluctuated above and below that level.

Since the end of the Devensian, 14000 years BP, the sea-level has risen with a generally increasing mean temperature, resulting in sediment deposition within over deepened valleys formed during the previous periods of low sea level stands. In response to the rapid temperature rise resulting in ice melting between 14000 and 11000 years BP sea levels rose. This period was punctuated by the Loch Lomond (Highland) Readvance which was the last significant cold phase between 11000 and 10300 years BP during which Cameron and Stephenson (1985) identified a minor lowering of global mean sea level. Subsequently

temperatures again increased and sea levels rose as the world's ice-masses melted. This initial period of relatively fast sea level rise has been termed the Flandrian Transgression by Godwin (1940) and extends between 10000 to 8000 years BP.

2.4.3 Flandrian Sea Level Curves.

Flandrian Sea level curves have been presented by a variety of authors. It is intended in this section to describe the merits and developments of relevant curves which cover a long (x1000 years) period and then to describe the Estuary development in relation to the pollen zone stratigraphic markers which cover more specific temporal periods, the recent archaeological data will be examined after this.

The first major sea level study of the Holocene was published by Fairbridge in 1961 (Fig 2.2). Fairbridge (1960, 1961) introduced sea level curves using radiocarbon ^{14}C dating which produced a generally rising sea level trend over this period, but with subsidiary oscillations. The fluctuations in sea level suggest that there would have been periods of transgression and regression which could significantly influence the nature of sedimentation which would occur in an estuarine environment undergoing a series of marine advances and retreats. Fairbridge used a worldwide spread of data for his curve, which has caused Lloyd (1989) to question his consideration of the validity of the height data. In considering a widespread series of sites the curve will also have been distorted by localised differences in tectonic regime and will effect the continuity of data. Problems with the construction of sea-level curves will be described later in this chapter.

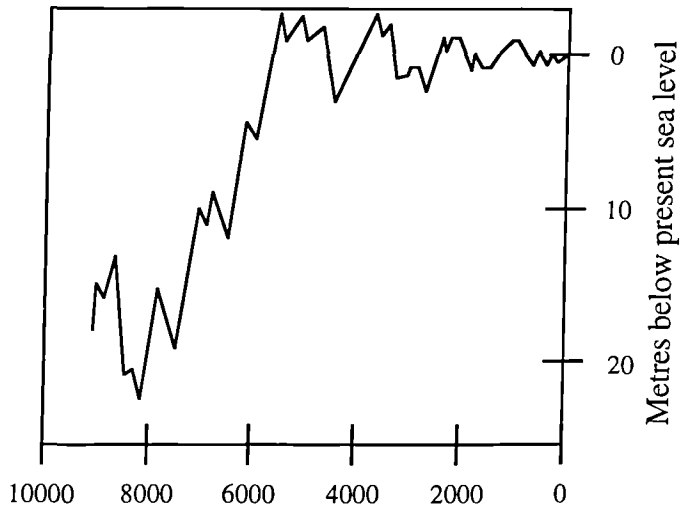

Fig 2.2. Sea level curve after Fairbridge (1961)

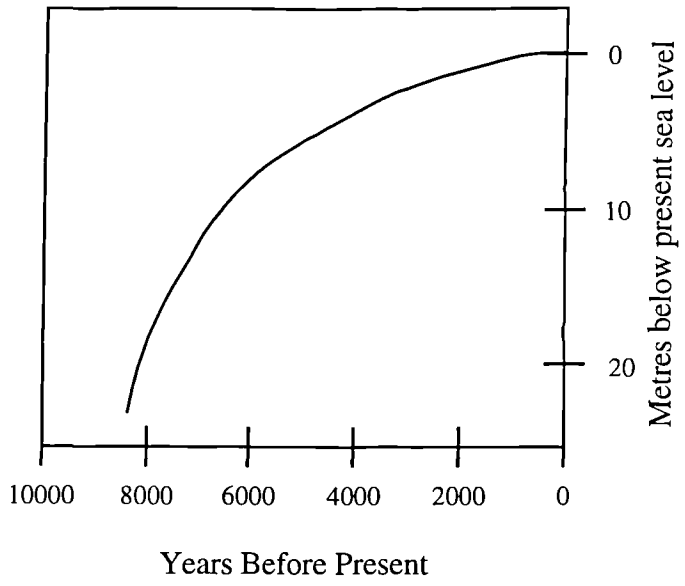

Fig. 2.3 Sea level curve for the North Sea/Netherlands, after Jelgersma (1969)

Jelgersma (1961) analysed samples from the Netherlands using data from a small area. This approach was adopted as it would give an accurate idea of sea level change specifically for the Dutch lowlands which are vulnerable to marine inundation. Jelgersma produced a smooth curve for sea levels, implying a steady rise in levels (Figure 2.3). However, Jelgersma's sampling was undertake on an inclined bedrock platform, for which it appears that she did not

thoroughly compensate. As a result samples of the same age will be found at increasing higher altitudes away from the tidal zone.

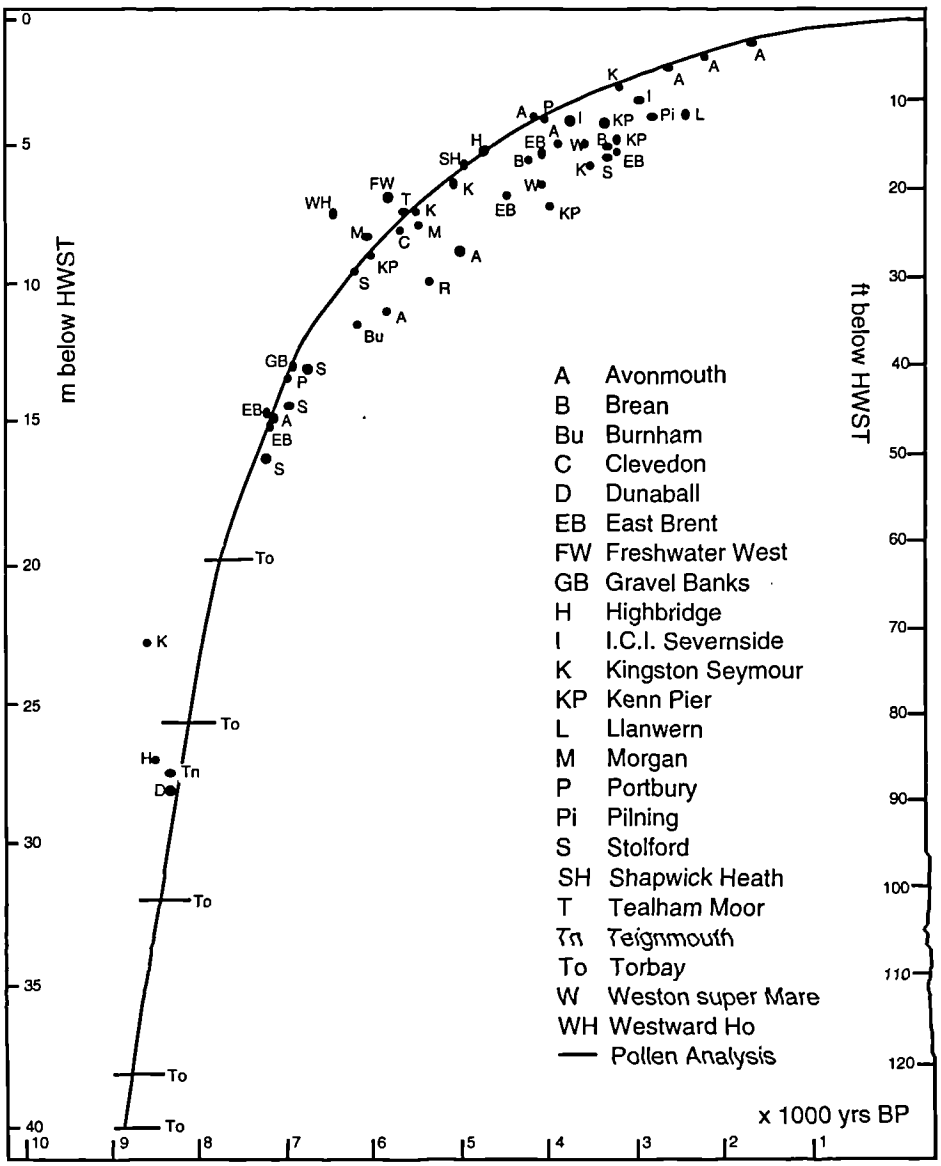

Fig.2.4 Sea Level Curve for Severn Estuary (from Hawkins, 1971) Locations of dated samples are shown.

Although there are significant differences between the curves of Jelgersma and Fairbridge, the differences can be attributed to the widespread origin of data for Fairbridge's study. Jelgersma's study is considered by many to represent global eustatic sea level change due to the area of analysis being tectonically inert. Morner (1969, 1971) also produced a different graph, but his study was specific to Scotland and Scandinavia which were prone to

isostatic rebound, of which he gave due cognisance to this very difficult interrelationship.

Hawkins (1971) supports a steady rise using data from the Severn Estuary (Figure 2.4). The sea level curve for the Severn Estuary by Hawkins was supported by Heyworth and Kidson (1982) which was used by Shennan (1983) to produce his curve for the Severn region (Fig 2.5).

Both the sea level curves produced by Shennan and Hawkins show a steep sea level rise between 7000 and 9000 years BP slowing in a similar fashion to the Jelgersma curve after this period. The period between 9000 and 7500 shown on the curve by Hawkins is based mainly on pollen analysis and slightly conflicting dated samples. With age the certainty of these points becomes less. However, the early part of the graph can be considered the most reasonable representation available.

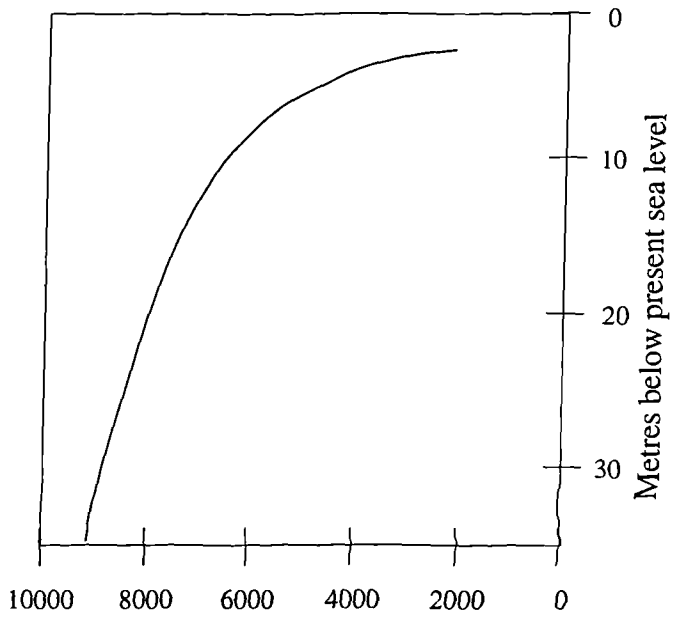

Fig 2.5 Sea level curve for the Severn Region by Shennan, 1983 (After Heyworth and Kidson , 1982)

2.4.4 Comparison of published sea level curves.

There are a number of studies that have been undertaken in the UK and Europe. The

International Geological Correlation Programme (IGCP) proposed the establishment of a global sea level curve to cover the period of deglaciation to the present. UK studies were also spurred by the Geologists Association (Proceedings, vol. 93) and the Engineering Group of the Geological Society (QJEG vol. 21, 1984). However, many of these curves are for different areas of the UK and show enormous variations due to the difficulty in separating the rebound following glacial retreat and the change due to eustatic rise. Further problems in comparison of the sea level curves results from differences in the techniques and interpretation of the various authors. Table 2.6 summarises the findings of several authors in the UK and relates them to the curve types described in Section 2.4.2.

Author	Date	Area of study	Sea level curve description
Godwin	1940 1943	Swansea Somerset Levels	Fast steady rise slowing after 4000BP, but punctuated by the Romano-British Transgression.
Godwin	1940	Fenlands	Steady rise from 7000BP, becoming oscillatory after 4000BP.
Jelgersma	1961	*Holland*	Smooth curve, fast rise from 7500 BP slowing asymptotically to present.
Fairbridge	1961	Worldwide	Highly variable, reached present level at about 6000BP and has varied erratically since.
Greensmith & Tucker	1973	Thames Estuary	Rising to present level in erratic fluctuating manner.
Devoy	1977	Thames Estuary	Fast fluctuating rise to 4000BP steadier rise to present level since.
Devoy	1978	South West England	Smooth curve very similar to Jelgersma.
Hawkins	1984	South West England	Smooth curve similar to Jelgersma

Table 2.6. Comparison of some UK sea level studies.

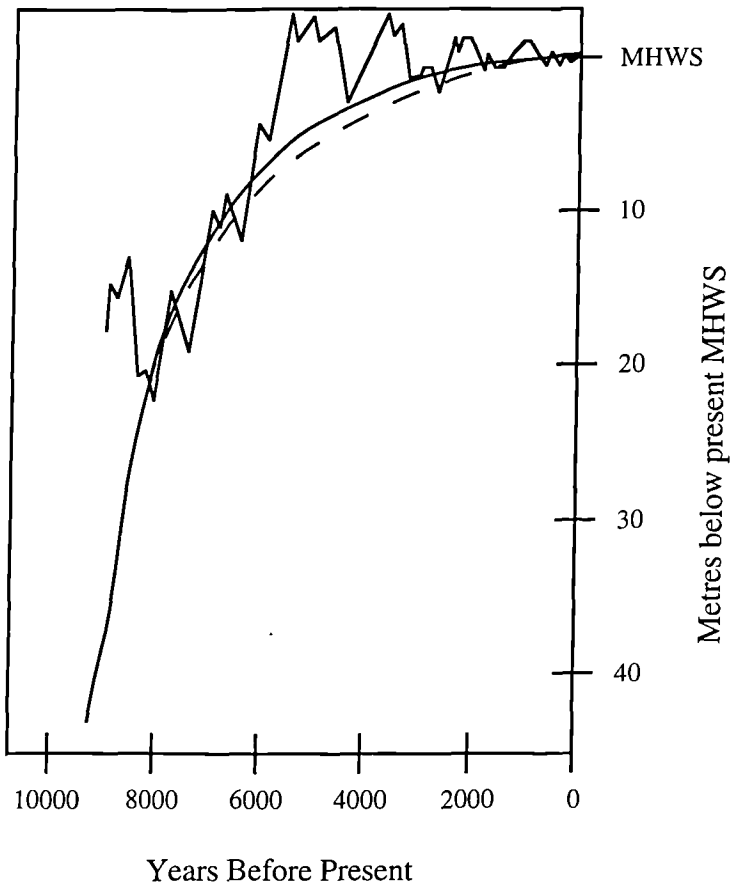

Fig 2.6. Graphical comparison sea level estimates by Fairbridge (1961) - jagged, Jelgersma (1961) - dashed curve and Hawkins (1971) - solid curve.

Most of the sea level studies agree that there has been a rise from greater than -40m AOD since around 10000BP. Since this time some authors have argued that there has been a relative sea level rise, which has been smooth in the South of the UK but has fluctuated up to 10m in the North of the UK where there have been regressive periods due to sea level falls, probably due to isostatic rebound as the north tries to recover from the loading the former ice sheets imparted upon the land. The curves constructed for the eastern coast of the UK are also affected by isostatic movements of the European landmass, although Devoy (1979) also suggested that oscillations in his curves could be attributable to fault movement in eastern England and in the southern North Sea. For the purposes of this thesis it is not necessary to describe in detail all the available sea level curves. In order to consider global sea level changes and the sea level changes relevant to the Severn Estuary, the works of Hawkins, Jelgersma

and Fairbridge are sufficient. A comparison of the three sea level curves is illustrated in Figure 2.6.

The curves of Hawkins and Jelgersma show a striking correlation, as would that of Shennan (1983) and Devoy (1979) if added to the graph. It is difficult to otherwise relate the curve of Fairbridge in any other way than stating that sea level has generally risen during the period of the Holocene.

2.5 Stratigraphic Zones of the Flandrian and Sea Level Rise.

The Flandrian has been divided into a series of pollen zones which reflect the prevailing climatic conditions of the time. These zones are chrono-stratigraphical positions and can be used as a frame to assess the degree of sea level rise. The curves already presented are based upon the evidence of floral and fauna remains in peat bands linked to their position. Thus if pollen of zone VII was found in a peat band at a depth of 'x' metres below Ordnance Datum, the approximate mean sea level would have stood at about this point at that time. Similarly radio-carbon dating is used as an alternative time frame.

Period Name	Time	Pollen Zone	Approximate Sea Level Rise
Boreal	10200 to 9500 BP	IV	
	9500 to 9000 BP	V	
	9000 to 7500 BP	VI	15 mm/yr
Atlantic	7500 to 5000 BP	VIIa	2 to 6 mm/yr
Sub-Boreal	5000 to 2500 BP	VIIb	1 to 2 mm/yr
Sub-Atlantic	2500 BP to Present	VIII	0.1 to 4 mm/yr

Table 2.7 Flandrian Pollen Zones and Sea Level Change in the Severn Estuary.

Periods, times and sea level changes of the Flandrian in the Severn Estuary are summarised in Table 2.7 while the following sections describe the periods in more detail. The sea level changes in this table are related to dateable peats within the Severn Estuary, although it should be noted that in some cases there can be no direct correlation between peats of a similar age because of their position in the Estuary and tidal frame. A theoretical improvement on this method is introduced later in the chapter.

2.5.1 Boreal Period.

The Boreal period is deemed to have extended over the pollen zones IV to VI. Pollen Zone IV is an intermediate stage between 10200 to 9500 years BP following the Highland Readvance. Pollen zone V lasted from 9500 to 9000 years BP and pollen zone VI from 9000 to 7500 years BP. At this time the sea level would have stood 40 to 50m below the present level, accordingly the coastline would have been some distance out to sea. Clark (1966) identified pollen zone IV and V peats off Torquay at -42.7m OD.

Godwin (1940) was the first to produce a reasonable study of sea-level change for the Severn Estuary. He based his interpretation on the pollen present in samples, the age of which was determined by a considering stratigraphic position with estimated prevailing temperature in which the fauna would have been likely to grow. Using borehole samples from Swansea in the Severn Estuary region, Godwin found that four of six significant organic bands had accumulated in Pollen Zone VIb. The peat bands within this zone spanned a vertical height of 9m approximately lying between -17 and -8m OD, a schematic relationship for these layers is shown in Figure 2.7.

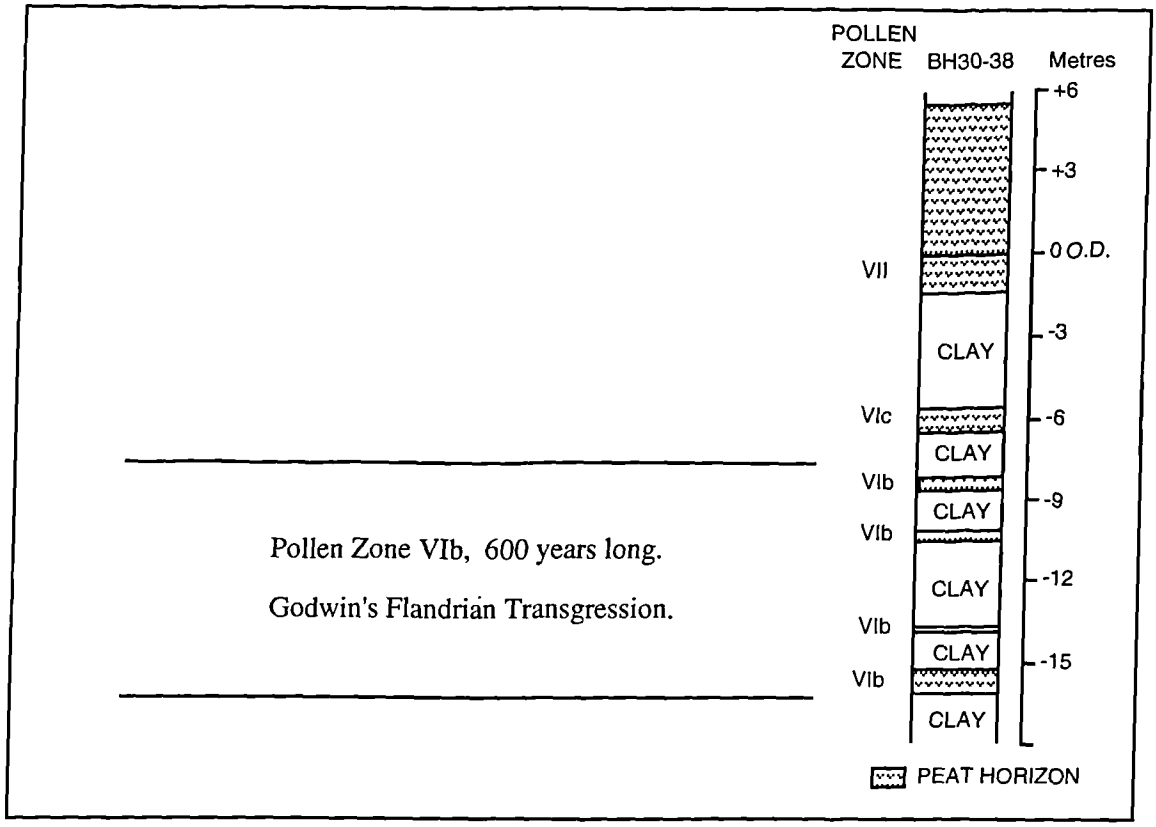

Fig. 2.7. The Flandrian Transgression from Pollen Analysis, after Godwin 1940.

Godwin concluded that 9m of sediment had therefore accreted over the period of around 600 years represented by this zone. Godwin related this evidence to a sea level rise during this period to be at a rate of 1.5m/century (15mm/yr). Godwin at the time acknowledged that his theory was partially flawed because although the assumption made when considering accretion and sea level rates is that the two rates are identical, he saw that peat formation may not have been exactly related to contemporary mean sea level, but at possible depositional positions above this height. This view was subsequently affirmed by Clark (1966) in submarine sampling off Torquay which identified five pollen zone VI peat bands spanning heights between -39.6 to -16.8m OD (a range of 22.8m) over an age of around 1500 years which indicates a rate of nearly 1.5m/century.

Within the Somerset Levels, peat bands have been dated at approximately 8360 and 8690 years BP at depths of -20.7m OD (Dunball) and -14.6m OD (Kingston Seymour) respectively. Borehole evidence of the buried valleys beneath the present alluvium suggests little evidence that there are any deposits below -25m OD in the Severn Estuary and Bristol

Channel, from which it can be deduced that the alluvial deposits in the region are less than 9000 years old.

It should be noted that for the two peat bands mentioned in the previous paragraph, the older peat band is present at a height above the younger one. There is an inherent danger in relating sea levels to the absolute height of the peat bands, even with closely located sampling sites. Godwin (1940) realised that fresh water peats were developing in hollows over a broad expanse of time and were only inundated when the sea-level reached a sufficient height. In effect dateable peats may have been accumulating for a considerable time before the sea level had reached the height at which they had been accumulating. Jeffries, Willis and Yemm (1968) identified pollen zone III peats around 2m above OD in the south of the Gordano Valley which could be attributed to a back bar environment, independent of sea level.

2.5.2 Atlantic Period.

The Atlantic Period which is represented by pollen zone VIIa lasted about 2500 years from 7500 to 5000 years BP and saw a slowing in the rate of sea level rise after the initial Boreal Period of fast rise.

Three peats were found by Buckley and Willis in Bridgwater Bay at -9.1, -7.6 and -6.1 m OD which were radiocarbon dated to have approximate ages of 7360, 7060 and 6890 years which suggests a rise of approximately 0.64 metres per century.

During the Atlantic Period the rate of sea level rise slowed considerably and as a result widespread organic horizons were able to develop. A peat band at Burnham-on-Sea has been found at -4.6m OD and attributed an approximate age of 6262 years (radiocarbon) by Godwin and Wills (1959) representing a rise of 0.24m per century since the earlier Atlantic aged samples from the Somerset Levels, however, this assumes that the samples formed in a correlative position to each other. Hawkins (1971) studied similar Atlantic aged peats in southern England and confirms that a degree of tilting has occurred towards the east of Southern England in the region of 6 metres in the last 6000 years.

2.5.3 Sub-Boreal Period.

The Sub-Boreal Period is represented by pollen zone VIIb and is deemed to have lasted between 5000 and 2500 years BP.

Godwin and Wills (1959, 1961) identified a succession of fibrous and humic peats inland in the Somerset Levels lying directly upon estuarine silts and clays. Neolithic trackways indicate the spread of primitive man in the region. Dating of the peats indicate an approximate rate of accumulation of 0.14 m per century between 4000 to 5000 years BP. However, these peats are some distance inland of the present coast and are freshwater in origin and cannot be related to any tidal frame and do not directly represent a relative sea-level movement but a rate of rise of the water table which is linked to the sea level rise.

There are numerous dated peats above Ordnance Datum for this period in near coastal localities such as Kingston Seymour (+0.15m, 5600 years BP), Llanwern (+3.1m, 4240 years BP) and Portbury (+3.4m, 4240 years BP) indicating a rise of around 0.22 to 0.24 m per century over this period. Comparison of the Sub-Boreal aged peats at Kingston Seymour and Burnham-on-Sea to the Atlantic Period peats from the same localities indicates a rise of 0.28m per century between these times.

2.5.4 The Sub-Atlantic Period.

The Sub-Atlantic Period is represented by pollen zone VIII lasting from approximately 2500 years BP to the present. This period has been analysed using archaeological data, historic evidence and tide gauges.

The last two millennia of dateable positions have been ones of controversy based on archaeological data and from data after the Industrial Revolution. These sources have provided the bulk of information as reliable radiocarbon dating becomes limited due to the near absence of wood and peat which would assist in interpreting the stratigraphy. Dating of Roman artefacts has been found to be generally reliable, although misleading positions have occurred. Similarly the erection of sea wall protection from Roman times onwards has led to sedimentation being limited to the seaward side of the defences giving an impression of an

increased rate of sea level rise. It is only relatively recently that reliable data from tide gauges has become available.

These sources of evidence indicate that the rate of rise of global mean sea level has slowed considerably within the last few millennia although it generally tends to be upwards in southern Britain, attributable to the collapse of the forebulge of the Pleistocene ice sheets (Lambeck 1987, 1990).

Early work on the Severn Estuary region based on archaeological evidence has brought mixed results. Roman remains have been found at depths of 1.7m to 4.3m below the ground surface in the Somerset Levels, but due to the distance inland it is hard to relate these finding to any sea-level change. Romano-British and later marine and estuarine clays in the Somerset, Wentlooge, Caldicot and Severnside Levels cover the entire coastline, with deposits being present up to 24km inland in the Somerset Levels at up to 4.3m thickness. Allen and Rae (1988) and Allen (1991) provided important data for the sea level changes of the last 2000 years within the Severn Estuary. They used three methods of ascertaining sea level changes;

- Marsh height differences.

A sea wall acts as a barrier starving the landward side of tidal sediment unless overtopped, as a result there is a height difference between the starved (internal) geomorphic surface and the actively accreting marsh (external geomorphic surface). The height difference between the two surfaces represents the amount of active accretion which has occurred since the seawall was built. Allen states that if the date at which a sea-wall has been built can be found to a reliable degree through the presence of buried artefacts or through archaeological evidence present in archive records or maps, then the time over which accretion outside the wall had occurred is known and can thus be related to sea level rise.

- Dateable geomorphic surfaces.

Where excavations or active erosion has taken place the previous buried internal geomorphic surfaces may be exposed. These represent a time when the area was starved of sediment, but consequently has become buried as a result of the seawall being breached or abandoned. The thickness of sediment which has developed on top of the old surface can be

used as another reference of accretion, if the time of the breach is known.

- Geochemical zones.

With the event of the Industrial Revolution in the mid-19th century, increased water borne pollution has occurred which have enabled the definition of a number of geochemical zones (chemzones), relating to the type and concentration of heavy metals (zinc, copper and lead) which have been deposited on the marsh surfaces.

Allen defines three zones; Zone I is pre-industrial and carries relatively low metal concentrations; Zone II is industrial and contains a gradually rising content of metal concentrations dated as being during the period of 1840-1850 AD using lead-210 chronology referenced to radiometrically dated cored samples from Swansea Bay by Clifton and Hamilton (1979); Chemzone III shows a slight wane in metal concentrations and is stated to begin at 1940-1950 A.D.

Allen and Rae's (1988) findings can be divided into four historic points; The Roman Period which is nominally dated as around 150 AD; The Medieval Period at about 1250 AD, and the base of chemzones II and III at 1845 and 1945 AD. These studies have been used to construct the graph presented as Figure 2.8.

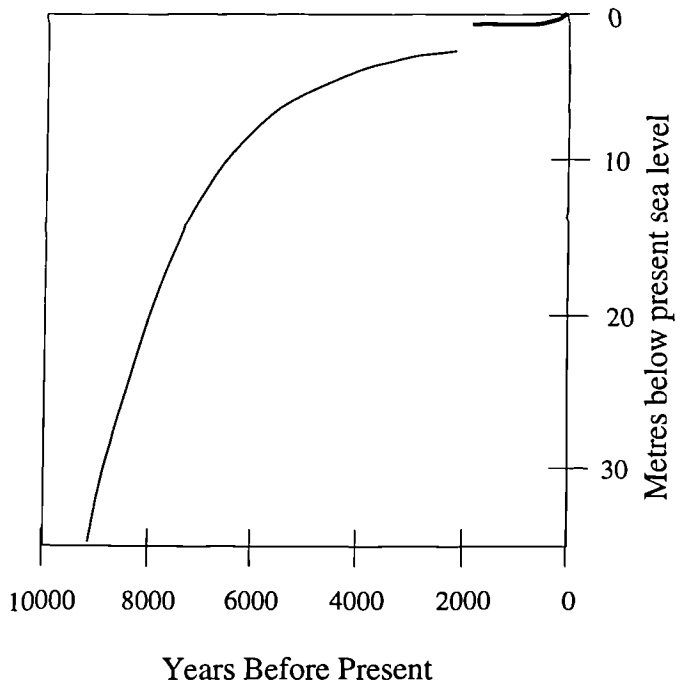

Fig 2.8 Allen's (1990) sea level curve (right hand side of graph) plotted in relation to Shennan (1983).

It is interesting that Allen has plotted his curve in relation to the curve of Shennan. Shennan's graph had an origin 0.5-0.6m above the local level of MHWS, but is reduced in the diagram to allow the maximum compatibility with the Allen curve. Nonetheless there is a discrepancy of about 0.8 m between the start and end of the two graphs which Allen (1990) suggests may be due to the difference in methods and the difference in positions of the sample localities. In comparison the Allen curve shows a greater correlation with the curves of Hawkins and even Jelgesma's Dutch based curve. It is concluded that Shennan's data may give an underestimation of the height of the sea over the period between 5000 and 2000 years BP.

In conclusion Allen and Rae (1988) and Allen (1991) suggest that using values averaged for the entire Severn Estuary that salt marsh accretion has amounted to 1.22m since the Roman Period, 1.05 since the Medieval Period, 0.54 since 1845 AD and 0.21 since 1945 AD. This data derives the sea level trends presented in Table 2.8 for the minimum rates of rise and Allen's 1991 revision of these figures.

Approximate Period	Rate of Rise (Allen and Rae)	Rate of Rise (Allen)
Roman - Medieval (150 - 1250 AD)	0.15 mm/year (0.015 m/century)	0.4 mm/year (0.04 m/century)
Medieval - Modern (start) (1250 - 1845 AD)	0.86 mm/year (0.086 m/century)	0.79 mm/year (0.079 m/century)
Modern - 1945 AD (1845 - 1945 AD)	3.3 mm/year (0.33 m/century)	1.49 mm/year (0.149 m/century)
Late Modern (1945 - 1988/91 AD)	4.8 mm/year (ca. 0.48 m/century)	4.65 mm/year (ca.).47 m/century)

Table 2.8. Rates of sea level rise for the Severn Estuary after Allen and Rae (1988) and Allen (1991).

The implication of Allen's findings is that sea level has been rising at an appreciable rate over the last two thousand years but is increasing at a rate greater than the present eustatic trend (Wigley and Raper, 1987), although this is not supported by tide gauge records, eg Rossiter (1967) or Woodworth (1996, pers.comm). Average trends in tide guage data, eg. Emery and Aubrey (1985) and Woodworth (1987) tend to show similar patterns to sea levels determined from geological data at similar positions, such as low or even negative rates of rise in areas undergoing isostaic rebound and the larger positive trends in southern England. Unfortunately the longer term averaging which is generally associated with the geological data will not provide the same detail of short term changes indicated by tide guage analysis.

2.6 Problems associated with Sea Level Curves.

Archaeological data is used based on the position of buried artefacts, the estimated age of civilisation from which they came and the assumption that these can be related to the prevailing sea level. However the literature frequently does not provide adequate data on which assumptions have been made. Unfortunately archaeological findings elsewhere may find that the assumptions of age may be invalid. Consolidation of the sediments will give height lower than their original altitude of deposition, in practice this is difficult to account for, although reliability can be increased by taking samples from near to the bedrock, above basal gravels or at the base of the organic bands where less consolidation would have occurred (Hawkins, 1984).

2.6.1 Peat Bands and Sedimentation.

The extreme tidal range of the Severn causes some problems in the production of the sea level curve as the sediments have to be assumed to be deposited relative to a position in the tidal range. For instance the highest astronomical tide (HAT) is theoretically the highest normal tide the Estuary will encounter and determines the highest altitude at which sediment could be laid as it is in suspension or being carried by the tide in question. However, an HAT may occur only every four years or so and sedimentation is known to occur on the salt mashes more

commonly than this. The height of the marshes is approximately at the mean high water spring tide (MHWS or HWST) which is deemed to be the controlling factor in the salt marsh formation where organic bands generally form. Hawkins' curve is based on peat samples taken relative to MHWS. This system, whilst being the best available, is further complicated by the height at which the peat may be forming along the marsh levee, peat bands may possess a gentle dip away from the main channel, or thicken inland, in which case fresh water peats may be present or forming below the MHWS level. Tidal pills cut the salt marshes and have often been infilled with thick organic deposits, causing peat bands to vary in thickness within a small area. The height of MHWS is not constant along the estuary but rises as the system narrows towards the estuary head. Comparing the Severn Estuary to other areas needs these aspects to be carefully considered, something which is not always present in some literature. Even within a single estuary, changes in the tidal regime may vary, the disparity shown between sea level curves in Figure 2.8 may be related to a lack of due cognisance being taken of the tidal regime.

2.6.2 Tectonics and Isostacy.

Sea level curves created for northern latitudes such as Scotland and Scandinavia (Morner) would be within an area of isostatic rebound where the land mass is responding to the removal of the overlying load of ice that had been present during the glacial cold periods. In such areas the sea level curve may be attenuated by the apparent upward and episodic movement of the land. Similarly the slow Tertiary and Quaternary collapse of the North Sea Basin affects the evaluation on the east coast of Britain and Western European coasts. Southern England is considered to be lying within the collapsing forebulge from the last glaciation and is tilting north eastwards on an axis approximately running through Swansea Bay (Churchill, 1965). Sea level curves for tectonically active areas should also be treated with care, unless due cognisance is paid to the neotectonic environment, in areas such as the north eastern Mediterranean it would be would be difficult to justify the level at which a deposit was laid due to the degree of neotectonic activity and synsedimentary deformation affecting the lateral consistency of the sediments.

2.6.3 Consolidation.

Hawkins (1971) was selective in the points that he used in creating his graph indicated in Figure 2.4, leading his curve through the more reliable points where a minimum of consolidation had occurred. As a result numerous points lie to the right of the line, the position of which is attributed to the consolidation of peat bands and sediments. The worst case ignoring the sample reliability, indicates that four metres of consolidation may have occurred within 4000 years. Hawkins rightly suggests that when dating organic samples it is preferable to take the material from where it will have consolidated the least, above basal gravels, at the base of the peat, or at the top and bottom.

2.7 Pre-Flandrian Sedimentation in the Severn Estuary.

2.7.1 Pleistocene.

Ice advances have caused morphological change in the Severn Estuary through a number of mechanisms. The ice masses themselves cause the erosion of weak underlying strata overdeepening bedrock channels and depositing glacial moraine and till. As water is 'tied up' in the enlarged polar ice caps, sea levels fell worldwide and existing rivers incised deep valleys into the bedrock in an attempt to equalise energetically with the lowered eustatic sea level base. Localised icefields may act as barriers redirecting preglacial stream courses which is a process evident in the stream course of the present Severn and it's tributaries. The cold temperatures lead to the formation of ice wedges which are subsequently infilled and similar superficial features.

The drainage of the Severn River system underwent a considerable expansion during the Quaternary due to river diversions. The original Severn flowed northwards into the Dee drainage system, diverting south at the end of the Wolstonian Glaciation, although the Warwick Avon had been diverted south prior to this from the Trent. Shotton (1953) suggests that the Warwick Avon was diverted during the late Wolstonian and early Ipswichian periods, the apparent reversal of flow explains why the main tributaries of the Avon within the

Cotswolds flow northwards. The course of the Severn through the gorge at Ironbridge in Shropshire was identified by Beckinsale and Richardson as originally belonging to that of the Dee or Trent. The Teme diverted into the Severn Basin more recently during the last (Devensian) glacial period from its original course into the River Wye system.

These glacial and interglacial periods resulted in the deposition of a number of river terraces, named the Power House, Worcester, Main and Kidderminster Terraces by Wills (1938) and Mitchell *et al.* (1973) in many areas of the Severn system.

There is evidence for glacial erosion on the eastern margin of the Severn, where the buried 'old channel' floor shows a broad open relief akin to glacial erosion rather than a sharper incised morphology representative of a new river erosion. Glacial till rich in Mercia Mudstone has also been found sporadically over the area, some of which has been described as 'head' on the 1963 Special Edition (Bristol) geological sheet. Glaciogenic deposits are also located at Portishead Down at 90m AOD (Hawkins 1992) and Failand Ridge (Colbourne, Gilbertson and Hawkins, 1974). Outwash sands and gravels have been identified to fill valleys up to 25m deep in the M5 road cutting at Court Hill Col and in the Tickenham Col (Hawkins & Kellaway, 1971). Unfortunately Quaternary deposits are only poorly exposed along the coastline of the Severn at Middle Hope (Gilbertson and Hawkins, 1977) and on the Chepstow promontory (Wills, 1938 and Hawkins, 1968). The majority of Quaternary sections, however, appear as temporary exposures only in road cuttings, boreholes and construction works.

The Quaternary deposits of the Chepstow promontory at NGR ST (551 905) are identified on the geological map as being the No.2 Terrace (Wills, 1938) but can be seen as a glacial type deposit (Hawkins, 1968) which comprise gravelly silts with boulders up to a ton in weight. Nearby deposits to the west of Chepstow, shown on the map to be the No.4 Terrace contain chalk like material. There is a lack of correlation in the nature of the similarly numbered terrace deposits either side of the Estuary, the origin of some has been proved to be glaciogenic, thus Hawkins (1968) points out the Terraces after Wills (1938) are misleading, neither they, nor the inferred positions on the geological map should be taken as being absolutely correct.

Appreciable differences in the morphology of the Lower Severn can be traced to the Wolstonian glacial cold period during which the course of the Severn had eroded a channel

over a kilometre to the east of the present course in the area of Severn Beach and Avonmouth (Hawkins 1971). This area is illustrated in Figure 2.9 as are the estimated base level contours showing a depth of up to -12m OD. Similar although less substantial deposits are also located in the Kenn Levels, Clapton and Tickenham gaps. At the end of this period of glaciation the main channel was infilled with fluvioglacial deposits and the Severn diverted westwards into a course believed to have been originated by Mounton Brook which subsequently formed the area of the present day 'Shoots'. The nature of sedimentation in this buried valley has been recorded by in Richardson, (1887), ApSimon and Donovan (1965), Gilbertson and Hawkins (1977) and Narbett (1992).

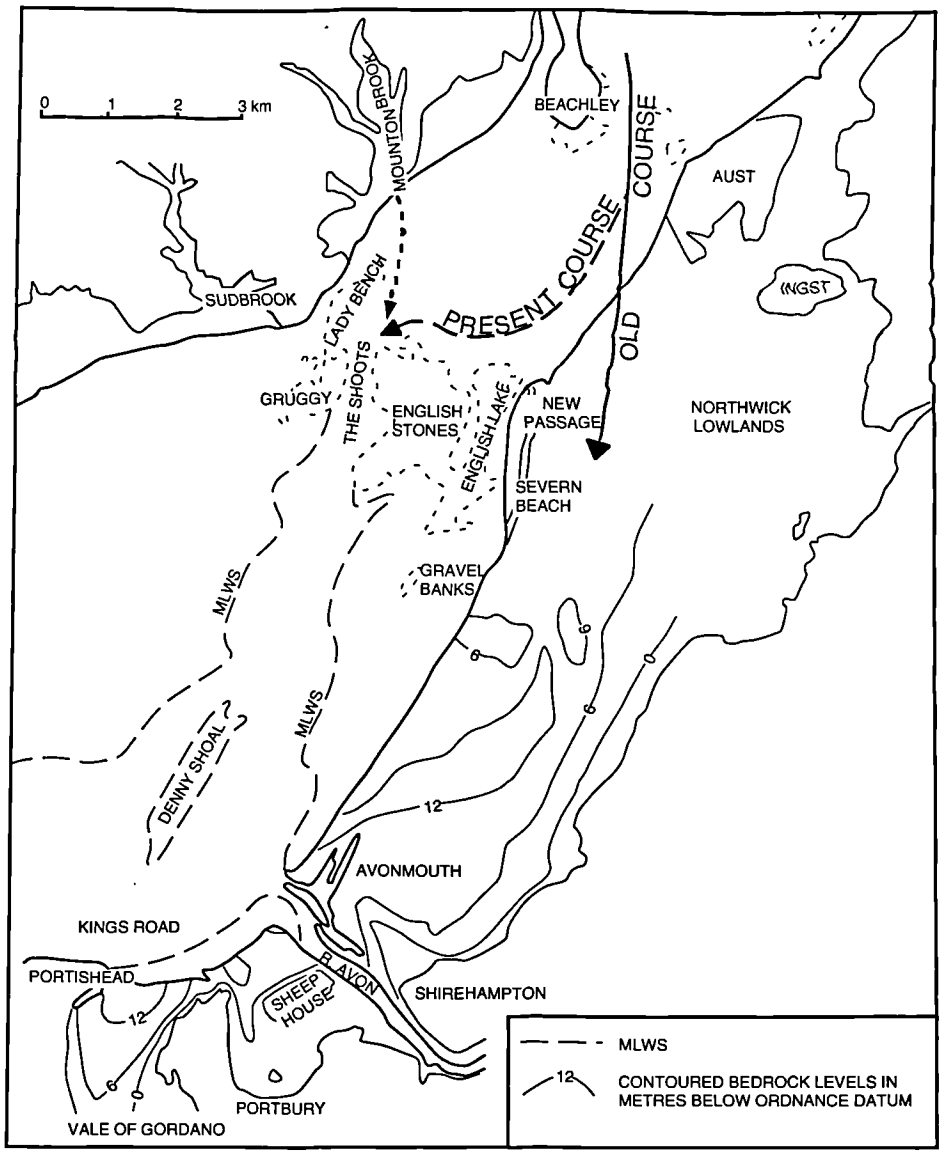

Fig 2.9. The Former Course of the Severn in the Severnside Levels.

The Clevedon Gap, Court Hill and Tickenham channels were eroded during the Anglian cold period at a time when an ice barrier was impeding the Bristol Avon which was being diverted through the Flax Bourton Gap forming the present Avon Gorge (Harmer, 1907). Knowing that the lowest bedrock level within the Flax Bourton Gap is about 44m AOD and using likely bed level gradients, it is probable that the Clevedon Gap channel must reach to a level of about 35m OD.

The glacial deposits within the Kenn Levels seem to comprise outwash gravel in the east and tills to the west, indicating that the ice sheets will have moved towards the east from the Bristol Channel. These deposits may be of Wolstonian age, overlain by early Ipswichian interglacial deposits with channels of Ipswichian age showing freshwater fauna (Welch, 1955; Kellaway, 1971; Gilbertson and Hawkins, 1978 and Andrews, Gilbertson and Hawkins, 1984). Davies (1983) claims that by using amino acid analysis on samples from the Gower Peninsula (South Wales) that some raised beaches formed during the Ipswichian contained reworked material from the Hoxnian.

2.7.2 Devensian and Late Devensian.

During the last glacial period, approximately 23,000 to 14,000 years BP in the Severn Estuary region, the Welsh ice fields reached as far south as Newport or even Uskmouth. At this time the mean sea level would have stood at about 100 to 110 m below OD (Fairbridge, 1961; Catt, 1977; Hawkins, 1984) with the broad Severn valley being incised by meandering channels. The area of the Shoots would have been eroded to a level of about -30m OD. Similarly the main deep water channels of the present Severn at Kings Road off the coast at Portishead and the Bristol Deep would also have been scoured deeper. Rock platforms were also eroded underneath the Caldicot and Wentlooge Levels, although dating of basal fauna has proved to give inconsistent ages for the same samples (Andrews et al, 1984). Admiralty Charts, assuming only minor post glacial erosion, can be studied to show that the Severn coastline would have stood some distance south of the Isle of Lundy in the Bristol Channel at the maximum low sea level and would not have reached Swansea until levels had risen to about 40m below the present level. Towards the late Devensian tundra conditions prevailed with

wind blown loess type deposits being deposited in many areas of Somerset, the sediment source of which appears to have been from the continental shelf, rather than by modern analogy, winds blowing from the north (ApSimon, Donovan and Taylor, 1961). A soil survey by Finlay (1965) found that many of the soils in the Somerset Levels were aeolian.

Unfortunately there has been no complete review of the pre-Flandrian sedimentation in the Severn Estuary region and it is not considered important to extend the discussion here, apart from noting that Hawkins and Tratman (1977) and all the previously mentioned works together contribute to much of the state of knowledge of these sediments at present.

2.8 Flandrian Sedimentation.

During this period the base of the original glacial Severn Valley and Bristol Channel would have dropped seawards towards the ancient sea level base which was some 110m below the present. As the Flandrian transgression progressed, sedimentation would have occurred first at the Estuary mouth and would have worked upstream with time. In effect the transgression began in the lower realms of the estuary about 8250 years BP but would not have reached the Gloucester area until much later.

To add to the problem of diachronous sedimentation, an estuary is in a dynamic equilibrium of marine and fluvial sedimentation. Sediment types vary according to the source area, whilst the coarseness of the sediments varies according to the depositional regime. By broad comparison, fine grained sediments tend to be deposited towards the mouth of an estuary whereas coarser sediments are lain in the upper region of the estuary due to the over riding fluvial velocities. This is very much a one dimensional philosophy and does not seem to apply to the Severn Estuary. Much of the sediment below 5m depth appears to have been transported into the Estuary from the south, based upon foramnifera studies (Murray and Hawkins, 1976). Furthermore tidal or fluvial flow velocities vary within the realms of the conducting channel with higher flow velocities producing coarser sediments. Slack waters and even marine or brackish conditions occur in back bar conditions where a tributary channel may be in near proximity.

Prior to the onset of the Flandrian transgression, approximately 8250 years BP there existed a broad channel eroded into the bedrock, which would become inundated as accretion began. These processes (with allowance for morphological changes) must have occurred several times with the various ice ages, although only the buried valley infills in the Severnside Levels and Somerset Levels appear to be well preserved.

The sediment pile at a single locality in the Estuary can be related to the sea level curve. In general three distinct sediment types related to their age of deposition can be defined and are described in the following sections. As will be explained later some of these sediment types may not be present locally, especially in upstream regions of the Estuary.

2.8.1 Pre-Inundation.

Before inundation by the transgressing sea, the late glacial landscape would have comprised an organic rich layer overlying the bedrock with glacial tills or fluvioglacial gravels. The organic layer would have comprised resistant vegetation growing as a result of the climatic warming and damper conditions, which would have represented arctic tundra before this.

2.8.2 Inundation.

During the period of initial fast sea level rise, high energy conditions occurred with the erosion and reworking of the underlying glaciogenic and organic sediments and the bedrock, resulting in the deposition of silty sands. Sollas (1883) and Murray and Hawkins (1976) identify the source of the early sands as being from the west Bristol Channel, generally migrating up the estuary as the sea transgressed.

The sand deposits would have formed sand bars and shoals similar to those seen in the modern estuary although with a broader relief and may have formed bars on the minor now buried tributaries. The period of sand deposition would have lasted until the rate of sea level rise and associated energy conditions decreased at about 6500 years BP, generally at a level around Ordnance Datum.

2.8.3 Reducing sea level rise.

As the rate of sea level rise decreased about 6500 years BP energy conditions in the Estuary reduced, resulting in the deposition of silty clays with peat bands and silty sand laminae. A peat band often occurs at the base of these deposits at around Ordnance Datum.

In the present tidal frame mud deposition occurs between the levels of MHWN and MHWS with the silty laminae being introduced as the result of storms, peaty sedimentation occurs when accretion has reached a level generally around MHWS and only a little inundation occurs.

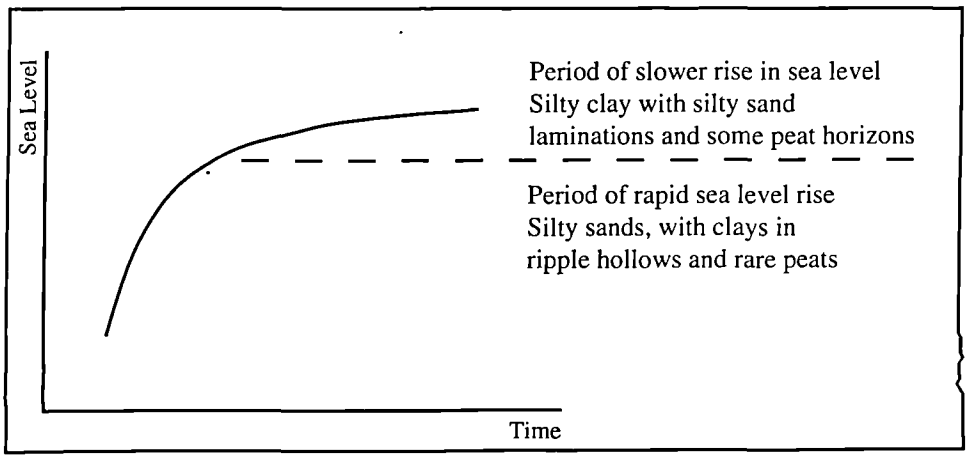

Fig 2.10 Sedimentation related to sea level curves.

The periods of deposition related to the tidal frame are ideallised in Figure 2.10. In reality all the sediments may not be present and sedimentation varies along the estuary axis and laterally away from the axis. The depositional sequence generally fines inland as the organic backswamps were starved of detrital sediment. The backswamp environments can be further complicated if riverine sediment is input, such as in the Somerset Levels. The period of fast sea level rise may not be represented upstream as the transgressing sea may not have reached this level of the valley before the rate of sea level rise had waned.

2.9 The Modern Sedimentary Environment.

As a consequence of the high tidal range and velocities created, high turbidity or well-mixed conditions occur in the Severn Estuary (Hamilton 1979, Uncles 1982, 1984). Hamilton (1979), Kirby and Parker (1980) and Harris (1988) identify three to five sedimentary environments in the Severn.

2.9.1 Bedrock Environment.

Bedrock is generally encountered in sub to intertidal areas of the Bristol Channel and locally on the rock platforms of the English Stones, at Oldbury, Hills Flat and Lydney. As a result of net sediment accumulation most of the pre-existing glacial bedrock valleys have been infilled, thus there is little bedrock exposure in the Severn.

2.9.2 Sand Environment.

The sand environment of the Severn is highly varied but may be separated into general areas:

- The sands of the Inner Bristol Channel which are generally sub-tidal, forming large cross stratified bedforms (Davies 1980, Harris and Collins 1985).
- The Outer Severn Estuary Region (Aust to Cardiff) shows large areas of bank detached sub and inter tidal shoals with large cross bedded reversible bedforms (Hawkins and Sebbage, 1972).
- The sand deposits of the Middle Severn Estuary just upstream of Aust are prone to the fastest currents and greatest turbidity, as a result of which the dune fields tend to be destroyed and show planar stratification with localised ripples occurring at slacker water which may be destroyed (along with any mud drape) on the onset of the next tide.
- The sand deposits of the Upper Severn Estuary around the meandering bends tend to be bank attached on the inside of the bends having planar bedding as a result of the upper stage currents.

2.9.3 Mud Environment.

The mud environment is very widespread. The subtidal areas of the Inner Bristol Channel and Outer Severn Estuary show settled and fluid mud characteristics, relating to a suspended sediment front (Kirby and Parker, 1982) or null point. Recent borings taken by 'jack up rigs' for the preliminary ground investigations of the Second Severn Crossing have found up to 2m of suspended mud and effluent directly upon the bedrock valley. The principle mud environment is the intertidal mudflats and alluvial wetlands which will be described in a later chapter

2.10 Estuarine Retreat.

As the present Severn system developed during the Flandrian the infilling of the valley was essentially diachronous with the transgressing sea depositing material in the lower regions earlier than in the main River System (now the Upper Estuary). The consequences of which will be explained later in this chapter.

Figure 2.11 shows an averaged bedrock profile of the Severn and the sea level curve for the Flandrian in the Severn (after Hawkins). By relating the two curves it can be deduced at what time MHWS, which is the approximate level of accretion in the tidal mudflats, reached different parts of the Estuary. Data for constructing the bedrock has been taken from a number of sources including channel surveys and ground investigation data, however, the graph cannot be considered to represent anything more than a simple model.

It is assumed that the present day bed level can be approximated to represent the buried valley floor, although clearly the buried flats adjacent to this deep channel will be slightly higher than the bedrock channel. Borehole evidence indicates it is the case that the bounding flats tend to be higher than the main channel, except in or near to deeper abandoned buried channels. From the two examples illustrated in Figure 2.11 it can be seen that the estuarine retreat of the Severn would have reached 50km downstream of Gloucester City (Llanthony) by 7000 years BP and 32.5 km downstream by 5000 years BP. Although it is not indicated on the

figure, the transgressing sea would have reached 120km downstream of Gloucester by 8000 years BP.

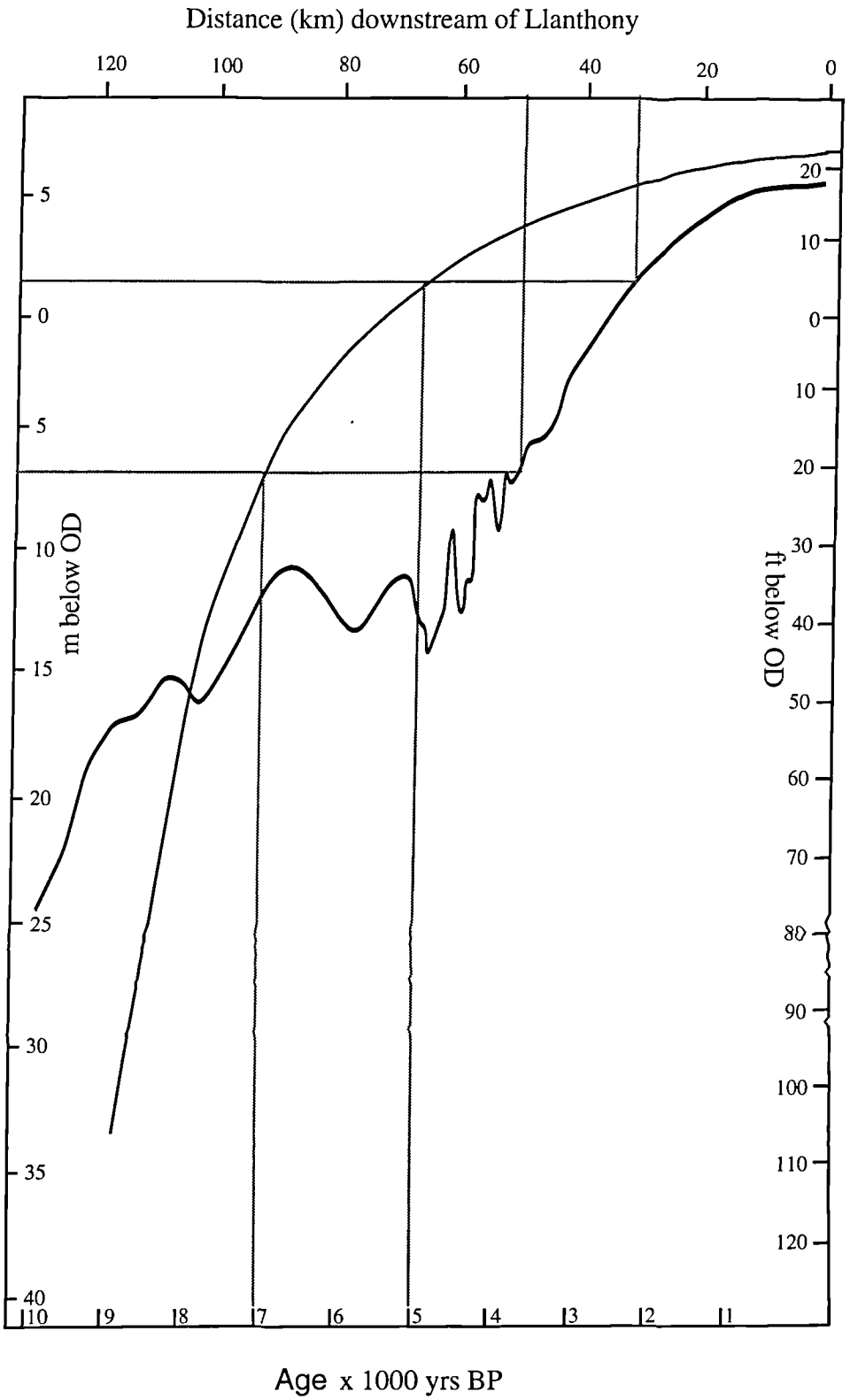

Fig 2.11 Sea level curve and bedrock profile (bold) for the Severn Estuary.

Using the height of mean high water spring as the present day level of the estuarine mudflats, it can be shown what thickness of sediment may have forseeably accreted since the onset of inundation of the old valley floor (Table 2.9). The construction of this table assumes that no riverine sedimentation has occurred, which will effect the values especially in upstream areas. Another factor to be noted is that areas deprived of clastic sedimentation will form considerable organo-sediments in response to the rising water table which is related to the sea level, thus considerable peat deposits especially upstream and away from the main channel must be expected, showing dominantly freshwater fauna and flora, but can still be considered to be part of the estuarine flood plain.

Distance (km) downstream	Place (approximate)	Time of innundation (years BP)	Sediment thickness (m)	Apparent sea level rise (mm/yr)
120	Porlock	8000	25.25	3.16
50	Avonmouth	7000	13.75	1.96
32.5	Littleton	5000	5.25	1.05
20	Sharpness	3600	2.75	0.76

Table 2.9 Innundation of the Severn Valley.

The apparent rates of sea level rise would be the values calculated from dividing the expected sediment pile thickness by the period over which it has accreted. Therefore the value calculated at Porlock is averaged over the initially high (15mm per year) rise of Godwin's to the period of much lower sea level rise. This is something which other peoples work does not necessarily take into account when constructing sea level curves.

Earlier, Figure 2.10 demonstrated that as the rate of sea level rise reduced, sedimentation changed from predominantly sandy to a finer nature. This cut off point occurred when mean sea level was around Ordnance Datum approximately 5500 years BP according to the graph, when inundation would have reached a position about 35km downstream of Gloucester (Figure 2.11). Therefore none of the higher energy sediments associated with the period of rapid sea level rise should be expected up the valley from about 35km south of Gloucester. Table 2.10 shows the expected thickness of estuarine sands and estuarine clays

which may be found at selected positions in the Estuary. The author believes that the prevalence of the 'Ordnance Datum Peat' or similar deposits in the Estuary suggests that the inflexion point in the sea level curve which is deemed to indicate a change in sediment type may have been a short period of regression or more likely a sea level stand at the same level before the sea level began rising again.

Distance (km) downstream	Place (approximate)	Total sediment thickness (m)	Thickness of 'sands' (m)	Thickness of 'clays' (m)
120	Porlock	25.25	18.5	6.75
50	Avonmouth	13.75	7.0	6.75
32.5	Littleton	5.25	0*	5.25
20	Sharpness	2.75	0*	2.75

Table 2.10. Approximate thickness of expected sediments. * denotes that some basal gravel or sand is likely.

Unfortunately reliable data to either confirm or disprove the model of accretion presented in Tables 2.9 and 2.10 is scarcer than would first appear. The majority of the data for the Severnside Levels is affected by the buried channel so borehole logs can be misinterpreted. Generally the sediment thickness is greater than would be expected, although areas away from the old channel which are closer to the modern day channel show a reasonable correlation. Limited logs on the Welsh side of the Severn in the Caldicott Levels seem to indicate a well formed coastal platform with a buried Triassic cliff line running along the approximate line of the Newport to Sudbrook railway line. The cone penetrometer results from a sea wall improvement scheme along the Caldicott Levels confirm the suggested model, although it would be easy to make the data fit the model when there is not enough substantive evidence. Seawall improvements at Whale Wharf near Littleton and near Shepperdine show a good correlation, although the number of exploratory holes is not sufficient to say so with any great certainty.

The present limits of alluvial deposits are represented by a break in slope, often in Mercia Mudstone, and are mapped approximately to the 10m contour line on the Bristol

Geological Sheet (BGS Sheet No 264). Examination in the field and from using aerial topographic surveys confirm that this is a reasonable approximation.

2.11 Future Sea Level Changes.

2.11.1 Contributory Factors.

Although the topic of future sea level changes was the motivation behind much of this thesis, it is stressed that the subject itself remains a contentious issue. There is evidence of a local and indeed global sea level rise from a variety of data sources which are at no point criticised in any detail in this work.

There are two ways of changing sea level on the human time scale. Either by changing the amount of water in the oceans by changing the mass of land based ice, or by making the existing water occupy more or less volume by changing the oceanic temperature. When considering sea level change, an important consideration is the rate at which it occurs. A one metre rise in one day is quite disastrous, while one metre in a million years would be irrelevant on the human scale.

The 'players' which may affect the global sea level are summarised as follows;

- Thermal Expansion

As water is heated it undergoes a small expansion. The atmosphere and sun only warm the top 100m or so of water. However, complex currents and density imbalances result in the circulation and mixing of the warmer surface layers to greater depths up to about 500m or more. The IPCC suggest that this would equate to a mean sea level rise of 0.1 metres per degree centigrade rise in an order of decades. Some scientists have been quoted that they believe that a single centigrade temperature rise may cause a 0.7m sea level rise, although it is not clear whether this is solely from thermal expansion of the world's oceans.

- Ice Reservoirs

The five major ice reservoirs are sea ice, mountain glaciers, the Greenland Ice Sheet, East Antarctic Ice Sheet and the West Antarctic Ice Sheet.

The melting of sea ice such as the North Pole will add insignificant amounts to the ocean levels as the difference will be reliant on the slight density difference due to the different salinities of the sea ice and the oceans. Mountain glaciers also are unlikely to contribute much to global sea levels as they appear to be too small, although some authors aver that their part is underestimated.

The Greenland and Antarctic Ice Sheets would contribute significantly to a sea level rise if temperatures were increased. The amount of ice tied up on one of the ice sheets is balanced between the loss through the melting or calving of icebergs and the accumulation through precipitation. Although an increase in global temperature may increase precipitation as more moisture may be held by the atmosphere, the melting in the zone of ablation in an ice field will increase even more because of the greater melt area produced from an upward rise in the snowline. It is interesting that if the Greenland Ice Sheet were to melt for whatever reason, even under the present climatic conditions it could not be regrown. This ice sheet is atypical because it is confined by the surrounding topography which protects it from melting and thus has not depleted as much as similar latitude ice fields.

The East Antarctic Ice Sheet is a desert and very cold. It can be assumed that unless a substantial global temperature rise was to occur then if anything, the ice sheet would grow as the warmer global temperature will probably trap more water in the atmosphere and increase precipitation. With conditions similar to Greenland, the high topography around the ice sheet provides a natural protection from ablation.

The West Antarctic Ice Sheet poses the greatest risk to sea level rise as it has an unstable configuration. Its main protection are the bounding ice sheets which are in a quasi-equilibrium state and vulnerable to any changes in the climate. If these defences were to collapse then a domino effect may occur further into the ice sheet.

It is difficult to qualify any perceptible effect of global warming on the prementioned 'reservoirs', however, the British Antarctic Survey has found that in the Antarctic there have been a number of significant changes in recent years. By observing flora, they have found that some frozen seeds are now starting to grow, indicating a temperature rise which is estimated to be in the order of 1 degree Celsius within the last thirty years. In addition the Antarctic summer

is now considered to be 50% longer than the equivalent in the 1970's, also based on floral evidence. This information was quoted in the Daily Telegraph (19/9/94) with no source.

A sea level rise in the Severn Estuary and around the South-west of Britain has been identified from a number of sources and for a number of reasons. Allen (1991) suggests that the source of a 'recently' accelerated sea level rise of about 4mm per year is due to the collapsing foreland bulge resulting from the previous ice age(s). Rossiter's analysis of tide gauge data records in the 1960's confirmed that there may be a sea level rise in excess of that assumed over the last 4 millennia as he concluded that the sea level rise over the period of reliable tide gauge information at Avonmouth was about 2.4mm per year. The NRA have a series of values based on recent observations of the rate of sea level rise which needs to be accounted for in the design of flood defences in coastal areas, the value for the Severn is 5mm per year.

The 'Green House Effect' and 'Global Warming' are contentious issues at best. However, this thesis uses up to date estimates of sea level rise to predict how future tides in the Severn may be affected. At no point does the author either affirm or dismiss the reliability of the 'greenhouse' predictions. Modelling of the possible effects of the postulated Greenhouse Effect have had mixed and controversial results. The basis of the models is that a rise in mean global temperature will cause a sea level rise due to the thermal expansion of the sea, glacial and polar melting. This is to an extent balanced by increased cold climate precipitation which may effectively tie up extra moisture as snow and ice. Modelling results so far have shown that if the greenhouse warming is occurring then there is a thermal inertia from the onset of the temperature rise to the resultant sea level change in the order of 30 years. It is worth remembering that if a suitable explanation of sea level and temperature behaviour can be derived, then some of the apparent discrepancies between Quaternary sea levels, fauna and flora may be explained.

2.11.2 Future Sea Levels in the Severn Estuary.

This section introduces a basic method of assessing the the approximate high tidal levels which may be attained at different locations within the Severn Estuary with an increase in

global mean sea level. The model presented makes a broad assumption that the high tides toward the mouth of the Bristol Channel are unaffected by tidal resonance and can be directly related to mean sea level rise. Readers should not take the figures derived in this section as definite and must refer to Section 7.6 for a description of the methodology used and it's shortfalls. Complex coastal shelf models suggest that while this model does not represent the true behaviour of the Severn system, the figures derived broadly correlate.

Estimates of global sea level rise have been given by Clayton (1990) and the IPCC (Warrick and Oerlemans, 1990) and are presented in Table 2.11.

	Clayton (1990-2030)	**Warrick & Oerlemans (1985-2030)**
High estimate	365 mm (9.1 mm/yr)	289 mm (6.4 mm/yr)
Best estimate	164 mm (4.1 mm/yr)	183 mm (4.1 mm/yr)
Low estimate	26 mm (0.65 mm/yr)	87 mm (1.9 mm/yr)

Table 2.11 Estimate of eustatic rise by 2030 postulated by Clayton (1990) and Warrick & Oerlemans (1990)

This section considers how these potential rises in sea level would change the tide at the mouth of the Severn and the nature of distortion upstream. For a tidal curve relatively unaffected by the distortion or shallow water effects which occur upstream, it can be assumed that an increase in mean sea level will approximate to an increase to the extreme levels of the tide, while the curve remains almost symmetrical. As the tide progresses upstream the curve will become much more distorted.

The high water levels indicated in Figure 2.12 for the area of the Severn covered by reliable Admiralty data show a linear increase in the high water levels upstream. Considering the rises from a neap to a spring and a spring to an astronomical high tide, a multiplication factor can be derived for the change in high water height as it increases upstream. Obviously the highest astronomical tide is calculated from a mathematical relation between the neap and spring tides. However, where data is available the observed values of HAT correspond closely to the calculated values. In simple terms if the difference between a mean high water

neap tide and a mean high water spring tide at the Estuary mouth is 1m and is 1.5m at a location 100km upstream then the multiplication factor at the upstream locality is 1.5 for this difference. The operation is repeated for the spring to astronomical tide and the neap to astronomical tide and the multiplication factor is derived through a line of best fit.

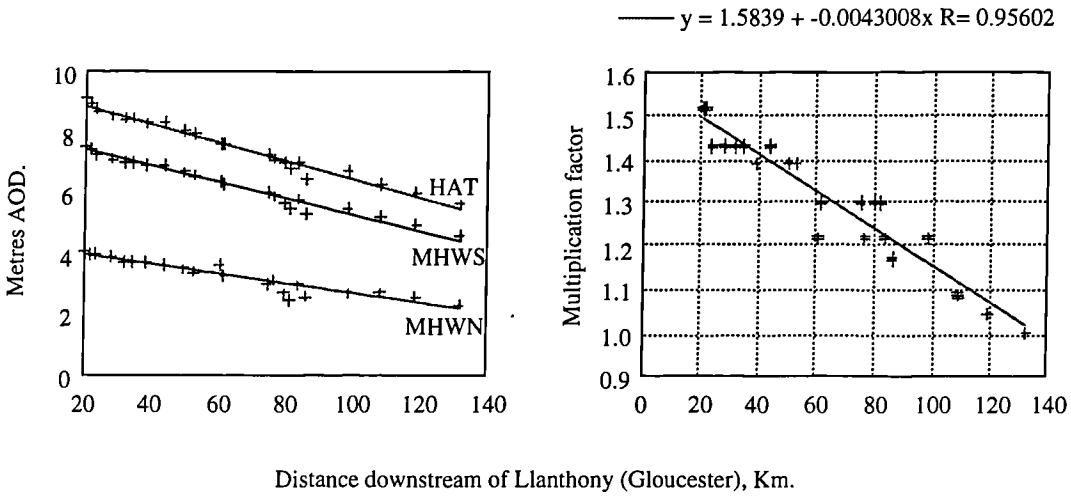

Fig 2.12 Multiplication of sea-level rise on high tide levels in the Severn Estuary.

		Clayton			Warrick and Oerlemans		
Place	km	Max (m)	Best (m)	Min (m)	Max (m)	Best (m)	Min (m)
Lynmouth	132	4.97	4.77	4.63	4.89	4.79	4.69
Watchet	99	5.92	5.69	5.53	5.84	5.71	5.60
Weston S-M	75	6.46	6.21	6.03	6.36	6.23	6.11
Avonmouth	50	7.20	6.92	6.74	7.10	6.95	6.82
Aust	39	7.42	7.13	6.94	7.31	7.16	7.02
White House	28	7.68	7.39	7.19	7.57	7.42	7.28
Sharpness	22	8.01	7.71	7.51	7.90	7.74	7.60

Table 2.12 Estimated heights of mean high water spring in 2030.

This simple model assumes that the postulated figure of global sea level rise would result in a constant value added to the high and low levels for a tide relatively unaffected by shallow water effects, i.e. Ilfracombe in the Bristol Channel. This 'unaffected rise' progressively increases upstream by the multiplication factor. The estimated maximum levels

of the high water spring tide in the Severn Estuary using the multiplication of the change in high water for the years 2030 and 2100 are given in Tables 2.12 & 2.13.

		Clayton			Warrick and Oerlemans		
Place	Km	Max (m)	Best (m)	Min (m)	Max (m)	Best (m)	Min (m)
Lynmouth	132	5.62	5.06	4.67	5.35	5.08	4.82
Watchet	99	6.66	5.98	5.57	6.35	6.05	5.75
Weston S-M	75	7.26	6.57	6.09	6.93	6.60	6.28
Avonmouth	50	8.07	7.32	6.80	7.71	7.35	7.00
Aust	39	8.32	7.54	7.00	7.94	7.57	7.21
White House	28	8.61	7.81	7.25	8.23	7.84	7.47
Sharpness	22	8.96	8.14	7.58	8.57	8.17	7.80

Fig 2.13 Estimated height of mean high water spring in 2100.

These values are calculated from figures based on the latest Admiralty data which is evaluated from a series of observations of tides at given positions. Admiralty data is not reliable north of Sharpness as this is the head of commercial navigation in the Estuary. As the areas bounding the great bends to the north of Sharpness tend to be the most liable to flood and are not reliably covered by the Admiralty predictions, it was decided that a tidal model of the Severn should be devised to predict future levels within the Estuary to Gloucester and that this model be applied to a number of engineering and hypothetical situations.

The height of the seawalls used in NRA modelling of the extreme tides in 1989 and 1990 for both banks of the Estuary are given in Table 2.13 for comparison with predicated future levels. The figures of the 'best' estimated highest astronomical tides are used in this table as they are a closer representation, although an underestimate, of the '100 years wave' to which the seawalls should be designed. The design level should also include an additional 0.5m for wave run-up. This table indicates that, with the exception of the seawall levels at Avonmouth, the remaining seawalls would, even at this very conservative estimate, be under threat of inundation if they were not improved. However, there have been seawall improvements at Aust and near the Whitehouse while Sharpness for the moment is relatively 'safe' as it lies upon a natural high area. The seawall improvements along the flanks of the

Lower and Middle Estuary undertaken during the early 1990's would require further improvements if the more extreme estimates of global sea level rise are correct.

Place	Seawall crest (m)	Present HAT (m)	Best 2030 (m)	Best 2100 (m)
Avonmouth	9.3 & 9.3	8.1	8.32	8.72
Aust	8.7 & 9.0	8.3	8.53	8.94
Whitehouse	9.9 & 9.3	8.6	8.83	9.25
Sharpness	10.5 & 10	9.0	9.24	9.66

Table 2.13 Estimated levels of future HAT compared to seawall levels in 1990.

2.12 Conclusions.

This chapter has provided an overview of the Quaternary history of the Severn, with particular reference to the Flandrian, both in relation to its position in the tidal frame and its gross sedimentological structure. Furthermore the present tidal regime was briefly analysed and used to predict future high tidal levels in Severn given present estimates of global sea level rise. This found that the future predicted sea levels are dangerously high with respect to existing, and in many places, newly raised flood defence levels. For a more accurate appreciation of this problem a computer model of the Severn was deemed necessary. This numerical simulation of tidal behaviour is described in the following four chapters, which describe the theoretical, computational and practical aspects of the model development and the validation and application of the results.

CHAPTER 3

HYDRAULIC THEORY OF MATHEMATICAL MODEL.

3.1 Introduction.

This chapter will introduce the relevant hydraulic theory behind a mathematical model of the Severn Estuary, which are derived during the chapter. Following a brief preamble and the history of apposite fluid dynamic theory, the chapter will proceed to identify the nature of solutions required and explain the relevant terminology and then proceed to derive a mathematical model based on the De Saint-Venant assumptions of unsteady flow in open channels. The De Saint-Venant equations are the basis of many mathematical models of river and estuarine flow.

The chapter covers a brief history of fluid mechanics in Section 3.2, the modelling needs considered prior to construction of the model in Section 3.3, describes one dimensional unsteady flow in Section 3.4, the De St.Venant equations and assumptions in Section 3.5 and proceeds to define the elements of integral and differential equations of fluid flow in the remaining sections.

3.1.1 Philosophical Preamble.

Mathematical models of open channel flow are accepted engineering tools. They have developed from hydraulic and mathematical theory and can be seen as the 'child' of hydraulic scale models. Hydraulic scale models were used with success in the previous century and first half of the twentieth century. Their development has in turn improved statistical, hydraulic and laboratory practice. Hydraulic models were superseded by mathematical ones when the hydraulic problems considered became too complex and it became necessary to understand the interaction of an engineering structure with its immediate surroundings and with the entire river, basin or region. Mathematical models only overtook hydraulic models in popularity when technology had advanced sufficiently so that the digital computer was able to analyse the

problems in an economical manner. Fortunately hydraulic models are still in common usage as it has been realised that numerical simulations are not infallible, nor are they at present capable of modelling many of the complex phenomena of interest to the engineer.

The author believes that after having studied many of the suitable techniques of simulating estuarine flow, in particular the numerical solution methods, that it would be easy for an engineer to simply 'piratise' parts of contemporary models and construct his own model using these pieces. However, this method, the 'black box' approach, is highly irresponsible. Such analysis may give satisfactory results to the engineer, but the method of formulation and solution is alien to him. Thus how the results are arrived at, and their validity, are uncertain to him and this becomes important when arguing whether the model has actually modelled anything of use. It is important to understand the physical processes and the reliability of the results. Another common pitfall is to become over zealous, developing a mathematically complex, yet under practical model where except to the modeller himself the system and documentation may be completely incomprehensible. A comprehensive review of previous literature highlighted the pitfalls that such attitudes can meet. A combination of unintelligible language, unfathomable solution techniques (mainly due to an unwillingness or incapability to follow a whole solution through) and very commonly, the typographical error, will in the majority of cases propagate fatal errors which the new designer will be unable to locate. It is absolutely vital that a system designer fully understands all the techniques he is to employ and then to design the system completely to his specifications, keeping the same notation and solution techniques throughout. One reason why the full description of a model may not be available is because economics play a considerable role in the extent to which a designer will reveal the analytical capabilities of his model, a successful tender may rely on what he has 'up his sleeve' and is unwilling to divulge.

3.2 Historical Development of Fluid Flow Theory.

The complete model of tidal simulation which this thesis describes consists of two mathematical stages, one is the derivation of the governing equations of fluid flow, so is predominantly an exercise in fluid mechanics, described in this chapter, and the second is the

adoption of the numerical method of solving these equations by computation, of which there are many types, which is described in Chapter 4. Although the two elements have been separated in this thesis, a designer must consider the suitability of the numerical solution technique and the flow equations in tandem when selecting the course of the model development.

This section briefly passes through the main history of hydraulic theory relevant to the design of a mathematical model of fluid flow. It is impossible to review and encompass all elements of hydraulics which are peripherally important to this thesis. However, the most important stages in theory can be attributed to the mathematicians of the eighteenth and nineteenth centuries. Whilst termed 'mathematicians' many of these scientists had interests or even academic positions in subjects ranging from astronomy to fluid mechanics and anatomy!

Like many physically based sciences, hydraulics has developed from the work of Isaac Newton. Most principles of fluid flow are based upon his laws of force and motion. Whilst only qualitative in approach Newton devised several theories of hydraulics and tidal flow. Daniel Bernoulli the Swiss mathematician published '*Hydrodynamica*" in (1738) and subsequently his (1741) work on Equatorial and Mediterranean tides significantly advanced Newton's work. The Bernoulli equation is important in steady state flow and is also used as an approximation in unsteady flow when modelled channel reaches need to be simplified. Bernoulli's father, with whom he had a constant rivalry, published '*Hydraulica* ' at a similar time, however, little new was introduced and the work proved less popular than that of Bernoulli Jnr. Bernoulli worked with Leonard Euler at St. Petersburg, developing an important form of mechanics (*Eulerian Mechanics*) which involves the analysis of the state of a fluid at particular locations within the flow. Treating a fluid as a continuous substance is the basis of analysing fluid flow in this thesis.

Laplace (1776) further developed fluid theory which was subsequently advanced by Lagrange in the 1780's who explained wave propagation in shallow water. His work is important in describing the speed and distortion of an incoming tide in an estuary, as explained in chapter two. However, unlike Eulerian type methods, *Lagrangian Mechanics*, involves the description of the motion of a body in time and space (e.g. a projectile type problem) and is

unsuitable for the description of fluid motion in a river or estuary, unless describing the motion of a wave or bore.

The Nineteenth Century work of De Chezy and the German engineer, Eytelwein into the effects of friction and the interaction of channel irregularities are of great importance, both in the study of the attenuation of an incoming tidal wave and the influence of structures, such as bridges on hydraulic flow. As a result the use of hydraulic models became increasingly popular and was best utilised by Froude.

The mid Nineteenth Century saw the greatest advancement of hydraulic flow simulation with the works of Partiot (1858, 1861, 1871) on wave motion in estuaries, Russell (1837, 1842-1843) on fluid flow and waves, Basin (1862, 1865) and Boussinesq (1872, 1873, 1877) also on wave motion. The publications of De Saint-Venant (1870, 1871) are considered most relevant to this thesis as he managed to marry the theory of unsteady hydraulic flow with mathematics. It is upon his two equations of momentum and continuity that unsteady flow problems are solved. The two equations have since been amended slightly by a variety of authors for greater completeness of a hydraulic solution, however, these departures have proved to be of minor significance. It must be stressed that all the authors mentioned in this paragraph worked very closely and whilst De Saint-Venant is accredited with being the 'father' of unsteady flow formulation, his works were not substantially different to those of his contemporaries.

The development of mathematical techniques has significantly improved the range and accuracy of applying fluid-dynamic equations, predominately in the twentieth century. The evolution of the digital computer has enabled models to become increasingly complex. Designing a modelling system itself requires a wide knowledge of classical hydraulics, calculus, numerical analysis, programming, data processing and conceptual modelling.

3.3 Identification of Modelling Needs.

Before a model designer can begin construction of his mathematical model, he must first identify just what problem he is to solve and in what detail he must proceed to give a realistic solution that satisfies the design needs. It must be stressed that mathematical models

are approximations of real and very complex phenomena, thus there will always be a degree of unmodellable inaccuracy. The modeller must balance the need for accurate results, against over-complicating the model where design and computer time may be vastly increased to give a result no more satisfactory than a much simpler model (and hence cheaper to design and run). In general a model will only incorporate the most important flow influences and ignore those of secondary importance. These unknown or ignored factors may or may not be important. Neither may they be readily identifiable, for instance the use of a friction value to evaluate the conveyance of a channel section which is described in Chapter 5, is an important way of 'tuning' a model, so that the computed results match those measured in reality in the natural river. However, the final frictional values may bear no resemblance to those which should have been entered for the natural channel, hence the 'tuned' or even 'fixed' values the computer program may output may have been compensating for an unknown effect in the channel so the programme has not been modelling physical reality. The friction problem will be returned to in chapter six.

3.3.1 Design Criteria.

The raw data available for the Severn Estuary which could be utilised in the model included channel cross-sections, fresh water flow at selected sites upstream and tidal curves at sites toward the estuary mouth, the details of which are discussed in chapter six. The following criteria were considered in the design stages of the mathematical and computer models.

- The simulation should give representative values of tidal height throughout a tidal period in the modelled reach, the high tidal heights were considered the priority.
- Tidal heights would identify flood hazard locations along the Severn Estuary, so sea wall heights would need to be included within the model design.
- The simulation would give new tidal heights within the Estuary as a result of sea-level change.

- The effect of man on channel morphology could be broadly established to ascertain the potential of tidal sumps in reducing tidal altitudes.
- The model could be run within the capabilities of the existing computing facilities in the Department of Geology, University of Bristol.
- The model could be developed at a later date to refine the modelling accuracy, by considering extra physical phenomena if required.
- The numerical solution could be adapted to solve for other estuaries

The latter three design criteria are predominantly concerned with practical aspects of the computer model, whereas the earlier ones are hydraulic phenomena which must be encompassed by the theoretical development of the mathematical model. After consideration it was decided that a one dimensional model of unsteady flow would be required, a description of which will be given in the succeeding section. To solve the mathematical model, a finite difference solution method was selected and will be described in Chapter 4.

3.4 One Dimensional Unsteady Flow in Open Channels.

This section introduces some of the terminology involved with the fluid flow model, the terms unsteady flow, open channel flow and one-dimensional flow.

3.4.1 Open Channel Flow.

An open channel is the term applied to a conduit for flow where a contained liquid which has a free surface present, this being a boundary exposed to the atmosphere. The free surface in a river is the interface between water and the air. Flow in a pipe which is not totally full is another example of open channel flow. A filled pipe does not have a free surface and flow within the pipe is described as confined.

3.4.2 Channel Types.

Dividing channel types may seem a little pedantic. However, when considering friction terms (in Chapter 5) the difference between a natural and man-made channel may be quite significant. A *natural channel* is one which is deemed to have developed naturally with a minimal human influence. Man made or *artificial* channels are self explanatory and include canals, gutters and ditches. Natural channels are sometimes referred to as 'real' channels, but this is a poor description. As the system to be modelled is an estuary it is a natural channel. Phenomena in natural channels tend to be much more complex than those in artificial channels, which are designed to obtain the maximum possible flow efficiency. To fully describe all the attributes that may be met in a natural channel is almost impossible, unnecessary and would encompass fields including geology, geomorphology, hydraulics and hydrology. Artificial channels are divided into several categories described in French (1986).

3.4.3 Unsteady Flow.

The flow in an open channel can be described by a variety of classifications, based on differing criterior. The simplest guideline for describing flow is the variation of the depth with respect to time. If the depth of a flow does not vary with time then it is said to be *steady*, however, if the depth does vary with time then it is said to be *unsteady*. Unfortunately this definition is not straightforward as the relative position of the observer can give a differing perspective on the definition. This difference in mechanical out look (Eulerian and Lagrangian) can be demonstrated by an idealised 'bore' passing up along a river which itself is unchanging in dimensions and has no bed slope variation. To the observer on the bank the flow will seem to be unsteady as the bore passes him, however, for someone standing at the crest of the bore, travelling along with it, (for instance a surfer!), then the height of the flow will remain constant and he will see no variation of depth with time and will see the flow as steady. Such an enigmatic situation is described as *spatially varied* or *discontinuous flow*, which unfortunately requires a different numerical approach to the model developed in this thesis. It is noted that the Severn Bore would not be shown in the modelled results here.

Similarly the variation of the depth of flow may also be considered with respect to space only. If the flow depth does not vary along the distance of a channel then it is said to be *uniform.* It is *non uniform* if the depth does vary with distance. The term uniform generally implies that the flow is steady as non uniform steady flow is physically a near impossibility. Non uniform flow is generally described as varied and can be further differentiated as *gradually* and *rapidly varied flow.* This is an arbitrary differentiation dependant on the rate of change of depth with distance. An example of the rapidly varied flow would be the flow over a weir or a bore, whereas gradually varied flow would describe a flood wave (Chow 1959).

The flow terms that have been given are far too rigid to describe the flow of even a small river, so the terms have been relaxed so that they can encompass real flow systems. For this purpose the gross flow conditions are considered, using the average velocity and depth at a point. *Unsteady flow* is now defined as a flow where the mean velocity at each point in the considered reach is not constant with time. This is obviously the case for an estuary where a tide enters and leaves the river, causing flow to increase, reduce and reverse during the period of the tide. It is unlikely that the freshwater flow at the estuary head will stay constant, especially if a storm drains into the system, superimposing additional non-steady flow effects.

3.4.4 One Dimensional Flow.

One dimensional flow is a convenient simplification of natural flow, considering flow conditions to only vary along one principle spatial axis. In reality fluid motion is three-dimensional with motion or displacement occurring in all three of the primary directions in space.

In a channel the fluid is constrained within boundaries, i.e. the channel sides and floor, which limit flow in two or even one dimensions. A simple treatment of fluid flow is to consider it one-dimensional where there are no property changes in two of the dimensions. This means that one dimensional flow in a channel is considered to be only up and down the channel axis, so that there is a uniform velocity throughout the water column and no transfer toward the sides of the channel.

Figure 3.1 shows how in a real fluid, the velocity reduces toward the channel floor where frictional shear at the boundary reduces flow velocity. To one-dimensionalise the flow, the variation throughout the column is averaged over the depth.

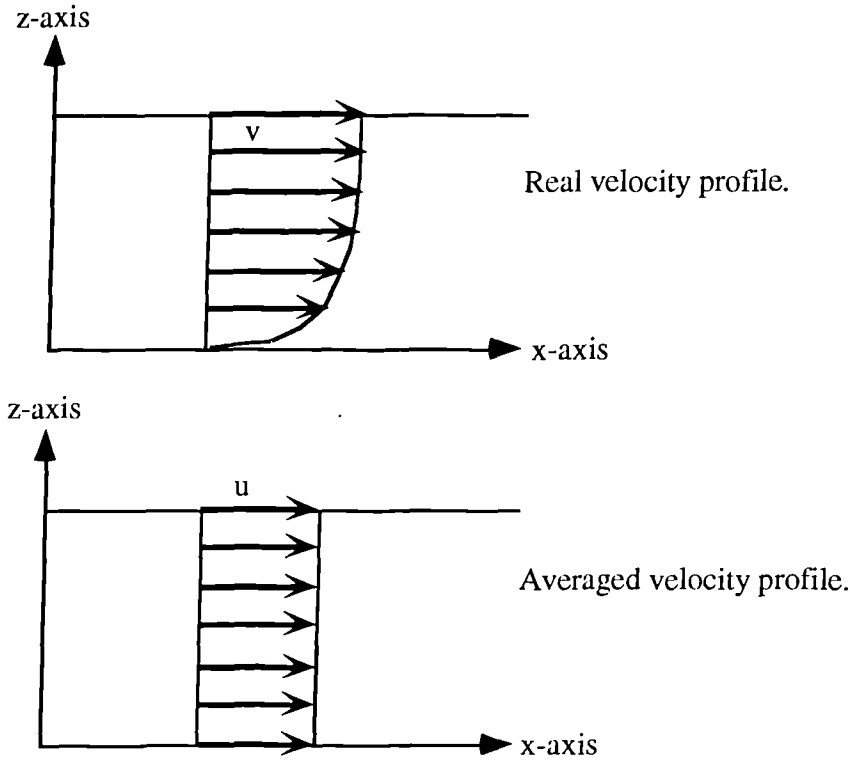

Fig. 3.1. Velocity profiles in a real and One-dimensional channel.

The value of v represents the local flow velocity at a position in the water column, in real flow conditions, whereas u is the depth averaged velocity of these "v" components, both u and v are in ms^{-1}. The value of u is related to the actual volume flow rate (Q) passing a given point of cross sectional area (A) so that the average velocity can be defined by equations 3.1.

$$u = \frac{1}{h} \int_{o}^{h} v \, dv$$

$$u = \frac{Q}{A} \qquad \textbf{(3.1)}$$

Where Q is the quantity of flow in $m^3 s^{-1}$

A is the cross sectional area in m^2

h is the depth in m.

This relation will become important later in the chapter, when explaining how the mathematical model is developed and how the presented model differs slightly in terminology from the basic equations of unsteady flow derived by De Saint-Venant.

In plan view a funnel-shaped estuary mouth and a narrower river channel show one dimensional flow (assuming that there is no velocity change within the water column), but this becomes a less valid assumption as an estuary widens, where circulation becomes more prevalent. It must be stressed that when approximating an estuary to limited dimensional flow, in reality a real river will show non-consistency with the assumption on a variety of scales, from small eddies, flow around banks and shoals, to circulation cells formed by river morphology and/or the Coriolis Effect. A modeller must decided at what point the river or estuary's behaviour becomes too complex to satisfy the dimensional approximation he has adopted. The validity of ignoring certain aspects of real estuarine flow from the general assumptions of the model designed are discussed Chapter 5.

A one-dimensional model is considered sufficient as the priority of modelling was to get tidal altitudes along the Estuary axis. Although there may be slight differences from a bank on one side of the channel to the opposite, the difference between either side within the modelled area would probably be minimal and to model in two dimensions would not add any valuable information, especially considering the quality of data in digitising the tidal curve, river flow or cross-section profiles and neglecting the effect of wind. Neither was it deemed important to consider velocity variations with depth. In this chapter and Chapter 4 there will be additions to the basic model to allow for quasi-two dimensional flow, which will allow for flow over seawalls and the addition of tributaries entering the main channel, problems which are solved with one-dimensional theory but give a simple description of two dimensional effects.

3.5 The De Saint-Venant Equations of Fluid Flow.

De Saint Venant (1871) presented two equations for one-dimensional unsteady flow in open channels. His derivations were based on a series of assumptions made about the flow conditions. It is upon these rules that integral and then differential forms of fluid flow can be derived. These two equations express the basic fluid flow laws for a continuous medium.

It is not intended to describe the De Saint Venant Equations but to follow his assumptions and derive a similar set of equations which are of an easier form to model and are more applicable to this thesis.

3.5.1 De St Venant Assumptions.

Barrie De Saint-Venant gave the following assumptions about fluid flow that governed his derivation of his flow equations.

- The flow is one dimensional, with the velocity being unvaried over a given cross section perpendicular to the channel axis. The free surface is considered to be horizontal across the section.
- The pressure is hydrostatic.
- Frictional and turbulent behaviour can be accounted for using analogous steady state flow laws.
- The channel bed slope is small so that the cosine of its inclination with the horizontal is considered unity.

From these assumptions a series of integral relations can be derived to describe the various elements of fluid flow considered in the eventual mathematical model.

3.6 Integral Relationships of Unsteady Flow.

The relationship of the flow equations relies upon the conservation of mass and momentum. The equation of the *Mass Continuity* is derived using the rule that between two sections there should be no overall change in mass and any losses that occur may be accounted for by overflowing the river defences. The *Conservation of Momentum* is derived with the constraint that momentum losses may be accounted for by loss over the defences, frictional resistance and unknowns.

By assuming that the water density does not change between sections, i.e. neglecting salinity and temperature effects, and that the fluid is not compressible, the equations can be derived by a control volume method. Such a method is used in Cunge *et al* (1980) and was derived from Liggett (1975) who used a unit width method of analysis which is similarly used in French (1986) but does not show an integral definition. All derived Equations are for a one dimensional system.

Before deriving the Equations is it necessary to introduce some of the nomenclature adopted (Fig 3.2).

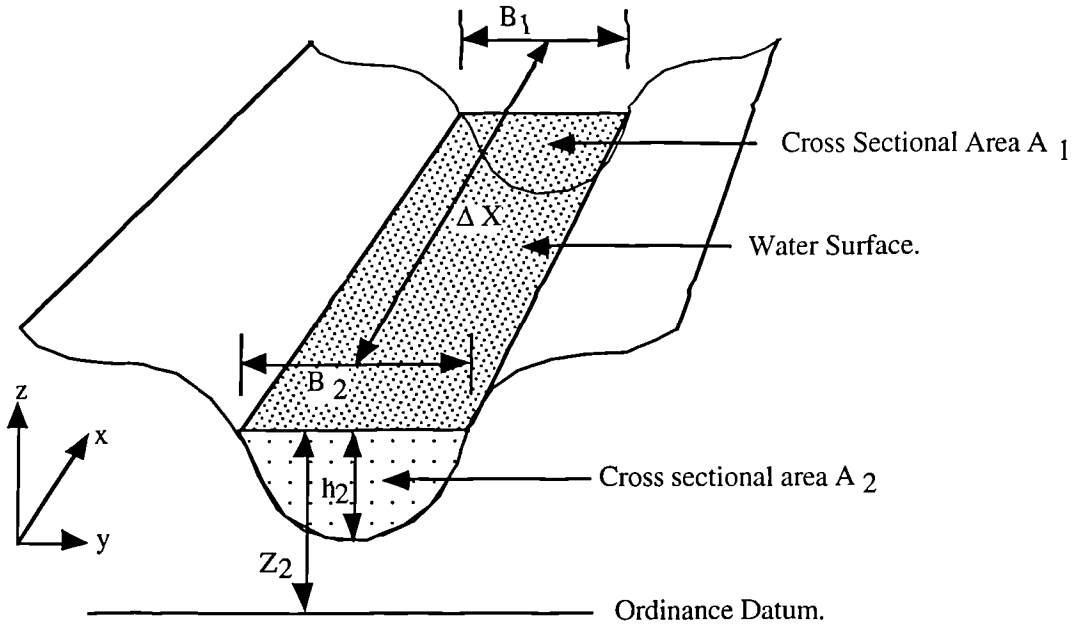

Fig 3.2. Simple channel between two end sections.

Where x_1 and x_2 = the positions along the channel axis of cross sections 1 and 2 at either end of a reach.

B_1 and B_2 = the breadths (m) of the water surface of the two cross sections.

A_1 and A_2 = the cross sectional areas (m^2) of the two cross sections.

Δx = the distance (m) between the two cross sections or the length of the reach measured along the main channel axis.

h_2 = the depth of the water at cross section 2.

Z_2 = the water surface elevation (m) above a given datum at cross section 2.

The two cross sections are at positions which will be a computational point in the finite difference solution which will be described in the next chapter. Considering the depth of flow in terms of the value Z with a constant datum level throughout the modelled area is easier than using the depth, especially in low lying areas such as an estuary. The convenient datum chosen was Ordinance Datum (Newlyn).

In addition the flow is assumed to be sub-horizontal, so that the angle of the channel bed with the horizontal tends towards zero and that the cosine of the angle is approximated to unity.

The *control volume* is a term applied to the total volume of water between the two cross sections. The behaviour of this volume in time and space is what helps us derive the integral Equations of flow, the mass continuity and the conservation of momentum.

3.7 Mass Continuity.

The continuity of mass must satisfy the condition that the net inflow of mass is equal to the change in storage. This means that for a mass of water entering or leaving the control volume over a certain time there must be a corresponding change in storage in the control volume. The net inflow or outflow of mass into the control volume is the difference of mass flow rates entering or leaving the control volume, i.e. the change at the first section $(\rho\ u\ A)_{x1}$ and at the second section $(\rho\ u\ A)_{x2}$ integrated with respect to time. As can be deduced from Equation 3.1, the terms $\rho\ u\ A$, can be expressed in the form of $\rho\ Q$ and are in Kg s^{-1}. The

value of net mass inflow is given in Equation 3.2a. The change in storage is the mass of the new volume added or subtracted to the original control volume over the integrated time period and is given by Equation 3.2b.

$$\text{Net inflow rate of mass} = \int_{t_1}^{t_2} [(\rho Q)_{x_1} - (\rho Q)_{x_2}] \, dt \qquad (3.2a)$$

Which must be equal to;

$$\text{Change in storage} = \int_{x_1}^{x_2} [(\rho A)_{t_2} - (\rho A)_{t_1}] \, dx \qquad (3.2b)$$

Continuity of mass can be demonstrated when *steady flow* conditions prevail, where there is no change in flow velocity, hence no change in the quantity of flow at either end cross section of the control volume. In this case the mass entering cross section 1 will not differ with time, neither will the mass leaving cross section 2. The net inflow rate over this period of time will be zero, as no extra mass has either entered or left the control volume. As there is no change in mass, the control volume will not have increased or decreased to accommodate a change in mass and thus there will be no change in storage. The water level will thus remain constant over the period of time, indicating steady non-variable flow.

An example of *Unsteady flow* is depicted in Figure 3.3 where there are two simplified rectangular cross-sections at either end of a channel reach, akin to cross sections 1 and 2. Cross Section 1 is nominally termed the upstream section. There are two time stages representing the initial and end time level over which the equations are integrated t_1 and t_2. At the start of any time level a mass of flow, ρQ_1 (which may change over the period of time), enters the control volume through the first section, at the same time a mass equal to ρQ_2 leaves the control volume downstream through section 2. If these two values are not equal then there will be a gain or loss in mass within the control volume and thus a change in the volume. The sum of these changes over the period of integration gives the net inflow rate and the change of storage. The change in volume is shown in the diagram and the mass of which is the storage change.

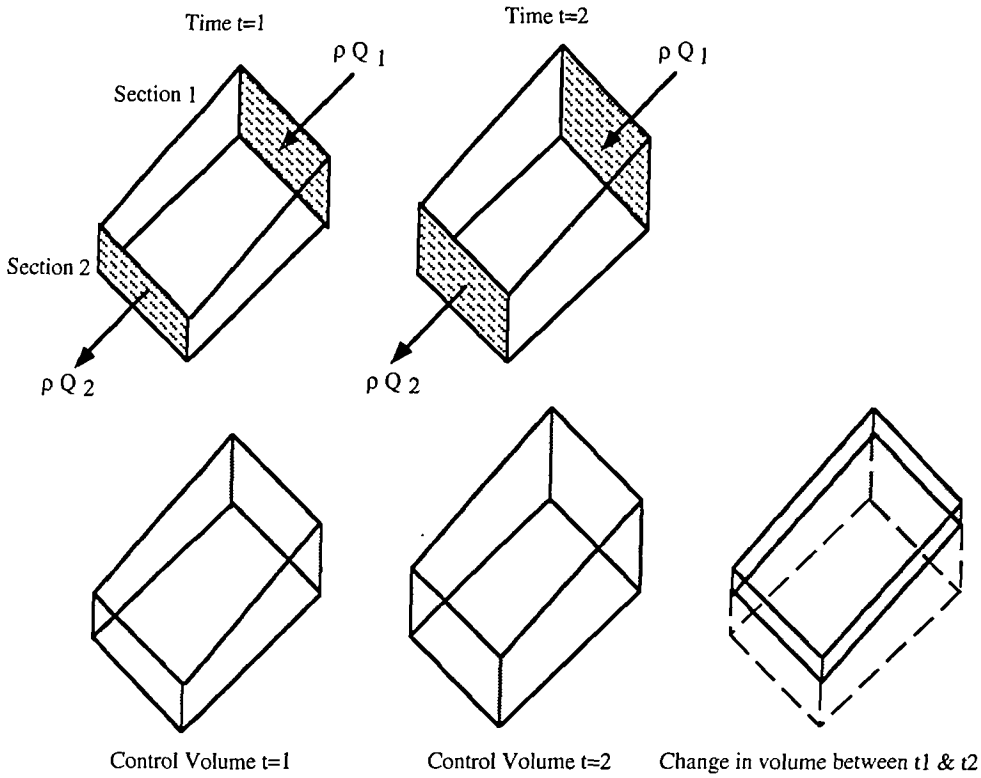

Fig 3.3. Continuity of mass showing change in storage when a greater mass of water enters the upstream cross section than leaves the downstream one.

From rearranging the two equivalent Equations 3.2a and 3.2b, a mass continuity relationship is derived by considering a constant fluid density between the two sections which eliminates ρ giving Equation 3.3.

$$\int_{x_1}^{x_2} [\,(A)_{t_2} - (A)_{t_1}\,]\,dx + \int_{t_1}^{t_2} [\,(Q)_{x_2} - (Q)_{x_1}\,]\,dt = 0 \qquad (3.3)$$

The previous expression does not allow for any loss of mass within the control volume, such as flooding over sea-walls or propagation up a tributary, lateral inflow and outflow will be considered later. A differential form of Equation 3.3 will be used as one part of the final mathematical model presented later in this chapter. The equation for the continuity of mass is commonly referred to as the Equation of Continuity.

3.8 Conservation of Momentum.

The conservation of momentum requires that the change of momentum in the control volume between the two times must be equal to the net inflow of momentum into the control volume added to the sum of the external forces acting over the control volume over this time.

ΔM is the change in momentum over period of integration

= Net momentum flux (M_F)+ Sum of external forces acting on control volume over period of integration.

There are a much greater number of components to this equation and subsequently it is a much harder to derive. A modeller must only consider what he thinks to be the major influences on the fluid motion, thus the momentum equation may differ from one model to another as various terms are ignored. Similarly some authors use differing terminology to describe the same processes thus a derived set of equations may look different but are essentially the same.

3.8.1 Net Momentum Flux, M_F.

From Newton's Second Law, momentum is defined as the mass of a body multiplied by its velocity in the units of Kg m s^{-1}. The momentum flux through a section is the product of the mass flow rate (ρ u A or ρ Q) and the velocity. The hydraulic pressure force detailed in the following section is frequently included in the momentum flux.

The momentum flux at a section, at any time, $M = \rho u Q$ **(3.4)**

The net momentum flux within the control volume over the period of integration is equal to the momentum flux entering at one section minus the momentum flux leaving the other integrated with respect to time (Equation 3.5). The net momentum flux represents the amount

of momentum to have entered or left the control volume over the period of integration between times t_1 and t_2 through both end cross sections.

Net momentum flux:

$$M_F = \int_{t_1}^{t_2} [(\rho u Q)_{x_1} - (\rho u Q)_{x_2}] \, dt \qquad (3.5)$$

The forces acting on the control volume are described as the hydrostatic pressure force, the force due to breadth change, the gravitational force and the frictional resistance force, which are described in sections 3.8.2 to 3.8.5.

3.8.2 Hydrostatic Pressure Force, F_H.

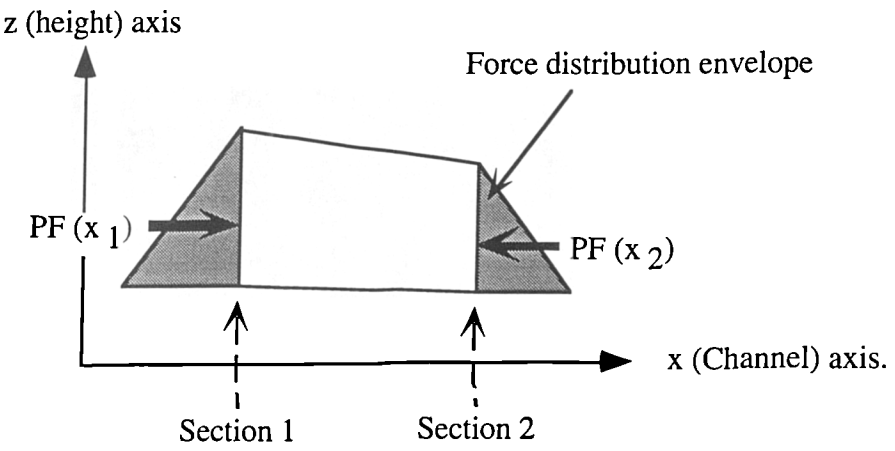

Fig 3.4. Pressure forces at end sections of a channel.

The mass of water at either end of a reach exerts a hydrostatic pressure force at the cross-section. The net pressure force, NPF_H, acting upon the control volume is equal to the difference of pressure forces at either end of the reach. The subscript H in the previous abbreviation signifies that the net pressure force being considered is related to the hydrostatic pressures. The two pressure forces are shown diagrammatically in Figure 3.4, which is a cross-section through the control volume, bounded at either ends by the two sections x_1 and

x_2 . The shaded triangles in Figure 3.4 show the distributions of hydrostatic pressure forces at the two sections, the arrows labelled PF (x_1) and PF (x_2) indicate the assumed (depth averaged) mean value of these pressure forces at the sections.

The pressure force at any cross section, with a free surface elevation of Z can be calculated from hydrostatic distribution laws (Equation 3.6). The notation for this Equation is presented in the following diagram (Figure 3.5). The liquid depth at the section is termed h, η is the depth integration variable along the z axis and $\sigma(\eta)$ is the width of the cross section at the depth η, so that $\sigma(h)$ is equal to the breadth of the liquid at the free surface (B).

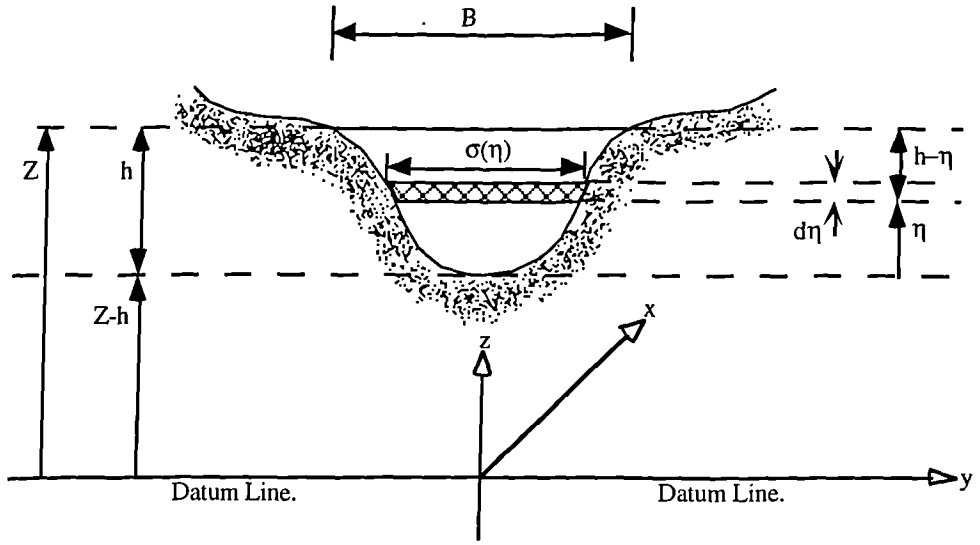

Fig 3.5. Notation for a cross-section for pressure forces.

The pressure force at a section is given by *Equation* 3.6, which is shown as an equivalence relationship of $I_1 g \rho$, where I_1 represents the integral term.

Pressure force at a single section due to hydrostatic pressure, PF_H:

$$PF_H = g \int_0^h \rho [h - \eta] \sigma(\eta) \, d\eta \equiv I_1 g \rho \qquad (3.6)$$

The net pressure force NPF_H is the difference of the two hydrostatic pressure forces at either end of the control volume. The time integrated Equation of the hydrostatic pressure force is shown below in Equation 3.7 and is the total hydrostatic pressure force, F_H.

Total pressure force due to hydrostatic pressure, F_H:

$$F_H = g\rho \int_{t_1}^{t_2} [(I_1)_{x_1} - (I_1)_{x_2}] \, dt \qquad (3.7)$$

3.8.3 Force due to Breadth Change, F_B:

Additional pressure forces are introduced by a variation in width of the channel reach. The Equations which derive this force rely on such a change being gradual. A sudden width variation invalidates the basic hypothesis that the stream-line curvature is considered negligible. If such a case is found in the real river being modelled then an internal boundary condition will need to be added at that point where additional modelling is required to satisfy the localised flow conditions.

The increase in pressure force over a small channel length due to width variation is given by Cunge et al. (1980) as the increase in wetted area (local cross-sectional area of liquid) for a constant water depth, $h = h_o$, $d\sigma . d\eta$, multiplied by the distance of it's centroid from the water surface, $(h - \eta)$, which are shown in Figure 3.5, multiplied by the density and acceleration due to gravity (Equation 3.8).

Pressure force due to breadth variation, PF_B:

$$PF_B = \rho g \left[\frac{\partial \sigma}{\partial \eta} \, dx \, . d\eta \right]_{h_o} (h - \eta) \qquad (3.8)$$

The force presented in Equation 3.8 is integrated over the depth at a given cross-section and over the distance between the two bounding cross-sections to give the total force acting at

the sides of the volume. This is subsequently integrated over the period of time under consideration to give the total pressure force due to breadth change, F_B, in Equation 3.9.

Total pressure force due to breadth variation, F_B:

$$F_B = \int_{t_1}^{t_2} \int_{x_1}^{x_2} \rho g \int_0^{h(x)} (h(x) - \eta) \left[\frac{\partial \sigma (x, \eta)}{\partial x} \right]_{h_o} d\eta \, dx \, dt$$

$$F_B \equiv \int_{t_1}^{t_2} \int_{x_1}^{x_2} \rho g I_2 \, dx \, dt \qquad (3.9)$$

Where h (x) represents the depth at a cross section, position x, σ (x, η) represents the value of σ at the section x and elevation above channel bed. The term h_o indicates that the depth at the section is kept constant to a value of h_o for which the bracketed term is to be integrated.

3.8.4. Gravitational Force, F_G.

The gravitational force acts down the slope of the channel and represents the weight component of the control volume along the channel axis. The channel slope S_o is shown in Equation 3.10, where Z_b represents the bottom elevation above a datum (Z - h).

$$\text{Channel Slope, } S_o = \frac{\partial Z_b}{\partial x} = \tan \alpha \qquad (3.10)$$

The channel section is shown diagrammatically in Figure 3.6 which indicates the components of the gravitational forces acting on the mass of the control volume.

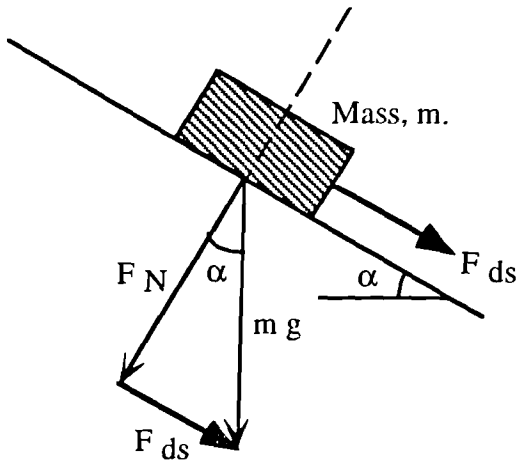

Fig. 3.6. Accelerating forces acting on a mass on a slope.

For a mass, m, there is a vertical force component downwards equal to m g. On a slope of angle α, there are two force components, the normal force F_N acting in a direction normal to the slope and the force down slope (F_{ds}), This force in fluid flow is the same as the force on the bed slope due to gravity. The force down slope can be evaluated by Equation 3.11.

$$F_{ds} = m\, g \sin \alpha \qquad (3.11)$$

One of the De Saint Venant assumptions of these derivations is that the channel slope is very small, thus as a low angle is approached then $\tan \alpha \approx \sin \alpha$. The channel bed slope is equal to the tangent term and so can be replaced for the sine term in Equation 3.12, to give the relation given in Equation 3.12.

$$F_{ds} = m\, g\, S_o \qquad \mathbf{(3.12)}$$

The total gravitational force, F_G, is the result of integrating Equation 3.12 with respect to time and is given by Equation 3.13.

Total Gravitational Force, F_G:

$$F_G = \int_{t_1}^{t_2} m g S_o \, dt = \int_{t_1}^{t_2} \int_{x_1}^{x_2} \rho g A S_o \, dx \, dt \qquad (3.13)$$

Assuming a cosine of unity would leave the tangent and sine of the bed slope as zero, thus S_o would be equal to zero, so there could be no equatable gravitational force. Indeed some modellers ignore the gravitational forces but in general the force is evaluated and the bounding assumptions are slightly compromised. It was found that the model did not provide reasonable results ignoring the gravity terms.

3.8.5 Frictional Resistance Force, F_F.

Whilst evaluating the gravitational force, frictional resistance was ignored. In the simplified diagram, fig 3.6, there was no frictional force indicated. However, in reality there would be a frictional resistance to motion from the base of the mass in the direction of the slope in opposition to the gravitational force downhill/stream. With water flow this resistance is considered to be from boundary shear forces at the juncture of the liquid and the channel sides and floor. To evaluate the shear force, it is necessary to introduce the friction slope, S_f, which is the energy gradient required to over come the frictional resistance in steady flow. This is obviously a case where the assumptions for steady flow are considered valid for unsteady flow. Chow (1959) determined that the frictional force on a unit length of channel was given by $\rho g A S_f$, which integrated over the length of the channel reach and the period of interest gives the total friction force, F_F, in Equation 3.14.

Total Frictional Resistance Force, F_F:

$$F_F = \int_{t_1}^{t_2} \int_{x_1}^{x_2} \rho g A S_f \, dx \, dt \qquad (3.14)$$

3.8.6 Change in Momentum.

The change in momentum between the two time levels in the control volume is shown in Equation 3.15.

Change in momentum, ΔM:

$$\Delta M = \int_{x_1}^{x_2} [(\rho Q)_{t_1} - (\rho Q)_{t_2}] \, dx \qquad (3.15)$$

The change of momentum can be described by the momentum flux and the effects of the pressure forces described in sections 3.8.2 to 3.8.5 are shown in Equation 3.16 which is a form of the Conservation of Momentum Equation.

$$\Delta M = M_F + F_H - F_B + F_G - F_F \qquad (3.16)$$

Equation 3.15 can be rearranged by removing the assuming constant density and writing in terms of the time integrals of the pressure forces which simplifies the gravitational and frictional force terms and leads to the derivation of the integral form of the conservation of momentum (3.17).

$$\begin{aligned}\int_{x_1}^{x_2} [(Q)_{t_1} - (Q)_{t_2}] \, dx = & \int_{t_1}^{t_2} [(uQ)_{x_1} - (uQ)_{x_2}] \, dt \\ & + g \int_{t_1}^{t_2} [(I_1)_{x_1} - (I_1)_{x_2}] \, dt \\ & - g \int_{t_1}^{t_2} \int_{x_1}^{x_2} I_2 \, dx \, dt \\ & + g \int_{t_1}^{t_2} \int_{x_1}^{x_2} A(S_o - S_f) \, dx \, dt\end{aligned} \qquad (3.17)$$

The two Equations 3.4 and 3.17 represent the integral forms of De Saint Venant's equations of unsteady flow, the Continuity of Mass and the Conservation of Momentum respectively. These two Equations are often referred to as the *Continuity* and *Momentum* equations. In neither equation was the effect of lateral inflow considered, but will be added later into the differential form of the flow equations.

The integral relationships derived in sections 3.7 and 3.8 are a series of addition sums which did not require the functions they contain to be continuous. Unfortunately in simulating a natural river it is unlikely that there will be enough data to furnish a solution based such relationships. The numerical solution of these equations requires them to be in differential forms where they may be represented by any of a series of numerical discretisations which may in turn be solved mathematically. The computational aspects of solving differential equations are described in Chapter 4. Section 3.9 shows how the family of differential equation can be derived based on the integral relations described previously.

3.9 Differential Equations of Flow.

Differential equations require that the dependant variables of a system are continuous. Dependant variables described so far include the variables, Z and Q and A, u, B, etc. Where Z and Q are considered primary variables because the knowledge of the values of them at a cross section enables the evaluations of all of the other variables if the cross-sectional geometry, area, breadth etc. have been digitised. Digitisation in this instance is the process of analysing the cross sectional data received and evaluating the various hydraulic properties at given water elevations, described in Chapter 6. Differential equations can be derived from the integral equations if the flow variables are continuous. A way to demonstrate the meaning of this is to consider the simple schematic cases of continuous and discontinuous flow.

If the flow was continuous then there may be a flow entering one section, and leaving at the next. As time progresses the flow may increase at one section (the upstream one) with a subsequent rise in the water level and flow velocity. With time this increase would reach the second section and there would be a subsequent rise in levels, velocity and outflow at the downstream section. The increase in free surface elevation and velocity would be gentle

between the two sections and the envelope of the free surface would be smooth between the two sections with no sudden jumps. This may be modelled by integral and differential methods if enough data were available.

A discontinuous situation, albeit an unrealistic case, may have a channel reach between two sections where there is a large pipeline at one end that can discharge large volumes of water in pulses. Continuous flow conditions may prevail between the two sections until the pipe discharges. This will cause a sudden increase in the volume of water and free surface level, which will be a sudden jump from the level immediately downstream. Obviously this invalidates the De Saint-Venant assumption that the streamline curvature is negligible, vertical accelerations are not negligible and the hydrostatic pressure distributions complicated. The integral relations may sum the flow properties entering and leaving the control volume and furnish reasonable answers, however, a differential equation is unsuitable. There are discontinuous solutions available for the solution of such problems, including the simulation of bores and dam breaks.

3.9.1 Taylor Series Expansions of a Function.

To obtain differential forms of the Continuity and Momentum Equations, it is necessary to first introduce how a function is described in a differential form. For a given function of any variable 'x', $f(x)$ can be represented by a Taylor Series expansion shown by Equation 3.18.

$$f(x) = f(x_0) + (x - x_0) f'(x_0) + \frac{(x - x_0)^2}{2!} f''(x_0) + \ldots\ldots + \frac{(x - x_0)^n}{n!} f^{(n)}(x_0) + \ldots\ldots \qquad (3.18)$$

The Taylor Series expansion with respect to time of the flow variable Q can be derived by knowing the value of Q at time t_2 (so that $f(x)$ in equation 3.18 is substituted by Q_{t_2}), by knowing an initial value of Q at time t_1 which is similarly substituted, knowing that the time period (Δt) is equal to $t_2 - t_1$ and by adopting the form $\frac{\partial Q}{\partial t} = f'(Q)$ to give Equation

3.19. The expansion with respect to distance (x) is derived by the same method and shown in Equation 3.20.

$$Q_{t2} = Q_{t1} + \frac{\partial Q}{\partial t}\Delta t + \frac{\partial^2 Q}{\partial t^2}\Delta t^2 + \ldots\ldots\ldots \qquad (3.19)$$

$$Q_{x2} = Q_{x1} + \frac{\partial Q}{\partial x}\Delta x + \frac{\partial^2 Q}{\partial x^2}\Delta x^2 + \ldots\ldots\ldots \qquad (3.20)$$

The theory behind the differential series of equations is that Δx and Δt approach zero, i.e. describe an infinitely small distance or time step, which is not a constraint of the integral relationships. If these two terms are very small, then their square and higher order terms are negligible, thus only the first order derivatives are assumed to have any significant value and the rest are ignored.

3.10 Continuity of Mass, Differential Form.

The Taylor Series expansions given in section 3.9.1 are the basis of converting the integral equations used earlier into a differential form. The technique for the mass equation is described in more detail than the dynamic equation in the next section because it is assumed that one example is sufficient to understand the method.

The continuity equation given in equation 3.4 can be split into two parts which are shown in Equations 3.21 and 3.22.

$$\lim_{t_2 \to t_1} \int_{x_1}^{x_2} [(A)_{t_2} - (A)_{t_1}]\, dx = \int_{x_1}^{x_2} \int_{t_1}^{t_2} \frac{\partial A}{\partial t}\, dt\, dx \qquad (3.21)$$

$$\lim_{x_2 \to x_1} \int_{t_1}^{t_2} [(Q)_{x_2} - (Q)_{x_1}]\, dt = \int_{t_1}^{t_2} \int_{x_1}^{x_2} \frac{\partial Q}{\partial x}\, dx\, dt \qquad (3.22)$$

From the previous terms the continuity of mass equation may be expressed in the form of Equation 3.23.

$$\int_{x_1}^{x_2} \int_{t_1}^{t_2} \left[\frac{\partial A}{\partial t} + \frac{\partial Q}{\partial x} \right] dt \; dx \qquad (3.23)$$

With a system which is considered continuous, the increments of Δt and Δx being considered infinitely small and the equation for the continuity of mass given as 3.23 considered to apply for a control volume also of infinitely small volume, the equation can be written in a differential form as equation 3.24.

$$\frac{\partial A}{\partial t} + \frac{\partial Q}{\partial x} = 0 \qquad (3.24)$$

The differential form of the momentum equation is shown in section 3.11, however, this section will continue to describe how the continuity equation is adapted until it represents the final form of the continuity equation used in the mathematical model.

The time derivative of the area function can be replaced so that it may be expressed in terms of Z, the elevation above datum of the free surface. It is preferable to try and develop the equations in terms of the primary flow variables, as they are both easier to understand and eventually compute.

$$\frac{\partial A}{\partial t} = \frac{\partial A}{\partial Z} \times \frac{\partial Z}{\partial t} = B \frac{\partial Z}{\partial t} \qquad (3.25)$$

The rate of change of area with free surface elevation is equal to the breadth which is crudely demonstrated by the aid of Figure 3.6 on a simple trapezoidal section.

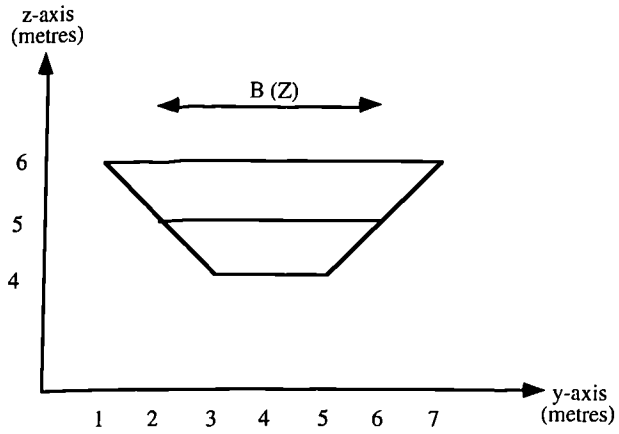

Fig 3.6 Trapezoidal section, area, elevation and breadth evaluation.

Considering the value of the breadth at a free surface elevation of 5m, we take the value of the areas at two elevations either side of this level, to get the rate of change of area with height:

Free surface elevation (Z) 6m Area (A) $8m^2$

Free surface elevation (Z) 4m Area (A) $0m^2$

$$\frac{\partial A}{\partial Z} = \frac{8 - 0}{6 - 4} = 4 = \text{Breadth (B) at surface elevation Z = 5m.}$$

It is noted that this adaptation of the breadth term and stage rather that the cross sectional area is a digression from the computational models used as comparisons, the HRS LORIS and ISIS models and Binnine and Partner's model. However, during running of the model derived for this thesis it was possible to compare the effect of the two alternative terms (breadth x rate of change of stage with time and rate of change of area with time) and was found to show little difference.

3.10.1 Other Effects.

The final adaptation to the continuity equation is to allow for mass lost laterally in the channel. This will occur in two types of cases, the first being flow up a tributary which must

be treated algorithmically and is described in Chapter 4 and the second being lateral inflow or outflow such as over-topping of seawalls, river banks, evaporation and seepage. Although *Lateral inflow* is the term adopted this also accounts for lateral outflow as well. The continuity equation is rewritten in a non-conservative form, so that extraneous mass losses may be accounted for by the lateral inflow variable, L. This section only deals with the theoretical aspects of including lateral inflow and Chapter 5 describes the practical aspects of inclusion.

Lateral inflow, L, is defined as the volume of inflow per unit length of channel per unit time and is in $m^2 s^{-1}$. This assumes that the density of the inflowing liquid is equal to that of the liquid in the channel. The lateral inflow term was not added at the integration stages because it is a value which is not considered to vary between the two time stages t_1 and t_2 and is an averaged value over the channel reach between section x_1 and x_2. As will be discussed in Chapter 6, the addition of lateral inflow into the equations has a major effect on high tide levels once the stage is sufficiently high enough to breach a seawall. A problem in the estimation or calculation of the value of L is that it is prone to a degree of error and may be the source of greater modelled error than any uncertainty that it resolves.

With the substitutions made previously, Equation 3.26 presents the final modelled version of the continuity equation.

Continuity of Mass:

$$B \frac{\partial Z}{\partial t} + \frac{\partial Q}{\partial x} = L \qquad (3.26)$$

Where L = lateral inflow (m^2/s)

3.11 Continuity of Momentum, or Dynamic Equation, Differential Form.

This section will convert the integral relationship of section 3.8 to give the differential form of the momentum equation. It is assumed that it is not necessary to describe the transformations used as they are the same as those used to derive Equations 3.21 to 3.24.

The integral equation of momentum (Eq.3.17) is represented as Equation 3.27 once Taylor series substitutions are applied.

$$\int_{x_1}^{x_2} \int_{t_1}^{t_2} \left[\frac{\partial Q}{\partial t} + \frac{\partial}{\partial x} \frac{Q^2}{A} + g \frac{\partial I_1}{\partial x} - g I_2 - g A S_o + g A S_f \right] dt\, dx \qquad (3.27)$$

Using the same principles as described in section 3.9, the momentum equation can be expressed in differential form, given in equation 3.28.

Conservation of momentum:

$$\frac{\partial Q}{\partial t} + \frac{\partial}{\partial x} \frac{Q^2}{A} + g \frac{\partial I_1}{\partial x} - g I_2 - g A S_o + g A S_f = 0 \qquad (3.28)$$

The differential form of the momentum equation given above can be written in a divergent form, equation 3.29, where the terms to the right hand of the equality sign, may account for momentum sources or sinks. If the sum of these terms is zero for a given position in the calculations, then momentum is said to be conserved with frictional, gravitational acceleration and breadth variations having no net affect on the flow.

$$\frac{\partial Q}{\partial t} + \frac{\partial}{\partial x} \frac{Q^2}{A} + g \frac{\partial I_1}{\partial x} = g I_2 + g A S_o - g A S_f \qquad (3.29)$$

A simplified model of flow may be used by ignoring the terms in the right hand side of equation 3.29, however, this would be very unlikely to occur naturally due to the complexity of natural river flow and so was not considered in the modelling process.

Equations 3.28 and 3.29 do not give readily calculable values for the two integrals I_1 and I_2 or the values of S_o and S_f. The rest of this section discusses these terms and the effect of lateral inflow on the momentum equation.

3.11.1 Hydrostatic pressure force integral, I_1.

The integral I_1 defined by equation 3.6 is rewritten below in Equation 3.30 after the gravity and density coefficients have been removed from the former equation.

$$I_1 = \int_0^h [\, h - \eta \,]\ \sigma(\eta)\ d\eta \qquad (\ \mathbf{3.30}\ )$$

Two substitutions made before analysing this equation are given below in equations 3.31.

$$\sigma(x, \eta) = B(x) \qquad (\ \mathbf{3.31}\ )$$

Where $\eta = h$ (the depth)

$\int_0^h \sigma\ d\eta = A$, i.e. the sum of all breadth elements added over the depth.

The Leibnitz Theorem is used to obtain the differential of an integral. Leibnitz's theorem states that if any two functions $f(x)$ and $g(x)$ are n times the differential real valued functions in the interval between the limits a to b, then it can be said that the relations in equations 3.32 are valid.

$$\frac{\partial^n}{\partial x^n}(f\,g) = \sum_{i=0}^{n} \binom{n}{i} \frac{\partial^{n-i}}{\partial x^{n-i}} f \cdot \frac{\partial^i}{\partial x^i} g \qquad (\ \mathbf{3.32a}\ )$$

When n is equal to unity then this leads to the relation below commonly termed the product rule (3.32b).

$$\frac{\partial}{\partial x}(f\,g) = g\frac{\partial f}{\partial x} + f\frac{\partial f}{\partial x}\ (\text{Product Rule}) \qquad (\ \mathbf{3.32b}\ )$$

The integral given by equation 3.30 can thus be represented by equation 3.33, using the substitutions given by the relations in 3.31.

$$\frac{\partial I_1}{\partial x} = \frac{\partial}{\partial x}\int_0^{h(x)} [\, h(x) - \eta \,]\ \sigma(x, \eta)\ d\eta$$

$$= \frac{\partial h}{\partial x}\int_0^{h(x)} \sigma(x, \eta)\ d\eta + \int_0^{h(x)} [\, h(x) - \eta \,]\ \frac{d\,\sigma(x, \eta)}{d\,x}\ d\eta$$

$$= \frac{\partial h}{\partial x}\ A(x) + I_2 \qquad (\ \mathbf{3.33}\ )$$

Substituting into equation 3.29 gives the momentum equation given in the form of Equation 3.34.

$$\frac{\partial Q}{\partial t} + \frac{\partial}{\partial x}\frac{Q^2}{A} + g A \frac{\partial h}{\partial x} - g A S_o + g A S_f = 0 \qquad (\ \mathbf{3.34}\ )$$

The momentum equation given above is not in a divergent form because all the terms on the left hand side of the equation add up to zero. This means that they account for all the sources or losses of momentum, which is unlikely to be a *true representation of momentum* conservation. It is for this reason that this equation is often referred to as the *Dynamic Equation.*

As with the *Continuity* Equation, it is preferable to describe the components of the equations in terms of the primary variables, Z and Q.

Using;

$Z_b = Z - h$ = bottom elevation.

$h = Z - Z_b$ = water depth

and that

$$\frac{\partial h}{\partial t} = \frac{\partial Z}{\partial t}$$

Then Equation 3.35 can be derived;

$$\frac{\partial h}{\partial x} = \frac{\partial Z}{\partial x} - \frac{\partial Z_b}{\partial x} = \frac{\partial Z}{\partial x} + S_o \qquad (3.35)$$

Which can be substituted into Equation 3.34 to give Equation 3.36.

$$\frac{\partial Q}{\partial t} + \frac{\partial}{\partial x}\frac{Q^2}{A} + g A \frac{\partial Z}{\partial x} + g A S_f = 0 \qquad (3.36)$$

The effect of lateral inflow has not been added until the end of the derivation. Inflow into a channel or out of one will be a further momentum source or sink. It is common to neglect the inflow term in the dynamic equation because the term tends to be much less important than the already derived terms. It was decided that it would be better to introduce the term, observe it's affect on the modelled results and then decide upon it's computational necessity. Adding a continuous lateral inflow per unit length, the dynamic equation is finally presented in the form of Equation 3.37. The inflow term in this case assumes that anything entering or leaving the system being represented by the lateral inflow term is doing so at right angles to the assumed channel axis.

$$\frac{\partial Q}{\partial t} + \frac{\partial}{\partial x}\frac{Q^2}{A} + g A \frac{\partial Z}{\partial x} + g A S_f - L\left(U_L - \frac{Q}{A}\right) = 0 \qquad (3.37)$$

3.12 Summary.

This chapter has introduced the hydraulic theory chosen as apposite to the modelling requirements of the thesis. The two derived equations of unsteady flow are rewritten as equations 3.38 and 3.39 and together are termed a *'mathematical model'*. They are two partial differential equations based on integral equations presented in sections 3.7 and 3.8 and the governing assumptions given in section 3.5.1.

$$B \frac{\partial Z}{\partial t} + \frac{\partial Q}{\partial x} = L \qquad (3.38)$$

$$\frac{\partial Q}{\partial t} + \frac{\partial}{\partial x}\frac{Q^2}{A} + g A \frac{\partial Z}{\partial x} + g A S_f - L\left(U_L - \frac{Q}{A}\right) = 0 \qquad (3.39)$$

This chapter has derived two governing equations of fluid flow by mathematically representing what were considered to be the most important contributions to the flow to be modelled. Although different in appearance they are almost the same as De St. Venant's original equations but have been derived in a form favourable to the author from a computational and practical point of view.

Chapter 4 describes the computational method selected to solve these equations whilst Chapter 5 will consider some of the techniques and problems evolved from modelling rivers and estuaries, such as how data availability and type effect the design of the system, how friction problems are considered and whether they are truly valid and how natural flow digresses from the basic assumptions to a point where the equations derived in this chapter become no longer valid.

CHAPTER 4

MATHEMATICAL SOLUTION OF UNSTEADY FLOW EQUATIONS.

4.1 Introduction.

Two equations of fluid flow based upon the assumptions of Se Saint-Venant which form a mathematical model of unsteady flow in an open channel were derived in Chapter 3. This chapter described the numerical methods by which the mathematical model can be solved to give a simulation of tidal phenomena in the Severn Estuary.

This chapter discusses the relevant history of solution techniques in Sections 4.2 and 4.3, before describing the finite difference scheme selected as being the most appropriate method of evaluation and the application of the method to solution of the mathematical model.

4.2 Historical Development.

Mathematical models of flow in tidal rivers are now accepted engineering tools. They involve the solution of mathematical equations describing fluid flow. The development of these models owes much to the existence of physical scale hydraulic models, popularised by Froude in the Nineteenth Century which were still in common use in the early half of this century (e.g. Gibson 1933). However, logistical problems due to increasingly complex design criteria led to the scale models becoming less popular as they neared their limits of application. Mathematical models were developed as cheaper and more convenient solutions, especially with the advent of the modern digital computer in the 1950's. These models utilised the theoretical and experimental techniques from which the scale models were designed. However, hydraulic models are still in common usage as they can display complex hydraulic phenomena which are as yet mathematically unsolvable.

In addition to the harmonic system of tidal prediction used for tidal calculations by the Hydrographer of the Navy in Admiralty Charts and tide tables, there are three closely related mathematical model types; The method of characteristics, finite difference and finite element

methods. An engineer designing a system must fully understand the applications and limitations of the chosen design system. All three simulation methods involve the solution of mathematical formulae expressing known hydraulic relationships. Although the mathematical theory behind the solution of differential equations such as the De Saint-Venant equations had been established early in the Nineteenth Century, early attempts to apply mathematics to tidal problems were frustrated by the errors evolved from the inaccurate measurements of cross sections, friction values and the bulk of calculations required.

Massau (1889) applied the newly developed method of characteristics to solve shallow water tidal problems. This paper was poorly received because of its complexity and the characteristic method was only popularised after Courant, Friedrichs and Lewy (1928), Schönfeld (1951), Richtmyer (1957) and others demonstrated practical applications of the method. It is from the work of Massau that most solution techniques employed today have developed. The method of characteristics involves the solution of hyperbolic partial differential equations such as the De Saint-Venant equations by graphical characteristic curves based on the form of the parent equations or numerical schemetisations of the curves. Reviews of characteristic methods are contained in Dronkers (1964), Mahmood and Yevjevich (1975) and Cunge *et al* (1980).

One of the first applications of finite difference solutions of shallow water equations was by stoker Stoker (1957). This system is very similar to the characteristic method and involves the solution of the original partial differential equations, rather than the characteristic form of the equations. The finite difference scheme has proved to be the most convenient method of resolving shallow water problems because it can be easily programmed onto a digital computer.

As computing facilities have become more advanced a further system of simulation, the finite element method has become popular at an exponential rate. It is impossible to review all the aspects of the numerical techniques.

4.3 Numerical Solution Techniques.

The equations of flow derived in Chapter 3 or any similar differential or integral relationships are the mathematical model of unsteady flow. However, they are too complex to solve by analytical methods in such forms because they describe a continuous function. It is necessary to develop a numerical solution technique which will solve these equations to the satisfaction of the model design criteria. The technique will be developed in this chapter.

The modelled solution of a tidal simulation, gives values of water stage and discharge. These two properties are functions of both time and space, but are not immediately available from the equations given in Chapter 3. The differential equations must be approximated to give stage and discharge values at a number of discrete points within the time-space domain which physically represent the height and flow at a cross section in the river and it's variation with time.

Taking discrete points in a continuous solution is termed discretization. The finite difference method described in this thesis is just one of a whole host of other discretization techniques such as finite element, characteristic and polynomial expansion methods. The finite difference method itself has a sub-family of similar but strategically varying solution methods. As will be discussed later these differing techniques may vary in validity over differing flow conditions, although to decide why isn't always documented or indeed obvious.

4.3.1 Benefits of the Three Principal Methods of Solution.

The three methods of solution are an evolution of mathematical thinking and thus show many similarities. The three principal families of solution are in reality a series of new generations of solutions based on the existing methods. The Characteristic methods came first and are analytical solutions of numerical functions which may be solved using graphical methods or by a numerical method of solving the characteristic curves of the equations. The finite difference methods were an advance on the numerical calculations of the characteristic type solutions, which allowed the representation of much more complex equations. However, in many ways the finite difference and characteristic solutions can be very similar. The finite

element solutions are similar to the finite difference solutions and use similar numerical methods, although much more complex solution 'nets' can be used to represent very complex systems or can be used to analyse the finer detail of a system that cannot be resolved by one of the other methods. Table 4.1 presents the benefits and drawbacks of the principal numerical methods which are applicable to the derived equations of fluid flow in Chapter 3.

Method	For	Against
Characteristics	Believed by some to be more accurate than other methods. Most applicable to 'shock fitting' solutions.	Not as suitable to computer applications.
Finite Difference	Easily applied to computer applications. Many solution methods available .	Can give the least accurate representation of a modelled system.
Finite Element	Most modern. Best representation of modelled system.	Can be numerically complex, leading to time consuming calculations.

Table 4.1. Three principal numerical solution methods.

The finite difference model is considered to be the most applicable method of solutions for this thesis due to the relative easiness in which it can be analysed by computer. The finite difference method has two major types of solution, the implicit and explicit method, which are briefly summarised in Table 4.2. The explicit method of solution is not as useful for the analysis of the tidal problems required by this study because of the nature of the 'real' data available, thus the implicit method has been selected. Unfortunately there are a great many methods of implicit finite difference schemes which vary in nature in subtle to quite vast amounts from each other. Whilst this study has considered many of the available methods, it is not possible to discuss each one on merit, so the chapter describes the overall theory of the

finite difference method and the derived method of solution. The References section at the end of this thesis details some works which are not directly referenced in the main body of text, but are relevant to the overall literature study and initial design of the numerical solution techniques used.

Method	For	Against
Explicit	Gives the simplest and quickest solution.	Requires much data which may not be available. Can be unstable.
Implicit	Stable in most conditions. Does not need as much natural data as an implicit method.	Can be slower to compute. Tolerance of solution method may hide errors in raw data.

Table 4.2 The two families of finite difference methods.

4.4 The Finite Difference Method.

A finite difference solution method has been chosen because of its suitability tocomputer application. Before introducing the solution of fluid flow, the author deems it apposite to introduce the basis of the finite difference method in this section.

The finite difference method involves the replacement of the original differential equations by finite difference equations. Finite difference equations are functions of the originally continuous arguments applied to a number of points forming a grid within the domain of applicability of the differential equations.

A very simple method of demonstrating the finite difference method is to consider a continuous function such as a curve which is varying in an x-y plane as represented by Equation 4.1, where $\frac{dy}{dx}$ is the gradient to the curve.

$$\frac{dy}{dx} = e^{-x^2} \quad \text{where } y = 0 \text{ when } x = 0 \qquad (\mathbf{4.1})$$

It is almost impossible to solve Equation 4.1 analytically. A finite difference method will give an approximate answer to this equation and will provide a technique which can solve other equations by the same method, making it a valuable numerical tool.

On a well behaved curve, the Mean Value Theorem can be applied to give the numerical value of the gradient, as shown in Equation 4.2.

$$\frac{dy}{dx} = \frac{\text{difference in y}}{\text{difference in x}} = \frac{y_i - y_{i-1}}{x_i - x_{i-1}} = \text{gradient at } x_{i-1/2} \qquad (4.2)$$

The term $\frac{dy}{dx}$ is the differential equation and the $\frac{y_i - y_{i-1}}{x_i - x_{i-1}}$ term is the finite difference form of that equation about the point $x_{i-1/2}$. Figure 4.1 demonstrates the difference between the real and mathematical gradients to the curve.

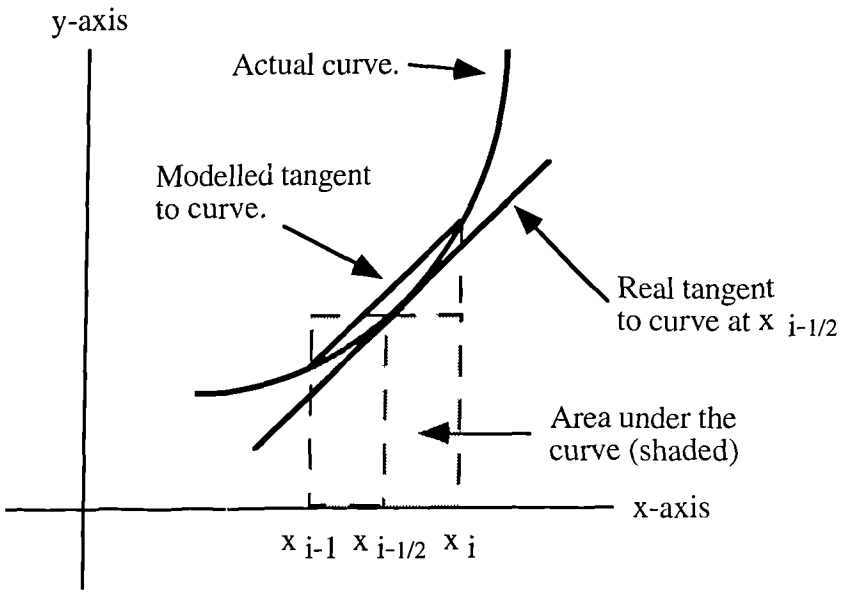

Fig 4.1. Graphical representation of real and modelled curves.

The original function of equation 4.1 may be solved by using the relationship depicted in Equation 4.2 to give a solution in the form of Equations 4.3 or 4.4.

$$\frac{y_i - y_{i-1}}{x_i - x_{i-1}} = e^{(-x^2_{i-1/2})} \qquad (4.3)$$

and thus

$$y_i = y_{i-1} + (x_i - x_{i-1})\, e^{(-x_{i-1/2}^2)} \qquad (4.4)$$

The solution given by Equation 4.4 is the result of integrating Equation 4.1. As long as $x_i - x_{i-1}$ is small enough, the real and modelled gradient will tend towards becoming the same line and thus the solved value of y will be accurate. The original continuous equation has been replaced by a finite difference scheme (albeit a very basic one). Starting at x = 0 and knowing that y = 0, Equation 4.4 is used to give successive values of y as x increases. In this example there is only one independent variable which is allowed to vary (x) and one dependant variable (y) which varies as a function of x. There are numerous methods of numerical discretion techniques, all of which can be called a finite difference scheme.

The solution to the flow in an estuary which is to be developed in this chapter is much more complex than the scheme shown above because the De St. Venant equations have a larger number of variables. Although the values of breadth, area, conveyance and wetted perimeter vary throughout the tidal cycle, they are dependant on the water stage, thus there are only two primary dependant variables (Z and Q) and two independent variables (t and x) in the flow equations.

4.5 The Finite Difference Computational Grid.

A finite difference grid defines all the points for which a numerical operation will occur. In a one dimensional channel these points represent the cross sections where flow variables will be evaluated during the period of simulation. This set of points is called the domain and is divided into the computational grid which is depicted in Figure 4.2, where the x-axis defines the spatially varying points, i.e. the cross sections in the real river and the t-axis defines the temporal positions. The salient features of these axes are described in the sub-sections of text below along with the initial conditions which define the flow at the beginning of simulation and the boundary conditions which are time dependant properties at the end of the modelled reach.

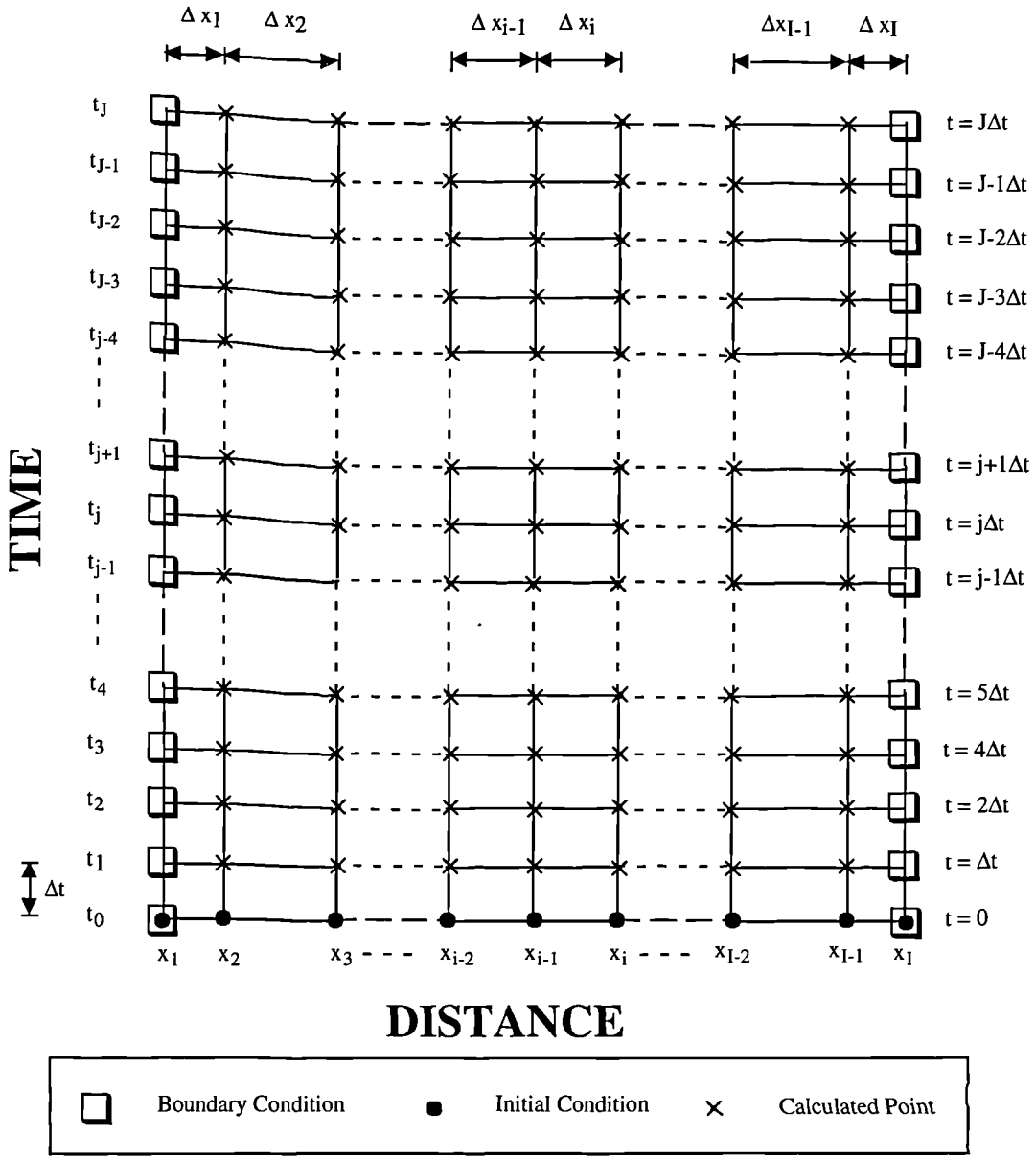

Fig 4.2. The finite difference grid.

4.5.1 Distance Axis.

Points along the distance axis are assigned the subscript i for the ith section and points along the time axis the superscript j. There are I points along the x-axis, starting at x_1, ending at x_I and thus there are I-1 space intervals. Each discrete point along the x-axis represents a schemetized cross-section in the natural river. It is common for the x-axis to possess equal spacing (Δx) between points. In this thesis the selected solution method allows the distance spacing to be varied. It is beneficial to allow the distance spacing to vary as the

model is not constrained to use cross sections at regular intervals, but to select points more representative of the river morphology or points of greater interest or flow variation. The cross sections are separated by a distance Δx_i between the adjacent sections x_i and x_{i+1}, thus it can be written that $\Delta x_i = x_{i+1} - x_i$. The set of points describing the x-axis is defined as $W_x = \{ i \Delta x , i = 1, 2, \ldots, I \}$.

4.5.2 Time Axis.

The time axis begins at t = 0 and ends at time $t = J\Delta t$, there are J+1 points and J time steps each of a period Δt. The adopted scheme will permit uneven time steps. Time spacing reductions may be of use when a model approaches a less stable stage, for instance towards low tide levels where small depth problems may occur. When steady flow conditions prevail a larger time spacing will reduce computer time. However, as a tide in an estuary does not occur simultaneously, it is unlikely at any one time that there will be any part of the estuary in which rapidly varying flow is not occurring. As rapidly varying conditions require closer time steps it was found that an even and short time spacing was the most convenient. The set of points discretized in time can be written as $W_t = \{ t_j = j \Delta t ; j = 0 , 1, \ldots, J \}$.

4.5.3 Grid Boundaries.

The boundaries of the computational grid are the seaward and landward ends of the river system or the distance sections x_1 and x_I. It is assumed that at least one flow property at these boundaries is known throughout the period to be modelled, or at least can be extrapolated from sporadic stages during the simulation. These boundaries can be found from tidal curves, rating curves or flood hydrographs and will be values of flow (Q) or height (Z) in most cases. A model designer may be constrained by the quality and type of data available at the boundaries and might be unable to consider certain finite difference schemes because of this.

4.5.4 Initial Conditions.

The initial conditions represent the state of flow at the onset of the simulation at time = 0. These take the form of either the flow or height at each cross-section when the modelling begins.

The computational grid comprises a set of points, $W = W_x \times W_t$. At all points within the grid with exception of the initial and boundary values, either flow, height or both will need to be calculated.

4.6 The Priessman Finite Difference Method.

There are a variety of finite difference schemes in which the difference functions are discretized in subtly differing manners. The method involved in this thesis is based on Priessman's four point system (1961) and is similar in form to that of Wallis *et al* (1989), which was used as part of a simulation of the Tay Estuary. The four point system solves the De St. Venant equations by discretising the flow equations with respect to two consecutive points in the channel at the present and next time level, which are the points A, B, C and D in Figure 4.3.

The discrete approximations of the differential terms in the Priessman scheme are based around the four points ABCD (fig. 4.3). The equations are solved by taking a point within the four other points. The $\frac{\partial f}{\partial x}$ term is a central difference which makes an approximation mid-way between two points x_i and x_{i+1}. The time derivative $\frac{\partial f}{\partial t}$ is weighted using the time difference operator $(\phi)\Delta t$, where $0.5 < \phi \leq 1$. The functions and derivatives can be expanded to give finite differences which describe the relationships of the four points in the Preissman scheme.

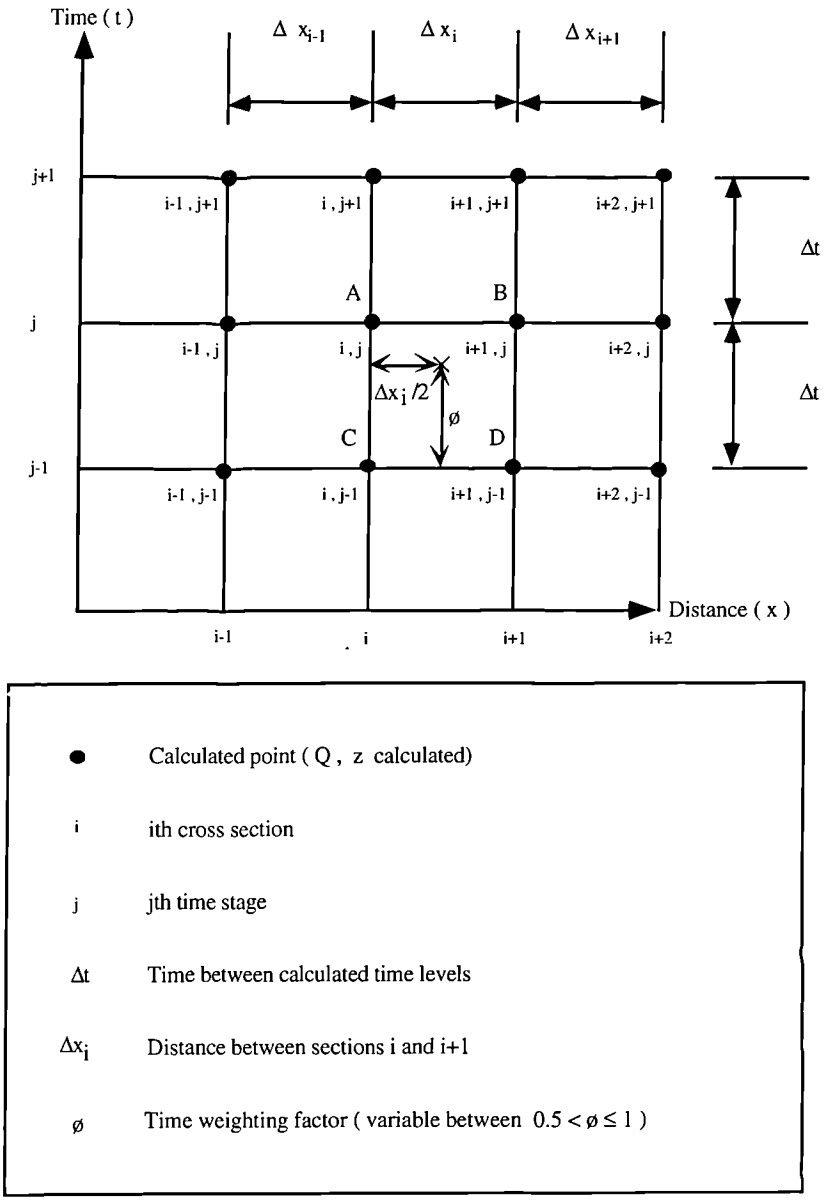

Fig 4.3 The computational grid for the Preissman discretisation.

4.6.1 Finite Difference Expansions of Functions.

The following finite difference operators are used to approximate to the time and distance gradients of a given function (f).

i) Temporal gradient;

$$\frac{\partial f}{\partial t} \approx \frac{1}{2\Delta t}\left(f_{i+1}^{j+1} + f_{i}^{j+1}\right) - \frac{1}{2\Delta t}\left(f_{i+1}^{j} + f_{i}^{j}\right) = \left[\frac{\partial f}{\partial t}\right]_h \qquad (4.5)$$

ii) Spatial gradient;

$$\frac{\partial f}{\partial x} \approx \frac{\phi}{\Delta x_i}\left(f_{i+1}^{j+1} - f_i^{j+1}\right) + \frac{1-\phi}{\Delta x_i}\left(f_{i+1}^{j} - f_i^{j}\right) = \left[\frac{\partial f}{\partial x}\right]_h \qquad (4.6)$$

iii) The function 'f' is similarly expanded to replace the coefficients in the differential equations;

$$f \approx \frac{\phi}{2}\left(f_{i+1}^{j+1} + f_i^{j+1}\right) + \frac{1-\phi}{2}\left(f_{i+1}^{j} + f_i^{j}\right) = [\, f \,]_h \qquad (4.7)$$

Where the grid function f_i^j is the value of the function $f(x,t)$ at point x_i and t_j

Δx_i is the ith distance step

Δt the time step

ϕ is the time weighting coefficient

The term on the right of the statements in square brackets is the shortened form for the discretized operator.

The superscript j denotes that the value of f is for the time j

The superscript j+1 denotes the following step (time $t+\Delta t$)

The supscript i denotes the value of the function is for the ith distance step

One advantage of the Preissman method is that it allows for the computation of both flow quantities and tidal elevation at the same point in the finite difference grid, rather than a staggered system where flow and height are calculated at alternating points, which is common in many of the other finite difference models. At the boundary positions, if flow is given then it is only necessary to compute the elevation or*Vice Versa.*

4.7 Convergence, Approximation Errors and Stability.

When validating a modelling system it is necessary to ascertain that the approximations involved are satisfactory and consistent with the analytical solution. The order of approximation is a theoretical method of demonstrating the accuracy of a discretised system and

a useful method of comparing differing schemes, although it does not necessarily demonstrate that the system is accurate. A modelling scheme must be tested for convergence (Cunge *et al.* 1980) which determines whether the approximated scheme approaches an exact solution of the original continuous function.

4.7.1 Approximation Errors.

By calculus the definition of a continuous function in time and space, $f(x, t)$ is;

$$\frac{\partial f}{\partial x} = \lim_{\Delta x \to 0} \frac{f(x + \Delta x,t) - f(x,t)}{\Delta t} \quad . \qquad (4.8)$$

In finite difference methods Δx is never infinitely small and has the length Δx_i as described earlier. The functions $\frac{\partial f}{\partial x}$ and $\frac{\partial f}{\partial t}$ must be replaced by a discrete space and time derivatives, which can be represented in various forms.

The use of finite difference replacement for differential expressions is subject to a truncation error of a given order. The order of solution helps to compare the theoretical accuracy of different discretizing schemes.

A function of time and space $f(x,t)$ can be represented by a Taylor series expansion;

$$f(x,y) = f(a,b) + \left[(x-a)\frac{\partial}{\partial x} + (y-b)\frac{\partial}{\partial y} \right] f + \frac{1}{2!}\left[(x-a)\frac{\partial}{\partial x} + (y-b)\frac{\partial}{\partial y} \right]^2 + \ldots\ldots\ldots + \frac{1}{(n-1)!}\left[(x-a)\frac{\partial}{\partial x} + (y-b)\frac{\partial}{\partial y} \right]^{n-1} f + R_n(x,y) \qquad (4.9)$$

Where $f(x,y)$ represents the function at point (x,y) and $f(a,b)$ is the value of the function at a nearby point (a,b). R_n represents the remaining approximation error.

A finite difference system can be expanded using a Taylor series. The Preissman method considers a series of points (A, B, C, D) and the time-weighted, central difference point E (Figure.4.4).

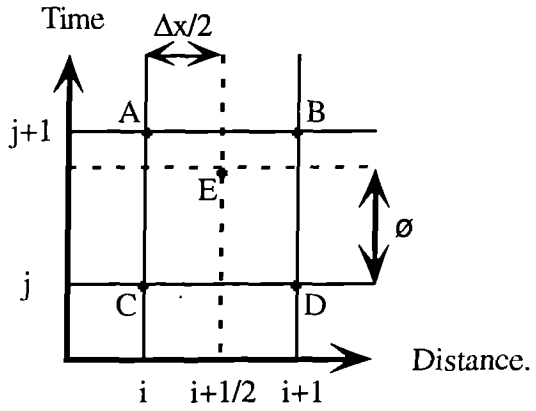

Fig 4.4 Four point family for Preissman schemes.

The Taylor series expansions of the functions approximated near to the point E, the grid co-ordinates for which are (i+1/2 , j+ø) are shown in the family of Equations 4.10.

$$f(i,j) = f(i+\tfrac{1}{2}, j+\phi) - \left[\frac{\Delta x}{2}\frac{\partial f}{\partial x} + \phi\Delta t \frac{\partial f}{\partial t} \right]$$
$$+ \frac{1}{2!}\left[\frac{\Delta x^2}{4}\frac{\partial^2 f}{\partial x^2} + \phi^2\Delta t^2 \frac{\partial^2 f}{\partial t^2} + \Delta x\, \phi\, \Delta t \frac{\partial f}{\partial x}\frac{\partial f}{\partial t} \right]$$
$$- \frac{1}{3!}\left[\frac{\Delta x^3}{8}\frac{\partial^3 f}{\partial x^3} + \phi^3\Delta t^3 \frac{\partial^3 f}{\partial t^3} + \frac{3\Delta x^2\, \phi\Delta t}{4}\frac{\partial^2 f}{\partial x^2}\frac{\partial f}{\partial t} + \frac{3\,\Delta x\, \phi^2\Delta t^2}{2}\frac{\partial^2 f}{\partial t^2}\frac{\partial f}{\partial x} \right]$$
$$+ R_n(i,j)$$

$$f(i+1,j) = f(i+\tfrac{1}{2}, j+\phi) + \left[\frac{\Delta x}{2}\frac{\partial f}{\partial x} - \phi\Delta t \frac{\partial f}{\partial t} \right]$$
$$+ \frac{1}{2!}\left[\frac{\Delta x^2}{4}\frac{\partial^2 f}{\partial x^2} + \phi^2\Delta t^2 \frac{\partial^2 f}{\partial t^2} - \Delta x\, \phi\Delta t \frac{\partial f}{\partial x}\frac{\partial f}{\partial t} \right]$$
$$+ \frac{1}{3!}\left[\frac{\Delta x^3}{8}\frac{\partial^3 f}{\partial x^3} - \phi^3\Delta t^3 \frac{\partial^3 f}{\partial t^3} - \frac{3\Delta x^2\, \phi\Delta t}{4}\frac{\partial^2 f}{\partial x^2}\frac{\partial f}{\partial t} + \frac{3\,\Delta x\, \phi^2\Delta t^2}{2}\frac{\partial^2 f}{\partial t^2}\frac{\partial f}{\partial x} \right]$$
$$+ R_n(i+1,j)$$

$$f(i,j+1) = f(i+\tfrac{1}{2}, j+\phi) + \left[-\frac{\Delta x}{2}\frac{\partial f}{\partial x} + (1-\phi)\Delta t \frac{\partial f}{\partial t} \right]$$
$$+ \frac{1}{2!}\left[\frac{\Delta x^2}{4}\frac{\partial^2 f}{\partial x^2} + (1-\phi)^2\Delta t^2 \frac{\partial^2 f}{\partial t^2} - \Delta x\,(1-\phi)\,\Delta t \frac{\partial f}{\partial x}\frac{\partial f}{\partial t} \right]$$
$$+ \frac{1}{3!}\left[-\frac{\Delta x^3}{8}\frac{\partial^3 f}{\partial x^3} + (1-\phi)^3\Delta t^3\frac{\partial^3 f}{\partial t^3} \right.$$
$$\left. + \frac{3\Delta x^2(1-\phi)\Delta t}{4}\frac{\partial^2 f}{\partial x^2}\frac{\partial f}{\partial t} - \frac{3\,\Delta x\,(1-\phi)^2\Delta t^2}{2}\frac{\partial^2 f}{\partial t^2}\frac{\partial f}{\partial x} \right]$$
$$+ R_n(i,j+1)$$

$$f(i+1,j+1) = f(i+\tfrac{1}{2}, j+\phi) + \left[\frac{\Delta x}{2}\frac{\partial f}{\partial x} + (1-\phi)\Delta t \frac{\partial f}{\partial t} \right]$$
$$+ \frac{1}{2!}\left[\frac{\Delta x^2}{4}\frac{\partial^2 f}{\partial x^2} + (1-\phi)^2\Delta t^2 \frac{\partial^2 f}{\partial t^2} + \Delta x\,(1-\phi)\,\Delta t \frac{\partial f}{\partial x}\frac{\partial f}{\partial t} \right]$$
$$+ \frac{1}{3!}\left[\frac{\Delta x^3}{8}\frac{\partial^3 f}{\partial x^3} + (1-\phi)^3\Delta t^3\frac{\partial^3 f}{\partial t^3} \right.$$
$$\left. + \frac{3\Delta x^2(1-\phi)\Delta t}{4}\frac{\partial^2 f}{\partial x^2}\frac{\partial f}{\partial t} + \frac{3\,\Delta x\,(1-\phi)^2\Delta t^2}{2}\frac{\partial^2 f}{\partial t^2}\frac{\partial f}{\partial x} \right]$$
$$+ R_n(i+1,j+1) \qquad \textbf{(4.10)}$$

These expansions can be substituted into the discrete form of the time derivative (Equation 4.5) giving the relationship shown in Equation 4.11.

$$\frac{\partial f}{\partial t} \approx \left[\frac{\partial f}{\partial t}\right]_h = \frac{\partial f}{\partial t} + (1-2\phi)\Delta t\frac{\partial^2 f}{\partial t^2} + (1 - 3\phi + 3\phi^2)\,\Delta t^2\frac{\partial^3 f}{\partial t^3} + O(\Delta t^3) \qquad \textbf{(4.11)}$$

Where $O(\Delta t^3)$ groups all the higher order terms and $\left[\frac{\partial f}{\partial t}\right]_h$ symbolically represents the discretised form of approximation to the derivative. Thus the left hand term in Equation 4.11 (the derivative) is approximately equal to the central term (the difference operator), which is equal to the right hand term (which is the discretized form after a Taylor series expansion is substituted). The value of $\left[\frac{\partial f}{\partial t}\right]_h$ is not equal exactly to $\frac{\partial f}{\partial t}$ but subject to an error equal to the terms multiplied by Δt and higher orders of Δt which are ignored by the finite difference scheme and are termed the truncation error. The difference operator in this case is said to be of the 'first order' because the first ignored term is a derivative multiplied by Δt to a single power.

There is however a special case when $\phi = 0.5$, when the first order term will disappear, leaving the solution a second order one.

Similarly the discrete form of the distance derivative (Equation 4.6) can be represented by Equation 4.12.

$$\frac{\partial f}{\partial x} \approx \left[\frac{\partial f}{\partial x} \right]_h = \frac{\partial f}{\partial x} + \phi (1-\phi) \frac{\Delta t^2}{2} \frac{\partial^2 f}{\partial t^2} \frac{\partial f}{\partial x} + \frac{\Delta x^2}{3!\,4} \frac{\partial^3 f}{\partial x^3} + O(\Delta t^3, \Delta x^3)$$

(4.12)

This solution is second order, regardless of the value of ϕ, because the point E is exactly mid way between the two x-axis points.

The schemetisation of the function f (Equation 4.7) is shown by Equation 4.13, which is also of a second order of approximation.

$$f(x, t) \approx [\, f]_h = f(i+\tfrac{1}{2}, j+\phi) + \tfrac{1}{8} \Delta x^2 \frac{\partial^2 f}{\partial x^2} + \tfrac{1}{2} \Delta t^2 \phi (1-\phi) \frac{\partial^2 f}{\partial t^2} + O(\Delta t^3, \Delta x^3)$$

(4.13)

For the entire finite difference scheme to be second order both the temporal and spatial discretisations need to be second order (i.e. $\phi = 0.5$).

The error of approximation is considered to be small, as are Δt and Δx so that they will become negligible when raised to higher powers. Halving the distance or time spacing reduces the error of approximation by two for a first order scheme and by four for a second order scheme, thus a higher order approximation will converge quicker to a solution. However, since Δx and Δt are not infinitely small, especially on a coarse grid, or where the function f(x,t) varies rapidly, the error evolved may be sufficient to render a second order scheme no more accurate than a first order one (Cunge 1980). Reducing the time weighting factor to 0.5 can produce instabilities in the calculations.

4.7.2 Convergence.

The essence of a finite difference scheme is that it must approach the exact solution of the original flow equations. When there is no way of ascertaining the analytical solution of the flow equations it is hard to compare the model's results with those of reality. Richtmyer

(1957) and Godunov and Ryabenki (1964) presented methods of determining the accuracy and convergence of some finite difference schemes. A convergent system should approach the analytical solution with little or no error as the time and space increments approach zero.

Consider the differential form of the Continuity Equation (Eq.3.39);

$$B\frac{\partial Z}{\partial t} + \frac{\partial Q}{\partial x} = 0$$

Let G represent this equation and G_d represent the discretised form, at point E as indicated in Figure 4.3, where x=i+1/2, t=j+ø and leaving 'B', the breadth, unexpanded to aid clarity; the resultant discrete form gives Equation 4.14.

$$G_d = B\left[\frac{\partial Z_{i+1/2}^{j+\phi}}{\partial t} + O(\Delta t)\right] + \left[\frac{\partial Q_{i+1/2}^{j+\phi}}{\partial x} + O(\Delta t^2, \Delta x_i^2)\right] \qquad (4.14)$$

For the solution to converge, as Δx and Δt reduce then $(G_d - G)$ must approach zero as depicted in Equation 4.15.

$$G_d - G = B\left[\frac{\partial Z_{i+1/2}^{j+\phi}}{\partial t} - \frac{\partial Z}{\partial t}\right] + \left[\frac{\partial Q_{i+1/2}^{j+\phi}}{\partial x} - \frac{\partial Q}{\partial x}\right] + O(\Delta t, \Delta x_i^2)$$

$$= O(\Delta t, \Delta x_i^2) \quad (\text{for } \phi \neq 0.5) \qquad (4.15)$$

As Δt and Δx become closer to zero, the O truncation error approaches zero, as does the $G_i - G$ term. It can now be said that the finite difference approximation is *consistent* with

the original differential form, with an order of approximation of $O(\Delta t, \Delta x_i^2)$ for $\phi \neq 0.5$, or $O(\Delta t^2, \Delta x_i^2)$ for $\phi = 0.5$.

4.7.3 Stability Analysis

There are a variety of methods of stability analysis using differing assumptions and degrees of mathematical intricacies, however, the majority of all authors reach a similar conclusion in the analysis of the four point implicit scheme. It is therefore thought unnecessary to repeat the method. Attention is thus drawn to Cunge *et al.* 1980 for a simple method of stability analysis.

The implicit finite difference schemes are unconditionally stable for $\phi \geq 0.5$ (Cunge, 1966; Vreugdenhil, 1973; Liggett and Cunge, 1975), although some authors quote a value of $\phi > 0.5$. The reason for this slight contradiction is that one method is analysing the solution with a theoretical viewpoint and the other (giving the value of $\phi > 0.5$) has allowed the results of model simulations to affect their evaluation of the ϕ. It is reasonable to say that the system is unconditionally stable for values of ϕ equal to 0.5 and above, although in practice, mathematical instabilities bound the value of ϕ to be greater than 0.5. It is also possible that a system analysed for stability by a linear method (Cunge *et al.*, 1980) may well converge at inexact values compared to real non-linear systems. It may also be proved that for a value of $\phi = 1$ that the system behaves like an explicit one and would be bounded by the Courant condition of computational stability which is described in Chapter 5.

4.8 Finite Difference Expansion of Flow Equations.

The discretisation of the basic De St Venant equations varies according to authors and the modelling scheme adopted. The discretisation of coefficients must be chosen carefully as it affects the properties of the finite difference scheme (Cunge *et al.* 1980). In the same work, shortfalls of the technique are highlighted with the problems of the time weighting coefficient

(ø) and more importantly the choice of discretisation of a given term. The examples in this work show that the mathematical expansions of a given term must be checked with as many relevant hydraulic laws as possible to be certain that term is correct.

The basis of the finite difference scheme are the two De St Venant type equations which are expanded using the Preissman formulation in Section 4.4.

4.8.1 Discretisation.

Let us consider the form of the De St. Venant equations introduced in the third chapter (Equations 3.39 and 3.40), although the friction slope is represented below in a form compatible with the friction and conveyance laws described in Chapter 5, so the equations in this chapter may be expanded correctly.

- Continuity:

$$B\frac{\partial Z}{\partial t} + \frac{\partial Q}{\partial x} = L$$

- Dynamic:

$$\frac{\partial Q}{\partial t} + \frac{\partial}{\partial x}\left(\frac{Q^2}{A}\right) + g A \frac{\partial Z}{\partial x} + \frac{g A Q|Q|}{K^2} + L\left(\frac{Q}{A} - U\right) = 0$$

The adopted discretisations of the derivatives and functions in the continuity and dynamic equations are listed below in the set of Equations 4.16.

$$B\frac{\partial Z}{\partial t} \approx \left[\frac{\phi}{2}\left(B_{i+1}^{j+1} + B_i^{j+1}\right) + \frac{1-\phi}{2}\left(B_{i+1}^{j} + B_i^{j}\right)\right] \times \left[\frac{1}{2\Delta t}\left(Z_{i+1}^{j+1} + Z_i^{j+1}\right) - \frac{1}{2\Delta t}\left(Z_{i+1}^{j} + Z_i^{j}\right)\right]$$

$$\frac{\partial Q}{\partial x} \approx \frac{\phi}{\Delta x}\left(Q_{i+1}^{j+1} - Q_i^{j+1}\right) + \frac{1-\phi}{\Delta x}\left(Q_{i+1}^{j} - Q_i^{j}\right)$$

$$L \approx \frac{\phi}{2}\left(L_{i+1}^{j+1}+L_i^{j+1}\right)+\frac{1-\phi}{2}\left(L_{i+1}^{j}+L_i^{j}\right)$$

$$\frac{\partial Q}{\partial t} \approx \frac{1}{2\Delta t}\left(Q_{i+1}^{j+1}+Q_i^{j+1}\right)-\frac{1}{2\Delta t}\left(Q_{i+1}^{j}+Q_i^{j}\right)$$

$$\frac{\partial}{\partial x}\left(\frac{Q^2}{A}\right) \approx \frac{\phi}{\Delta x}\left[\left(\frac{Q^2}{A}\right)_{i+1}^{j+1}-\left(\frac{Q^2}{A}\right)_i^{j+1}\right]+\frac{1-\phi}{\Delta x}\left[\left(\frac{Q^2}{A}\right)_{i+1}^{j}-\left(\frac{Q^2}{A}\right)_i^{j}\right]$$

$$gA \approx g\left[\frac{\phi}{2}\left(A_{i+1}^{j+1}+A_i^{j+1}\right)+\frac{1-\phi}{2}\left(A_{i+1}^{j}+A_i^{j}\right)\right]$$

$$\frac{\partial Z}{\partial x} \approx \frac{\phi}{\Delta x}\left(Z_{i+1}^{j+1}-Z_i^{j+1}\right)+\frac{1-\phi}{\Delta x}\left(Z_{i+1}^{j}-Z_i^{j}\right)$$

$$\frac{Q|Q|}{K^2} \approx$$

$$\frac{\left[\frac{\phi}{2}\left(Q_{i+1}^{j+1}|Q|_{i+1}^{j+1}+Q_i^{j+1}|Q|_i^{j+1}\right)+\frac{1-\phi}{2}\left(Q_{i+1}^{j}|Q|_{i+1}^{j}+Q_i^{j}|Q|_i^{j}\right)\right]}{\left[\frac{\phi}{2}\left(K^2{}_{i+1}^{j+1}+K^2{}_i^{j+1}\right)+\frac{1-\phi}{2}\left(K^2{}_{i+1}^{j}+K^2{}_i^{j}\right)\right]}$$

$$L\left(\frac{Q}{A}\right) \approx \left[\frac{\phi}{2}\left(L_{i+1}^{j+1}+L_i^{j+1}\right)+\frac{1-\phi}{2}\left(L_{i+1}^{j}+L_i^{j}\right)\right] \times \left[\frac{\phi}{2}\left(\left(\frac{Q}{A}\right)_{i+1}^{j+1}+\left(\frac{Q}{A}\right)_i^{j+1}\right)+\frac{1-\phi}{2}\left(\left(\frac{Q}{A}\right)_{i+1}^{j}+\left(\frac{Q}{A}\right)_i^{j}\right)\right]$$

$$LU \approx \left[\frac{\phi}{2}\left(L_{i+1}^{j+1}+L_i^{j+1}\right)+\frac{1-\phi}{2}\left(L_{i+1}^{j}+L_i^{j}\right)\right] \times \left[\frac{\phi}{2}\left(U_{i+1}^{j+1}+U_i^{j+1}\right)+\frac{1-\phi}{2}\left(U_{i+1}^{j}+U_i^{j}\right)\right]$$

(4.16)

4.8.2 Linearisation of equations.

The derivatives presented can be rearranged in terms of the future values with respect to time (i.e. to the i+1 time level). It is at this stage that the model presented here deviates from the 'pure' Preissman type models by solving for the Z_{i+1}^{j+1}, Z_i^{j+1}, Q_{i+1}^{j+1} and Q_i^{j+1}

the 'pure' Preissman type models by solving for the Z_{i+1}^{j+1}, Z_i^{j+1}, Q_{i+1}^{j+1} and Q_i^{j+1} values rather than ΔZ_{i+1}, ΔZ_i, ΔQ_{i+1} and ΔQ_i values, where $\Delta Z_i = Z_i^{j+1} - Z_i^j$ etc.

For clarity the future (j+1) value of any variable will now be represented with an asterix (*) superscript, whilst the present (j) value will have no superscript. This is to avoid confusion with similar figures in the text. Thus Q_i represents the quantity of flow at position i and the present (j) time step and Q_i^* the value of flow at the same section, but at the next (j+1) time step.

The continuity equation is rearranged to the form of Equation 4.17.

$$Q^*_{i+1} - Q^*_i + \frac{c2_i\ c5_i}{4}\left(Z^*_{i+1} + Z^*_i\right) = c6_i + c3\left(Q_i - Q_{i+1}\right) + \frac{c2_i\ c5_i}{4}\left(Z_{i+1} + Z_i\right) \qquad (\mathbf{4.17})$$

The dynamic equation is rearranged to the form of Equation 4.18.

$$Z^*_{i+1} - Z^*_i + Q^*_{i+1}\left[\frac{c2_i}{c1_i} + \frac{2\,Q^*_{i+1}}{c1_i\,A^*_{i+1}} + \frac{|Q|^*_{i+1}}{c4} + \frac{\phi\,c6_i}{c1_i\,A^*_{i+1}}\right] + Q^*_i\left[\frac{c2_i}{c1_i} - \frac{2\,Q^*_i}{c1_i\,A^*_i} + \frac{|Q|^*_i}{c4_i} + \frac{\phi\,c6_i}{c1_i\,A^*_i}\right]$$

$$= c3\left(Z_i - Z_{i+1}\right) + \frac{c2_i}{c_i 1}\left(Q_{i+1} + Q_i\right) - \frac{c3}{c4_i}\left(Q_{i+1}|Q|_{i+1} + Q_i|Q|_i\right) + \frac{2\,c6_i\,c7_i}{c1_i} - 2\frac{c3}{c1_i}\left[\frac{Q^2_{i+1}}{A_{i+1}} - \frac{Q^2_i}{A_i}\right] - \frac{\phi\,c6_i\,c3}{c1_i}\left[\frac{Q_{i+1}}{A_{i+1}} + \frac{Q_i}{A_i}\right] \qquad (\mathbf{4.18})$$

The coefficients c1-c7 have been used to simplify the form of the equations, the actual values of which are shown in the family of Equations 4.19.

$$c1_i = g \left[\phi \left(A^{*}_{i+1} + A^{*}_{i} \right) + \left(1 - \phi \right) \left(A_{i+1} + A_i \right) \right]$$

$$c2_i = \frac{\Delta x_i}{\phi \, \Delta t}$$

$$c3 = \frac{1 - \phi}{\phi}$$

$$c4_i = \frac{\left[\phi \left(K^{2\,*}_{i+1} + K^{2\,*}_{i} \right) + \left(1 - \phi \right) \left(K^{2}_{i+1} + K^{2}_{i} \right) \right]}{\Delta x_i}$$

$$c5_i = \phi \left(B^{*}_{i+1} + B^{*}_{i} \right) + \left(1 - \phi \right) \left(B_{i+1} + B_i \right)$$

$$c6_i = \frac{\Delta x_i}{\phi} \left[\frac{\phi}{2} \left(L^{*}_{i+1} + L^{*}_{i} \right) + \frac{1 - \phi}{2} \left(L_{i+1} + L_i \right) \right]$$

$$c7_i = \frac{\phi}{2} \left(U^{*}_{i+1} + U^{*}_{i} \right) + \frac{1 - \phi}{2} \left(U_{i+1} + U_i \right)$$

(4.19)

The coefficients defined in Equations 4.19 have been introduced to aid clarity, although in the computer model they also prevent repetition of calculation (thus time saving during programme execution) and typing.

When the equations are to be solved it must be noted that the value of any variable with the asterix superscript will be the value which the computer programme has calculated to that point in the iterations and not necessarily the final converged value.

The rearranged equations are now represented by the following two linear equations similar in form to Dronker's third implicit scheme (1969) and are shown in Equations 4.20 and 4.21.

- Continuity

$$Q^*_{i+1} - Q^*_i + \delta_i Z^*_{i+1} + \delta_i Z^*_i = \varepsilon_i \qquad (4.20)$$

- Dynamic

$$\alpha_i Q^*_{i+1} + \beta_i Q^*_i + Z^*_{i+1} - Z^*_i = \gamma_i \qquad (4.21)$$

These two equations can be represented in a matrix form (Figure 4.5), where the odd rows represent the solution of the continuity equation and the even ones the dynamic equation.

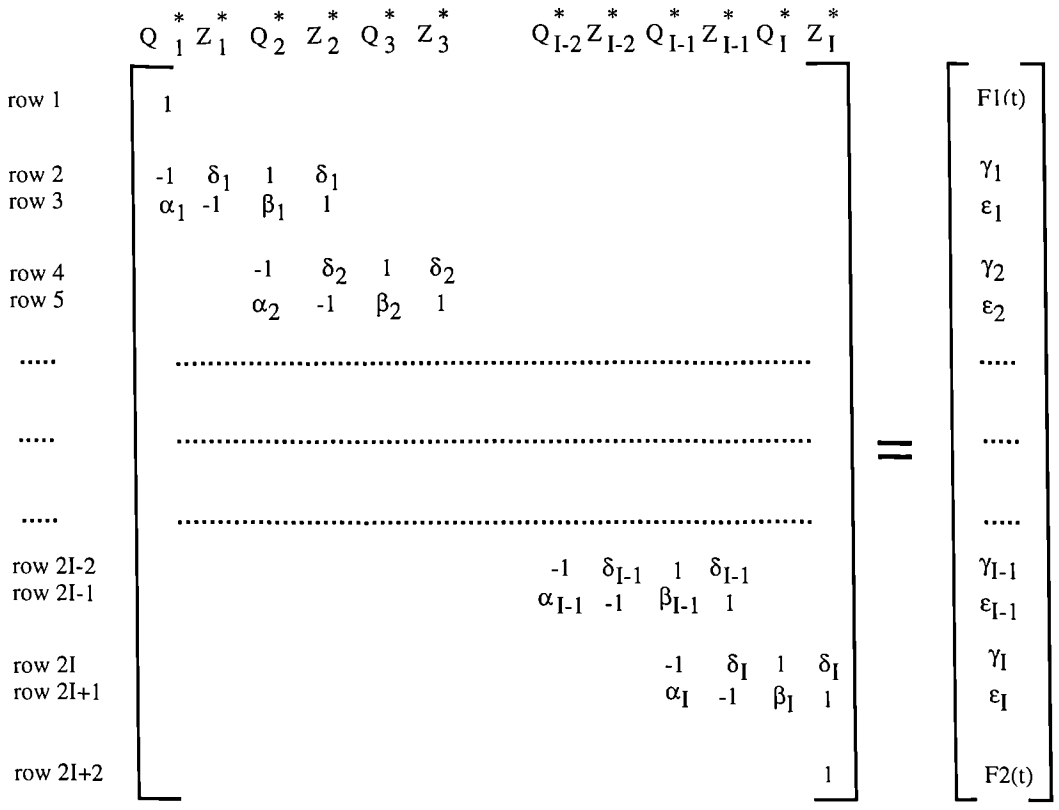

Fig 4.5. Matrix representation of rearranged dynamic and continuity equations.

The first and last rows in Figure 4.5 are the boundary conditions at the ends of the channel reach. In this case F1(t) is the value of Q^*_1, which means that the first channel section (i = 1) will be the upstream (river flow) end. The model originally used the tidal downstream

section as i = 1, in accordance with Dronkers (1969) who states that this the normal case and so has been adopted by many other works as the acceptable standard, however, when branches were added to the model it was found preferable to use the upstream limit(s) as i = 1 and to redesign the solution algorithm.

In the solution of the two equations 4.20 and 4.21 there are 2I+2 equations to be solved (the number of rows in the matrix of figure 4.5), with the first and 2I+2 values only being known (the boundary conditions).

4.8.3 Recurrence Relationships.

To solve these equations it is necessary to set up a pair of recurrence formulae which may be solved by the double sweep method of solution which is a commonly used numerical method of solution of these types of finite difference equations. It is assumed that at the downstream end of the channel (where i = 1) that the quantity of flow is always known from an hydrograph or similar. Thus it can be defined that $Q_1^* = F1(t)$. The boundary conditions at this point are linearised so that Q_1^* is a function independent of the water surface elevation (Equation 4.22).

$$Q_1^* = F1(t) = r_1 - (p_1 Z_1^*) \qquad (4.22)$$

Using boundary conditions of $p_1 = 0$ and $r_1 = Q_1^*$, the boundary value of Q becomes independent of Z for this point. The significance of the variables p and r will become clear when they are used in further substitutions.

By taking the second and third rows from the matrix in Fig. 4.5 two linearised equations of flow in terms of Z_1^*, Z_2^*, Q_1^* and Q_2^* can be derived (Equations 4.23 and 4.24)

$$Q_2^* - Q_1^* + \delta_1 Z_2^* + \delta_1 Z_1^* = \varepsilon_1 \qquad (4.23)$$

$$\alpha_1 Q_2^* + \beta_1 Q_1^* + Z_2^* - Z_1^* = \gamma_1 \qquad (4.24)$$

After substituting Q_1^* into Equation 4.24 using Equation 4.23, Equations 4.25 can be derived once rearranged.

$$Z_1^* = \frac{\varepsilon_1 + r_1}{p_1 + \delta_1} - \frac{\delta_1}{p_1 + \delta_1} Z_2^* - \frac{1}{p_1 + \delta_1} Q_2^*$$

or $$Z_1^* = s_1 - q_1 Z_2^* - t_1 Q_2^* \qquad \textbf{(4.25)}$$

The second form of 4.25 is substituted into Equations 4.22 and 4.24 to give the second recurrence relation shown by Equation 4.26a.

$$Q_2^* = \frac{\gamma_1 - \beta_1 r_1 + s_1 (p_1 \beta_1 + 1)}{\gamma_1 + t_1 (p_1 \beta_1 + 1)} - \frac{1 + q_1 (p_1 \beta_1 + 1)}{\gamma_1 + t_1 (p_1 \beta_1 + 1)} Z_2^* \qquad \textbf{(4.26a)}$$

Which by comparison to Equation 4.22 is equivalent to Equation 4.26b.

$$Q_2^* = r_2 - p_2 Z_2^* \qquad \textbf{(4.26b)}$$

The two recurrence relations can be similarly proved for all other values of i, giving the two relations (Equations 4.27 and 4.28) using the substitution of the coefficients, p, q, r, s and t, furnishing an upper tri-diagonal matrix (fig 4.6), where the main coefficients lie along the main diagonal band.

$$Z_i^* = s_i - q_i Z_{i+1}^* - t_i Q_{i+1}^* \qquad \textbf{(4.27)}$$

$$Q_{i+1}^* = r_{i+1} - p_{i+1} Z_{i+1}^* \qquad \textbf{(4.28)}$$

The matrix represented in Figure 4.6 shows that there are 2I+2 equations to be solved for each time level, although the two boundary conditions are known (F1(t) and F2(t)) leaving 2I unknown equations to be solved. The recurrence relations are solved by the double sweep method of solution, solving for all sections in the modelled system before proceeding to the next time level.

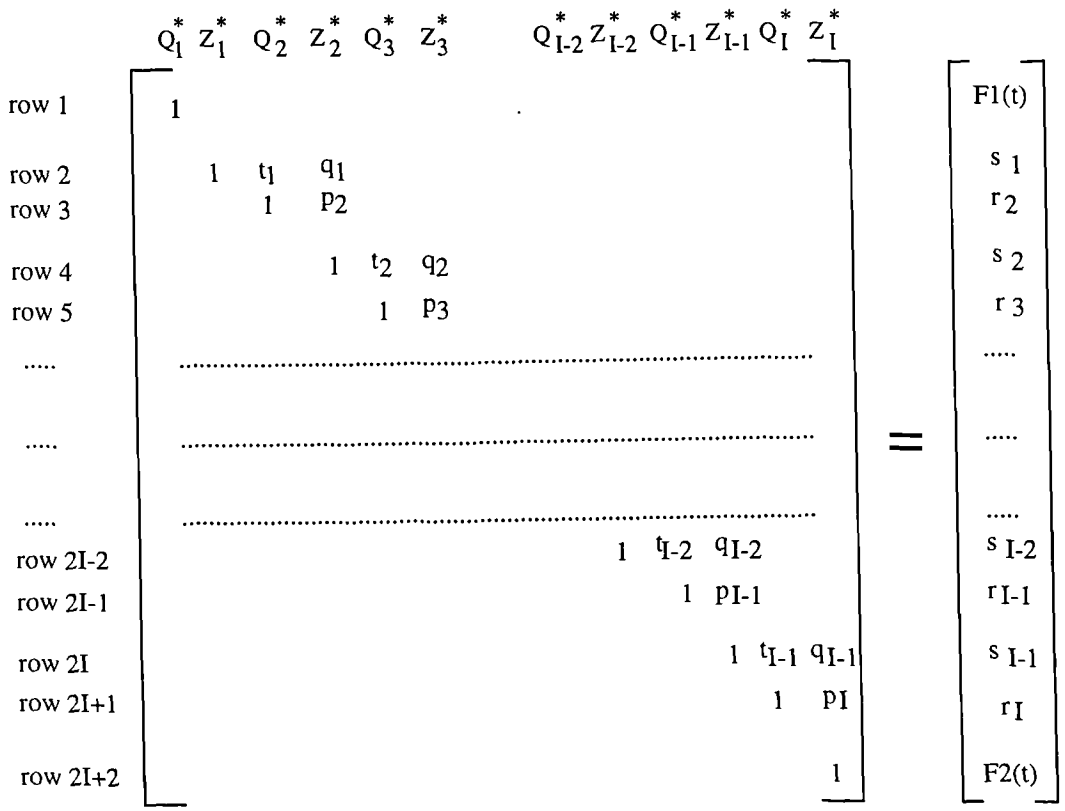

Fig 4.6. Tri-diagonal matrix form of recurrence relationships.

4.9 The Double Sweep Method of Solution.

The double sweep method involves the solution of a sparse tri-diagonal matrix (Fig. 4.5), for a one dimensional river system. When a branched system is introduced the method differs slightly and will be described in Section 4.10. As is common with most finite difference schemes (excepting six-point schemes which have been used by some workers), a

single computational point is only linked to the two points either side of it in the channel, hence the sparseness of the matrix in Fig. 4.5.

4.9.1 First Sweep.

The first sweep of the solution begins at one boundary end of the system, nominally termed section i = 1, the upstream boundary in this case. The values of p_1 and q_1 are calculated directly from the know flown at that point, with values of $p_1 = 0$ and $r_1 = Q_1^*$. The values of s_1, t_1 and q_1 are then calculated. The first sweep proceeds from section to section downstream, calculating the values of s_i, t_i, q_i, p_{i+1} and r_{i+1} at each point until the opposite boundary is reached.

4.9.2 Second Sweep.

Once the first sweep is complete, the method returns from the downstream boundary end. Q_I^* is calculated from Equation 4.28 using the known boundary value of Z_I^* and p_I and r_I. The value of Z_{I-1}^* is then calculated from Equation 4.29. The sweep continues back moving from successive grid points in the reverse manner to the first sweep until the upstream boundary is met, where only Z_1^* is calculated from the already known value of Q_1^*. Once the second sweep is completed the system moves onto the next j+1th time level, assuming that the solution has converged. The double sweep solution is symmetrical so it is unimportant which end of a channel the method starts at as long as the flow is sub-critical (Abbot, 1979). In this model the flow is considered not to become supercritical apart from over weirs if present, where upon a computer programme sub-routine is used to account for flow that cannot be represented by De St Venant relationships.

4.10 Branched Solutions.

After the model was first developed it was found that it would be preferable to include river branches, specifically for the partition of the East and West Channels, just south of

Gloucester City as previously the scheme allowed modelling of only the West Channel which proved to not be accurate enough. As mentioned previously the programme needed to be re-written so that the upstream end would be the initial grid points. There are now two upstream boundaries, Westgate Bridge (East Channel) and Maisemore Weir (West Channel), for which hydrographs were needed for both. Due to the data available it was found unnecessary to continue the model further north where the two reaches meet above Gloucester at the Upper Parting and develop a looped system of solution which is computationally more complex than a branched system.

The branched solution varies only slightly from a simple single channel solution, but requires that a given order must be kept in the solution technique. Three compatibility relations used to define conservation of flow and energy are also required at the juncture of the tributaries.

The schematic branched river system (Fig 4.7) in this case has three tributaries labelled A, B and C. It is assumed that the flow (Q) is known at the upstream ends of A and B and the elevation (Z) is known at the downstream end of C so that these are the boundary points.

The first sweep begins at point 1 on branch A, assigning p_1 and r_1 as described previously to the known value of flow. The sweep continues to the end section (A,I) of branch A. The sweep then jumps at the first point of branch B and operates in the same manner calculating the recurrence coefficients.

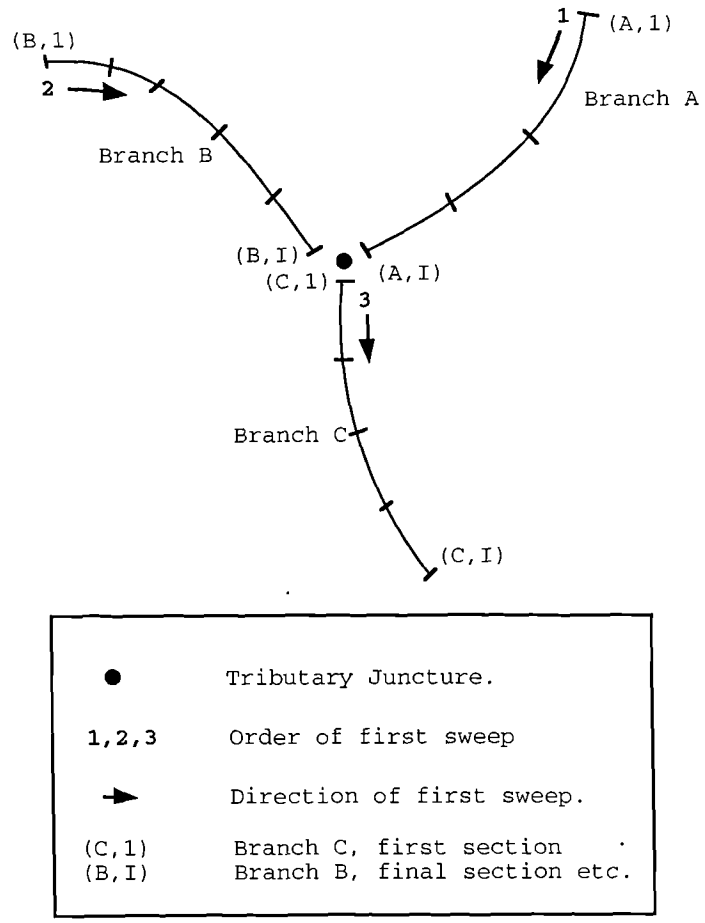

Fig 4.7 Branched river system.

In order to proceed down the third channel it is necessary to introduce a set of compatibility conditions (Equations 4.29a-c). Equation 4.29a in simple terms shows that the quantity of flow in the downstream channel is equal to the sum of the two branches entering it. The two other relations are derived from steady flow theory, simplifying the channel reach between the nearest upstream channel cross sections to the branch point. These equations are based upon the Bernoulli Equation and represent the head loss in the reach, which must be kept as small as possible as the equations are not rigorous simulations of flow, so their influence on the modelled solution must be kept as low as possible.

$$Q^{*}_{(C,1)} = Q^{*}_{(A,I)} + Q^{*}_{(B,I)} \qquad \textbf{(4.29a)}$$

$$Z^{*}_{(A,I)} + \frac{1}{2g}\left[\frac{Q^{*}_{(A,I)}}{A^{*}_{(A,I)}}\right]^2 = Z^{*}_{(C,1)} + \frac{1}{2g}\left[\frac{Q^{*}_{(C,1)}}{A^{*}_{(C,1)}}\right]^2 \qquad \textbf{(4.29b)}$$

$$Z^{*}_{(B,I)} + \frac{1}{2g}\left[\frac{Q^{*}_{(B,I)}}{A^{*}_{(B,I)}}\right]^2 = Z^{*}_{(C,1)} + \frac{1}{2g}\left[\frac{Q^{*}_{(C,1)}}{A^{*}_{(C,1)}}\right]^2 \qquad \textbf{(4.29c)}$$

Where (C, 1) represents the first grid point of branch C, (A, I) and (B, I) represent the last sections of branches A and B respectively. Introducing the coefficients, branchα, branchβ and branchγ into equations 4.29a and 4.29b gives the simpler form of Equations 4.30.

$$Z^{*}_{(A,I)} + \text{branch}\alpha\, Q^{*}_{(A,I)} = Z^{*}_{(C,1)} + \text{branch}\gamma\, Q^{*}_{(C,1)}$$

$$Z^{*}_{(B,I)} + \text{branch}\beta\, Q^{*}_{(B,I)} = Z^{*}_{(C,1)} + \text{branch}\gamma\, Q^{*}_{(C,1)} \qquad \textbf{(4.30)}$$

Where $\text{branch}\alpha = \frac{1}{2g}\frac{Q^{*}_{(A,I)}}{\left[A^{*}_{(A,I)}\right]^2}$ etc.

From the first sweep along the two branches A and B, the coefficients of p and r are known at the end sections of these two branches. Equation 4.28 is rearranged so that the values of $Z^{*}_{(A,I)}$ and $Z^{*}_{(B,I)}$ can be inserted Equations 4.31).

$$Z^{*}_{(A,I)} = \frac{r_{(A,I)} - Q^{*}_{(A,I)}}{p_{(A,I)}}$$

$$Z^{*}_{(B,I)} = \frac{r_{(B,I)} - Q^{*}_{(B,I)}}{p_{(B,I)}} \qquad \textbf{(4.31)}$$

Substitution of Equations 4.31 into Equations 4.30a-b derives Equations 4.32.

$$Q^{*}_{(A,I)}\left[\text{branch}\alpha - \frac{1}{p_{(A,I)}}\right] + \frac{r_{(A,I)}}{p_{(A,I)}} = Z^{*}_{(C,1)} + \text{branch}\gamma\, Q^{*}_{(C,1)}$$

$$Q^{*}_{(B,I)}\left[\text{branch}\beta - \frac{1}{p_{(B,I)}}\right] + \frac{r_{(B,I)}}{p_{(B,I)}} = Z^{*}_{(C,1)} + \text{branch}\gamma\, Q^{*}_{(C,1)}$$

(4.32)

From Equations 4.32 the values of $Q^{*}_{(A,I)}$ and $Q^{*}_{(B,I)}$ can be found which can then be substituted into the compatibility Equation 4.29a to give Equation 4.33.

$$Q^{*}_{(C,I)}\left[1 - \frac{\text{branch}\gamma}{\text{branch}\alpha - \dfrac{1}{p_{(A,I)}}} - \frac{\text{branch}\gamma}{\text{branch}\beta - \dfrac{1}{p_{(B,I)}}}\right]$$

$$= \left[\frac{1}{\text{branch}\alpha - \dfrac{1}{p_{(A,I)}}} + \frac{1}{\text{branch}\beta - \dfrac{1}{p_{(B,I)}}}\right] Z^{*}_{(C,I)}$$

$$- \left[\frac{\dfrac{r_{(A,I)}}{p_{(A,I)}}}{\text{branch}\alpha - \dfrac{1}{p_{(A,I)}}} + \frac{\dfrac{r_{(B,I)}}{p_{(B,I)}}}{\text{branch}\beta - \dfrac{1}{p_{(B,I)}}}\right]$$

(4.33)

This last equation can be arranged to give a similar form to Equation 4.28, to give the values of $p_{(C,1)}$ and $r_{(C,1)}$ for the third branch of the junction. The first sweep continues downstream along channel C from this point in the usual way starting with these values of p

and r, which can be considered internal boundary conditions representing the 'upstream end' of channel C.

The second sweep returns up the same channel to give values for $Z^*_{(C,1)}$ and $Q^*_{(C,1)}$ and the 'upstream' end of the channel. The second sweep must now return up branch B using the exchange Equation 4.34, derived by replacing $Q^*_{(C,1)}$ and $Q^*_{(B,I)}$ in terms of p, r and Z and then substituting into Equation 4.29b.

$$Z^*_{(B,I)} = \frac{(1 - p_{(C,1)}\text{branch}\gamma)\, Z^*_{(C,1)} + r_{(C,1)}\text{branch}\gamma - r_{(B,I)}\text{branch}\beta}{1 - p_{(B,I)}\text{branch}\beta} \qquad (4.34)$$

The second sweep then continues up branch B until reaching the upstream boundary point. The solution then returns to the point of juncture of branch A, where $Z^*_{(A,I)}$ is calculated with an equation derived in the same manner as Equation 4.34 (Equation 4.35).

$$Z^*_{(A,I)} = \frac{(1 - p_{(C,1)}\text{branch}\gamma)\, Z^*_{(C,1)} + r_{(C,1)}\text{branch}\gamma - r_{(A,I)}\text{branch}\alpha}{1 - p_{(A,I)}\text{branch}\alpha} \qquad (4.35)$$

The second sweep proceeds up channel A until meeting the end boundary point. The modelled results are then checked for computed convergence, which if satisfactory allows the computations to move to the following time stage.

It should be realised that the compatibility relations given by Equations 4.29b and 4.29c are adopted from steady flow theory and represent the energy equation or Bernoulli Equation. In effect the solution of the branch problem in this case is setting up a region of internal boundary conditions at the juncture of the tributaries and assuming that from the junction to the next section on a given branch that steady flow conditions give a reasonable enough approximation of the flow for the small distance between the section and junction. If cross sections for all the channels at the point of convergence are known and are very close together

then a simpler, although less correct compatibility relationship could be used which sets the relevant water stages as being equal.

4.11 Conclusions.

This Chapter has presented the numerical solution to the mathematical model of flow derived in the previous chapter using a simple four point discretisation, adapted for a branched flow system. In many commercial packages and academic publications, the mathematical solution of the differential equations is often neglected, leaving it difficult for a reader to justify the validity of some of the modelled results. The numerical solution of the derived equations is as important a facet of the computer model as the flow equations, hence the two fold division of Chapters 3 and 4. However, they are not remotely independent as some forms of flow equations or numerical solution methods are not compatible, and therefore the flow equations, solution techniques and the 'add on' subroutines which model flow conditions for which the De St Venant equations are not applicable have to all be considered together from the onset of the model design.

CHAPTER 5.

ASPECTS OF FLOW IN NATURAL RIVERS.

5.1 Introduction.

This chapter will introduce the practical considerations of modelling tidal flow in an estuary, which encompasses a wide variety of aspects. It will describe the data availability for constructing the river cross-sections and how conveyance is calculated. The accuracy and aptness of boundary data of known flow conditions will then be described, before developing flow equations when the continuous functions described in Chapter 3 and Chapter 4 become invalid, such as flow over weirs. Chapter 5 can be seen as a precursor to Chapter 6 which will show the validity of modelling from a mathematical and theoretical sense. It is obvious that a model at its best can only be as accurate as the quality of the initial data permits. This is a major factor in considering how many components of fluid flow need to be modelled, as the inaccuracies in the data available may be of a magnitude great enough to negate the need for 'fine tuning' the model with over elaborate flow calculations.

For this analysis the river system needs to be digitised into a form solvable by the computer. There are two forms of discretisation to represent the physical properties of the river for the model. Firstly there is *Geographic Discretisation* which is the process of describing the selection of model elements, such as branched flow and weirs over the area of the modelled system, while *Hydraulic Discretisation* describes the hydraulic and topographic elements of the river cross-sections.

5.2 Geographic Discretisation.

Geographic Discretisation describes the process that the modeller uses to select the kind of elements he is to employ to represent the layout of the system to be simulated, such as the channel links, branched networks, looped networks, hydraulic structures and flood plain cells.

5.2.1 Channel Links, Looped and Branched Networks.

This part of the Geographical Discretisation process has been described in the previous chapter to some extent. To model a system it is necessary to divide it into a series of computational zones, over which a number of mathematical processes may be employed to describe a realistic, but computationally simple passage of flow. The basic pattern of decision making involved is as follows.

- Choice of one, two or three dimensional flow.

True multi-dimensional modelling was rejected at an early stage because of computational power, time, cost and accuracy considerations. As the problems to be modelled are relatively simple scenarios and involved a number of hypothetical situations where the lack of certainty in the data could not justify a very complex model, a one dimensional model was selected as being suitable for the problem solving required.

- Looped, Branched and Floodplain Networks.

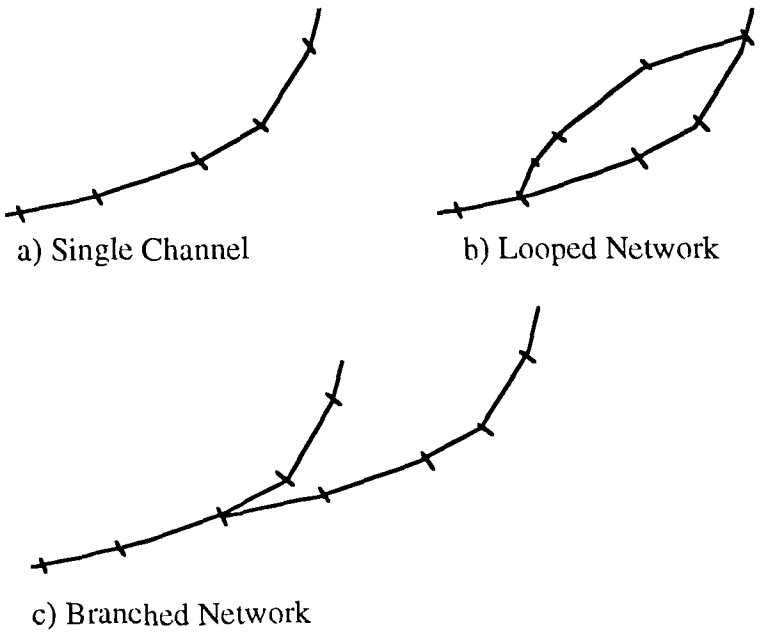

Figure 5.1. Single channel, looped and branched networks.

Three differing networks which may be modelled by finite difference means are shown in Figure 5.1. By comparison to the area of the Severn which is being modelled between Gloucester and Avonmouth, a looped network was not required, but after consideration of the early modelled results using a simple single channel extending from Maisemore Weir to Avonmouth, it was decided that a branched system to encompass the division of flow in the East and West Channels at Gloucester provided a more realistic simulation of flow than a single channel model, such as that used by Binnie and Partners during the 1980's. It was found that during the verification of modelling (see Chapter 6) that addition of the branched system provided greater computational stability to the model especially during low flow periods and computation was not noticeably slower than the single channel model. The computational aspects of branched flow have been described in the previous chapter.

Modelling of flood plain flow was not required because most of the flow within the area being modelled tended to be contained within the seawalls in an area where the spatial extent of the flood plains is generally small. However, two features of ignoring this aspect have been considered in the analysis of the results, firstly modelling of floodplain flow would have been advantageous when considering the flow of water back into the river system when the seawalls had been overtopped and the tide had subsequently waned. Secondly the modelling of historical tides when the seawalls had not been built encompasses large flood plain areas. However, the uncertainties in conditions, such as the tidal regime, channel positions, channel depth and extent of some of the flood plain areas meant that the modelled results should only be treated qualitatively and thus it was not deemed necessary to try and model complex flow. Mapping and analysis of the floodplain would have increased the amount of work required for the model and would have considerably extended the scope of work although the computational aspects of modelling floodplain flow are relatively simple.

- Weirs.

There are two weirs in the Severn Estuary in the modelled zone. One weir is at Maisemore and forms the 'boundary' section of the West Channel at Gloucester. This weir was not modelled, as the hydrological data available for the West Channel applied to Over Bridge which is actually downstream of Maisemore. A second weir on the East Channel at

Llanthony has been modelled. The hydrological aspects of modelling a weir are described in the Hydraulic Discretisation sections.

5.2.2 Sources of Cross-sectional Data.

A total of 84 channel cross sections were constructed from the relevant data sources extending from Barry Island to the two upstream points at Maisemore Weir and Westgate Bridge. However, after initial modelling it was found that a smaller model extending from Avonmouth to the same upstream points was suitable, especially as there was more tidal data available for Avonmouth which limits the number of sections used to 67. The data was obtained from two sources of information, the Admiralty Charts published by the Hydrographer of the Navy and from cross sections obtained from the National Rivers Authority which represent a survey carried out on their behalf by the Hydraulics Research Station (HRS) in 1976. The section locations and names are located in Appendix E and show which source of information was used. In general data from the Admiralty Charts was used for sections downstream of Sharpness and the HRS. survey upstream of this point. As Sharpness Docks are considered to be the head of commercial navigation on the River Severn the Admiralty data ceases at this point.

The constructed cross sections must be perpendicular to the general flow in the channel which is considered to be the channel axis to satisfy the assumptions concerning one dimensional representation. The axis of the channel is taken to be at a level between mean and high tidal levels because at lower stages the channel may narrow and diverge from a perpendicular angle to the assumed section. This problem is exacerbated in the sections higher upstream, where narrow ebb channels may wind a considerably different course to the channel at high tide or diverge. The distance between sections is also an important factor to consider as too great a distance between cross sections will not give an accurate reflection of the channel and may also be computationally invalid when considering gradually or highly varied flow, whilst sections too close together may be a computational extravagance. Although it is not considered a computational necessity to use the Courant condition of stability with the model which has been adopted, it was found that it was sensible to use this equation as a guideline

for deciding the maximum distance between cross sections, see sections 5.3.1 and 5.3.2. In areas where greater variation in flow conditions, or areas of greater interest, sections were chosen closer together.

The two subsections 5.2.3 and 5.2.4 describe how the data was collected from the two data sources.

5.2.3 Cross-sections obtained from Admiralty Charts.

A map showing the cross-sections collected from the Admiralty Charts is presented as Figure 5.2.

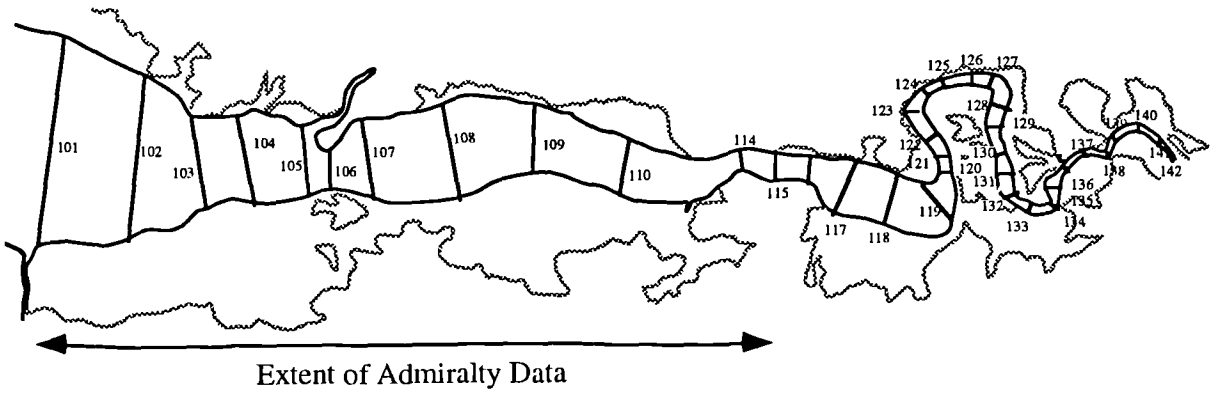

Figure 5.2. Cross sections in Lower and Middle Severn Estuary, showing extent of sections derived from Admiralty data. Diagram not alligned to grid north.

The cross sections in the Estuary from between Avonmouth (Portbury Docks) to Sharpness were constructed by drawing a line across the Admiralty charts and taking the values of soundings and elevations relative to chart datum. These levels for the channel bed are then converting to an elevation relative to Ordnance Datum which is the datum line used for all values of elevation in this thesis. An example section is given as Figure 5.3. The values adopted were those immediate to the section line. In areas of sparse data readings an inverse square calculation using points within a representative sphere of influence was used to give an average value of the bed level. This sphere of influence was decided by eye depending on the number and variability of the data values within the immediate area. The data was analysed

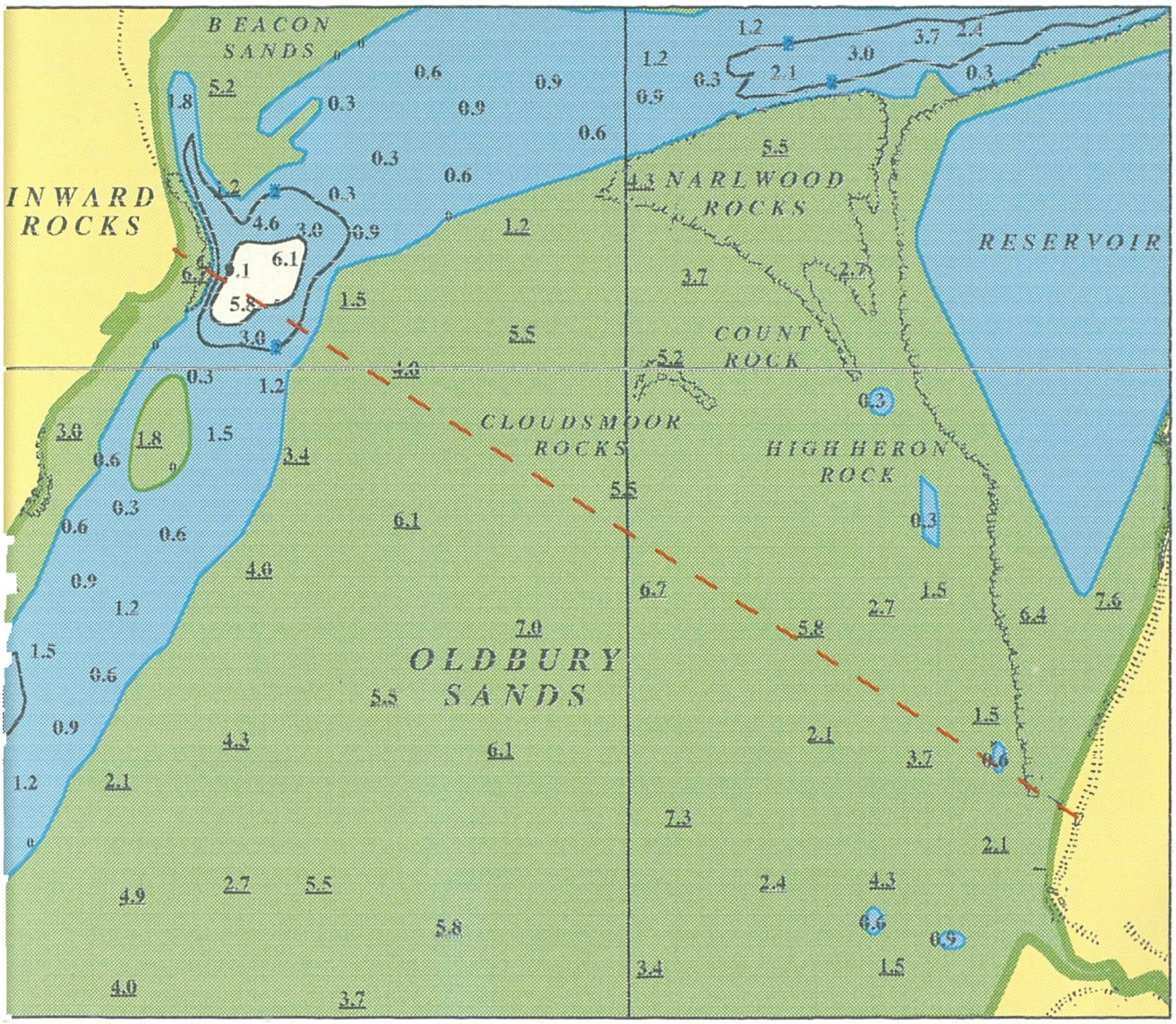

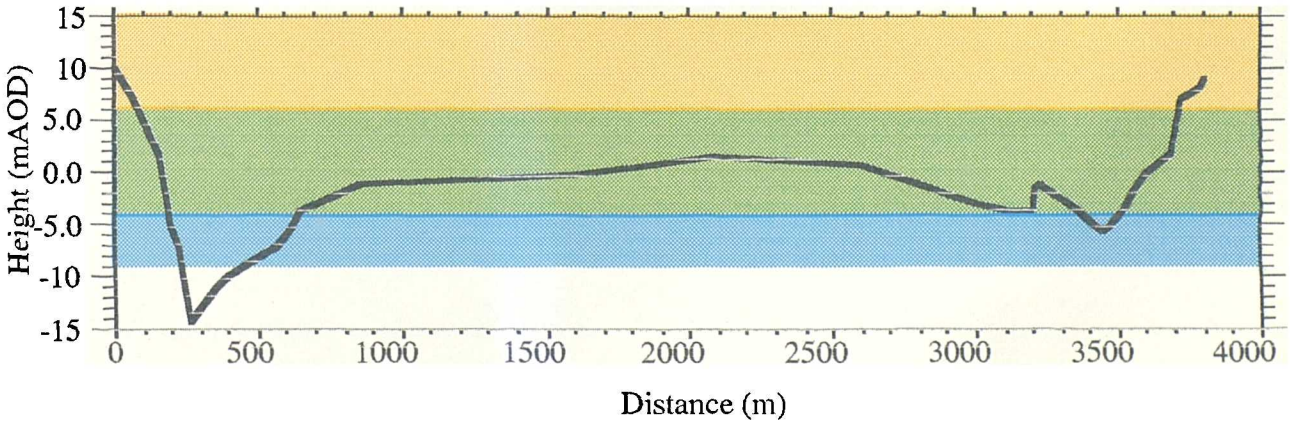

Fig 5.3 Example cross section from Admiralty Chart.

using KaleidaGraph™ on an Apple Macintosh computer which statistically evaluated the density of points along the cross section so areas where there was little representative data could be identified and examined to see whether any further information should be obtained. Viewing the profiles in KaleidaGraph also identified any gross errors in the data which may have arisen as the result of typing.

The Admiralty Charts are published for the interests of navigation so that there are a dense number of soundings within the main channels, but much sparser information for the sand and mud banks and drying shoals which are generally less navigable. When areas of low data density exist, previous Admiralty Charts were consulted to find whether there were any additional soundings were available. In some cases the estuary was visited at low tide to ascertain the general trend of the floor to enable bedlevel elevations to be estimated from nearby soundings marked on the Admiralty Charts. Low density points tend to be in areas which dry at low tide so this was a satisfactory method.

The Severn Barrage report by the Institute of Civil Engineers (1980) presented results of a number of sonar studies of the floor of the Estuary and Bristol Channel. These contoured Figures were reduced to bedrock levels from where the best reflections had been recorded. In this survey it was stated that there had been no attempt to correlate these charts to those of the Admiralty. Inspection of the two showed that there were discrepancies up to 4m in difference between them. In some cases the sonar charts showed bedrock at a significantly higher level than the Admiralty soundings which were marked on the chart as mud and sands (of unknown thickness). Consequently the echo soundings were used as a guide but not for absolute Figures. Similarly available sidescan and traditional sonar profiles showed the sea floor to be much more irregular than would be interpreted from the Admiralty charts. One problem with the sonar images is a distorted vertical scale and 'noise' from the method, the sections taken from Admiralty charts would effectively smooth the floor by taking representative values approximate to the mean heights of the floor indicated in the sonar surveys. Due cognisance of this problem was taken, namely by noting that in areas of high irregularity that the wetted perimeter would be greater than a value interpreted from the Admiralty constructed sections and that the floor would be rougher than expected when considering the friction value.

5.2.3 Cross-sections obtained from HRS surveys.

The Hydraulics Research Station undertook a channel survey of the Severn from Avonmouth northwards to above Worcester, to be used with LORIS, their own predictive model of the Severn, specifically for the Gloucester to Worcester (generally non-tidal) reach. The HRS cross-sections from Avonmouth to Gloucester were made available by the National Rivers Authority, Lower Severn Division, (Tewkesbury). These surveys and occasional resurveys made the following year give heights relative to Ordnance datum of the channel floor at selected cross sections along the river. Data is generally available at 2 m intervals along the length of each cross section, with survey points being closer when near to topographical inflexion points.

Re-surveying of the original HRS sections in the following year showed that there were significant rises in the bed level following a summer of drought and that sand had accumulated in some of the sections north of Slimbridge to a thickness of over 1 metre in some parts. This rise in the bed levels will cause some problems with the modelling of steady flow at low tide as it is not possible to change the original section details to account for what are effectively ephemeral and unpredictable changes to the channel morphology. Thus it is acknowledged that following the instance of a dry summer, bed levels and hence low tide levels may be higher in reality than those modelled. Similarly the opposite is possible if the modelled sections have higher bed levels than the natural ones at the time of observations. However, analysis of the sections which the HRS did resurvey indicates that there are no significant changes in the hydraulic characteristics of the channel at medium to high tidal levels.

In a number of cases the HRS surveys are incomplete. Two sections had been lost, which had to be ignored, because the model can allow for an appreciably varied spatial separation between points this does not present an undue mathematical difficulty. In other instances the sections themselves were incomplete, further data to construct these sections was obtained from an aerial survey of the estuary flood plain which has mapped much of the river flood plain to a 0.25m accuracy, also obtained through the NRA. When necessary the sections were also levelled in the field if no other data was available. If the aerial survey had been

employed then selective positions along the profile were field levelled as were positions on a number of the HRS cross sectional survey to check the accuracy.

5.3 Hydraulic Discretisation.

To model a river system it is necessary to divide it up into a number of representative computational points, akin to the x axis points on the finite difference grid in the previous chapter. The term 'representative points' assumes that the flow equations satisfy the De St Venant assumptions at and between the Estuary cross sections used in the modelling process. In places where the De St Venant assumptions are invalid, for instance over a weir, then different laws are applied, the relevant ones which are contained in the sections on geographic discretisation.

If the De St Venant hypotheses are valid for a reach of a channel then a cross-section must be selected at either end of the channel which are computational points and must be analysed to represent as accurately as possible, the topographic and hydraulic properties of the channel reach. The features required are the cross-sectional area, breadth and wetted perimeter of the section, described as a function of the water elevation (stage).

Rozenberg and Rusinov (1967) highlighted the dangers of time saving by limiting the number of sections, so that a reach may not be accurately represented. They showed that width is the important factor in the wave propagation speed which becomes an important consideration when there is a local widening in the channel.

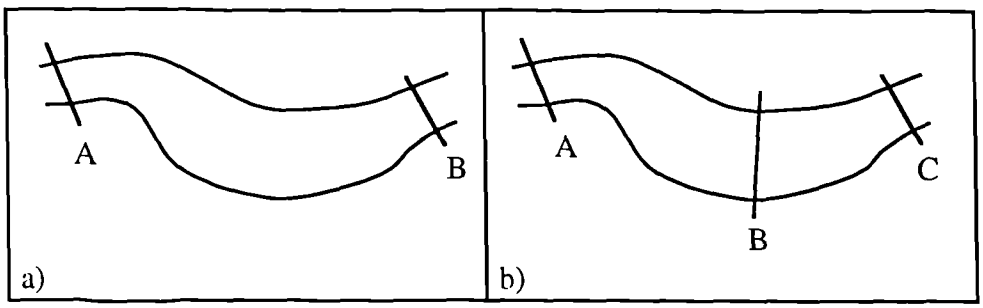

Figure 5.3a and b. Consideration of cross section positions on a widening reach.

If a section of a river was represented by the detail shown in Figure 5.3a using sections A and B, then a wrong propagation speed would be produced by the calculations. Figure 5.3b would give a better impression using the three sections A, B and C, where an extra section has been added where the river widens. It should be noted that large changes in the river breadth or area invalidate the De St Venant assumptions and thus need additional mathematical solutions.

Choosing closer and more numerous section locations are more beneficial but also time consuming in production. The modelling system adopted allows for distances between the sections to be varied, as opposed to a regular grid which is commonly used in other models, so that in complex, variable reaches the sections can be closer together. It often occurs that cross sections are only available for the narrow parts of the channel so that the model needs to be adapted for embayments and coastal irregularities between sections. The Binnie and Partners model used in the 1980's took this into account but only using a volume consideration and ignored the breadth changes. Again adapting analysed data to give what is in the opinion of the model operator a more accurate solution can fall into the trap of creating more significant errors than those which were first being corrected. It is more acceptable to have a model that gives a nearly correct solution than to have one which outputs results which exactly match the 'real' observations, but is based upon incorrect assumptions or schemetisation.

5.3.1 Distance Step.

As a rule of thumb, but not an essential requirement, the maximum distance step between the modelled cross sections may be calculated in the following manner, based upon the speed of an incoming tide (treated as a wave) and the section spacing.

Consider the approximate dimensions of the Severn Estuary, assuming that the average water depth is 10 metres;

$$\text{Speed or celerity of wave, } c = \sqrt{(\text{depth} * \text{acceleration due to gravity})}$$

$$= \sqrt{(10*10)}$$

$$= 10 \text{ m/s}$$

Given a tidal period of 12 hours this would mean that the wave would travel 432 km. If 100 points per wave length is considered a suitable resolution then the maximum spacing between points should be no more that 4.32 km. The maximum spacing in the model used was 4.6 km which is greater than the estimated maximum allowable distance between sections. However, this occurs only once in the model between the two most seaward cross sections and is only just larger the guidance value, given the greater depth here it is not likely that this spacing will compromise the model's resolution. The distance step in critical areas should be reduced much more to suit the data and purposes of the simulation, the minimum distance step was 106m in the upper area of the modelled system.

5.3.2 Time Step.

Although the time step is not part of the hydraulic discretisation, the relationship between the time and distance steps can have an effect on the stability and accuracy of a solution. Although many authors believe that the method adopted is unconditionally stable, the Courant Condition is used as a guidance to time step. The Courant Number is given as Equation 5.1.

$$\text{Courant Number} = CR = c\,\Delta t \,/\, \Delta x$$

$$= \sqrt{(\text{depth} * \text{acceleration due to gravity})}\,\Delta t \,/\, \Delta x \qquad (\ \mathbf{5.1}\ )$$

The Courant Number in explicit systems is limited to a maximum value of 1, but may be larger in implicit systems such as this model. If CR is allowed to equal 3, then the maximum time step is limited to 22 minutes using the assumed depth and distance spacing calculated in Section 5.3.1, however, this value would lead to a very coarse modelling of the tide, which in the case of a macrotidal estuary such as the Severn, would not give an accurate representation of the tidal curve.

Time Step (min)	Distance (m)	Depth (m)	Courant Number
1	3000	25	0.31
5	3000	25	1.58
1	1000	8	0.53
5	1000	8	2.68
1	200	4	1.89
5	200	4	9.48

Table 5.1. Courant number for different situations.

The approximate Courant Number for different time steps, distance between sections and depths relevant to the modelled areas of the Estuary are given in Table 5.1. It is noted that decreasing the spacing between sections increases the Courant Number, it is therefore only a guidance. If the maximum Courant Number (arbitrarily set to three) is exceeded, then it is better to do so by decreasing the distance between sections. Finer resolution required by the modelling denotes that the time step should be smaller. Reducing both the time step and the distance between sections where a rapid variation in the breadth or cross sectional area occurs may help the modelled system conform to the De St Venant assumptions and not require any additional calculations.

5.4 Pre-processing of Cross-Sections.

The cross sections obtained need to be analysed to give the data which is required by the computer model, which is the cross-sectional area, breadth and wetted perimeter for each of the model cross sections for every tidal level. These values are all a function of the tidal height or stage. As the tidal height at a given cross-section is a variable continuous function, there are an infinite number of values of the cross-sectional area, breadth and wetted perimeter which can be calculated between the lowest bedlevel and a theoretical maximum tidal level. It is not feasible to calculate all these values during running of the main programme so to save time

the sections are digitised and pre-processed. The pre-processing of the sections used to provide data for the modelling described by the thesis calculates the cross sectional area, breadth and wetted perimeter at metre elevations of the tidal surface from the lowest bed level (conveyance and non-homogenous flow is also accounted for, but are addressed in a separate section). The values of the functions are saved to computer disc at the metre intervals so that they can be read by the main programme which calculates the intermediate values which fall between the calculated metre spaced values by interpolation

5.4.1 Cross-Sectional Area.

The cross-sectional area is defined as the area of the channel which is actively conveying fluid in a cross section perpendicular to the flow bounded by the channel floor and sides. In some studies the cross section is divided into a 'live' cross-sectional area, representing the active area of the channel which is transporting the majority of flow and a 'total' cross sectional area which represents the entire section underwater including the flanks which may be flood plains which are merely storing water and not transporting it to any appreciable degree (Figure 5.4).

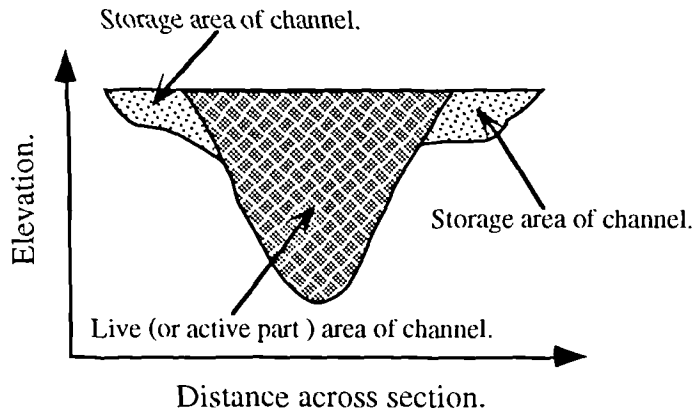

Fig 5.4 Engineering 'live' and 'storage' areas in a channel cross-section.

Attributing different hydraulic properties to *different packages of the channel cross* section is a diversion from the one-dimensional theory and the De St Venant assumptions, in

some studies there is sometimes an 'effective' breadth defined representing the breadth of the live area of the channel. This study considered dividing the channel into areas of live flow and storage, but rejected this approach after some preliminary modelling because it was thought that the considerable amount of additional time required for defining such areas did not justify the relatively insignificant improvements to the model. During flow in the Severn in the present day tidal regime there is relatively little flood plain flow due to the presence of the sea walls which confine the flow to the salt marshes on the seaward side, which apart from at very high tides are small components of the total cross sectional area of the section and relatively small components of the breadth. It is deemed that dividing storage and live areas would have little effect on the model accuracy although such an approach may, however, be more significant in the breadth term. When considering historical flow when the sea walls had not been constructed there would have been considerable areas of flood plain involved in the estuarine regime, so defining live and storage areas would be a preferable method. This approach could not be adopted for these historic flows because it was deemed that the degree of uncertainty in the historic tides was sufficient to render any results of modelling as being semi-quantitative, thus the extra time in reprogramming the main computer programme and to an even greater degree, the time required to define active and storage areas and re-analysing the cross sections was not justified in this research. It is also noted that there is no mathematical definition of live and storage areas, so it is the arbitrary judgement of the engineer to define such areas which involves an amount of guesswork, is considerably time consuming and may create as many problems as it solves.

After consideration of the requirements of the programme, the cross-sectional areas were evaluated for water levels at metre elevations from the lowest bed level to 12 mAOD which was anticipated to be beyond the highest elevation of the tidal surface which would be modelled. Figure 5.5 shows how the cross sectional area varies with the water stage.

The cross sectional area is calculated using the trapezium rule, systematically calculating across the section for a given tidal elevation using variable slice widths defined by the relevant survey points of the channel floor and the water level when it truncates a slice between survey points (Figure 5.6).

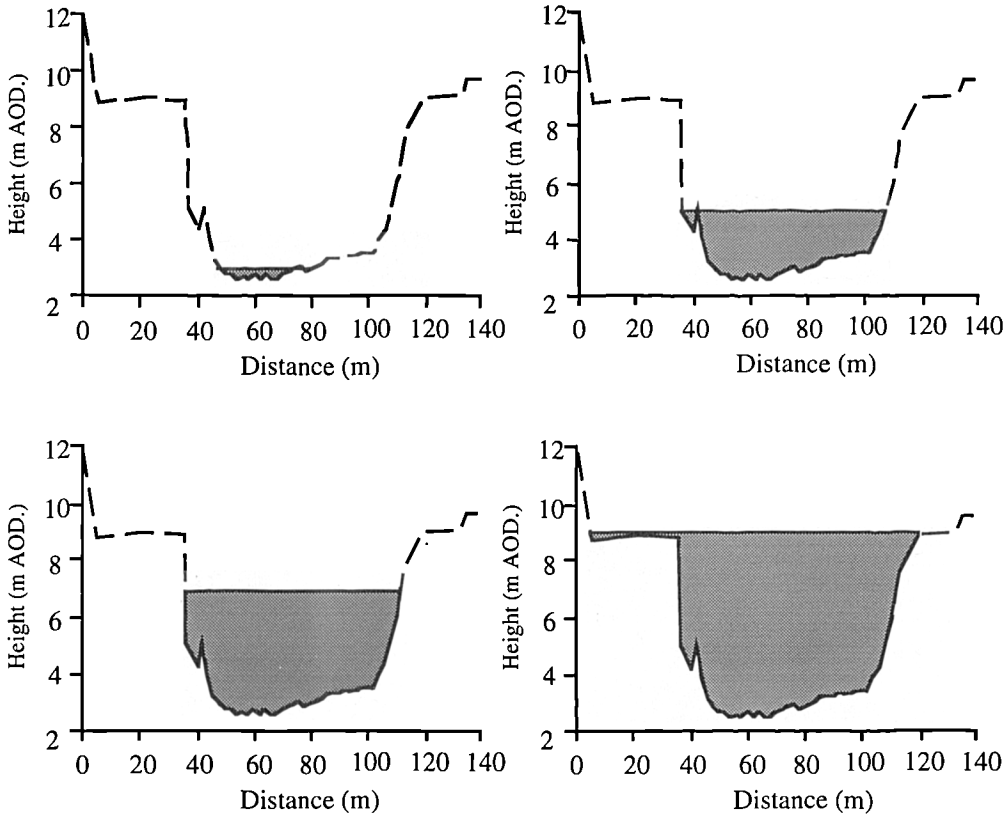

Fig 5.5. Cross section at Windmill Hill at 3, 5, 7 and 9 m water stages, values of cross sectional area, breadth and wetted perimeter are given later in text.

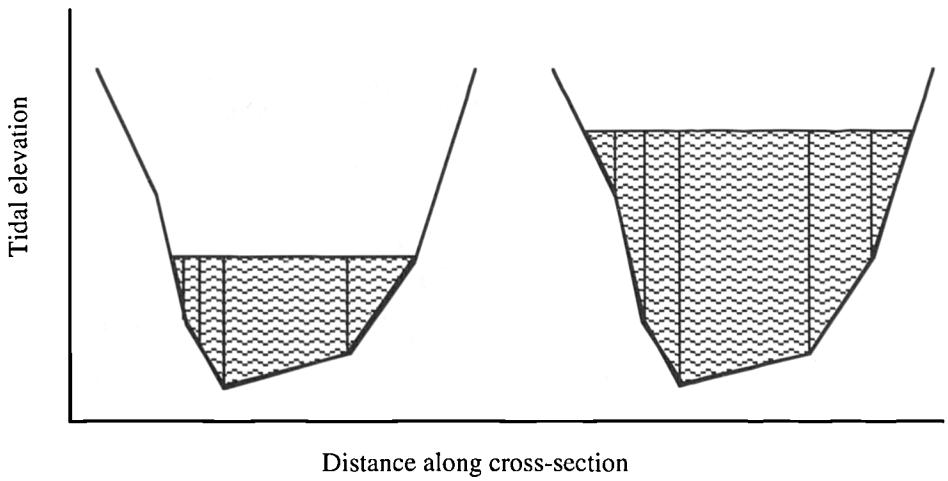

Fig 5.6. Cross-sectional areas and vertical slices for two different tidal levels.

Two potentially time and computer memory saving methods of evaluating the cross-sectional areas and other flow variables were also investigated and are described briefly in this paragraph. Simplifying the sections to a rectangular system means that easier calculations could be done (Figure 5.7), however, such a method was found after only a small number of analyses of cross sections to give unsatisfactory representations of the hydraulic properties for low flow levels. The method proved to be time consuming and involved an appreciable degree of decision making to construct the schematic sections, which again tends to move away from modelling reality and can introduce a degree of error.

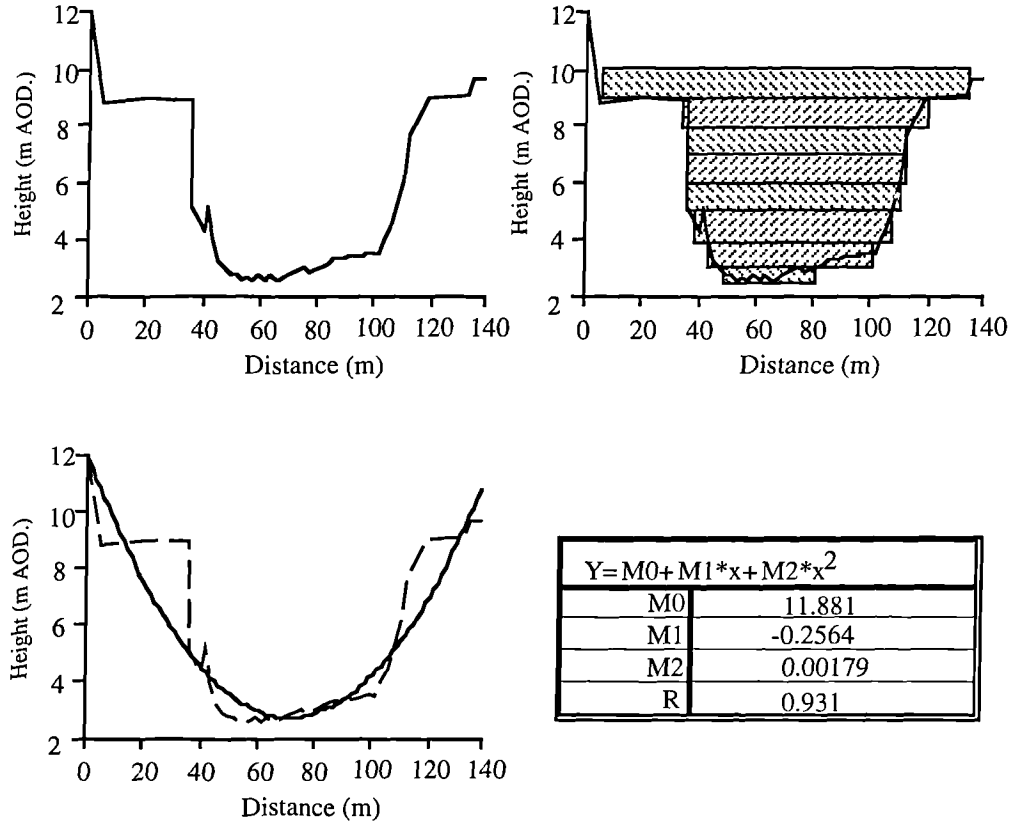

Fig 5.7 Original cross-section and approximation by rectangles and simple polynomial curve.

An easier way was to approximate the shape of the cross-section to a polynomial curve, thus an equation rather than a large data set could be entered into the programme (Figure 5.7) which could solve the cross sectional area for a given water surface elevation. An advantage of this technique is that there is no need to tabulate values at metre intervals and that intermediate

values can be calculated. However, the curve fitting method also proved to be too inaccurate due to the irregularity of the channels. To evaluate the parameters required would need an equation solving and integration routine within the main programme, which could result in the speed of calculation becoming slow for high order polynomials.

Both methods can be applied with relative success to man made channels which tend to have a more regular nature. A comparison of the results obtained from the three methods of evaluating the cross sectional area of the section illustrated in Figure 5.7 is show in Table 5.2. In this table the 'actual' values refer to the cross sectional area calculated by small slices which was considered the best available representation.

	Cross Sectional Area (m^2)		
Height (m AOD)	Actual	By Rectangles	By Curve fitting
2	0.00	0.00	0.00
3	9.04	15.625	5.20
5	124.37	140.625	109.98
7	271.34	291.975	281.08
9	431.22	453.125	498.42

Table 5.2. Results of different evaluation methods for determining the cross sectional area.

5.4.2 Breadth

The value of the breadth is defined as the distance across a cross section perpendicular to the flow along the free surface from the two external boundaries which are the channel sides, although internal boundaries such as islands must also be deducted from the total breath. For the simulations the value of the breadth is also tabulated at metre intervals into a cross sectional data file which is read by the main simulation programme. As before with the area calculations there could be a division of a 'live' and 'storage' breadth within the channel representing the breadth over which the section is actively conveying the bulk of fluid. During the analysis of

the rectangular and curve fitting techniques referred to in the previous section the effect on the breadth was examined and is shown in tabular form for the three different methods for the same cross section in Table 5.3.

	Breadth (m)		
Height (m AOD)	Actual	By Rectangles	By Curve Fitting
2	0.00	0.00	0.00
3	34.22	31.25	25.92
5	69.96	67.50	71.70
7	75.65	76.25	98.04
9	114.08	85.00	118.66

Table 5.3. Different calculations of the channel breadth using cross section illustrated in Figure 5.5 and 5.7.

5.4.3 Wetted Perimeter.

The wetted perimeter is defined as the length of contact of the fluid with the channel sides and floor along the cross-section and thus tends to be a similar value to the breadth in simple shallow sections. During the construction of the channel cross sections it is vital to find out the relative importance of the effect of the wetted perimeter on the flow calculations as it prone to being the most difficult to ascertain from the sections taken from the Admiralty Charts. At a very high water level for a theoretical section analysed from the Admiralty Charts, say at Avonmouth, the wetted perimeter varies by only a matter of metres from the breath. Inspection of the echo sound profiles in various publications of the channel floor seaward from here, shows the bottom to be much more irregular and hence for the Admiralty derived sections, the wetted perimeter must be considered an underestimate, especially in highly irregular sections which will tend to have a bedrock substrate.

	Wetted Perimeter (m)	
Height (m AOD)	Actual	By Rectangles
2	0.00	0.00
3	24.29	32.25
5	70.98	72.50
7	75.65	85.75
9	114.08	98.50

Table 5.4. Calculated values of wetted perimeter from different methods.

The drawback of using a simplified curve technique to give the wetted perimeter is that the integration for an arc of a function can be quite complex, during the preliminary digitisation of the cross sections it was found that two differing commercial mathematical integration solutions gave different results to the solution of the same problem. These results are therefore not illustrated in Table 5.4. as they were unreliable and the curve fitting method was deemed inaccurate and rejected before a different analysis method was derived.

5.4.4 Friction Laws.

In order to evaluate the conveyance which is pre-processed or calculated during execution of the main programme, it is necessary to establish friction values representative of the resistance to flow of the channel sides and floor.

The friction values and hence the conveyance calculations are the only truly adjustable values in the modelling system and may be used to tune the model to fit existing data. Using steady uniform theory and the assumption that this can be applied to unsteady flow problems, one can build up a suitable resistance law. The form of a simple relationship between flow and frictional resistance is shown as Equation 5.2.

$$U = C R^{i} S^{j} \qquad (5.2)$$

Where U = Average cross sectional velocity of flow.

R = Hydraulic Radius

S = Channel slope

C = Resistance coefficient.

i and j = Coefficients.

There are two popular formulae used to describe this semi-empirical uniform flow relationship, the Chezy Equation which was first published in 1769 and the Manning Equation published in 1889. The Manning Equation is derived empirically from a curve fitting processes and experimental observation, whilst the Chezy Equation is derived from theoretical principals. The Manning Equation has been selected as being applicable to this thesis because there is more literature available over its limit of applicability and estimated friction for the Severn. However, it is acknowledged that it is by no means a better representation than some other methods based on different principals. The Manning Equation is given in Equation 5.3.

$$U = \frac{1}{n} R^{2/3} S^{1/2} \qquad (\mathbf{5.3})$$

Where U = Average cross sectional velocity of flow

n = Manning Roughness Coefficient.

R = Hydraulic Radius

S = Friction Slope

As an aside, it was found that a degree of caution must be taken if imperial 'English' units are being used as this affects the numerical values of the equation and a multiplier of 1.49 must be added to the equation. It is not always clear in literature as to which units of measurement have been adopted.

5.4.5 Estimation of 'n' Values.

There are a number of factors which are involved in the selection of the Manning roughness coefficient. For convenience it is preferable to use a single non-varying value of n, this is only applicable if fully rough turbulent flow as defined by the Reynolds Number is occurring (ASCE, 1963). Assuming that this condition is the case then the selection of the Manning coefficient is then a qualitative estimation based on a number of controlling factors, indicated below;

- Surface Roughness

The surface roughness of the channel provides the most important factor in estimating the value of n. The value of Manning's roughness increases with the coarsening of grain size of the material lining the channel in contact with the flowing medium. However, with coarser sediments particularly when gravels or boulders form the substrate, the value of n varies considerably with the depth of flow, typically there are high n values at low depths of flow due to the turbulence created within the water column. The effect of the roughness becomes less important at greater depths. Although it is desirable to accurately represent such flow behaviour it must be remembered that at present complex turbulent behaviour is not readily solvable by mathematical means but can be better represented by hydraulic models.

- Vegetation

The value of n should account for the effects of vegetation in retarding flow, with a more retardant vegetation covering causing an increase in the value of n. This is an effect strongly dependant upon the depth of flow and the vegetation's density and distribution. Bushy vegetation seems to impede flow to a greater extent than individual tree trunks, although a series of closely spaced tree trunks can exponentially increase the turbulent effects due to the complex current flow around the trunks.

- Channel Irregularity

Variations in the channel floor between sections generally tend to be of a degree unimportant to the selection of the Manning coefficient although sudden changes in morphology such as large scours or recent deposition may give higher values of n than would be expected from the surface roughness due to the increased turbulence that could result. In some cases such as weirs or constrictions, the flow equations and Manning Formula are not valid and different flow laws are applied to create internal boundary conditions. Urquhart (1975) draws attention to the considerations involving active or abandoned erosional or sedimentary processes within a channel reach.

- Meanders

Persistent channel curves of large radius do not effect the values of n to as great an extent as the channel substrate but tighter or more variable curvature in the channel course can increase the channel roughness significantly. Curvature can cause uneven water surface levels at either side of the channel and momentum effects. Rossiter and Lennon (1969) approached this subject in a basic way using an additional coefficient within the flow equations rather than adjust the friction values. However, American authors have developed a system to adapt Manning values according to the curvature of the modelled system.

- Discharge and Stage

The value of roughness generally decreases with an increase in stage and discharge. At low flow depths channel irregularities may significantly disrupt the flow, becoming minor as the depth of flow or discharge increases. However, if the stage reaches a height above the level of the flood plain then the friction value may increase due to vegetation, especially if the flood plain flow is of a small depth. In these cases it may be necessary to consider modelling composite cross sections, which are described later in the chapter.

5.4.6 Soil Conservation Service's Method of Deriving Manning's Roughness Coefficient.

The initial values of the Manning's roughness coefficient for the modelled area of the Severn Estuary were evaluated for this work by using an amended version of the Soil Conservation Service (SCS) method of roughness estimation (1963). This technique uses a methodical consideration of modifying influences whilst acknowledging that evident turbulent processes within the channel are good indicators of flow retardation.

This method of estimation of roughness values adopts a systematic approach which proceeds by selecting a basic value and modifying it when extraordinary conditions prevail. The initial Manning Coefficient is selected from the assumed channel roughness based on tabulated values of the Manning Coefficient for different types of material in the channel. The SCS values for the likely channel conditions within the Severn are given in Table 5.5.

Channel Character	Basic Manning's n
Channel in earth	0.020
Channel in rock	0.025
Channel in fine gravel	0.024
Channel in coarse gravel	0.028

Table 5.5. SCS values of basic Manning's Coefficient of Roughness, n, for different channel types.

The basic value is then adapted for any influence which vegetation may exert upon the flow through retardation around leaves, stems, branches and trunks. Although vegetation may effectively reduce the channel width, additional factors to be considered when deciding upon modifications to the Manning value are the vegetation's resistance to bending, vegetation height in relation to the depth of flow, vegetation density, distribution and the season. In the case of the Severn the majority of the vegetation encountered are grasses or reeds upon the mudflats and tidal marshes and vegetation within the flood plain with trees and larger vegetation

tending to be a sub-ordinate consideration. Values for the relevant effects due to vegetation given by the SCS which are encountered in the Severn Estuary are shown in Table 5.6.

Vegetation and flow conditions.	Degree of effect on n.	Range of modifying values.
Dense growths of flexible turf, grasses or weeds, with an average depth of flow 2 to 3 times greater than the height of the vegetation.	Low	0.005 - 0.010
Turf grasses where the average depth of flow is 1 to 2 times the height of vegetation, or stemmy grasses and weeds where the average depth of flow is 2 to 3 times greater than the height of vegetation Young bushy growths along side of channel.	Medium	0.010 - 0.025
Young bushy growths with weeds in growing season or older bushy growths out of season.	High	0.025 - 0.050
Turf grasses where the depth of flow is one half the height of vegetation. Growing season trees, weeds and brush.	Very High	0.050 - 0.100

Table 5.6. SCS correction factors for vegetation.

Corrections for channel irregularities are based upon changes in the cross sectional area and shape. Area changes, if gradual have a minor effect on the roughness, whilst channel movements from one side to another will cause greater changes, especially if eddies and reverse currents are created which are features that are more likely to occur at small depths of flow. SCS modifying values for channel irregularities relevant to the Severn Estuary are given in Table 5.7.

Character of change in size and shape of channel reach.	Modifying value.
Gradual changes in size or shape.	0.000
Large or small cross sectional areas alternating occasionally or shape changes causing occasional shifting of main flow from one side to another.	0.005
Large and small sections alternating frequently or shape changes causing frequent shifting of main flow to one side or the other.	0.020

Table 5.7. Modifying values for changes in size and shape of cross sections.

Using the SCS system the value of the roughness is modified for meanders by summing the already defined modification factors to give a present subtotal (n'). The straight length of the channel reach in consideration is deemed L_s and the meander length L_m and the values of modification are tabulated for differing ratios of L_m / L_s which are given in Table 5.8.

L_m / L_s	Degree of meandering	Modifying value
1.0 - 1.2	Minor	0.00
1.2 - 1.5	Appreciable	0.15 n'
> 1.5	Severe	0.30 n'

Table 5.8. Modification values for channel meandering.

The total value for the Manning Roughness Coefficient is thus the sum of n' and the modifying value for meandering. Appendix C summarises the modifying channel factors using the SCS technique for the modelled area of the Severn and the final values of n, derived by this methods. In later chapters it will be shown that the friction values vary appreciably from the theoretical values which should be used and are generally lower than expected. This has been

found to be the case for other modelling studies of the Severn, although no adequate explanation for this has been given by the previous works.

5.4.6 Chow's Method of determining Manning's Roughness Coefficient.

Chow (1959) presented a second system to evaluate the value of the Manning's roughness coefficient, tabling n values for different channel types. This method is particularly suited to the design of man-made or channels which are regularly maintained. Chow's values pertinent to the flow generally encountered within the Severn Estuary are summarised in Table 5.9.

Type of channel and description.	Minimum	Normal	Maximum
D. Natural Streams			
D1. Minor Streams (with maximum flood width <30m.)			
Clean, straight, no rifts or deep pools.	0.025	0.030	0.033
As above with more stones and weeds.	0.030	0.035	0.040
Clean, winding, some pools and shoals.	0.033	0.040	0.045
As above with more stones and weeds.	0.035	0.045	0.050
As above with even more stones.	0.045	0.050	0.060
Clean, winding, some pools and shoals with lower stages and more ineffective slopes and sections.	0.040	0.048	0.055
Sluggish reaches, weedy, deep pools.	0.050	0.070	0.080
Very weedy, deep pools and underbrush.	0.075	0.100	0.150
D2. Flood Plains.			
Pasture, Short grass.	0.025	0.030	0.035
Pasture, High grass.	0.030	0.035	0.050

Brush, Scattered with heavy weeds.	0.035	0.050	0.070
Brush, light with trees in winter.	0.035	0.050	0.060
As above in summer.	0.040	0.060	0.080
Dense brush in winter.	0.045	0.070	0.110
As above in summer.	0.070	0.100	0.160
Trees stumps, cleared land.	0.030	0.040	0.050
Trees, fallen trees, some undergrowth, stage below branches.	0.080	0.100	0.120
As above with stage reaching branches.	0.100	0.120	0.160
D3. Major Streams (top width at flood stage > 30m): n Values less than that for minor streams of similar description (due to less effective bank resistance).			
Regular section with no boulders or brush.	0.025		0.060
Irregular and rough sections.	0.035		0.100

Table 5.9. Manning's roughness coefficient for selected channel types (after Chow, 1959)

According to the ASCE (1963) a non-varying value for the Manning coefficient can be assumed if fully rough flow is occurring, defined by the relationship given in Equation 5.4.

$$n^6\left[\frac{A\ S}{W}\right]^{0.5} > 1.9 \times 10^{-13} \qquad (\ \mathbf{5.4}\ )$$

Where A = cross sectional area.

S = slope of channel.

W = wetted perimeter.

n = Manning coefficient.

For values less than that given in Equation 5.4, the Manning Coefficient varies with the Reynolds number. Equation 5.4 has been used as a justification of the Manning Coefficient and as a guideline for the minimum value assuming the criterion of fully rough flow is being met. Such a justification was used by analysing the model using a debugging tool and stopping the programme to check the conditions of Equation 5.4.

The representation of friction in one-dimensional flow may be argued about at considerable length, it is possible to get lost in theoretical considerations and lose track of the overlying principal that this form of modelling is an approximation of complex phenomena and is prone to errors. It is the responsibility of the engineer to reduce these errors to an acceptable level, but also to know when to cease. As will be mentioned in the following chapter, it is possible to constantly retune the model so that the results fit the natural data very closely, however, the friction values entered may bear no semblance to reality.

The importance of the friction value is in the evaluation of the conveyance of the channel cross sections. In the following section on conveyance, the effects and merits of composite channels will be examined, where the friction values change longitudinally across a section and effect the total channel conveyance.

5.4.6 Conveyance.

The conveyance factor (K) of a section is defined as the *Section factor*, defined by Equation 5.5.

$$K = A R^{2/3} \qquad (5.5)$$

Which can be related to the discharge (Q) by Equation 5.6.

$$Q = K (S_f)^{0.5} \qquad (5.6)$$

Where K = the conveyance,

S_f = the friction slope

Q = the discharge (from steady flow theory).

A = the cross sectional area

R = hydraulic radius (= area / wetted perimeter)

Assuming that the value of K increases with increasing depth for every discharge in a section there is thus a unique value for the depth at which uniform flow occurs. The value of the conveyance of the channel can be calculated both as a function of the (intermediate) stage during the main programme or tabulated at metre intervals as per the cross sectional area and be interpolated in the same manner as the area, breadth and wetted perimeter variables.

The conveyance of the channel, through changes in the friction values, is the only truly adjustable function in the model. There are several formulae for the value of the conveyance which have distinct advantages over the other ones in certain circumstances, as mentioned previously the model adopted the Manning Formula because of the availability of data and because it has been used very successfully by others in the past.

The following subsections introduce two ways of evaluating the conveyance of a channel by considering the variation of friction, and hence conveyance, with the flow regime. One method is an approximation for compound channels and the other for frictional variations with the depth of flow.

- Conveyance in Compound Channels.

Conveyance, hence the friction value, can vary with the shape of the channel, for instance the 'live' part of the channel will convey more than the 'storage' part. With overbank or flood plain flow, friction values are generally higher, due partially to the lower depth of flow and its interaction with the vegetation and the like. In evaluating the conveyance of a section one can give Manning values for frictional resistance, representative for areas of the cross section. Take the example compound section given in Figure 5.8 in which there are a number of regions where the friction values can be considered, which are described after the figure.

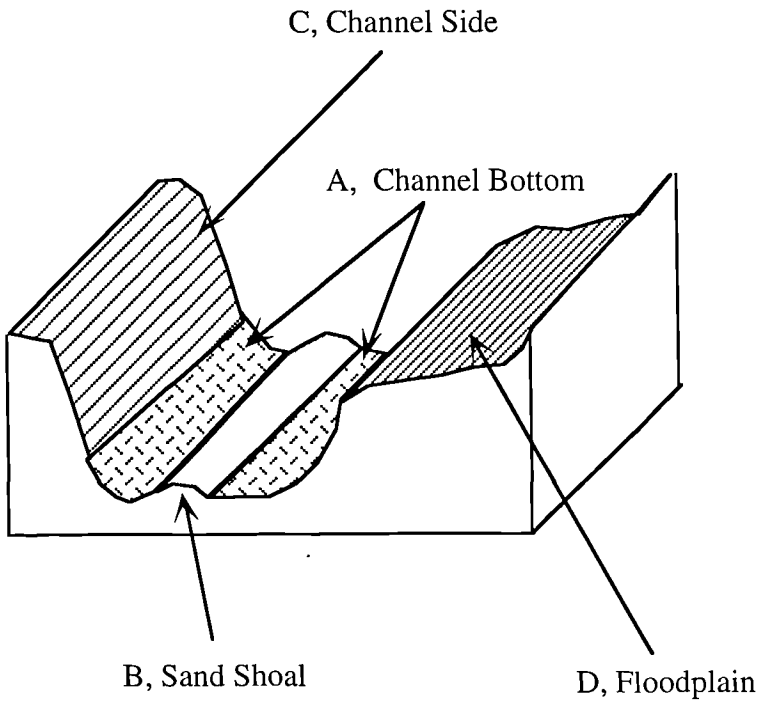

Fig 5.8. Simple channel section with different areas of resistance to flow.

A) Channel bottom

Fine sediment with relatively low friction value (e.g. $n \approx 0.025$).

B) Channel bottom

Sand shoal with higher friction value than fine sediment channel bottom because of increase frictional resistance resulting from increased grain size. Further turbulence may be created by eddies, etc. around the topographical change, especially at low flow levels, increasing the friction (e.g. $n \approx 0.03$).

C) Channel sides

Friction values should be related to the grain size, although retardation of flow is greater due to irregular shape. Under some conditions the flow can be in a reverse direction to the mean flow because of eddies. Choose higher value than that of A (or B depending on grain size).

D) Flood plain flow

Highest friction values because of low flow and vegetation effects, values bear little semblance to those expected when considering purely grain size.

Once the values of friction across the channel section have been decided the channel conveyance is calculated using Equation 5.7.

$$K = \sum_i n_i^{-1} b_i h_i^{5/3} \qquad (5.7)$$

Where K = the conveyance.

b = the finite width of a vertical slice.

h = the depth of the slice.

n = the friction value of the slice.

i = the slice number.

The author has noticed that in some models that when this approach has been adopted the value of the depth has not been averaged per slice when the channel bottom differs on either side of the slice giving a false impression of the conveyance. Equation 5.8 gives another form for conveyance calculations for complex channel types, but was not found to be as useful as the earlier calculation of conveyance in compound channels.

$$K = \left(\frac{(A_1 + A_2 + A_1)^5}{(W_1 + W_2 + W_3)^2} \right)^{1/3} \frac{W_1 + W_2 + W_3}{n_1 W_1 + n_2 W_2 + n_3 W_3} \qquad (5.8)$$

Currently the mathematical modelling of flow in composite sections is not really possible because of the great complexity of the system. Figure 5.9 shows how flow velocities which are related to the local friction and turbulence can vary to a complex degree. This schematic example indicates the slowing of the flow towards the channel sides and a general retardation of flow within the flood plain area.

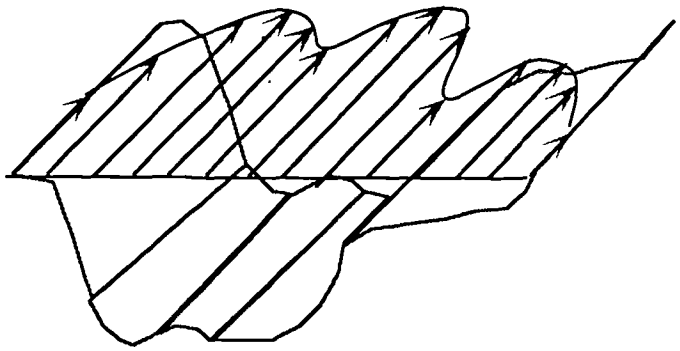

Fig 5.9. Velocity envelope of mean flow for simple compound channel.

One interesting feature of flow within this type of channel is that there is a substantial retardation of the flow in the area where the floodplain meets the main channel. Here eddies can form through turbulent interaction which is a phenomenon which is best modelled using hydraulic scale models. A hydraulic model nonetheless may not truly reflect the hydraulic behaviour of natural rivers where the pattern of flow can change from day to day, depending on the wind and hydraulic conditions and under such conditions flow predictions might as well be determined using chaos theory.

- Conveyance in relation to flow depth and velocity.

As has already been stated, the friction due to turbulent interaction varies with the flow depth. At low flow depths there is greater relative interaction with the channel floor, until a given volume of fluid passing the spot has a large enough mass to negate many of the internal flow effects within the column. Obviously if a modeller wishes to use a higher friction value at low

flow levels, he must be able to determine a cut off point or transitional area where the flow reaches a depth at which the low flow resistance can be neglected. This will depend on the channel size, shape and roughness. To achieve such an approach requires the frictional values used to be arbitrary figures dependant on the modeller's judgement rather than a well-defined mathematical law. Two approaches were derived, giving higher friction values for the lowest part of the channel floor throughout the flow simulation (a crude simplification and not satisfactory at greater flow depths) or to adopt a power law reducing the friction at given points in the cross section as the depth of flow increases.

A similar flow related effect is that the bed forms within a channel or area of the channel also change as flow velocities change. Current ripples may create more turbulence than the sediment grains of which they are made. High flow velocities at low depths should have lower friction values than lower velocities at the same depth, as the channel bedforms will tend to be planar bedding at the higher velocities and rippled at lower ones. Again this will become a function of the velocity, grainsize and cohesion of the bed sediments. This phenomenon is too complex to attribute true values to, even with the aid of laboratory flume studies and it was up to the author to set representative approximations of the flow, if deemed necessary. Two approaches to this problem were modelled but were found to have little effect on the computed results, one involved raising the friction value if flow reached a given height (say less than one metre) above the lowest point of the channel, another used varying values of friction for different parts of the channel to account for high turbulence on shallows including shoals and flood plains, the latter being very time consuming to pre-process cross sections. A third method modifies the estimated fricition value by $n.e^{(\text{max depth - flow depth})}$ where n was varied by trial and error. However it was difficult to be convinced that unrealistic values were not being produced by this method.

5.4.6 Non-Uniform Velocity Distribution.

Schonfield (1951) introduced a simple method of integrating velocities to account for non linear velocity variations, for instance the retardation of flow adjacent to the channel sides.

Using a similar method to the derivation of conveyance from compound sections, the non-linear coefficient of velocity variation (ß) can be evaluated using Equation 5.9.

$$ß = \frac{A \sum_i n_i^{-2} h_i^{7/3} b_i}{\left(\sum_i n_i^{-1} h_i^{5/3} b_i \right)^2} \qquad (5.9)$$

The value of ß, often called the Boussinesq Coefficient, is calculated by the pre-processing programme and tabulated at stages of the water elevation, in the same fashion as the conveyance, breadth, etc. The Boussinesq Coefficient can be placed in the two flow equations defined in the previous chapter before the Q^2/A terms. However, by adopting this term the equation also become incompatible with the earlier equations as they are formed using different hypotheses to the De St Venant assumptions. To reach near compatibility the storage area and breadth of the cross section must be very small compared to the 'live' component. It was found impractical to edit the mass of stored cross section information and re-preocess the sections to give new tabulated values of the hydraulic properties. The method was used for approximately 200 to 300 model runs and was not found to produce any significant variations to the runs not using this modifier.

5.5 Lateral Inflow.

The addition of varying friction values within a compound channel cross section and non-uniform velocities which can also be expanded to account for vertical velocity distributions, is part of a number of exercises which produce quasi two- or three-dimensional flow simulations, without the time and computer expenditure considerations involved in a true multi-dimensional model requiring solution of a much greater number of equations. Other examples of simple modelling of complex multi-dimensional phenomena using adaptations of one-dimensional theory are the addition of a branched river system, as described in the

previous chapter and the allowance for water transfer into and out of the channel termed lateral inflow.

Lateral inflow accounts for the exchange of water from a channel section to an area other than the normally modelled conductive relationship between adjacent sections along the channel reach such as the over-topping of seawalls, outlets, pipes and small pills. Unfortunately river tributaries cannot be modelled by using a lateral inflow type calculation as the lateral inflow is simplified to being a point source. However, there is no rigorous criteria for deciding when a river becomes significant enough to be added as a branch. Although lateral inflow effectively is considered as a point source it is mean averaged per unit length of the distance between adjacent channel cross sections.

Lateral inflow or outflow in the context of this work has been modelled only for the overtopping of the sea walls by high tides. It may seem that the volume of water overtopping the seawalls at any one time even on an extremely high tide within the Estuary is much less important than say the flow of the River Wye in to the system. However, the water input of the Wye is less than 1% of the total water volume in that section of the Severn Estuary and would not effect the water heights other than locally which cannot be resolved in a one-dimensional model. The splitting of the West and East Channels at Gloucester, whilst flow quantities are much less than that of the Wye, comprise a much more significant proportion of the total flow. It is possible to add the effects of outflow pipes and pills to the model as has been implemented in the NRA's use of the LORIS model, however, it is not feasible in the context of this work to have surveyed, gauged or obtained discharge information for such structures. As it was found that lateral inflow may have a significant effect on tidal heights, there may have been greater error in the modelled results due to poor levelling data of these structures, than any improvement to the model's accuracy they may have brought. Indeed during the review of the NRA Severn model there were some unreal situations where it appears that the model has been tuned to fit the known results at the expense of realism.

The flow equations can be adapted to include the continuous inflow terms by considering the quantity of flow and velocity per unit length from or towards the channel axis. Chapter 3 introduced the final flow equations including these two terms, which are reproduced as Equations 5.10 and 5.11. The non-linear velocity distribution described in Section 5.4.6 is

not included in these equations as it was found that the volume of work required to re-evaluate cross sections for this effect did not warrant the negligible changes to the modelled results.

$$B \frac{\partial Z}{\partial t} + \frac{\partial Q}{\partial x} = L \qquad (5.10)$$

$$\frac{\partial Q}{\partial t} + \frac{\partial}{\partial x}\frac{Q^2}{A} + g A \frac{\partial Z}{\partial x} + g A S_f - L\left(U_L - \frac{Q}{A}\right) = 0 \qquad (5.11)$$

It was necessary to find the sea wall heights on either bank of the Severn for the entire length of the modelled system at reasonable spacings. During the time span of the modelled tidal events, the sea walls in places have been improved and heightened so it was necessary to compile a set of sea wall heights at the times of the various modelled events through archive searches of aerial photographs, flood plain mapping, design records, seawall surveys and any additional field levelling which was required. To calculate the lateral inflow over a reach requires four values which are representative heights of the upstream and downstream seawall crests on either side of the channel. For the purpose of this work, troughs and pills between the locations of the section ends are effectively ignored so that the representative heights used, accounted for the most reasonable height which is usually the average crest height of the length of seawall to either side of the cross sectional point rather than the absolute height at the position of each cross sectional point. It was thus necessary to walk most of the seawalls bounding the Estuary between Gloucester and Avonmouth on the English and Welsh banks to determine that satisfactory representations had been collected and to level the crest heights where necessary. This was undertaken after the initial computer runs with a lateral inflow subroutine had been added showed that the overtopping of seawalls was a major contributor to the modelled results. This element of research alone took over two months.

It is difficult to describe the method of calculation of the flow overtopping the sea walls which has been derived for this work. Figure 5.10 illustrates how a 'normal' length of seawall between channel cross sections (x, y) is represented by a modelled seawall profile which has been divided into six equal sections divided by the points 1 to 6. To calculate the spillage out of the system over the seawall the reach is divided into 3 imaginary weirs (A, B & C) which

have sill heights equivalent to the calculated heights of the mid points (points 1, 3 & 5) of the three divided lengths forming a 'staircase' geometry of adjacent weirs.

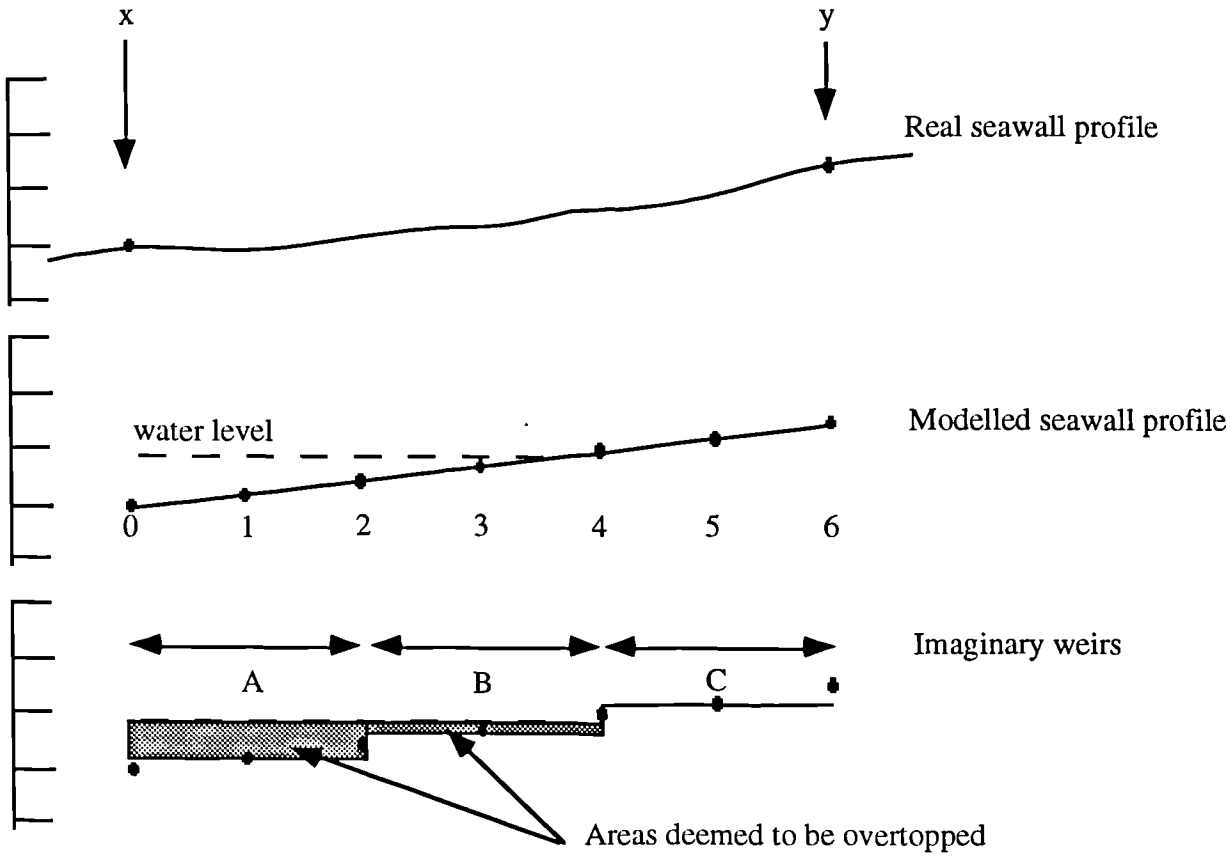

Fig 5.10. Schematic representation of seawalls for lateral inflow calculations.

In the example shown in Figure 5.10 the water level is above the crest of the seawall over nearly two thirds of its length and is deemed to be flowing over the seawall within the shaded areas indicated, the quantity of which is calculated using a weir flow equation which is indicated in Section 5.6. In this example there is slight over-estimate of the amount of flow in the area of weir B, however, this may also have been an underestimate of the flow had the water level been slightly lower than point 3. In reality it is not necessary to divide the length of the seawall up too greatly due to local dips and peaks in its length, however, if greater mathematical reality was required the section could be divided into more of the imaginary weirs to increase the definition.

In order for the inflow value to be correctly applied to the computer simulation the total flow is calculated for both sides of the channel and summed. This figure is divided by the total

length of the channel reach to give the lateral inflow per unit length. As the lateral inflow figures were found to sometimes add instabilities to the modelled solution, effectively because the sudden addition of a large lateral inflow was a 'shock to the system', the lateral inflow values were smoothed using the values calculated in the present and previous two time steps. A maximum outflow of $0.3m^3/s$ was permitted, which was obtained from the NRA's modelling of lateral inflow. The velocity of the lateral inflow was calculated in a simple manner by dividing the quantity of flow by the depth of water over the seawall at each imaginary weir divided by the length of the channel wall.

5.6 Weir Flow.

There is only one weir that needs to be modelled in the area of interest of the Severn, at Llanthony in the East Channel at Gloucester. The disruption to the overall flow regime caused by a weir in a river system of the size being modelled may be considered very small and may only affect the immediate area up and downstream of the weir. For this reason the weir problem was at first ignored and added to the computer model later and even then the weir was not modelled to a great deal of accuracy.

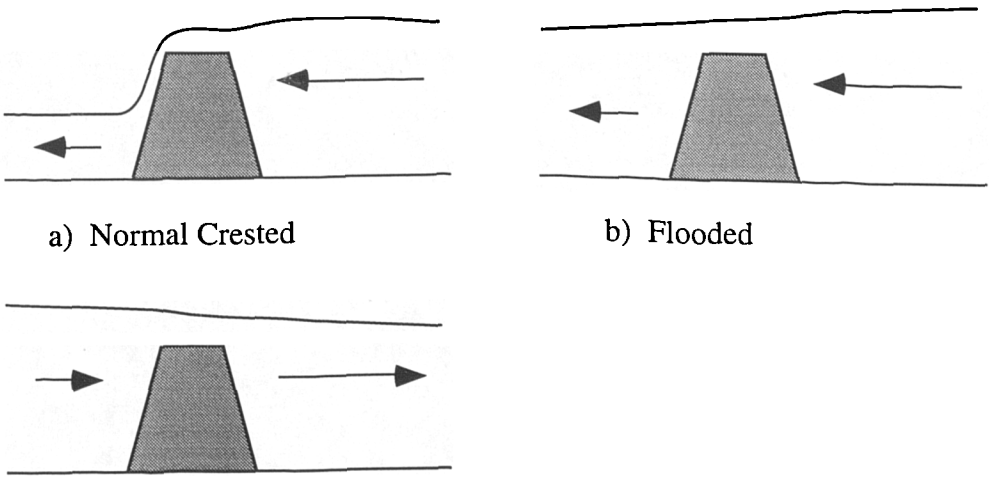

Fig 5.11. Simplified Weir Types.

The three weir flow conditions which need to be considered in this thesis are illustrated in Figure 5.11 and require different equations to solve the flow conditions occuring.

- Normal Crested Weir.

Flow over a normal crested weir is described by Equation 5.12 and is the most common occurrence in the area of interest.

$$Q_{us} = \mu_1 B_w (2g)^{1/2} (Z_{us} - Z_w)^{3/2} \qquad (\mathbf{5.12})$$

- Flooded Weir and Reverse Flow

Flow over a flooded or drowned weir is given by Equation 5.13 and can commonly occur when a very high tide penetrates the Upper Estuary or if the River Severn is in flood.

$$Q_{us} = \mu_2 B_w (2g)^{1/2} (Z_{ds} - Z_w) (Z_{us} - Z_{ds})^{1/2} \qquad (\mathbf{5.13})$$

Where Q_{us} = flow immediately upstream of weir

Z_{ds} = height of free surface immediately downstream of weir

Z_{us} = height of free surface immediately upstream of weir

Z_w = height of weir crest

B_w = width of weir

μ_1 and μ_2 = weir flow coefficients

The upstream and downstream terms do not refer to the geographical position of the cross section, but to the direction of flow. In most cases a cross section on the side towards the estuary mouth would be deemed the downstream section, however, if the flow is dominated by a riding tide coming up the estuary and flooding a weir, the cross section on the seaward side of the weir is considered to be the downstream section in a mathematical sense.

Computation of weir calculations can become quite complex depending upon the position in the process of calculations. For instance in the example of the normal crested weir when the upstream flow, downstream flow and upstream heights are known, then the

downstream height can be calculated using an internal boundary condition. The flooded weir case is much more complex and requires a subroutine to solve the relevant heights with a Newton iteration method. Although many of the sub-routines devised in the computer model are simple to follow, it is deemed necessary to describe the solution of the weir problem in this section.

A compatibility relationship is required which states that the quantity of flow upstream is equal to the flow downstream, i.e. $Q_{ds} = Q_{us}$. The computer programme decides whether the flow is reverse or normal and sets the values accordingly. The solution techniques do not allow that the height of the water surface is equal upstream and downstream, or that if the two values are very similar that the downstream height is calculated to be higher than the upstream one. The three cases are then treated as follows;

- Normal Crested Weir.

In the case of the weir at Llananthony and the direction of the solution methods in the two sweeps, the values downstream of the stage may be calculated but not the upstream heights. The downstream quantity of flow is therefore set to be the same as the latest calculated value of the upstream flow and the upstream height is solved using a Newton iteration method where the value of a function is solved with Equation 5.14.

$$Z_{new} = Z_{latest} - \frac{f(Z)}{f'(Z)} \qquad (5.14)$$

Thus solving for the upstream value of the stage where Q can be represented by (r - p Z)

$$Q_{ds} = Q_{us} = (r_{us} - p_{us} Z_{us})$$

$$f = \mu (Z_{us} - Z_w)^{1.5} - Q$$
$$= \mu (Z_{us} - Z_w)^{1.5} - (r_{us} - p_{us} Z_{us}) \qquad (5.15)$$

$$f' = 1.5 \mu (Z_{us} - Z_w)^{0.5} + p_{us} \qquad (5.16)$$

Where $\mu = \mu_1 B_w (2g)^{1/2}$, thus;

$$Z_{us} = Z_{us} - \frac{\mu (Z_{us} - Z_w)^{1.5} - (r_{us} - p_{us} Z_{us})}{1.5 \mu (Z_{us} - Z_w)^{0.5} + p_{us}} \qquad (5.17)$$

- Flooded Weir and Reverse Flow.

The relevant functions required to calculate the upstream values or downstream values of flow are shown in Equations 5.17 to 5.20.

$$f = \mu (Z_{ds} - Z_w) (Z_{us} - Z_{ds})^{0.5} - \text{abs}[(r_{us} - p_{us} Z_{us})] \qquad (5.18)$$

$$f' = 0.5 \mu (Z_{ds} - Z_w) (Z_{us} - Z_{ds})^{-0.5} + \mu (Z_{us} - Z_{ds})^{0.5} + p_{us} \qquad (5.19)$$

Where $\mu = \mu_2 B_w (2g)^{1/2}$, thus;

$$Z_{us} = Z_{us} - \frac{\mu (Z_{ds} - Z_w) (Z_{us} - Z_{ds})^{0.5} - \text{abs}[(r_{us} - p_{us} Z_{us})]}{0.5 \mu (Z_{ds} - Z_w) (Z_{us} - Z_{ds})^{-0.5} + \mu (Z_{us} - Z_{ds})^{0.5} + p_{us}} \qquad (5.20)$$

Following these calculations the value of Q is updated using p, r and the new value of Z.

5.7 Low Flow Conditions.

A problem inherent with all modelling methods of this type is that the model may predict surface altitudes less than or close to the bed level. In this case an additional calculation must be added to correct for this effect. To satisfy a simple model such as the one designed it is necessary that hydraulic continuity is maintained within the system. This is obviously not the case in the Severn where there are a number of topographic highs in the bed level which

effectively cut off flow between sections at extremely low tides. For the purposes of modelling a low flow method is added. Three systems were considered;

- Set a minimum flow level permitted and add a 'sweetening' flow.
- Use low flow calculations described in Cunge *et al* (1980).
- Treat low flow as a weir unit.

It was found after some 650 validation runs that a simple weir style calculation using Equation 5.21 or a modified weir equation such as the one used in the HRS LORIS study (Equation 5.14), gave the most satisfactory results. In no case were levels or quantities of flow expected to fully match reality, but low flow corrections are a vital necessity to maintain numerical stability in the modelled system.

$$Q = \mu_3 \left(\frac{g\,A}{B}\right)^{0.5} \qquad (\ \mathbf{5.21}\ )$$

5.8 Boundary Conditions.

A number of boundary conditions are required so that modelling can proceed, these include the external boundary conditions which represent the data such as the tidal curves and flood hydrographs at the upstream and downstream sections and the internal boundary conditions which mark 'breaks' in the continuity of the modelled system, where the De St Venant Equations are no longer valid.

5.8.1 External Boundary Conditions.

For the sub-critical conditions assumed to generally represent the flow conditions to be modelled in the Severn Estuary, an independent boundary condition is required at the upstream and downstream ends of the model. The following are thus required to lead to a proper solution of the proposed model equations.

- Discharge hydrograph upstream and stage hydrograph downstream, or
- Discharge hydrograph upstream and rating curve downstream.

It is easiest to use discharge hydrographs at the upstream limits of the system and stage hydrographs at the downstream limits in the context of this work. Rating curves are difficult to define and can be based on discharge hydrographs at the downstream end, which although implemented by Amien and Fang (1970), are dismissed by Cunge *et al* (1980) as they cause instabilities. The sets of external boundary conditions are responsible for the uniqueness of solution, thus irregularities in the data need to be carefully examined and smoothed if necessary. It was found in preliminary testing of the model that unsmoothed hydrographs at the downstream end of the model could cause fatal instabilities during modelling. The external boundary conditions modelled were digitised at five minute intervals and then linearly interpolated to give minute long intervals within the computer programme. The sources for the external boundary conditions were taken from NRA and Admiralty Data, although it must be stressed that the flood (flow) hydrographs obtained for the upstream boundaries were found to be inaccurate. The NRA has since developed a real time monitoring system which is far more reliable for upstream flow quantities.

5.8.2 Internal Boundary Conditions.

The are a number of internal boundary conditions, namely at low flow conditions, weir flow and at the junction of branched tributary systems which are solved by internal methods within the computer programme itself. The calculations impose discharge and stage relationships which are not represented by the flow equations defined in Chapter 3.

5.9 Initial Conditions.

Initial conditions describe the flow and tidal altitudes at the beginning of the model simulation. A benefit of the implicit scheme developed is that these values do not have to be particularly accurate. For simplicity the model run was started at the beginning of a high tidal

cycle so approximately high tidal values were used at all the cross sections, although the time of high tide is obviously not synchronous. Zero rates of flow, assuming the tide was on the turn were used as the quantity of flow at the initiation of analysis. There were a few problems encountered during the modelling associated with these assumptions especially if weir calculations are used in the simulation, such problems are described in the next chapter.

5.10 Rapidly Expanding Cross Sections.

In river systems where any of the values of breadth, wetted perimeter or cross sectional area change rapidly from one cross section to the next, then the De St Venant equations are no longer valid so internal constrains on the flow conditions are required. This is usually the case for cross sections where the breadth varies quickly due to a constriction or widening of the channel. However, the small time step adopted for this model (1 minute or 5 minutes) reduces some of the need for these additional corrections in some locations. It is difficult to define when the change in breadth from one section to the next is so great that an additional calculation is required. It was not found, however, that such adjustments made any major effect to the modelled output in this work and a subroutine developed for this purpose was not required in the final version of the computer programme.

5.11 Conclusions.

This chapter has introduced the practical aspects and data needs of the mathematical and computational models derived in Chapters 3 and 4. The following chapter describes how the assumptions used in the modelling process and the data reliability effect the outcome of the model simulation. It is the problems which have been discussed within this chapter that cause the greatest deviation from reality, rather than the original equations of flow and computational solution of those methods described in the previous chapters. So whilst it may appear that the greatest work effort is required in considering the actual theory of hydraulic flow and solution technique, it is the expertise of the model designer in establishing the validity of the raw data

being analysed and how it is treated in conditions where the flow no longer can be represented by the De St Venant equations which makes one model differ in reliability to another.

CHAPTER 6

COMPUTER MODEL AND VERIFICATION.

6.1 Introduction.

This chapter introduces the computer model developed and how it has been adapted to give the most satisfactory results. The computer model developed was subject to more than six months of verification testing to evaluate the sensitivity, stability, accuracy and computational necessity of a variety of mathematical procedures. Although it is not practical to reproduce most of the modelled results because of the shear volume of data involved all the major variations in analysis will be described and discussed upon merit.

6.2 The Computer Program.

A copy of one of the most frequently used forms of the computer program developed is listed in Appendix D of this thesis. The computer program has been adapted during its development, both becoming more complex, for instance in the development of a branch network of channels and becoming simpler when it was realised that some factors were not necessary in view of the detail of information available for insertion in the model. A breakdown of the program is given in the following sections as well as a flow diagram of the model's execution. The program has been written in the FORTRAN (ANSI -77) programming language because of the 'number crunching' capabilities of the language and has been run on Sun (SPARC) workstations. Program editing was undertaken using the 'VI' text editor and debugging using 'DBX'. The program has not been designed to conserve memory by using small array sizes. Therefore, although debugging was easier as there were many data values preserved within these arrays which could be examined, running time in debug was very slow and could not be undertaken in the user friendly 'Sunview' windows mode.

6.3 Program Description.

A flowchart describing the execution of the program is given as Figure 6.1 whilst the program that it describes is given in Appendix D. This flow chart shows only the major subroutines and decision making parts of the program.

The following sections describe the relevant executable parts of the program, giving reference to their theoretical origins in earlier chapters. When considering the process of the modelling procedure it is necessary to consult the flow chart in Figure 6.1 and the FORTRAN program itself. A list of notation used in the computer model as well as the preceding chapters is presented in Appendix B.

6.3.1 Program Initialisation.

The first part of the computer program initialises the model by declaring the variables to be used and by reading all the external data files where the information to be manipulated by the program is stored. The initialisation process can be divided into the following;

- Declare Variables.

This section of the program defines the variables used in the main body of the program, including the relevant arrays according to FORTRAN (ANSI -77) protocol. A description of the variables used in the program is given in the initial lines of the computer listing.

- Declare Common Blocks.

This part of the program declares the common blocks used by the program which is a convenient memory management system and to a minor degree a time saving exercise in producing the program. The common blocks are used to 'hold together' the frequently used variables in the program which are exchanged between the main program and subroutines during execution.

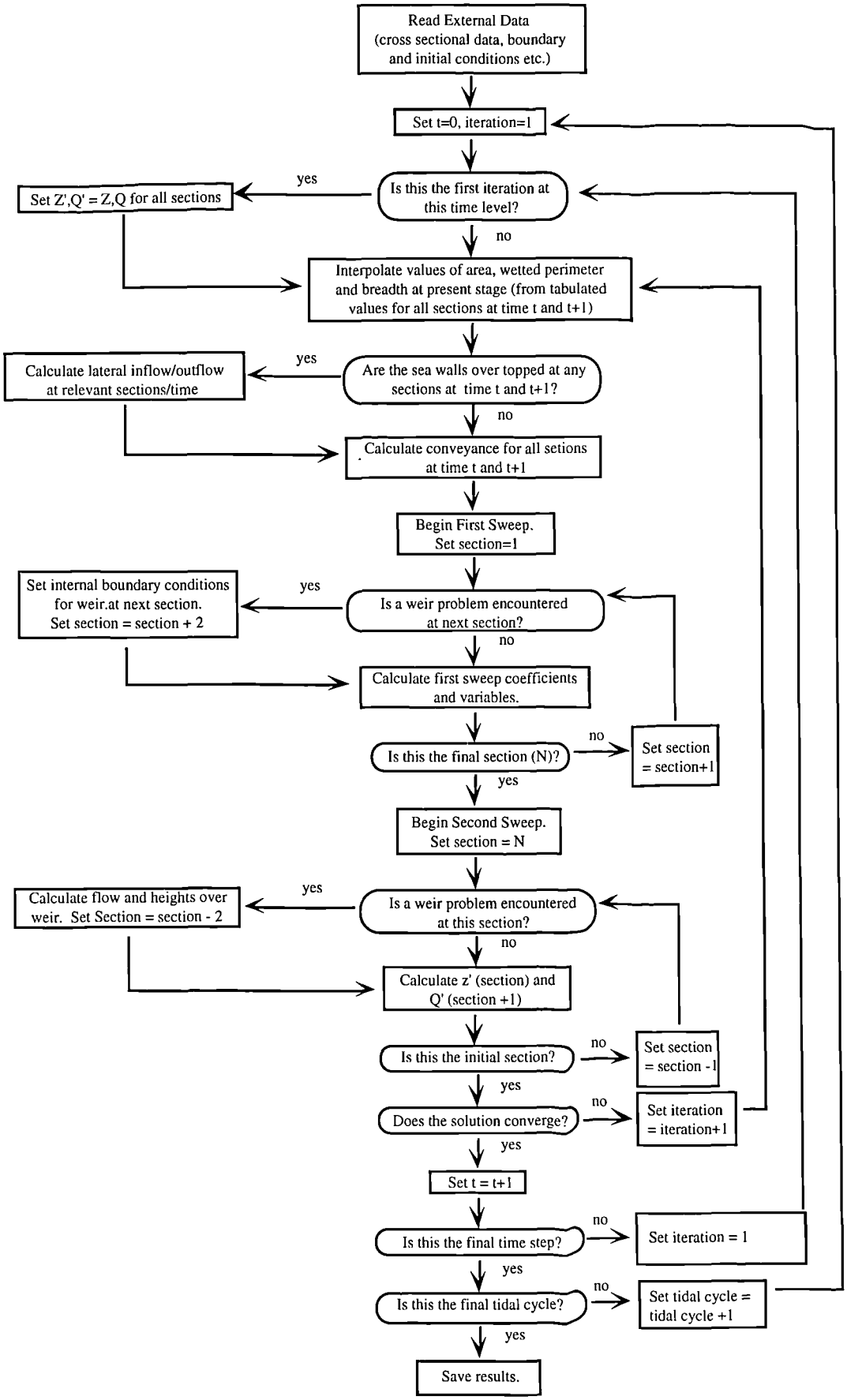

Fig 6.1. Flowchart for Computer Program Execution.

The common blocks used in the program are the following:

hthydro saves all the height dependant values of the area (a), breadth (b) and wetted perimeter (wp) for each section. These tabulated values are read from the external cross sectional data files and are at metre intervals, calculated in the manner specified in the previous chapter. Each of these parameters is stored in an array of the form a(b, n, h) where b represents the branch number, n the number of the cross section and h the height in metres AOD. Therefore a(1, 10, 9) will store the value of the cross sectional area at section number 10 on branch 1, when the water surface height is 9 mAOD.

thydro stores the time dependant values of area, breadth, wetted perimeter, conveyance and friction for each section. These variables change during the program apart from the friction when a constant global friction value is specified to represent the hydraulic properties of an entire section. Apart from the friction value, these variables are stored in the form of branch number, section number and time step. Thus area (1, 10, 9) stores the value of the cross sectional area that has been calculated for cross section number 9 on branch 1 at the 9th time stage. In the program in Appendix D, friction is not time dependant but remains constant during the period being modelled at any section.

weight is a small common block that stores together the time weighting factor (theta) and time increment (tinc) in seconds.

inf is the common block that groups together the calculated and tabulated values involved in the calculation of the lateral inflow or outflow namely the quantity of outflow (l), velocity (ul) and the sea wall heights on either side of the channel (lh, rh) at each cross section.

weirdo is an enigmatically named common block describing the relevant description of the weir parameters, namely the weir position (weirpos), weir height (weirht) and weir breadth (weirb) for all weirs.

dependants groups together the two dependant variables which are the backbone of the model solution which are the height (z) and the quantity of flow (Q) for each cross section.

coefficients is a 'bucket' common group that contains the other commonly used and transferred coefficients within the program and subroutines, namely the values of the calculated variables p, qq, r, s and tt.

- Read External Data Files.

This part of the program tells the computer 'what to do' and 'where to do it from', i.e. where to find the relevant files to read, open them and set up the parameters used throughout the program. It can be divided into the following subsections:-

- Read Weir Information.

The information about the weirs to be modelled is saved on an external file in the following form;

i) Whether a weir calculation (weirprob) is to be used and the number of weirs in modelled system (noweirs)

ii) The position of the weirs in the form of the branch number (branch) and section number (sect) where the weir is present.

iii) The height of the weir (weirht) and breath of the weir (weirb) at the weir position.

Stages (ii) and (iii) are repeated for each weir (noweirs times). A variable at the position of the weir (weirpos) is assigned the value 1 (or logically 'true') to denote to the main program that when this position is met then a weir problem will be encountered if the weir problem is to be evaluated, otherwise the program skips the position.

- Read Time Increment, Time Weighting, Convergence Tolerance and Number of Tidal Cycles to be evaluated.

This section reads a simple external file to give the necessary coefficients and convergence criteria and also includes the number of tidal cycles to be calculated before the solution is deemed to be satisfactory.

- Read Data from General Branch Files.

The data contained within these files for each of the branches of the modelled network comprises the following form:-

i) Number of sections on branch (nosects).

ii) Name of section (names), distance of section reach (xdist), global friction value for section (friction) and seawall heights (lh, rh) on either side of channel.

Part (ii) is repeated for each section along the branch, i.e. nosects number of times.

- Read Individual Section Files.

For each section the following information is read:-

i) The value of the minimum elevation of the channel bed (least) in metres AOD.

ii) The maximum height (mx) to which the channel properties are tabulated on the external file which is generally 12m AOD.

iii) The values of the sea wall heights on the left hand (lh) and right hand (rh) sides of the channel in metres AOD (there is an option to use seawall heights read earlier in the program).

iv) The cross sectional area of the channel (a) at every tabulated (metre interval) water surface stage, in square metres.

v) The breadth of the channel (b) at every tabulated (metre interval) water surface stage, in metres.

vi) The wetted perimeter of the channel (wp) at every tabulated (metre interval) water surface stage, in metres.

These individual section files also include the tabulated values of the non-uniform velocity variation and calculated values of conveyance using compound channels of varying friction. The cross sectional data which is processed to give the values of i) to vi) above is stored after the tabulated values in the form of the distance, channel elevation and friction of that slice of the channel, although this is not used in the main program example given. The methodology for computing the hydraulic properties has been given in the previous chapter, Figures 6.2 and 6.3 illustrate a sample data file for a cross section (Gatcombe).

Row 1	-1.02 12 11.82 12			
Row 2	0.0956250000000	258.97551373626	695.33246785714	1395.9681111111
Row 3	2526.2772500000	3678.0233779461	4845.2765833333	6051.2397391304
Row 4	7266.2914942792	8486.3089191457	9724.4885150502	10977.566552954
Row 5	12235.556519509	13499.384000000		
Row 6	9.5625000000000	418.57197802198	471.67785714286	1008.8527777778
Row 7	1144.0083333333	1159.4839225589	1178.1083333333	1211.8927536232
Row 8	1217.1901601831	1225.5349351640	1250.6220735786	1255.5340022297
Row 9	1260.4459308807	1268.2000000000		
Row 10	9.5628776654482	418.62144719037	471.80625493389	1009.0806667597
Row 11	1144.3700047301	1159.9791272206	1178.7360504831	1213.4575197354
Row 12	1219.8345615966	1229.2442370510	1255.3560761130	1261.3407847947
Row 13	1267.3254934764	1276.1193786216		
Row 14	0.2959008339179	15689.655071309	72186.351234325	174178.08027738
Row 15	358212.18557126	615731.27195826	936359.99565875	1314240.0510217
Row 16	1748387.9580292	2233908.6513883	2768505.2757290	3350630.9539883
Row 17	3978316.8856026	4650048.4048459		
Row 18	1.0000046051808	1.0531348509211	1.0235522705345	1.0994913329456
Row 19	1.1088944572165	1.0771124198460	1.0579251653273	1.0511817697249
Row 20	1.0450738313969	1.040751111i2071	1.0389280268747	1.0382437332751
Row 21	1.0377270560588	1.0374564560131		

Fig 6.2 Sample cross section data file (part 1).

The data stored in the section of file indicated in Figure 6.2 is described below in terms of the rows illustrated;

Row 1:	Minimum bed level, maximum tabulated stage, left seawall height and right seawall height.
Rows 2 to 5:	Areas at metre intervals of the water stage from -1 mAOD to 12 mAOD.
Rows 6 to 9:	Breadths at metre intervals of the water stage from -1 mAOD to 12 mAOD.
Rows 10 to 13:	Wetted Perimeter at metre intervals of the water stage from -1 mAOD to 12 mAOD.
Rows 14 to 17:	Conveyance at metre intervals of the water stage from -1 mAOD to 12 mAOD, using compound channel calculations.
Rows 18 to 21:	Bossinesq coefficient of variable flow velocity at metre intervals of the water stage from -1 mAOD to 12 mAOD.

Row 22	0.	11.820000000000	3.5000000000000D-02
Row 23	4.6000000000000	11.640000000000	3.5000000000000D-02
Row 24	19.200000000000	8.6500000000000	3.5000000000000D-02
Row 25	35.500000000000	8.4900000000000	3.5000000000000D-02
Row 26	43.700000000000	7.9200000000000	3.5000000000000D-02
Row 27	48.900000000000	7.5600000000000	3.5000000000000D-02
Row 28	52.900000000000	6.4200000000000	2.8000000000000D-02
Row 29	62.600000000000	5.1600000000000	2.8000000000000D-02
Row 30	92.600000000000	4.9800000000000	2.5000000000000D-02
.	.	.	.
.	.	.	.
Row 40	230.00000000000	1.7900000000000	1.5000000000000D-02
Row 41	244.00000000000	1.8900000000000	1.5000000000000D-02
Row 42	258.00000000000	1.8900000000000	1.5000000000000D-02
Row 43	272.00000000000	1.8900000000000	1.5000000000000D-02
Row 44	290.50000000000	1.6800000000000	1.5000000000000D-02
Row 45	309.00000000000	1.6900000000000	1.5000000000000D-02
Row 46	324.00000000000	1.4800000000000	1.5000000000000D-02
Row 47	338.00000000000	1:4800000000000	1.5000000000000D-02
Row 48	358.00000000000	1.3300000000000	1.5000000000000D-02
Row 49	378.00000000000	1.2500000000000	1.5000000000000D-02
Row 50	398.00000000000	1.2500000000000	1.5000000000000D-02
.	.	.	.
.	.	.	.
Row 70	693.50000000000	1.8300000000000	1.5000000000000D-02
Row 71	710.00000000000	1.7800000000000	1.5000000000000D-02
Row 72	719.00000000000	1.7800000000000	1.5000000000000D-02
Row 73	728.00000000000	1.7800000000000	1.5000000000000D-02
Row 74	736.50000000000	1.7100000000000	1.5000000000000D-02
Row 75	745.00000000000	1.6600000000000	1.5000000000000D-02
Row 76	761.00000000000	1.6100000000000	1.5000000000000D-02
Row 77	777.00000000000	1.2100000000000	1.5000000000000D-02
Row 78	793.50000000000	0.2100000000000	1.5000000000000D-02
.	.	.	.
.	.	.	.
Row 100	1146.0000000000	-0.9200000000000	1.3000000000000D-02
Row 101	1169.0000000000	-0.9700000000000	1.3000000000000D-02
Row 102	1191.5000000000	-1.0200000000000	1.5000000000000D-02
Row 103	1214.0000000000	-0.2200000000000	1.5000000000000D-02
Row 104	1230.0000000000	1.1800000000000	1.5000000000000D-02
Row 105	1246.0000000000	1.5800000000000	1.5000000000000D-02
Row 106	1268.0000000000	5.1000000000000	2.5000000000000D-02
Row 107	1268.2000000000	12.000000000000	3.5000000000000D-02

Fig 6.3 Sample cross section data file (part 2)

The data stored in rows 22 to 107 of the cross section data file indicated in Figure 6.3 is the channel survey, giving the distance across the cross section, the bed level elevation in mAOD and the estimated Manning's friction for the point in each row.

- Read Digitised Values of the Boundary Conditions.

These are read from external files giving the values of the tidal curve at the seaward end and the upstream values of flow. The values of the tidal heights at the initial downstream section are read from a pre-processed digitised tidal curve, where the height of the water surface is stored at five minute intervals. The program interpolates (linearly) between these values to give the tidal heights at the downstream section at minute intervals. The upstream boundaries represented by quantities of flow are similarly pre-processed and saved as an external file and are also read at five minute intervals. The program again interpolates linearly to give the values as minute intervals.

- Read Initial Conditions.

The values of flow (Q) and stage (z) are read for each section for the very first time level (t=0). As the solution rapidly moves away from these values they only need to be approximate to start the program off, especially in the case of the height, with the program beginning at high tide, the values of z to start with at each section are approximate to the estimated high spring tide at each point. The quantity of flow in similar models is usually set at zero and assumes that the tide is on the turn. However, if a weir problem is encountered it is preferable to have a nominal amount of flow at the weir section for computational purposes, hence the initial values of the flow are set to the initial value of flow at the upstream boundary of the relevant branch and to the sum of the branches for the main channel.

- Read Values of Lateral Inflow.

Originally this part of the program was to read time dependant lateral inflow values for the sections to account for small additions to the system such as outflow pipes and pills, utilising known data or information from previous model runs. However, it was found satisfactory to set all values of lateral inflow to zero at the start of program execution.

- Read Stations.

As it is not practical to save all the tidal data generated for every channel cross section, because of the demands on computer file space, a number of representative sections have been selected

and the modelled flow and stage through out the tidal cycle saved to file for these stations after completion of the modelling.

6.3.2 Program Calculations.

The process of execution by the program is shown in a simplified form by the flow chart illustrated in Figure 6.1. The individual sections of the program are described in a general manner in the following paragraphs. Further details of sections of the computer program deemed necessary to describe are included in the more technical section, 6.6, later in the chapter.

- Set Values for First Iteration.

If this is the first iteration at any time step, then the values of z and Q for the next time step have to be set, otherwise they will be equal to zero, or the values calculated at the same time step on the previous tidal cycle. This is obviously an estimated value, so they are set to be equal to the values of z and Q at the present time step, i.e. $Q^* \& z^* = Q \& z$ for all sections on the first iteration.

- Interpolate values of area, wetted perimeter and cross-sectional area.

All the data for the hydraulic properties of the sections are saved on external files, where the cross sectional area, etc. are stored at metre intervals of the water stage. During the program execution the stage will fall at intermediate heights between these metre spaced values so that the values of variables describing the hydraulic properties have to be determined by interpolation. The subroutine *Interpol* uses a simple linear interpolation calculation to do this. In the literature review of similar models it was found that many models use a too great a separation of tabulated heights, often at 2m intervals or more, so that the interpolated values are prone to considerable error. When the stage approaches the heights near to where the flood plain lies, during a metre increase in stage, the area, and especially breadth and wetted perimeter may increase at an exponential amount with the free surface elevation. Similarly

when the water stage approaches the bed level, large changes in the hydraulic properties can occur with a small rise in the stage.

- Calculate any Lateral Inflow or Outflow.

Every section is checked whether the seawalls are overtopped on either side of the channel at the section. If this is the case, then the subroutine *Inflow* is summoned which calculates the lateral inflow by the method described in the previous chapter.

- Calculate Conveyance.

The conveyance at all the sections at the present and following time steps is calculated using the Manning Roughness Coefficient in the subroutine *Convey* using one of the friction laws described earlier in the work.

- First Sweep.

The first sweep ultimately calculates the exchange variable used in the second sweep to calculate the values of stage and quantity of flow at the next time level. The first sweep proceeds in the following manner;

i) Checks to see whether a weir problem is required by the program at the given section. If the weir problem is necessary then an internal boundary condition is deemed to be present and the values of the exchange variables, p and r are set accordingly via the subroutine *Sweep1weir*.

ii) When a weir calculation isn't relevant to a section, the program calls the subroutine *Sweep1* to evaluate the following coefficients derived in Chapter4.

a. The coefficients c1 to c7.

b. The variables alpha to epsilon.

c. The exchange variables branchalpha, branchbeta and branchgamma if a branch in the channel is encountered The exchange variables p, r, tt, qq and s which are passed back to the

main program. The exchange variables p to s are calculated for all sections or set at the relevant boundary sections.

- Second Sweep.

The second sweep calculates the values of the stage and discharge at the next time level in the following order using the coefficients calculated in the first sweep subroutine.

i) Checks to see whether a weir problem is required by the program at the given section. If this is the case then the program calls the subroutine *Sweep2weir*, which works by calculating the height using the present estimate of the quantity of flow and the type of weir.

ii) If a weir problem is not encountered then the program proceeds through the subroutine *Sweep2*, which runs in the following manner;

a. Calculate the value of the stage at the next time level at the river branch if encountered.
b. Calculate the value of the discharge and height at consecutive sections (the order of which depends on the branch where the section is situated).
c. Checks to see whether the stage is at a level below the bed level at the section, assigns a small nominal flow if this is the case.
d. Checks whether a low flow calculation is required (i.e. depth < 0.4m) and calculates the discharge accordingly.

The second sweep calculates the stage and discharge for all the sections, with the exception of the relevant external boundary conditions.

- Check for Convergence.

The program uses a crude, but satisfactory convergence criteria within set tolerance limits for the variation of Q and z, and checks whether a further iteration is required, or whether the computations can move to the next time step.

6.3.3 Output Final Data to File.

Once calculations are complete the program saves the calculated data to file in the following forms.

a) Time, stage, discharge, velocity and lateral inflow, giving the values at ten minute steps. These files are saved for the sections stipulated in the initial reading of the data in the stations file.

b) Distance, maximum stage, minimum stage, time of maximum stage, time of minimum stage, maximum lateral outflow, section name for the modelled system.

6.4 Model Development.

There were several distinct stages in the development of the model where major re-programming was required due to the addition of a new feature to be simulated. The growth of the model was related to collecting new data, such as seawall surveys being completed and to the growing knowledge of the designer. Several distinct phases of the model developed are described as follows.

- Single Channel Model.

The very first analyses were undertaken on a theoretical channel comprising of a number of simple trapezoidal sections to test whether the designed model functioned realistically and to try and assess the effect of varying time steps and time weighting factors on the model results. The first simulation of the Severn was a simple model which only considered the West Channel at Gloucester and ran to Brean Down at Weston-Super-Mare. The modelled reach was curtailed due to the tidal curve availability (i.e. the Admiralty figures) for Avonmouth, so downstream of Avonmouth was omitted. Similarly this omission was also justified because of the two dimensional circulation patterns in the wider mouth of the Estuary and the problems with giving a realistic value for the wetted perimeter and considerations for the embayments.

- Single Channel Model, Non-Homogenous Velocity Variations.

The first model adopted a global friction value for a cross section of the channel which represented the entire frictional characteristics of the cross section and was used to evaluate the conveyance within the main program. The effects of varying friction values across the section and thus non-homogenous velocity variations (using the Boussinesq correction) were determined by calculating the conveyance and Boussinesq correction in the pre-processing of the cross sections. It was found that there was no benefit in undertaking these additional calculations and that the time taken to adjust a cross section's characteristics, if required, was such that it did not merit pursuing the effect of compound channels.

- Branched Solution.

A branched solution was adopted because it was thought that it would add a greater deal of realism and numerical stability especially at low flow levels. The model was easily adapted for branch solution, although it must be noted that in the computer program presented in Appendix D, the solution is based specifically for the network assumed for the Severn, rather than a 'model system' which may be used for any river system. This process was adopted to save time during the model development. It is important to note that the solution considers the branched system around Gloucester only, although the outflow of the Wye and Frome are much greater than those considered for the East and West Channels. However, the selection of tributaries to be modelled is based upon the proportion of the total channel discharge the river represents at the point of inflow. Although the River Wye is the largest of the tributaries to flow into the modelled area of the Severn, the Wye system represents about 1% or less of the total channel discharge at its inflow, so it was deemed that to model the Wye as a branch would have no discernible effect upon the required results and would increase computational time. Hence the effect of this tributary's flow was not modelled. In addition, no reliable cross sections were available for the Wye and similar tributaries so it would have been difficult to justify any further consideration. The two channels at Gloucester, however, have been surveyed and although the West Channel conveys much of the flow the East Channel can commonly convey one third of the total flow above the confluence at Lower Parting.

- Weir problems adopted.

There are two weirs in the modelled area of the Severn, Maisemore Weir, which is used as a boundary section and Llanthony Weir which was modelled as a 'normal' section. The weir problem calculations were added to give a more representative flow over the weir at Llanthony, and in dealing with low flow over what might be theoretically deemed to be a weir sill represented by a rock bar in the channel. The results of considering the weir problem are given in Section 6.5 and it can be seen that the effect of modelling weirs increased computational time considerably without affecting the modelled heights. This might provide an argument that modelling weirs in this system is a computational luxury, however, the modelled discharges proved to be much more realistic. Weir calculations in a system as big as the Severn are in essence a minor perturbation of the overall flow so it is the modeller's responsibility to decide whether a weir denotes a significant factor in the channel flow.

- Lateral inflow/outflow.

This was added at a late stage, mainly due to the problem of obtaining the relevant data any earlier. Early levelling of the sea-walls came from the HRS after some time. These heights are in many cases lower that the present seawall heights as there has been a gradual improvement policy of the tidal defences of the Severn Estuary. This presented several difficulties in the modelling process. Firstly in the verification of the model, using already known tidal curves or discharges, the heights of the seawalls when the known tides occurred had to be used, so it was necessary to work through all the data available (improvement plans, levelled surveys, council records, etc.) to get an acceptable chronology of the seawall improvements. Subsequently for modelling later tides the new seawall heights had to be used, in many cases it was necessary to go into the field and level the wall crests. The evaluation of the lateral inflow or outflow does not take into account local depressions in the seawall between sections. It was also found that the outflow (i.e. spillage over the walls) could be modelled with ease, yet it was almost impossible to account for how, where and at what rate, the water returned back to the main channel from behind the walls without expanding the model considerably to include flood plain flow cells. Two options were available; one was to ignore the inflow, effectively losing any water which flowed over the seawalls on the high tide as this creates problems when

low flow levels were encountered. The second option was to instruct the program to deliver the spillage back to the system at low tide at a similar rate to which it left the system at high tide, which of course, is not particularly natural. It was found satisfactory to adopt the former.

6.5 Preliminary Analysis and Validation.

The first stage in model validation, based on the work of Howes (1985) and Sargent (1982) is the *Mathematical Model Verification* stage which is achieved during the model development stage. This involves a subjective process of assuring that the assumptions adopted in the mathematical model represents the behaviour of the real system which it simulates. In the case of this model the De St Venant assumptions have been adhered to as the main source of derivation of the flow equations, with the additional quasi-two dimensional effects listed in the previous chapters. Many of the required stages of the verification of the mathematical model have already been addressed in the earlier chapters, although some additional simplifications which were thought to be unrealistic, but adopted once their effect had been determined through modelling, will be mentioned in this chapter.

Before the model was used a series of verification tests were undertaken to define the overall effect of all the variables entered into the system and their co-variance, so the mathematical stability and sensitivity of the model could be assessed. A model which is insensitive to data differences may 'pass' erroneous data with the user being unaware that non-reality was being modelled. For instance, if a tidal cross section should have been $500m^2$ but an error caused this to be one tenth of the value, then a program which is relatively insensitive may calculate as normal, indicating that for some instances the data fed into the program has little influence on the result. Until the model had been developed to a stage where there was confidence in the accuracy of the input and output data, checking for erroneous processing could only be made by examining all the calculated data for 'glitches' or errors flagged up by the computer. With further insight into the nature of the program the need to double check all the results reduces as the modeller can anticipate where errors are occurring. At least 1500 runs were made during the early stages of analysis on a series of simple and then increasingly more

complex simulations. It is obviously not feasible to present all these simulation results, so the factors affecting the modelled results are described and shown graphically or tabulated only where apposite. In general this section will present the overall findings of the model runs, and highlight the 'worst case' diversions from the expected model behaviour, namely secondary oscillations brought about by instability in the solution.

6.5.1 Verification of Computer System Consistency.

The second phase in validation is termed the *Computerised Model Verification* stage which is designed to check that a program carries out the processes expected of it, thus correctly representing the designed model. Effectively this stage is the 'debugging' stage of the program where the compiled computer code is checked that it works correctly, by detecting typing errors, particularly wrong numbers in calculations and the order of execution is correct. This exercise was undertaken using a debugger and following the code execution line by line. A compiled program needs to be checked for repeatability of results (Hermann, 1967). Although it seems unlikely, the model needs to be run several times with the same input data to assess whether the same results are being output each time. Initially the model was run several times to validate the repeatability of the analysis when any input data or programming was changed, but at later stages the model was run only once unless reprogramming had been undertaken. No occasions of non-repeatability were encountered, thus the model is considered internally valid. Brately *et al* (1983) suggested that results from small computer simulations should be checked against hand calculations to verify the computer code. Although this approach did not identify any significant errors, it did help validate that using 'real' numbers, i.e. to eight decimal places, rather than double precision numbers in the program was acceptable, i.e. no problems were being generated through rounding errors which can be associated with using less memory intensive real numbers. However, the sheer bulk of calculations within the model meant that only subroutines, or even parts of subroutines could be tested and checked by manual methods.

The verification of the computer model system proceeded by testing the rigour of the model by adjusting many of variables used in the program. Commonly hidden errors in the

program code or indeed in the mode of behaviour of the program only appear when extreme parameter values are entered. Such testing of the model is called sensitivity analysis and is demonstrated in the next sections. Analysis of the sensitivity of a model uses two rationales; the Deterministic Approach looks at the effect of changing the individual parameters on the modelled output, whilst a Stochastic Approach looks at the overall effect on the scheme when the input parameters, defined by a likely distribution, are all co-varied.

6.5.2 Effect of Time Increment.

The computer model has been run at 10, 5 and 1 minute time steps. It was found that the longer time steps generally were calculated quicker, due to the lesser number of mathematical operations required. However with larger time steps the peak high waters could be damped by up to 10 cm, because they were effectively missed, i.e. fell between the calculation points, so that the short time step produced a higher resolution.

In this and additional sections of the chapter the run time of the computer program is referred to. However a direct comparison of computer run times is difficult because the overall running time is dependant on the number of other tasks the computer is running and thus the demand on the operating system. It was also found that different machines (with similar operating system capabilities) had differing run-time characteristics, due to different installed software and network demands. Running times were generally less than fifteen minutes.

6.5.3 Time Weighting Coefficient.

The time weighting coefficient, ø, referred to in Chapter 4, was varied to find it's effect on the modelled results. It was found that higher values of ø, above 0.8, damped the data slightly, to an order of about 10 cm total on the largest tidal ranges modelled, but provided smoother tidal curves especially towards low flow periods. At values of ø less than 0.52 secondary 'noise' or small instabilities occurred, generally at low tide (due to shallow depth calculations being incurred at some point in the model). It was found that adopting a value of 0.5 for the time weighting coefficient was not practical because of fatal instability

problems. In the final tidal simulations a time weighting factor of 0.66 was adopted, as it provided the greatest accuracy, with little or no instability problems.

6.5.4 Effect of Friction.

The friction values used to describe the characteristics of the channels are the single most important factor in influencing the eventual results of the simulation. The behaviour of the friction values can be summarised as follows.

- High friction values amplify the tide less than lower ones, thus simulations show a smaller tidal range by reducing the tidal maxima and raising the tidal minima compared to simulations run with lower friction values.
- Higher friction values retard the progression of the tide more than lower values when a tidal influence is encountered.
- High friction values raise both the tidal maxima and minima in upstream reaches when a significant tide does not penetrate, i.e. during steady river-like flow or gradually varying flow conditions.

The effect of friction values adopted for the Estuary for a tide approximately representing a spring and neap tide are demonstrated in Figures 6.4 and 6.5, where the same friction value has been used for every section.

Figure 6.4 clearly shows that the high tide does not significantly penetrate more than about 42km upstream of Avonmouth (Newnham) on a neap tide, above which the Estuary is dominated by river flow. The river flow heights are higher in the Upper Estuary when higher friction values are used. The greatest change in bed levels occurs between 30 to 45 km upstream of Avonmouth, when the acceleration along the gradient is such that the friction values have little effect upon the low tide height, whereas between 20 to 30km upstream of Avonmouth, at Slimbridge and the Noose, the widening, shallowing and reduced bed level gradient means that friction values can cause approximately 0.75m difference in the height of

the base flow. For a neap tide, friction values have little effect on the height of the high tide in the Lower Estuary, thus the graphed high tides are nearly similar.

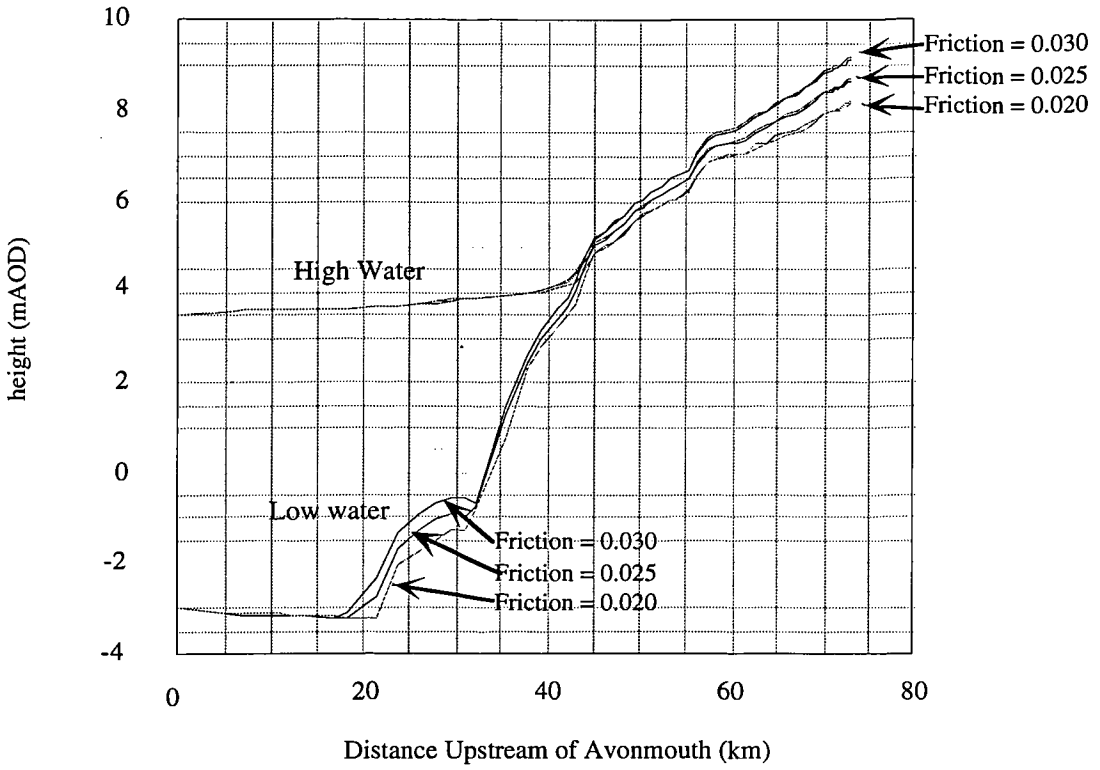

Fig 6.4 Effect of friction on a 'neap' tide.

Figure 6.5 shows the importance of friction values on the height of high tides which penetrate the Upper Estuary as they become increasingly amplified and that significantly lower tides are also calculated in the Lower Estuary, which can lead to low flow problems in the Lower and Mid Estuary. There is a vast difference in the low water levels in the Lower Estuary about 19km upstream of Avonmouth at Narlwood rocks which is constricted by the Oldbury Reservoir. However, when additional schemetisation (an extra cross section) was added, or a schematic section which did not include the reservoir, i.e.was modelled as the channel before the structure was built, then this problem was not solved. It seems that the simulation is unable to cope fully with the sudden rise in the channel bed upstream of Narlwood and the invoked low flow calculations cannot account for extreme low flow in this area. However, when the final modelling was completed, sensible friction values

downstream meant that this problem was generally minor and did not significantly affect the overall modelled results. It was found that on a spring tide, if friction values were set to less than 0.022 (Manning) for all sections downstream of Berkeley, then a fatal instability occurred through a non-correctable low flow problem when tides had a range in excess of the spring tide.

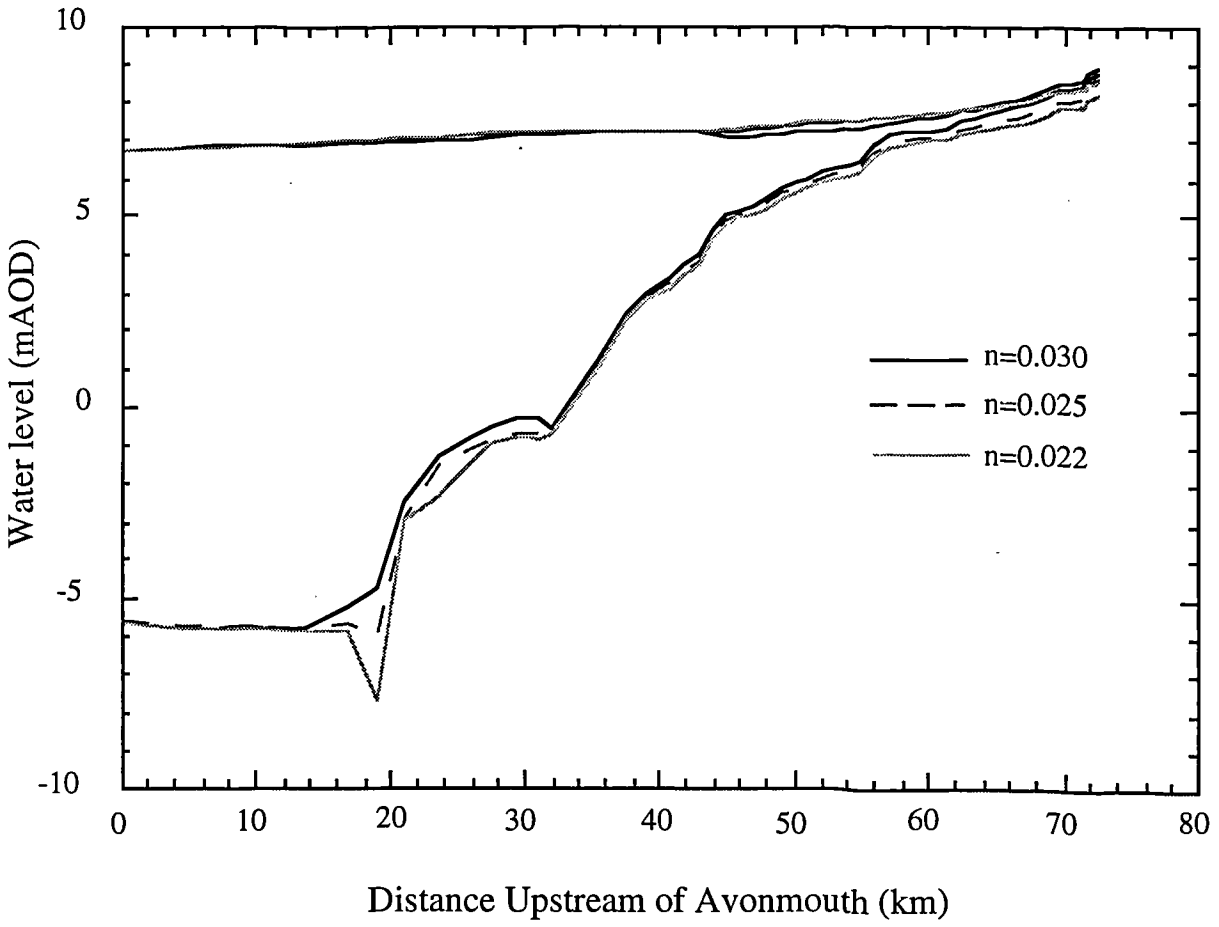

Fig 6.5 Effect of friction on spring tide heights.

6.5.5 Effect of Weir Calculations

Using weir calculations does not affect the high or low tide levels in the system other than by about 2 cm in the region of the weir (either higher or lower) in all modelled cases. However, the quantity of flow in the proximity of the weir is different, and bears a greater

semblance to reality in the upper modelled regions both upstream and downstream of the weir, but is generally more time consuming in analysis, as the model takes longer to converge to a solution.

When steady flow conditions prevail, then a simulation that does not use a weir calculation provides smoother results of the quantity of flow. If the weir calculation is invoked then spiky 'noise' oscillations, of less than 1.5% of the total amount of flow occur around the value calculated by the simulation not accounting for weirs. Although this suggests that on neap tides or tides which do not penetrate far up the Estuary, ignoring weir flow conditions provides a better solution, the 1.5% error in modelled flow quantities are far less than the errors in the measurement of flow at the upstream boundary. It was found that there was no difference in the modelled tidal levels when weir calculations were used and that in nearly all conditions it was found that calculating for weirs was a computational luxury, except when reverse flow occurs.

6.5.6 Effect of Upstream Boundary Conditions.

The effect of upstream boundary conditions (quantity of river flow) for a simple example for both a non tidal simulation and a tidal simulation are shown in Figures 6.6 and 6.7. These graphs show the effect of the quantity of flow at the upstream boundary on the neap and spring tide heights. The graphs are labelled by the approximate total flow of the East and West Channels when they converge at the Lower Parting As for all the graphs in this chapter, the distances upstream of 71 km from Avonmouth apply to the East Channel heights, heights in the West Channel are generally similar. Channel flows at Lower Parting are in m^3/s in the two figures.

- Spring Tide.

The Spring Tide (Figure 6.6) illustrates how the quantity of upstream flow can effect the high and low tidal heights from about 36km upstream of Avonmouth to the Estuary head. The effect on low flows is around 2.6m at Westgate Bridge, the upstream boundary of the East Channel, while the high tidal levels are effect by a maximum of about 1.8m. The differences generally

tend to get greater upstream. The range between the tidal maxima and minima is about the same in each case.

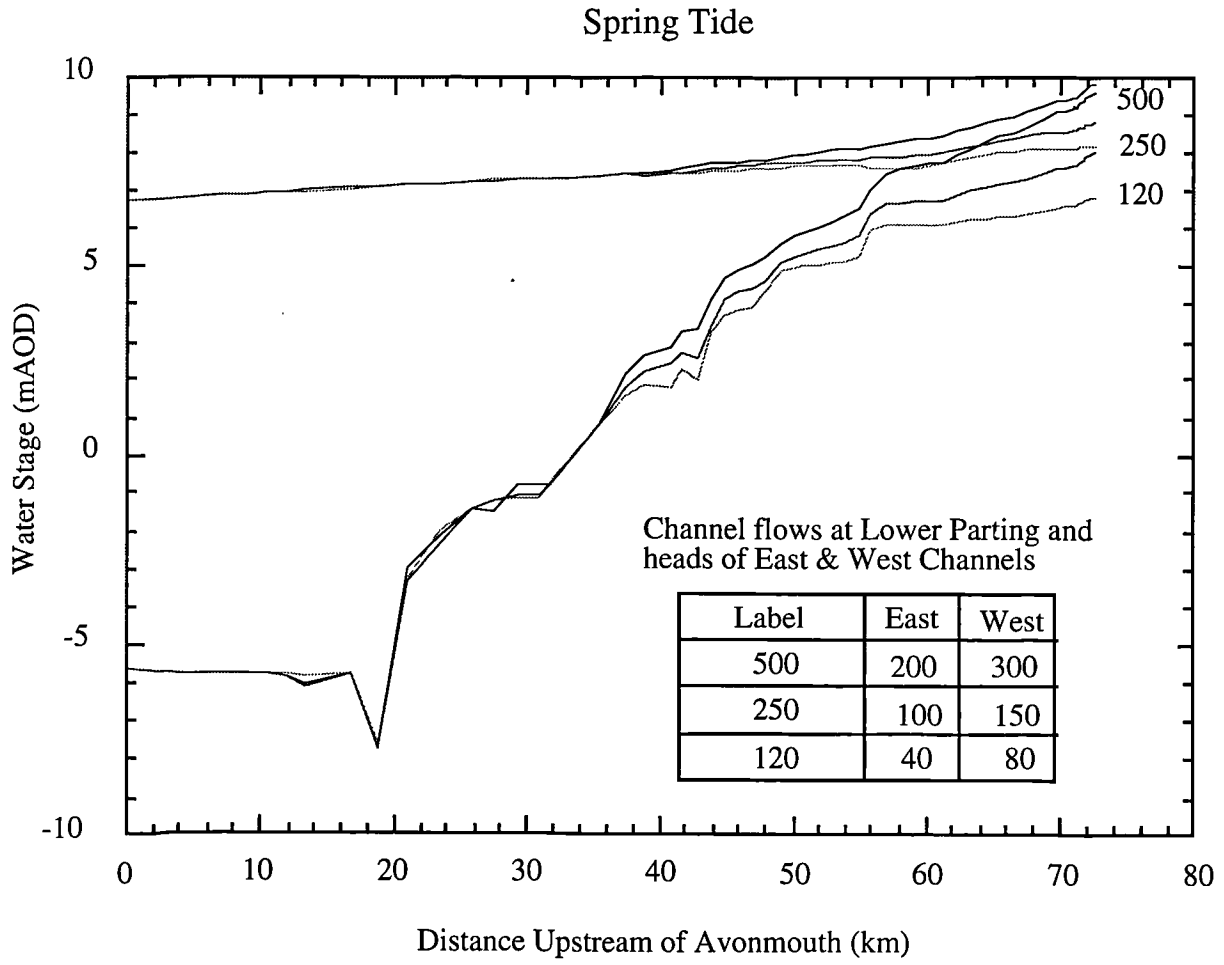

Fig 6.6 Effect of upstream flow on spring tide heights.

- Neap Tide.

The Neap Tide (Figure 6.7) illustrates that the water level also influenced from 26km upstream of Avonmouth to the estuary head, although this reach is non tidal. The steady flow level is nearly identical to the Spring tide low water, with the disparity of the two only becoming appreciable downstream of about 30km from Avonmouth.

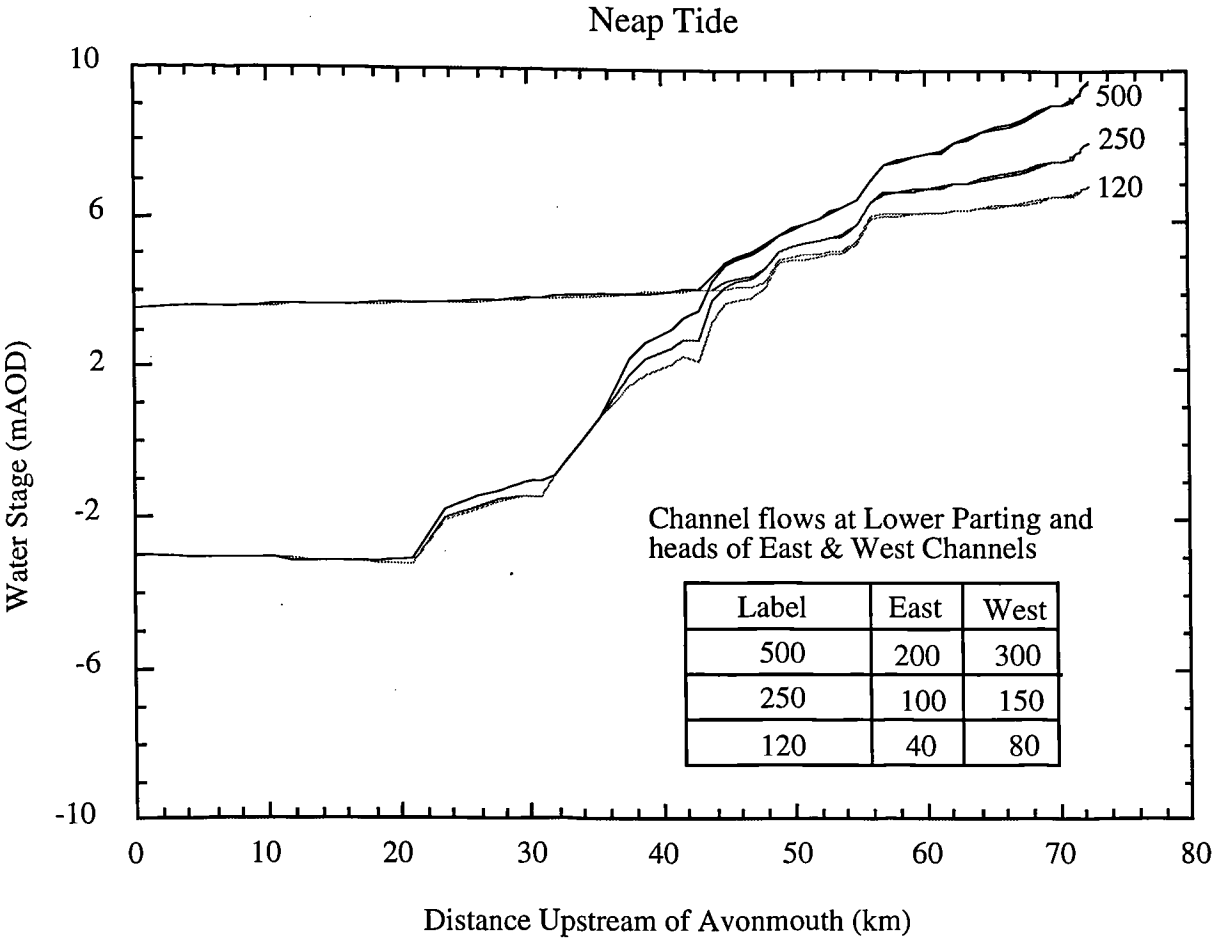

Fig 6.7 Effect of upstream flow on neap tidal heights.

The two previous examples have been modelled using a constant inflow from the upstream end which does not vary during the tidal cycle. Obviously this may change with the flow of the river north of the boundary points. A more significant flow at the boundary points occurs when a high tide penetrates and passes beyond the two upstream sections. This effect needs to be investigated as for many of the design events to which the model is to be applied there are no upstream hydrographs, the scenarios being hypothetical. Therefore a strategy for modelling the effects of the upstream input was developed as follows:

a) Model 1990 Surge where known upstream hydrographs had been constructed for a model used by the Hydraulics Research Station (HRS) to ascertain tidal heights. This tide is described later in the chapter.

b) Model same tide with a constant upstream inflow equal to the mean of the data which occurred over the modelling period.

It was found that a constant value of flow is sufficient to give identical high water heights, although naturally there is a slight error in the modelled and observed flow rates. Uncertainty in the base data negates concern over this discrepancy as the hydrograph values were based on sparse readings (4 No.) and were then read from a graphed curve which had been provided by the NRA with an uncertain scale. It would be preferable when very rapidly varying conditions in the upstream flow are encountered, or an extremely high tide enters the Upper Estuary, that a hydrograph be used. However data availability was such that this cannot be attained, therefore a further model technique was used.

c) After the model has 'settled down' after three runs though the tidal cycle with constant upstream flows, allow the boundary conditions at the upstream sections to vary with the calculated flow at the section immediately downstream and model over several more tidal cycles. After 2 cycles the model was found to settle with new boundary conditions, which represent the incoming tide if it penetrates sufficiently. These modelled results were then compared to the HRS hydrograph and were found to be within 10 minutes of the observed flow peaks and troughs. This can be accounted for by retardation of the flow within the system due to the selected friction values. The tidal heights again were within 20cm of the heights modelled by either of methods a) and b) above at the upstream section where the height was most pronounced, whilst the newly calculated hydrographs were much closer to the observed data. The hydrographs showed that, whilst the tide was ebbing, the flow was almost identical to the initial input values of upstream flow, whilst a tide entering the section shows a reduction in the flow rate. Allowing the boundary conditions to change gave a slightly higher height and it seems that it allows the crest of the high tide to pass the section. Stages (a), (b) and (c) were repeated for any other event where the hydrograph was known. As the method was successful, it can be used to predict an upstream hydrograph when the flow is only approximately known, to give an idea of the flow that can be passed into the Severn River System, if any.

Therefore it was found that reasonable simulations can be made with either constant flow rates at the upstream end equal to the mean of the inflow or that the boundary conditions may be allow to fluctuate.

6.5.7 Effect of Low Flow Calculation.

The low flow calculation is necessary when the simulation has calculated a level close to or indeed below the bed level, when cross sectional areas become very small. The calculation is crude and is not intended to model reality, but to stabilise the model which would otherwise calculate impossible flow variables thus preventing convergence to a solution.

The model has been run with several different calculations to allow for low flow (see Chapter 5) when the calculated water stage was within 0.4m of the minimum bed level of a cross section. It was found that the simplest method of adding a sweetening flow equivalent to the average of the flow upstream and downstream of the section did not add enough stability to the model and often fatal errors occurred. Solution methods for low flow used in Cunge (1986) proved a good method and were used for many of the earlier calculations until it was found that the method used in the HRS LORIS model using a simplified weir calculation proved by far the most stable, fastest and least likely method to introduce numerical instabilities into the modelling. This method is detailed in the previous chapter.

The model becomes unstable, even with low flow calculations when a combination of a high tidal (spring or greater) is modelled with Manning friction values of less than 0.02 downstream of Berkeley.

6.5.8 Using Pre-processed Values of Conveyance, Composite Sections and Coefficient of Non-Homogenous Flow Variations.

Composite sections using friction values which vary at differing parts of the channel were pre-processed and the conveyance and non homogenous velocity variation (Boussinesq Coefficient) calculated. These were read by the program from file and interpolated as per the breadth, cross sectional area and wetted perimeter. Use of tabulated conveyance had little effect

on the tidal characteristics evaluated compared to when the conveyance alone is calculated within the program. Both the tabulated conveyance and the non-homogenous velocity allowance generally caused a slight reduction in maximum tidal altitudes when large areas of flood plains were encountered, due to a higher friction value for the flood plains. The effects were minimal, however, in the order of less than 5cm on the tidal heights This method of modelling was dropped when it became apparent that a large amount of data processing was required if a section's characteristics were altered prior to a simulation. The method of assessment of these compound sections has been derived in the previous chapter.

6.5.9 Effect of Lateral Inflow Calculations.

Overtopping of seawalls was found to be important in influencing the calculated high tidal values upstream of an area where the wall had been overtopped. The difference between a calculation where the walls were allowed to be overtopped and an infinitely high sea wall preventing outflow are discussed in the next chapter. Inflow of the water 'lost' at high tide over the seawalls back to the channel at lower levels was not modelled, as it would have required additional flood plain modelling and/or a more complex modelling system, although such a calculation would add to the stability of the model at lower flows.

6.5.10 Instabilities.

A problem with the justification of the model verification is the presentation of data. There are many aspects which can be altered and affect the final calculations, many of which have a co-dependence. It is not feasible to present all this data, for instance checking all the tidal curves for each section on every run and checking for instabilities. In terms of this work instabilities can be considered as two families, one is the fatal instability where the program cannot handle the calculations and creates invalid data. Such an error is a division by zero, but in this model this is only encountered at low flow where the continuity of the system is broken. Non-fatal instabilities occur on different levels. The least significant is an oscillation around a value, especially the tidal height at low flow, where the model tends to vary between values

about 5cm either side of the general average level. This fluctuation appears to have been as much as 0.4m in the earlier Binnie and Partners modelling. More significant errors occur when the low flow calculation is used, when flow is approximated to ensure modelling continuity. This instability usually appears as significant oscillations in the quantity of flow, which if too large, can cause a domino effect on values modelled over the entire system leading in some cases to a fatal instability. The low flow instability is caused by low friction values (<0.022 Manning) in the ten most downstream sections. Another instability which appears in all of the other models which have been used on the Severn is the 'late ebb instability', where just before the onset of the incoming tide, an abnormally low level is computed. This can be avoided to some extent by using higher friction values downstream or a higher time weighting coefficient. Comments on the small instabilities will be made in the next chapter. However, at this point it is worth mentioning that instabilities were used as one of the main guidelines to ensuring that the most reliable friction values, weir simulations and low flow calculations were used. As many of the computations undertaken have a large co-dependence, this assurance is very painstaking as it not only requires that each individual 'module' has to be checked, but that the influence on the other variables and calculations has to be ascertained.

6.6 Summary of Factors Effecting Calculations.

6.6.1 Computerised Model Verification

Section 6.5 and it's subsection have demonstrated some of the effects of varying the input parameters using a generally deterministic approach. It is much more difficult to completely assess the model using a stochastic approach as there are so many input parameters which may be varied and many outputs which need to be analysed. In order to analyse the system in such a manner requires selecting the input parameters randomly from a (normal) distribution curve of their expected range of applicability. Thus a limited number of parameters were selected and the ranges within which the values could be chosen are defined as follows;

Tidal Range at Avonmouth;	Neap to Astronomical (3.5 to 8.1m)
Time weighting coefficient;	0.50 to 0.99
Friction values;	0.012 to 0.045
Upstream flow rate;	40 to 700 m^3/s
Weir Calculation;	Off / On
Time step;	1, 5 or 10 minutes
Low flow calculations;	Different methods
Weir flow coefficients;	0 - 1

As there are two primary output values, the height and quantity of flow at every cross section, it is not possible due to time constraints to produce an equation showing the covariance of each parameter on the output results. The approach adopted to overcome this was to apply a stochastic approach but not to analyse the results in detail. It was preferred to investigate graphical output of a high and low water height graph for the entire estuary and comparing with other results, and height & flow rate vs time graphs for every five sections. It is not practical to demonstrate all the effects and influences on the calculated flow regime from the variation of all the variables in the computer model, although at least 6 months of modelling was almost solely involved with the testing of the model for stability and influence of the varying factors used in the model. Table 6.1 indicates qualitatively the influence of the variables and calculations used with reference to their effect on the modelled results.

Factor	Lower Estuary	Middle Estuary	Upper Estuary	Extra Notes
Time Step	3	3	3	2 (Speed)
Time Weighting (ø)	3	3	3	Unstable at ø=0.5. High value smoothes calculated tidal curves.
Friction	3 (HW) 1 (LW)	2 (HW) 1 (LW)	1 (HW)* 1 (LW)	Low friction in Lower Estuary can cause low flow instability.
Weir Calculations.	3	3	2 (HW)* 3 (LW)	Generally only effects flow quantities 1 (Speed)

Upstream Boundary Conditions	3	2 (HW)' 2 (LW)	1 (HW)' 2 (HW)* 1 (LW)	
Low Flow Calculation.	1 (LW)*	2 (LW)	3	
Compound Sections	3	3	3	Not fully considered.
Overflow of seawalls	3 or 1‡	1 (HW)*	1 (HW)*	

Table 6.1 Influence of individual factors used in the modelling process on tidal levels and flows.

Where 1 denotes 'major effect', for instance >15cm change on tidal heights

2 denotes 'moderate effect', for instance 5 to 15cm change on tidal heights

3 'minor or no effect', for instance less than 5cm on tidal heights

(HW) effect on high water level or flow

(LW) effect on low water level or flow

* 'Spring' tides only.

' 'Neap' tides only.

‡ Substantial differences were encountered using HRS survey data and research derived data, see later in this Chapter.

6.6.2 Operational Validation.

The previous sections have described the general influence of various factors on the modelled results, the remaining sections show how the model was verified by comparing modelled data with real events which is termed the *Operational Validation* stage of verification. Both the HRS and Binnie and Partners works appear to have considered, incorrectly, that this stage is the only one required to validate the model, although it is assumed that some degree of in-house verification must have occurred. The stages of model testing before this stage were vital as the general characteristics of the model could be evaluated. For instance the effect of

varying friction on difference flow heights is indicated on Figures 6.4 and 6.5, this information was used to create a strategy for 'tuning' the friction values of the model. The final stage of verification is the application of the model using known data and comparing the results with the 'real' data. The philosophy was to choose initial values based on the two methods described in Chapter 5 and to adjust these slightly at each section to give a closer fit of the calculated results to the known data, although it was also ensured that the friction values used did not diverge too far from those that could be considered feasible. The prevalidation set up of the model was accomplished in the following manner;

a) Model neap tide, setting friction values to most accurately reflect low tide levels, i.e. to model the 'river flow' levels in the Upper Estuary when unaffected by tides.
b) Check neap high levels and adjust friction if required to near Admiralty predictions.
c) Model spring tide using these values and compare spring high and low levels and change friction values to give closest match.
d) Check new values against the neap tide again, then the spring if required.

Naturally the effects on stability, changing the time weighting and other variables were all checked at each stage. The next chapter shows the spring and neap tides, both modelled and Admiralty predications in some detail, so to avoid repetition are not shown here.

6.8 Validation of Model with Known Tidal Events.

Once the basic characteristics of the model were established and their effect on the flow calculations understood, the model was set up so that the selected values of time weighting factor, etc. would give the greatest accuracy whilst remaining stable over the widest range of conditions. This model was then used to validate the results against known tidal events in the Estuary, with the friction values being set and adjusted to give tidal heights matching the tidal events as closely as possible. However, the model was not over tuned so that the calculated data matched perfectly the known tidal data, using unrealistic friction values, which is a tendency of many other model users. Unlike many physically based models the relative lack of

complexity of this model is such that the primary object is to set up the model so that it gives the best approximation of the flow conditions, which are repeatable in the most conditions. Once representative friction values have been established for every section, they were kept at these values for every model run encompassing many different tidal events in the Severn such as the ones described in the next chapter, which also comment upons the friction values and their reality to natural conditions.

The modelled tides used in the calibration and validation were as follows;

- August 27th 1976
- October (7th to 14th) 1979
- December 12th 1981 tidal surge
- February 3rd 1990 fluvial flood
- February 26th 1990 tidal surge

The more recent tides were used in the initial calibration events as the data available was more continuous and accurate. The individual modelling events are described in the following sections.

6.8.1 The 1990 Tidal Surge.

The 1990 tidal surge on February 26th, is an event which brought media attention to the problems of flooding within the Severn Estuary, the upper reaches of which and the Severn River System had already been flooded from the slightly earlier fluvial flood (see section 6.8.2) and flooding in October of the previous year. The downstream boundary conditions were obtained from NRA data for this event, which had in turn been obtained from the City of Bristol Conservancy and Pilotage Department, which comprised the tidal curve constructed from the gauge readings at the port of Avonmouth. The tidal surge at Avonmouth reached a maximum height of 8.79m AOD, the highest level since tide records began at the port, although the gauge itself was damaged during the storm which caused the surge, so the

peak values have been reconstructed from a gauge at Portbury, which also ceased to function during the storm.

The upstream discharges at Gloucester were obtained from the NRA modelling of the event which provided a flood hydrograph, but were subsequently rescaled using the very limited 'real time' observations of four flow readings. The upstream flows at Haw Bridge or Saxon's Lode were also obtained and used as additional guidance. It was found that because the event was tidally controlled, a steady river input was suitable as its effect was significantly less than that of the tide on the heights and flows generated.

Tidal heights observed and calculated are given in Tables 6.2 and 6.3, as sea walls were over topped the tide was modelled using the data provided by the NRA (HRS survey data) and the slightly contrasting data obtained during this study.

Place	Tide	Observed	Modelled	Difference
Epney	Highest	10.16	10.02	-0.14
	Lowest	c. 5.15	5.35	+0.20
Minsterworth	Highest	9.77	10.01	+0.24
	Lowest	c. 5.80	6.46	+0.66
Gloucester Dock	Highest	9.57	10.10	+0.53
	Lowest	c. 7.25	7.52	+0.37

Table 6.2. 1990 Tidal Surge, modelled using aerial survey and levelled sea wall heights.

Place	Tide	Observed	Modelled	Difference
Epney	Highest	10.16	9.98	-0.18
	Lowest	c. 5.15	5.35	+0.20
Minsterworth	Highest	9.77	9.80	+0.03
	Lowest	c. 5.80	6.44	+0.64
Gloucester Dock	Highest	9.57	9.91	+0.34
	Lowest	c. 7.25	7.52	+0.37

Table 6.3 1990 Tidal Surge modelled using HRS data for seawall heights.

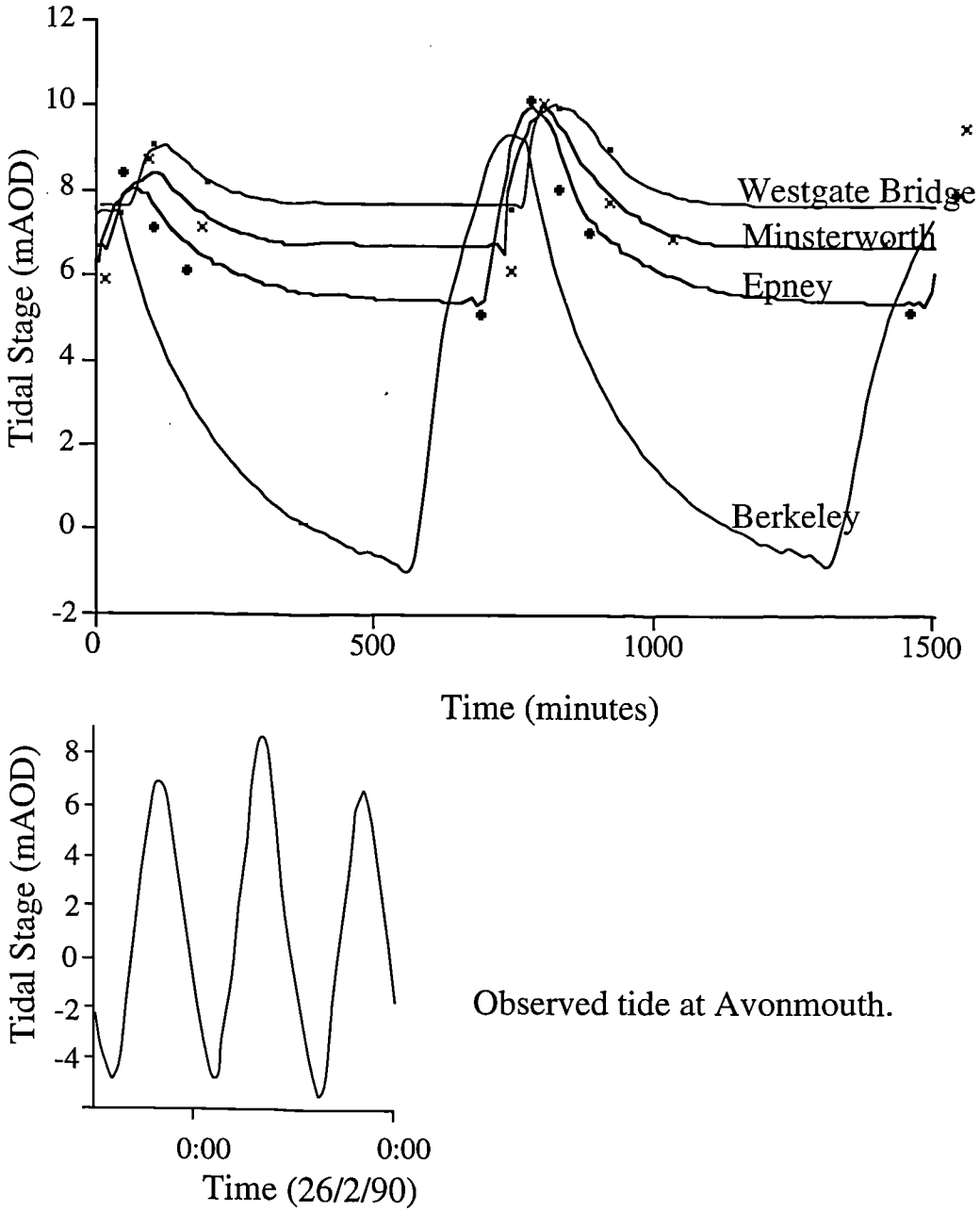

Fig 6.8 Modelled (solid line) and observed (points) tidal curves for 1990 surge.

The model produced an acceptable fit to the observed data (Figure 6.8), although the peak levels modelled on the high tide before the surge tended to be higher in most cases. Timing of the modelled events was generally good in comparison to reality giving a general confirmation of the friction values used. The timing of events (although not so much with very

high tides) can be varied considerably by the model friction values used. It is noted that the least correlation with the observed values is at Epney where the timing of the tidal heights is not accurate and the low flow is higher than that observed. The low flow height at Minsterworth is higher than expected too, suggesting that too high a friction value was being used in the Middle Estuary. The graph also illustrates some of the non-fatal instabilities which are generated at low flow, where the curves are not fully smooth, the 'late ebb instability' is also identifiable on the curve for Minsterworth.

It was found that after the model had been tested for the flood tide of 1990 (Section 6.8.2) that too high friction values were accounting for poor correlation in the Middle Estuary. The modelled friction values were readjusted for lower friction in the Middle Estuary, producing a closer fit to the low tidal levels (Table 6.4). Manning friction values were lowered by 0.04 between Newnham and Lower Parting.

Place	Tide	Observed	Modelled	Difference
Epney	Highest	10.16	10.21	+0.05
	Lowest	c. 5.15	5.27	+0.12
Minsterworth	Highest	9.77	10.03	+0.26
	Lowest	c. 5.80	6.18	+0.38
Gloucester Dock	Highest	9.57	10.10	+0.53
	Lowest	c. 7.25	7.38	+0.13

Table 6.4 1990 Surge Tide, evaluated for lower friction values in the Middle Estuary, using aerial survey and levelled values for seawall heights.

Place	Tide	Observed	Modelled	Difference
Epney	Highest	10.16	10.15	+0.01
	Lowest	c. 5.15	5.22	+0.07
Minsterworth	Highest	9.77	9.87	+0.10
	Lowest	c. 5.80	6.03	+0.23
Gloucester Dock	Highest	9.57	9.96	+0.39
	Lowest	c. 7.25	7.39	+0.14

Table 6.5 1990 Tidal Surge using lower friction values and HRS data for seawall heights.

6.8.2 The 1990 Fluvial Flood.

The modelling of the 1990 fluvial flood which was at its peak on the 3rd of February was less important for the area of the Severn Estuary being considered than the high tidal levels encountered during the surge event. However, modelling of such an event aids the analysis of the physical reality of the model and the rigour of the analyses over a varied set of flow conditions. The fluvial flood after a period of prolonged rainfall was most noticeable north of Gloucester to Worcester where large areas of land were flooded and hadn't fully drained when the surge tide occurred later in the month. The tide which occurred in the Severn during the fluvial flood had a relatively small range, so that there were no pronounced tidal effects in the Upper Estuary.

For this modelling event, upstream current flow gauge readings were available for the West Channel at Over Bridge and in the East Channel at Westgate Bridge. The Over Bridge readings were used to represent the upstream boundary conditions at Maisemore Weir.

As the driving tide which occurred during this event had a relatively small range, the effect upstream of the tide becomes minimal. The available benchmarks for this simulation are relatively sparse, taken from NRA gauging stations. The following modelled and observed calculations are available for direct comparison (Table 6.6).

Place	Tide	Observed	Modelled	Difference
Epney	Highest	c. 6.40	6.93	+0.53
	Lowest	c. 6.20	6.87	+0.67
Minsterworth	Highest	c. 8.10	8.31	+0.21
	Lowest	c. 7.65	8.29	+0.64
Gloucester Docks.	Highest	10.37	10.25	-0.12
	Lowest	c. 10.20	10.23	+0.03

Table 6.6 1990 Flood Tide.

These results were not found to be satisfactory, suggesting that too large friction values were being used for the Middle Estuary because the low tide levels were too high, although the

figures matched the upstream levels very closely. However, as the simulation of the surge tide of the same year indicated, upstream high tide levels were defined to a substantial degree by the over topping of sea walls. To re-evaluate the data for the flood tide the NRA recalculated river flow values which were reconstructed from upstream hydrographs. This quantity of flow at the upstream boundaries varied with time rather than the single value which was the average of the peak flow over the period of the simulation which had been used before. This was found to reduce the low flow levels but not substantially, so the model was rerun with lower friction values in the Middle Estuary and gave closer results, which are depicted in Table 6.7.

Place	Tide	Observed	Modelled	Difference
Epney	Highest	c. 6.40	6.53	+0.13
	Lowest	c. 6.20	6.37	+0.17
Minsterworth	Highest	c. 8.10	8.11	+0.01
	Lowest	c. 7.65	7.76	+0.11
Gloucester	Highest	10.37	10.27	-0.10
Docks	Lowest	c. 10.20	10.25	+0.05

Table 6.7. 1990 Flood Tide, Recalculated results in mAOD.

The model had then to be re-evaluated for the surge-tide, where it again was found that there was closer agreement with the observed tides (Tables 6.4 & 6.5) although the effects on the values calculated were not as significant as the effects on the river flood calculations. In all cases where the modelling event is adjusted then a full analysis of computational stability, by changing the time weighting factors, etc., has been undertaken.

6.8.3 The 1979 Tidal Events.

The October 1979 tidal event was modelled using sparse data from a Binnie and Partners (confidential) report. The computer model had to be adapted slightly to account for the larger number of tides involved rather than the smaller periods of tides, usually three high waters, it had previously been modelling. Some of the data available was sparse so that the

period of 7/10/1979 to 12/101979 was modelled as one set of tides, and the 13th and 14th were modelled as a separate set, but some of the downstream boundary conditions were approximate so that less reliance is given to the values modelled on these days. The results of modelling these tides are shown in Tables 6.8 & 6.9.

Date	Portbury Observed	Portbury Modelled	Berkeley Observed	Berkeley Modelled	Epney Observed	Epney Modelled
7	+7.82	+7.82	+8.42	+8.49	+9.26	+9.35
	-6.10	-6.10	-1.82	-1.96	+5.03	+5.32
	+7.96	+7.96	+8.61	+8.67	+9.45	+9.42
8	-6.12	-6.12	-1.85	-1.95	+5.06	+5.27
	+7.45	+7.45	+8.08	+8.17	+8.80	+8.83
	-6.01	-6.01	-1.89	-1.93	+5.01	+5.28
	+7.56	+7.56	+8.17	+8.29	+8.89	+8.93
9	-5.70	-5.70	-1.83	-1.87	+5.06	+5.27
	+7.21	+7.21	+7.80	+7.77	+8.50	+8.55
	-5.48	-5.48	-1.86	-1.85	+5.05	+5.29
	+6.82	+6.82	+7.40	+7.41	+7.94	+7.86
10	-5.29	-5.29	-1.84	-1.82	+5.02	+5.25
	+6.35	+6.35	+6.91	+6.85	+7.34	+7.33
	-4.91	-4.91	-1.90	-1.80	+4.94	+5.23
	+6.04	+6.04	+6.52	+6.65	+6.90	+6.82
11	-4.56	-4.56	-1.89	-1.78	+4.91	+5.23
	+5.49	+5.49	+5.98	+6.03	+6.33	+6.41
	-4.14	-4.14	-1.94	-1.78	+4.84	+5.21
	+4.93	+4.93	+5.34	+5.37		
12	-3.78	-3.78	-2.02	-1.81	+5.68	+5.78
	+4.56	+4.56	+4.95	+5.04	+4.78	+5.19
	-3.37	-3.37	-2.02	-1.83	+5.27	+5.45
	+3.95	+3.95	+4.29	+4.44		

13	-2.90 +3.67 *	-2.90 +3.67 *	-2.07 +4.06 -2.01	-1.80 +4.12 *	+4.73*	+5.19 *
14	+3.17 -2.16 +3.20 -2.03	+3.17 -2.16 +3.20 -2.03	+3.45 -1.97 +3.50 -1.95	+3.49 -1.83 +3.27 -1.84	+4.69*	+5.19

Table 6.8. October 1979, low and high water heights, modelled and observed, (* denotes no data, or maximum level recorded).

Date	Portbury Observed	Portbury Modelled	Berkeley Observed	Berkeley Modelled	Epney Observed	Epney Modelled
7	0 735	0 735	30 775	30 770	100 835	110 840
8	1485 2220	1485 2220	1510 2260	1500 2240	1575 2315	1590 2330
9	2955 3695	2955 3695	2985 3730	2970 3730	3055 3805	3060 3800
10	4430 5175	4430 5175	4465 5205	4450 5200	4540 5285	4550 5300
11	5905 6655	5905 6655	5940 6675	5920 6660	6025 6775+	6020 6800
12	7380 8125	7380 8125	7405 8150	7410 8150		7520
13	8865	8865	8890	8890	*	
14	9635 10385	9635 10385	9670 10405	9650 10390	* *	

Table 6.9. Time of high tides in minutes after first high tide at Avonmouth, October 1979. Modelled times are to the nearest 10 minutes. (* denotes no data, + falls on 12/10/79)

The times of low tide were not entered on Table 6.9 as the timing of the low tide is an arbitrary thing. When near steady flow conditions, i.e. river flow, prevail then low water

levels can occur over a substantial period of time. This is apposite for the readings at Epney, although less so for Berkeley. Although not totally conclusive this table also indicates how the high water on a spring tide, which is slightly less the tides on the 7th and 8th, reaches the secondary ports quicker than a tide with a smaller range, such as the ones on the 11th and 12th.

6.8.4 The August 1976 Tidal Event.

The 1976 tidal event on the 26th of August showing observed and modelled events at Avonmouth, Sharpness, Newnham and Epney are shown in Figure 6.9 and Table 6.10. Data for this model has not been verified and assumes that the data source (Binnie and Partners) is reliable, although it has been read from graphs within their report and is therefore subject to some error.

	Avonmouth (Observed)	Sharpness (Predicted)	Sharpness (Observed)	Newnham (Predicted)	Newnham (Observed)	Epney (Predicted)	Epney (Observed)
HW	c. 7.1	7.87	c. 8.0	8.21	c. 8.3	8.45	c. 8.4
LW	c. -6.1	-0.97	c. -1.4	3.46	c. 2.9	5.66	c. 5.4

Table 6.10 August 1976 Tidal Surge, water level figures.

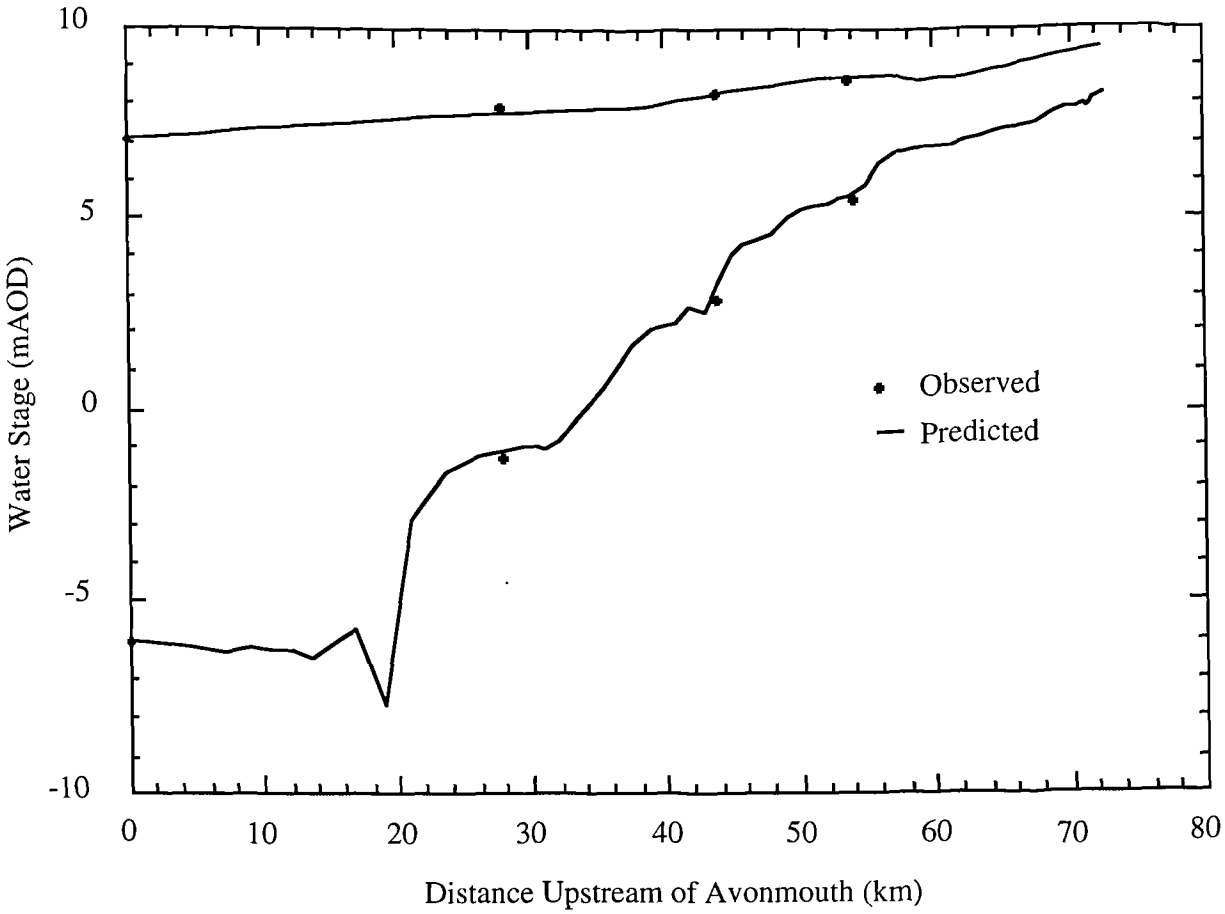

Fig 6.9 August 1976 Tidal Surge Water Levels

The tidal levels in Figure 6.9 appear to be a close fit, although the results in Table 6.10 show that there is an appreciable discrepancy in the low water levels, especially at Newnham and Sharpness. This difference may not be accounted for in the differences in the bed levels at the time of the event and when the channels were surveyed, which is mentioned later in this chapter. It should thus be argued that the friction values assigned to the cross sections in the Middle Estuary are too high, thus causing a higher than observed base flow. Modelling by Binnies and the HRS indicate that exceptionally low friction values were required to accurately model the high tide levels in Middle Estuary; it appears that this zone is the most sensitive to changes in the friction values. The Binnie model actually under predicted low tidal levels by over a metre at Epney, yet also under predicted the high levels by about 30cm for this tide. This is hard to equate as an underprediction of one level over predicts the other. The timing of the Binnie peak levels actually implies that too high friction values were used in the area of Epney as the tide had been delayed in comparison to the observed peak. However, this could

have been a function of the weather at the time as well as a substantil amount of siltation which had happened before the event but after the channel surveying.

The modelling of this tide is interesting as it leaves two choices, to retune the model with lower friction values and assess the the effect on all other modelling simulations, or whether to accept the errors produced, bearing in mind the reasonable representation.

6.8.5 The 1981 Tidal Surge.

Data for the 1981 tidal surge on the 12th of December was collected from similar sources to the 1990 surge. Again the tide gauge at Avonmouth was damaged (this time it jammed) during the event, so the peak high tidal level of 8.75 mAOD was also constructed from the Portbury gauge. The readings for both this event and the 1990 surge could not take into account the effect of wave action on the gauged readings. It was noted that tidal improvements had been undertaken between the 1990 and 1981 events so differing seawall levels were used for the two. The results of modelling this tide are included in Table 6.11. The first table is a run using the HRS printed data for river bank heights in their 1991 report, Table 6.12 shows the same simulation using heights obtained from the aerial survey and in the field measurements. The model run using the HRS seawall heights identified considerable areas of seawall breaching between Avonmouth and Berkeley.

Place	Tide	Observed	Modelled	Difference
Berkeley	Highest	+9.64	+9.33	-0.31
	Lowest	c. - 1.5	-1.64	-0.14
Epney	Highest	+10.16	+9.94	-0.22
	Lowest	c. +5.1	+4.99	-0.11
Gloucester Dock.	Highest	+9.33	+9.92	+0.59
	Lowest	c. +6.7	+6.72	+0.02

Table 6.11. Modelled results, 1981 tidal surge in mAOD, using HRS seawall data.

Place	Tide	Observed	Modelled	Difference
Berkeley	Highest	+9.64	+9.49	-0.15
	Lowest	c. - 1.5	-1.66	-0.16
Epney	Highest	+10.16	+10.09	-0.07
	Lowest	c. +5.1	+4.99	-0.11
Gloucester Dock.	Highest	+9.33	+9.81	+0.48
	Lowest	c. +6.7	+6.72	+0.02

Table 6.13 Modelled results for 1981 tidal surge in mAOD, using levelled and aerial survey data for seawalls.

6.8.6 Hybrid Model

The modelling of the events from the 1990 tidal surge and the 1981 tidal surge indicates that the greatest model accuracy would come from a hybrid model using the HRS data for the upper half of the Estuary and the Aerial survey and levelling data for the lower half of the Estuary. It was not feasible to measure all the levels derived by the HRS for the levels upstream, however, levelling of limited stretches north of Minsterworth indicated that the HRS data was probably closer than that derived during this research for the seawall heights in this area.

Results of a 'hybrid' model for the 1990 and 1981 surge are contained in Tables 6.13 and 6.14.

Place	Tide	Observed	Modelled	Difference
Berkeley	Highest	+9.64	+9.49	-0.15
	Lowest	c. - 1.5	-1.62	-0.12
Epney	Highest	+10.16	+10.09	-0.07
	Lowest	c. +5.1	+4.99	-0.11
Gloucester Dock.	Highest	+9.33	+9.72	+0.39
	Lowest	c. +6.7	+6.72	+0.02

Table 6.13. 1981 Surge tide using hybrid set of sea wall heights.

Place	Tide	Observed	Modelled	Difference
Epney	Highest	10.16	10.15	+0.01
	Lowest	c. 5.15	5.22	+0.07
Minsterworth	Highest	9.77	9.87	+0.10
	Lowest	c. 5.80	6.03	+0.23
Gloucester	Highest	9.57	9.96	+0.39
Dock	Lowest	c. 7.25	7.39	+0.14

Table 6.14. 1990 Tidal Surge .

6.9 Comparison with Existing Models.

Although data was available for modelling different events to those presented in Section 6.8, it was thought that a direct comparison of the results with similar numerical models would provide a benchmark to compare this model with the already established ones, which are accepted as being accurate. It is noted, however, that both sets of data for comparison have been made available from confidential sources. The NRA have provided their own copies of the user manual for the 'LORIS' modelling system and the River Severn Flood Plain Report (1991) on an 'in confidence' basis, while the Binnie and Partners data was obtained from an 'interlibrary loan'. However these reports are marked 'commercial in confidence' and it has not been ascertained whether the reports still maintain this status, although it is thought unlikely. It is therefore decided that a comparison of the three models will be made on a relatively non-critical basis. In all cases modelled data from other sources generally concentrated on only three to four cross sections in the Severn for practical reasons in displaying data.

It is very easy to concentrate the verification method on the positive aspects of a computer simulation, rather than comparing every aspect of the modelled results. Unfortunately it is difficult to draw direct comparisons without the raw data being available. Evidence from graphed results may not reveal the true story due to detail being hidden by having graphs of differing scales and possibly with smoothed curves. However, a qualitative comparison of the three model's behaviour is given in Sections 6.9.1 to 6.9.5.

6.9.1 Binnie and Partners Model.

The computer program used by Binnie and Partners (1981) is a four point half time step implicit method, similar to the model developed in this thesis, called FWAVE, although it calculates on a storage area and 'live' cross sectional area basis, the theory of which is briefly described in Chapter 5. Cross sections are analysed by a program called HYDAN, tabulating the data at two metre intervals. The model was used to analyse the potential effects of a barrage on the Severn Estuary , and so extends further seawards than the model used in this thesis. This model was used to calculate the 1976 and 1979 tidal events.

- 27th. August 1976.

This high spring tide was used to calibrate the Binnie and Partners model. During their calibration it was found that the friction values required to manage a reasonable match with the observed data needed to be as low as 0.012 (Manning) between Frampton-on-Severn and Longney, which had also been found to be the case in the earlier modelling by the HRS. The simulation found that times and heights of the high tide matched well, as did the curve of the flood tide, although there was poor correlation between the shape and levels of the ebb tide and low water heights. The modelled low water heights were considerably less than those observed. Binnie's principally attributed this to siltation which had occurred during the drought of 1976, one year after the channel survey by the HRS in 1975, up to 1 metre of siltation was reported near Newnham.

- October 1979.

The modelling of the October tides from 1979 found that in the Upper Estuary, that low flow levels were too low around Epney. The low water levels were attributed in part as being due to numerical instabilities, although the timing of high water which was up to 40 minutes too early at Epney and the modelled heights suggest that friction values were slightly too low. Results were about 0.2m too great at high water and low water levels were 0.9m too Modelled events for tides after the 12th of October where the high water did not penetrate the

Upper Estuary showed that the model oscillated around the nearly constant observed results by 0.4m.

6.9.2 HRS Model.

The HRS model uses the HRS software package LORIS and was first used in 1981 to carry out a study of tides between 1975 and 1981. After further instructions from the National Rivers Authority (Severn Trent) in 1991, the HRS constructed a new model, based on the 1981 study. Both models are part of the Avonmouth to Worcester Flood Alleviation Study. The HRS model is much more complicated than either the model derived for this study or the Binnie model, as it simulates flood plain flows, loops, weirs, outflow pipes and man made structures and their influence on the flow regime. A summary of the HRS modelled calibration events are summarised in the following paragraphs.

- 1981 Tidal Surge.

The model predicted peak elevations to within ± 0.1m at Berkeley and Epney, but under predicted maximum levels upstream by about 0.3m. There was a lag of what appears to be an hour on the modelled peak results at Berkeley.

- 1990 Fluvial Flood.

The text of this report states that the model predicted peak levels to within ±0.1m at Epney and Gloucester Docks, but over predicted the peak level at Minsterworth by about 0.3m. However, inspection of the graphed modelled results provided in the accompanying report suggests that there is a substantial discrepancy in the modelling of events prior to the fluvial flood (25th January to 1st February 1990) with an over prediction of low water levels of the order of 0.5m on some tides at Gloucester Docks.

- 1990 Tidal Surge.

Showed similar characteristics to the fluvial flood event, although the actual peak tides show a reasonably good correlation, there is some discrepancy on the tides beforehand. At

Epney, Minsterworth and Gloucester Docks the shape of the ebb tide curve was significantly different to the observed curves, especially upstream. The largest difference being at Gloucester Docks, where the ebb tide curve which was modelled was sluggish in reducing to low water level. This was partially due to the modelled low water levels being approximately 0.4m too high.

6.9.3 Model Accuracy - Tidal Maxima and Minima.

There is a justification in all cases to say that the modelled high water heights are good, with correlation to within 0.1m, not dissimilar in many instances to the accuracy of the tide gauges themselves. Low water heights prove much more difficult to justify, being much harder to model accurately. The most obvious explanation for the poor correspondence of low water levels is the effect of bed level changes, which will be investigated in the following chapter.

It seems that the model developed for this thesis and the friction values adopted can accurately reproduce tidal maxima in most of the Estuary, although high events towards Gloucester may over predict levels. This is probably because outflow from the system along pills and similar cannot be accounted for. Similarly the model tends to generally over predict low water levels in the Middle Estuary, it is therefore concluded that the early HRS studies and Binnie and Partner's studies may be correct when they use abnormally low friction values in these reaches. However, the modelling of the 1990 tides by the HRS found that friction values, in some cases double that used in their previous study were applicable. Therefore it is concluded that modelling of this type, whilst it adopts a relatively rigorous schematisation of the system, cannot be considered to represent a physically based model, but a best approximation to very complex processes which are occurring. It is just as acceptable to have model results which do not perfectly fit the natural data and acknowledge the short comings, than to try to perfectly match the data, with incorrect friction values.

6.9.4 Model Accuracy - Timing.

The timing of the modelled events is almost as important as the calculated levels in validating the model, as the friction values not only define the degree of tidal amplification but also the time in which the tide takes to penetrate upstream. Unfortunately the 'commercially' modelled events, quite naturally are concerned with significant high tides, ones which have caused flooding within the Estuary. It appears from modelling less significant tides that it is easier to model the time of high water when there is a large tidal range, because of the faster speed of propagation due to the extra water depth. The shape and correspondence of the modelled and observed 'tail' of the tidal curve showing the ebb tide in the opinion of this author, is of little importance in verifying the model if the low water level is not accurately represented as the two appear to be co-variant. However, matching the timing and heights of the ebb flood and the relatively constant low water levels when steady flow conditions are being approached, probably gives the best representation that the friction value chosen is "correct". It is noted that during the course of a tide that the value of friction could change due to changes in the bedform morphology.

6.9.5 Model Stability.

All three models show signs of numerical instability in their graphical output. It is not possible to comment upon the significance of the instability of the HRS and Binnie models, because the base data is not available. It may be the case that the curves produced in the confidential reports use data separated by significant time steps, thus some instabilities may be missed, it also possible that the data has been smoothed, especially the Binnie data as this was hand drawn. Certainly the Binnie model, which by nature of its age is the most simple, seems to create the most instabilities. The HRS model and the one developed for this work show very similar characteristics, such as secondary oscillations near low flow and the 'late ebb instability'. Unfortunately it is not possible to reproduce the modelled graphs of the other works because of their confidential nature.

6.10 Summary of Verified Model.

The final model used to simulate flow in the Severn Estuary has been set up with the following parameters and functions which have been described in this and the previous chapters and has been used unaltered for the model runs used in the next chapter:

- Branched System
- Downstream Boundary = Avonmouth (tidal curve)
- Upstream Boundary = Maisemore (West Channel)
- Upstream Boundary = Westgate Bridge (East Channel)
- Time weighting factor (ø) = 0.66
- Time step = 1 minute
- Friction Values listed in Appendix E
- Weir calculation used as described in Chapter 5
- Upstream boundary conditions set as constant values initially but allowed to vary
- Upstream inflows initially given as $100m^3/s$ in East Channel unless otherwise specified
- Upstream inflows initially given as $150m^3/s$ in West Channel unless otherwise specified
- Low Flow Calculation invoked when flow depth is less than 0.4m
- Lateral inflow calculations used as described in Chapter 5
- Seawall heights based on 'hybrid' model of HRS and data collected in this study

The following features have been deemed *unnecessary to the final model:*

- Non-homogenous flow variations
- Compound sections with differing friction values
- Changes in friction values with flow depth and velocity
- Most river inputs and outflow pipes, etc.
- Floodplain and return flow into system after seawalls have been overtopped
- Looped network around Gloucester

The following additional aspects of computation which have been adopted in some more complex models were not considered as they are beyond the capabilities of the model:

- Two-dimensional modelling, especially in Estuary mouth
- Low flow channels diverging from one-dimension schematisation
- Bedform changes and bedform migration
- Effects of wind stress on flow and wave build-up
- Salt balance and exchange
- True mathematical modelling of the Severn Bore
- Waves, except for tidal long wave.

6.11 Conclusions.

Chapters 3 to 6 have described the theory, mathematical analysis, data needs and verification of a tidal model of the River Severn. An accuracy of within 10cm at high water was thought to be good prior to the modelling when the data accuracy, the requirements of the model and the actual similarity to reality which the modelling assumptions represent are considered. The model met this criterion in most cases, only showing any significant discrepancies between modelled and observed low water levels, which are considered less important. Although the model results cannot be expected to simulate every tide accurately as there are limitations in the data and differences in the tidal and meteorological conditions the model is a good tool in predicting the high water heights which could be encountered from normal tidal and surge tide conditions.

Over 2000 verification runs of the model were undertaken during its development. Often a simple change to the data required the analysis of 10 to 20 additional runs checking the stability, sensitivity and accuracy of the model. Although this chapter has presented some of the results of the verification runs, the bulk of data and hence the problems with showing this data and the limitations of computer disc storage space, limits the amount of information which can be reasonably reproduced in this thesis.

The model has been developed from the verification runs to give the closest result to all the tides used for comparison with an identical set up. Thus can be considered the most representative solution which can be made using this type of mathematical modelling and the data available. The next chapter describes the applications for which the model has been used and reproduces many of the events mentioned in this chapter in more detail.

CHAPTER 7

MODEL RESULTS.

7.1 Introduction.

This chapter presents the results of the simulation of a variety of different tidal conditions, including hypothetical historical and future tides. These model runs have been undertaken using the model set-up described in Chapter 6, unless otherwise indicated. This chapter will describe the modelling of the existing neap and spring tides in the Severn Estuary and the tidal surge of the 26th February 1990. These tides are used for comparison to describe similarities and variations which occur over the present day tidal regime. Observations of the present day tidal regime are used to construct a new spring tide boundary curve at Avonmouth for potential future tidal events which may occur in the Severn in the next 105 years. Historic tides are also calculated and compared to the future and existing events to assess how the model may be used in the observations of sea level change. The chapter concludes by assessing the present day tidal defences of the Severn and demonstrates how the use of a tidal 'sump' may significantly reduce high water levels in the Estuary.

7.2 Spring Tide.

The present day spring tide has a range of 12.2m at Avonmouth (Admiralty Tide Tables, 1993) with a high water level of 6.7 mAOD and a low water level of -5.5 mAOD . An idealised tidal curve for the spring tide at Avonmouth is summarised in Table 7.1.

Event	Time	Height (m)
High Water	0:00	6.7
Low Water	6:50	-5.5
High Water	12:10	6.7
Low Water	19:00	-5.5

Table 7.1 Idealised spring tide times and heights at Avonmouth.

The tide shown in this table has been used as the downstream boundary conditions to calculate the behaviour of a spring tide in the Severn. The upstream boundary conditions selected were $100m^3/s$ at Westgate Bridge and $150m^3/s$ at Maisemore Weir. The modelled and observed high and low tidal levels are shown in Figure 7.1 and the times of the tides in Figure 7.2. Table 7.2 indicates the timing of the modelled and Admiralty predicted spring tidal events.

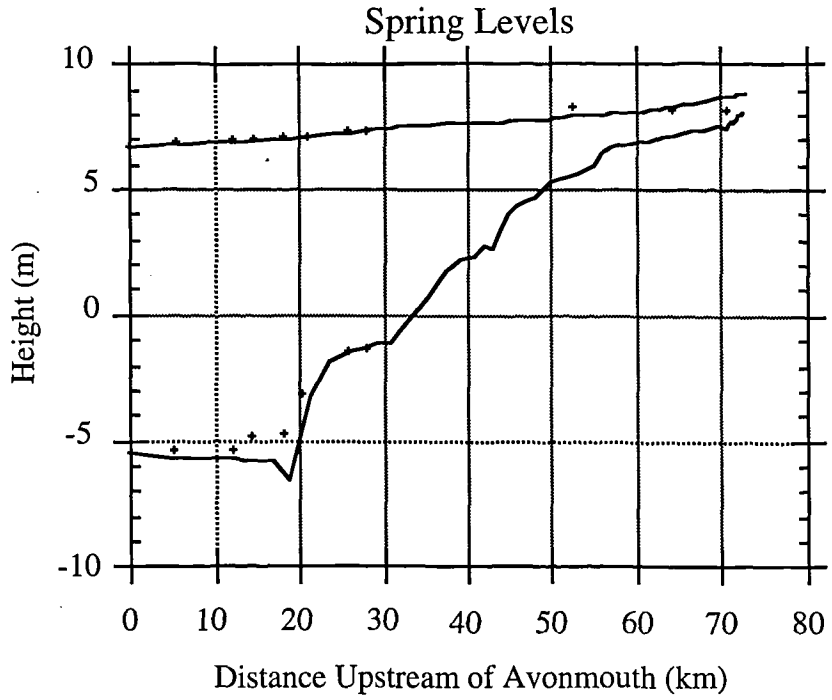

Fig 7.1 Modelled Spring tidal heights, Admiralty predictions shown as crosses.

Place	Time HW (predicted)	Time HW (Admiralty)	Time LW (Predicted)	Time LW (Admiralty)
Avonmouth (0 km)	730	730	410	410
Sharpness (29.3 km)	769	765	563	575
Epney (53.0 km)	819	820	742	No data
Llanthony (71.2 km)	864	865	743	No data

Table 7.2 Spring tide times in minutes, predicted by model and Admiralty Tables.

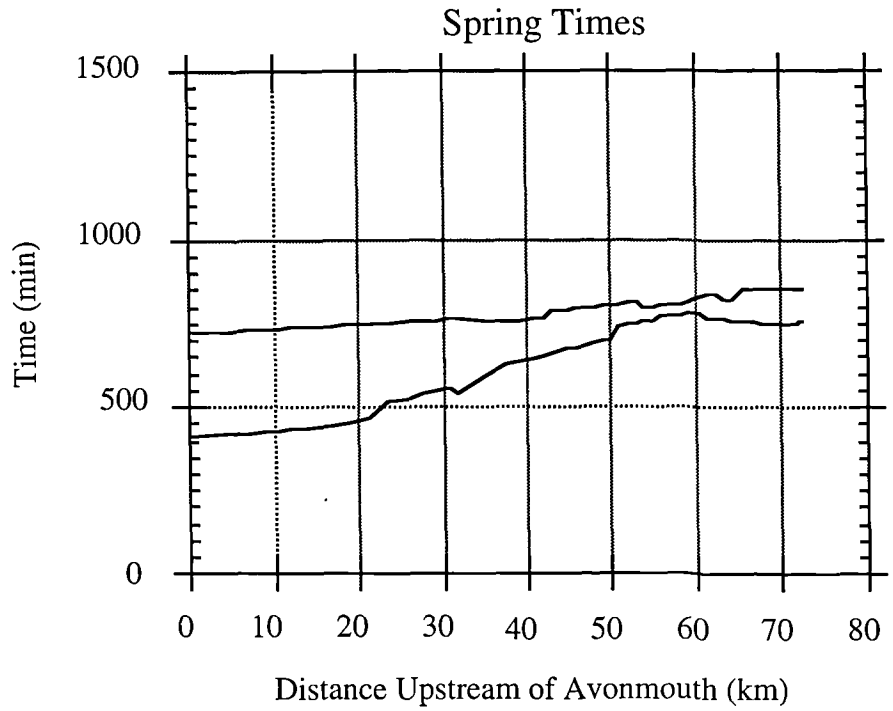

Fig 7.2 Spring tide times.

7.2.1 Analysis of tidal heights and times.

A direct comparison of the spring tide, modelled and predicted by the Admiralty charts is difficult as the Admiralty figures are based upon a series of observed events averaged over a period of time (see chapter 1). Thus an ideal spring tide as would be defined by the Admiralty figures does not occur as a single tide. The Admiralty observations are based on tides which may or may not be affected by wind, which causes wave build up on coasts facing the prevailing wind and by the river flow conditions. It seems that from these predictions the times of the tidal highs are relatively similar, indicating that overall the effect of the modelled friction and the river inflow is good. However, Figure 7.1 indicates that the predicted levels at Llanthony and Minsterworth are slightly higher than the Admiralty predicated values (indicated as crosses on the graph). This may be because the majority of Admiralty observations are for river flood which is generally less than used in the model. The modelled high water level at Epney (52 km upstream) is considerably lower than the Admiralty predicted levels, this may be because the friction values selected downstream of here are too high. However, it is more

likely that the bend of the river, causing momentum effects on an incoming tide, and the narrowing of the river cause the observed tidal heights to be slightly higher than those predicted. The low tide results do not correlate well in the Lower Estuary, because of the low flow problems encountered, which have been described in the previous chapter. This discrepancy has to be accepted as one of the limitations of the model. However, another aspect is the difficulties in schematising the river at these levels, when the ebb channels digress from the 'full' channels. The only way of truly reflecting this change would be to schematise the river in a different manner when low stages occur, involving a much more complex model. Therefore it is concluded that the model in its present state is sufficient, bearing in mind the model objectives to give representative high water heights. The sensitivity of the model to this low flow problem can be illustrated by modelling the ideal spring tide given in the 1993 Admiralty tide tables (Figure 7.1) and the 1992 curve. The figures are the same for high water levels, but the low water level given for Avonmouth is 0.1m lower for th 1992 tide. This causes a much more significant deviation from the Admiralty data. The problem has been highlighted in the previous chapter for modelling of a 'spring' tide, when the 1992 figures have been used as they give a better reflection of the model limitations in this area.

The timings of high water, however, are very close to the Admiralty predictions, suggesting that the friction values and schemetisation closely represent the natural conditions. There are no Admiralty figures for the time of low tide in the Upper Estuary as low flow conditions exist over a long period of time and therefore the choice of a time of low water is arbitrary. The modelled data does give a time of low tide which represents the lowest tide before the onset of the incoming tide.

It is considered that the modelled and Admiralty heights and times have a sufficient correlation to say that the modelled results of the spring tide are a good representation of the real event.

7.2.2 Analysis of Flow.

The variation of the tidal heights and mean flow with time can be deduced from the model data for any selected schemetised cross section. Figures 7.3a to 7.3f show the flow and stage relationships for some cross sections over the period of simulation.

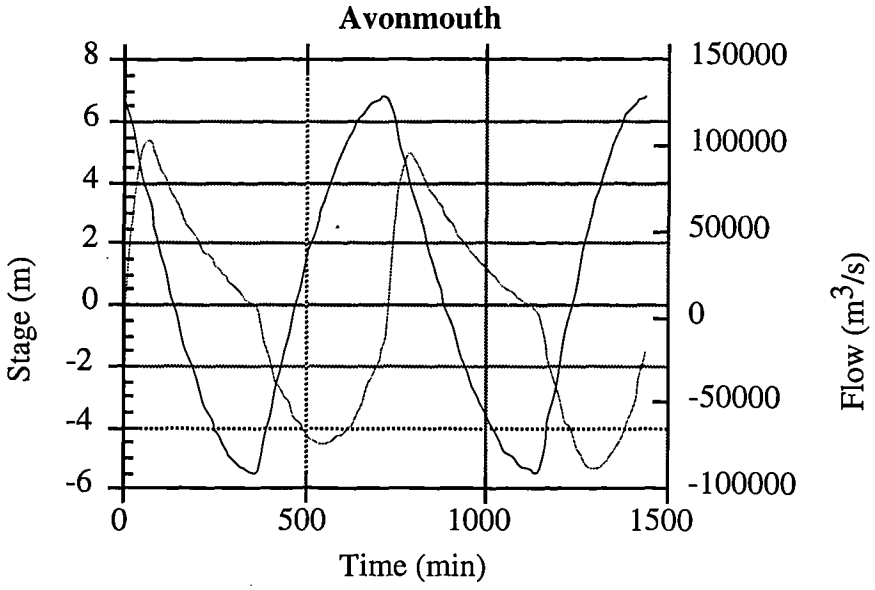

Fig7.3a Tidal stages and flow for a spring tide at Avonmouth.

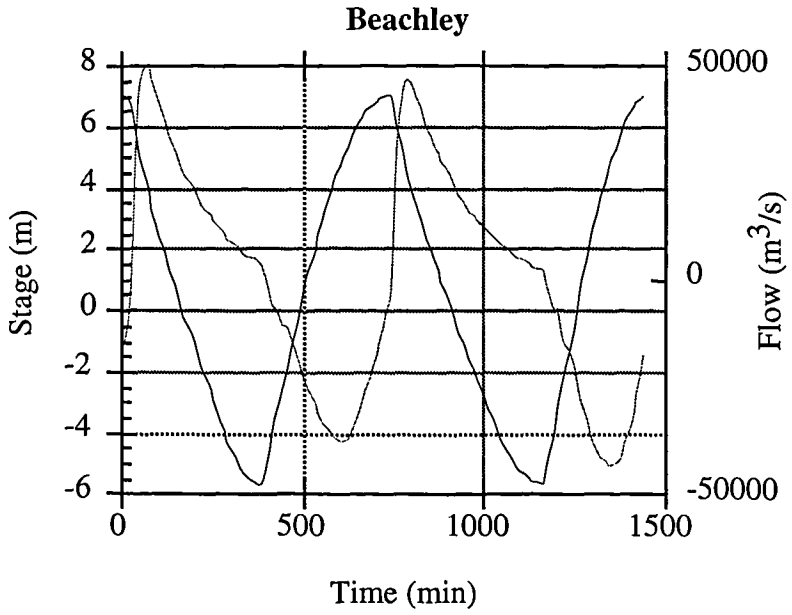

Fig7.3b Tidal stages and flow for a spring tide at Beachley.

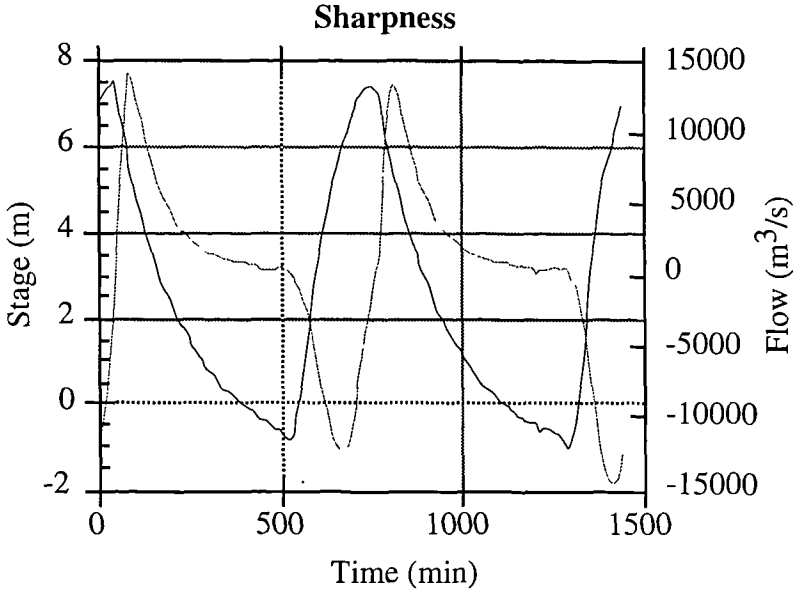

Fig7.3c Tidal stages and flow for a spring tide at Sharpness.

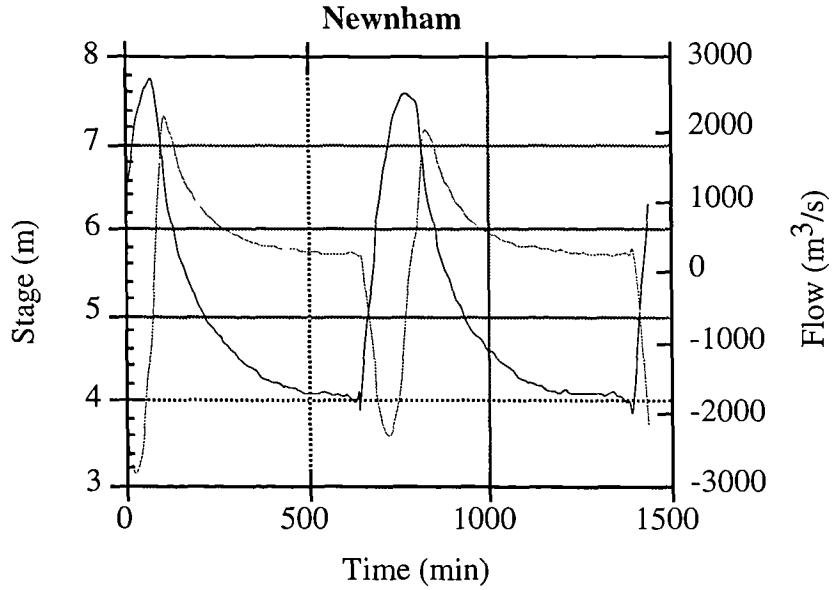

Fig7.3d Tidal stages and flow for a spring tide at Newnham.

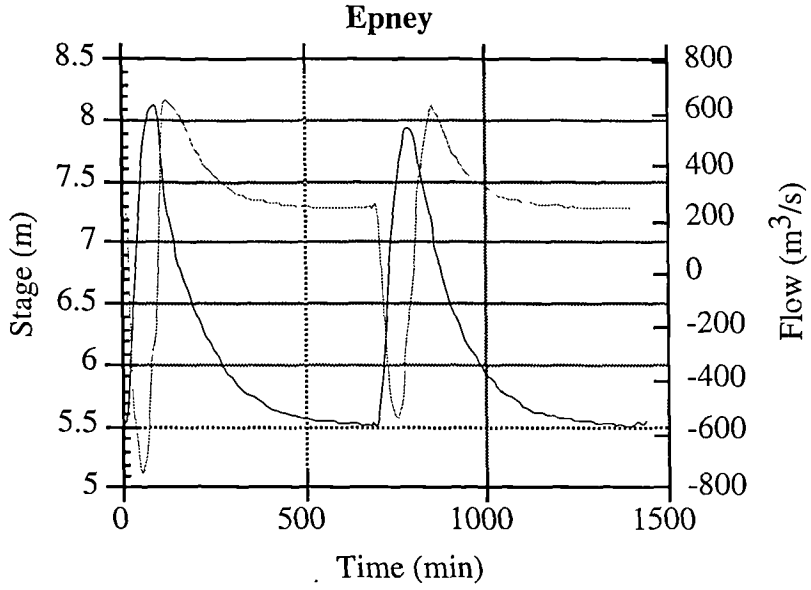

Fig7.3e Tidal stages and flow for a spring tide at Epney.

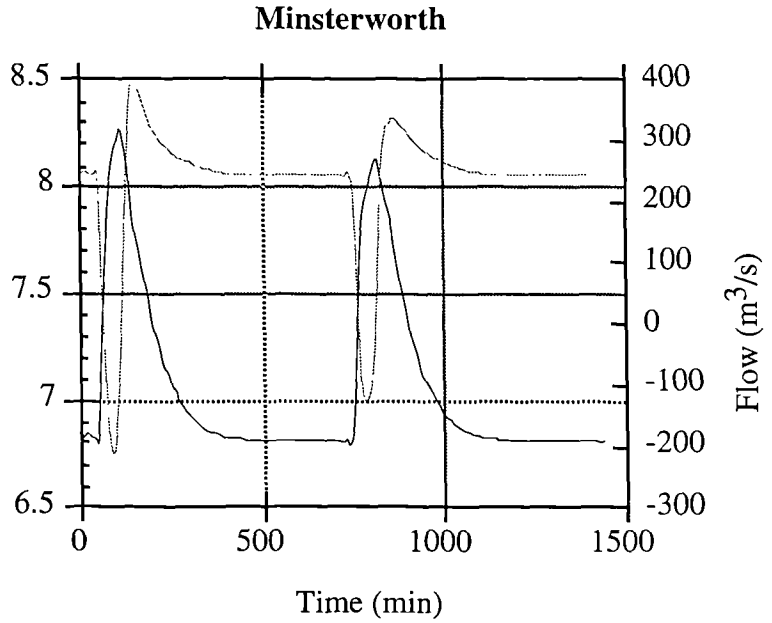

Fig7.3f Tidal stages and flow for a spring tide at Minsterworth.

The family of graphs which comprise Figure 7.3 illustrate the tidal curves and flows (feint line) for six representative cross sections in the Estuary. Unfortunately the apparent lack of smoothness in some areas of the curves is caused by the limitations of the software used to

display them and the printer, rather than representing small oscillations in the data, although all the curves, especially the one for Newnham, show some minor oscillations at low tide. It may have been preferable to display all these figures at the same time scale although as a result much of the detail would be lost on the upstream sections

The graph for Avonmouth (Fig 7.3a) clearly shows the nearly sinusoidal stage curve used as the downstream boundary for the idealised spring tide. The peak flow occurs some 150 minutes before the high tide, up to a maximum of about -90000 m^3/s, while the maximum ebb flow occurs some 100 minutes after high water, reaching quantities of about 90000 m^3/s. Once the maximum ebb is reached it slowly dies down to nearly nothing just around or after low water before the onset of the next tide. Whilst there is almost the same maximum flood and ebb flow, the period of flood, indicated as negative flow on the graphs, is slightly less than the ebb. It is noted that the calculated flood is greater after the second high tide, while the ebb maximum is slightly higher after the initial high tide. This appears to be a function of the model. The discrepancy can be reduced by running the model over more tidal cycles to allow the model to 'settle down'. However, the effect is not deemed to be of any great consequence to the analysis of results.

The curve for Beachley, where the Severn Road Bridge crosses at a natural constriction of the Estuary, shows a similar tidal curve to that of Avonmouth although high water is slightly higher. The maximum flow, however, is about one half of that calculated at Avonmouth. The timing of the changes in flow rate are similar to Avonmouth although the maximum ebb flow follows sooner after high water, as would naturally be expected. The period of flood flow is also reduced by about 30 to 50 minutes.

Further upstream at Sharpness (Fig 7.3c) the tidal curve starts to show distortion due to shallow water effects, with the period of rising tide and flood being considerably less than the ebb flow. This is again illustrated by a very rapid rise in the tidal heights, midway through which the maximum flood flow occurs (at about 650 minutes into the simulation). After this the rate of flow seawards rapidly decreases with the onset of the ebb tide. Ebb flow levels reach a maximum about an hour to an hour and a half after high water and then decline rapidly to nearly nothing. The period when the tide is 'on the turn' or slack water at low tide when there is almost no flow in either direction lasts about 4 hours, while there is almost no slack

water at high tide. Although it appears that there is no flow at low water, there is the component of river flow seawards occurring, but this is so small compared to the rates of flow generated by the tide, that it cannot be easily distinguished on the graph. The next incoming tide is then marked by a rapid increase in landward (negative) flow which lasts about 200 minutes.

The curve for Newnham shows increasing distortion, with a very small period of flood and longer ebb. Characteristics of the tidal curves are similar to those at Sharpness as are those at Epney and Minsterworth (Figures 7.3 e&f). The latter two curves show the component of river flow which could not be distinguished earlier. In these curves the flood flow lasts only about 2 hours while ebb flow and river flow lasts for about 10 hours. Between Epney and Minsterworth the maximum ebb becomes appreciably greater than the maximum rate of flood flow because riverine flow is becoming a dominant factor. A curve for the upstream boundary would show near steady conditions with flow rates equal to that of the boundary flow with a slight disturbance in water levels (about 20cm) representing the high water. The peak which represents this is a well-defined curve of small duration.

The mean cross sectional velocities generated during the spring tide (Figures 7.4 & 7.5) can be calculated by dividing the rate of flow by the areas of the channel cross section.

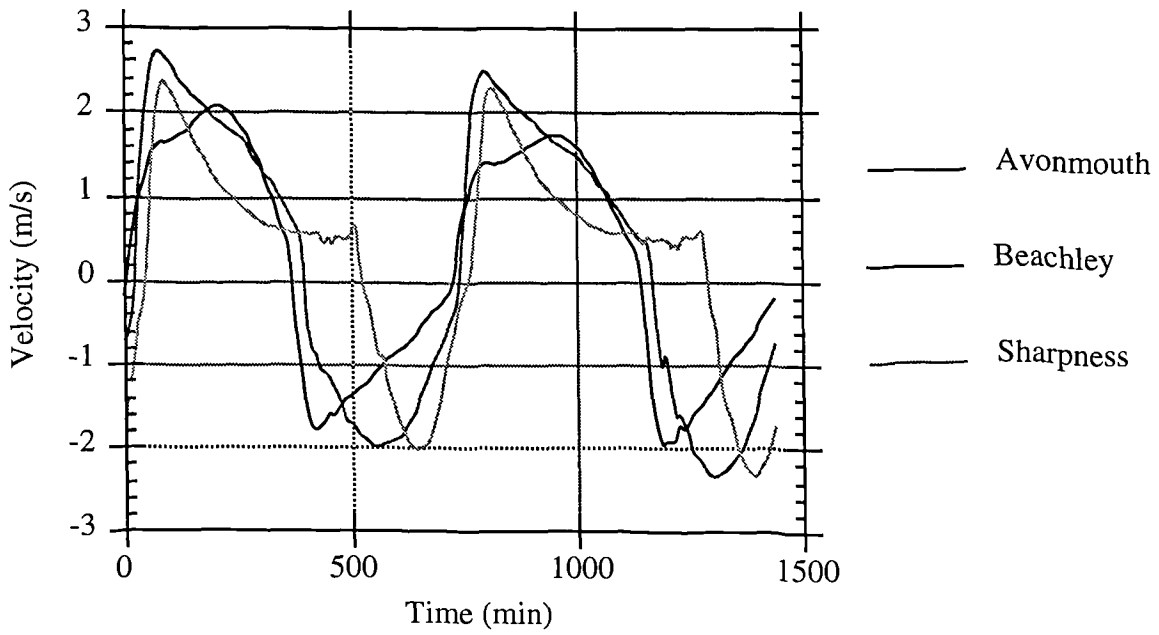

Fig 7.4 Flow velocities on spring tide, Avonmouth, Beachley & Sharpness.

The velocities indicated on Figure 7.4 show that the maximum tidal velocity generated at these sections is about -2.3 m/s on the flood at Beachley and about 2.4 m/s on the ebb at the same spot. The constriction at Beachley of the Estuary naturally amplifies the velocities and from there to Sharpness causes the maximum turbidity in the Estuary. The velocities generally mimic the flow curves for the sections in shape, with the exception of the curve for Avonmouth which shows very abrupt changes in the rates of flow at the onset of both the flood and ebb tides. The peak velocities of the ebb flow on the Avonmouth curve seem to be 'truncated' in comparison to the other two, with a slight wane in the rate of change of the flow velocities about an hour before the maximum flow velocities are calculated. The peak velocity at Avonmouth is recorded some time after the peak ebbs at Beachley and Sharpness. The maximum velocity at the latter is just after the high tide when the greatest ebb flow is occurring, while the greatest velocities at Avonmouth on the ebb tide are about 2 hours later, when the tide is halfway towards slack water and has about 2.5 metres to fall to low water. Thus it seems that the maximum velocities recorded at Avonmouth are a combined function of the quantity of ebb flow and the capacity of the channel to take the flow. A comparison of the calculated velocities and tidal stream velocities indicated upon the Admiralty Charts for Avonmouth is given in Table 7.4.

Hours	Admiralty Velocity (m/s)	Modelled Velocity (m/s)
-6	1.5	0.7
-5	0.3	-1.5
-4	-2.2	-1.5
-3	-2.4	-1.2
-2	-1.6	-0.9
-1	-1.3	-0.5
HW	-1.0	-0.2
1	0.3	1.3
2	1.1	1.4
3	1.2	1.6
4	1.5	1.7
5	1.6	1.5
6	1.6	0.7

Table 7.3 Admiralty and modelled flow velocities at Avonmouth (spring tide).

It is noted that the Admiralty figures are based upon the tidal stream in the main channel near the mouth of the Avon whereas the modelled figures represent the averaged cross sectional velocity. These values cannot therefore be expected to correlate with the Admiralty figures. The greatest correlation would be expected towards low water when the model cross section is smallest, thus flow is being modelled as if it is conducted along the narrow channel where the Admiralty tidal stream is measured. However, it has been mentioned previously that the schemetisation of the low water channel is prone to diverge the most from reality. The modelled higher water flow rates can be expected to be less than the Admiralty figures as the modelled results encompass slow flow rates over the mud banks and shoals, the Admiralty figures being based on observations in the fast water channel only. There is a suggestion from the tabulated figures that the model seems to calculate the reversal in flow at Avonmouth as occurring rather more suddenly than in reality. No reliable explanation can be given for this.

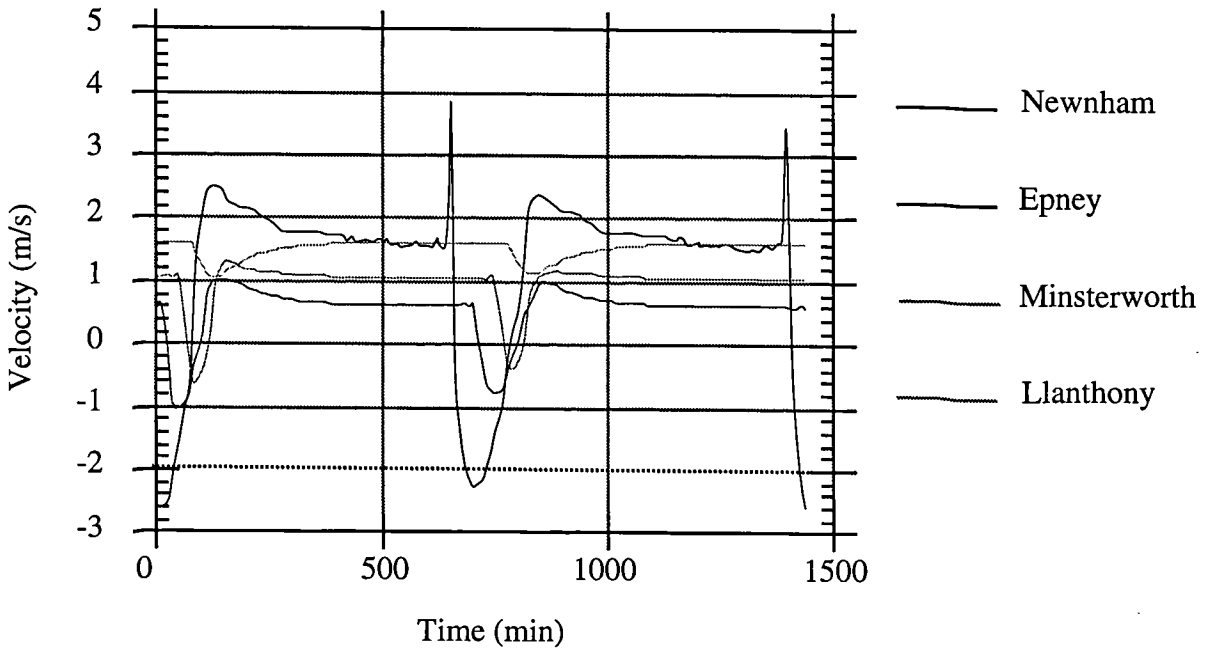

Fig 7.5 Flow velocities on spring tide, Newnham, Epney, Minsterworth & Llanthony.

The velocity curves shown in Figure 7.5 indicate that nearly steady flow conditions prevail in most of the sections and that the incoming tide represents a relatively short lived period of up-estuary flow. Steady flow conditions show an initial period of high velocity flow

towards the sea after the high tide has entered and passed the section. This settles down to a constant flow velocity which is defined by the rate of river flow and the capacity for flow of the channel. Thus cross sections which are either shallow or narrow show the greatest flow velocities. The curve for Newnham shows some 'noise' towards low water level, followed by a high peak, which is an effect of the 'late ebb' instability described in the previous chapter. It is also noted that flow in this modelled simulation is not affected significantly by low flow calculations, thus the peak is a mathematical anomaly rather than an inapplicable mathematical subroutine for low flow. This peak flow indicated to be nearly 4 m/s which seems to be caused by the combination of low river levels (hence cross sectional area) and the imminent onset of the next tide, which is represented by a very quick rise in water levels. This aspect of the model behaviour seems to indicate mathematically the very quick change in conditions which the macrotidal estuary produces is too great to be truly represented by this form of mathematical model. A shock capturing finite difference method such as the Lax Scheme is more apt for this condition. This feature is further confirmed in that increasing the time weighting factor helps to remove the noise and late ebb instability. It was found that the 'late ebb' instability only occurs in relatively few modelled conditions, and is usually due to too low friction values in the local vicinity of the cross section where it is seen. Very minor changes to the friction values at the cross section, which have no overall effect on any other modelled results, usually remove the rogue values. It is also noted that Griffiths (1974) found very similar behaviour downstream near Slimbridge.

One of the most important aspects of presenting modelled results has been highlighted in Figure 7.5 on the curve for Newnham. It is easy to show peak and low water levels or flow rates only as a comparison in data tables, in which case a flow of 4 m/s would be presented for Newnham at a time when a steady flow rate of under 2m/s is more representative of the flow in this part of the system. This lack of care taken in questioning the output results is quite apparent in other model studies.

7.3 Neap Tide.

The present day neap tide has a range of 6.0m at Avonmouth (Admiralty Tide Tables, 1993) with a high water level of 3.3 mAOD and a low water level of -2.7 mAOD. An idealised curve for the neap tide occurring at Avonmouth is given in the tide tables and is presented as Table 7.4.

Event	Time	Height (m)
High Water	0:00	3.3
Low Water	6:20	-2.7
High Water	12:30	3.3
Low Water	18.50	-2.7

Table 7.4 Neap tide times and levels.

The tide shown in Table 7.4 has been used as the downstream boundary conditions to calculate the behaviour of a neap tide in the Severn Estuary. The upstream boundary conditions selected were the same as for the spring tide simulation in Section 7.2. The calculated high and low water levels are shown in Figure 7.6 and the times of the tides in Figure 7.7. Table 7.5 indicates the timing of the observed and predicted tidal events.

Place	Time HW (Predicted)	Time HW (Admiralty)	Time LW (Predicted)	Time LW (Admiralty)
Avonmouth (0 km)	740	740	380	380
Sharpness (29.3km)	799	790	492	565
Newnham (43.9 km)	Tidal Limit	-	Tidal Limit	-
Epney (53.0 km)	-	-	-	-

Table 7.5 Modelled and observed neap tide times.

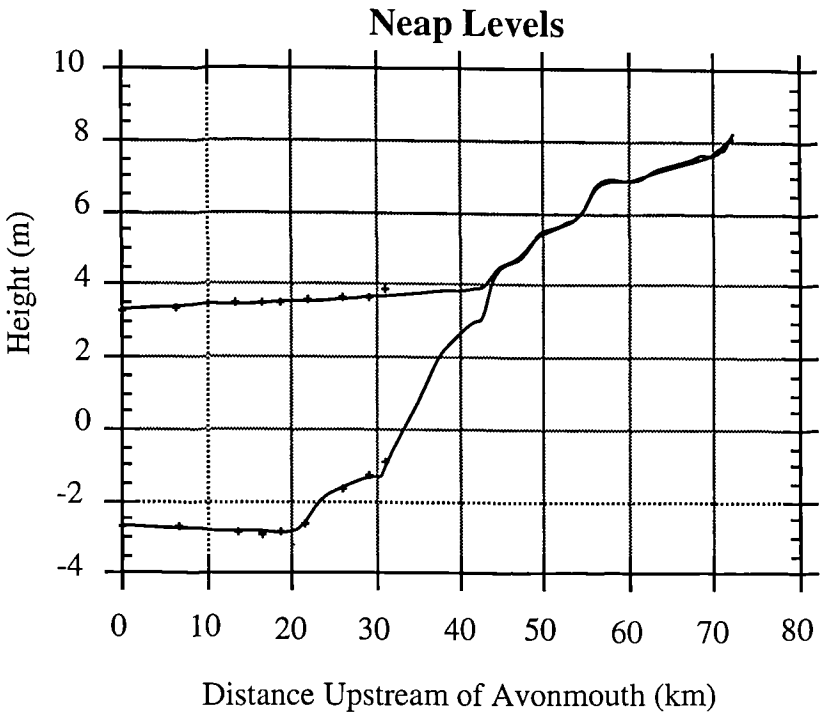

Fig 7.6 Neap tidal heights, Admiralty predictions indicated as crosses.

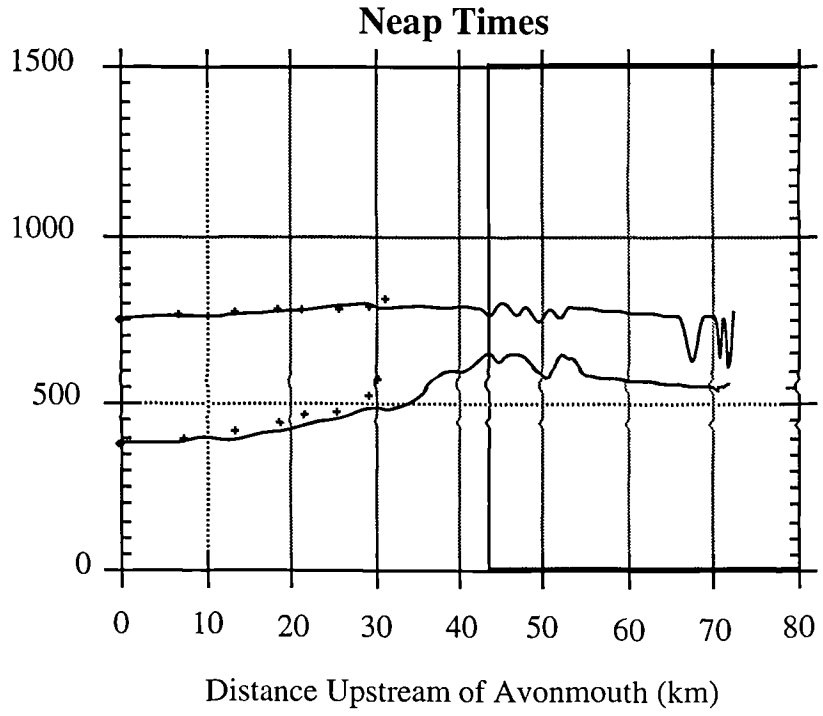

Fig 7.7 Neap tide times, shaded area is non tidal.

7.3.1 Analysis of Tidal Heights and Times.

The modelled neap tide levels show good correlation with the Admiralty observations, even with the problems discussed in Section 7.2 of resolving the observed levels and an idealised tide. Admiralty figures are illustrated as points on Figure 7.6 against the continuous line of the modelled results. The timings of high and low water are not as close as the spring tide calculations, especially at low water neap where the model seems to be predicting low water about half an hour to an hour earlier than encountered. However, as there is a longer period of slack water on a neap tide, this is not unacceptable. The modelled tide levels show close agreement to the Admiralty figures, in contrast to the modelled spring tide in the Lower Estuary, highlighting the findings of the model verification that the spring low tide level causes low flow modelling problems in the area. Again it is concluded that the model and observed levels and times show a sufficient correlation to say that the simulated neap tide is a good representation of the real event.

7.3.2 Analysis of Flow.

The variation of tidal heights and mean flow with time have also been deduced for selected cross sections on the neap tide and are illustrated in Figures 7.8a to 7.8c. The graphs of tidal heights and quantity of flow illustrated in these figures show similar characteristics to the spring tide graphs of the same properties, although naturally, the tidal range and flow quantities are about one half of those generated on the spring tide. A more direct comparison of the spring and neap characteristics is given in Section 7.4. One feature of note is that these graphs indicate that the maximum ebb flow on a neap tide is appreciably greater than the flood flow on the same tide. There are differences of a similar order on the spring tide flow, although they appear much less significant given the greater range of flow. The flow levels indicated on Figures 7.8a to 7.8c are indicated as the feint curves on the graphs.

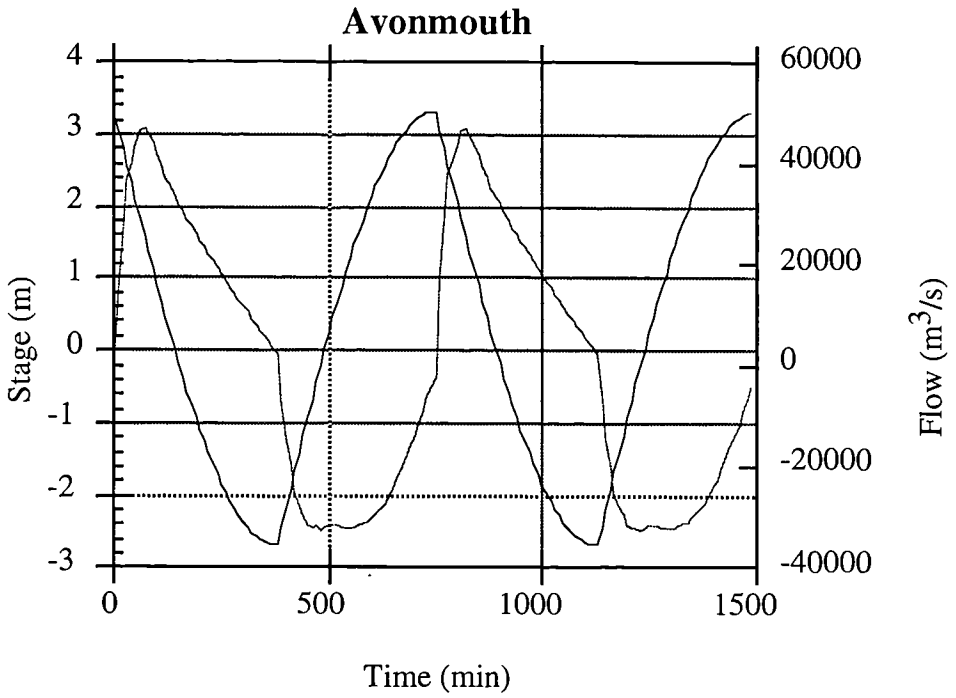

Fig 7.8a Tidal stages and flow for a neap tide at Avonmouth.

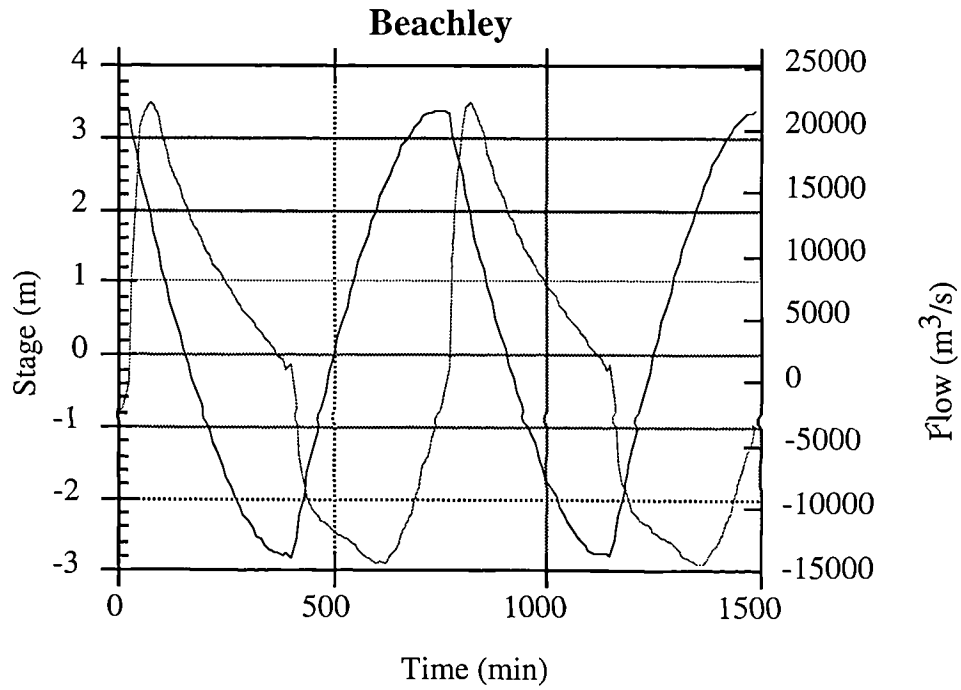

Fig 7.8b Tidal stages and flow for a neap tide at Beachley.

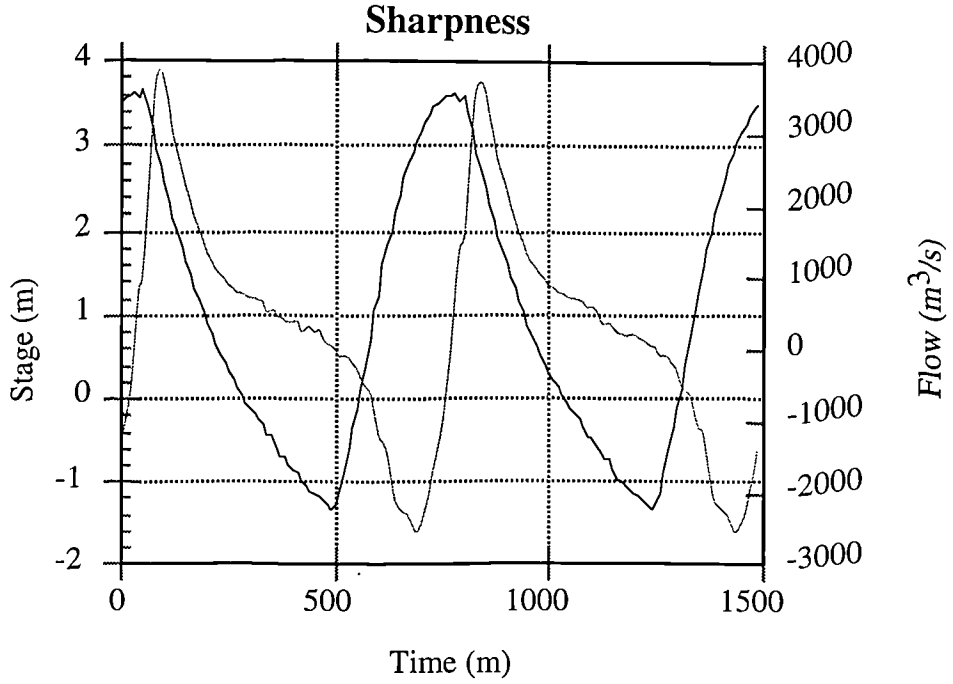

Fig 7.8c Tidal stages and flow for a neap tide at Sharpness.

As the neap tide only penetrates the Estuary to Newnham it is not necessary to present the stage and flow curves for the stations upstream of here as they approximate to a straight line at a steady level. The steady flow levels for the stations used as a comparison in Section 7.2 were, Newnham (3.9 mAOD), Epney (5.5 mAOD), Minsterworth (6.8 mAOD) and Llanthony (7.9 mAOD), with velocities being almost the same to those on the spring tide. The flow rate for Minsterworth was 150 m/s and 100m/s at Llanthony.

The mean cross sectional velocities generated on a neap tide are illustrated in Figure 7.9 for three cross sections. This figure illustrates how the maximum velocities on a neap tide are again generated at Beachley on ebb flow, which is calculated to be nearly 1.5 m/s which is 1.5 times the maximum flood flow velocity. The curve for Avonmouth indicates that lower velocities are generated compared to the other two sections, being in the region of 1 m/s. The velocity curve for Avonmouth, as with the spring tide shows less peakedness than the other two, although unlike the spring curve, the highest velocities are calculated to occur just after the onset of the ebb tide. Whereas at Avonmouth the maximum flood velocities occur just after low water and slow in a linear fashion immediately afterwards, the maximum flood velocities at Beachley occur over a much longer period of time, perhaps as much as 4 hours, before

waning at a quicker rate than at Avonmouth. The explanation for this is that the flood flow, although being driven up the Estuary by natural forces, is retarded by the constriction at Beachley, which is unable to carry all the flow. This means that the tide effectively 'backs up' behind the narrowing. The opposite effect seems to happen on the ebb tide.

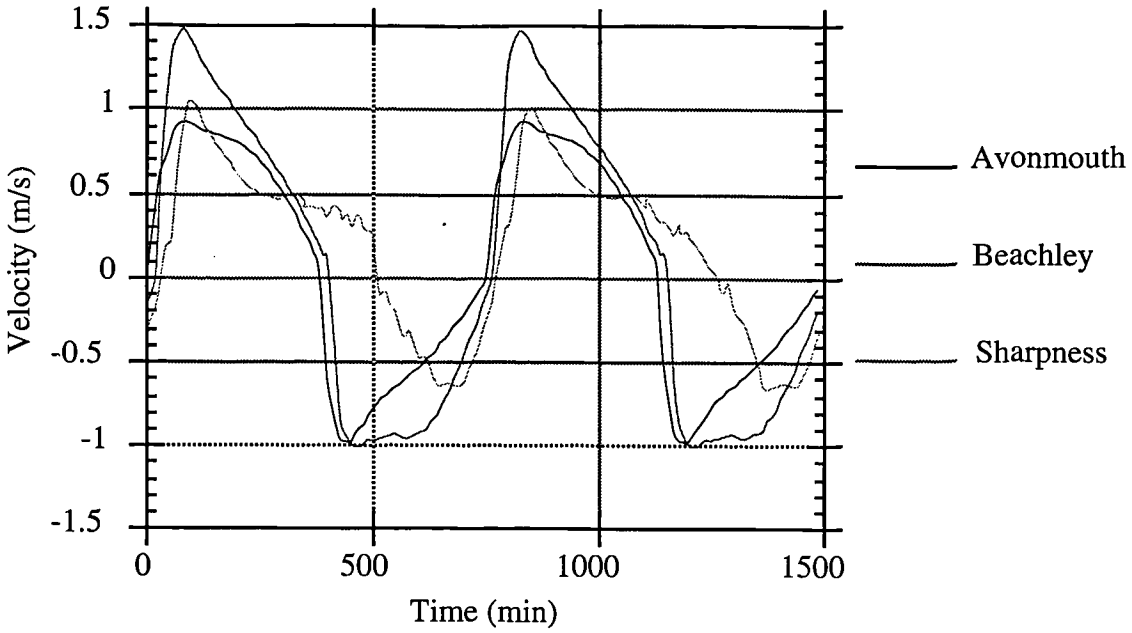

Fig 7.9 Tidal velocities at Avonmouth, Beachley and Sharpness calculated on neap tide.

A comparison of Admiralty tide stream and modelled velocities for a neap tide is given in Table 7.6 for Avonmouth. As can be seen in Table 7.6, the magnitude of flows is similar for both sets of data. The computer simulation, however, computes maximum flood velocities 2 hours after high water, while the Admiralty figures indicate the greatest flow velocities near to low water. As the Admiralty observations are in the middle of a channel it is likely that at low flow much of the water is conducted through this route and that velocities would be higher than those modelled. The ebb flow is modelled as beginning slightly before the Admiralty tide stream data and quickly reaches maximum velocities after the change. When observing the tides near Avonmouth to the Severn Bridge after the tide has changed it is possible to see the tide behaving in a very complex manner with channels still appearing to be carrying a flood flow whilst other areas appear to be ebbing. To model this behaviour is far

beyond the capabilities of the simulation but does help to explain the difference between the model approximation and complex natural phenomena.

Hours	Admiralty Velocity (m/s)	Modelled Velocity (m/s)
-6	0.9	0.2
-5	0.2	-0.9
-4	-1.2	-0.8
-3	-1.2	-0.6
-2	-0.8	-0.5
-1	-0.7	-0.3
HW	-0.5	-0.1
1	0.2	0.8
2	0.6	0.9
3	0.6	0.8
4	0.8	0.7
5	0.9	0.5
6	0.9	0.1

Table 7.6 Admiralty tidal streams and modelled velocities for a neap tide at Avonmouth.

The tidal velocities generated for the constant flow at the upstream example stations were as follows; Newnham (1.51 m/s), Epney (0.6 m/s), Minsterworth (1.04 m/s) and Llanthony (1.43 m/s).

7.4 Comparison of Simulated Neap and Spring Tides.

The previous two sections in this chapter have described the modelled spring and neap tides. This section compares the salient features of both to highlight the principal differences and similarities between the two events. The two tides represent the two end members of nearly all the tides which occur in the Estuary.

	Spring Tide				Neap Tide			
Place	Hours	Height (m)	Max.* Flow (m^3/s)	Max.* Velocity (m/s)	Hours	Height (m)	Max.* Flow (m^3/s)	Max.* Velocity (m/s)
Avonmouth HW	0:00	6.7	-89000	-2.0	0:00	3.3	-32800	-1.0
LW	-6:50	-5.6	103600	2.1	-6:10	-2.7	45600	0.9
Beachley HW	0:12	7.0	-43000	-2.3	0:17	3.4	-14400	-1.0
LW	-5:36	-5.9	48000	2.7	-5:41	-2.8	22000	1.5
Sharpness HW	0:39	7.3	-14700	-2.3	0:49	3.7	-2600	-0.7
LW	-3:31	-1.1	14300	2.3	-4:09	-1.7	3700	1.0
Newnham HW	1:11	7.5	-2800	-2.7	-	-	-	-
LW	-1:05	3.4	2200	2.5	-	3.9	250	1.5
Epney HW	1:19	7.8	-750	-1.1	-	-	-	-
LW	0:12	5.5	660	1.0	-	5.5	250	0.6
Minsterworth HW	1:35	8.0	-220	-0.7	-	-	-	-
LW	0:20	6.8	400	1.3	-	6.8	250	1.1
Llanthony HW	2:14	8.6	98	1.1	-	-	-	-
LW	0:13	8.0	100	1.6	-	7.9	100	1.4

Table 7.7 Comparison of modelled spring and neap events. * denotes max. on flood or ebb tide, not necessarily at high or low water.

As can be seen in Table 7.7, a spring high tide progresses up the Estuary at a faster rate than the neap because the celerity of the incoming long wave is greater due to the deeper depth of water. The maximum rates of flow on a spring tide are typically 2.5 to 3 times greater than those on a neap in the area penetrated by both tides. In the tidal Lower Estuary the ebb flow generally reaches greater velocities and has a higher maximum flow rate than the flood, which is surprising as the flood duration is less.

The shape of the neap and spring tidal curves are essentially the same except that much less water is being transported on the neap flow and that some reaches are non tidal on the neap. However, the low neap tidal levels correspond much better with Admiralty figures in the Lower Estuary because of shortcomings in the model's capabilities to accurately model very low flows.

The modelled results presented in Table 7.7 are to the nearest 0.1m. The model results actually predicted a low water spring level in the Middle and Upper Estuary, slightly above the low water neap level by 0cm to 5cm. In nature the low water spring levels are higher than the neap ones as so much water enters the Upper Estuary that it is unable to drain sufficiently as water is stored on floodplains and in pills. The computer simulation of this aspect is not particularly convincing. However, a two dimensional model may be able to simulate this effect to greater satisfaction.

7.5 Tidal Surges.

As the tidal surges used as verification events in Chapter 6 are essentially similar in range and nature, this section will only consider the February 1990 surge as it is the best documented event. This tidal event recorded the highest level at Avonmouth since 1883 and is depicted in Table 7.8.

Event	Hours	Height
High Water	0:00	7.15
Low Water	7:00	-4.8
High Water	12:10	8.79
Low Water	19:10	-5.5
High Water	24:00	7.15

Table 7.8 February 26th 1990 tidal surge at Avonmouth. Hours do not refer to actual time of occurrence on the day.

7.5.1 Analysis of Tidal Heights and Times.

The calculated surge heights are shown on Figure 7.11 and show reasonable agreement with the limited numbers of observed levels, although there is a slight underprediction of levels at Minsterworth, c. 62km upstream of Avonmouth. Figure 7.12 shows reasonable agreement

with the times of the tides. Although the low tide which occurred after the surge was some 0.7m lower at Avonmouth than the low water before the surge, the observed data showed that levels were slightly lower on the low tide which occurred before the tidal surge, rather than afterwards from about 50 km upstream of Avonmouth. However, levels were very similar in this region at low water either side of the surge. This is because river flow waned during the course of the events, but was not modelled to do so.

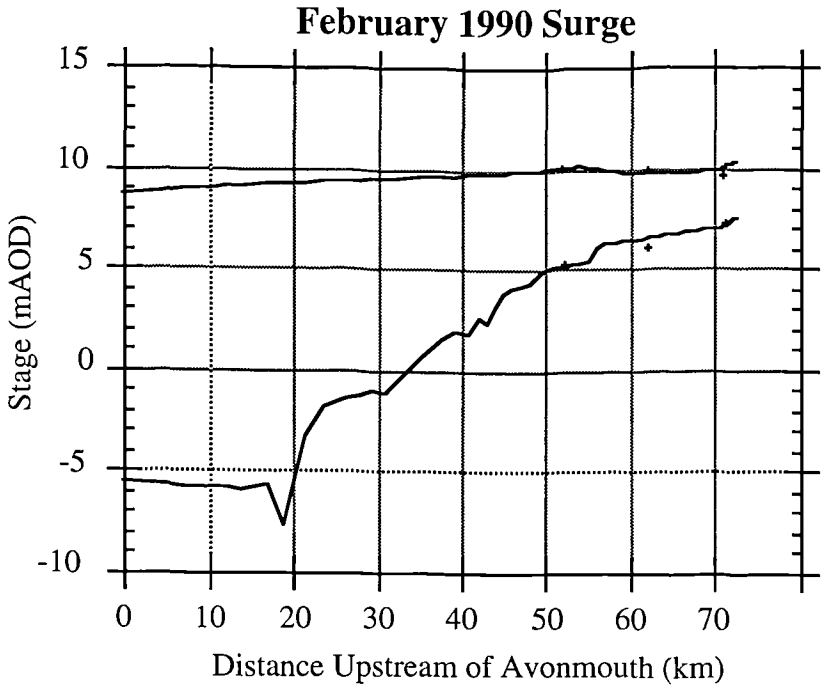

Fig 7.11 February 1990 tidal surge levels, calculated and observed (crosses).

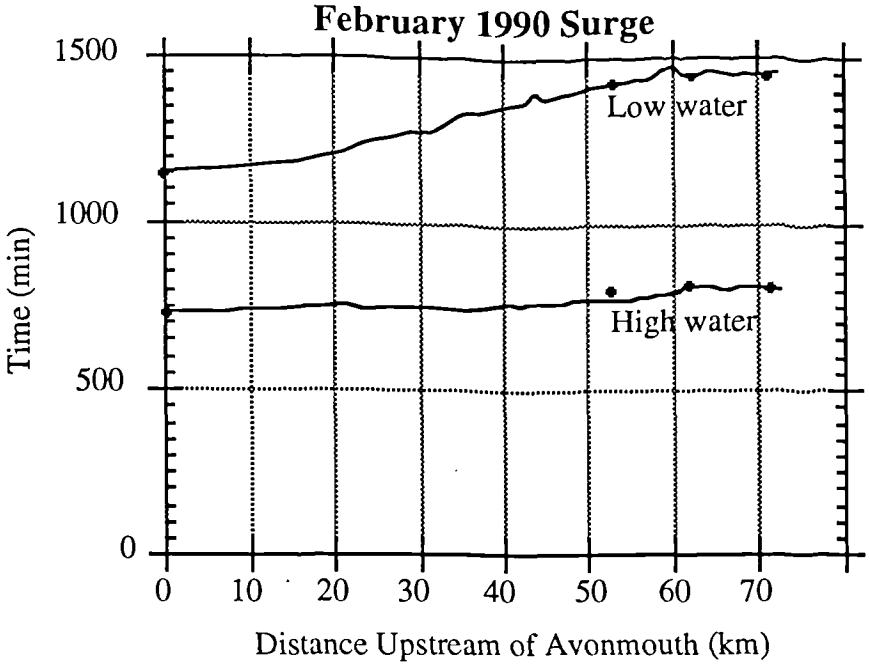

Fig. 7.12 Times of February 1990 surge, modelled and observed (points).

7.5.2 Analysis of Flow.

It is easier to compare the modelled and observed events at individual sections when data is available. It is deemed important to show the quality of the model through such a comparison as the 1990 tide is the best yardstick by which to measure the accuracy and capabilities of the model because it is the best recorded extreme event. The individual tidal curves and calculated flows are given in Figures 7.13a to 7.13g, with any observed levels placed upon the graphs for visual correlation of the real and modelled events. The flows are illustrated as faint curves on the graphs.

Many of the features of these curves such as their shape and timing are similar to that of the spring and neap tides, although the tidal heights and flows are naturally higher. This tide is the first to demonstrate the penetration of the entire modelled areas of the Severn Estuary and so demonstrates the capability of the weir calculation module.

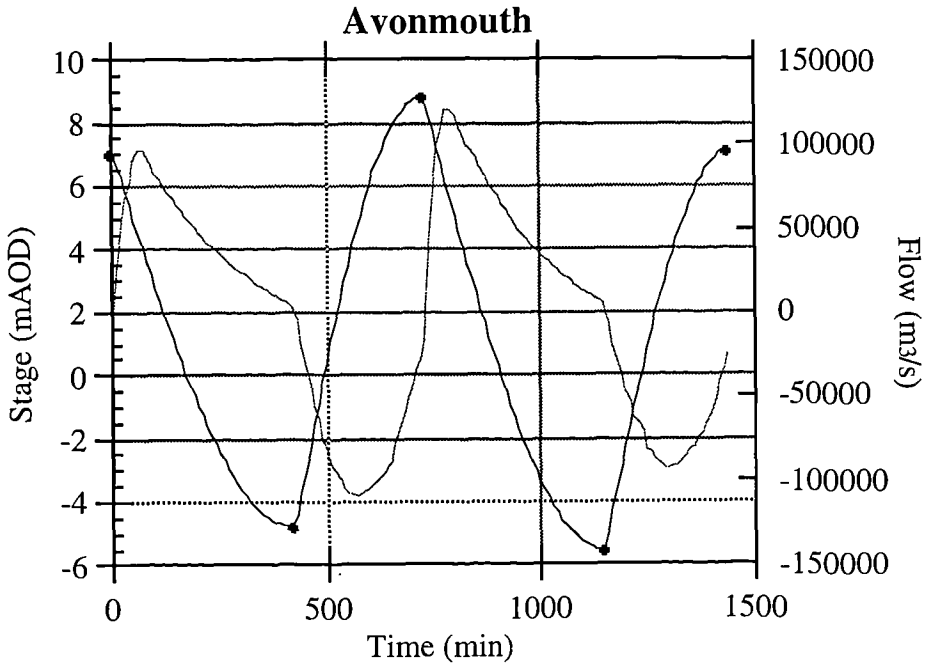

Fig 7.13a 1990 tidal surge calculated for Avonmouth, points show observations.

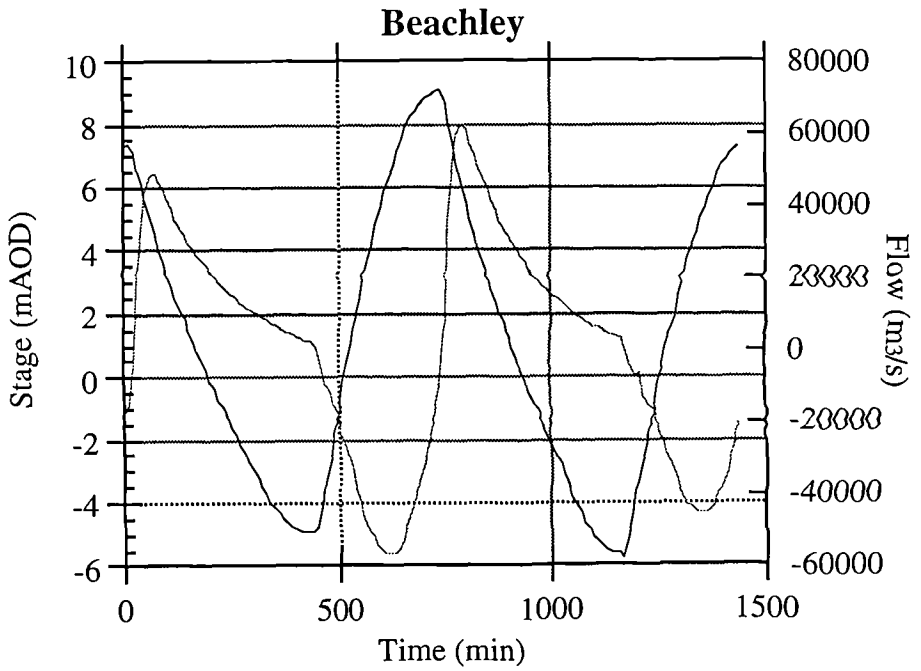

Fig 7.13b 1990 tidal surge calculated at Beachley.

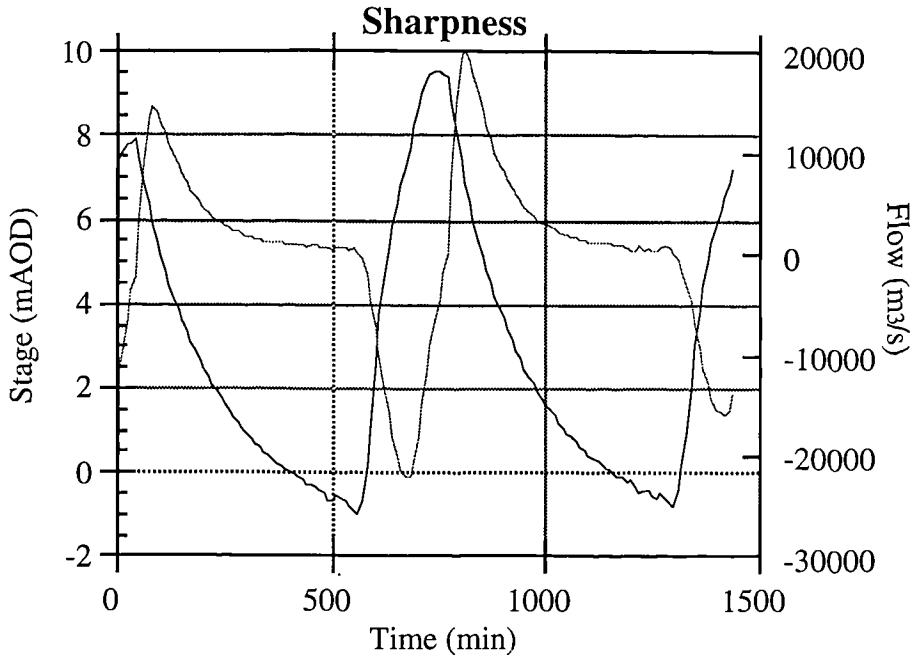

Fig 7.13c 1990 tidal surge calculated at Sharpness.

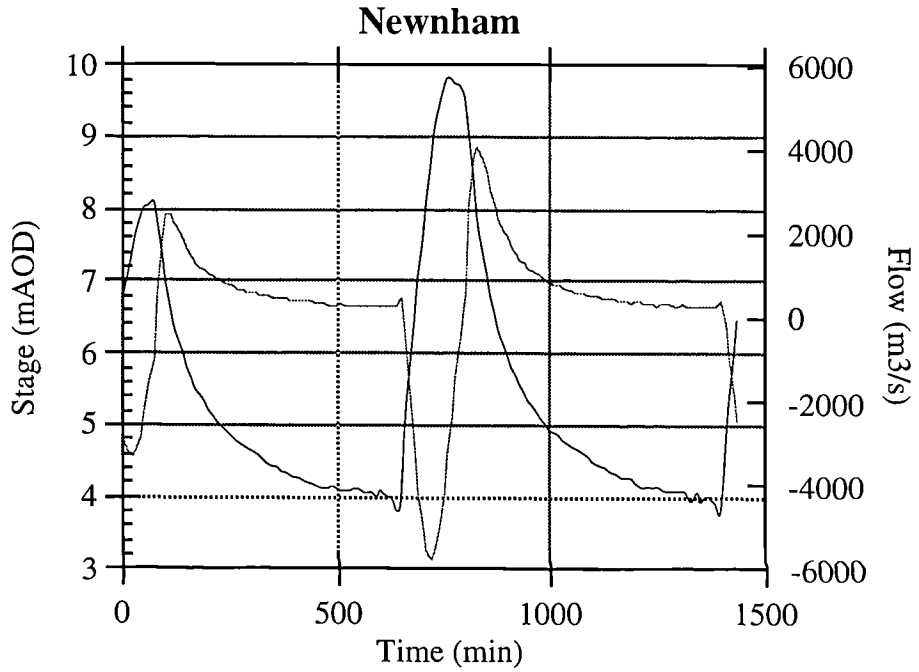

Fig 7.13d 1990 tidal surge calculated at Newnham.

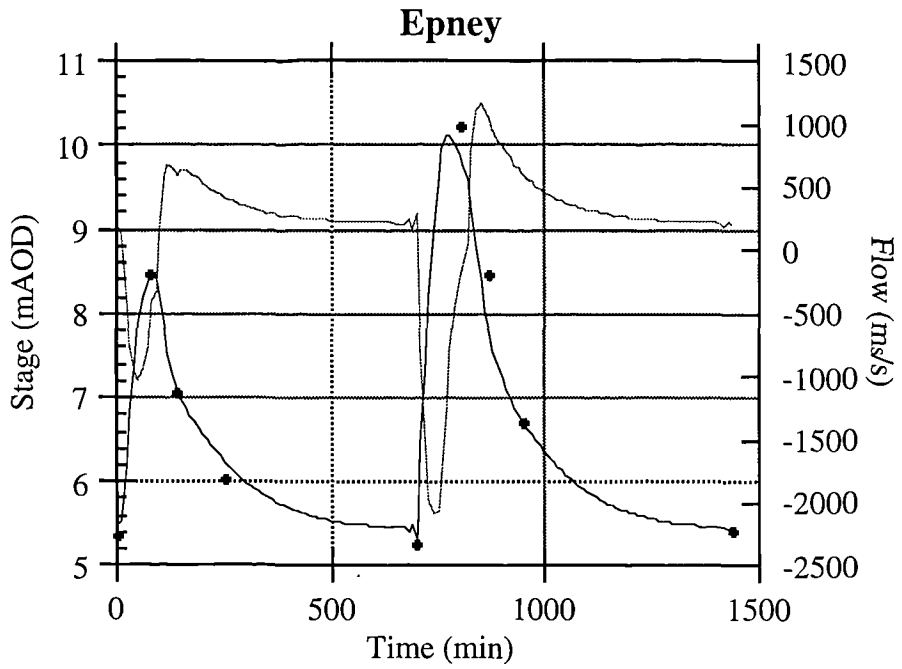

Fig 7.13e 1990 tidal surge calculated and observed at Epney.

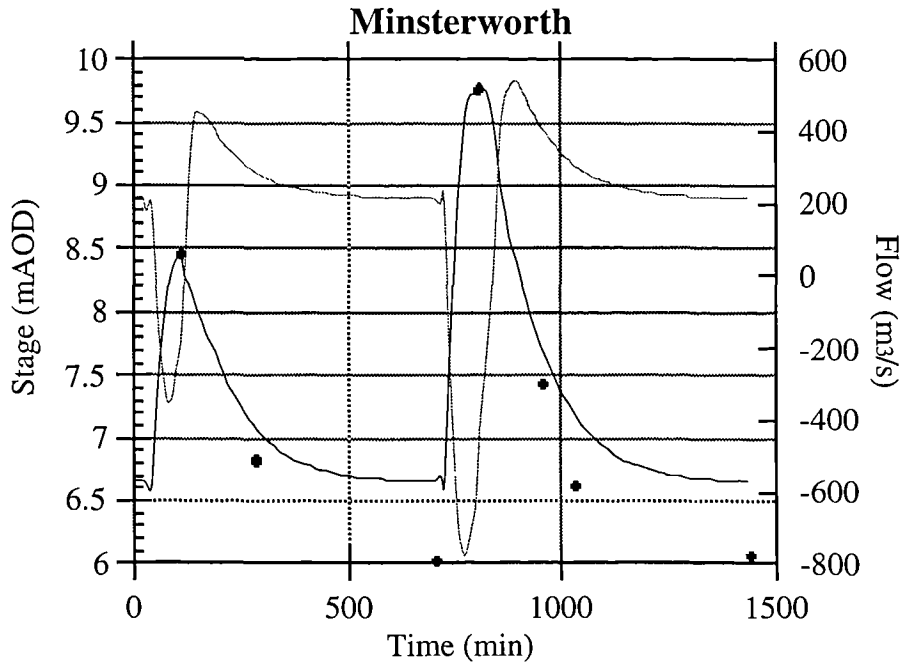

Fig 7.13f 1990 tidal surge calculated and observed at Minsterworth.

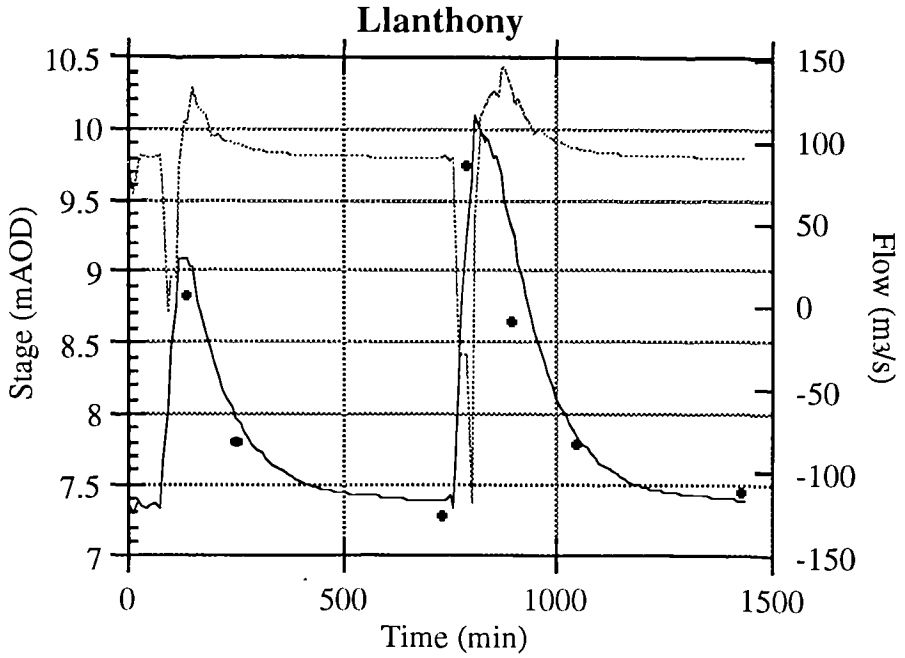

Fig 7.13g 1990 tidal surge calculated and observed at Llanthony.

The graphs of stage and flow in Figures 7.13a to 7.13g show the tidal behaviour at each section. The peak of the tidal surge at Avonmouth rises upstream reaching a peak at about 52km further upstream near Epney. Unfortunately there is only observed data available for Epney, Minsterworth, Llanthony and the tidal curve at Avonmouth by which to compare the results.

The shape of the tidal curve at Avonmouth is similar to that of the spring tide, other than the maximum flood flow is about 110000 m^3/s, as opposed to being about 90000 m^3/s on a spring tide. The peak ebb tide flow is similarly greater than that on a spring tide. What is interesting is that the low water level at Avonmouth is similar to that of a spring low water level, which has previously caused a low flow problem in the Middle/Lower Estuary. The low flow problem is usually indicated by abnormally low water levels between 15 and 20 km upstream of Avonmouth, accompanied by minor instabilities or 'noise' in the stage-time graphs at low water. However it is less pronounced in the modelling of the surge tide. It appears that the great quantity of water which is modelled to have entered the Estuary upstream provides a greater ebb base flow at low water as it takes longer to drain this volume and so creates less low flow problems. This seems to confirm the steady flow levels observed in the

Middle Estuary, where spring low water levels are higher than the neap. however, this is not borne out in the calculated steady flow levels which are similar to, if not slightly lower than the spring levels in most locations. It is noted that the upstream boundary conditions used for the spring simulation in Section 7.2 have greater flow rates than the boundary conditions used for the surge. The spring boundary conditions are slightly high to represent a modal value for flow at Gloucester.

The curves for Sharpness and Beachley show similar behaviour to that at Avonmouth when compared to the spring tide graphs. It is clear, however, that in the surge simulation the maximum flood flow occurs before the surge high water and the maximum ebb just after it. This may seem obvious, but the spring tide graphs presented in Section 7.2 showed discrepancies either side of a symmetrical tide in the ebb and flood maxima. This appears to be a function of the solution method which could not be resolved. It also implies that the maxima and minima calculated during the surge tide simulation may be slightly damped (before surge) or amplified (after surge) due to this behaviour of the model. The calculated maximum flood flow at Sharpness of nearly -25000 m^3/s is noted to be considerably higher than that on the spring tide which generates a maximum flow of about -12500 m^3/s.

The maximum flood flow at Newnham is nearly three times that of the spring tide and the ebb flow twice the rate, thus unless water is allowed to spill over sea walls, this area of the Estuary which is relatively narrow must generate significantly high tidal velocities. These are discussed in the next section.

The observed levels at Epney seem to indicate that the modelled tide reaches this point slightly earlier than in reality although the calculated levels were in very close agreement. The times of high water compared on the surge and spring are best seen by reference to Figure 7.12 and Figure 7.2. The latter has a much steeper gradient indicating that the higher tides penetrate the Estuary at much quicker rates, leaving a longer period of ebb afterwards. The surge tide at Epney is indicated to be about 2.4m higher than the spring as compared to a difference of 2.2m at Avonmouth.

The observed and modelled data at Minsterworth also show good correlation with respect to tide times and heights, although the low water level is calculated to be higher than the observed level by about 0.6m. This may be due changes in the bed levels of the channels

or an incorrect friction setting for the general area. Unfortunately the channel bed could not be surveyed to determine any discrepancies between the used model sections and the present day ones. An aspect of this discrepancy in modelled and observed levels at Minsterworth is that the stage curve appears to reach low water conditions later than observed. This is not the case as the modelled low water level is higher than the observed level, so modelled and observed low water conditions occur at a similar time but appear to be different because of the steady flow levels they attain.

The model over predicted high water levels at Llanthony (Fig 7.13g) by about 0.3m, although the modelled high water occurs later than the observed event which partially contradicts the effects that friction would have on these levels. Low water levels show a good correlation at this location. The graph for Llanthony shows the most distortion compared to the smooth curves generated for other sections as the effect of the calculations to simulate Llanthony Weir immediately downstream cause some noise as they are only an approximation to flow and disrupt the continuity of the flow equations. The effect is relatively minor, however, so it is arguable that the local disturbance to the modelled results in this area is as acceptable as a mathematically continuous solution which does not simulate the weir. It was determined during the verification processes that the instabilities caused by the weir calculations are not propagated significantly to other cross sections thus the reliability of the model is not affected. At Llanthony there is a very sudden reversal of flow as the high tide enters. However, it is very short lived in the order of an hour before the system ebbs. The period of tidal ebb before steady river-like flow conditions occur is also short lived, in the order of 3.5 hours, whilst steady flow conditions last for a further 9 hours or more.

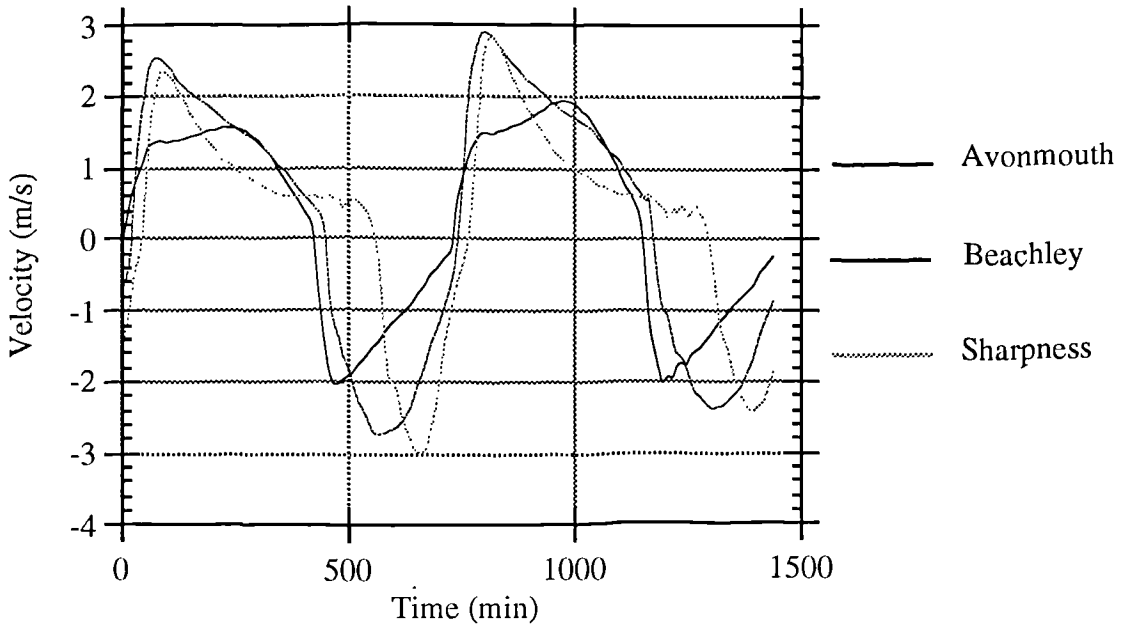

Fig 7.14 Flow velocities calculated for 1990 surge tide, Avonmouth, Beachley & Sharpness.

The mean cross sectional velocities calculated are illustrated in Figure 7.14 for the three example stations in the Lower Estuary. These curves indicate that maximum flood velocities in the order of -2 m/s, -2.7 m/s and -3 m/s are generated for Avonmouth, Beachley and Sharpness respectively. The velocity at Avonmouth is not significantly different to that generated on a spring tide and the ebb velocities were modelled to be slightly less than those generated on a spring tide. This can be explained through the relationship of the water stage, cross sectional area and quantity of flow. Although greater quantities of flow are calculated on the ebb tide of the surge than a spring, the water stage and thus the cross sectional area is greater, so the channel has a greater capacity at high water during the surge. The flood tide at Sharpness and Beachley reaches significantly higher velocities on the surge tide than on the modelled spring tide because the channel capacity does not increase enough with the stage to conduct flow at the same velocity as on the spring.

There is a significant progression in the time of the maximum flood velocities, occurring first at Avonmouth, then nearly two hours later at Beachley and a further two hours later at Sharpness. Maximum ebb velocities at all three sections are of a similar magnitude to spring velocities. The maximum ebb velocities occur nearly simultaneously at Sharpness and

Beachley and rapidly die down. The ebb at Avonmouth again shows a depressed ebb curve, as do other cross sections in the vicinity which are not natural constrictions.

There are two distinctive curve types which illustrate the velocities computed during the tidal cycle for the Lower Estuary sections as illustrated in Figure 7.14 which appear to be a 180 degree rotation of each other. These can be summarised as follows and be roughly related to natural phenomena, although it is appreciated that in reality it is much more complex than described.

- Broad Channel Cross Section.

A broad channel cross section such as that at Avonmouth exhibits velocity behaviour which produces the maximum velocities on an ebb tide, some time after high water has occurred and produces the maximum velocities on the flood tide soon after low water. The characteristic shape of the velocity curve is rounded during ebb flows and pointed during flood. When an ebb tide begins the high water level is such that there is a large channel area and hence conveyance. Velocities do not need to be large to move the driven tide through the cross section, until the water surface has dropped to a level that the cross section cannot conduct the driven tide without speeding the tidal flow. The flood tide occurs after water levels have dropped and the conveyance is low, so that initially high velocities are required until the stage has increased to such a level that the conveyance is great enough for the velocity to drop.

- Narrow Channel Cross Sections.

These sections such as Beachley and Sharpness show the highest ebb velocities soon after high tide, which slowly die down with the tide. The flood velocities increase in a slower fashion, giving the impression of a sharp point during the ebb and a rounded curve during the flood on the velocity graph. Flow velocity in such a cross section is directly related to the flow rate caused by the tide as the cross sectional area, thus the conveyance, does not vary to as great an extent as in a broad section.

The sections in the Middle and Upper Estuary exhibit different velocity characteristics as the tide becomes more distorted. Figure 7.15 indicates the velocity characteristics at

Newnham, Epney, Minsterworth and Llanthony. These graphs show that the highest velocities are generally generated on the flood tide which is relatively short lived. The ebb tide has longer to drain the water which has entered on the flood tide and generally generates lower velocities than on the flood, which die down to a velocity representing the river flow. Obviously upstream penetration becomes less with distance and the effect of the incoming flood reduces. The curve for Newnham again shows a high ebb velocity just before the onset of the high tide as the cross sections here and nearby become very shallow and approach critical flow conditions.

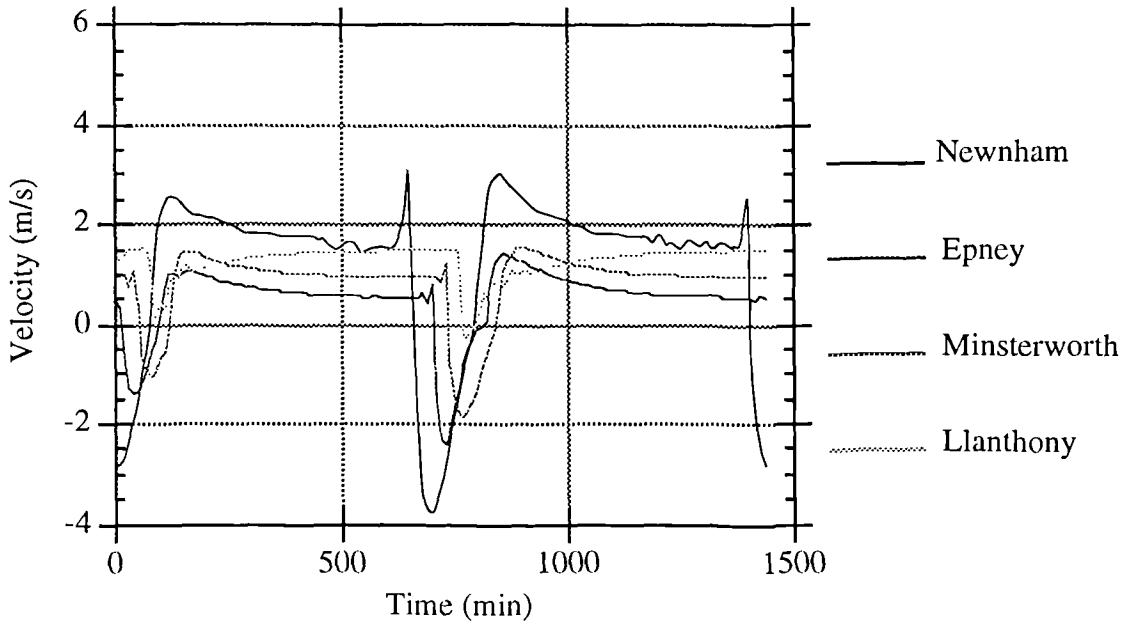

Fig 7.15 Flow velocities calculated for 1990 surge tide, selected positions in the Middle and Upper Severn Estuary.

The surge tide gives a good opportunity to follow the changes in the channel characteristics during a tide, such as the relative changes in area and breadth. Figure 7.16 indicates the change of areas in the Lower Estuary which identically mimic the behaviour of the tidal curves for each section. As can be seen on this figure the maximum areas vary more substantially than the minimum areas of the three sections. Table 7.9 summarises the maximum and minimum areas which were used in the simulation of the 1990 surge.

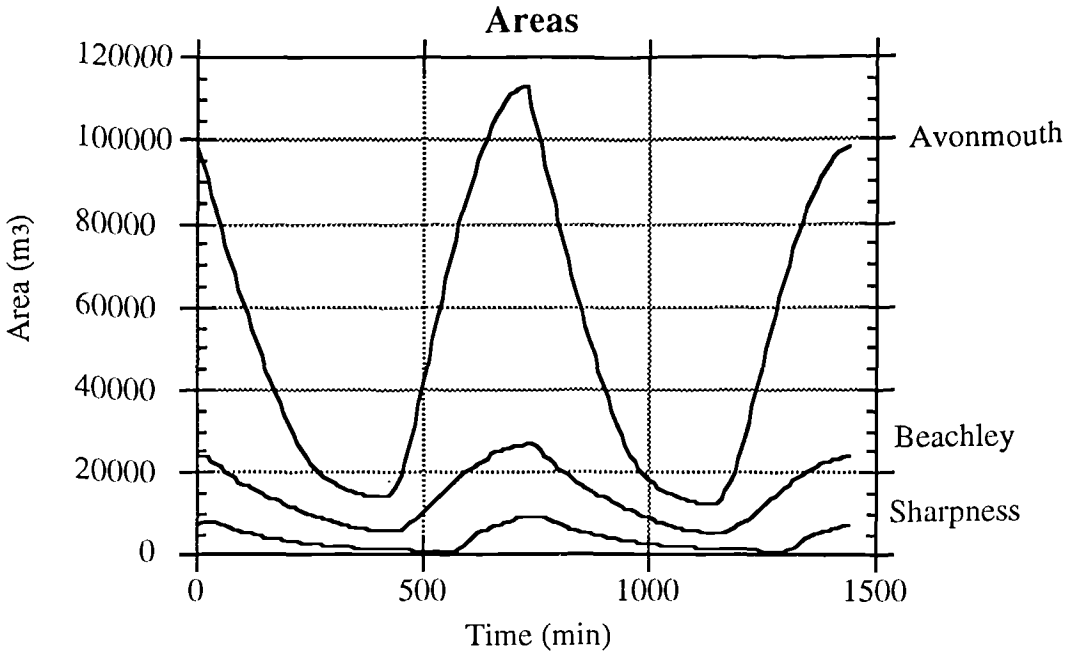

Fig 7.16 Areas of cross sections in the Lower Estuary calculated during tidal surge of 1990.

Place	Maximum Area (m^3)	Minimum Area (m^3)
Avonmouth	112900	12200
Beachley	27200	5400
Sharpness	9400	900

Table 7.9 Maximum and minimum areas during 1990 tidal surge, rounded to nearest $100m^3$

The areas during the tide vary with the tidal stage. Table 7.9 shows that there is nearly an order of magnitude difference in the maximum and minimum areas at each section and that the areas of the cross sections decrease rapidly upstream. The cross sectional area at Avonmouth is approximately four times greater than that at Beachley and 12 times the area at Sharpness at high tide, whereas the low tide area at Avonmouth is just over twice that at Beachley, but over thirteen times greater than the area at Sharpness.

The variation of the cross sectional areas for the remaining example sections further upstream during the tidal surge of 1990 is illustrated upon Figure 7.17, which indicates that

the incoming tide causes a rapid variation in areas, with the maximum areas reducing at each section upstream. What is clear on this figure, however, is that the low tide areas are not related to position in the Estuary as the low tide area at Newnham is considerably less than that at Epney and Minsterworth. This is because the bed level is relatively high at Newnham and thus the area at low water is small, leading to the high velocities at late stages of low water and the apparent 'late ebb' instability as the conveyance of the channel is low.

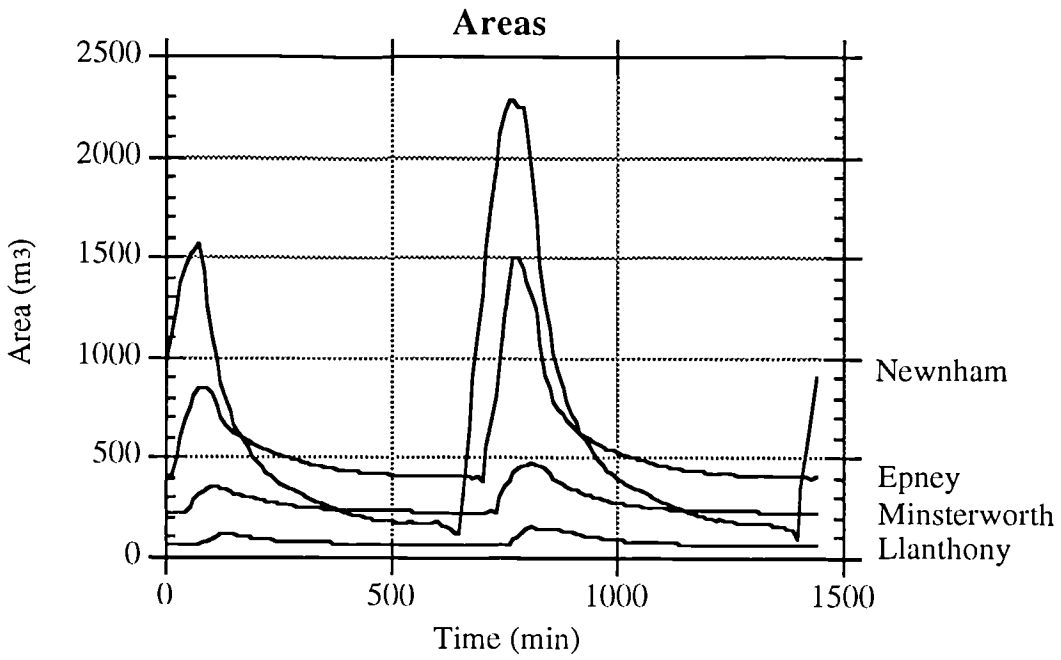

Fig 7.17 Cross sectional areas in Mid and Upper Estuary during 1990 tidal surge.

Place	Maximum Area (m^3)	Minimum Area (m^3)
Newnham	2292	119
Epney	852	381
Minsterworth	468	215
Llanthony	59	28

Table 7.10 Maximum and minimum cross sectional areas, Mid and Upper Estuary during 1990 tidal surge.

The maximum and minimum cross sectional areas at Newnham differ by a factor of nineteen, while the minimum areas for the remaining cross sections are about half the maximum values.

An outcome of analysing the variation of areas and breadths over all the tides which have been simulated during this work, is the realisation that the schemetisation of some cross sections was to the minimum resolution possible with this method of modelling relatively rapidly varying flows. The principle example is the 'noise' or stepped nature of the stage curves at Sharpness for instance. This noise was initially attributed to low flow problems in adjacent areas. However, on more detailed analysis of this and many other sections, it appears that the steps in the graphs are due to the 1m resolution which has been used during the pre-processing of the sections. When sections vary very rapidly in either area or breadth, the cross sectional data which is calculated from the data digitised at 1m intervals of the tidal stage, appears to be too rough an approximation, which suggests that increased resolution would be better. This is an important consideration as many models use 2m stage levels for the pre-processing of the cross sections, which appears to be too great an interval. This effect, however, is complicated further by the nature of the cross sections and appears confined to the narrow cross sections, rather than the broad ones such as Avonmouth.

The variation of the breadth with time during the surge tidal cycle at the example sections is indicated in Figures 7.18 and 7.19 and are summarised in Table 7.11. The breadth can be seen in these figures to vary with the tidal stage, showing a considerable rate of change during the main rise and fall of the sea level, but little change during, just before, and after the slack water periods at high and low water. All three sections illustrated on Fig 7.18 show that there is a more rapid change in breadth near low water than towards high water as would be expected because of the much wider channel and flood plain.

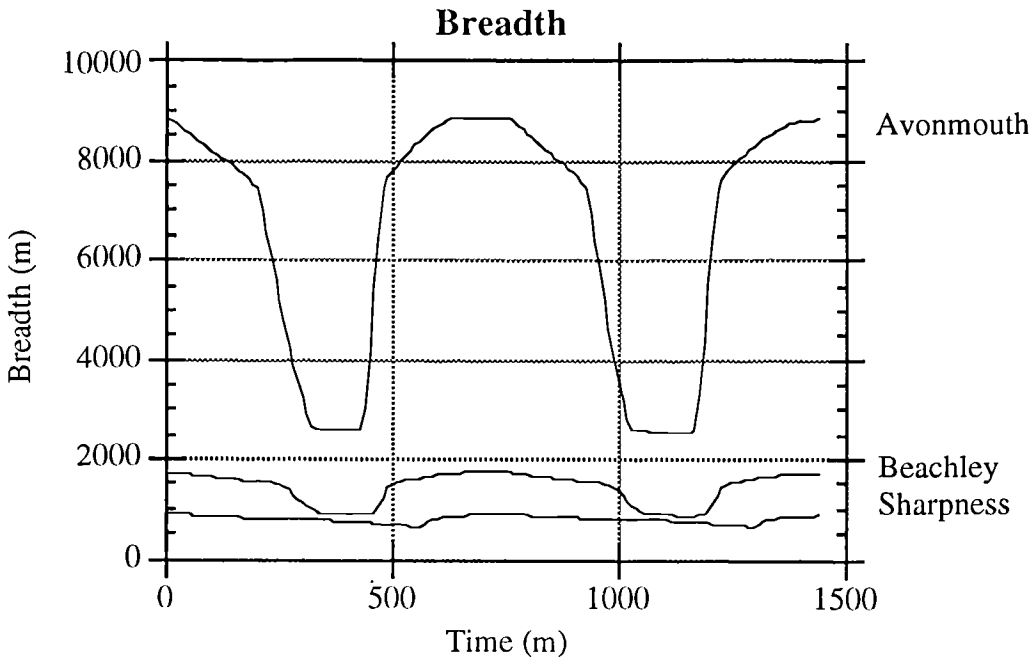

Fig 7.18 Change in breadth with time during 1990 surge tide in Lower Severn Estuary.

The change in the breadth for the sections higher upstream indicated in Fig 7.19 and Table 7.11 show very rapid variation with time due to the relatively short lived duration of the incoming tide. However, this comparison is made bearing in mind the size of the channels, as the rate of change of breadth for the Lower Estuary sections is much greater because of their size. The breadth curves for Llanthony and Minsterworth do not show much variation between the maximum and minimum values because the difference in stage is relatively small and because the flow is confined to a narrow channel. The graph for Epney shows a very rapid change in the breadth as the tidal stage rises which indicates a narrow low water channel which broadens out considerably at higher levels. The curve for Newnham shows a rapid decrease in the breadth at the end of the ebb tide as flow is confined to a small shallow ribbon-like channel, followed by a smooth curve which corresponds in shape to the stage curve.

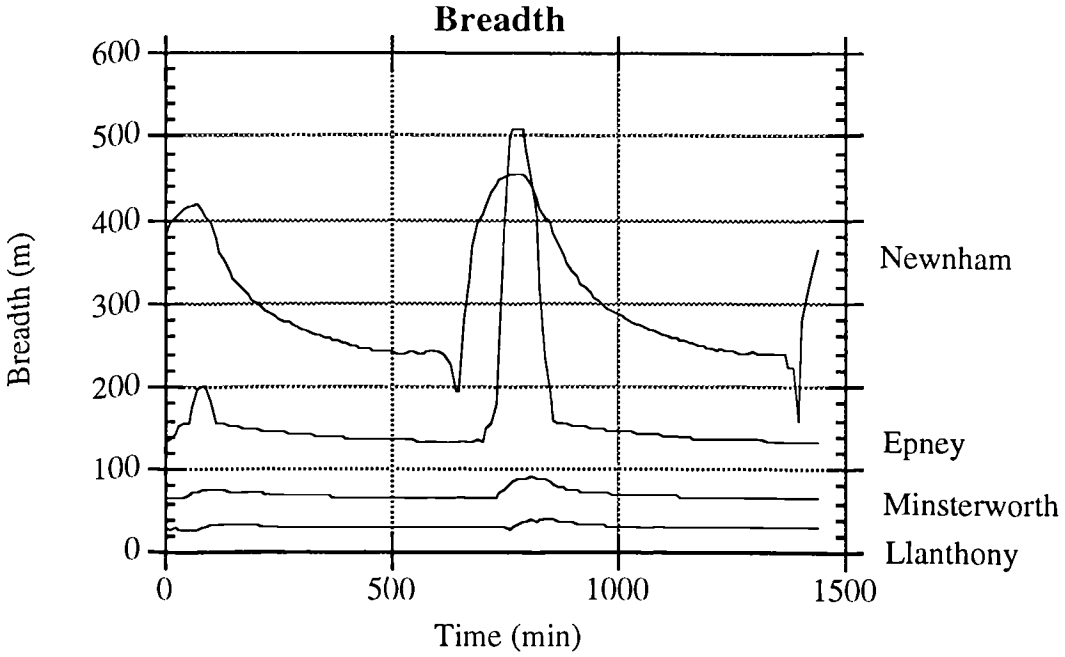

Fig 7.19 Change in breadth with time during 1990 surge tide in Mid and Upper Severn Estuary.

Section	Maximum Breadth (m)	Minimum Breadth (m)
Avonmouth	8839	2529
Beachley	1736	851
Sharpness	897	612
Newnham	453	193
Epney	508	132
Minsterworth	70	64
Llanthony	41	28

Table 7.11 Maximum and minimum calculated breadths during 1990 tidal surge.

In summary, the breadth curves of the sections which are penetrated by the most tides, i.e. the Lower Estuary and Middle Estuary area show a greater correlation to the stage time graphs. The cross section at Epney shows a relatively high rate of change of breadth considering the cross sections size, which bears testament to the deep narrow valley which has formed in the channel at this point (see Section 7.8).

7.5.3 Inundation.

The surge tide on February 26th 1990 caused considerable flooding in the Severn Estuary, which was still recovering from flooding caused by the fluvial flood earlier in the month. Flooding on the surge tide occurred north of the first bend at Frampton to Gloucester, although localised flooding also occurred at Severn Beach. Severn Beach was visited during the Flood when it was seen that much of the flooding which occurred was due to waves breaking over the seawall rather that the tide exceeding the seawall height.

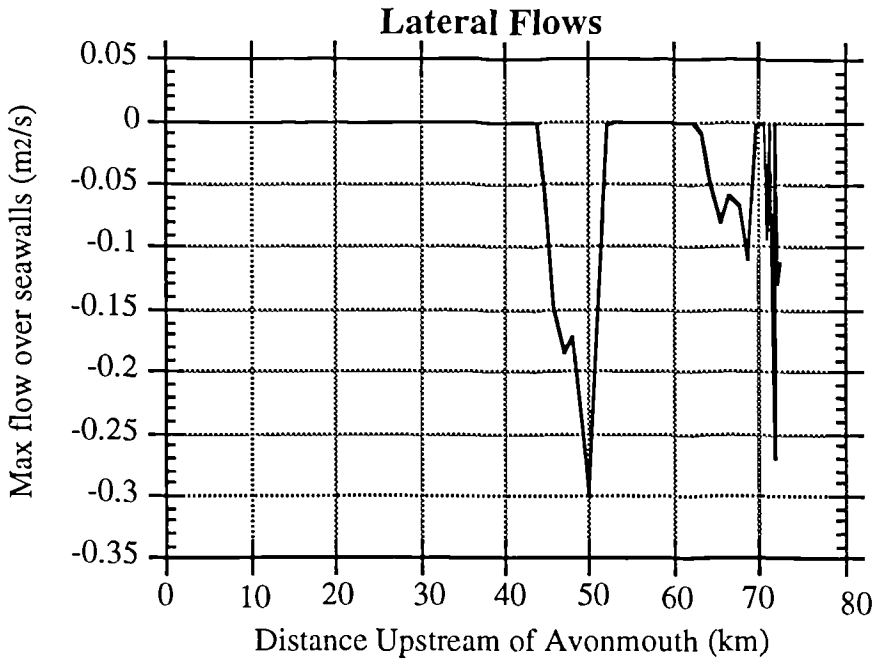

Fig 7.20 Calculated lateral flow over seawalls on 1990 tidal surge.

The peak values of outflow over the seawalls is indicated in Fig 7.20 based on the hybrid model of seawall heights. As can be seen the flooding of the Estuary is predicted to have occurred about 44km upstream of Avonmouth, which is just upstream of Newnham to Epney. The greatest predicted outflow, which is the maximum rate permitted of -0.3m^2/s by the computer model, was at Framilode where the greatest degree of flooding occurred in reality. Incidentally, the seawall improvements at Framilode after this tide comprised the

addition of an extra breeze-block to the seawall. Although this sounds a futile exercise, the defences at this point are limited spatially because of the position of the hamlet's access road. Further major flooding, predicted by the model occurred between 63 and 70km upstream of Avonmouth, between Minsterworth and Lower Parting, and on Alney Island from both the East and West Channels, which was also borne out by aerial photographs of the flood.

7.6 Predicting Future Spring Tide Levels.

7.6.1 Introduction.

Chapter 1 introduced a basic model of predicting new spring tide levels in the Estuary, using published figures of potential sea level change. By analysis of the potential change in mean sea level, it is possible to construct a new spring tidal curve for Avonmouth for the years 2030 and 2100 AD. The methodology used to construct this curve and the results of modelling the effects of the new levels on the Estuary are described within this section.

The method used to predict new tide ranges in this thesis is very simplistic and the results do not correlate with the predicted values produced by complex coastal shelf models. In this thesis the seaward boundary conditions at Avonmouth have been calculated using the following methodology;

- Future or historical tides at Lynmouth are simplified to represent the present day tide raised (or lowered) by a change in global mean sea level only. Lynmouth is considered for the purposes of the study to be the most distant point from the head of the Estuary within the Severn/Bristol Channel system.
- Low water levels for the boundary conditions of the model at Avonmouth are calculated to be equal to the present low water level plus the change in global mean sea level.
- High water levels for the boundary conditions of the model at Avonmouth are calculated by adding the change in mean sea level multiplied by the difference of published high water levels at Avonmouth, divided by the difference of equivalent high water levels at Lynmouth. This is based upon the present day tidal conditions of the Estuary.

While the tide levels used in this thesis are acceptable, it must be remembered that they are calculated from the assumption that the change in levels at the mouth of the Bristol Channel is simply related to the change in global mean sea level. In reality the Bristol Channel is too close to resonance for this to be the case. As a result the values output from the model for simulations using these boundary values cannot be considered definitive but an indication of the tidal regimes which could occur. The seaward boundary conditions used in this thesis are too simplistic to provide exact solutions for the assessment of the Severn coastline. For such information to be derived it would be imperative that a model encompassing the entire Bristol Channel, or preferably an even greater extent of the coastal shelf be used, although this was not practicable for this thesis.

7.6.2 Method of predicting the new spring tide at Avonmouth.

It is assumed that the spring tide at Lynmouth in the Bristol Channel is relatively unaffected by shallow water effects, hence any changes in mean sea level will be a simple addition of the sea level rise to the low and high tidal levels. Lynmouth has been selected as it is the most distant port that is considered to be a subsidiary port within the family of ports for which Avonmouth is the main port in the Admiralty Tide Tables. Equations 7.1 and 7.2 describe the relationship of the existing levels and future levels at this port.

Mean Sea Level (MSL) ≈ Mean Tidal Level (MTL)

= Average of mean spring and neap high and low water levels

$$= \frac{(MHWS+MLWS+MHWN+MLWN)}{4} \qquad (7.1)$$

Change in mean sea level = ΔMSL = ΔMTL, which can be added to high and low water levels;

$$\text{Future MTL} = \frac{(MHWS+MLWS+MHWN+MLWN)}{4} + \Delta MSL \qquad (7.2)$$

In effect this means than the mean high (MHW) and mean low water (MLW) levels will each increase by the predicted mean sea level rise, thus for Lynmouth, the new sea levels are indicated in Equations 7.3.

$$\text{New MHW} = \text{MHW} + \Delta\text{MSL};\ \text{New MLW} = \text{MLW} + \Delta\text{MSL} \qquad (7.3)$$

Unfortunately these levels get distorted as a tide enters the Estuary, thus it is necessary to determine the new tidal levels for the model curve at Avonmouth. Figure 7.21 shows the Admiralty predicted low water levels for Lynmouth to Avonmouth, the latter being 82.3 km upstream of Lynmouth.

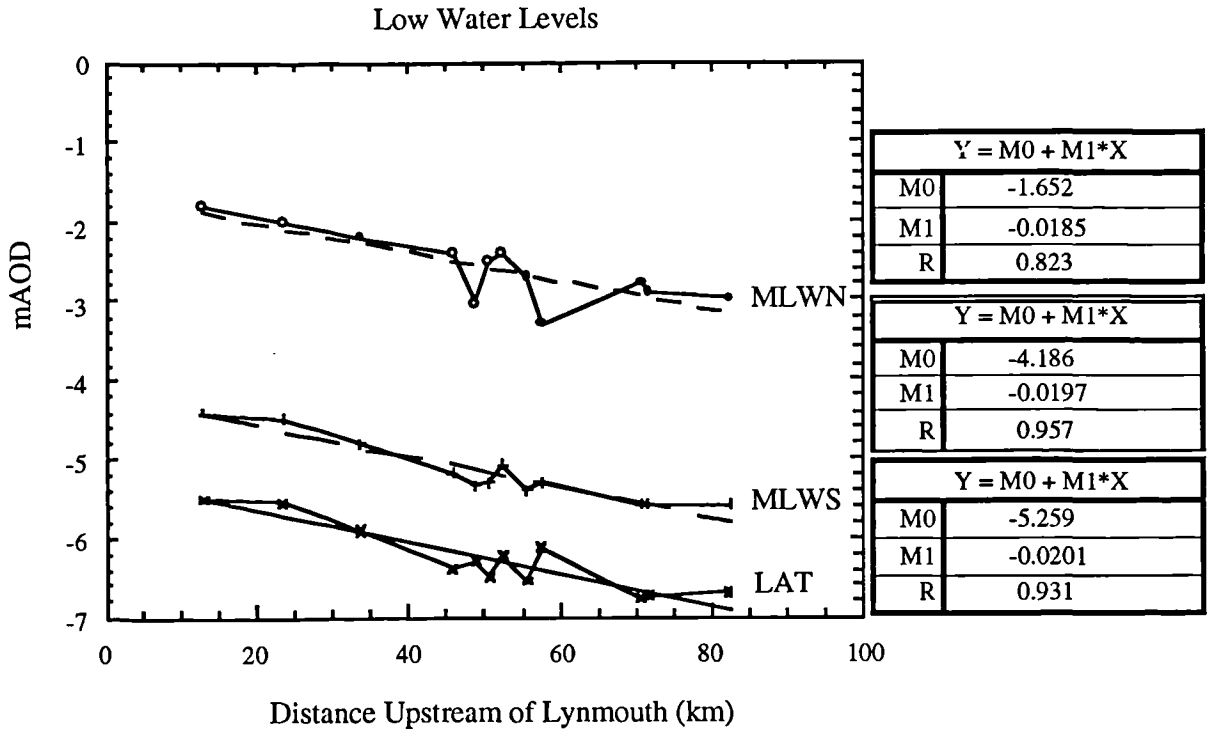

Fig 7.21 Low water levels on neap, spring and astronomical tide, Lynmouth to Avonmouth.

Figure 7.21 presents a simple straight line curve fit for the lowest astronomical tide (LAT), mean low water spring (MLWS) and mean low water neap (MLWN) tidal levels, as can be seen the gradient (M1) term is very small and similar in each case. As in Chapter 1, a

multiplication factor of the low water levels can be derived by considering the drop in the levels from each tide. The mathematic derivation of the multiplication factor is given as Equation 7.4.

Difference in levels at seaward end = Level 1 - Level 2 = Δ Level

Difference in levels at upstream point = Level 1(us) - Level 2 (us) = Δ Level (us)

$$\text{Multiplication Factor, MF} = \frac{\Delta \text{ Level (us)}}{\Delta \text{ Level}} \qquad (7.4)$$

Where Level 1 and Level 2 can represent the LAT, MLWS or MLWN at Lynmouth, and Level 1(us) and Level 2(us) the same tidal events at an upstream port. Figure 7.22 shows the multiplication factors of the following relationships plotted in relation to position in the Estuary;

$$MF1 = \frac{MLWN(us)-LAT(us)}{MLWN-LAT} ; MF2 = \frac{MLWN(us)-MLWS(us)}{MLWN-MLWS} ; MF3 = \frac{MLWS(us)-LAT(us)}{MLWS-LAT}$$

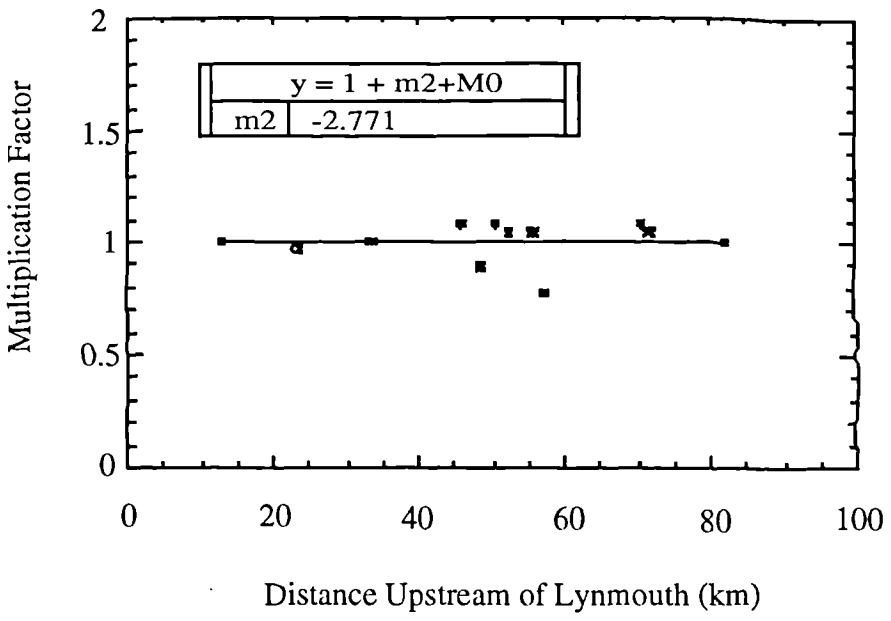

Fig 7.22 Multiplication of low water levels, Lynmouth to Avonmouth.

As there is almost no gradient to the line of best fit for the relationship of the multiplication factor and the distance from Lynmouth, it is deemed that for this part of the

Estuary, there is no apparent increase or decrease in the amount that the seaward low water changes. Thus if mean sea level is to change at Lynmouth then the low water levels would each rise by ΔMSL, this rise would be the same for all the ports to Avonmouth. Therefore Equation 7.5 summarises the new low water levels which would be found at Avonmouth.

$$MLW(new)_{Avonmouth} = MLW(existing)_{Avonmouth} + \Delta MSL \qquad (7.5)$$

The high water heights are not as simple to determine as there is an apparent increase in the effect of any sea level change up the Estuary. Figure 7.23 shows the high water levels between Lynmouth and Avonmouth.

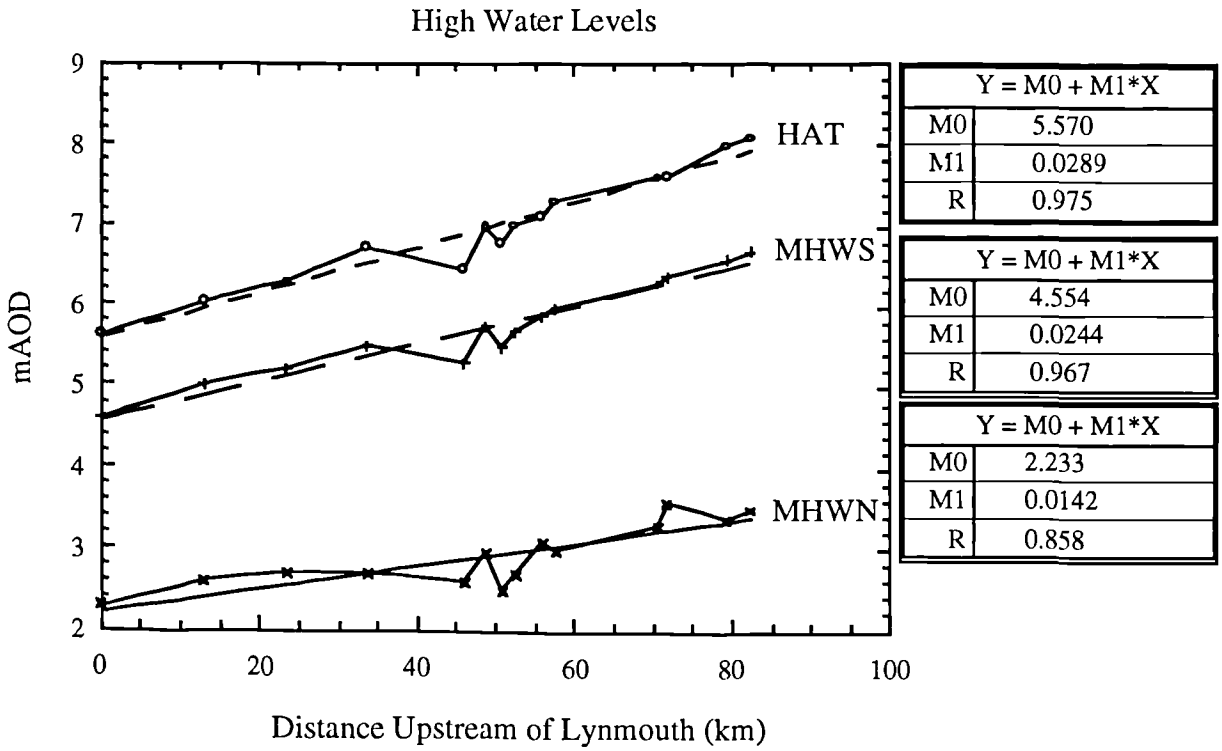

Fig 7.23 High water levels, Lynmouth to Avonmouth.

The important feature of the best fit line for the high water levels is that the gradient (M1) increases with the higher tides, thus the difference between the LAT and MHWN at Avonmouth is more than that at Lynmouth. Figure 7.23 shows the multiplication factor which

can be derived for these high waters by replacing the equivalent high water term in Equation 7.4.

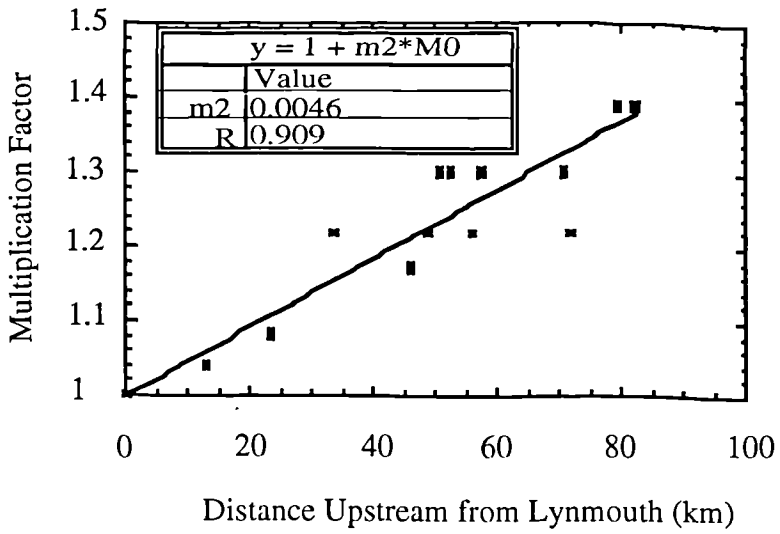

Fig 7.24 Multiplication of high tides between Lynmouth and Avonmouth.

The best fit line on Figure 7.24 is used to derive the new high water heights at Avonmouth (Equation 7.6 and 7.7)

$$\Delta MSL_{Avonmouth} \text{ (high water)} = (1 + (0.0046 \times \text{Distance})) \times \Delta MSL \qquad (7.6)$$

Where the distance between Avonmouth and Lynmouth is 82.3 km.

$$MHW(new)_{Avonmouth} = MHW(existing)_{Avonmouth} + \Delta MSL_{Avonmouth} \text{ (high water)} \qquad (7.7)$$

The new spring tides are thus calculated from the change in predicted mean sea level to give new spring tide curves at Avonmouth. It is more difficult to assign the times at which high and low water will occur on these predicted spring tides. For the purposes of modelling it has been assumed that the present day times of high and low water on a spring tide at Avonmouth can be used for the predicted springs, with the acknowledgement that this is only an approximation and that the high water is likely to occur some minutes before the present day one due to the greater depth of water, thus increased celerity of the tidal long wave.

7.6.3 Future Spring Tides at Avonmouth.

The potential future spring tides which may encountered at Avonmouth have been calculated using the method specified in Section 7.6.2, using the predicted changes in mean sea level given by Warrick and Oerlemans (1990) and Clayton (1990). Changes in the value of mean spring level and the equivalent rise to the high water spring level at Avonmouth are given in Table 7.12. These can be used to construct the new spring tide maxima and minima given in Tables 7.13 and 7.14, using Equations 7.5 and 7.7.

Author	Estimate	Predicted rate of rise (mm/yr)	Rise by 2030 ΔMSL (mm)	Rise in high water at Avonmouth (mm)	Rise by 2100 ΔMSL (mm)	Rise in high water at Avonmouth (mm)
Clayton	High	9.1	364	501.8	1001	1380.0
	Best	4.1	164	226.1	451	621.8
	Low	0.65	26	35.8	71.5	98.6
Warrick & Oerlemans	High	6.4	288	397.0	736.0	1014.7
	Best	4.1	184.5	254.4	471.5	650.0
	Low	1.9	85.5	117.9	218.5	301.2

Table 7.12 Predicted changes in mean sea level and the rise in high water levels at Avonmouth, for 2030 and 2100 AD.

		HAT	MHWS	MHWN	MTL	MLWN	MLWS	LAT
	Present	**8.1**	**6.7**	**3.5**	**0.4**	**-3.0**	**-5.6**	**-6.7**
Clayton	High	8.60	7.20	4.00	0.83	-2.64	-5.24	-6.34
	Best	8.33	6.93	3.73	0.60	-2.84	-5.44	-6.54
	Low	8.14	6.74	3.54	0.44	-2.97	-5.57	-6.67
Warrick & Oerlemans	High	8.50	7.10	3.90	0.73	-2.79	-5.31	-6.41
	Best	8.35	6.95	3.75	0.62	-2.82	-5.42	-6.52
	Low	8.22	6.82	3.62	0.51	-2.91	-5.51	-6.61

Table 7.13 Predicted tide levels at Avonmouth, 2030 AD.

		HAT	MHWS	MHWN	MTL	MLWN	MLWS	LAT
	Present	**8.1**	**6.7**	**3.5**	**0.4**	**-3.0**	**-5.6**	**-6.7**
Clayton	High	9.48	8.08	4.88	1.59	-2.00	-4.60	-5.70
	Best	8.72	7.32	4.12	0.94	-2.55	-5.15	-6.25
	Low	8.20	6.80	3.60	0.49	-2.93	-5.53	-6.63
Warrick & Oerlemans	High	9.11	7.71	4.51	1.28	-2.26	-4.86	-5.96
	Best	8.76	7.35	4.15	0.71	-3.53	-5.13	-6.23
	Low	8.40	7.00	3.80	0.66	-2.78	-5.38	-6.48

Table 7.14 Predicted tide levels at Avonmouth, 2100 AD.

The new predicted spring tide levels have been used to simulate the tides which may occur in the Severn Estuary which are analysed in the following sections. The tide depicted as the present day tide refers to the Admiralty Figures for 1992.

7.6.4 Modelling of Future Spring Tide Heights.

The spring tides derived for 2030 and 2100 AD have been modelled to give a range of high water spring levels which could be expected in the Estuary at these dates. In the following sections it is only necessary to talk in terms of the modelled levels as there are only relatively minor changes to the timing, flow quantities and velocities generated. Upstream boundary conditions of $150m^3/s$ and $100m^3/s$ have been used for the West and East Channels respectively. No changes are necessary to the general set up of the model for the 2030 tide, particularly the sea wall heights as the spring tides modelled do not exceed any of the seawall crests. The tide for 2100 would exceed the seawalls in some places. However, new sea wall heights anticipating future constructions have not been added. Considerations of sea wall constructions are discussed later in this chapter.

7.6.5 Spring Tide, 2030 AD.

The calculated ranges of high water that may be expected on a spring tide using the tidal curves described earlier is illustrated Figure 7.25.

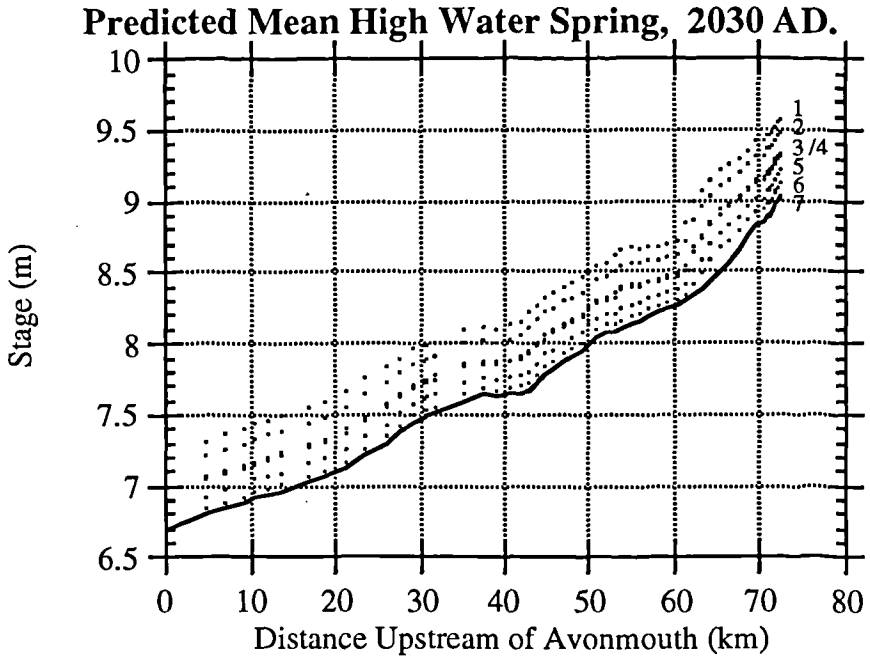

Fig 7.25 Calculated MHWS levels, 2030 AD.

1. Clayton (High); 2. Warrick & Oerlemans (High); 3/4 Clayton (Best), Warrick & Oerlemans (Best); 5. Warrick and Oerlemans (Low); 6. Clayton (Low); 7. Existing.

The calculated heights and existing modelled heights of the spring tide are also shown in Table 7.15, which gives the differences between the new modelled high tide level and the existing one. It can be seen in Table 7.15 and Figure 7.25 that the apparent rise in sea level at Avonmouth results in a rise similar or slightly higher at the upstream sections, with the exception of the sections between 50 and 60km upstream of Avonmouth. The apparent rise in these sections is less than that at Avonmouth because flow is no longer confined to the main water channel but is spilling onto the river flood plain (within the seawalls). It is most likely that if sea level was to change in this nature, there would be erosion in the reach 50km to

60km upstream of Avonmouth as the channel would try to adapt to the new levels by increasing the area of the main channel.

Place	Existing	Clayton			Warrick and Oerlemans		
		High	Best	Low	High	Best	Low
Avonmouth (0 km)	6.70m	7.20m +0.5m	6.93m +0.23m	6.74m +0.04m	7.10m +0.40m	6.95m +0.25m	6.82m +0.12m
Beachley (11.9 km)	6.93m	7.47m +0.54m	7.18m +0.25m	6.98m +0.05m	7.36m +0.46m	7.20m +0.27m	7.06m +0.13m
Sharpness (29.3 km)	7.45m	7.96m +0.51m	7.69m +0.24m	7.49m +0.04m	7.86m +0.41m	7.71m +0.26m	7.58m +0.13m
Newnham (43.9 km)	7.72m	8.27m +0.55m	7.98m +0.26m	7.77m +0.05m	8.17m +0.45m	8.00m +0.28m	7.86m +0.14m
Epney (53.0 km)	8.08m	8.62m +0.54m	8.33m +0.25m	8.13m +0.05m	8.51m +0.43m	8.35m +0.27m	8.21m +0.13m
Minsterworth (61.3km)	8.30m	8.85m +0.55m	8.51m +0.21m	8.34m +0.04m	8.72m +0.42m	8.54m +0.24m	8.41m +0.11m
Llanthony (71.2 km)	8.89m	9.46m +0.57m	9.19m +0.30m	8.98m +0.09m	9.37m +0.48m	9.22m +0.33m	9.07m +0.18m

Table 7.15 Modelled high water spring tide levels, 2030AD

7.6.6 Modelled Spring Tide, 2100AD.

The predicted high water spring levels for 2100AD are given in Table 7.16 and illustrated in Figure 7.26. The latter indicates that there is a drop in predicted levels between about 56km and 60km upstream of Avonmouth for the best and high estimates, near Longney where the river expands considerably, so the progression of the higher tides is being influenced by the increase in breadth and flood plain flow. Tidal levels upstream of 68km are also reduced for the high estimate as the predicted levels are greater than the seawall crests. This is a serious consideration as it illustrates that the existing tidal defences would require considerable reconstruction if the high estimate of global sea level change was to occur.

Place	Existing	Clayton			Warrick and Oerlemans		
		High	Best	Low	High	Best	Low
Avonmouth (0 km)	6.70m	8.08m +1.38m	7.32m +0.62m	6.80m +0.10m	7.71m +1.01m	7.35m +0.65m	7.00m +0.30m
Beachley (11.9 km)	6.93m	8.35m +1.42m	7.59m +0.66m	7.04m +0.11m	7.98m +1.05m	7.61m +0.68m	7.21m +0.28m
Sharpness (29.3 km)	7.45m	8.82m +1.37m	8.08m +0.63m	7.56m +0.11m	8.46m +1.01m	8.11m +0.66m	7.76m +0.31m
Newnham (43.9 km)	7.72m	9.21m +1.49m	8.40m +0.68m	7.84m +0.08m	8.81m +1.09m	8.41m +0.69m	7.88m +0.16m
Epney (53.0 km)	8.08m	9.54m +1.46m	8.75m +0.67m	8.19m +0.11m	9.16m +1.08m	8.77m +0.69m	8.21m +0.13m
Minsterworth (61.3km)	8.30m	9.72m +1.42m	9.01m +0.71m	8.39m +0.09m	9.44m +1.14m	9.04m +0.74m	8.40m +0.10m
Llanthony (71.2 km)	8.89m	9.89m +1.00m	9.58m +0.69m	9.05m +0.16m	9.81m +0.92m	9.60m +0.71m	9.07m +0.18m

Table 7.16 Predicted high water spring, 2100AD and change from present.

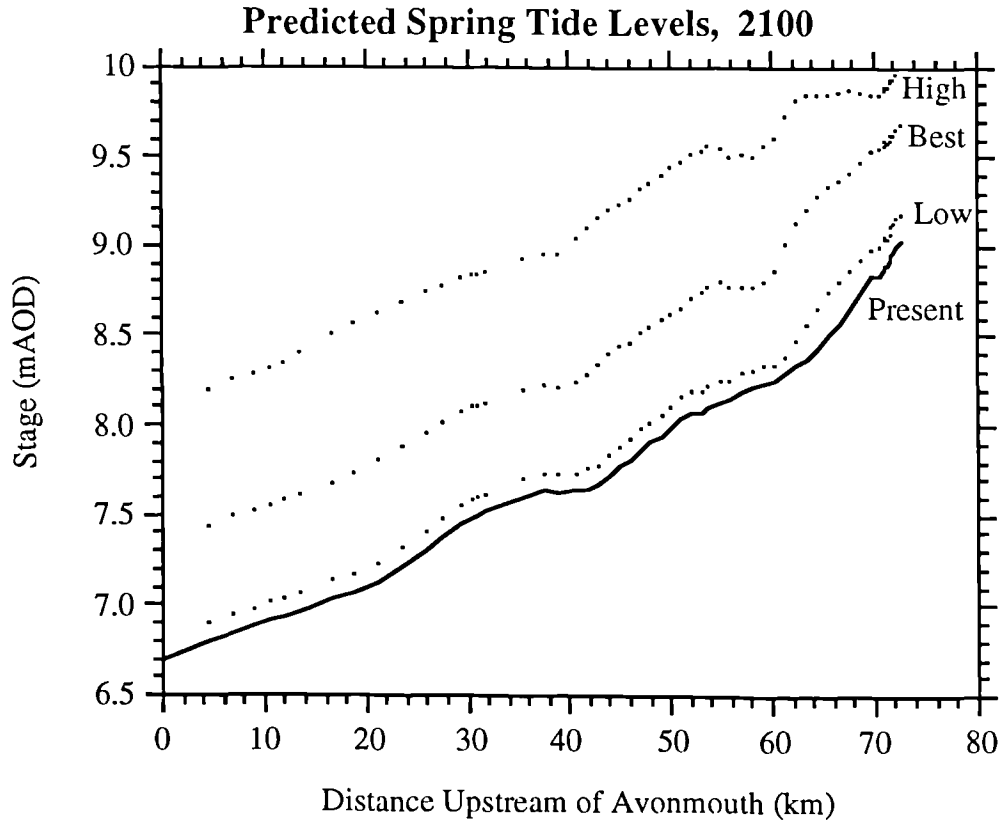

Fig 7.26 Predicted range of high water springs, Clayton High, Best and Low estimates.

7.6.7 Discussion of Modelling.

The tides which have been modelled as potential future tides have been constructed using the assumptions and basic model given in Sections 7.6.2 and 7.6.3. This tidal curve constructed for Avonmouth can be considered to be an estimation only. However, the model was run using additional seawards sections and a near symmetrical curve in the Bristol Channel using sections to Barry Island, to ascertain whether the estimated spring tide at Avonmouth was a reasonable representation. Given the limitation of the model developed to include the Bristol Channel sections it was found that the newly constructed curve was a good approximation, although the larger model cannot be considered reliable as the model had not been verified properly in this form.

The modelled changes in sea level rise can be compared to the predicted levels given in Chapter 2 for sections to Sharpness. The computer model predicted levels about 4 to 5cm higher at Beachley (Aust) and 2 to 4cm lower at Sharpness for the 2030 tide. The computer model similarly predicted higher levels at Beachley by 2 to 5cm and lower levels at Sharpness by 2 to 14cm.

The modelled results are likely to be under-estimates for most of the Estuary as the model, especially on the spring tides for 2100AD, indicated that the river spilled into the wider flood plain which lies between the main channel and the seawalls. In reality this part of the flood plain is likely to build up with the rise in the sea level thus keeping the flow predominantly in the main channel.

7.7 Historic Tides.

7.7.1 Introduction.

Historic spring tide levels in the Severn can be modelled using Allen's (1991) estimates of sea level change, although there have been changes in the seawalls and channel morphology. Allen's postulated changes in sea level rise are presented in Table 7.17. These

values have been obtained for positions upstream of Avonmouth, through levelling of marsh heights near to high water spring level. To construct a new spring tidal curve at Avonmouth it is thus necessary to use Allen's change in sea level as an indicator of the change in sea level at Avonmouth, not downstream at Lynmouth. Thus it is necessary to back calculate the change to the low water levels using the theory introduced in Section 7.6, using the re-arranged Equations 7.8 and 7.9.

$$\Delta MSL = \frac{\Delta MSL_{Avonmouth}}{(1+(0.0046 \times Distance))} \qquad (7.8)$$

$$MLWS(old)_{Avonmouth} = MLWS(existing)_{Avonmouth} - \Delta MSL \qquad (7.9)$$

Period	Rate of Rise	ΔMSL (Avonmouth) from present	Change in Low water at Avonmouth
1945-1995	4.65 mm/y	-0.23m	-0.17m
1845-1945	1.49 mm/y	-0.38m	-0.28m
1250-1845	0.79 mm/y	-0.85m	-0.62m
150-1250	0.40 mm/y	-1.29m	-0.94m

Table 7.17 Historic sea level changes calculated from Allen (1991).

Time	MHWS (m)	MLWS (m)
Present	6.70	-5.60
1945	6.47	-5.77
1845	6.32	-5.88
1250	5.85	-6.22
150	5.41	-6.54

Table 7.18 Estimation of historic spring tides at Avonmouth.

The new changes in sea level can be applied to the existing spring tide curve to give the ancient spring tides as depicted in Table 7.18, using the times of the present day spring tide as an approximation.

It was found that during the verification of the model that the tidal range contributes to the severity of the low flow problem. For instance a tide as low as -6.22mAOD could be used for the 1250AD tide (a range of 11.85m) without significant instabilities occurring, whilst a tide as low as -6.54m (a range of 11.6m) could be modelled for the 150AD tide. As a comparison it has been shown that the present day spring tide with a low water of -5.6m (range 12.3m) is close to producing fatal low flow instabilities. Thus it appears that the low flow problem is partially attributable to the rate of change of the flow conditions, the low water levels used at Avonmouth and the friction values which affect both the rate of change and heights. To complicate this argument further, it is noted that the astronomical tide may be calculated under present day conditions too, even with a lower water level at Avonmouth and tidal range considerably greater than the spring tide. In this case the volume of water draining the Estuary is sufficient to keep enough of a base flow to prevent the 'fatal' low flow calculation.

An important issue in the modelling of these historic tides was also the extent of the salt marshes and flood plains at the time of the events. The earliest modelled tide for 150AD would have occurred in an Estuary which was broad and almost unreclaimed from its original extent. For this tide, the modelled cross sections were reconstructed to the entire width of the now reclaimed and starved flood plain. This was achieved through re-analysing the present day sections, removing any tidal embankments and using the level of the flood plain behind the sea wall as the original height of the broad estuarine plain, prior to empoulderment. This is obviously prone to many errors, such as consolidation of the sediments and the relatively unknown degree to which the marshes built up from 150 AD to their reclamation. Similarly there have almost certainly been changes in the channel morphology which cannot be accounted for. Indeed the model for this period could not incorporate sections to the north of Minsterworth as it becomes unclear, even from borehole evidence, as to what size or direction the Estuary flowed. Therefore the upstream boundary condition for this simulation was set to 250m^3/s at Minsterworth.

Allen has published much data in the late 1980's and early 1990's, encompassing the progressive reclamation of the Middle and Upper Estuary since Roman Times. These models have been used as 'snapshots' of the Estuary for the 1250 and 1845 tides, and cross sections have been adapted accordingly to his work where possible. However, some sections for these tides have had to be left as they are today as no reliable information or interpretation of the historic sections could be used.

7.7.2 Modelled Results

The results of modelling the predicted historic tides are included in Table 7.19.

Place	Existing	1945	1845	1250	150
Avonmouth (0 km)	6.70m	6.47m -0.23m	6.32m -0.38m	5.85m -0.85m	5.41m -1.29m
Beachley (11.9 km)	6.93m	6.68m -0.25m	6.54m -0.39m	6.10m -0.83m	5.67m -1.26m
Sharpness (29.3 km)	7.45m	7.16m -0.29m	7.01m -0.44m	6.51m -0.94m	6.03m -1.42m
Newnham (43.9 km)	7.72m	7.39m -0.33m	7.22m -0.50m	6.74m -0.98m	6.37m -1.35m
Epney (53.0 km)	8.08m	7.72m -0.36m	7.57m -0.51m	6.98m -1.10m	6.65m -1.43m
Minsterworth (61.3km)	8.30m	7.92m -0.38m	7.78m -0.52m	7.06m -1.24m	6.92m -1.38m
Llanthony (71.2 km)	8.89m	8.44m -0.55m	8.27m -0.62m	7.78m -1.11m	----

Table 7.19 Predicted high water springs for historic tides with comparison to present day spring level.

Table 7.19 clearly shows that the difference between the historic high water spring tide and the present day one at Avonmouth become much greater upstream for each of the tides, other than the earliest tide where there is less consistency in the increase. This has extremely important ramifications for the measurement of sea level change in an Estuary which is

described in the following section where the results of modelling historic and future tides are discussed.

7.8 Analysis of Modelled Spring Tides; Past, Present and Future.

7.8.1 General

This section analyses the spring tides which have been modelled during this chapter in terms of sea level rise in the last 1850 years. Models of sea level rise for this period are generally based upon the amount of sediment which has accreted since a dateable event, such as Allen's chemzones, reclamations, identified buried surfaces and artefacts. This section provides a different analysis based upon modelling data, although it is acknowledged that there are many unknown factors to be accounted for in the model.

7.8.2 Difficulties in Modelling.

There are a number of practicalities which cannot be easily resolved in this model due to the nature of the data available and the applicability of some of the assumptions made. This section will describe some of the possible sources of error which may be introduced in the analysis of the past and future tides.

- Model Cross Sections

The mean spring high water is considered to be the principal control on the general height of a salt marsh. Thus it is used by Hawkins (1971) and others as the surface in which to correlate sea level change. Figure 7.27 illustrates the differences which may occur between an actual channel cross section and the section used for modelling in the event of a change in the mean spring high water.

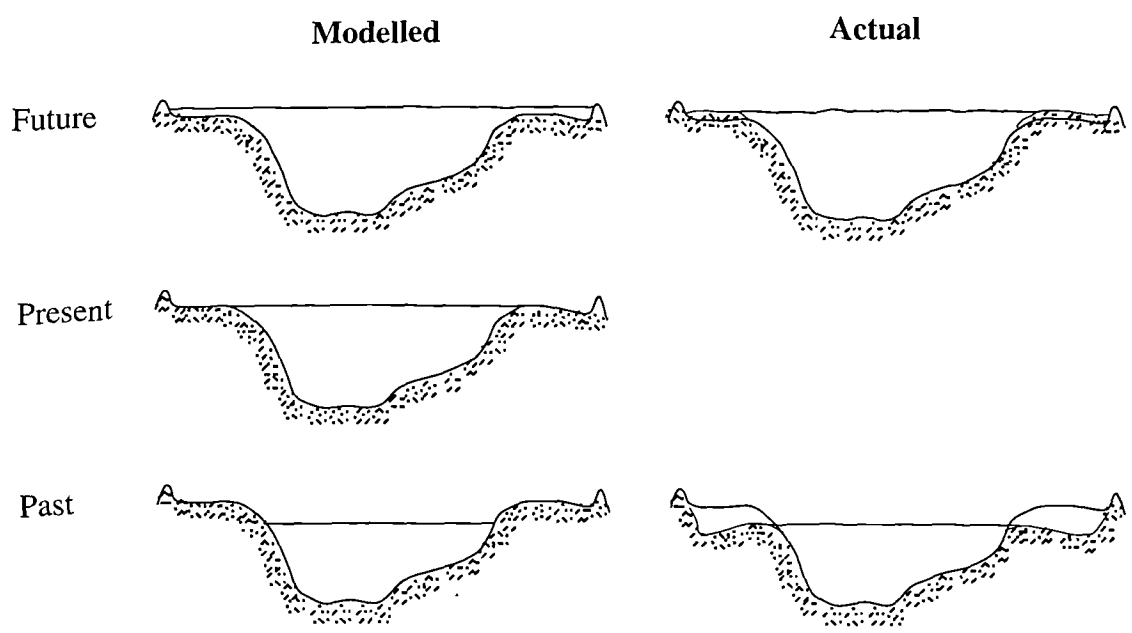

Fig 7.27 Variations in cross sections with progressive changes in mean high water spring tide for a schematic section.

A model cross section for the present day is in dynamic equilibrium with the tidal environment. In an idealised situation, the height of any flood plain inside of the seawalls is governed by the mean high water spring level. Thus the tide spills onto the level adjacent to the channel depositing sediment on tides higher than the mean spring flood.

The modelling of tides in the future has used the cross sections derived for the present day morphology of the Severn Estuary. Thus with a rise in MHWS, the modelled tides are more likely to overflow towards the seawalls (Fig. 7.27) whereas in reality sedimentation, unless unable to keep up with the sea level changes, will occur between the seawall and the channel at a height of around the prevailing MHWS. Thus the real and likely ('actual') channel cross sections will show significant variations in the modelled breadths; the modelled sections are likely to be broader at high tide. This has been identified earlier as being a significant factor in he propagation of a tide. It is likely that in the future that tides will be kept within the main channel more than the model predicts due to the accretion, thus it is assumed that the future tides predicted by the model are under-estimates of the potential tides.

It is easier to represent the historic format of the Severn from the data already available on morphological change, however, in places sections will be similar to the modern day ones because of the lack of data. In this case the model section will hold the older, lower tide

within the present day channel morphology, whereas the probable morphology of the channel will have been broader than today as accretion to today's levels would not have occurred (Fig 7.27). This presents a problem as there are two opposite effects which may be generated from this simulation. Firstly, if the tide is confined to the present day morphology of the channels, then the predicted levels are likely to be too high, but conversely if the reconstructed sections had flood plains which were too low in relation to the predicted tide, then excess spillage would occur onto the flood plain, thus giving an impression of high tide levels being lower than expected. The extent of the problem was ascertained by running the analysis for the 1250AD tide with the modern day channel cross sections and comparing the results to a model run with the channel cross sections constructed for the 150AD extent of the Estuary. These two simulations can be seen as two extremes, with the modelled results given in Table 7.19 as being an intermediate prediction using the nearest estimate to the shape of the Severn, which at the time had been reclaimed in many places. Thus for this simulation there are some broad and narrower sections.

Place	'150AD Layout'	'1250AD Layout'	'1993 Layout'
Avonmouth (0 km)	5.85m	5.85m	5.85m
Beachley (11.9 km)	6.10m	6.10m	6.11m
Sharpness (29.3 km)	6.50m	6.51m	6.49m
Newnham (43.9 km)	6.72m	6.74m	6.75m
Epney (53.0 km)	6.95m	6.98m	7.12m
Minsterworth (61.3km)	7.01m	7.06m	7.34m
Llanthony (71.2 km)	---	7.78m	7.89m

Table 7.20 The 1250AD spring tide, high water levels, modelled using different channel layouts.

The comparison of the three models of the 1250 tide are given in Table 7.20, in which it is clear that there is little difference in the modelled levels of this tide even with three different schemetisations in the Lower Estuary. However, differences become greater further

upstream, where it becomes obvious that the larger historic floodplains had some appreciable control on the progression of the tide, causing attenuation of the high levels.

- Changes to Cross Sections.

The problems with modelling cross sections with respect to sea level change have already been described in terms of change in the marsh heights with sea level. However, with the simulation of future sea level curves the effect of erosion is also difficult to assess. One major feature is that many of the salt marshes in the Severn Estuary are being eroded at their toe by dominant currents and are thus retreating at an appreciable rate. This retreat cannot be modelled within the scope of this work, nor can the effect of scouring or deposition in the channel bed. The model has shown that currents and amount of flow may be 1.5 to 2 times the present values for the two tides in the future. This would naturally cause greater erosion and widening of the channel cross sections. Similarly it is impossible to assess the degree that the bed of the Severn has eroded since the historical events of the past, where it is likely that the main channel cross sections were narrower or shallower.

- Tidal curves.

The tidal curves input to the model at Avonmouth have been based upon a simple mode of determination. The curves based upon future sea level changes have been described earlier, whereas the historical changes have been based on the sea level changes suggested by Allen (1991). These figures are for observations in the Middle Estuary and so may reflect a greater sea level change than was present at Avonmouth. However, this is the best estimate available.

7.8.2 Comments on the Observations of Sea Level Change in the Severn Estuary.

The events which have been simulated from 150AD to 2100AD can be used to show how a change in sea level may appear in different parts of the Estuary. Figure 7.28 shows the predicted heights of mean high water spring along the Estuary for the various periods of

history, the future tides being the values modelled on Clayton's 'best' estimate of sea level change.

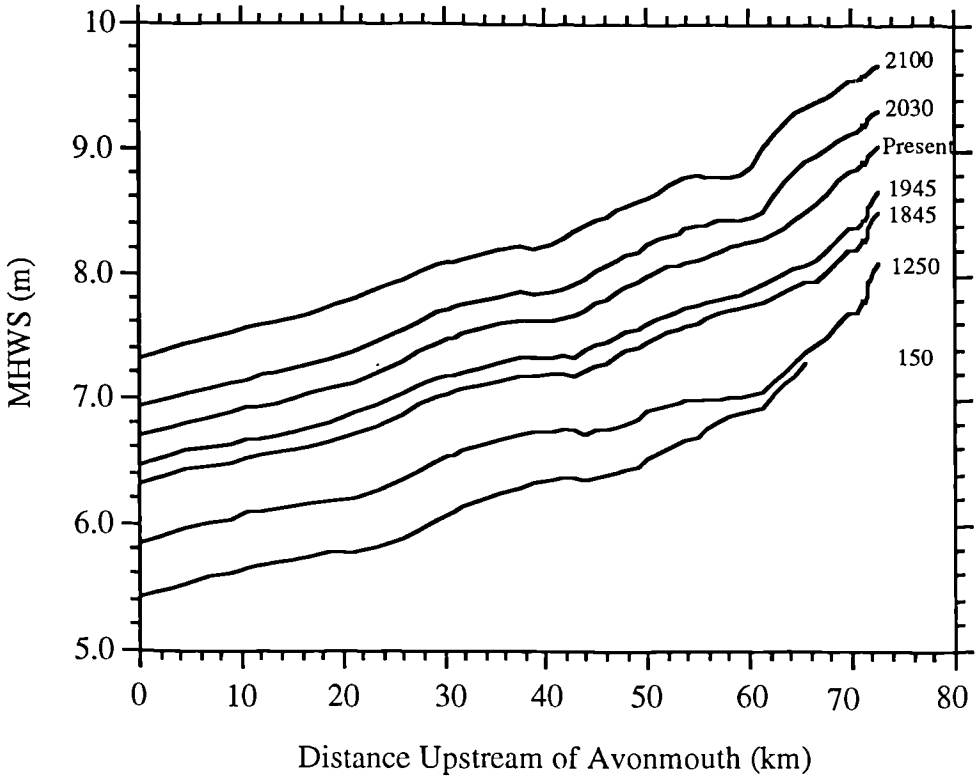

Fig 7.28 Predicted MHWS for different times in history.

Figure 7.28 illustrates the gradual increase in MHWS with time at all locations. The figure also indicates that there is little difference in the spring tide maximum upstream of about 60km in 150 and 1250 AD, this is because this represents the approximate area of the tidal limit of the spring tide at those times. If the heights of two consecutive MHWS are subtracted and divided by the age between the two predicted levels, then the amount of accretion, assuming the basic model of accretion level matching MHWS, can be calculated for each period, giving the apparent rate of sea level rise which would be measured from geological evidence of deposition at each section (Figure 7.29).

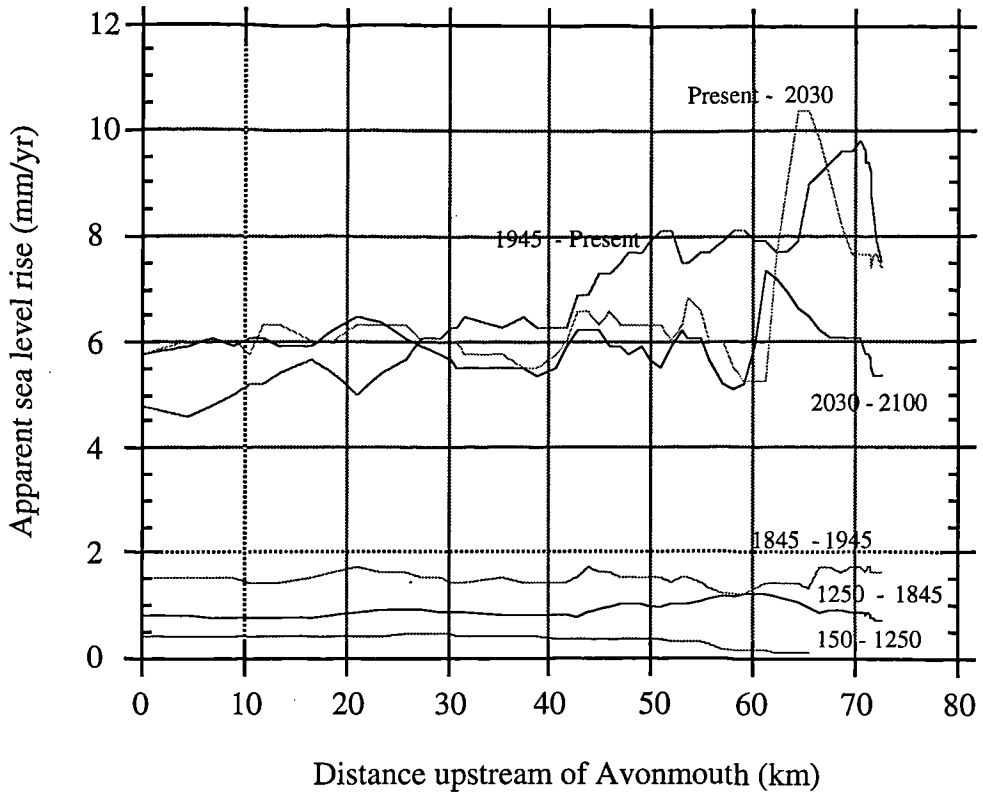

Fig 7.29 Apparent sea level changes along the Estuary.

There is little apparent change in sea level rise along the Estuary for the three early periods of time. It would be difficult to predict any considerable accretion rate for the period between 150 and 1250, more than 57km upstream of Avonmouth because of the relative lack of tidal influence. For the period 1250 - 1845 the modelling indicates that the general rise in sea level at Avonmouth would be reflected in most of the Estuary, although a slightly greater rise might be reflected between 53km and 66km upstream of Avonmouth. The period between 1845 and 1945 also seems to generally reflect the sea level change at Avonmouth over the entirety of the Estuary.

The graph of apparent sea level change between 1945 and the present day is the best indicator of the way that sea level change is reflected in the Estuary as the sections constructed are the most reliable. This graph shows a general increase upstream in the amount of accretion which could have occurred along the Estuary. Ignoring the abnormally high points, it could still be said that up to twice the amount of accretion which could be expected adjacent to the channel on the saltmarsh at Avonmouth could occur further upstream. The graphs for the two predicted future tides, begin by showing a general rise in the apparent rate of sea level change

as would be measured moving up the Estuary from Avonmouth to about 20km upstream. The two graphs then fluctuate around the rate which would be seen at Avonmouth, because of the difficulty in modelling the sections where the modelled breadth will be greater than might be expected in reality.

7.8.3 Summary

The modelling of past, present and future tides has provided an estimate of the apparent sea level change which may occur at any point in the Severn Estuary These indicate that the rate of rise calculated is dependant on the position in the Estuary. Taking the difference in modelled MHWS since 1945 to the present as being the most typical example of such behaviour in an Estuary (as the set up of the simulation most truly reflects the physical reality of the Severn) it can be said that a general increase in the measured rate of sea level would be seen up Estuary. Therefore construction of any sea level curves in an estuary with a large tidal range should take into account the position that measurements were made. This is complicated much further by lateral changes in mudflat geometry and that inundation times are not taken into account.

7.9 Inundation of Salt Marshes.

The inundation of salt marshes is demonstrated by taking three sections across a salt marsh in the Lower, Middle and Upper Estuary and comparing them to the tidal curve for the sections. So far the level of MHWS has been deemed to control sedimentation, so this tide is used as the comparative tide in this section. However, without considering tidal surges, the level of HAT ultimately dictates the maximum height of a salt marsh, unless excessive plant derived (peat) sedimentation is occurring.

7.9.1 Upper Estuary.

Two example sections for the Upper Estuary are illustrated in Figure 7.30 to show the high water spring and astronomical tide.

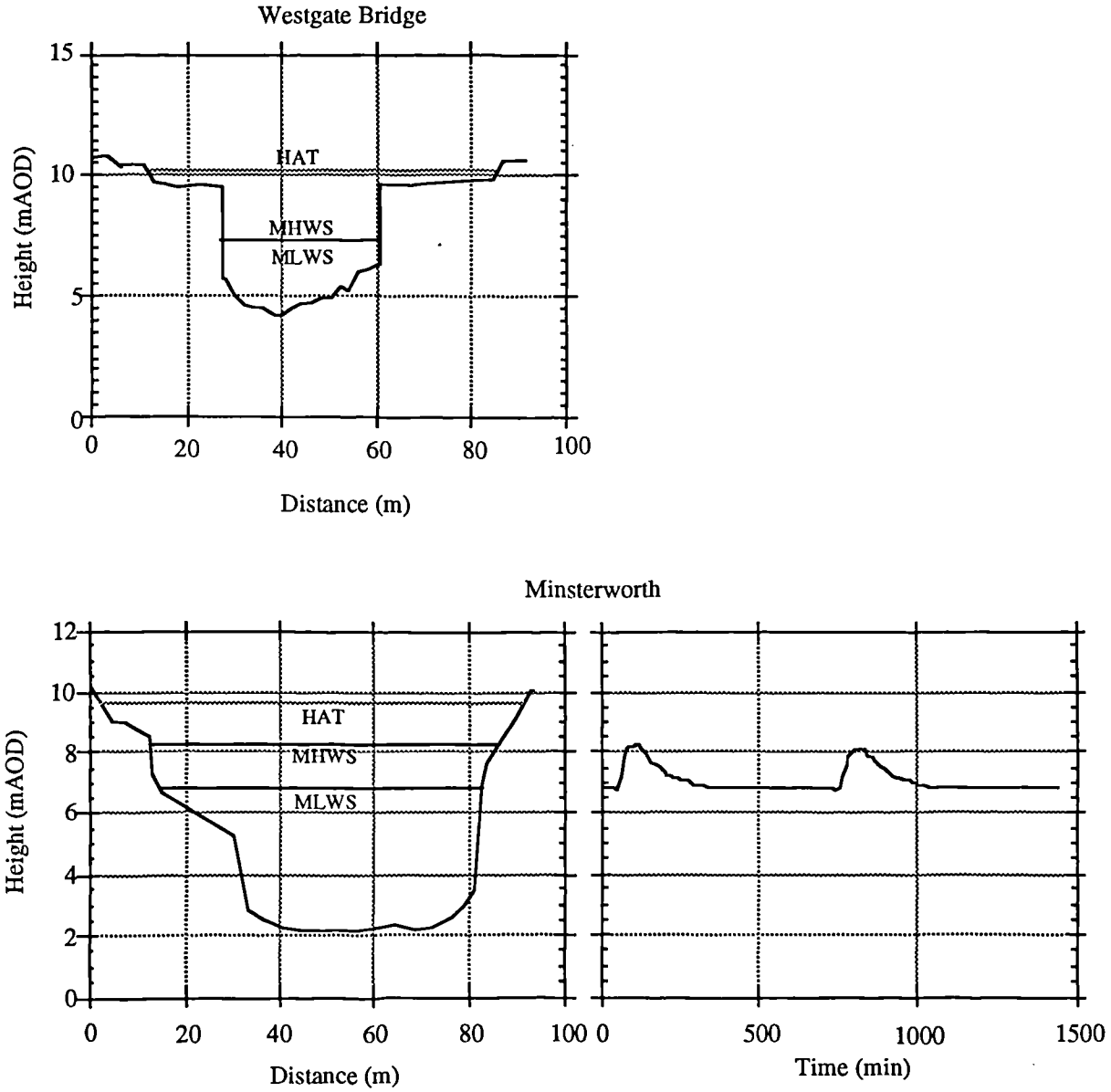

Fig 7.30 Estuary sections at Westgate Bridge and Minsterworth, spring curve to the right if relevant.

Two sections illustrated in Figure 7.30 indicate that the spring tide is totally contained within the main channel, unless there is excessive river input. The highest astronomical tide,

does spill out of the channel onto the flood plain, which is most clearly indicated in the Westgate Bridge section, where the HAT is held within the seawalls. This is not the case for some other sections of the East and West Channels, where spillage onto Alney Island occurs. The HRS modelling of the 1990 river flood calculated considerable flow on Alney Island during this event. Inundation of the flood plain at Westgate Bridge on an Astronomical tide would be up to 0.75m deep, but relatively short lived, about 80 minutes.

These two sections are typical of Upper Estuary sections, where the height of the flood plain within the seawalls, if present, is above the level of MHWS but below the Astronomical maximum.

7.9.2 Middle Estuary.

Two example sections in the Middle Estuary are shown in Figure 7.31. These again show similar features to the Upper Estuary section, i.e. the flood plain levels being at a level between the high water spring and astronomical levels. The cross section at Epney shows how the channel has been incised to considerable depth at one side, with the remaining impounded flood plain being on the other (west) side. Inundation of this part of the flood plain would be to a maximum depth of about 0.5m and would last 55 minutes, when flooding would extend over 300m inland to the seawall from the main channel. Accepting that the flood plain within the seawalls is at a height of 9.0m, the approximate duration and depth of flooding can be assessed (Table 7.21).

Time (min)	Height of tide (m)	Depth of floodplain inundation (m)
onset	9.00	starts
+10	9.18	0.18
+20	9.41	0.41
+30	9.50	0.50
+40	9.41	0.41
+50	9.39	0.39
+55	9.03	0.03

Table 7.21 Floodplain inundation at New Inn (Epney) HAT.

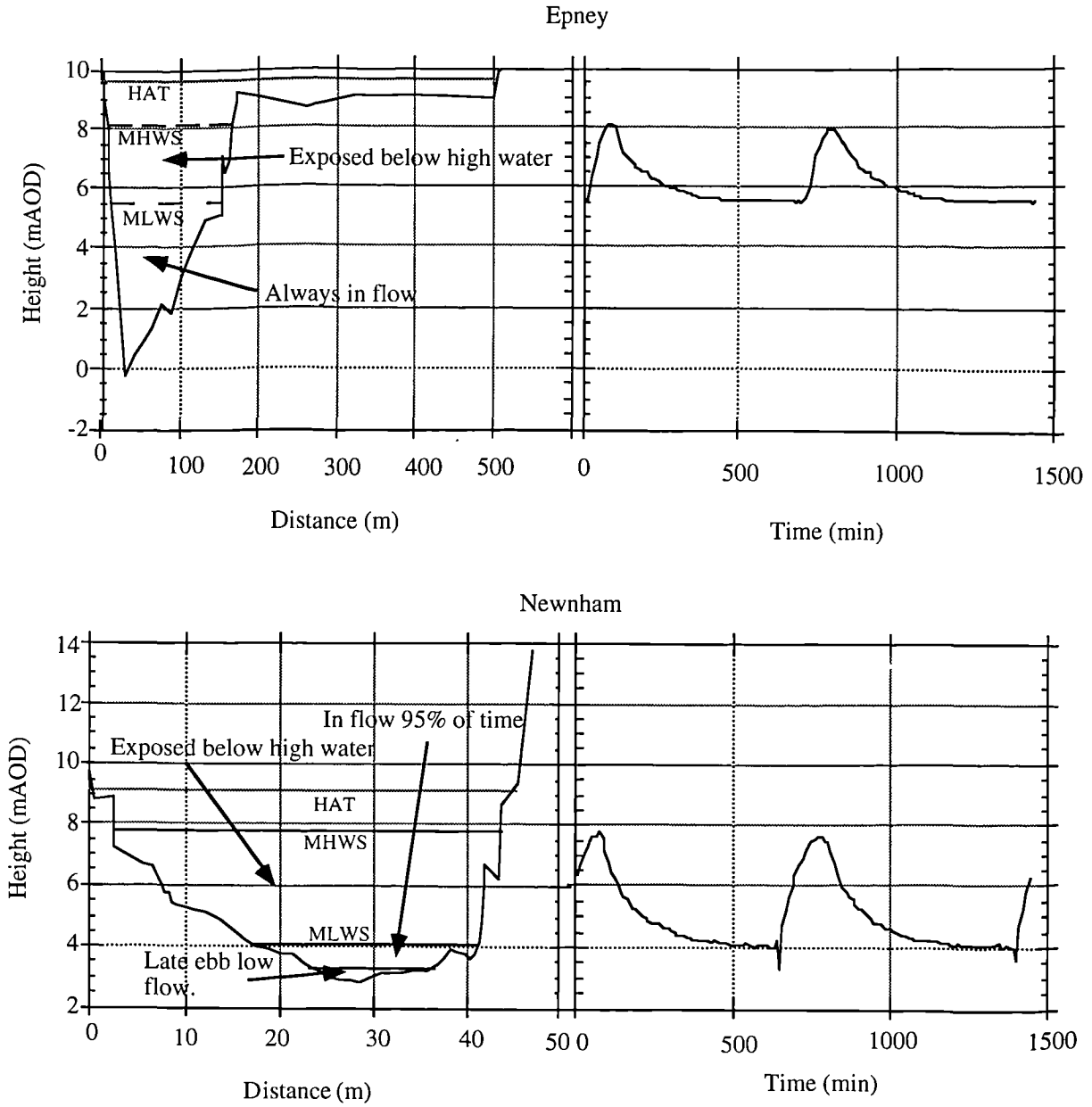

Fig 7.31 Channel sections and spring tide curves, Middle Estuary Locations.

It has been found from modelling tidal heights between the HAT and MHWS at Avonmouth, that a tide in excess of 7.5mAOD at Avonmouth would cause inundation of the flood plain at Epney. Such tides occur an estimated 22 times a year, using Allen (1990) as a guide. The vertical rate of water rise on this flood plain, on an astronomical tide, would be about 0.017m/minute. Assuming an average gradient of the flood plain surface of 0.001 would mean that the tide would appear to move at 0.3m/s across the flood plain on the rising tide.

The example section at Newnham demonstrates how the channel is almost totally confined by seawalls, with little or no flood plain. The 'relict' flood plain inside of the seawalls is again only flooded by tides in excess of the MHWS. Figure 7.31 also indicates the small flow area which conducts the flow at low water.

7.9.3 Lower Estuary.

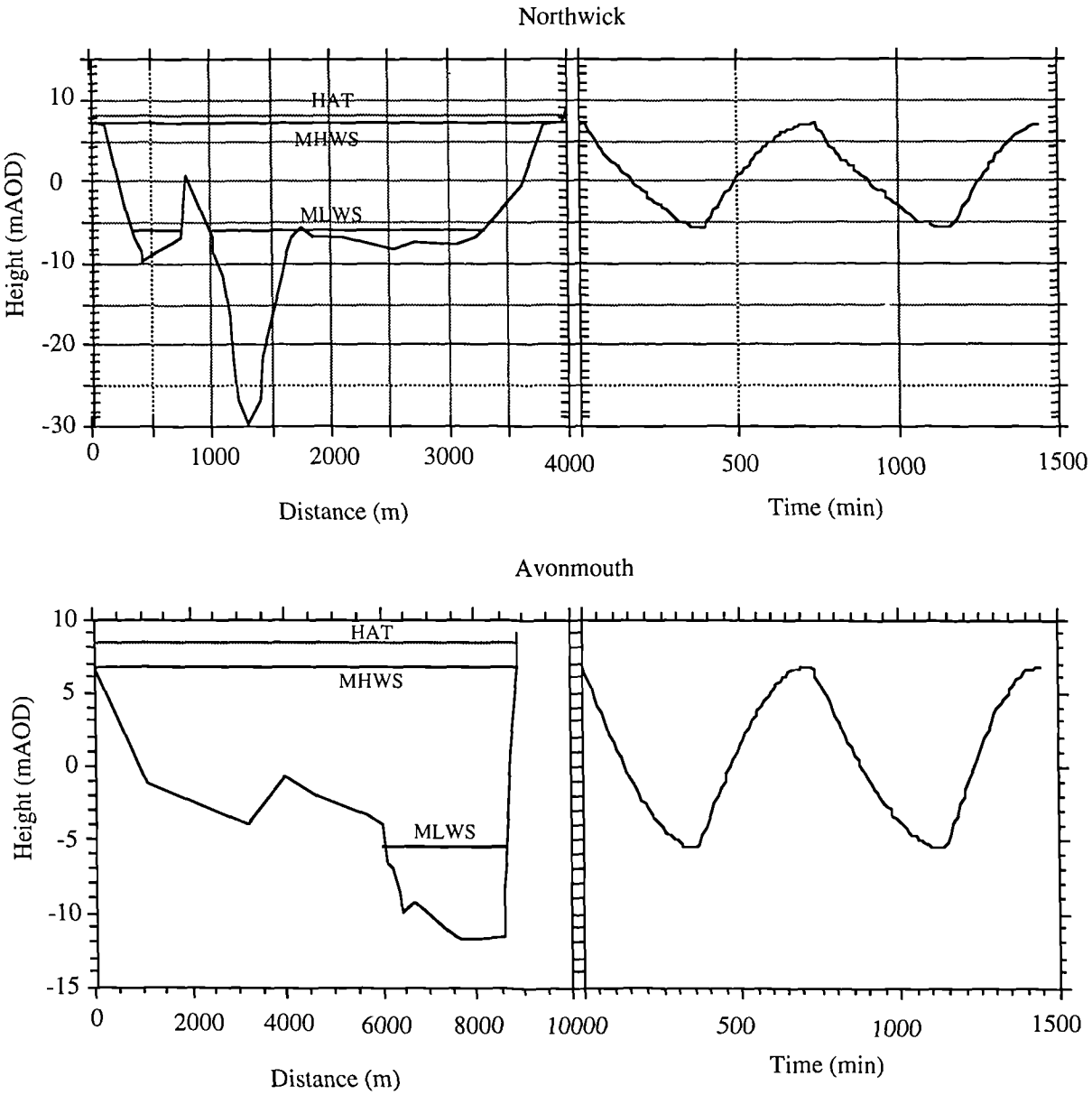

Fig 7.32 Channel sections and spring tide curves at Northwick and Avonmouth in the Lower Estuary

Two example sections in the Lower Estuary are illustrated in Figure 7.32. These illustrate the deep channel which has formed at Northwick which is just upstream of the Shoots. The height of MHWS at Northwick is 15cm greater than the level of the marsh adjacent to the channel and so is flooded on many more tides, in the order of 140 (Allen, 1990) to 213 (Narbett, 1993) times a year. Northwick Wharf provides a good example of a stepped morphology salt marsh, where plateaux of a similar height are separated by small vertical alluvial cliffs. The morphology of these marshes are described in the next chapter. The section at Avonmouth illustrates that the tide is entirely empounded by the seawalls at high tide. At this section there is considerable drying of the mudflats to the west of the main channel (0 to 6000m on Figure 7.32), where this area is exposed for nearly five hours during a tidal cycle.

7.9.4 Summary

The comparison of the modelled spring and astronomical high tides has found that the salt marshes in the Severn Estuary fall into two categories; saltmarshes in the Middle and Upper Estuary are at a height above the MHWS level, but below the HAT level, whereas marshes in the Lower Estuary fall at about MHWS or Lower, adjacent to the main channel. Further aspects of the morphology of the salt marshes and a model of accretion are described in Chapter 8. It appears the position in the Estuary must be taken into account when analysing mean sea level change, through changes in the rate of accretion as the tidal range gets increasingly amplified upstream. The height at which the marshes are accumulating must also be considered. Using the MHWS level as a reference datum as the position of accretion, may be the best estimator, but is obviously not the definitive level at which salt marsh accretion has taken place. Therefore, with the complexity of accretion measurement in the Estuary, tidal curves constructed within the last two millennia, must be prone to considerable error, and non-continuity between positions. Allen and Rae (1988) constructed a sea level curve based upon the mean of the measured amount of accretion at positions in the Estuary at different periods in history. These errors, were in the range which could be expected at different positions, both along the Estuary axis and away from the main channel from the evidence of

the modelling and salt marsh morphology. For sea level curves constructed from such methods employed by Allen and Rae (1988) and Allen (1991) it is recommended that the recorded data be reduced to give a level representative to Avonmouth, or the Bristol Channel, to give a true representation of the sea level change. This would be easy from the analysis presented in this thesis for the change in heights of the various high water events in the present day environment and the comparison with the predicted 1945 levels. However, the modelling of historical tides was not conclusive as to the merits of the method.

7.10 Tidal Defence.

7.10.1 Introduction.

This section describes the modelling of tides in the Severn, with a view to the existing tidal defences and assesses their suitability.

Defence banks along the Severn Estuary and its tributaries are designed to prevent salt-water flooding because of the adverse effect it has on the low lying land and are built to resist all but extreme surge tides. In the uppermost reaches of the tributaries and the Severn, the flood banks are designed to limit the overtopping of freshwater due to fluvial flood. The crests of the seabanks rise up-estuary and in front of 'strategic' developed land, such as power stations and where places are exposed to severe wave attack, such as Frampton, where south-westerly winds can cause a wave build up of over 0.5m above the predicted tidal levels. Many of the banks are Mediaeval in age and are below design levels because they have settled or have not been adequately repaired.

The crest levels of the defences are under constant review, in light of surge tides, wave attack and floods. Sea wall levels in the Severn are devised using a hydraulic model operated by the HRS, new frequency analysis of extreme events and computer modelling. Although there has been substantial redevelopment of the sea defences in the Severn, much of the data available was before the 'Greenhouse Effect' was fully understood, so the levels are still under review, in light of the potential for the present tidal regime becoming potentially more threatening in the future.

7.10.2 Abnormally High Sea Levels.

Abnormally high sea levels are used in the assessment of sea defences and are only considered in the Severn, when sea levels are above land levels, even for relatively short period of time (<2 hours). Presently used figures for high sea levels are based upon the research of Lennon (1963), Graff (1980) and Price (1976) which are unmodified values as each have argued that they have not identified evidence of long term trends in the rise of high water levels. However Lennon suggested an average rise of 200mm/Century for the Severn, based on tide gauge records, of which half he accounted for as being due to land subsidence. The NRA now allow 5mm/year as the rise for the Severn region. The results of the three works are presented as Table 7.22 for the predicted one in a hundred years height at Avonmouth.

Author	1/100 years height (m)	Method
Lennon	8.60	Linear Log
	8.90	Gumbel
	8.53	Normal Frequency
	8.47	Barricelli
	8.41	Jenkinson
	8.50	Adjusted Normal Frequency
Graff	8.33 to 8.49	Jenkinson (different periods of observation)
	8.45	Jenkinson
Price	8.60	Adjusted Normal Frequency
	8.63	Wessex Water Authority

Table 7.22 Predicted one in one hundred years tidal heights at Avonmouth.

Price (1976) corrected an error in Lennon's calculations, to derive a return period of 30 years to a 8.5mAOD tide at Avonmouth and 8.6mAOD for the hundred year return.

The most extreme tide recorded in the Severn (Plate 1) was on the 30th January 1607 which was estimated to have been 9.2m AOD at Avonmouth and another tide of 9mAOD on the 8th December 1703. The tide level of the 1607 event is marked on buildings in both the Somerset levels and in Wales. This tide was estimated to have comprised of a 'normal' tide, 0.1m below the astronomical high tide, combined with a 1.2m surge at the time of high tide. Price estimated that there was a return period of about 850 years on this tide, Wessex Water Authority and the NRA now ascribe a 1 in 500 year frequency for the 1607 tide. It is noted that the largest surge actually occurred at low tide on the 16th March 1947, when a surge of 3.7m was measured, this would have been devastating if it was to have occurred at high water on a large tide.

Lennon also analyses the frequency of surges occurring in the Severn. He predicted a 2.35m surge as the one in a hundred years return and 2.56m as the 200 years return, although such measurements must be extremely difficult to justify given the high tidal range and complexity of the Severn. It is also noted that Lennon's analysis suggest that surges are twice as likely on the neap tide, suggesting that there may be an unexplained interaction at spring tides reducing surge levels (Binnie, 1981).

The surge of February 1990 was higher than the 30 year and 100 year return events, although the tidal range was less. However this tide is attributed a 70 year return by the HRS, highlighting the problems in the frequency analysis of tide levels.

7.10.3 Seawall Heights

The Welsh Water Authority accepted seawall heights in the 1980's at design levels which rise from 8.8m at Cardiff to 9.5m at Sudbrook. Crest heights in the Caldicott levels have since been reviewed, especially where unprotected by saltmarshes and prone to wave attack, where levels now are built to over 10mAOD. These levels are based upon the 100 years return sea level, with an allowance for wave attack. Wessex Water Authority, use the same criterion, with a recommended minimum level of 8.63m at Avonmouth, although Severn Trent Water used 8.5m for Avonmouth previously, the 30 year return value, but only 0.1m less that the 100 years return.

7.10.4 Waves.

A wave run up of 0.5m is used as a general allowance for seawall design. Wave heights in excess of 1.7m during force 9 gales have been identified by the HRS at Severn Beach and levels between this and 1m for the 'English' coast from Avonmouth to Frampton.

7.10.5 Flood Defence Construction.

Sections of sea walls prone to wave attack are invariably defended by a seawards protection of rock rap, although precast reinforced asphalt or cast in situ-concrete are common in the Somerset Levels. Older seawalls are generally small and grassed on both sides, relying on protection from fore-bounding saltmarshes or mudflats. These often have nearly vertical faces and a susceptible to breaching when overtopped by still water or during extreme wave attack.

7.10.6 Modelled Events.

The following tides have been modelled to assess flood defence levels in the Severn Estuary;

- 30 years event, 8.5mAOD at Avonmouth (range 14.8m)
- 100 years event, 8.6mAOD at Avonmouth (range 14.9m)
- 500 years event, 1607 tide, 9.2mAOD at Avonmouth (range 15.4m), average winter flow.

With a river flow of $150m^3/s$ at Maisemore and $100m^3/s$ at Westgate Bridge (average winter flow) and also $500m^3/s$ at Maisemore and $235m^3/s$ at Westgate Bridge (5 years flood).

- 70 years event, 1990 tidal surge, 8.8m AOD at Avonmouth (range 14.3m)

The results of modelling the abnormal tides during average winter flow and during the five years river flood are illustrated on Figures 7.33 and 7.34.

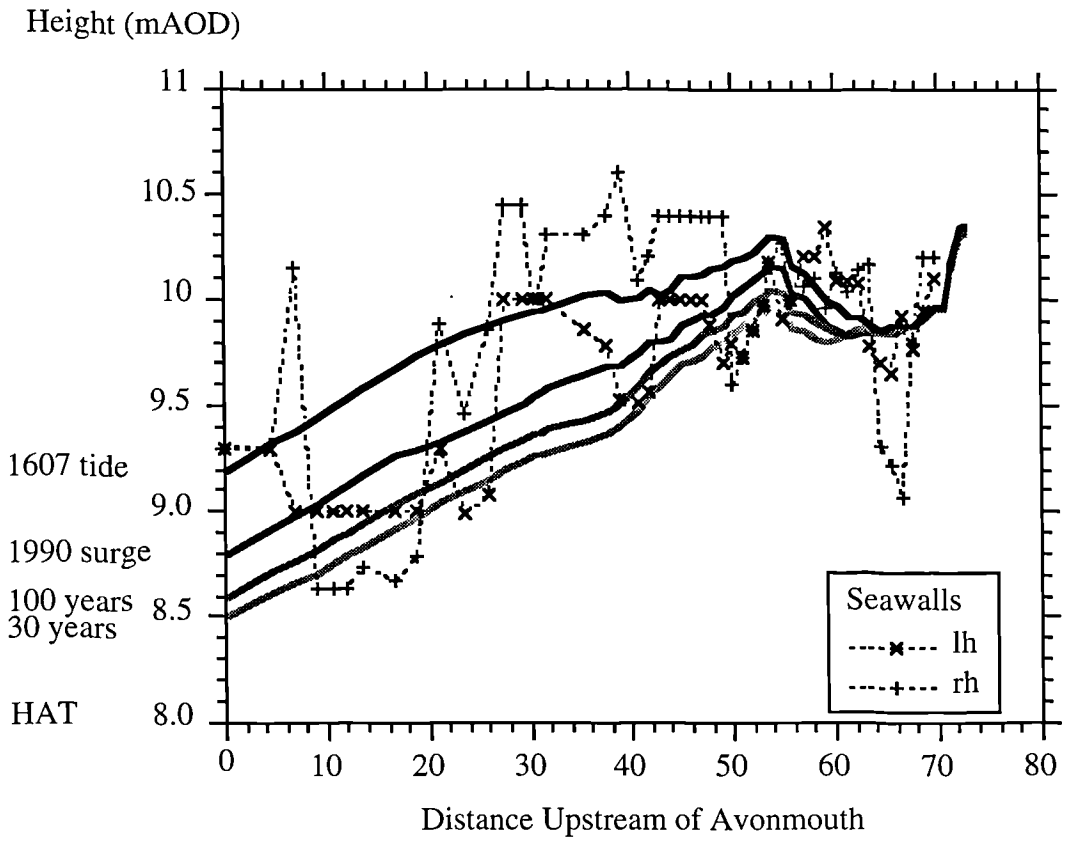

Fig 7.33 Abnormal tides during average Winter flows.

Figure 7.33 shows how the predicted extreme tides often exceed the seawall heights. The figure illustrates the HRS survey of seawall heights, which have been improved in the Lower Estuary, between 9 and 20km upstream of Avonmouth, hence high water levels are not affected by overflow over the walls, as the new wall heights have been used in modelling. From inspection of this graph is can be found that the 30 years event would flood the left hand (English) bank at about 22km distance upstream, both sides at about 50km and upstream of 62km. These positions are near to Berkeley, Framilode and in areas upstream of Minsterworth. The seawall at Berkeley has recently been improved because of flooding, where a substantial reinforced soil wall and rock wrap has been added to the existing structure. The higher events would flood even greater areas to a larger degree, although the seawall

improvements north of Avonmouth to about 20km upstream would only be overtopped by the extreme 1607 tide, which would breach about a third of the Estuary's present defences.

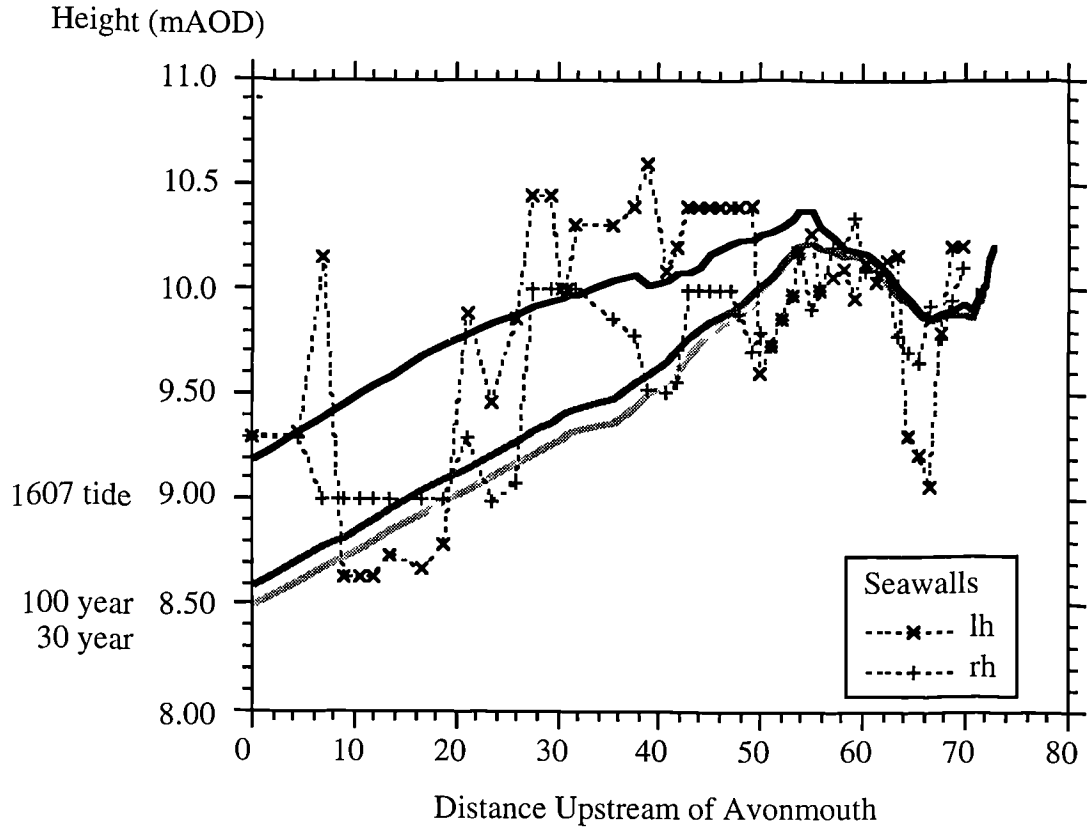

Fig 7.34 Abnormal tides during 5 year river flood.

The combination of extreme high water and high river flood indicates that high water levels will be raised by up to 0.2m between 40km and 60km upstream of Avonmouth compared with the events during normal winter flow.

When assessing the defences in the Estuary, it is worth considering what level seawalls should be built to if no flooding is to occur on the 100 years wave. The model was set up so that the seawalls were infinitely high so that the height of a 100m event in the Estuary could be fully assessed. This is illustrated in Figure 7.35, which shows the height of the 30 and 100 years tide with an allowance made for waves on the 100 years tide which is the NRA guideline height. This clearly shows that many of the seawalls, especially on the right hand bank, upstream of Slimbridge (35km) and from Lower Dumball (50km) on the left bank would be overtopped and that the sea defences in the Upper Estuary are considerably lower than required. However, flow across Alney Island is likely to retard extreme levels passing

upstream into the Severn River north of Gloucester, hence may be considered an acceptable sacrifice. Allowing the walls to be overtopped may be a necessary evil, given the requirement that any further seawall work must not have an adverse effect on the Severn River system, which is naturally immune to river flood inundation.

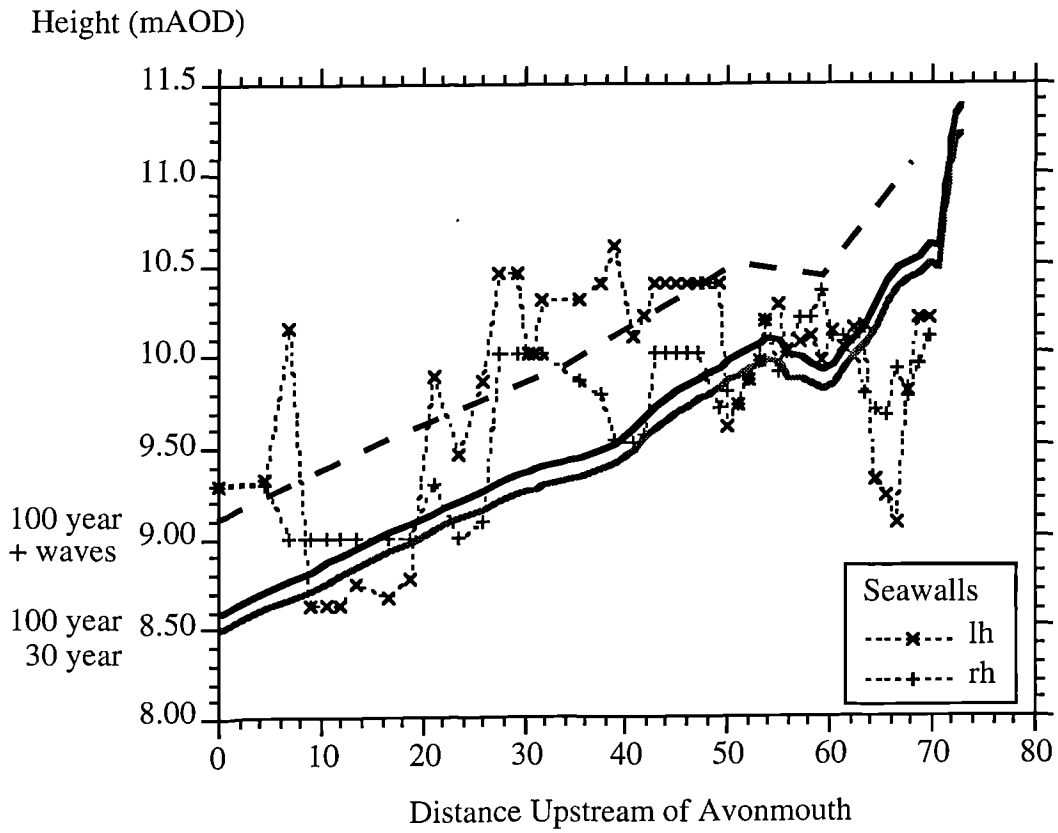

Fig 7.35 30 and 100 year events, with no seawall overtopping.

A critical consideration is the defence of the City of Gloucester, which can flood quite severely between the East and West Channel. However, defences adjacent to the built up areas are at about 10.5mAOD, which would flood on the extreme tides. Figure 7.36 illustrates the topography near Gloucester, where it is deemed that high tides greater than 10.5m at this location, would threaten areas lying less than 10mAOD.

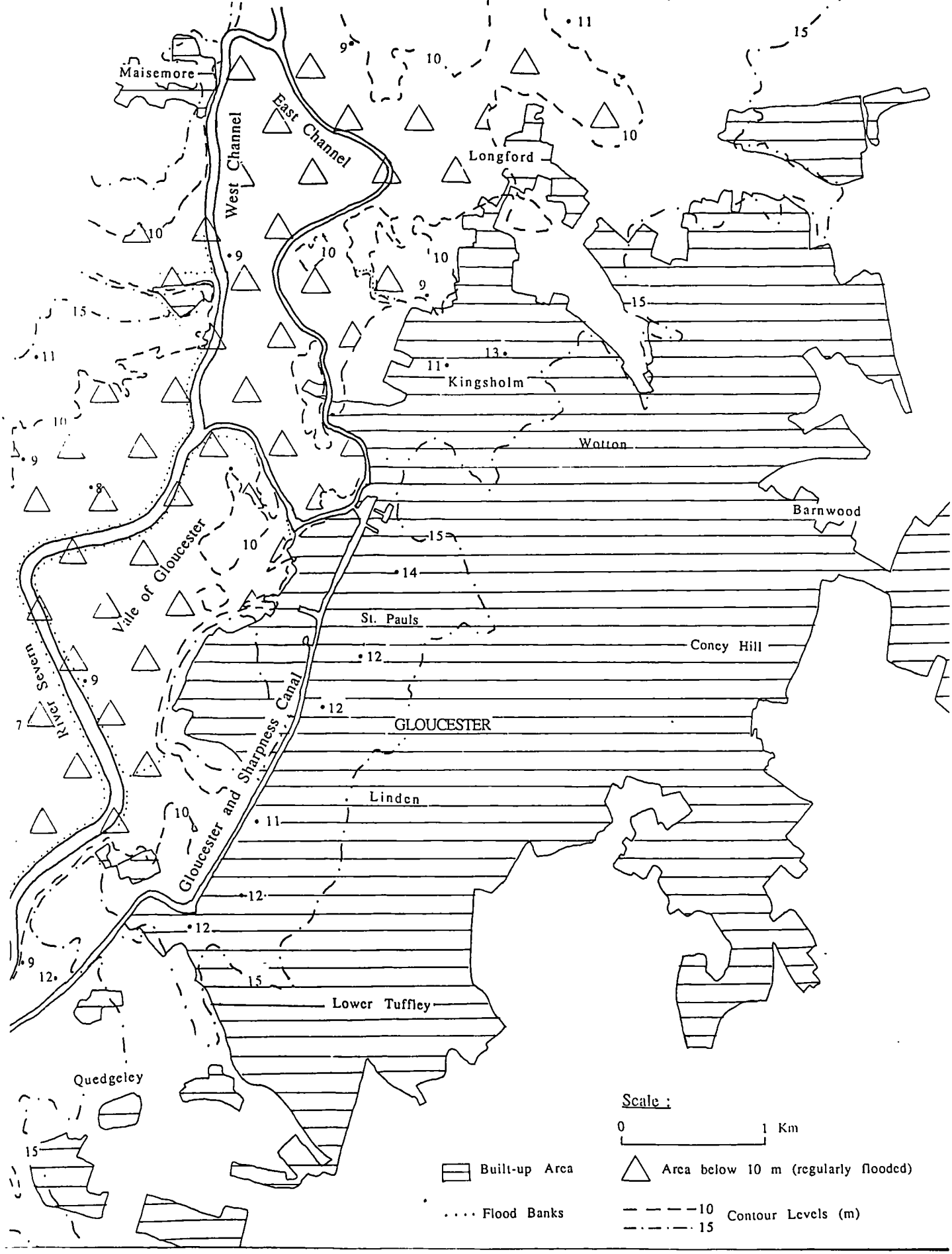

Fig 7.36 Low lying areas of Gloucester City.

Gloucester is a City which is vulnerable to the effects of tidal interactions with large river flows (Hawkins and Taylor, 1991). Both the model study in this work and Binnie and Partners modelling of the Estuary without the attenuating effects of flow over the seawalls, indicate that seawalls in excess of 11.3m (this work) and 11.6m (Binnie model) above Ordnance Datum would be required to contain the thirty years tide at Gloucester, when combined with an average winter flow of about 200 to 250m^3/s. The relatively unrealistic scenario of the 1607 flood occuring with a 5 year river flood, would cause levels in excess of 12.5m at Gloucester if all the seawalls were built up to prevent flooding. The current situation would dictate that tidal levels of the 30, 70 or even 100 years events would not, according to the model, vary significantly at Gloucester. However, this is a reflection of the flooding over the seawalls occuring, naturally the higher the tidal event the more severe any flooding would be.

Protecting the City of Gloucester would become increasingly difficult if sea levels, hence the frequency of extreme tidal events, were to increase as protection of the City also hinders the drainage of waters flowing from the Cotwolds to the east of the City. Large scale developments, now being constructed in the East of the City at Barnwood and Coney Hill, will increasing require delaying resevoirs to prevent a severe risk of flooding.

7.10.7 Tidal Sumps

The effect of allowing the eastern bank of the bend at Arlingham to flood has been assessed during the course of this work. A proposed method of creating a tidal sump involved the removal of the existing sea defences and allowing an area of land up to the residential properties at Arlingham to flood. Two different heights of the reclaimed land allowed to flood were assessed; a ground level of 7 mAOD, slightly lower than existing levels and a ground level of 5 mAOD which would require excavation of material to over 2m depth. The area where earthworks may be undertaken is illustrated on Figure 7.37. It is estimated that to complete such works that 1.8 million m^3 of material would need to be removed for the first project, and about 9.4 million m^3 for the second project.

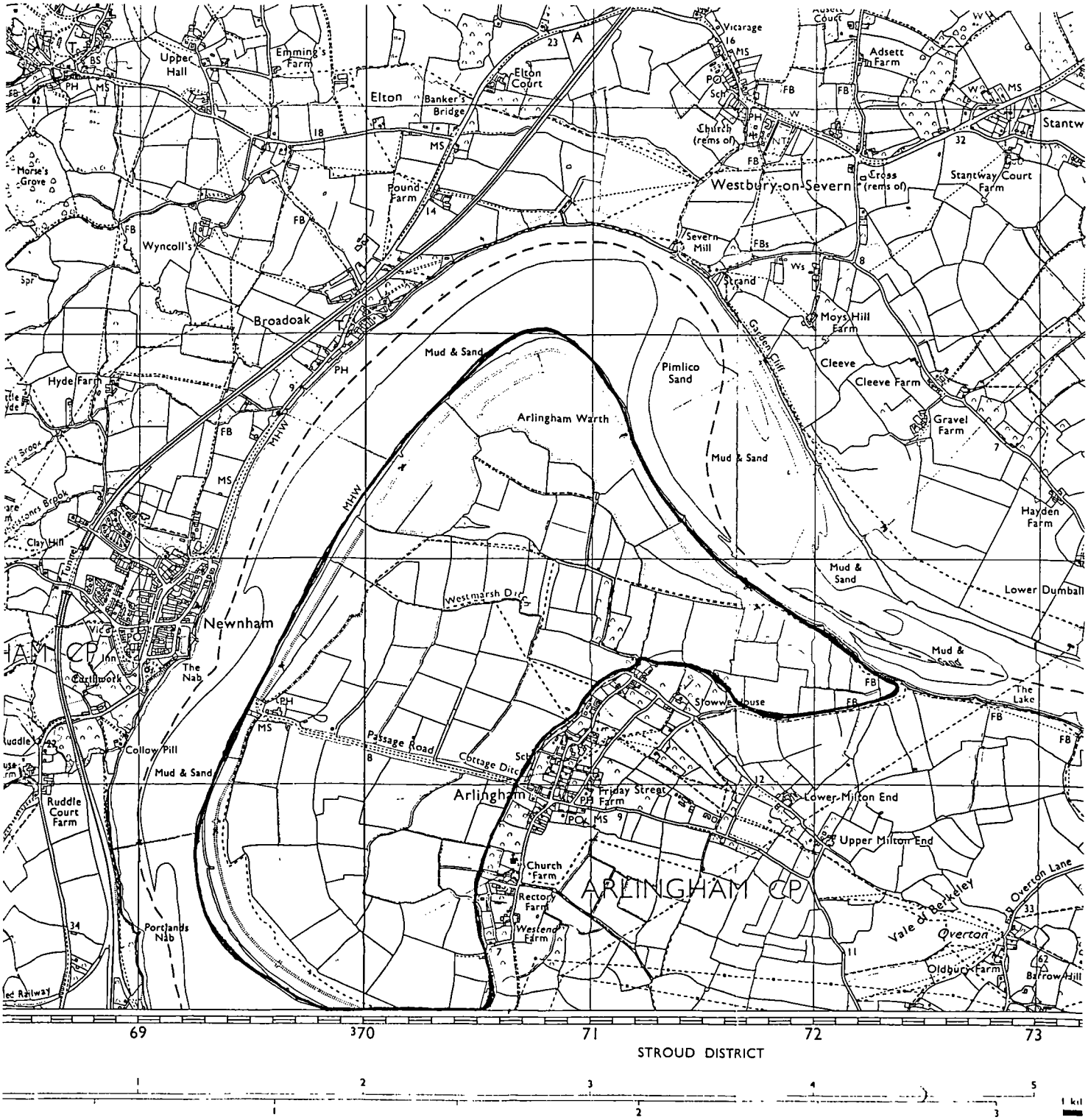

Fig 7.37 Area disturbed by earthworks, where new cross sections have been constructed.

The modelled effects of these large scale earthmoving operations on the high water levels on a spring and astronomical tide are illustrated in Figure 7.38.

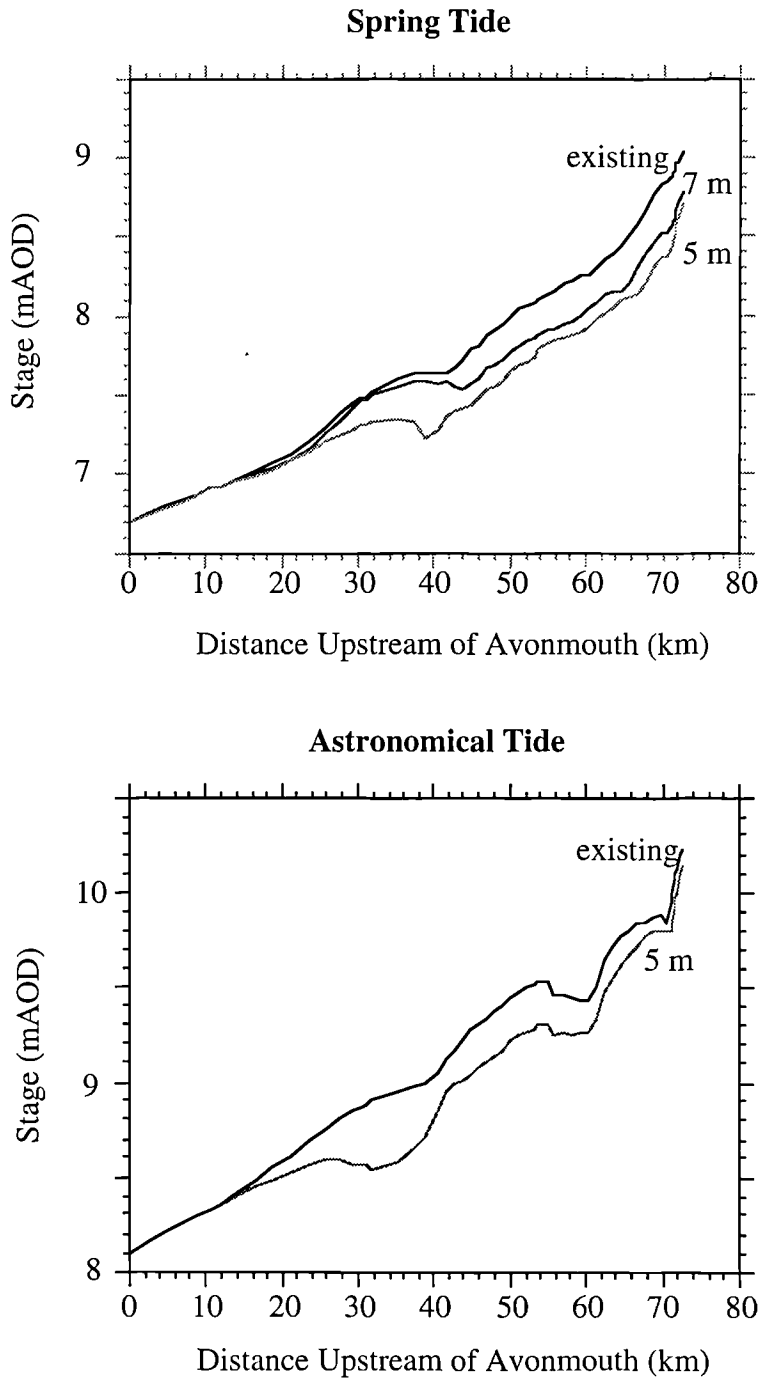

Fig 7.38 Effects of introducing 'tidal sump' on the Arlingham bend.

The simulation of this tidal sump on the effects on the spring and astronomical tides reveals that the project would reduce tidal levels from 30km upstream of Avonmouth almost to

the Estuary head. The model predicted a number of seawall breaches upstream of Minsterworth on the unaffected astronomical tide. The reworking of the bend to 5mAOD predicted only very minor breaches in four locations. It was found that the levels of the high astronomical tide were reduced the most downstream of the theoretical earthworks at Slimbridge and Frampton, where a maximum change of 37cm was recorded. In general the change was a reduction of 0.25m upstream of Arlingham for the excavation to 5mAOD. Low water levels were generally higher by less than 10cm in most of the Estuary, or slightly greater downstream of Sharpness to Oldbury Reservoir. Maximum velocities were reduced to about two thirds of the predicted 'normal' velocities, while the time of high tide was delayed by about 3 to 18 minutes, upstream of Sharpness.

In conclusion the model predicts that the use of a tidal sump could reduce the risk of flooding in considerable areas of the Severn. There are several other localities where there are no substantial residential properties within extensive reclaimed flood plain areas which could be considered for a similar project. The effect on the ecologically strategic mudflats at Slimbridge would be relatively small, as the value as a wildlife reserve relies upon the drying of the mudflats for bird feeding. As the low water levels are relatively unaffected this habitat would not be threatened. However, the overriding practicality would be one of money, if such a project was considered. The cost of moving and as importantly disposing of the quantity of material required would almost certainly render any such project unfeasible. A cheaper plan would be to simply let the existing floodplain area be allowed to flood by removing the seawall and protecting the village at Arlingham with a new seawall. The cost of this would be relatively low, although the cost to farming and 'political correctness' of such work cannot be assessed. The study of this strategy is considered the limit to which a computer model can be applied to coastal engineering, as the overall effects on the Severn Estuary would need to be considered by way of a hydraulic scale model.

7.10.8 Changing Bed Levels.

The channel surveys and modelling undertaken by the HRS revealed that bed movements had occurred between the assessment of the cross sections and the modelled

events. It is impossible within the scope of this work to assess how bed levels may change with time, however, a brief assessment of the effect of changed bed levels could be made. The greatest difference that the change in bed levels could make would be in the Upper Estuary where the rises and falls, found to be as great as 1.6 m between 1975 and 1986 for a section upstream of the model boundaries, greatly affected the capacity of the channel. The HRS found that the majority of bed level fluctuations occurred upstream of the two weirs at Maisemore and Llanthony. The model was therefore run with the lowest bedlevel raised by 0.5m or dropped by 0.5m from Minsterworth to the upstream boundaries, with the section properties re-evaluated. The results of this modelling found that for high tide levels, the bedlevel did not effect the high water level for most tidal events, but if bed levels were raised then a substantial fluvial flood showed higher levels, even with a tidal influence. Low water levels were always increased, in the range of 0.75m.

7.11 Conclusions.

This chapter has reproduced the results of modelling the existing tidal regime in the Severn Estuary for the spring, neap and surge tides. The salient features and differences between which have been discussed.

Future tidal levels, based on predicted global sea level changes have been presented which predict a worse case rise of about 0.5m of high water levels at Avonmouth by 2030AD and in the order of 1.4m by 2100AD, although the 'best estimate' of sea level rise predicts levels about 0.2m and 0.6m for these two periods. Modelling predicts that similar or slightly greater rises would be recorded further upstream, although it is believed that the model will underpredict such changes, due to unaccountable changes in the salt marsh morphologies.

Historic tides have also been modelled, with the morphology of the Estuary being reconstructed from archaeological information. These modelled events indicate that the drop in high water spring levels is increased upstream. For instance, the predicted high water spring level at Avonmouth is estimated to have been 5.41mAOD in 150AD, which is 1.29m less than at present, but would be between 1.35 to 1.43m less than the existing levels in the Middle Estuary. It is clear from the modelling, however, that there will be significant systematic

spatial variation in the accreted depth of sediment and thus the calculated rate of sea level rise. Using the high water spring level as the control on the height of the salt marsh accretion, this indicates that the rate of accretion, hence sea level change, would appear greater upstream. However, modelling of this effect was inconclusive because the rate of sea level rise was so small for the early tides that differences in the calculated change of sea level rise upstream were imperceptible.

Comparison of the high water levels and the channel morphologies indicated that the saltmarshes are not accreting at the level of mean high water spring, but are generally above this level in the Middle and Upper Estuary, and below the level in the Lower Estuary. This difference can be partially attributable to the constriction of the Estuary by seawalls, narrowing the sections and reducing flood plain flow in the Middle Estuary, and by the minerogenic deposition of sediments, which will tend to be coarser grained upstream.

Modelling of abnormally high tides has confirmed that the sea defences of the Severn estuary are barely adequate, and require review, if sea level is to rise at greater rates than are considered at present. MAFF standards for coastal protection suggest that works should be constructed to allow for a tide+surge+wave action with a 200 to 300 year return, or a tide+surge with a 1000 year return. The tidal defences of the Severn are designed to a less conservative value based upon the 100 years tide, with an allowance for wave attack. This is not considered sufficient for the Severn Estuary, although proper evaluation must include a cost assessment of the value of rebuilding seawalls to a greater height compared to the damage caused by inundation. An example of an innovative technique of allowing an area of the Estuary to flood to act as a tidal sump has been demonstrated as being a method which can attenuate high water levels in much of the Estuary.

CHAPTER 8

SALTMARSHES

8.1 Introduction.

The previous chapter has illustrated how the Severn Estuary is vulnerable to extreme tides from innundation and from the fast currents generated. The alluvial plains and saltmarshes bounding the Estuary are the most sensitive environment to tidal influences and in light of the research on sea level change in this work, are addressed in this chapter. The chapter describes the sedimentology of the saltmarshes, the morphology of some the marshes in the Lower Estuary and how they have developed with the changes in the hydrodynamics of the Estuary. The vulnerability of the coastline and seawalls in the Estuary are assessed at the end of the chapter.

8.2 Saltmarsh Stratigraphy and Morphology.

Allen (1985) describes the generalised stratigraphy of the saltmarshes of the Severn, dividing them into five lithostratigraphic surfaces and associated units. Revisions of this model (Figure 8.1) are shown in Allen (1987) and Allen and Rae (1987) which introduce these units and the typical staircase geometry they form. The lithostratigraphic units may overlap one or more of the older buried units.

Name	Description
Wentlooge Formation	Basal unit up to 16m thick of mainly bluish grey and green silts with thin peats
Rumney Formation	Pink grading to grey silty clays up to 3m thick
Awre Formation	Well laminated grey silty to sandy clays
Northwick Formation	Well laminated grey silty to sandy clays
Intertidal Mudflats	Laminated grey silty clays

Table 8.1 Generalised description of lithostratigraphic units.

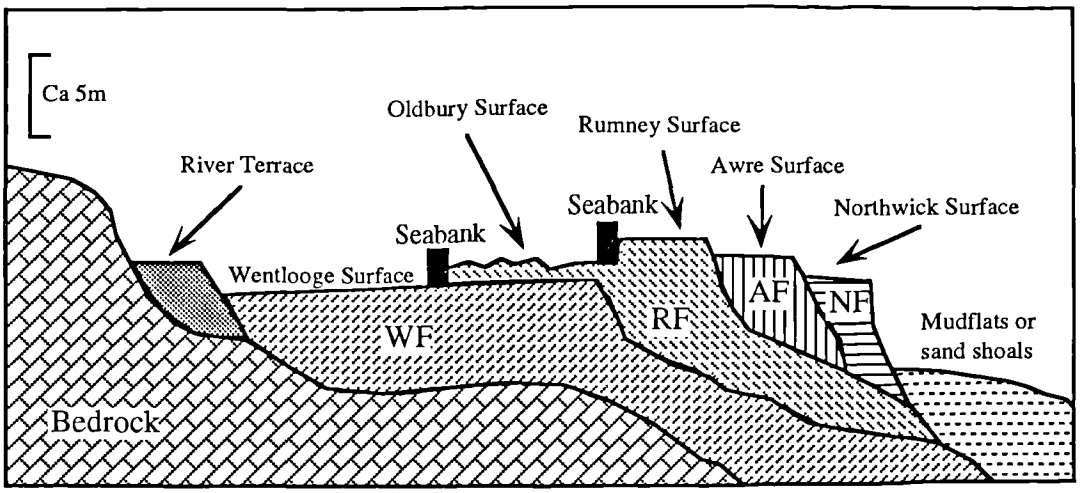

Fig 8.1 Figurative illustration of Allen's alluvial stratigraphy. (WF - Wentlooge Formation; RF - Rumney Formation; AF - Awre Formation; NF - Northwick Formation)

Name	Age	Status
Wentlooge Formation	Isolated in Roman Times by embankments	Wentlooge surface isolated and not accreting
Rumney Formation	Partially isolated by early mediaeval reclamation	Oldbury surface isolated and not accreting (characteristic ridge and furrow topography) Rumney Surface accreting besides sea walls forming highest geomorphic surface on saltmarsh
Awre Formation	Industrial Revolution	Awre Surface still accreting forming middle saltings
Northwick Formation	Early 20th Century	Northwick Surface still accreting, forming lowest surface of saltmarsh
Intertidal Mudflats	?	Youngest, forming soft sediment tidal platform at foot of Awre formation.

Table 8.2 Age and status of lithostratigraphic units.

The deposition of these units has been attributed to sea level or climatic fluctuations by Allen. From archaeological information he has derived general ages for the onset of accretion of these units (Table 8.2). It is noted, however, that not all units or formations are present in a saltmarsh, indeed Narbett (1992) stated that the simplified model by Allen is not rigorous enough to apply to Northwick Warth in detail.

8.3 Physical Controls.

Allen and Pye (1992) state that the location, character and dynamic behaviour of saltmarshes are controlled by four physical factors;

- Sediment Supply
- Wind and Wave Climate
- Tidal Regime
- Movement of Relative Sea Level

The following sections describe how these factors influence the morphology of the saltmarshes in the Severn Estuary.

8.3.1 Sediment Supply.

There are three principal sediment sources in the Severn Estuary similar to those identified by McManus (1979):

- Fluvial - Thought to be predominantly suspended and in solution in the present day lower energy conditions of the Severn. Collins (1987) identified from mineralogical comparisons that the fine sediments presently brought into the Severn Estuary have a fluvial origin.
- Marine - These may enter the Estuary from the Bristol Channel as a traction load or in suspension. Early sandy sediments, deposited in general below 0 mAOD were identified

by Murray and Hawkins (1976) as originating from the Celtic Sea, accompanying the initial period of the Flandrian Transgression and higher energy conditions.

- Redeposition - Internal erosion and deposition processes can recycle sediment with an estuary. This process is obviously limited in general to the soft sediment alluvial coastline of clifflets and mudflats.

An estuary can be a net importer or exporter of sediment (Kelly, 1987, O'Conner, 1987) depending on the degree of infilling which has taken place. During the early stages of the Flandrian Transgression to 6000 BP the Severn would have been a net importer of sediment with little erosion taking place. Allen (1990) assesses the current status of the Severn Estuary as being nearly at capacity with no appreciable difference between export and import. This was an important consideration in the assumption of not applying sediment transport in the modelling of the Estuary, which would have required a complex model. Kirby and Parker (1982), Collins (1987) and Allen (1990) suggest that about 1.63×10^6 tonnes of fine sediment are discharged per year into the Bristol Channel from fluvial sources and that three times this amount is held in suspension. A total of 1.16×10^{10} tonnes of fine sediments is estimated to have been introduced into the Severn in post-glacial times.

Some of the most important suppliers of the present day sediments are the existing mudflats and probably saltmarshes which are reworked as an internal supply of sediment. Allen (1988) describes the theoretical processes of reworking and deposition up-estuary as it transgresses with rising sea level.

8.3.2 Wind and Wave Climate.

The wind and wave climate principally effects the erosion of the soft sediment clifflines. Erosion tends to be greater in the Autumn and Winter due to the stormier weather. Erosion of the alluvial clifflines is predominantly controlled by waves breaking against the cliffs exploiting desiccation cracks formed during the Summer, whilst scouring at the foot of these cliffs can undermine them. The different modes of cliffline erosion and failure are described by Allen (1987).

The winds and waves are also a major consideration in the building of sea defences. As mentioned in the previous chapter, wave effects in the order of 0.5m minimum should be considered above the 100 years tide when designing sea defences. Exposed coastlines in the Severn Estuary are predominantly on the English side between Severn Beach and Frampton, whose aspect make them vulnerable to south westerly winds, which are generally the strongest encountered in the Severn and frequently are associated with the storms that drive tidal surges.

8.3.3 Tidal Regime.

The tidal regime of the Severn Estuary has already been covered in some detail in this thesis, so is not repeated in any great detail here. The macrotidal tidal regime, drives spring tides into the Estuary with heights that increase upstream. The height of the high water spring equates roughly to the height of the saltmarsh surfaces, an aspect which is considered later in this chapter. The level of the mean high water neap is sometimes considered to be at a similar level to the base of the saltmarshes, with mudflats or sand shoals being present at lower altitudes. Obviously estuaries with larger tidal ranges will tend to form higher saltmarsh cliffs under these conditions at the wet margin with the estuary.

Another important aspect of the tidal regime is the currents generated and the angle of incidence of these flows with the saltmarshes. Marshes where rapid prolonged currents sweep towards them will have a greater potential to erode than ones in less direct contact with the dominant currents. The relationship between saltmarshes and the currents in the Lower Severn Estuary will be described later in the chapter.

8.3.4 Movement of Relative Sea Level.

Mature saltmarshes accrete within the prevailing tidal frame. Unless the rate of change of the prevailing sea level is too great for the marsh to match, the surface will rise with a rise in sea level, or will become exposed if sea level was to drop.

There is little evidence of reductions in the post glacial sea levels in the Severn Estuary. Such events would cause widespread exposure of saltmarshes and would lead to the formation

of the alluvial 'crust' as described by Narbett (1992), which would subsequently become buried with the onset of the next period of sea level rise. Geotechnical information from boreholes shows no evidence that the present day alluvial pile has any stiffer layers indicative of buried crusts.

A rise in mean level will be approximately matched by the rate of rise of the saltmarsh surfaces. It has already been demonstrated that the amount of apparent sea level rise increases upstream. The rise in the relative sea level also influences the retreat of the Estuary upstream as illustrated by Allen (1988) and the nature of infill of the Severn Estuary (Hawkins, 1984).

8.4 Accretion of Sediments.

8.4.1 Measurement of Accretion.

Saltmarsh accretion in the Severn Estuary within the last 2500 years has been analysed using a variety of techniques which have developed by Allen and Rae (1988). These measurements include the following;

- Height differences related to reclamations.

As seawalls have been built the flood plain behind the defences have been starved of sediment supply, hence if the date of reclamation is known, the height difference between the marshes in front and behind the wall can be used as a guide to the amount of accretion which is assumed to directly relate to the sea level change. However, such a theory is prone to a variety of errors. Whilst the following sentences seem to criticise the method it is stressed that the method is still one of the most reliable of the methods applied to the Severn.

As seabanks maroon the older and larger floodplain, the near channel and still free to flood saltmarshes may build up at a greater rate because the former area of inundation is severely attenuated. Allen (1991) acknowledged this as a small error but argued that the hydraulics of an estuary are such that compensations downstream would result in little if no discernible increase in the effect of this factor. This seems to have been borne out by the modelling of the 1250AD tide with a narrow reclaimed saltmarsh geometry to the Estuary and a

broad alluvial plain geometry. The difference between modelling the two showed only minor increases to the spring tide heights when the Estuary was restricted. However, greater volumes of flow and velocities were generated during the 'restricted' scenario, suggesting greater sediment would be carried if an estuary was suddenly reclaimed, leading to an initial period of fast accretion in front of the seawalls, this could be counteracted by increased erosion.

Allen also assumes that the saltmarshes are mature prior to reclamation. This may be true for some areas of the Estuary but cannot be considered definitive. If a seawall was emplaced there may be an initial period of rapid accretion, which would slow down as the saltmarsh attains a high level in the tidal frame. This effect would definitely be greater for seawalls placed on lower alluvial surfaces, closer to the main channel.

Narbett (1992) also argued that Allen made no account for the seawalls being overtopped during extreme events and depositing sediments behind the seawalls. Whilst this holds true, it is not likely that the amount of sediment which would be carried over the walls would be sufficient to cause any significant difference in the measured accretion. However, localised places where a seawall may have been built, suffered severe damage and was not repaired for some time might have post-reclamation sediments of an appreciable thickness. Although the area was not studied in detail, the excavation of a 'borrow pit' near Aust Warth mentioned by Narbett (1992) showed two distinct layers where calcareous nodules had formed separated by over 300m of alluvium close to, but behind, the seawall. As it is difficult to date these horizons, it must be assumed that the two deposits are of a relatively similar age, given their nature. Calcrete horizons form relative to the groundwater table and zone of capillary rise. Although this apparent change in conditions due to a sudden influx of sediment because of a long to moderate term failure of the seawall cannot be discounted, it is more likely that installation of some form of land drainage caused a drop in the water table to allow formation of the lower horizon or that the water table was allowed to rise after some form of groundwater abstraction had ceased. No anecdotal information from the owner of the area, or the NRA could be found to substantiate any of these ideas. Much of the land drainage in the area is pre- or just after the war, therefore it is possible that relatively mature calcrete horizons can form within 50 years.

It was found during the construction of the cross sections of the Estuary and flood plains for the computer model the surfaces of the old mature marshes behind and in front of the sea wall formed levees. This is a natural phenomena caused by the over flowing sediment rich waters onto the flood plain, both during major periods of inundation and through wave breaking. In places in the Middle Estuary surveying of the land clearly shows the new post reclamation levee superimposed upon the larger older levee. The older levees, whilst showing a much larger height difference between levee crest and low points, generally have a smaller surface gradient, suggesting that there is some interaction between the present day levee, recent tidal regime and the constriction of the Estuary.

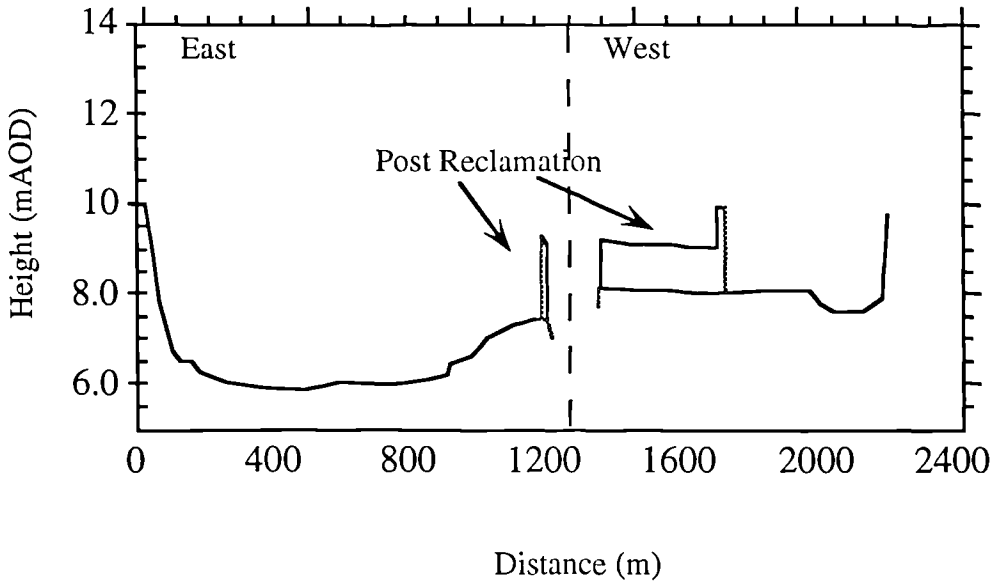

Fig 8.2 Existing and pre-reclamation flood plain near Epney.

Figure 8.2 indicates the old and present reclaimed flood plain near Epney. This clearly shows the small extent of the present day flood plain within the seawalls and that over one metre of accretion has occurred since its reclamation. The rapid rise of the ground surface on either side of the old flood plain is due to the outcrop of the bedrock. This figure shows the pre-existing levee which had developed prior to reclamation, which is lower and steeper on the east side of the main channel. This difference may be due to different times of reclamation, although no authoritative historical data could be found to confirm this. An investigation using

a hand auger was also undertaken to see whether the sediments indicated that one side or the other had been an overflow channel, where either excessive scour or deposition had occurred during ancient inundation. However, the results, primarily due to the sampling technique were inconclusive. This investigation could not identify whether the topography was due to excess settlement on the east side, possibly indicating the presence of a buried channel. It is clear that if a levee, either post or pre-reclamation is eroded by the channel spreading outwards, then the high part might be removed resulting in a lower apparent rate of sedimentation, although this is countered by an increase in the rate of sedimentation on the part of the floodplain which had been protected by the levee and would be more prone to flood than before.

This dating of buried surface is also prone to error for the reasons listed by Narbett (1992), although it appears that Allen's research in the main has followed an acceptable methodology in this respect. Allen's chemzones, however, are criticised by Narbett, who believes that the post industrial geochemical markers are unreliable because of the ability of organic matter to concentrate these pollutants, as he found a high correlation between organic content (assumed to indicate the presence of *spartina* grass trapping sediment) and the metal concentrations. It is also noted that the organic content of alluvial soils can commonly decrease with depth (disbarring any peat type sedimentation) because of the breakdown of organic materials and limitations of test methods.

Allen's proposed rates of sea level rise have been included in Chapter 2 and been accepted as the basis for modelling historical tides, especially as no better estimates have been proposed. The model therefore predicts sea levels in the Severn Estuary which are prone not only to the potential methodology errors and incorrect assumptions mentioned previously, but to the following factors highlighted by Narbett (*1992*);

- The sharp upturn in sea level within the last 150 years proposed by Allen (1988 and 1991) may be due to the ability of vegetation to promote sedimentation rather than a dramatic increase in sea levels.
- The construction of sea defences along the Estuary margin in the last 500 years has altered the depositional regime, hence may influence the apparent rate of change of sea level.

- Shipping movements can significantly affect the channel morphology and hence the sedimentological characteristics of the Estuary (Hawkins, 1984).

8.4.2 Accretion in the Severn Estuary.

Allen (1988) indicates the amount of accretion he has measured between several of his chronological markers in positions in the Estuary. In his study he suggests that the following amounts of accretion have occurred in the Severn, which have been compared to the modelling of the mean high water spring level predicted by the model studies.

- Roman time to present.

Allen found that accretion in the region of about 0.9 to 1.7m had occurred in this period, showing a minimum amount of accretion near to Aust increasing upstream and downstream, although the downstream prediction may not have enough data to fully back the assumption. The model studies predicted the apparent change in sea levels from the present to Roman times would be greater upstream of Aust which was the locality where the lowest change was predicted. Allen used a quadratic polynomial curve to show the changes in sea level from this time to the present along the Estuary, the modelling did not confirm this type of behaviour. The model predicted changes in the order of 1.26 to 1.43m with less spread than Allen's figures.

- Medieval to present.

Allen proposed a straight line fit suggesting greater accretion up-estuary between about 0.6m and 1.6m for this period of over 700 years, with the maximum accretion occurring upstream. This type of behaviour was confirmed by the model simulation if sedimentation was closely related to the high water levels, although again the predicted change in spring tide levels is less than that of Allen.

- 1845AD to present.

Allen again predicts a polynomial distribution of accretion between about 0.4m at Aust, increasing rapidly upstream to a maximum of about 1.2m. Model studies did not show such a trend in the spring high tide heights, again a nearly linear change of about 0.4m at Aust to 0.6m near Gloucester.

- 1945AD to present.

Allen indicates that the accretion of sediments in the Estuary increase in a linear fashion upstream from about 0.2m to 0.3m. Modelling studies show close agreement to this in all but the Upper Estuary.

Some of the discrepancies of the modelled and Allen's measured heights are explained by the complexity of the depositional system, especially as it has already been shown the mean high water spring is not necessarily the level of the marsh height and that major differences in sedimentation can occur within small distances due to the position of the saltmarsh in either an erosive or deposition part of the channel (see later in the chapter). As a conclusion it is deemed that Allen's work although flawed, is not unacceptable and certainly must be embraced at present as the best guidance for historic sea level changes. However, the model studies and Narbett's comments on the chemzones used as stratigraphy since the mid Nineteenth Century do seem to suggest that the extreme rates of accretion up to 1.2m that Allen has recorded are not due to the prevailing changes in sea level, but to methodology errors or unknown physical conditions.

8.4.3 Model of Accretion on Saltmarshes.

Allen (1992) and Allen & Rae (1987) both highlighted that the lithostratigraphic units present on the Estuary flanks showed the sensitivity of the soft sediment coastline to small changes in the tidal regime. Allen (1990) proposed a simple one-dimensional model for the vertical growth of a saltmarsh or alluvial surface. Allen's model is a differential equation describing the principal controls on the rate of saltmarsh accretion (Equation 8.1).

$$\frac{dE}{dt} = \frac{dS_{min}}{dt} + \frac{dS_{org}}{dt} + \frac{dA}{dt} - \frac{dM}{dt} - \frac{dP}{dt} \qquad (8.1)$$

Where $\frac{dE}{dt}$ = rate of change in surface elevation, relative to tidal datum (LAT)

$\frac{dS_{min}}{dt}$ = Rate of accretion of minerogenic sediment

$\frac{dS_{org}}{dt}$ = rate of accretion of organogenic material

$\frac{dA}{dt}$ = rate of change in amplitude of the astronomical tide (increase is positive)

$\frac{dM}{dt}$ = rate of change in relative mean sea level (upwards trend is positive)

$\frac{dP}{dt}$ = rate of change in surface level due to consolidation of sediments.

As estuarine sediments are analogous to river floodplain sediments, the minerogenic term can be expanded using Equation 8.2 for the addition of fine sediment through diffusive and convectional processes, summing the relevant effects over the period of accretion on a single tide and the sum of these tides over the yearly period.

$$\frac{dS_{min}}{dt} = \frac{K}{1 - P} \sum^{year} \sum^{T} C(H,t)\, W(t) \qquad (8.2)$$

Where K = fraction of remaining sediment thickness at the end of a year

P = fractional porosity of material deposited

T = duration of surface wetting during astronomical tide

C = fractional volume concentration of mineral matter in the water

H = height of tide

t = time relative to the start of the average tidal year

W = terminal settling velocity of suspended particles.

The term for minerogenic deposition decreases rapidly as the surface elevation of a marsh increases. Without considering abnormal tides, the highest astronomical tide defines the maximum level at which a saltmarsh can accrete through minerogenic sedimentation.

The rate of organic sedimentation depends on the amount of retained root and surface vegetation debris. This term is a function of the tidal elevation as vegetation is zoned within the tidal frame. Often saltmarshes with steppped surfaces have different types of dominant species upon each level. This term is most important in the upstream sections of the Estuary floodplain where they are starved of mineral sediments because of the levee. In such locations it would be natural to expect appreciable thicknesses of organic material, namely freshwater peats.

The height of the astronomical tide has been demonstrated to rise in the Severn Estuary at a rate greater than mean sea level, so the effect of sea level change will vary in different places of the Estuary, albeit by a relatively small amount. It is unlikely that the long term consolidation term adds appreciably to the overall calculation of Equation 8.1. Allen divides saltmarsh accretion into three principal growth modes based upon Equation 8.1.

- Mode 1 Growth.

$$\frac{dS_{org}}{dt} + \frac{dA}{dt} - \frac{dM}{dt} - \frac{dP}{dt} < 0$$

This mode requires the minerogenic deposition to be positive for the marsh to remain in an equilibrium state. Marshes in this mode of growth attain constant level below the highest astronomical tide after an initial early period of fast accretion. Such growth is best suited to by an upward trend in relative sea level.

- Mode 2 Growth.

$$\frac{dS_{org}}{dt} + \frac{dA}{dt} - \frac{dM}{dt} - \frac{dP}{dt} > 0$$

This mode illustrates that the marsh cannot manage equilibrium as it would require a negative input of minerogenic sediment. After the highest astronomical tide level is reached by

the marsh surface, accretion can only occur as organic coastal peat like formation. This mode of growth is favoured by conditions of steady or reducing sea level.

- Mode 3 Growth.

$$\frac{dS_{org}}{dt} + \frac{dA}{dt} - \frac{dM}{dt} - \frac{dP}{dt} = 0$$

This mode of growth occurs between the other two models of growth where equilibrium would occur after an infinite period, attaining the height of the highest astronomical tide.

8.4.4 Saltmarsh inundation at Northwick.

Allen's predictions of marsh maturation times are of the order of about 100's to 1000 years, implying that measurements on more recent marshes would over estimate the apparent rise in mean sea level as the marshes would still be accreting at an enhanced rate to the higher and older marshes behind. Narbett (1992) produced profiles of the saltmarsh at Northwick, a typical example of which is used in Table 8.3 to illustrate the inundation of the marsh on spring and astronomical tides, using figures from the computer modelling of the tides.

Surface	Elevation (mAOD)	Tide	Period of inundation (min)	Max depth of inundation (m)
Northwick	6.47	HAT	132	1.83
(Lower Marsh)		MHWS	83	0.56
Awre	6.83	HAT	117	1.47
(Intermediate Marsh)		MHWS	44	0.20
Rumney	7.26	HAT	95	1.01
(High Marsh)		MHWS	not flooded	not flooded

Table 8.3 Inundation of saltmarsh at Northwick, spring and astronomical tide.

The inundation figures for the saltmarsh at Northwick illustrate that only the Rumney formation has attained a height above the spring tide level and can be considered to be mature. Changes in tidal levels in excess of 0.6m in 10 minutes can occur on the astronomical tide leading to the marshes flooding at very high velocities. This change cannot be matched by the drainage of the marsh, so the water is slowly transferred to the Estuary via tidal pills on the ebbing tide. After a high tide water may be left to stand against the seawalls. Not only do the walls suffer erosion during the high water itself, but also from transverse flows of draining water exacerbated by the wind. Observations suggest than wind can cause boundary layers in the upper 1 to 5cm of the water column on flooded saltmarshes which appear to flow in excess of twice the velocity of the flooding waters.

When the saltmarshes are observed to flood it can be seen that the flow upon them is very turbulent and well mixed. Crude field experiments with ink dyes suggested there appeared to be no laminar flow close to the surface of the marsh. It is clear that the sedimentation of fine material on the marsh is low on a spring tide and that the vegetation is trapping a high percentage of this material, possibly up to 40 or 50%, with the remainder settling from the water column.

A more important contributor to the saltmarshes is the coarser silt fraction. Silt laminae can often be traced across the entire area of a single saltmarsh level. Studies for this work at Northwick using glitter as a marker at first proved difficult because the current velocity or turbidity was sufficient to resuspend the glitter and lose the marker horizon. However, a heavier glitter was found which proved more reliable. The tests analysed half metre square areas on each of the surfaces at Northwick for sedimentation over the period of 1.5 years. It was found that silt laminae up to 3mm thick deposited after storms could be traced quite continuously over the extent of the entire Northwick Surface close to the main channel. Continuity of the laminae became less toward the back of the surface and was found to be disrupted close to the cliff line with the Awre Formation due to interaction with the cliff. Silt laminae were found to be thinner on the Awre Surface and much less continuous. Of three major silt laminae on the Northwick Surface, only one could be detected on the Awre Surface and was less than half the thickness of its equivalent on the lower surface. No appreciable sedimentation could be detected on the high marsh. There was no conclusive proof of grading

of the silt laminae and overlying clay. Silt accounted for 70% of the sediment accumulated over the period of investigation. Sedimentation on average was measured at over a centimetre on the Northwick Surface and less than a centimetre on the Awre Surface during the period of observation.

In conclusion the small scale experiments at Northwick suggested that sedimentation on the lower marsh is in excess of the rise in mean sea level and is related to the frequency of storms and the sediment carried on a storm tide rather than on normal tides. The non-storm inundation of the marshes does deposit fine sediment of which much is trapped by the vegetation. No trends in sediment settling and concentrations over the extent of the saltmarsh could be ascertained as the velocities of inundation were such that sampling was hazardous. The intermediate marsh is accreting at rates similar to the present estimate of sea level rise (5mm/year) and the upper marsh at less than the prevailing rise of sea level, although it is noted that the period of observation is not sufficient to totally justify these statements.

8.5 Erosion of Sediments.

Sediment erosion in the Estuary takes place in a variety of locations and by different methods. This section will describe the erosional processes in brief as a precursor to later sections on saltmarsh morphology, cliff lines and coastal vulnerability.

8.5.1 Erosion of Alluvial Cliffs.

Alluvial cliffs bound over two thirds of the saltmarshes of the Severn Estuary and can be in excess of two metres high in places. These cliffs which are in retreat from the main channel may be reworked in a number of ways, described by Allen (1987) of which the most common are:

- Toppling of blocks loosened by desiccation cracks and columnar soil joints.
- Spalling of upper material bound by organic material.
- Rotational slips.
- Plane slips.

Stormy weather is a dominant control in the erosion of the cliff lines and tends to be greater in the autumn and winter, when larger waves exploit the desiccation cracks formed during the summer. Waves and currents exploit the cliffs through the scouring of the cliff bases, undercutting them and through the forcing of compressed air into cracks from breaking waves. Fallen blocks may be reworked by the currents, but can survive and become sediment traps. A number of blocks were loosened from a cliff line in the Caldicot Levels during a spring tide, where it was found that approximate 10% of the clumps survived four consecutive high tides although they had decreased in volume by about one half and were well rounded. The surviving clumps had the best developed and most penetrative colonisation by vegetation.

Narbett (1992) found that the cliff faces at Northwick Warth had retreated between 550 and 800mm over a two year period with the greatest erosion occurring at the top and foot of the cliffs. Allen (1990) suggests that the presence of these cliff lines indicate that the Estuary is widening at it's high water mark and retreating up the Severn Vale. Modelling studies have indicated that the tides predicted for the future would reach higher levels than at present, but more importantly the quantity of flow and current velocities on the flood and early ebb tide would be up to 1.5 times faster than at present. This would be likely to cause significant erosion of soft sediment clifflines in the Lower and Middle Estuary. As much of the Middle Estuary has been reclaimed there is little surviving saltmarsh between the seawalls and the main channel. In the future the channel will try to erode towards the seawalls to accommodate the additional flow, threatening the tidal defences. Indeed Gibson (1933) suggested that the Severn Bore is a sign of instability in the Estuary, and only the areas downstream of where the bore appears have adjusted to the tide and are stable.

8.5.2 Surface erosion.

Surface erosion is relatively minor in most areas due to the binding of the surface by vegetation. However, the turbid currents which can cross a saltmarsh surface during inundation can exploit desiccated features. Desiccation can form polygonal mudcracks and often mudflakes where the silty layers dry out and are easier to remove. Drainage water entering tidal pills may reach velocities which can cause scour and erosion in these features.

8.5.3 Mudflat Erosion.

Mudflat erodability is reduced by biotic stabilisation of the surface. Narbett (1992) found that the mudflats adjacent to Northwick Warth were eroding at a minor rate, although they can be plainly seen to be accreting in some areas adjacent to clifflines where there are either considerable amount of debris strewn against the cliff upon which the mud is draped, or where marsh grasses have colonised the mudflats.

8.6 Saltmarsh Morphology and Tidal Influences.

The shape of saltmarshes in the Severn Estuary fall within a continuous series bounded by two end member geometries which are termed a 'dynamic marsh' and an 'accreting marsh' for the purpose of this study.

8.6.1 Accreting Marshes.

Accreting marshes are so described as they are actively accreting without any signs of major erosional processes. These marshes have a characteristic shape with little or no neap tide cliffline. The marshes rise up smoothly as a wide levee from the mudflats at their toes, with the cessation of vegetation being the only significant difference between the two, sometimes marked by a very small cliff. Buried clifflines are almost non-apparent in these saltmarshes, are non-erosional and vegetated. Drainage of the flood waters on these marshes is by a series of narrow rills at the drainage apron which are aligned at right angles with the shoreline and deepen and open towards the coast. The rills have been described by Allen (1987) as being eroded ridges and furrows formed by the action of waves and coarse debris cutting into the drainage channels from the marsh levee. When observing the marsh drain it is clear that substantial velocities can be generated in these rills and the dominant erosion may be related to this flow rather than wave action.

8.6.2 Dynamic Marshes.

It is tempting to describe the dynamic marshes as erosive as they are bounded by a steep erosional cliffline, however, there may still be net accretion on the saltmarsh surfaces. These marshes show the classic stepped morphology described earlier, with internal clifflines which may be erosional if the tide reaches a suitable height on the marsh, produces sufficient velocities and are not well colonised by vegetation. Drainage from these marshes tends to be via tidal pills which may form near linear features such as those seen on accreting marshes, or be long meandering channels, especially in wider floodplains. The gradient of the individual surfaces in a dynamic marsh generally tend to be less than those on accreting marshes and can actually slope away from the wet margin of the saltmarsh. This grading away from the Estuary margin may be due to the formation of recent levees or eroding back though the bank of an older levee.

8.6.3 Saltmarsh Geometries in the Lower Severn Estuary.

The location of twelve saltmarsh localities around the Estuary are indicated on Figure 8.3 and the profiles of the saltmarshes on Figure 8.4. The former figure illustrates the dominant tidal flows which occur on the flood and ebb. These currents are responsible for the location of the soft sediment clifflines. The saltmarsh profiles form a continuous sequence between the end member saltmarsh types and are describe in terms of their position in the Estuary. These areas can be described in terms of the dominant erosional tides which are occurring (Table 8.4).

Area	Erosional processes
South of Sudbrook	Very minor flood erosion
North of Sudbrook	Considerable erosion from flood tide
South of Severn Beach	Very minor ebb & flood erosion
North of Severn Beach	Considerable erosion from ebb tide
North of Aust	Considerable erosion from flood tide

Table 8.4 Areas of tidal erosion of saltmarshes

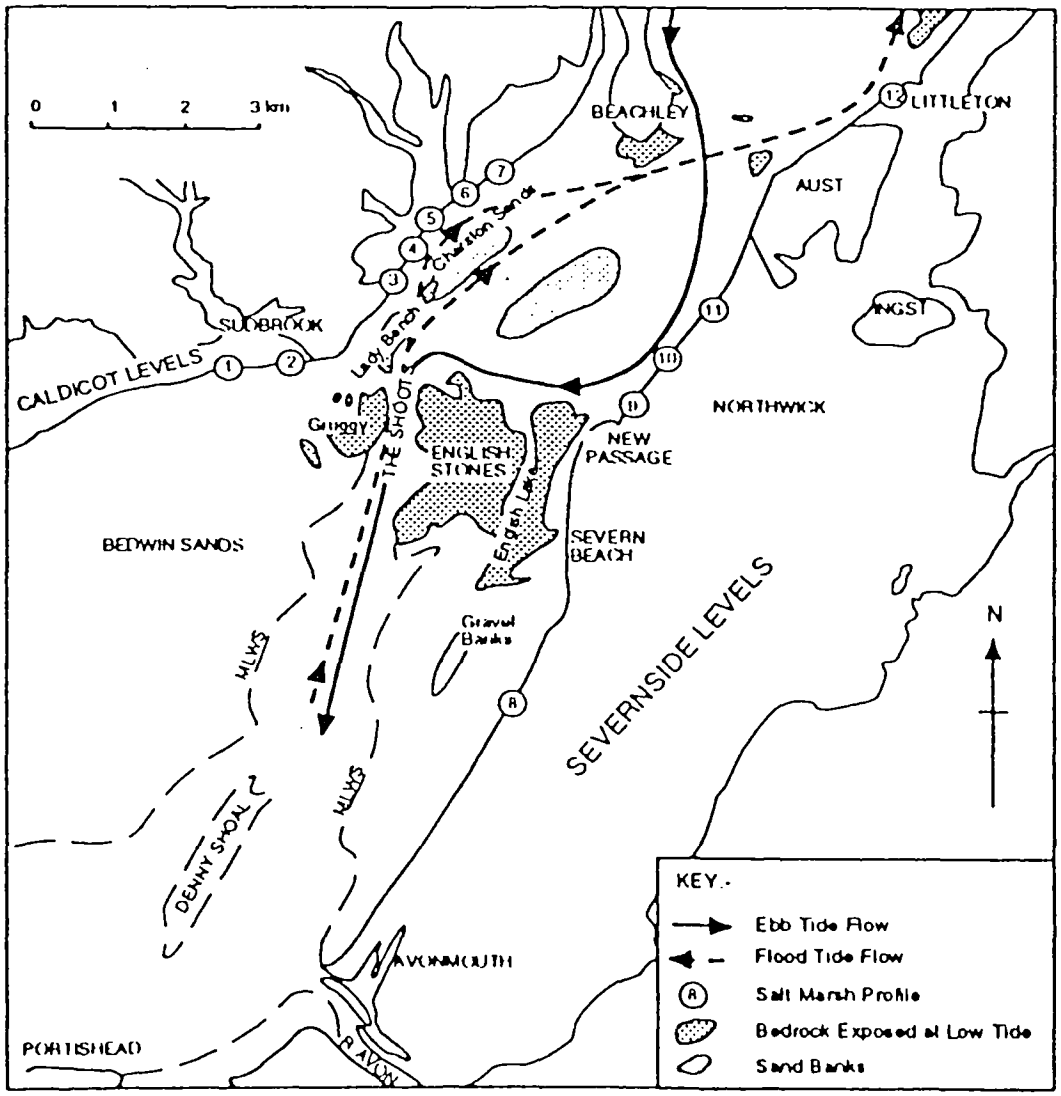

Fig 8.3 Location of saltmarsh profiles and dominant currents.

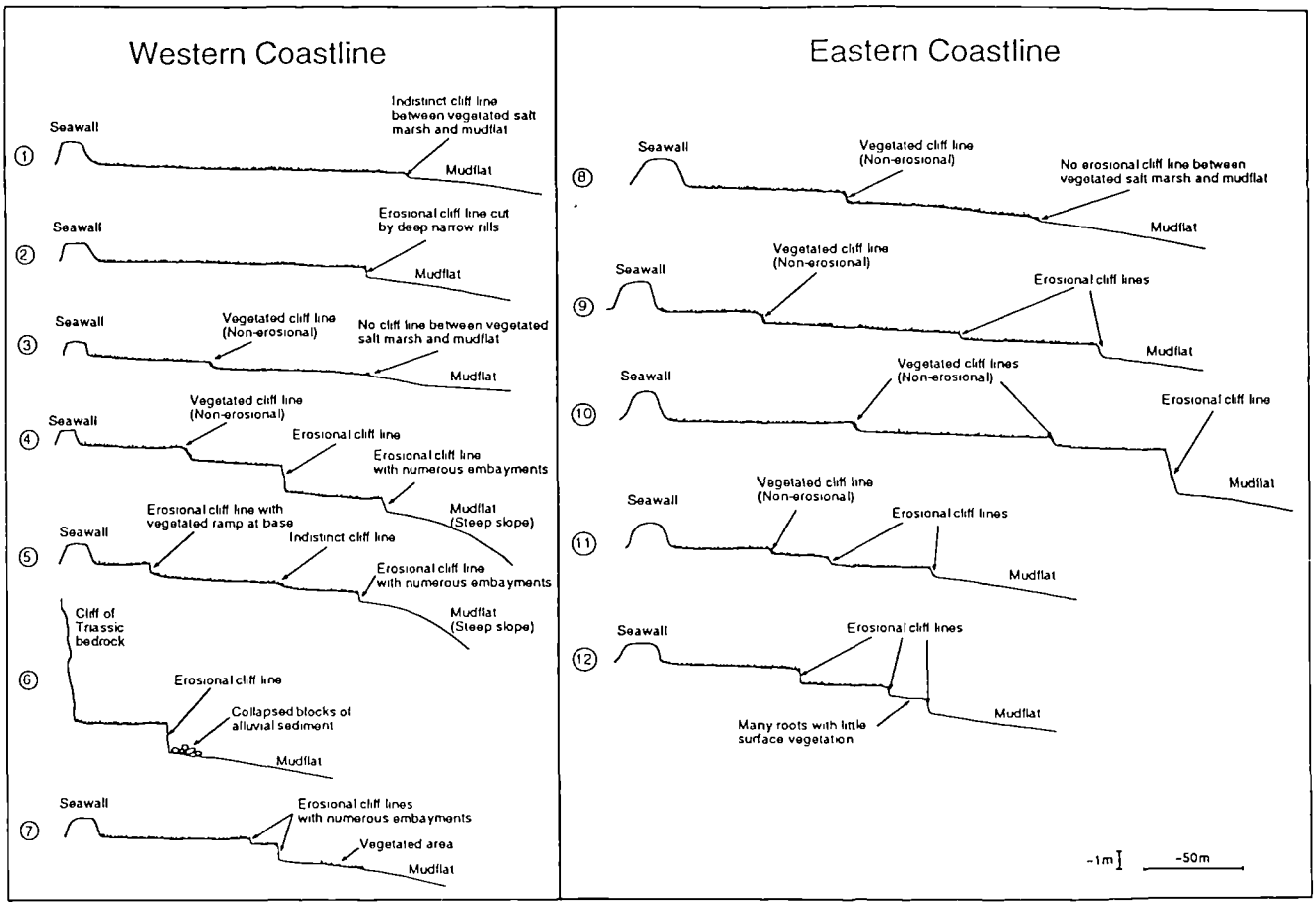

Fig 8.4 Saltmarsh profiles.

- South of Sudbrook.

The unstepped ("accreting") saltmarsh illustrated in profile 1 is in an area where the coast is protected by the recent deposits of the Bedwin Sands and the Black Bedwins. Here the wide expanse of the Bedwin Sands and their elevation close to high water spring means that current and wave attack is minimal (Hawkins, Narbett and Taylor, 1994). Profile 2 is on the same part of the coast but nearer to the headland at Sudbrook. This profile shows a small erosional cliffline cut by deep narrow rills. The rills have some shelly debris within them which appear to have been transported and deposited within the relative shelter of them. However, shelly lenses within the profile cut by the rills, appear to show past colonisation in low energy conditions. This marsh is affected slightly by the currents of the late flood tide which is partly diverted around the Gruggy, explaining the small erosional cliff line.

- North of Sudbrook.

Profile 3 shows no significant erosional features other than a vegetated, presently non-erosional cliffline about 0.3m high, which shows many embayments within the marsh. The marsh grades towards the mudflat with no distinct cliff line. The profile appears to be protected from the flood tide by Lady Bench. Profile 4 is immediately north of the line of the Shoots/Black Rock channel where the tide is restricted between the rocky outcrops of the English Stones and the Gruggy. The flood waters pass up through the Shoots, skirt Lady Bench, before being diverted either side of the Charston Sands onto the coast. This profile shows three distinct cliffs which seawards measure 0.5, 1.2 and 0.6m. The upper cliff is generally vegetated but is starting to show signs of erosion, while the lower cliffs are eroding at present. Profile 5 shows an indistinct middle cliff and the upper and lower cliffs which are actively eroding. There has been erosion of the seawall between profiles 4 and 5 where there is less protection from the saltmarsh. Profile 6, north of St Pierre Pill is in an area where the coast has retreated to within 50m of the outcropping Triassic bedrock and has a single, 1.5m high erosive cliff. There have been emergency remedial works to protect the seawall and the alluvial cliff line through the emplacement of large stone boulders in front of them to prevent erosion. However, it seems that close to this profile there is still some major erosion which

may threaten the railway line present behind the seawall. Profile 7 shows two closely separated clifflines. The coastal cliff appears to have retreated almost to the buried one. However, the large coastal cliff measured to be 0.9m high diminishes northwards as the flood tide diverts round the Beachley Peninsula and so there are slower and more oblique currents running along the coast causing less erosion. Erosional effects have abated to an extent that the mudflats have been partially colonised by vegetation and appear to be building up.

- South of Severn Beach.

The east coast of the Severn south of Severn Beach has been modified by developments on the Severnside Levels, however, profile 9 illustrates that the marsh is essentially accreting. There is a sign of an older cliffline although this is now heavily vegetated.

- North of Severn Beach.

Profiles 9 to 11 in this area show three clifflines at different distances from the tidal embankment. Profile 10 shows a coastal cliff over 2m in height above the mudflats. Studies have indicated that the marshes in this area are accreting rapidly although erosional effects are obvious too.

- North of Aust.

Profile 12 again shows three erosional cliff lines. The lower surface here is effectively unvegetated in winter although there is evidence of spartina roots and stems. This marsh highlights the sensitivity of the coastal environment to small climatic changes, as in summer when energy conditions are slightly less the marsh is colonised by spartina.

8.6.4 Model of Accretion at Northwick Warth.

The depositional history of Northwick Warth over the last two millennia has been proposed in a model by Narbett (1992) and is summarised and modified as follows:

- Prior to the mediaeval reclamation of the area just south of Aust a wide expanse of alluvial lowland was open to tidal inundation. The saltmarsh near to the Estuary margin was probably creek-like with numerous channels flanked by elevated areas of vegetation.
- Much of the alluvial plain was reclaimed in mediaeval times, leaving a narrow strip of marshland which has continued to accrete. Land behind the seawall will have remained essentially unaltered since its reclamation.
- Accretion of 0.75m of sediment has since occurred outside the seawall, initially at a fast rate, partially because of the restricted area, but then slowing as the marsh approached a mature equilibrium height in the tidal frame. Allen (1987) labelled this terrace, now the high marsh, the Rumney Formation.
- The face of the Rumney marsh underwent erosion at its boundary with the mudflats, forming a steep cliff, likely to be to a similar height as today's cliffline. This cliff was subsequently buried to leave a small remnant scar. The new vegetated saltmarsh level (intermediate marsh) was labelled the Awre Formation by Allen & Rae (1987). The new marsh level protected the cliffline behind where erosional processes waned.
- The intermediate marsh appears to have grown at a much faster rate than the Rumney Surface as it started low down in the tidal frame, undergoing juvenile growth in excess of the prevailing trends in sea level. Narbett (1992) identified that much of its formation was after the Industrial Revolution, based on heavy metal concentrations. Higher organic contents suggest that the marsh was well vegetated from its inception. This is not to say that the early buried deposits of the Rumney Formation did not grow at the same rapid rate as the Awre Formation.
- The face of the intermediate marsh was also eroded as another vegetated marsh grew in front. This marsh surface is called the Northwick Surface by Allen and is nominally dated by him as beginning to accrete toward the start of the century, although it may be as late as 1950. This marsh has similarly undergone erosion forming the present day cliff at the Estuary margin.
- There is an erosional scour at the foot of the cliff bounding the mudflats, which abuts a narrow zone of poorly vegetated mudflat which appears to be accreting, partially through the reworking of fallen blocks from the saltmarsh.

It can be seen in the south of Northwick Warth that the buried cliffline between the upper and intermediate marshes is still undergoing considerable erosion, while elsewhere it is colonised by patchy vegetation and less or non-erosive. This is because the Northwick (lower marsh) surface is lower in the south of the warth. Aerial photographs indicate that this area in the south was a small embayment in 1952 just before the onset of accretion of the Northwick Surface. The surface here therefore has had less time to grow and hence is lower. It appears that the embayment was due to current influence, because the shapes of the two buried cliffs are both are embayed, it is only the most recent deposition which is not embayed. Therefore if any residual trends in the currents still occur, raised velocities may reduce the rate of accretion at this point, possibly explaining the lower level of the Northwick Surface here. The highest cliff on Northwick Warth is in the centre of the exposure and is over 2m high (see profile 10 in Figure 8.4) which is clearly eroding at the greatest rate (400mm/year) along this coast due to the diversion of the ebb tide by the rock promontory at Beachley.

8.6.5 Origin of Cliffs.

The cliffs which can be seen in the modern day environment are clearly being eroded by the predominant tidal currents. South of the study area illustrated in Figure 8.3 on the west banks of the Estuary the main flood tide is bifurcated by the sand bands of the Middle Grounds. A significant portion of the tide passes northwards toward the mouth of the River Usk and the adjacent mudflats through the channel of the Newport Deep. It is this current, which has caused significant erosion of the sediments (up to 5m) that is causing the exposure of the submerged forest and peats near the level of Ordnance Datum. Within the study area north of Sudbrook, the flood tide is diverted by the rock outcrops and shoals of the Gruggy, Lady Bench and Charston Sands to the west and the English Stones to the east concentrating the flow through the Shoots. Current velocities within the Shoots can reach 6 to 8 knots at low water and even though velocities are significantly less against the coastline further north, the flood is clearly eroding the coast back towards the seawall when the dominant current hits the coast at an incident angle. The flood tide is deflected further north by the Beachley Peninsula towards the coast north of Aust on the east side of the Estuary to cause more flood dominated

cliff erosion. A well formed tidal cliff is also developed on the east banks of the Estuary between Severn Beach and Aust. Here the cliffs have been formed by the erosional effects of the Ebb flow which is diverted to the south-east by the Beachley Peninsula onto the coast.

The existing cliffs are concluded to be forming when there is a significant current striking the coast at an incident angle. Non-erosional coasts are either protected or the current is running in a more parallel manner to the coast and causing less erosion. The buried cliffs are in similar positions to the present day ones, so it is concluded that in general the tidal effects causing the present day erosion were similar in the past when the older cliffs formed. Naturally any of the clifflines could have eroded backwards to destroy the previous ones, hence not all of Allen's geomorphic surfaces are present on the dynamic marshes. The heights of the cliffs would have been defined by the potency of the erosional forces primarily, but would have also depended on the height of the old marshes and the position to which the erosion had backed into the pre-existing levee.

The accreting, non erosional mudflats are marked by a distinctly different morphology to the stepped dynamic marshes and show little or no sign of clifflines. The presence of buried clifflines within these marshes cannot be discounted, with later sediments lain on top to disguise the old features, possibly forming a ramp. However, it is as likely that the marshes have also been influenced by a similar tidal regime as today and do not show large erosional features. Therefore it is proposed that these marshes do not have the same internal features as the dynamic marshes and represent a layer cake type build up both in height and towards the wet margin. This cannot be backed up with field evidence at present.

The cliffs on the saltmarshes must vary with small changes in the tidal regime, such as diversions of the current through sandbank movements which would move the main position of erosion. The erosion of these features is important from an engineering point of view as they highlight the temporary nature of the coast and the vulnerability of the sea defences where a coastline may be retreating. The cliffs may also separate off-lapping strata which may differentially settle over the juncture of two units either side of a buried cliff. The cliff line itself can also be considered a geotechnical weakness in the subsurface. In places these cliffs may be very difficult to detect, especially in the accreting marshes, where if present they are no longer visible. It is also noted that the position of the present day buried cliffs on the

dynamic marshes may not represent the position of the two underlying formations as they may have eroded back some distance after the protective lower surface had accreted.

There is a problem in assessing why the stepped morphologies of the saltmarshes have formed, as it appears that there has been a cyclic series of erosion and accretion. Certainly the fact that there are often two buried cliff lines and an actively eroding cliff in widespread areas of the system suggests that the overriding control on sedimentation and erosion is a major estuary-wide effect. Apparently this could only be achieved through a change in the hydrodynamics of the Estuary or the climate. Hydrodynamic effects would be the wax and waning of the strength of the erosive current, possibly through small oscillations in the range of the tides. Climatic effects would control river inflow, although this is very unlikely to affect the downstream areas according to the model studies. The colonisation of vegetation in response to the climate is a more realistic factor, where the organics could bind the surface together to resist erosion. However, it is proposed that the process of erosion and accretion is a simultaneous effect under the same conditions with time. As a dynamic saltmarsh is eroding along the wet margin the mudflat in front is accreting to a small amount. Under the right conditions, for instance the colonisation of a pervasive marsh grass, accretion takes hold, building up rapidly in front of the present cliff line. As the mudflat builds up to form a juvenile saltmarsh, it protects the marsh behind, although some erosion, which dies down with time, of the now being buried cliffline occurs. The new juvenile marsh forms a cliff when it has reached a height and gradient that can no longer smoothly pass the currents over it and starts to erode. The cyclicity is simply explained by the height of the accreting strata at the wet margin, which once it has reached a critical height begins to erode and the process restarts. It is possible that the erosion processes could be triggered by a single wave event.

8.7 Coastal Vulnerability.

8.7.1 Introduction.

Coastal wetlands will be among the most severely affected ecosystems if sea levels were to rise. A marsh may maintain its aerial extent or even expand with rising sea level if

sedimentation can match the apparent rise. Extreme tides have already been discussed in this thesis. However, it is noted that the occurrence of present day extreme events will become much more frequent given an increase in sea levels. Coastal engineers in the Netherlands have concluded that at present a 4m surge has a return period of 250 years, however, if sea level was to rise by 1m then the return for this event would be about 1 in 50 years. Dykes in the Netherlands are designed to the 1 in 10000 years event in the centre of the country where failure of these defences would be a complete disaster. Were sea levels to rise by 1m, the return on the 1/10000 event would be close to 1 in 250 years (Goemans, 1986). Erosion of coastlines would be expected to increase with the increased volumes of water and velocities generated. Morphology changes can be assessed by the Bruun Rule (Bruun, 1983) which predicts that exposed coastal profiles erode to provide new sediment on the channel floor, so that the channel capacity remains the same throughout the sea level rise, i.e. the bed level rises at about the same amount as the sea level rise, whilst the channel banks retreat landward. This effect will be serious in the middle Severn Estuary where the channel is nearly against the seawalls and has little distance to retreat. As has been mentioned previously it is believed that the Middle and Upper Estuary are not stable at present and a trying to erode laterally to match the tidal conditions. This erosion may explain why some of Allen's lithostratigraphic units are not present upstream as they have been completely removed or were unable to form. Increased sea levels would increase the extent of saline intrusion threatening urban water supplies. Areas close to the prevailing sea level or water table may find a salinsation of the groundwater, especially in drainage ditches, which could threaten the present day ecosystem.

8.7.2 Assessment of Coastal Vulnerability.

A coastal vulnerability index can be calculated from Table 8.5 (Based on Gornitz, 1991) to compare the risk classes of various parts of the Estuary. The assessment is made based upon the following factors.

- Relief: Higher areas are less inclined to flood, even on extreme tides and are therefore at less risk. Although it is noted that erosion at the foot of the cliffs may destabilise the structure. The hazard index therefore decreases from levels close to the tidal frame.
- Rock type: The hazard index for the rock type is assessed on the strength and erodability allowing for discontinuities, etc.
- Landforms: The index for landforms depends upon the estimated erodibility of the various morphologies.
- Sea level change: The hazard associated with sea level change is assessed upon the change in tidal velocities and quantity of flow which can be expected from present with a prevailing sea level trend. Obviously this also affects the vulnerability of the coastline to inundation.
- Shoreline movement reflects the whether the coast is eroding or not. As there are not sufficient long term observations for this assessment, the presence of an alluvial cliff is seen to signify a high risk.
- Tidal range: This reflects the energy conditions of the Estuary, thus the erosional power and sediment transportability of the tides.

			Rank		
	Very Low	Low	Moderate	High	Very High
Variable	1	2	3	4	5
Relief (mAOD)	> 20	10 to 20	5 to 10	0 to 5	< 0
Rock / Sediment	Sandstone	Volcanic	Most rocks	Coarse superficial	Fine superficial
Morphology	Rock Cliff	Medium cliff & embayments	Low cliffs, glacial & protected saltmarshes	Beaches (pebble) & unprotected saltmarshes	Beaches (sand) & mudflats
Sea level Change (mm/yr)	< -1 (land rising)	-1 to 1	1 to 2 (normal eustatic)	2 to 4 (land sinking)	> 4
Shoreline movement (m/yr)	> 2	0 to 2	0 (stable)	-2 to 0	< -2 (erosive)
Tidal range (m)	< 1 (microtidal)	1 - 2	2 - 4 (mesotidal)	4 - 6	> 6 (macrotidal)

Table 8.5 Assessment of coastal vulnerability.

The coastal vulnerability index used for this work is calculated using Equation 8.3.

$$CVI = \{ (\frac{1}{6} (a_1 \times a_2 \times a_3 \times a_4 \times a_5 \times a_6) \}^{0.5} \qquad (8.3)$$

Where a_i = rank of each of the variables.

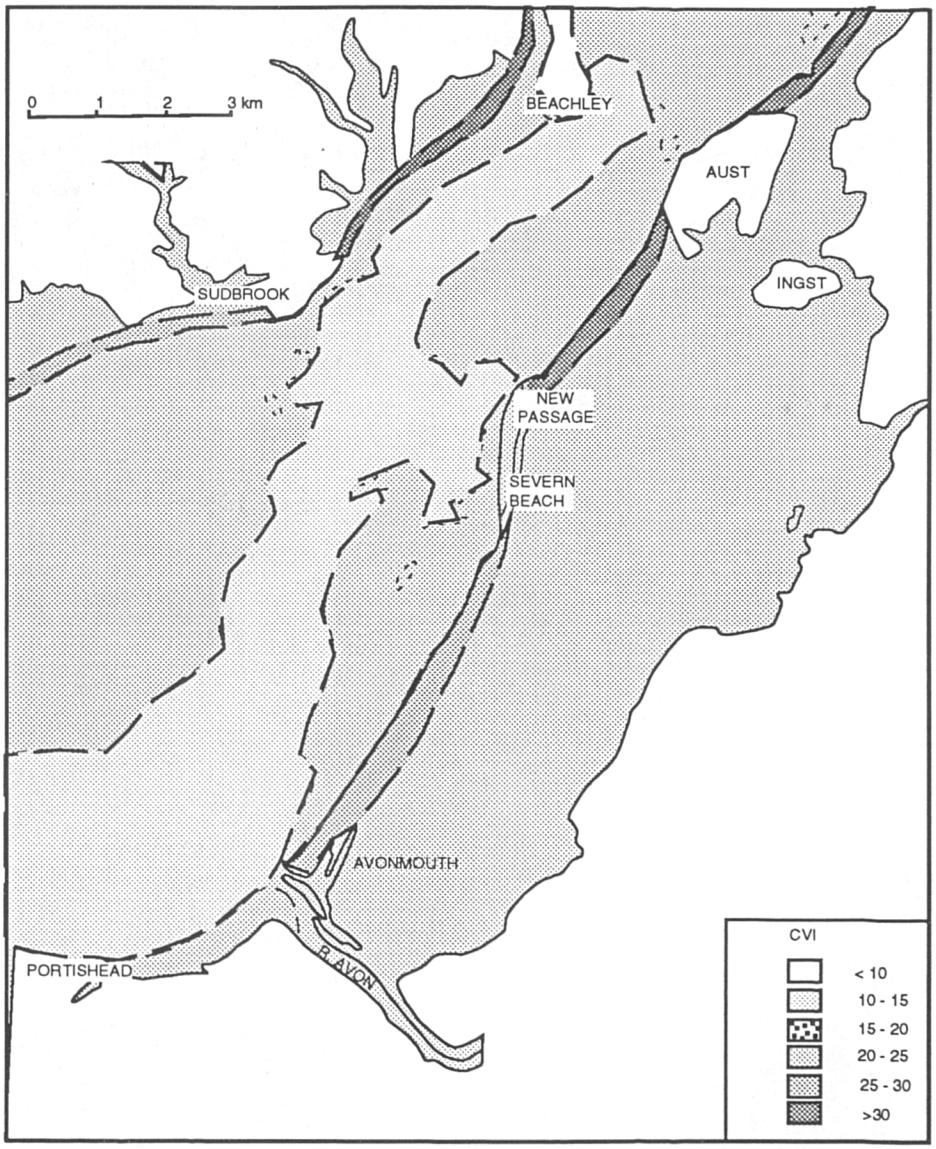

Fig 8.5 Coastal Vulnerability map, Lower Estuary.

A coastal vulnerability map for the Lower Estuary has been compiled as Figure 8.2. This figure is, however, a simplified map, but illustrates that the index can be used, and refined to provide comparative maps of the Severn. The index system can be adapted to

include wind effects, value of property, etc., and be incorporated onto a GIS data system. Coastlines with a vulnerability index in excess of 30 are deemed to be in need of review, vulnerability indexes greater than 20 are likely to be affected noticeably by medium to long term sea level change. Even with a quantifiable system of analysis of coastal vulnerability it is unlikely that the system could replace human judgement and the consideration of individual areas of specific areas of greater interest or importance.

8.8 Seawall Vulnerability.

The vulnerability of seawalls can be classified in a similar manner to the coastal vulnerability index. A seawall classification scheme proposed for this study is illustrated in Table 8.6.

Rank	1	2	3	4
Seawall height /waves	<100 years tide	<100 years tide +0.5m	<100 years tide +1.0m	>100 years + 1.0m
Extent of protective saltmarsh	<10m	10 - 50m	50 - 100m	>100m
Construction of seawall	grassed	grass + rock	rock wrap	Rock/concrete + reinforced earthworks
Erosion	seawall eroding	erosive cliff in front of bank	small cliffs on saltmarsh	None appreciable

Table 8.6 Assessment of seawall vulnerability index.

Seawall vulnerabilities have been calculated using Equation 8.4.

$$SVI = \{ \frac{1}{4} (a_1 \times a_2 \times a_3 \times a_4) \}^{0.5} \qquad (8.4)$$

Where SVI = Seawall Vulnerability index a_1 = weighting of variable

It is suggested that the seawall vulnerability index is categorised as follows;

$SVI \leq 2$	seawall extremely vulnerable
$2 < SVI \leq 4$	seawall vulnerable
$4 < SVI \leq 6$	seawall slightly vulnerable
$SVI > 6$	seawall OK.

Seawall vulnerabilities are shown in Table 8.7, which has accounted for seawall improvements in the 1990's since the HRS survey. The figures quoted are the average of three observations along the channel reach. If figures are quoted in brackets, it indicates that there are areas of poor seawall condition, with an SVI of that value.

The tables show that the seawalls are generally all right in the Lower Estuary especially on the east side where strategic developments are protected. The quality of the seawalls decreases upstream in the semi-rural areas of the Middle Estuary, often with vulnerability indexes lower than 4 close to residential areas.

SECTION	UPSTREAM DISTANCE (m)	LEFT BANK HEIGHT (HRS) (m)	RIGHT BANK HEIGHT (HRS) (m)	WEST BANK SVI	EAST BANK SVI
AVONMOUTH	0	9.3	9.3	6	6
SHOOTS	4588	9.32	9.3	6	6
SUDBROOK	6963	10.15	9	6 (2)	4
NORTHWICK	8963	8.63	9	6 (2)	5
AUSTWARTH	10538	8.63	9	5	6
BEACHLEY	11913	8.63	9	6	6
LITTLETON	13463	8.74	9	6	6
INWARD ROCK	16726	8.67	9	5	5
NARLWOOD	18813	8.78	9	5	6
WHITE HOUSE	21088	9.89	9.3	3	6 (4)
LYDNEY	23563	9.46	8.99	5	4
BERKELEY	25900	9.86	9.08	5	6
FAIRTIDE ROCKS	27550	10.45	10	7	7
SHARPNESS	29313	10.45	10	7	6
WELLHOUSE ROCK	30313	10	10	6	6
PURTON	30809	10	10	6	7
GATCOMBE	31833	10.3	10	6	5
SLIMBRIDGE	35291	10.3	9.86	7	5
FRAMPTON	37509	10.4	9.78	3	3
FRETHERN	38913	10.6	9.53	4	4
NORTHINGTON	40745	10.09	9.51	4	4
BOXGROVE	41812	10.21	9.56	4	4
BULLOPILL	42889	10.4	10	5	4
NEWNHAM	43882	10.4	10	6	4
HAWKING PILL	44843	10.4	10	5	4
ARLINGHAM WARTH	45855	10.4	10	4	3
PIMLICO SANDS	46995	10.4	10	5	3

SECTION	UPSTREAM DISTANCE (m)	LEFT BANK HEIGHT (HRS) (m)	RIGHT BANK HEIGHT (HRS) (m)	WEST BANK SVI	EAST BANK SVI
ARLINGHAM	47945	10.4	9.89	3	3
LOWER DUMBALL	49133	10.4	9.71	4	4
PRIDING	50031	9.61	9.8	4	3
FRAMILODE	50944	9.73	9.73	3	3
UPPER DUMBAL	51968	9.86	9.86	3	3
NEW INN (EPNEY)	53035	9.97	9.97	3	3
LONGNEY	53758	10.18	10.18	4	4
BOLLOPOOL	54920	10.27	9.91	6	5
CONSTANCE FARM	55892	10	10	4	4
HILL FARM	57022	10.06	10.2	3	3
THE FLAT	58120	10.1	10.2	3	3
DENNY HILL	59239	9.96	10.35	5	5
WEST MINSTERWORTH	60242	10.13	10.09	5	5
MIDDLE MINSTERWORTH	61319	10.04	10.09	5	5
EAST MINSTERWORTH	62407	10.14	10.08	4	4
WINDMILL HILL	63326	10.16	9.78	4	5
ELMORE	64361	9.31	9.7	2	4
CORNHAM	65501	9.22	9.66	2	3
UPPER REA	66504	9.07	9.92	2	3
MINSTERWORTH HAM	67560	9.8	9.77	2	2
MOOR FARM	68674	10.2	9.95	4	3
SUD MEADOW	69693	10.2	10.1	3	3

Table 8.7 Seawall vulnerabilities.

Seawall vulnerabilities are calculated using the present figures of the 100 years return wave. However, as new figures encompassing secular changes in sea level, believed to be a rise of at least 4mm/year, the walls should be reviewed as it is likely that the 100 years return event is likely to be a larger tide than the figures quoted in this thesis. Vulnerability analysis of the coastline and seawalls are simply a yardstick to assess the relevant stability of one part to another, there are no quantitative figures suggested for what may be unstable and what isn't, although a guidance for the seawalls has been proposed.

The assessment of seawall vulnerabilities has indicated that with the exception of a few small areas, the Lower Estuary is just suitable under todays conditions. Seawalls further up the Estuary are all in need of improvements or review. It is recommended that any such review is not undertaken to solely consider today's conditions but potential future conditions and the management of risk. For instance the modelling has shown that allowing innundation of some

areas of land may mitigate flooding problems elsewhere in the Severn. New seawalls might be better employed away from the present positions allowing occasional floods to help the overall wetlands management. Similarly it appears that the banks on the outside of the bends in respect to the flood tide are the most vulnerable as they may face 'super-high' levels caused by momentum effects of the incoming tide in the Middle Estuary particularly. These should be higher, stronger and closer to the channel than on the opposing side, unless the opposite side is particularly vulnerable to overtopping during river flood.

8.9 Conclusion.

The morphology, sedimentological and erosional processes on saltmarshes have been described in this chapter. It is hope that the chapter has conveyed some of the complexities of saltmarsh growth and the relationship to changes in relative sea level rise which could not be addresses in the earlier chapters. In particular the sensitivity of the saltmarshes to erosional forces and how the vulnerability of the coastline can be assessed.

Plate 2 Alluvial cliffline at Northwick Wharth.

Plate 3 Water stored on marsh levee after surge tide, 27 February 1990, Middle Estuary.

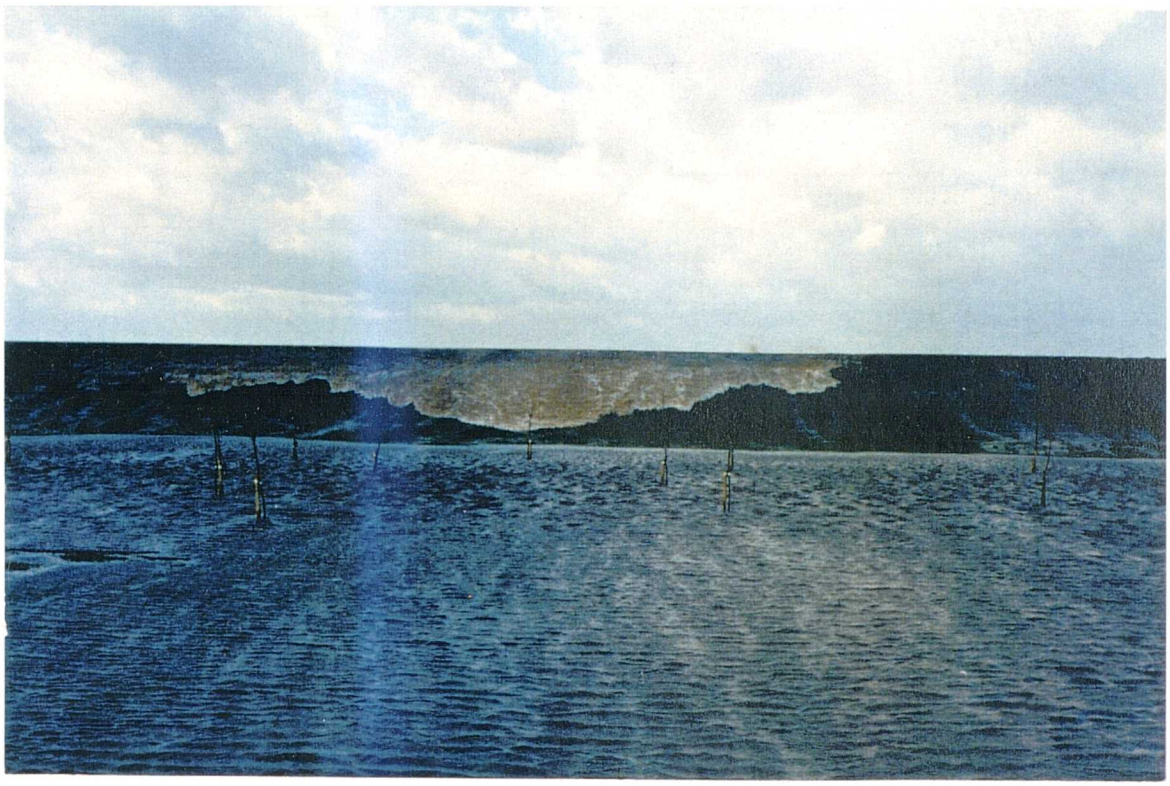

Plate 4 Wave break over seawall at Severn Beach.

Plate 5 Breach of Seawall at Northwick, February 27 1990.

CHAPTER 9

SUMMARY, CONCLUSIONS AND RECOMMENDATIONS

9.1 Introduction

The research in this thesis can be divided into a number of phases describing the course of the study and the conclusions made. The phases are described in the following sections and are summarised below:

- Phase 1; Flandrian sea level curves and the development of the Severn Estuary.
- Phase 2; Development and verification of a computer model of the Severn Estuary.
- Phase 3; Modelling results and applications in the Severn Estuary.
- Phase 4; Review of saltmarshes and recent sea level changes in the Severn Estuary.

9.2 Phase 1; Flandrian sea Level Curves and the Development of the Severn Estuary.

The present day morphology of the Severn Estuary has been moulded during the ice advances and retreats of the Pleistocene. The Flandrian Transgression which began in earnest some 10000 years before the present day is responsible for the inundation and infilling of most of today's Estuary. Overwhelming evidence seems to confirm the sea level curves of Jelgersma (1969), Hawkins (1971), Shennan (1983) and others, that the sea has risen in the form of a relatively smooth curve. The transgression began at a fast rate of sea level change, in the order of 15mm/year initially before slowing about 6000 years ago, to a rate of less than 2mm/yr about 2000 years ago. The widespread distribution of a peat, approximately at Ordnance Datum seems to mark the separation of the fast rate of sea level change and the appreciably slower rate thereafter. This period effectively separates two contrasting styles of sedimentation. An early period of coarser grained sandy material is only really evident in the Lower Estuary as the transgression had not necessarily reached the Upper Estuary by this time.

During this period the Estuary would have seen little or no erosion taking place with sediments being lain at a fast rate from a seawards source. The deposition of finer sediments after 6000 BP is estuary-wide, although coarser sedimentation has occurred upstream near Gloucester due to the interaction of riverine and estuarine waters. The period of slower sea level rise led to opportunities for peat bands and even forests to form, which subsequently were buried by younger alluvium. These organic bands are now exposed in some localities, especially the Caldicot Levels, in the soft sediment cliffs bounding the Estuary, highlighting the erosion of what must be considered recent sediments. While there is no conclusive geological or geotechnical evidence to support oscillatory sea level curves proposed by some workers, the author suggests the widespread 'Ordnance Datum Peat' may represent a sea level stand, where the rate of rise temporarily decreased, stopped or even reversed.

The thickness of sediment which may be expected in localities along the Estuary can be assessed by comparing the buried valley and a suitable sea level curve to produce a simple model of estuarine development. Such a comparison using Hawkins' (1971) sea level curve showed that estuarine sedimentation would have begun at Avonmouth in about 7000 BP, depositing a basal layer of sandy material of about 7m thickness, upon which a similar thickness of clayey strata would have been deposited. Further upstream, approximately at Littleton, the transgression would not have been truly represented until some 2000 years later, with nearly no early sand sedimentation, except for the former buried deeper water channels. Sedimentation further upstream is complicated by the influence of the Severn River and the apparent upstream thickening of sediments during the late stage infilling of the valley due to river interaction (Hawkins and Taylor, 1991).

The relatively recent stratigraphy of the Estuary has been constructed by Allen (1988, 1991) based on human events and a generalised morphological model of the recent sediments. He has derived rates of sea level change between Roman, Mediaeval, the Industrial Revolution and present day times which have implied an increase in the rate of sea level rise over these periods. It is noted that a significant rate of rise is proposed for times since the Industrial Revolution. This may be attributed to the warming of the atmosphere by man's activities. The increase in the rate of rise before this period is likely to be due to the

constriction of the Estuary by reclamations and through method errors in the analysis of later sediments (Narbett, 1992).

Modern research on the 'Greenhouse Effect' and recent sea level changes does confirm that the global mean sea level is rising. However, models of the effect of global warming are only just becoming plausible machines. A recent (1995) meeting of the Intergovernmental Panel on Climate Change has agreed that a global temperature rise of between 0.6 °C and 0.9 °C has occurred within this Century. Predicted global sea level changes vary from a rate of less than 1mm/year to in excess of 9mm/year. A best estimate of eustatic sea level change of 4.1mm/year has been suggested by both Clayton (1990) and Warrick and Oerlemans (1990). The Severn Estuary is subsiding due to post glacial land movements which will exacerbate the rate of sea level change, confirming the NRA guidance rate of 5mm/year as the best rate as to assess future sea levels. Such a rate would raise the level of the mean high water spring tide some 175mm in the Bristol Channel and 240mm at Avonmouth by the year 2030AD. A worst case prediction of a high spring tide of 9.0mAOD at Sharpness by the year 2100 would mean a rise in excess of 1.5m from the present would be observed at this port.

The heights of tides in the Severn which have been predicted by the early stages of this research were found to be of such concern with a view to tidal defence that it was decided that a more penetrative analysis of them should be carried out using a computer simulation of the Estuary.

9.3 Phase 2; Development and verification of a computer model of the Severn Estuary.

The research for the development of the computer model was initiated by an exhaustive literature search of sources as the field was entirely alien to this author. The solution has been divided into two discrete chapters on the fluid flow theory and mathematical solution methods although the two are inextricably linked in the model derivation process. It is often the case that work on such models are biased toward one of these disciplines and cannot be followed through fully from the conception to completion of the model. There are many stages in the development of the model based upon the availability of data, model requirements and

computing facilities. The starting block of the model derived and all other similar models are the De St Venant assumptions of unsteady flow. Although he derived his own equations of flow in a form different to those developed for this work, the two sets of equations are fundamentally the same, with additional calculations added in this work where required to account for effects not considered initially by De St Venant.

The process of deriving the best model for the requirements of the work was self deciding to some extent given the following thought process. It was easy to decided upon a one dimensional model of the system as there was no justified need for a more complex simulation, especially as the flow in the Severn can be observed to be very unpredictable in two and three dimensions. Computing facilities are available in the University to run a multidimensional model, but not in the Geology Department. Having decided upon the one dimensional model, the mathematical method of solution had to be decided and applied to the derived equations of flow. The finite difference and finite element methods of solution were the most applicable methods of solving the flow equations. The finite different methods were selected becuase of their simplicity and suitability to develop into a program. Having chosen to use the finite difference method it was necessary to use a solution system which could not only be applied to the mathematical equations, but also to the data which was to be input. Early in the work channel cross sections of some parts of the Severn Estuary were obtained through the NRA. These sections were unevenly spaced and meant that over one half of the available finite different schemes could not be used as they required regular spacing for their rigid computational grid. An explicit difference scheme could not be used either as they require simultaneous data during the simulation runs which could not be obtained for the problems to be addressed. The Preissman implicit four point scheme was thus chosen as the applicable method. This method of solution is quite popular and it was clear early in the research that it was going to be a viable tool for solution. However, an understanding of the model capabilities and limitations could not be made without a consideration of alternative methods.

After deciding upon the mathematical solution method the equations of flow have to be finalised to include all the extra functions it is estimated might affect the results of the simulation and give the best representation of physical reality in the modelling. The additions to the simplest set of De St Venant equations included non-uniform velocity distributions in the

channel, compound conveyance calculations, calculation of flow over weirs, over seawalls and a branched network of channels. All these additional routines diverge away from the original assumptions and are in some cases discontinuous functions. The apparent violation of the De St Venant assumptions adds further approximation errors to the modelled results which can only be justified by an increase in accuracy of the solution from the additional routines. The testing process of the model revealed that only the branch, weir and seawall calculations were justified in their inclusion into the model and the other routines were dismissed.

Once the equations of flow were finalised they required translating into a finite difference scheme through the process of discretisation, where continuous (differential) functions can be represented by finite mathematical operations. At this point all models will tend to diverge in nature to each other as the process has many different, albeit subtle, versions of discretisation. These solutions can then be tested for their theoretical accuracy and stability. At this stage the Preissman scheme is implicitly stable in all forms although functional instabilities may be encountered during the modelling process when abnormal flow conditions are met. The accuracy of the system has been proved to be of a first order for the final set up of the model.

The next stage of model development was the translation of the numerical solution to a computer program. As the complexity of the model and the demand on the operating systems of the department's computer hardware was unknown at the outset of modelling, the program was written in FORTRAN as this programming language could be easily transferred to a more powerful machine if required. The program in its final form takes about seven minutes to run a simulation on a SUN workstation. The debugging of the program was undertaken on model runs on a simple set of trapezoidal channel sections which found after initial programming errors were corrected that the model ran satisfactorily. At this point all computer code and workings out were checked from the beginning to ensure that no errors had been propagated through careless writing or programming.

The verification of the model was undertaken on the full model with channel cross sections derived from the data donated by the NRA, which was a survey of the channel cross sections by the Hydraulics Research Station in 1975 and from Admiralty Charts of soundings of the floor of the Severn Estuary. Seawall levels were available from a 1990 HRS publication

but were reanalysed from an aerial survey of the Estuary and from field levelling, as were incomplete HRS channel surveys. The quality of the HRS surveys were also examined by levelling in the flood plain and were found to be reliable. Verification of the model undertook a study of the effects of all the variables on the output results to find the sensitivity of the model to different computational conditions. This stage is the most difficult to convey to someone who is alien to the workings of the model as it involved a vast number of calculations with a variety of co-dependant variables. It was at this point that it was found that compound channel calculations and non-linear velocity distributions could be removed from the calculations as they had no discernible effect on the model results. It was found that the model was very sensitive to the selected friction values in the Lower Estuary, which if too small would cause the model to propagate fatal instabilities.

Once the program was working reliably it was verified and 'tuned' so that it could represent a broad number of hydrological scenarios, by comparing the output results to known tidal events in the Severn. It was found that the model could closely simulate a variety of tides from a neap to extreme surge and flood tides. Low water levels were sometimes misrepresented because of changes to the channel beds. It was also found that the height of the modelled seawalls was a major control on the height of the high water calculated on extreme events and the data provided by the NRA was not sufficient for some of the modelling requirements. Field levelled data and archive searches corrected the problem. Finally it was also found that the friction values used for simulation needed to be lower than expected in the Middle Estuary compared to an earlier analysis of the channel cross sections (see Appendices 3 and 5). This aspect of modelling was also reflected in previous studies by the HRS and Binnie and Partners, although it is noted that the model used for this work was closer to what were believed to be the ideal friction values than the other studies. After the model was verified and accepted as giving good representable results of the known tidal events, it was used to analyse tidal occurrences in the third stage of research.

9.4 Phase 3; Modelling results and applications in the Severn Estuary.

The model was applied to spring and neap tides as predicted by the Admiralty Tide Tables and showed very close agreement with the published figures. Modelling has shown that the Lower Estuary is ebb dominated with maximum flow rates of over 100000 m^3/s at Avonmouth on a spring tide (range 12.3m) and just under half of this (46000 m^3/s) on a neap tide (range 6.5m). Average velocities reach up to 2.7 m/s at Aust on the ebb flow which is directed towards the eroding saltmarshes at Northwick Warth. Modelling also shows the water brought in on the spring tide has not fully discharged downstream of Misterworth before the onset of the next high water. The modelling shows very clearly how the tide is distorted as it penetrates the Estuary and how the high water elevation increases upstream for as far as the tide reaches. Although the quantity of flow reduces rapidly upstream, being around half the figure at Aust than at Avonmouth on all tides, the maximum velocities in the system are generated between Beachley (Aust) and Sharpness as the Estuary narrows and has the greatest tidal ranges. The model also predicts that the Estuary is flood dominant in parts of the Middle Estuary around Newnham and Epney on a spring or higher tide. This is an important consideration in assessing the stability of the banks of the Estuary at this position as the flood current is deflected from the main axis which has formed through ebb and river flow and holds the opposite bend to the flood dominated sides.

Analysis of the tidal surge on February 26th 1990 confirmed the reliability of the model in that the modelled times and heights of the tide closely match the observed occurrences. This tide flooded considerable areas of the Severn Estuary which could be seen in aerial photographs lent by the NRA. The program identified the positions where the seawalls were breached almost perfectly. Flow velocities on the 1990 surge were predicted to reach nearly 3m/s at Sharpness on both the ebb and flood flow, while velocities at the shallow sections near Newnham in the Middle Estuary neared 4m/s on the flood.

Using a simple calculation of the seaward boundary conditions it is predicted that the mean high water spring tide at Avonmouth will reach 6.9m by 2030AD and would be up to 7.3mAOD by the end of the next century based upon the plausible estimates of sea level rise. A worse case prediction of a sea level rise at Avonmouth of 1.4m by 2030AD has been

proposed using the work of Clayton (1990) and his predictions of global sea level rise including influences due to the 'greenhouse effect'. Such a spring tide was modelled to flood the existing tidal defences in the Middle and Upper Estuary. It is proposed from the modelling studies of these tides that the Middle Estuary would erode considerably with the additional amount of flood flow which would enter on the tide and the higher velocities generated. However, because of the simplified seaward boundary conditions derived, the values of future tides predicted in this thesis should not be considered definitive. To be totally reliable a much more extensive simulation encorporating modelling of the Bristol Channel and coastal shelf seas is required.

Historic tidal levels have been developed using estimates by Allen (1991) of relative sea level rise although it is believed that his more recent estimates are subject to considerable error. It is predicted that the spring tidal curve at Avonmouth would have reduced in range with the high water level being 1.29m lower than the present in AD 150. In order to model these historic tides in the Severn it was necessary to construct the channel cross sections which existed at the time, using much of Allen's archaeological research augmented by levelling surveys and archive searches. It was found that the model predicted that although the high spring water at Avonmouth would have been 1.29m less than at present, the spring level would have been up to 1.45m lower than present in other parts of the Estuary. An even greater discrepancy was encountered when the spring tide was modelled for the period about 1250AD when high water would have stood a predicted 0.85m lower at Avonmouth but 1.25cm lower than at present at Minsterworth, 61km upstream of Avonmouth. It was modelled that the mean spring tide limit was about 65 - 70km upstream of Avonmouth (just below the branch of the Severn into the East and West Channels) until 1250 AD.

If the high spring tide is considered to be a good datum by which to directly compare the rate of accretion on a tidal marsh, the model predicts that no appreciable accretion would be recorded in the period 150 to 1250 AD more than 55km upstream as tidal effects were minor and that the maximum rate of accretion would be found at about 30km upstream of Avonmouth. The rate of accretion if measured between 1250 and 1845 AD would be greatest 60km upstream of Avonmouth as the Estuary transgressed into this area and it became more frequently tidal. Rates of rise would be expected to be 1.5 times greater at this point than

elsewhere in the Estuary, but still less than 1.5mm/year. The period from 1845 to 1945 also suggests that the increase in tidal heights is greatest in the Upper Severn Estuary at the model boundaries, 70 to 75 km upstream of Avonmouth. The rate of change of sea level rise from 1945 to the present appears to be amplified from 4mm/year at Avonmouth to over twice the amount upstream. These estimates of rise have already been discussed as being potential over estimates and it is likely that measurements of sea level rise would not reveal these figures on the mature saltmarshes. The modelling does illustrate how care must be taken when selecting positions to measure accretion, or substantial errors in the sea level change can be created by taking measurements on younger marshes at different places along the channel.

The model studies also indicate that the Middle and Upper Estuary marshes bounding the channel have grown to a higher position in the tidal frame. This is because they are generally older marshes which have been eroded into by the transgressing estuary. Younger marshes such as those seen at Northwick have not had chance to form upstream because of the velocities generated in the channel against the narrow alluvial plain in front of the older high marshes.

An assessment of the seawalls in the Estuary has indicated that many are below required design levels in the current tidal regime of the Severn. However, it is accepted that flooding of the mainly rural land to the south of Gloucester does alleviate potential problems in the city. It was found that for the Estuary to be entirely contained on the present (NRA) design level of the 100 years tide, with 0.5m being allowed for wave effects, all the seawalls over 50km upstream of Avonmouth, i.e. from Epney, would require raising by up to 2m. The highest recorded tide in the Severn occurred on January 30th 1607. This tide with a maximum height of 9.2mAOD at Avonmouth would flood over a third of the present tidal defences of the Severn if it were to happen again.

It was found that removal of the existing seawalls close to Arlingham on the first great bend in the Estuary could reduce flooding both up and downstream of the area. A large scale operation resetting the seawalls closer to the town and lowering ground levels to 5mAOD from the present height of between 7 and 8mAOD would cause reductions of between 25 and 50 cm on the highest astronomical tide in nearly 50km of the Estuary. However, the long term effects on the sedimentary environment of the Estuary cannot be assessed.

It is concluded that the present defences of the Severn are barely adequate at present, even without considering the possibility of additional rises due to global warming. It is necessary to review the potential problems of inundation from a view of either protecting all or most of the Levels through a substantial programme of seawall improvements or from a view of risk management where it may be necessary to abandon some of the reclaimed saltmarshes to alleviate problems elsewhere. Constant review of the sea levels is required in light of the research into sea level change. It is accepted that a rise in the order of 4 to 5 mm/year relative mean sea level is applicable at present to the Severn. However, predictions of up to twice this value have been made (Clayton, 1990).

9.5 Phase 4; Review of saltmarshes and sea level changes in the Severn Estuary.

The final stage of this work has brought together the detail of the saltmarshes especially in the Lower Estuary. Saltmarsh morphology has been described in terms of lithostratigraphic units described by Allen (1985). This description applies to a number of marshes within the Estuary which from an overlapping staircase sequence of surfaces lowering to the wet margin of the Severn. It has been shown in this study that this type of behaviour only occurs when a flood or ebb current strikes the coast at an incident angle. The diversion of the ebb and flood flows causes erosion of clifflines on opposing sides of the Estuary but on the opposite stages of the tide. It can be seen in sheltered areas that there is no stepped form to the saltmarshes but a gentle levee rising from the mudflat. There is no physical evidence that Allen's units exist on these marshes buried beneath the currently vegetated surface. The surface of these marshes appears in places to be the extension of the mudflats and may only be distinguished from them by the appearance of vegetation.

The growth of the saltmarshes has been described from which is can be seen than the newer marsh terraces close to the main channel have yet to reach maturity and are accreting at a rate greater than the relative sea level rise. However, as these accrete they are still being eroded at their toes. It is suggested that the stepped marshes do not reflect fluctuations in the tidal or climatic regime, but an interaction of the currents with the building up mudflats in front

of the saltmarshes. As the mudflats mature they can be considered saltmarshes upon colonisation be vegetation. Still uneroded they reach a critical height at which point toe erosion begins, whilst the marsh, although retreating builds up on its top surface.

This research has provided an indication of the coastal vulnerability of the Lower Severn Estuary and a ranking system to derive the values. Although only a qualitative system and in need of further research, it clearly defines the areas of coast most likely to be eroded or inundated. A higher resolution study of the Severn using this system or a modification of it could provide very detailed information about areas of the Severn which are considered vulnerable to any change in the tidal regime. The research has also categorised the tidal defences of the Severn in comparison to their likely performance against the 100 years wave. Many areas of sea defences can be considered extremely vulnerable or vulnerable to inundation or erosion.

9.6 Recommendations.

The most important requirement for further work in terms of this PhD is to derive more reliable seaward boundary conditions for tides for which there are no real time data, such as future spring tides based upon estimates of sea level change. Such boundary conditions can only be derived though modelling of the Bristol Channel, or even further seawards, so that the effects of tidal resonance in the Severn can be truely represented and the output results be considered reliable.

The computer model has been written in a form which is not user friendly. The program could be written in a form where it can be applied to a broad range of situations. Reprogramming should encompass the following items;

- User friendly environment so that the program can be run by inexperienced users.
- Restructuring of program to include more variable systems, including floodplain flow.
- Addition of relatively simple routines to account for aspects of flow, such as through bridges, not included in this study.

- Simple bulk sediment transport and salinity balance routines could be easily incorporated into the program but may require larger machine.
- Simulation of tidal heights, velocities and pressure effects on structures, especially seawalls.
- Simulation of effects of proposed Severn Barrage could be applied easily.

The research into the Severn Estuary has revealed that the seawalls and coastline are vulnerable to the effects of erosion and inundation. It is predicted that both these elements will get worse with time. As the Severn is very complicated and variable in nature, it is recommended that the following research could be undertaken to assess the vulnerability of the Severn.

- Review of coastal and seawall vulnerability methods with other studies to produce a rational system of index classification.
- Fine resolution survey of the Estuary flood plains to consider detailed coastal and seawall vulnerability index distribution.
- Implementation of survey onto Geographical Information System (GIS)
- Review of seawall heights and assessment of their suitability in light of vulnerability surveys.
- Review of seawall heights in light of potential sea level rises.
- Recommend action if required.

Research into the development and changes in the saltmarshes and alluvial plains need to be a continuous and well recorded process in order that any valuable long term assumptions can be made. This should include studies of type locations at half yearly intervals at least with good pictorial records of the changes occurring. As sea level rise remains a contentious issue and is not fully believed by many people it is necessary to identify as early as possible any consequences there might be so that adequate long term planning can be made for wetland management. Specific scientific research on the saltmarshes could include the following.

- Detailed monitoring of inundation times and velocities on saltmarsh surfaces.
- Detailed monitoring of sediment deposition on the saltmarshes, including the rate and type of sediment deposition and variations in the suspended sediment concentrations of flood waters.
- Changes to the sedimentary or erosional regimes through man made influences or natural transgression of the Severn.
- Identification of depth and shape of buried clifflines and their spatial relationship with visible cliffline scars.
- Much clearer comprehension of 'accreting' saltmarsh behaviour and underlying strata, especially the identification of buried cliffs if present.
- The influence of vegetation on the sedimentary processes and erosion resistance of saltmarshes.

The geotechnical properties of soft clays are being researched by many workers, not least by SERC funded research on the soft clay test bed site at Bothkennar in Scotland. There are still many aspects of geotechnical engineering which can be researched in this field. During this research a number of geotechnical studies were consulted which identified some interesting points which may be pursued including the following.

- Loss on ignition analysis of organic content.
- The use of the moisture condition value (MCV) on determining soft clay suitability for tidal embankments.
- The formation of the desiccated alluvial crust and methods of permanently increasing its thickness.
- Strengthening soft clays through lime stabilisation or vibro methods.
- The effects of groundwater changes with sea level.

REFERENCES

Abbott, M. B. (1966). *An Introduction to the Method of Characteristics*, Thames and Hudson, London and America, Elsevier, New York

Abbott, M. B. (1975a). Method of Characteristics, Chapter 3 of *Unsteady Flow in Open Channels*, Water Resources Publications, Fort Collins, Colorado.

Abbott, M. B. (1975b). Weak solutions of the Equations of Open Channel Flow, Chapter 7 of *Unsteady Flow in Open Channels*, Water Resources Publication, Fort Collins, Colorado.

Abbott, M. B. (1977). Commercial and scientific aspects of mathematical modelling, *Int. Conf. on Appl. Num. Modelling*, University of Southampton, England, July.

Abbott, M. B. (1979). *Computational Hydraulics; Elements of the Theory of Free Surface Flows*, Pitman Publishing Limited, London.

Abbott, M. B. and Cunge, J. A. (1975). Two dimensional modelling of tidal deltas and estuaries, Chapter 18 of *Unsteady Flow in Open Channels*, Water Resources Publications, Fort Collins, Colorado.

Abbott, M. B. and lonescu, F. (1967). On the numerical computation of nearly-horizontal flows, *J. Hyd. Res.*, 5, No.2, pp. 97-117.

Abbott, M. B., Marshall, G. and Ohno, T. (1969). On Weak Solutions of the Equations of Linearly Horizontal Flow, *Report Series 3, International Institute for Hydraulic and Environmental Engineering*, Delft.

Abbott, M. B. and Rodenhuis, G. S. (1972). A numerical simulation of the undular hydraulic jump, *J. Hyd Res.*, 10, No. 10, pp. 239-257.

Abbott, M. B, Rodenhuis, G. S. and Verwey, A. (1973), Sytem II-Siva, a design system for rivers and estuaries. pp207-214 in IAHR/AIRH Int.Symp.on river mechanics.

Abbott, M. B and Verwey, A. (1970), Four point method of characteristics, *JHD, PASCE,96*, pp 2549-2564.

Abramov, A. A. (1961). On the translation of boundary conditions for systems of linear ordinary differential equations (a variant of the sweep method), *URSS Comput. Math. and Math. Phys.*, No. I (in Russian).

Abramov, A. A. and Andrieyev, V. B. (1963). Application of the double-sweep method, *J. Applied Math. and Math. Phys.*, 3, No. 2 (in Russian).

Agassiz, L. (1840). *Etudes sur les glacies Neuchatel.* 346pp.

Agassiz, L. (1847). *Systeme glacaire au recheches sur les glaciers ptl.* Nouvel etudes et experiences sur les glaciers actuels. V1. 598pp.

Airy, G.B. (1842). *Tides Waves.*

Allen, J.R.L., (1985). Intertidal drainage and mas movement processes in the Severn Estuary; rills and creeks. *J.geol.soc.Lond.*, 142, 849-861.

Allen, J.R.L., (1987a). Late Flandrian shoreline oscillation in the Severn Estuary; the Rumney Formation at its typesite (Cardiff area). *Phil.Trans.R.Soc.Lond.* B315, 157-174.

Allen, J.R.L., (1987b). reworking of muddy intertidal sediments in the Severn Estuary, Southwestern U.K. - a preliminary study. *Sedimentary Geology,* 50, 1-23.

Allen, J.R.L., (1987c). Towards a quantitative chemostratigraphic model for sediments of late Flandrian age in the Severn Estuary, U.K., *Sedimentary Geology*, 53, 73-100.

Allen, J.R.L., (1988). Modern period muddy sediments in the Severn Estuary (southwestern U.K.); a pollutant based model for dating and correlation. *Sedimentary geology,* 58, 1-21.

Allen, J.R.L., (1989). Evolution of salt marsh cliffs in muddy and sandy systems; a qualitative comparison of Bristish west coast estuaries. *Earth surface Processes and Landforms*, 14, 85-92.

Allen, J.R.L., (1990a). The Severn Estuary in southwest Britain; its retreat under marine transgression and fine sediment regime. *Sedimentary Geology,* 66, 13-28.

Allen, J.R.L., (1990b). Constraints on the measurement of sea-level movements from saltmarsh accretion rates. *J.Geol.Soc.Lond.*, 147, 5-7.

Allen, J.R.L., (1990c). Saltmarsh growth and stratification; a numerical model with special reference to the Severn Estuary, southwestern Britain. *Marine Geology*, 95, 77-96.

Allen, J.R.L., (1991). Saltmarsh accretion and sea level movement in the inner Severn Estuary, southwest Britain; the archaeological and historical contribution. *J.Geol.Soc*, 148, 485-494.

Allen, J.R.L., (1992a). Fine sediment and its sources, Severn Estuary and inner Bristol Channel, southwest Britain. *Sedimentary Geology*, 75, 57-66.

Allen, J.R.L., (1922b). Tidally influence marshes in the Severn Estuary, southwest Britain. In Allen, J.R.L. & Pye, K. (Eds.) *Saltmarshes (Morphodynamics, Conservation and Engineering Significance)*, Cambridge University Press.

Allen, J.R.L. & Rae, J.E., (1986). Time sequence of metal pollution, Severn Estuary, southwestern U.K., *Marine Pollution Bulletin*, 17, 427-431.

Allen, J.R.L. & Rae, J.E., (1987). Late Flandrian shoreline oscillations in the Severn Estuary; A geomorphological and stratigraphical reconnaisance. *Phil.Trans.R.Soc.*, B315, 185-230

Allen, J.R.L. & Rae, J.E., (1988). Vertical saltmarsh accretion since the Roman Period in the Severn Estuary, southwest Britain, *Marine Geology,* 83, 225-235.

Amein, M. M. and Fang, C. S. (1970). Implicit flood routing in natural channels, *JHYD PASCE 96*, No.HY12, December.

Amein, M. M. and Chu Hsiao-Ling (1975), Implicit numerical modelling of unsteady flows, *PASCE, JHD.* 101, pp717-732.

Andrews, J.T., Gilbertson, D.D. & Hawkins, A.B. (1984). The PLeistocene succession of the Severn Estuary: A Revised model based upon amino acid racemization studies. *Jour.Geol.Soc.*, 141, pp967-974.

ApSimon, A. M. and Donovan, D. T. (1956) Marine Pleistocene Deposits in the Vale of Gordano, Somerset. *Proc U.B.S.S,* Vol., No.3, pp130-136.

ApSimon, A. M., Donovan, D. T. and Taylor, H. (1961). The Stratigraphy and Archaeology of the Late glacial and Post glacial Deposits on Brean Down, Somerset. *Proc U.B.S.S.* Vol.9, No.2, pp67-136.

ASCE (1963). Report of the American society of Civil Engineers, Task force on friction factors in open channels. *PASCE, JHD*, v89, No. HY2, pp97-143.

ASCE (1975). *Sedimentation Engineering, Manual and Reports on Engineering Practice*, No. 54.

Aubrey, D.G. and Spear, P.E. (1985). A study of non-linear tidal propagation in shallow water inlet and estuary systems, Pt 1 and Pt 2. In *Est.Coast.Shelk.Sci,* 21.

Balloffet, A., Cole, E. and Balloffet, A. F. (1974). Dam collapse wave in a river, *JHYD*, ASCE, 100, No. HY5.

Bazin, H., 1862, Experiences sur les ondes et la propagation des remous [Experiments with waves and the propagation of negative waves]: *Acad. Sci. [Paris] Comptes rendu*, v. 55, p. 353-357, [1862], and v. 57, p. 302-312, [1863].

Bazin, H., 1865, Recherches experimentales sur la propagation des ondes [Experimental research on wave propagation]: *Acad. Sci. [Paris] Mem..*, v. 19, p. 495-644. Also, Dunod, Paris, 1865, in second part of hydraulic researches of Darcy and Bazin.

Bender, M.L., Fairbanks, R.G., Taylor, F.W., Matthews, R.K., Goddard, J.G., and Broeker, W.S. (1979). Uranium series dating of Pleistocene reef tracts of Barbados, West Indies. *Geol.Soc.Am.Bull.*, 90, pp 577-594.

Bender, M.L., Taylor, F.W. and Matthews, R.K. (1973). Helium-uranium dating of corals from the middle Pleistocene Barbados reef tracts. *Quat.Res.*, 3, pp 142-146.

Benet, F. and Cunge, J. (1971). Analyse d'experiences sur les ondulations secondaires dues aux intumescences dans les canaux trapezoidaux, *J. Hyd.Res.*, 9, No. 1, pp. 11-13.

Binnie & Partners. (1980). One dimensional model studies of the Severn Estuary. *Severn Tidal Power. Report No. 54.*

Binnie & Partners. (1981).Land drainage and sea defence. *Severn Tidal Power. Report No. 84.*

Boussinesq, Joseph. (1871). Theorie de l'intumescence liquide appelee onde solitaire ou de translation, se propagent dans un canal rectangularaire [Theory of the liquid intumescence, called a solitary wave or wave of translation, propagated in a channel of rectangular cross section]: *Acad. Sci. [Paris] Compies rendus*, v. 72, p 755-759.

Boussinesq, Joseph. (1872). Theories des ondes et des remous qui se propagent le long d'un canal rectangulaire horizontal, en communiquant au liquide continu dans ce canal des vitesses sensiblement parallesles de la surface au fond [The theory of waves and backwaters which propagate along a rectangular horizontal canal, subject to continuous flow and having velocities in the canal that are approximately parallel to the bottom]: *Jour. Math. Pures et Appl. de M. Liouville [France],* s.2, v. 17, p. 55-108; additions, v. 18, 1873, p. 47-52.

Boussinesq, Joseph. (1873). Theorie des ondes liquides periodiques [Theory of liquid periodic waves]: *Acad. Sci. [Paris]* Memories presentes par divers savants, v. 20, p. 509-615.

Boussinesq, Joseph. (1877). Additions et eclaircissements au memoire intitule: Essai sur la theorie des eaux courantes [Additions and clarifications for the memoir with the title: Treatise on the theory of flowing water]: *Acad. Sci. [Paris] Mem.*, v. 24, s. 2, p. 51-58.

Boussinesq, Joseph. (1877). Essai sur la theorie des eaux courantes {Treatise on the theory of flowing water]: *Acad. Sci. [Paris] Mem.*, v. 23, p. 261-529.

Boris, J. P. and Book, D. L. (1973). Flux-corrected transport. I. SHASTA, a fluid transport algorithm that works, *J. Comput. Phys.*, 11, pp. 38-69.

Bouvard, M., Chollet, J-P. and Cunge, J. A. (1977). Progress recents et difficulte'sde simulation mathematique de rivieres alluvionnaires, *17th Congress of the IAHR*, Baden-Baden.

Bowen, D.Q. (1977). In 'The Quaternary history of the Irish Sea'. Ed. Kidson and Tooley, pp223-256. Steel House Press, Liverpool.

Bowen, D.Q. (1978). *Quaternary Geology.* Pergammon Press.

Brately, P., Fox, B.L. and Shrage, L.E., (1983), *A Guide to Simulation*, New York, Springer Verlag, 585pp.

Brebion, S., Lebrun, B., Chevereau, G. and Preissmann, A. (1971). Modeles mathematiques de la pollution, *IRCHA*, Centre de Recherche, 91 Vert-le-Petit, France, November.

Broecker, W.S., and Thurber, D.L. 1965: Uranium series dating of corals from Bahaman and Florida Key limestones. *Science* 149, pp.58-60.

Broecker, W.S, Thurber, D.L., Goddard, J., Ku, T.L., Matthews, R.K., and Mesolella, K.J. (1968). Milankovitch hypothesis supported by precise dating of coral reefs and deep sea sediments. *Science*, 159, pp.297-300.

Bruun, P., (1983). Review of conditions for the uses of the Bruun rule of erosion, *Coastal Engineering*, 7, 77-89.

Cameron, I.B. & Stephenson, D. (1985) The Midland Valley of Scotland. *BGS, HMSO*, London.

Cameron W.M. & Pritchard D.W. (1963) *Estuaries in the Sea.* Vol.2. J.Wiley. New York. pp 306-324.

Catt, J.A. (1977). Loes and Coversands. (In British Quaternary Studies, ed Shotton, F.W.) pp221-230.

Cavanna, J.m. and Swain, P.J. (1977) Wave overtopping of sheltered coastline. DEpt Civ.Eng., University of Bristol.

Chang, H. H. and Hill, J. C. (1977). Minimum stream power for rivers and deltas, *JHYD*, ASCE, 103, No. HY12, December.

Chappell, J. (1974). Geology of coral terraces, Huon Peninsula, New Guinea: A study of Quaternary techtonic movements and sea-level changes. *Geol.Soc.Am.Bull.*, 85, pp 553-570.

Chappell, J. (1983). A revised sea-level record for the last 300000 years from Papua New Guinea. *Search*, 14, pp 99-101.

Chappell, J., and Veeh, H.H. (1978): Late Quaternary tectonic movements and sea-level changes at Timor and Atauro Island. *Geol. Soc. Am. Bull.* 89, pp. 356-68.

Chen, Y. H. (1973). *Mathematical modelling of water and sediment routing in natural channels*, Ph. D. Thesis, Colorado State University, Fort Collins.

Chen, Y. H. and Simons, D. B. (1975). Mathematical modelling of alluvial channels, *ASCE Symposium on Modelling Techniques 'Modelling 75'*, Vol. I, San Francisco, Sept. 3-5.

Chevereau, G. and Gsu~hier, M. (1976). Use of mathermatical models as anapproach to flow control problems, *Proceedings of the Int. Symp. on Unsteady Flow in Open Channels*, BHRA Fluid Engineering, Newcastle-upon-Tyne.

Chevereau, G., Holly, F. and Preissmann, A. (1978). Can detailed hydraulic modelling be worthwhile when hydrologic data is incomplete? *Int. Conf. on Urban Storm Drainage*, University of Southampton, April.

Chollet, J. P. and Cunge, J. A.- (1979). New interpretation of some head loss-flow velocity relationships for deformable beds, *submitted to J. Hyd. Ret.*, 17,No. 1, pp. 1-13.

Chollet, J. P. and Cunge, J. A. (1980). Head loss-flow velocity relationtionships for deformable movable beds, *Appl. Math. Modelling*.

Chow, V. T. (1959). *Open Channel Hydraulics*, McGraw-Hill, New York

Churchill, D.M. (1965). The displacement of depositis fromed at sea level 6,500 years ago in southern Britain. *Quaternaria*, VII, pp239-249.

Clark, R.H. (1966). The sea-bed off southeast Devon. *Unpub. PhD thesis, University of Bristol.*

Clayton, K. M. (1990). Sea-Level rise and coastal defences in the UK. *Quarterly Journal of Engineering Geology*, 23, 283-287.

Clifton, R.J. & Hamilton, E. (1979) Lead-210 chronology in relation to levels of elements in dated sediment core profiles. *Est.Coast.Mar.Sci.*, Vol.8, 259-269.

Colbourne, G.J., Gilbertson, D.D. & Hawkins, A.B. (1974) Temporary drift exposures in the Failand Ridge. *Proc.Bris.Nat.Soc.*, 33, pp91-97.

Colin, E. and Pochat, R. (1976) One dimension open channel flow (dissipative operator), *Proceedings Int. Symp. Unsteady Flow in Open Channels.* BHRA Fluid Engineering, Newcastle-Upon-Tyne.

Collins, M.B. (1983) Supply, ditribution and transport of suspended sediment in a macrotidal environment; Bristol Channel, U.K., *Est.Coast.Mar.Sci*, 8, 259-269.

Collins, M.B. (1987). Sediment transport in the Bristol Channel; a review. *Proc.Geol.Assoc.*, 98, 435-474.

Coope, G.R. (1975). Climatic fluctuations in NW Europe since the last interglacial, indicated by fossil assembleges of Coeloptera in ice Ages ancient and modern. *Geol.Jour.Spec.Iss.6.*, Liverpool.

Coope, G.R. (1977). Quaternary Coleoptera as aids in the interpretation of environmental history. In *British Quaternary Studies: Recent Advances*. Ed. Shotton, F.W., pp 55-68.

Cooper, L.H.N. (1948). A submerged ancient cliff near Plymouth. *Nature*, London, 161, pp 280.

Corps of Engineers (1976). HEC-2 Water Surface Profiles, Users Manual with Supplement, Hydrologic Engineering Center, Corps of Engineers, U.S. Army, Davis, California, November.

Courant, R., Friedrichs, K. O. and Lewy, H. (1928). On the partial difference equations of mathematical physics. *Math. Ann.*, 100, p. 32 (in German). -

Courant, R. and Hilbert, D. (1953). *Methods of Mathematical Physics,* Vol. 1, Interscience Publishers, New York.

Crickmore, M.J. (1982). Data collection - tides, tidal currents, suspended sediment. In I.C.E. *Severn Barrage*, Thomas Telford, London.

Cronin, T.M., Szabo, B.J., Ager, T.A., Hazel, J.E. and Owens, J.P. (1981): Quaternary climates and sea levels in the US Atlantic Coastal Plain. *Science*. 211, pp. 233-40.

Cunge J. A. (1966). Etude d'un schema de differences finies applique a l'intergration numerique d'un certain type d'equation hyperbolique ecoulement. Unpublished PhD thesis, University of Grenoble.

Cunge J. A. (1975a). Applied mathematical modelling of open channel flow, Chapter 10 of *Unsteady Flow in Open Channels*, Water Resources Publications, Fort Collins, Colorado.

Cunge, J. A. (1975b). Two-dimensional modelling of flood plains, Chapter 17 of *Unsteady Flow in Open Channels*, Water Resources Publications, Fort Collins, Colorado.

Cunge, J. A. and Perdreau, N. (1973). Mobile Bed Fluvial Mathematical Models, *La Houille Blanche*, no. 7.

Cunge, J. A., Holly, F.A. & Verwey, A. (1980). *Practical Aspects of Computational River Hydraulics*. (Monographs and surveys in water resources engineering: vol 3). Pitman Publishing Limited, London.

Cunge, J. A. and Simons, D. B. (1975). Mathematical model of unsteady flow in movable bed rivers with alluvial channel resistance, *proceedings of the XVIth Congress*, IAHR, Sao Paulo.

Cunge, J. A. and Wegner, M. (1964). Integration numerique des equations d'ecoulement de Barre de St. Venant par un schema irnplicite de differences finies. Application au cas d'une galerie tantot eh charge tantot a surface libre, *La Houille Blanche*, No. 1, p. 33-39.

Davies, C.M. (1980) Evidence for the formation and age of a commercial sand deposit in the Bristol Channel. *Est.Coast.Mar.Sci.*, 11, 83-99.

Davies, J. A. and Fry, T. R. (1929) Notes on the Gravel Terraces of the Bristol Avon. *Proc. U.B.S.S.*, Vol. 74, 106-111.

Davies, K.H. (1983): Amino acid analysis of Pleistoncene marine molluscs from the Gower Peninsula. *Nature*. 302, pp.137-9.

De Saint-Venant, B. (1870) Demonstration elementaire de la formule de propagation d'une onde ou d'une intumescence dans un canal prismatique; et remarques sur les propagations du son et de la lumiere, sur les ressauts, aussi que sur la distinction des rivieres et des torrents [Elementary demonstration of the propagation formula for a wave or a translatory wave in a prismatic channel; remarks on the propagation of sound and light on hydraulic jumps; remarks on the distinction between rivers and torrents]: *Acad. Sci. [Paris]* Comptes rendu, v. 71, p. 186-195.

De Saint Venant B. (1871). Theorie du mouvement non-permanent des eaux avec application aux crues des rivieres et a l'introduction des marees dans leur lit, *Acad. Sci. Comptes Rendus*, 73, pp. 148-154, 237-240.

Devoy, R.J.N. (1978). *Phil.T.Roy.Soc.B.*, vol.285.

Devoy, R.J.N. (1979). Sea Level changes in the Thames Estuary. *Phil.Trans.R.Soc.Lond.*, B285, 255-410.

De Vries, M. (1973a). River Bed Variations - Aggradation and Degrodation, *Delft Hydraulic Lab., Publ. No. 107*, Delft, The Netherlands.

De Vries, M. (1973b). Application of Physical and Mathmatical Models for River Problems, *Publication No . 112, Delft Hydraulics Laboratory,* Delft, The Netherlands, April.

Donovan, D. T. (1962), Sea Levels of the Last Glaciation. *Bull. Geol. Soc. Amer.,* Vol.73, 1297-1298.

Dracos, Th. (1970). Computation of instantaneous flows in open channels of any geometry, *Schweizerische Bauzeitung*, 88, No. 19, May, pp. 21121-2118 (in German).

Dronkers, J.J. (1964). *Tidal computations in rivers and coastal waters*, 518pp, J.Wiley and Sons, New York.

Dronkers, J.J. (1969). Tidal computations for rivers, coastal areas and seas. *J.H.D.*, P.A.S.C.E., No. HY1, 95.

Dyer, K. R. (1973). *Estaries, A Physical Introduction.* 140pp.

Einstein, H. A. (1950). The bed load function for sediment transportation in open channel flows, *U.S. Dept. of Agriculture, Tech. Bull. 1026.*

Emery, K.O. & Aubrey, D.G. (1985). Glacial rebound and relative sea levels in Europe from tide gauge records. *Tectonophysics.* 120, 239-255.

Fairbanks, R.G. (1989). A 17,000-year glacio-eustatic sea-level record - influence of glacial melting rates on the younger dryas event and deep-ocean circulation, *Nature,* Vol.342, No.6250, pp 637-642.

Fairbridge, R. W. (1960). The changing level of the sea. *Sci.Am.*, 202, pp70-79.

Fairbridge, R. W. (1961) Eustatic changes in sea level, in 'Physics and Chemistry of the Earth 4', pp.91-187, Pergammon Press, London.

Findlay, D.C. (1965). The soils of the Mendip District of Somerset. *Mem.Soil.Surv.G.*B.

Flood Studies Report (1975) Volume III, Natural Environment Research Council, 27 Charing Cross Road, London

Forchheimer, Ph. (1903). Wasserbewegung in Wanderwellen [The motion of water in traveling waves]: *Akad. Wiss. [Vienna] Minutes Proc.*, sec. 2-a, p. 1697-1720.

Forchheimer, Ph. (1904) Wasserbewegung und Wanderwellen [Water movement and translatory waves]: *Gewasserkunde Zeitschr.*, v. 6, p. 321-339.

French, R.H. (1986) *Open Channel Hydraulics.* McGraw-Hill. 705pp.

Geike, J. (1894) *The great ice age and its relation ti the antiquity of man.* Stanford. London, 850pp. 3rd Edition.

Gelfand, 1. M. and Lokutsievski, 0. V. (1964). The double sweep method for solution of difference equations, *Appendix II to Godunov and Ryabenki.*

Gibson, A.H. (1933). Construction and operation of a tidal model of the Severn Estuary. *Severn Barrage Comittee Report*, ECA. HMSO, London.

Gilbertson, D.D. & Hawkins, A.B. (1974). Upper Pleistocene deposits and landforms at Holly Lane, Clevedon, Somerset. *Proc.Univ.Bris.Spaelaeol.Soc.* 13, pp 349-360.

Gilbertson, D. D. and Hawkins, A. B. (1977). The Pleistocene Succession at Kenn, Somerset. *Bull.Geol.Surv.Gt.Brit.*

Gilbertson, D.D. & Hawkins, A.B. (1977). The Quaternary deposits at Swallow Cliff, Middlehope, County of Avon. *Proc.Geol.Assoc.* 88, pp 255-266.

Godunov, S. K. and Ryabenki, V. S. (1964). *Theory of Difference Schemes*, North-Holland, Amsterdam.

Godwin, H. (1940) A boreal transgression of the sea in Swansea Bay. Data for the study of post-glacial history. *new Phytologist*, 39, 308-321.

Godwin, H. (1943). Coastal Peat Beds of The Bristish Isles and North Sea. *J.Ecol.*, 31, 199.

Godwin, H.& Wills, E.H. (1959,61,64). *Cambridge University Nat.Rad.Meas.*

Goemans, T. (1986). the sea also rises. The ongoing dialogue of the dutch with the sea, in *Effects of changes in statosphere ozone and global climate*, vol.4, sea level rise, UNEP AND U.S. EPA., 47-56.

Gornitz, V. & Lebedeff, S. (1987). Global sea level changes during the past century. in *Sea level fluctuation and coastal evolution.* (eds D. Nummedal, O. H. Pilkey & J. D. Howard), SEPM Special Publication No. 41.

Gornitz, V (1991) Global coastal hazards from future sea level rise. *Global Planetary Change,* Vol. 89, pp 379-398.

Goundunov, S.K. & Ryabenki, V.S.(1964) *Theory of difference schemes.* Amsterdam.

Graff, J. (1980) *An investigation of the frequancy distribution of annual sea level maxima at ports around Great Britain.* Institute of Oceanographic Sciences.

Graeff (1875). Memoire sur le movement des eaux dans les reservoirs a alimentation variable [Memoir on water movement in reservoirs with variable inflow]: *Acad. Sci. [Paris] Mem.,* v. 21, p. 393-583.

Graeff (1875). Memoire sur l'action de la digue de Pinay sur les crues de la Loire a Roanne [Memoir on the effect of Pinay Dam on the floods of the Loire at Roanne]: *Acad. Sci. [Paris] Mem.,* v. 21, p. 539-626.

Graeff (1875). Sur l'application des courbes de debits a l'etude du regime des rivieres et au calcul de d'effet produit par un systeme multiple de reservoirs [On the application of the hydrograph to the river regime and to the computation of the effect produced by a system of multiple reservoirs]: *Acad. Sci. [Paris] Mem.,* v. 21, p627-674.

Graeff (1883). Traite d'hydraulique [Hydraulics, chapter on flood forecast]: Paris, p. 438-442.

Greensmith, J.T. & Tucker, E.V. (1971) The effects of late Pleistocene and Holocene sea level changes in the vicinity of the River Crouch, East Essex. *Proc.Geol.Assoc.* 82, pp 301-322.

Greer, De H. (1940) Geochronologia sueccia principles. *K.SvenskaVetensk.Akad.Handle.* Ser.3, 18(6)

Griffiths, E.C. (1974). Sedimentary response to the tidal regime of the Upper Severn Estuary. *Unpublished PhD thesis,* University of Bristol.

Gunaratnam, D. and Perkins, F. E. (1970). Numerical Solutions of Unsteady flow in Open Channels, *Hydrodynamics Laboratory T.R. No. 127,* Dept. of Civil Engineering, MIT, Cambridge, Massachusetts.

Hamilton, D. (1979). the high energy, sand and mud regimes of the Severn Estuary, S.W. Britain. In Severn, R.T., Dineley, D.L. & Hawker, L.D. (Eds.), *Tidal Power and Estuary Management.* Scientechnica, Bristol, 162-172.

Hamilton, P. and MacDonald, K.B.(eds). Symposium on Estuarine and Wetland Processes and Water Quality Modelling, New Orleans. *Marine Sciences, Series II*, PLenum Press, New York.

Hansen, D.V. & Rattray, M. (1966). New dimensions in estuary classification. *Limnology and Oceanograpghy*, 11, pp319-326.

Harmer, F.W. (1907). On the origin of certain canon-like valleys associated with lake-like areas. *Q.J.G.S.* V63., pp470-514.

Harmon, R.S., Mitterer, R.M., Kriausakul, N., Land, L.S., Schwarcz, H.P., Garrett, P., Larson, G.J., Vacher, H.L. and Rowe, M. (1983): U-series and amino-acid racemization geochronology of Bermuda: implications for eustatic sea-level fluctuation over past 250,000 years. *Palaeogeogr., Palaeoclim.Palaeoecol.* 44, pp.41-70.

Harris, P.T. (1988). Large scale bedform as indicators of mutually evasive sand transport and the sequantial infilling of wide mouthed estuaries. *Sedimentary Geology,* 57, 273-298.

Harris, P.T. & Collins, M.B. (1985). Bedform distributions and sediment transport patterns in the Bristol Channel and Severn Estuary, U.K.*Marine Geology*, 62, 153-166.

Hawkins, A.B. (1968). The geology of the Portbury area. *Proc.Bris.Nat.Soc.*, 31, pp195-202.

Hawkins, A. B. (1971). The Late Weichselian and Flandrian Transgression of South West Britain, *Quaternaria,* 14, pp 115-130.

Hawkins, A. B. (1972). Sea level changes around South West England. Colston symposium on Marine Archaeology, *Colston Papers*, 23, 67-88.

Hawkins, A. B. (1979). Estuary Evolution: with special emphasis on the Severn Estuary. Colston Symposium on Tidal Power and Estuary Management. *Colston Papers*, 30, 151-161.

Hawkins, A. B. (1984). Depositional Characteristics of the Estuarine Alluvium: some engineering implications. *Quarterly Jounal of Engineering Geology*, 17, 219-234.

Hawkins, A. B. (1991). Implications of past and predicted sea level changes for coastal engineering, in*Developments in Coastal Engineering.* (eds Peregrine D. H. & Loveless J . H.), University of Bristol. 141-150.

Hawkins, A.B. (1992). Geology of the Avon Coast. In Crowther, P.R.(Ed.) *The Coast of Avon*, Bristol Naturalists Society Special Issue No.3.

Hawkins, A. B. and Kellaway, G. A., (1971). Filed meeting at Bristol and bath with Special reference to New Evidence of Glaciation. *Proc. Geol. Assoc.*, 82, pp 267-292.

Hawkins, A.B. & Sebbage, M.J. (1972) The reversal of sand waves in the Bristol Channel. *Marine Geology*, 12, M7-M9.

Hawkins, A.B., Narbett, R.W. & Taylor. D.R. (1994) Flandrian clifflines in the Severn Estuary.

Hawkins, A.B. & Taylor, D.R. (1991). Potential sea level rise and its implication for the City of Gloucester. *IAEG Conference on Urban Geology.*, Tunisia.

Hawkins, A.B. & Tratman, E.K. (1977). The Quaternary deposits of the Mendip, Bath and Bristol areas. *Proc.Univ.Bris.Spelaeol.Soc.*, 14(3), pp197-232.

Henderson, F. M. (1966) *Channel Flow*, McMillan Company, New York.

Hermann, L (1967) *Proc.ASCE.J.Eng.Mech.Div.* Vol.93

Heyworth, A. & Kidson, C. (1982) Sea level changes in southwest England and Wales. *proc.Geol.Assoc.*, 93, 91-111.

Holly, F. M. and Preissmann, A. (1977). Accurate calculation of transport in two dimensions, *JHYD ASCE*, 103, No. HYI I, November.

Houghton, J. T., Jenkins, G. J., Ephraums, J. J. *Climate Change.* Intergovernmental Panel on Climate Change (1990). Cambridge University Press. 365pp.

Howes, B.L. Dacey, J.W.H. and Wakeham, S.G. (1985) The effects of sampling technique on measurements of porewater constituents in salt marsh sediments. *Limnol.Oceanog.* Vol.30, pp 221-227.

Howes, B.L, Dacey, J.W.H. and Teal, J.M. (1985) Annual carbon mineralization and below ground production of spartina-alterniflora in a new-england salt-marsh, *Ecology*, Vol.6, no.2, 595-605.

HRS. (1980) Lower Severn Basin Study: Model Study.

HRS. (1981) A computational hydraulic model of the River Severn, *Report EX 945*, HRS Wallingford, March (3 volumes).

HRS. (1976) Lower Severn Basin Study: Wave Heights.

HR Wallingford (1991) *Loris (LOoped RIver Simulation)* , User Manual.

HR Wallingford (1991) *River Severn Flood Plain Avonmouth to Worcester, computational model study.* Report EX2252, March.

Imbrie, J. & Imbrie, K.P. (1979). *Ice Ages. Solving the Mystery*. Macmillan Press.

Ippen A.T. (Ed.), 1966. *Estuary and Coastal Hydrodynamics*, McGraw-Hill Book Co., Inc.

Ippen A.T.& Harleman. (1961). One dimension analysis of salinity intrusion in estuaries. *Tech.Bull.No.5*. Comittee on tidal hydraulics. US Army Corps of Engineers.

Isaacson, E., Stoker, J. J. and Troesch, B. A. (1954). Numerical Solution of Flood Prediction and River Regulation Problems (Ohio-Mississippi floods), Report II, New York University, *Inst. Math. Sci. Rept. IMM-NYU-20S.*

Jamieson (1865). On the history of the lAst geological changes in Scotland. *Geol.Soc.Lon.Quart.Journ.* V21., pp161-203.

Jeffries, R.L., Willis, A.J. & Yemm, E.W. (1968). The late post-glacial history of the Gordano Valley, north Somerset. *New Phytol.* 67, pp335-348.

Jeffrey, A. (1969). *Mathematics for engineers and scientists.*

Jelgersma, S. (1961). Holocene sea level changes in the netherlands. *Meded.Geol.Sticht.* Series.C. VII, 7, 1-100.

Jelgersma, S (1966). Sea Level Changes during the last 10,000 years. In *Proc.Int.Syp.World.Climate, 8000-0 BC.*, R.Meteorol.Soc.Lon. pp25-48.

Jelgersma, S (1969), In The Quaternary History of the North Sea, pp 233-248, *Acta.Univ.Ups.Symp.Univ.Ups.Annum.Quingentesimum Celebrantis,* 2.

Jobson, H. E. and Keefer, T. N. (1979). Modeling highly transient flow, mass and heat transport in the Chattahoochee River near Atlanta, Georgia, *USGS Open File Report 79-270*, NSTL Station; Mississippi 39529.

Kamphuis, J.W. (1970), Mathematical study of the St. Lawrence River. *JHD, PASCE,* 96, pp 643-664.

Kellaway, G.A. (1971). Glaciation and the stones of Stonehenge. *Nature*, 232, pp30-35.

Kerfve, B. (Ed.), *Hydrodynamics of estuaries, Vol.I.* Estuarine Physics. Crc Press, Florida.

Kidson, C. and Heyworth, A. (1973). The Flandrian sea-level rise in the Bristol Channel. *Proc. Ussher. Soc.* 2, pp189-191.

Kidson, C. and Heyworth, A. (1973) *Q.J.E.G,* 9 , pp 217-235.

Kidson, C. and Heyworth, A. (1976). The Quaternary deposits of the Somerset Levels. *Q.J.E.G.*, 9, pp 217-235.

Kirby, R. & Parker, W.R. (1982) A suspended sediment front in the Severn Estuary, *Nature*, 295, 396-399.

Kleitz, Ch. (1877). Sur la theorie du mouvement non-permanent des liquides et sur son application a la propagation des crues des rivieres [On the theory of unsteady flow of liquids, and on its application to the propagation of river floods]: *Ponts et Chaussees Annales (France)*, sem. 2, no. 48, p. 133-196.

Labeyrie, J., Lalou, C. and Delibrias, G. (1969): Etude des transgressions marines sur l'atoll de Mururoa par la datation des differents niveaux de corail. *Cah. Pacifique* 13, pp. 59-68.

Lagrange, I.L. (1781). Memoire sur la theorie du mouvement des fluides [Memoir on the theory of movement of fluids]: *Acad. Royal [Berlin] Mem.*, p. 151-198, [1783]; and p. 192-198 [1788].

Lagrange, I.L. (1788). Mecanique analytique [Analytical Mechanics]: *Paris, Bertrand's ed.*, pt. 2, sec. 2, act. 2, p. 192; or Oeuvres [Works] sec. 11, act. 36.

Lambeck, K. (1990) Late Pleistocene, Holocene and present sea-levels - constraints on future change. *Global and Planetary Change*, vol.89, no.3, pp205-217

Lambeck, K and Nakada, M. (1987). Glacial rebound and relative sea level variations - A new appraisal. *Geophys.Jour.Roy.Astr.Soc.*, vol.94, no.1, pp171-224.

Land, L.S., MacKenzie, T.F. and Gould, S.J. (1967): Pleistoncene history of Bermuda. *Geol. Soc. Am. Bull.* 78, pp. 993-1006.

Laplace, P.S.(1775-76). Researches sur quelques points du systeme du monde [Researches on some points of world system]: *Acad. Sci. [Paris] Mem.*, (complete works, v.9).

Lax, P. D. (1954). Weak solutions of non-linear hyperbolic equations and their numerical applications, *Comm. Pure Appl. Math.*, 7, pp. 159-193.

Lax, P. D. and Wendroff, B. (1960). Systems of conservation laws; *Comm. Pure Appl. Math.*, 13, pp. 217-237.

Leeder, M.R. (1982). *Sedimentology. Process and Product.* Allen and Unwin.

Leendertse, J. J. (1970). A Water-Quality Simulation Model for Well-Mixed Estuaries and Coastal Seas: Vol. I, *Principles of Computation, Rand Corporation Memorandum*, RM-6230-RC, February.

Lennon, G.W. (1963). A frequency investigation of abnormally high tidal levels at certain west coast ports. *Proc.Inst.Civ.Engs.* 25, pp 451-484.

Libby, W.F. (1955). *Radiocarbon Dating*. 2nd edition. Chicargo.

Ligget , J. A. and Woolheiser, D. A. (1967). Difference solutions of the shallow water equations. *JEMD, PASCE,* 93, pp 36-72.

Liggett, J. A. (1975). Basic equations of unsteady flow, Chapter 2 of *Unsteady Flow in Open Channels*, Water Resources Publications, Fort Collins, Colorado.

Liggett, J. A. and Cunge, J. A. (1975). Numerical methods of solution of the un-steady flow equations, Chapter 4 of *Unsteady Flow in Open Channels*, Water Resources Publications, Fort Collins, Colorado.

Lloyd, I.M.. (1989) *The location and investigation of a test bed site for research on soft clay*, Unpublished PhD Thesis, University of Bristol.

Long, S.P. & Mason, C.F. *Saltmarsh Ecology*. Blackie, London and Glasgow.

Lowe, J.J. & Walker, M.J.C. (1987) *Reconstructing Quaternary Environments*, Longmans, London.

Lyell, C. (1839). *Noveaux elements de geologie*. Paris.

Martin, M.H. (1992) A history of Spartina on the Avon Coast. In Crowther, P.R.(ed.) *The Coast of Avon,* Bristol Naturalists Society Special Issue No.3.

Mahmood & Jerjevich. (1975) *Unsteady Flow in Open Channels*. Water Resorces Publications.

Massau, J. (1889). L'integration graphique and Appendice au memoire sur l'integration graphique. *Assoc.des ingenieurs sortis des ecols specials de Gand, Belgium*, Annals, 12, pp185-444.

McDowell, D.M. and O'Connor, B. A. (1977), *Hydraulic behaviour of estuaries*, MacMillan

McManus, J. (1979). Sediments in estuaries. *Colston Papers*, 30, 190-187.

Meade, R.H. (1972). transport and deposition of sediments in estuaries. *Geological Society of America Memoir*, 133, 91-120.

Meijor, Th. Ji F. P., Vreugdenhil, C. B. and de Vdes, M. (1965). A method of computation for non-stationary flow in open channel networks, *Proceedings 11th Congress IAHR*, Leningrad, Paper 3.28.

Mitchell, G. F. (1960). The Pleistocene History of the Irish Sea. *Advan. Sci. Land*, 17, No.68, pp 313-325.

Mitchell, G. F. (1977). Raised beaches and sea level. In *British Quaternary studies, Recent Advances*. Ed. Shotton, F.W., pp 169-186.

Mitchell, G. F., Penny, L. F., Shotton, F. W. and West, R.G. (1973). Acorrelation of Quaternary Deposits in the British Isles. *Geol.Soc.Lond.*, Special Report No.4, 99pp.

Miller, W. A. and Cunge, J. A. (1975). Simplified equations of unsteady flow, Chapter 5 of *Unsteady Flow in Open Channels*, Water Resources Publications, Fort Collins, Colorado.

Morner, N.A., (1969). The late Quaternary history of The Kattegatt Sea and the Swedish west coast. *Sverig.Geol.Unders.* Ser.C, No.640, pp 1-487.

Morner, N.A., (1971). *Geol.Minjb.* 50, pp 699-702.

Morner, N.A., (1980) '*Earth Rheology, Isostacy amd Eustacy*', J.Wiley, Chichester.

Murray, J. W. and Hawkins, A. B. (1976). Sediment transport in the Severn Estuary during the past 8000-9000 years. *Jl. Geol. Soc. Lond.*, 132, pp 385-398.

Myers, W. R. C. (1978). Momentum transfer in a compound channel. *J. Hyd. Res*, IAHR, 16, No. 2.

Narbett, R.W., (1992). Geological and engineering properties of estuarine alluvium from the Severn Estuary. *Unpublished PhD Thesis*, University of Bristol.

Nemec, J. and Kite, G. W. (1978). Mathematical model of the upper Nile basin, *Int. Symp. on Logistics and Beneflts of using Mathematical models of Hydrologic and Water Resource Systems*, IIASA, Laxenburg.

Officer, C.B. (1976). *Physical Oceanography of estuaries (and associated waters).* 465pp, J.Wiley and Sons.

Patterson, W.S.B., *Koerner, R.M., Fisher, D., Johnsen, S.J., Clausen, H.B.*, Dansguard, W., Bucker, P. and Oeschage, H. (1977). An oxygen isotope climatic record from Devon Island Ice Caps, Actic Canada, Nature, 266, pp 508-511.

Parker, W.R. & Kirby, P. (1982) Sources and transport patterns of sediment in the inner Bristol Channel and Severn Estuary. In I.C.E. *Severn Barrage*, Thomas Telford, London.

Partiot, H.L. (1858). Memoire sur mascaret (Extrait par l'auteur) [Author's abstract: Memoir on the tidal bore]: Acad. Sci. [Paris] Comptes rendu, v. 47, p. 651-654.

Partiot, H.L., 1861, Etude sur les mouvements des marees dans la partie maritime des fleuves [Study on the movements of tides in the maritime portion of rivers]: Paris.

Partiot, H.L. (1861). Memoire sur le mascaret [Memoir on the tidal bore]: *Ponts et Chaussees Annales [French]*, sem. 1, no. 2, p. 17-48.

Partiot, H.L. (1871). Memoire sur les marees fluviales [Memoir on the tides in rivers]: *Acad. Sci. [Paris]* Comptes rendu, v. 73, p. 91.

Peltier, W. R. & Tushingham, A. M. (1989). Global sea level rise and the greenhouse effect: might they be connected? *Science*, 244, 806-810.

Peltier, W. R. & Tushingham, A. M. (1990). The influence of glacial isostatic adjustment on tide gauge measurements of secular sea level. *Journal of Geophysical Research.*

Penck, A. & Brucker, E. (1909) *Die Alpen im Eiszeitalte Tauchnitz.* Leipzig. 1199pp.

Pethick, J.S. (1981) Long term accretion rates on tidal salt marshes. *J.Sed.Pet.* 51, 571-577.

Pethick, J.S. (1992). Saltmarsh geomorphology. In Allen, J.R.L. & Pye, K. (Eds.) *Saltmarshes (Morphodynamics, Conservation and Engineering Significance)*, Cambridge University Press.

Pizzuto, J.E. (1987) sedimewnt diffusion during overbank flows. *Sedimentology*, 34, 301-317.

Preissmann, A., (1961). Propagaffon des intumescences dans les canaux et rivieres, *First Congress of the French Association for Computation*, Grenoble, September.

Preissmann, A. (1965). Difficulte's rencontrees dans le calcul des ondes detranslation a front raide, *Proceedings 11th Gongress IAHR*, Leningrad, paper 3.52.

Preissmann, A. and Chevereau, G. (1976). Remarques sur le choix des method etd'appre'ciation de la qualite' des divers systemes de regulation de canaux a surface libre, Symposium: *Fluid Motion Stability in Hydraulic Systems with Automatic Regulators*, Bucharest.

Preissmann, A. and Cunge, J. A. (1961a). Calcul des intumescences sur machines electroniques, *IX meeting of the UHRE*, Dubrovnik.

Preissmann, A. and Cunge, J. A. (1961b). Calcul du mascaret sur machine electronique, *La Houille Blanche*, No. 5, pp. 588-596.

Price, R.K.(1974). Comparison of four numerical methods for flood routing. *PASCE JHD.* 100, pp 879-900.

Price, R.K. (1976) Analysis of Avonmouth tide data. *Lower Severn Basin Study.* HRS

Price, R.K. and Samuels, P.G. (1980). A computational hydraulic model for rivers. *P.I.C.E.*, part 2, 69, MAr., pp 87-96.

Pritchard, D.W. (1955) Estuarine circulation patterns. *Proc.Am.Soc.Civ.Engrs,* 81, pp 1-11.

Pritchard, D.W. (1967). What is an Estuary: Physical Viewpoint. In *Estuaries*, G.H. Lauff (Ed). Am.Assoc.Adv.Sci.

Pritchard, D.W. & Carter, H.H. (1971). Estuarine circulation patterns. In Schubel (1971).

Pugh, D.T. (1987). *Tides, Surges and Mean-sea Level*, 472pp, J.Wiley and Sons, G.B.

Pugh, D.T. (1990) Is there a sea level problem. *Proc Inst.Civ.Engs.* Pt 1- Design and Construction. Vol. 88, June. pp347-366.

Reboull, H. (1833). *Geologie de la periode Quaternaire.* Paris.

Reece, G., (1986). *Microcomputer Modelling by Finite Differences*, MacMillan.

Richardson, C. (1887) The Severn Tunnel. *Proc.Bristol.Nat.Soc., Eng.section,* New Series, 5, 49-81.

Richtrnyer, R. D. (1957). *Difference Methods for Boundary Value Problems.* Interscience, New York.

Rossiter, J.R.(1967) An analysis of annual sea level variations in European Waters. *Geophys.Jour.R.Astro.Soc.Lond.* 12, pp 259-299.

Rossiter, J. R. (1972). Sea-level observations and their secular variation. *Philosophical Transactions of the Royal Society, London*, 272, 131-139.

Rozenberg, L. I. and Rudnov, M. I. (1967). Some singularities of schematization of channels with flood plains in unsteady flow computations, *CGI Trudy No. 140*, pp. 83-90

Russell, J.S. (Scott), 1837, Experimental researches into the laws of certain hydro-dynamic phenomena that accompany the motion of floating bodies, and have not previously been reduced into conformity with the known laws of the resistance of fluids: *Royal Soc. [Edinburg] Philos. Trans.*, v. 14, p. 47-109 [1840]. Published in French in Ponts et Chaussees Annales, sem. 2, p. 143-234, 1837.

Russell, J.S. (Scott), 1842-43, Report on waves: British Assoc. Adv. Sci. Proc. for 1844, p. 311-390 [1845].

Rusinov, M. 1. (1967). Influence of some parameters of prismatic channel with flood plains on the velocity of release wave crests, *GCI Tru, No. 140*, pp. 64-82

Sargent, R.G., (1982), verification and validation of simulation models, in *Progress in Modelling Simulation*, ed. Cellier, F.E., London Academic Press, pp 159-172.

Schaffranek, R. W. and Baltzer, R. A. (1978). Fulfilling model time-dependentdata requirements, *Symposium on Technical, Environmental, Socio-economical and Regulatory Aspects of Coastal Zone Management*, Water-ways and Harbors Division, ASCE, March.

Schonfeld, J. C. (1951), *Propagation of tides and similar waves*, thesis, Technical University, Delft, The Netherlands.

Schubel, J.R. (1971). *The Estuarine Environment.* Washington DC: Am.Geol.Inst.

Schubert, C. & Szabo, B.J. (1978). Uranium series ages of Pleistocene marine deposits on the islands of Curacao and La Blanquilla, Caribbean Sea. *Geol.Mijnbouw*, 57, pp.325-332.

SCS (1963) *Guide for selecting roughness coefficients 'n' values for channels.* US Dept. Agriculture, Soil Conservation Service, Washington.

Seddon, J.A. (1898). A mathematical analysis of the influence of reservoirs upon streamflow: *Am. Soc. Civil Engineers Trans.*, v. 50, p. 401-427.

Seddon, A.J. (1900). River hydraulics: *Am. Soc. Civil Engineers Trans.*, v. 43, p. 179-243.

Shennan, I. (1983). Flandrian and Late Devensian Sea-level changes and crustal movements in England and Wales. Ch.11 in Smith, D.E. & Dawson, A.G. (Eds.), *Shorelines and Isostacy*. Academic Press, London.

Shennan, I. (1989), Holocene crustal movements and sea level changes in Great Britain. *Journal of Quaternary Science*, 4, 77-89.

Shotton, F.W. (1953). The Pleistocene deposits of the area between Coventry, Rugby and Leamington Spa and their bearing upon the topographic development of the Midlands. *Phil.Trans.R.Soc.Lon.* Ser.B, 237, pp209-260.

Shotton, F.W. (1967). The problems and contributions of methods of absolute dating within the Pleistocene period. *Jour.Geol.Soc.Lon.*, 122, pp357-383.

SOGREAH (1961). *Compotison of the de St. Venant Equations and Muskingum Method on the Rhone River*, internal report.

Sollas, W.J.(1883). The estuaries of the Severn and its tributaries. *Q.J.G.S.*, 49, pp611-629.

Stearns, H.T. (1971). Geological setting of an Eocene fossil deposit on Eua Island, Tonga. *Geol..Soc.Am.Bull.*, 82, pp 2541-1552.

Stearns, C.E. (1976): Estimates of the position of sea level between 140,000 and 75,000 years ago. *Quat. Res.* 6, pp. 445-9.

Stearns, H.T. (1978). Quaternary Shorelines in the Hawaiian Islands. *B.P.Bishop Museum Bull. (Honalulu)* 237, pp 1-57.

Stephens, N. & Synge, F.M. (1966). Pleistocene shorelines. In *Essays in Geomorphology*, Ed. Dury, G.H., pp 1-51.

Stevens, M. A. and Simons, D. B. (1973). Manning's roughness coefflcients for the Padma River, *l5th Congress of the IAHR*, VOL. 1, Istanbul.

Stoker, J. J. (1957). *Water Waves*, Interscience, New York.

Stone, H.K., (1968) Iterative solution of implicit approximations of multidimensional partial differential equations, *Soc.Ind.Appl.Math.,Jour Numer Anal.*, 5, (3), pp 530-558.

Strelkoff, T. (1969). One dimensional equations of open channel flow, *JHD, PASCE*, 95, pp 861-876.

Strelkoff, T. (1970). Numerical solution of De St Venant Equations, *JHD, PASCE,* 96, pp 223-254.

Stumf, R.P. (1983) The process of sedimentationon the surface of a salt marsh. *Est.Coast.Shelf.Sci., 17, 495-508.*

Tooley, M.J. (1985). Sea levels. *Progress in Physical Oceangraphy*, 9, 113-120.

Uncles, R.J. (1981). A note on tidal Assymetry in the Severn Estuary, *Est.Coast.Mar.Sci.* 13, pp 419-432.

Uncles, R.J. (1982). Computed and observed residual currents in the Bristol Channel. *Oceanol.Acta.*,5, pp11-20.

Uncles, R.J. (1984). Hydrodynamics of the Bristol Channel. *Marine Pollution Bulletin,* 15, 47-53.

UNESCO/SOGREAH (1964). *Mekong Delta mathematical model Vol. II*, Preliminary Investigation, Sept.

UNESCO (1969). *Mekong River Delta Model Study*, Report Series 9, Paris.

Urquhart, W.J. (1975) *Hydraulics*. Eng.Field.Man. US Dept.Agriculture. Soil Conservation Service, Washington.

Vasiliev, O. F. (1970). Numerical solution of the non-linear problems unsteady flow in open channels, *Proceedings of thc 2nt International Conference on Numerical methods in fluid dynamics*. Berkeley. pp. 420-421.

Vasiliev, 0. F. and Godunov, S.K. (1963), Numerical method of computation of wave propaption in open channels; application to the problem of floods, *Dokl.Akad.Nauk SSSR, lSl*, No.3 (inRussian).

Vasiliev, O. F., Temnoeva, T. A. and Shugrin, S. M. (196S). Numerical rnethod for the calculation of unsteady flows in open channels, *Izv. Akad. Nauk SSSR*, Mechanics, No. 2.

Veeh, H.H. (1966): Th^{230}/U^{238} and U^{234}/U^{238} ages of Pleistocene high sea level stand. *J. Geophys. Res.* 71, pp. 3379-86.

Verwey, A. (1971). Mathematical model for flow in rivers with realistic bed configuration, *Report series No. 12, International Courses in Hydraulic and Sanitary Engineering*, Delft.

Von Neumann, J. and Richtmyer, R. D. (1950). A method for the numerical calculations of Hydrodynamic shocks, *J. Appl. Phys.*, 21, pp. 232.

Vries, De H., (1958). Variation in concentration of radiocarbon with time and location on Earth. *Koninkl.Nederlands.Akad.Wentensch.Proc.* Ser.B., 61, pp1-9.

Vreugdenhil, C. B. (1973). *Computational Methods for Channel Flow*, Publication No. 100, Delft Hydraulics Laboratory, Delft.

Wallace, S.G., Crowther, J.M. & Curran, J.C., (1989). Consideration of a one dimensional transport model of the Upper Clyde Estuary. *Advances in water modelling and measurement.* BHRA, Cranfield, Bedford.

Wallace, S. G. and Knight, D. W. (1984). Calibration studies concerning a one-dimensional numerical tidal model with particular reference to resistance coefficients. *Est.Coast.Shelf.Sci,* 19.

Ward, W.T. (1971). Postglacial changes in level of land and sea. *Geol.Mijnbouw*, 50, pp 703-718.

Ward, W.T. (1973). Correlations of Pleistocene Shorelines in Gippsland, Australia and Oahu, Hawaii. *Geol.Soc.Am.Bull.*, 84, pp 3087-3092.

Warrick, R. A. & Oerlemans, H. (1990). Sea Level Rise. In *Climate Change*. (eds J. T. Houghton, G. J.Jenkins, & J. J. Erphraums), Cambridge University Press, 263-281.

Water Pollution Research Lab. (1972). Water Quality in the Severn Estuary and recommendations for future investigations. *Water Pollution Research Lab. Report No.1276.* DoE.

Welby, W. (1607). *Lamentable newes out of monmouthshire in Wales. Contayning the wonderfull and most fearfull accidents of the great over-flowing of water....January last 1607,* London.

Welch, F.B.A. (1955) Notes on gravels at Kenn, Somerset. *Proc.Univ.Bris.Spelaeol.Soc.*, 7, pp137.

West, R.G. (1972). Relative land-sea level changes in southeastern England during the Pleistocene. *Phil.Trans.R.Soc.Lon.,* 272A, pp 87-98.

Wigley, T.M.L. & Raper, S.C.B. (1987). Thermal expansion of sea water associated with global warming. *Nature*, 330, pp127-131.

Willis, E. H., (1971), *Ann.N.Y.Acad.Sci.,* 95, pp 368-376.

Wills, L. J. (1938) Pleistocene development of the Severn from Bridgnorth to the Sea. *Q.J.G.S,* London, 94, pp 161-242.

Wiley, M.L., (Ed.). (1977). *Estuarine process Vol.II,* Cirulation Sediments and transfer of materials in the estuary, Academic Press, New York. International estuarine research conference, Galverston, 1975.

Wood, E., Harley, B. M. and Perkins, F. G. (1975). *Transient Flow Routing in Channel Networks*, Report RR-75-1, IIASA, Laxenburg.

Woodworth, P.L. (1987). Trends in UK mean sea level. *Marine Geodesy*, 11, 57-87.

Woodworth, P.L., Shaw, S.M. & Blackman, D.L. (1991). Secular trends in mean tidal range around the Bristish Isles and along the adjacent European coastline. *Geophys.Jour.Int.*, 104, 593-609.

Zanobetti, D., Lorgere', H., Preissmann, A. and Cunge, J. A. (1970). Mekong Delta mathematical model program construction, *J. Waterways and Harbors Division, ASCE*, 96, No. WW2, May.

APPENDIX A

LOCATION MAPS

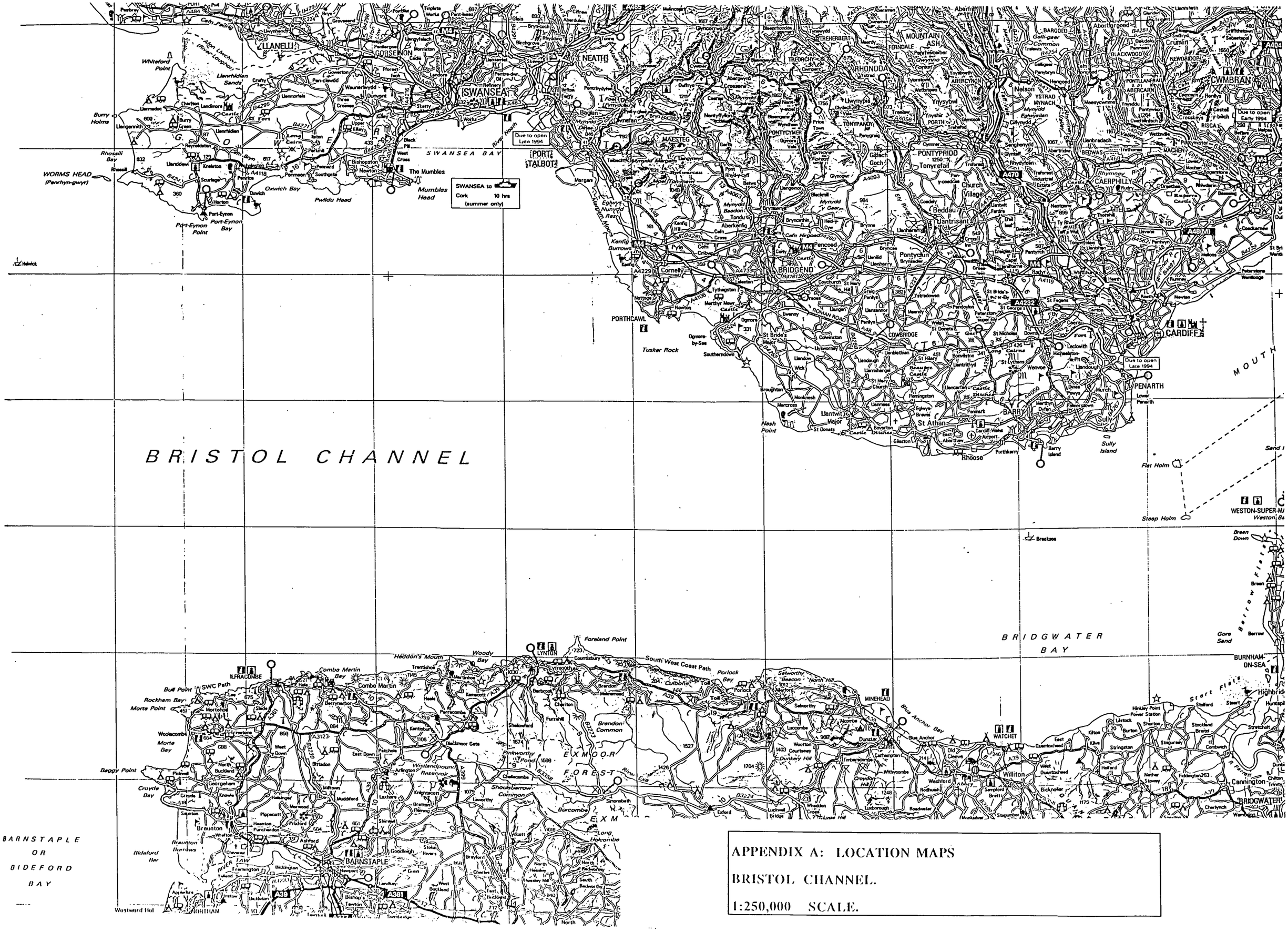
BRISTOL CHANNEL
SWANSEA BAY
BRIDGWATER BAY
EXMOOR FOREST
SWANSEA to Cork 10 hrs (summer only)
Due to open Late 1994
Due to open Early 1994
Due to open Late 1994
The Mumbles
Mumbles Head
WORMS HEAD (Penrhyn-gwyr)
Whiteford Point
Burry Holms
Rhossili Bay
Oxwich Bay
Pwlldu Head
Port-Eynon Point
Port-Eynon Bay
Tusker Rock
Nash Point
Flat Holm
Steep Holm
Foreland Point
Woody Bay
Combe Martin Bay
Bull Point
Rockham Bay
Morte Point
Morte Bay
Baggy Point
Croyde Bay
Braunton Burrows
Hubberstone Pt
Milford Haven
Breaksea
Barrow Flats
Gore Sand
Sand
Brean Down
Blue Anchor Bay
Porlock Bay
South West Coast Path
Heddon's Mouth
Brendon Common
Shoulsbarrow Common
Burcombe
Pinkworthy Pond
Wistlandpound Reservoir
Challacombe
Croydon Hill
Dunkery Hill
Cefn Pedol
Kenfig Burrows
Kenfig Pool & Nature Reserve
Eglwys Nunydd Reservoir
Llandegfedd Reservoir
Cefn Cribwr
Cefn Hirgoed
Mynydd Beacon
Mynydd-y-Gaer
Mynydd Baedan
Mynydd Carn-y-Cefn
Mynydd Eglwysilan
Mynydd Machen
Mynydd Maen
Mynydd Rhiw-saeson
Mynydd Ty-Isaf
Mynydd-y-Garn-Fawr
Mynydd-y-Grug
Mynydd-y-Llan
Mynydd-y-Rhiw
Mynydd-y-Twyn
Mynydd-y-Wern
Mynydd Bychan
Mynydd Carn-y-Cefn
Mynydd Eglwysilan
Mynydd Machen
Mynydd Maen
Mynydd Rhiw-saeson
Mynydd Ty-Isaf
Mynydd-y-Garn-Fawr
Mynydd-y-Grug
Mynydd-y-Llan
Mynydd-y-Rhiw
Mynydd-y-Twyn
Mynydd-y-Wern
Mynydd Bychan
Cefn Pedol
Kenfig Burrows
Kenfig Pool & Nature Reserve
Eglwys Nunydd Reservoir
Llandegfedd Reservoir
Cefn Cribwr
Cefn Hirgoed
Mynydd Beacon
Mynydd-y-Gaer
Mynydd Baed

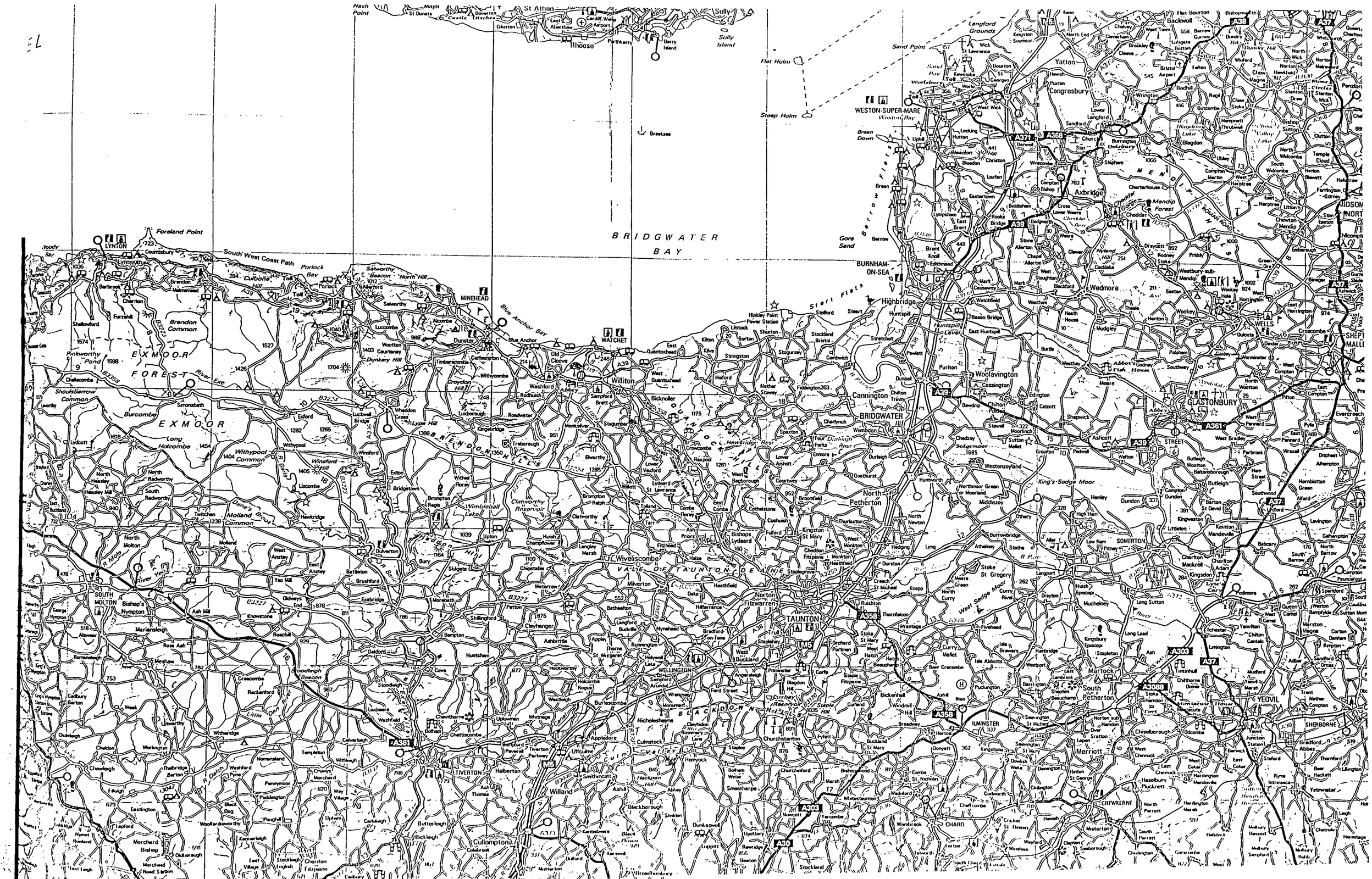
BRIDGWATER BAY
EXMOOR FOREST
EXMOOR
BRENDON HILLS
QUANTOCK HILLS
VALE OF TAUNTON DEANE
BLACKDOWN HILLS
MENDIP HILLS
Foreland Point
LYNTON
Countisbury
South West Coast Path
Porlock Bay
Porlock
MINEHEAD
Blue Anchor Bay
Blue Anchor
WATCHET
Hinkley Point Power Station
Stert Flats
Steart
Highbridge
Burnham-on-Sea
WESTON-SUPER-MARE
Weston Bay
Sand Point
Langford Grounds
Flat Holm
Steep Holm
Brean Down
Gore Sand
Barrow Fleet
Brean
Berrow
Burnham Flats
Breaksea
Nash Point
Minehead
St Donats
Gileston
St Athan
Cardiff Wales Airport
East Aberthaw
Porthkerry
Barry Island
Sully
Sully Island
Lynton
Lynmouth
Woody Bay
Brendon Common
Pinkworthy Pond
Shoulsbarrow Common
Burcombe
Long Holcombe
Withypool Common
Dunkery Hill
Selworthy Beacon
North Hill
Culbone Hill
Culbone Toll
Porlock Toll
Selworthy
Alcombe
Luccombe
Woolston
Courtenay
Timberscombe
Cleeve
Carhampton
Withycombe
Croydon Hill
Dunster
Old Cleeve
Washford
Abbey
Williton
Sampford Brett
Quantoxhead
East Quantoxhead
Kilton
Kilve
Stringston
Stogursey
Combwich
Stockland Bristol
Bicknoller
Nether Stowey
Fiddington
Holford
Dunball
Cannington
Chilton Trinity
Puriton
Woolavington
Cossington
Bawdrip
Bridgwater
Durleigh
Chedzoy
Sedgemoor
Westonzoyland
Goathurst
Huntworth
Northmoor Green or Moorland
Middlezoy
King's Sedge Moor
North Petherton
Bishops Lydeard
Cothelstone
Cushuish
Kingston St Mary
Fitzpaine
Monkton Heathfield
Durston
Creech St Michael
Knapp
Rushton
Thornfalcon
Stoke St Mary
West Hatch
Hatch Beauchamp
Taunton
Norton Fitzwarren
Heathfield
Milverton
Oake
Hillfarrance
Wellington
Sampford Arundel
Holcombe Rogus
Ford Street
Wiveliscombe
Langford Budville
Runnington
Thorne St Margaret
Applen
Ashbrittle
Cleeve Hill
Cleeve Abbey
Washford
Rodhuish
Monksilver
Stogumber
Elworthy
Crowcombe
Raspool
Lower Vexford
Vexford
Lydeard St Lawrence
Brompton Ralph
Clatworthy Reservoir
Huish Champflower
Upton
Wimbleball Lake
Brushford
Exebridge
Bury
Skilgate
Oldberry End
Knowstone
Molland
Anstey
Yeo Mill
Ash Mill
Bishop's Nympton
South Molton
Mariansleigh
Rose Ash
Romansleigh
Meshaw
Creacombe
Rackenford
Stoodleigh
Stoodleigh Beacon
Loxbeare
Westleigh
Burlescombe
Chevithorne
Uplowman
Whitnage
Tiverton Parkway
Tiverton
Halberton
Willand
Cullompton
Culm Valley
Culmstock
Hemyock
Churchstanton
Fyfett
Buckland St Mary
Broadway
Ilminster
Horton
Donyatt
Kingstone
Chiselborough
Merriott
Crewkerne
Haselbury Plucknett
Chard
Combe St Nicholas
Wadeford
Whitestaunton
Chaffcombe
Cricket St Thomas
Wayford
Seaborough
Dunkeswell
Upottery
Newcott
Broadhembury
Silverton
Bradninch
Cullompton
Crediton
Coppleston
Sandford
Uton
Hele
Stockleigh Pomeroy
Stockleigh English
Morchard Bishop
Morchard Road Station
Lapford
Eastington
Woolfardisworthy
Puddington
Pyne
Black Dog
Newton St Cyres
Brampford Speke
Thorverton
Cadbury
Barton
Thelbridge Barton
Chawleigh
Chulmleigh
Cheldon
Witheridge
Templeton
Calverleigh
Bothen
Chettiscombe
Sandford
Poughill
Penny Mire
Crown Mordred
Way Village
Westford
Nomansland
Workington
Urworthy
Dart River
Little Dart River
Taw River
River Yeo
River Mole
Molland Great Common
Duke's Pool
Wimbleball Lake
Clatworthy Reservoir
Hawkridge
Withypool
Winsford Hill
Exton
Withiel Florey
Bridgetown
Brompton Regis
Dulverton
Battleton
Brushford
Exebridge
Bampton
Huntsham
Oakford
Cove
Stoodleigh
Loxbeare
Westleigh
Burlescombe
Nicholashayne

APPENDIX A: LOCATION MAPS

SEVERN ESTUARY.

1:250,000 SCALE.

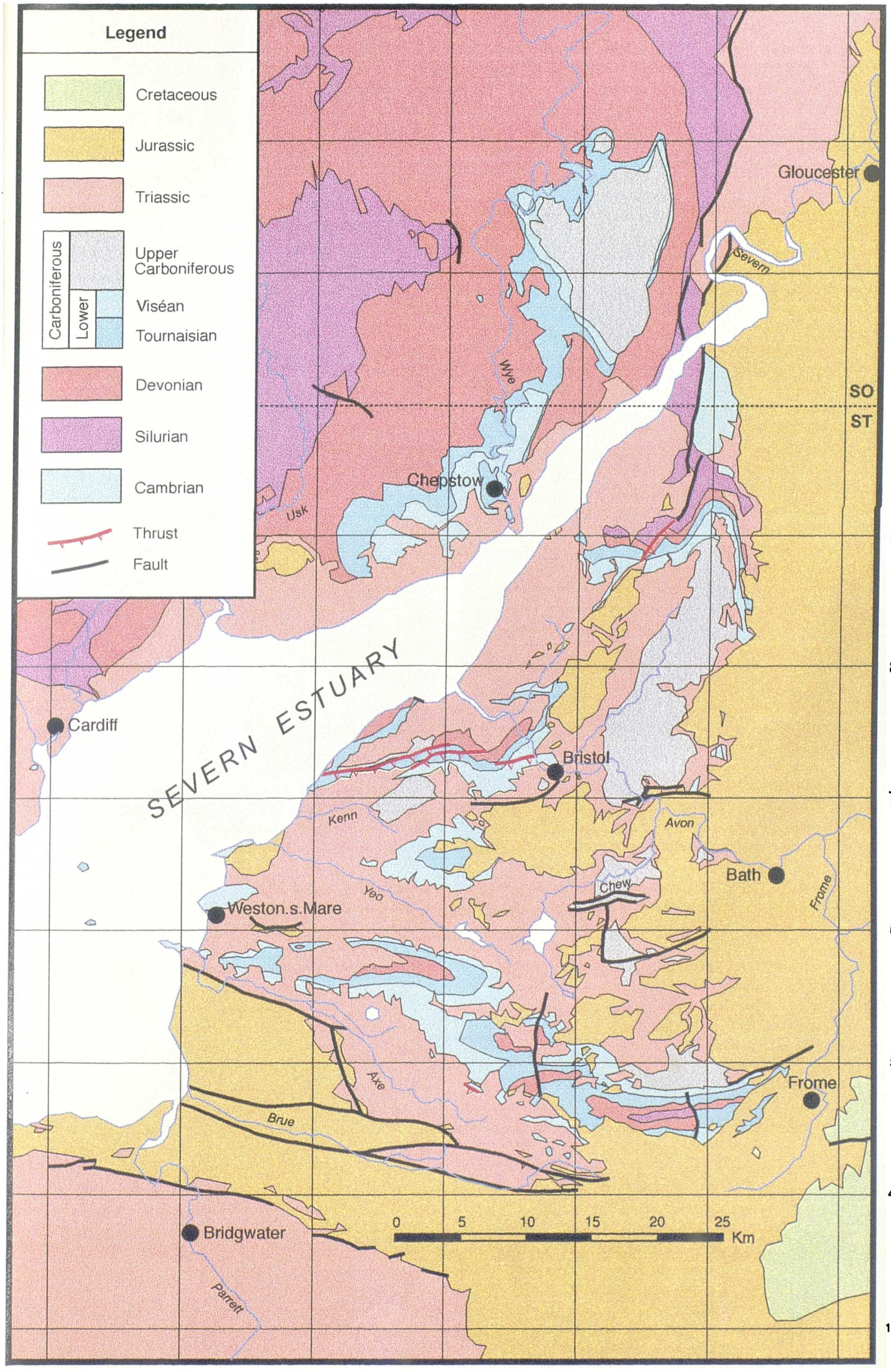
Legend
Cretaceous
Jurassic
Triassic
Carboniferous
Upper Carboniferous
Lower
Viséan
Tournaisian
Devonian
Silurian
Cambrian
Thrust
Fault
SEVERN ESTUARY
Gloucester
Severn
Wye
Chepstow
Usk
Cardiff
Bristol
Kenn
Avon
Bath
Chew
Yeo
Weston.s.Mare
Frome
Axe
Brue
Bridgwater
Parrett
0 5 10 15 20 25 Km
SO
ST
220
10
200
90
80
70
60
50
40
130
320
30
40
50
60
70
380

APPENDIX A: LOCATION MAPS

CROSS SECTIONS, AVONMOUTH TO BEACHLEY.

1:50,000 SCALE.

APPENDIX A: LOCATION MAPS

CROSS SECTIONS, BEACHLEY TO OLDBURY RESERVOIR.

1:50,000 SCALE.

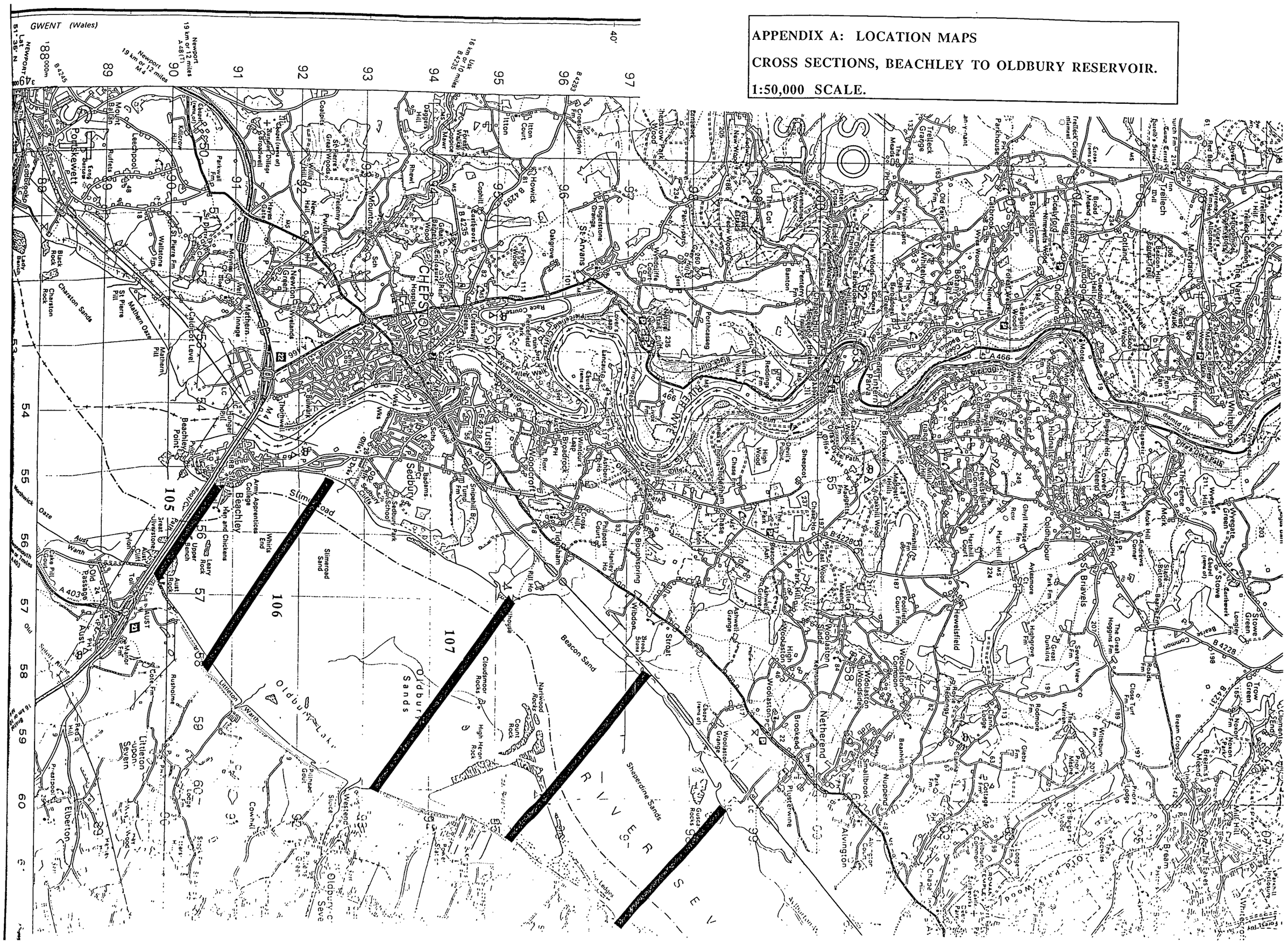
GWENT (Wales)
CHEPSTOW
RIVER WYE
RIVER SEVERN
Beachley
Beachley Point
Slimeroad Sand
Oldbury Sands
Beacon Sand
Shoperdine Sands
Oldbury Lake
Oldbury-on-Severn
Littleton-upon-Severn
Elberton
Aust
Pontskewett
Mounton
St Arvans
Tutshill
Sedbury
Woodcroft
Netherend
Alvington
Bream
Trelleck
Llandogo
Whitebrook
Broadstone
Catbrook
Parkhouse
Trelleck Grange
Trelleck Common
Llandogo Common
Whitebrook Common
Wyndcliffe Wood
Hale Woods
Ninewells Wood
Pentery Fm
Banton
Redding Fm
Lydcott Fm
Porthcasseg
Rogerstone Grange
Howick
Itton
Itton Court
Cross-Bleddyn
Daggers Hill
Cophill
Earthwork
Great Barbastelle Enclosure
Oakgrove
Wyndcliffe
Lover's Leap
Lancaut
Prior's Reach
Longshoppes Reach
Wye Valley Walk
Offa's Dyke Path
Offa's Dyke
Offa's Dyke Centre
Tidenham Chase
Devil's Pulpit
Sheepcote
Chase Fm
Tidenham Park
Tidenham Ho
Pulpits Court
Bulwark
Thornwell
Mathern
Mathern Oaze
Caldicot Level
Caldicot Pill
Mathern Pill
St Pierre Pill
St Pierre Fm
St Pierre's Great Woods
Waltstone Fm
Black Rock
Charston Rock
Charston Sands
Lady Barron
Pontskewett
Mount Ballan
Leechpool
Ruffets
Kilcrow Hill
Parkwall Fm
Hayes Gate
Broadwell
Coalpits
Willis Hill
New Hall
Twelveyric
Moorings
Newton Green
Wetlands
Sch
Chapel (rems of)
Turnpike Cottage
Tumulus
Cromlech
Standing Stone
Roman Villa
Roman Temple
Roman Road
Roman Camp
Ancient Camp
Ancient Settlement
Ancient Earthwork
Ancient Boundary
Ancient Trackway
Ancient Cross
Ancient Dyke
Ancient Ditch
Ancient Bank
Ancient Wall
Ancient Quarry
Ancient Pit
Ancient Mine
Ancient Shaft
Ancient Adit
Ancient Level
Ancient Tunnel
Ancient Well
Ancient Spring
Ancient Stream
Ancient River
Ancient Lake
Ancient Pond
Ancient Reservoir
Ancient Canal
Ancient Aqueduct
Ancient Bridge
Ancient Ford
Ancient Causeway
Ancient Embankment
Ancient Cutting
Ancient Tunnel
Ancient Shaft
Ancient Adit
Ancient Level

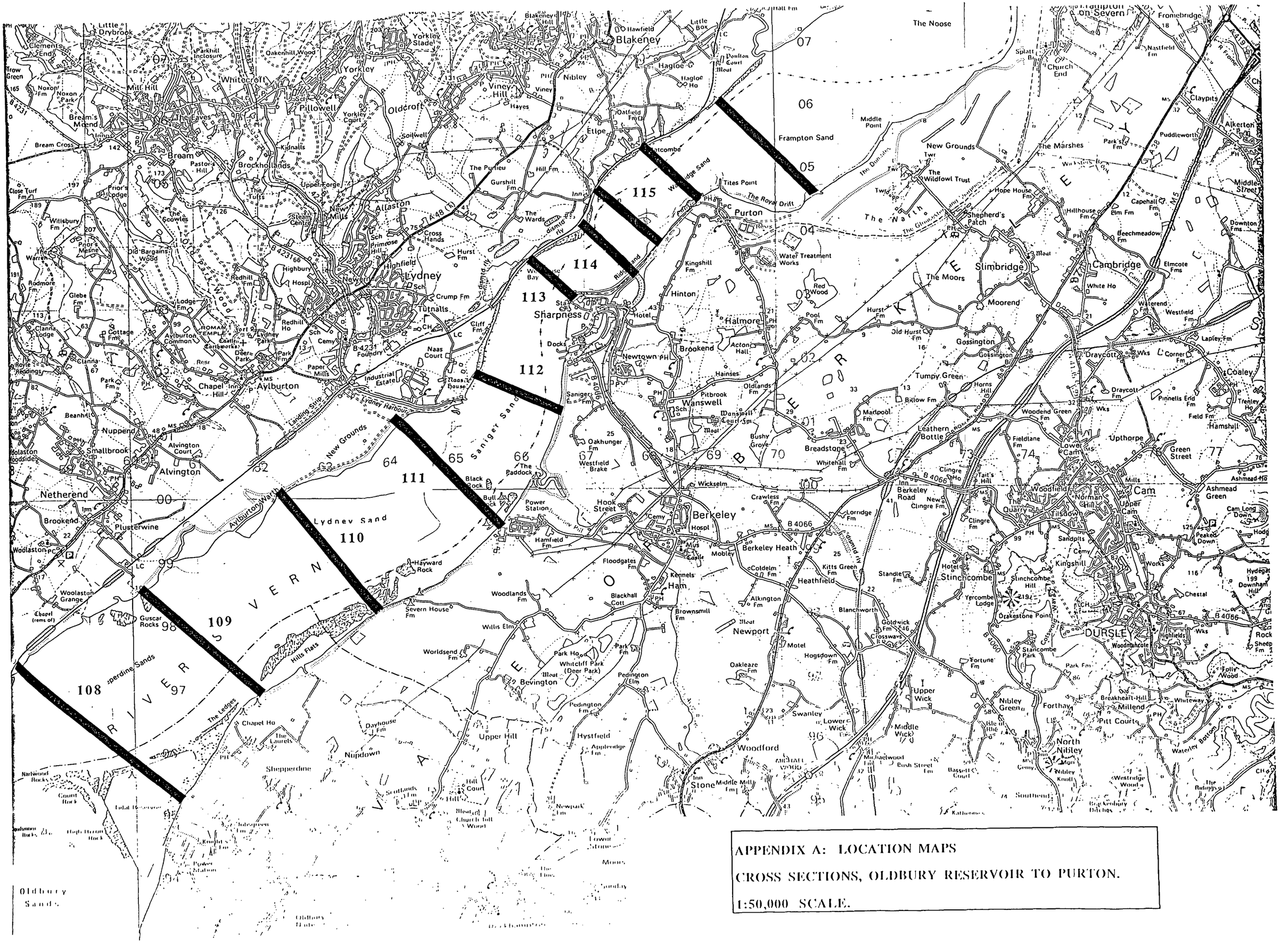
Lydney Sand
Lydney Harbour
Oldbury Sands
RIVER SEVERN
RIVER WYE
Blakeney
Purton
Sharpness
Berkeley
Lydney
Slimbridge
Cambridge
DURSLEY
Frampton Sand
Wainlode Sand
Ridge Sand
Saniger Sand
Perdine Sands
Hills Flats
Guscar Rocks
Narlwood Rocks
Count Rock
High Heron Rock
Oldbury Naite
Oldbury Power Station
Landing Slip
Aylburton Warth
New Grounds
Whitecroft
Pillowell
Oldcroft
Yorkley
Viney Hill
Nibley
Hagloe
Oatfield Fm
Etloe
Middle Point
The Noose
Frampton on Severn
Fromebridge
Claypits
Aikerton
Puddleworth
Middle Street
Capehall Fm
Downton Fms
Beechmeadow Fm
Elmcote Fms
Waterend Fm
Westfield Fm
Lapley Fm
Draycott
Coaley
Pinnells Erid Fm
Trenley
Hamshill
Upthorpe
Green Street
Ashmead Green
Cam Long Down
Peaked Down
Hydegate
Downham Hill
Rock Sheep Fm
Folly Wood
Whiteway
Waterley Bottom
Breakheart Hill
Millend
Pitt Courts
Forthay
Nibley Green
North Nibley
Westridge Wood
Blackbury Ditches
Stinchcombe
Stinchcombe Hill
Drakestone Point
Yercombe Lodge
Kingshill
Highfields
Woodmancote
Folly Wood
Fortune Fm
Standile Fm
Heathfield
Kitts Green Fm
Berkeley Heath
Berkeley Road
New Clingre Fm
Clingre Fm
Lorridge Fm
Crawlesss Fm
Hook Street
Hamfield Fm
Floodgates Fm
Kennels
Ham
Blackhall Cott
Brownsmill Fm
Alkington Fm
Blanchworth
Goldwick Fm
Crossways
Newport
Motel
Hogsdown Fm
Oakleaze Fm
Pedington Fm
Pedington Elm
Bevington
Park Hood
Whitcliff Park (Deer Park)
Park Fm
Worldsend Fm
Willis Elm
Severn House Fm
Woodlands Fm
Hayward Rock
Woolaston Grange
Woolaston Pc
Woolaston Woodside
Netherend
Brookend
Plusterwine
Smallbrook
Nuppend
Alvington
Alvington Court
Beanhill
Shepperdine
Nupdown
Upper Hill
Hystfield
Applelodge Fm
Dayhouse Fm
Chapel Ho
The Laurels
The Ledges
Knoll Fm
Jobsgreen Fm
Scotlands Fm
Church hill Wood
Newpark Fm
Lower Stone
Stone
Middle Mill Fm
Woodford
Middle Wick
Upper Wick
Lower Wick
Swanley
Michaelwood Fm
Bush Street Fm
Bassett Court
Southend
Nibley Knoll
Isle of Rhe
Tumpy Green
Horns Hill
Billow Fm
Marlpool Fm
Leathern Bottle
Woodend Green
Fieldlane Fm
Breadstone
Whitehall Fm
Bushy Grove
Oakhunger Fm
Westfield Brake
Wansell Court Fm
Wansell
Pitbrook
Oldlands Fm
Hainses
Saniger Fm
Newtown
Brookend
Acton Hall
Halmore
Hinton
Kingshill Fm
Water Treatment Works
Red Wood
Pool Fm
Old Hurst Fm
Hurst Fm
Moorend
The Moors
Gossington
Gossington Bridge
Shepherd's Patch
Hope House Fm
The Wildfowl Trust
New Grounds
The Marshes
Park's Fm
Tites Point
The Royal Drift
The Noose
Sharpness Docks
Docks
Naas Court
Naas House
Industrial Estate
Paper Mills
Foundry
Cliff Fm
Crump Fm
Tutnalls
Redhill Ho
Redhill Fm
Highbury
Hurst Fm
Primrose Hill
Cross Hands
Allaston
Newerne
Lydney Park
Lydney Park Woods
Roman Temple
Camp
Earthworks
Deers Park
Park Fm
Aylburton Common
Aylburton
Chapel Inn
Hill
Lodge Fm
Glebe Fm
Rodmore Fm
Prior's Mesne
Old Bargains Wood
The Warren
Prior's Lodge
Close Turf Fm
Willsbury Fm
Bream's Mead
Bream Cross
Bream
Pastors Hill
Brockhollands
The Tufts
Upper Forge
New Mills
Steam Centre
The Scowles
Iron Age Camp
Kidnalls
Soilwell
Yorkley Court
Yorkley Slade
Oakenhill Wood
Parkhill Inclosure
Dean Forest Fm
Mill Hill
Noxon Fm
Noxon Park
Trow Green
Clements End
Little Drybrook
Hawfield
Blakeney Hill
Little Box
Poulton Court Moat
Hagloe Ho
Viney
Hayes
The Purlieu
Gurshill Fm
Hill Fm
The Wards
Inn
Pc
Purton
Kingshill Fm
Hinton
Halmore
Brookend
Newtown
Hainses
Oldlands Fm
Pitbrook
Wansell
Marlpool Fm
Billow Fm
Tumpy Green
Horns Hill
Leathern Bottle
Woodend Green
Fieldlane Fm
Breadstone
Whitehall Fm
Bushy Grove
Oakhunger Fm
Westfield Brake
Wansell Court Fm
Saniger Fm

APPENDIX A: LOCATION MAPS

CROSS SECTIONS, PURTON TO LONGNEY.

1:50,000 SCALE.

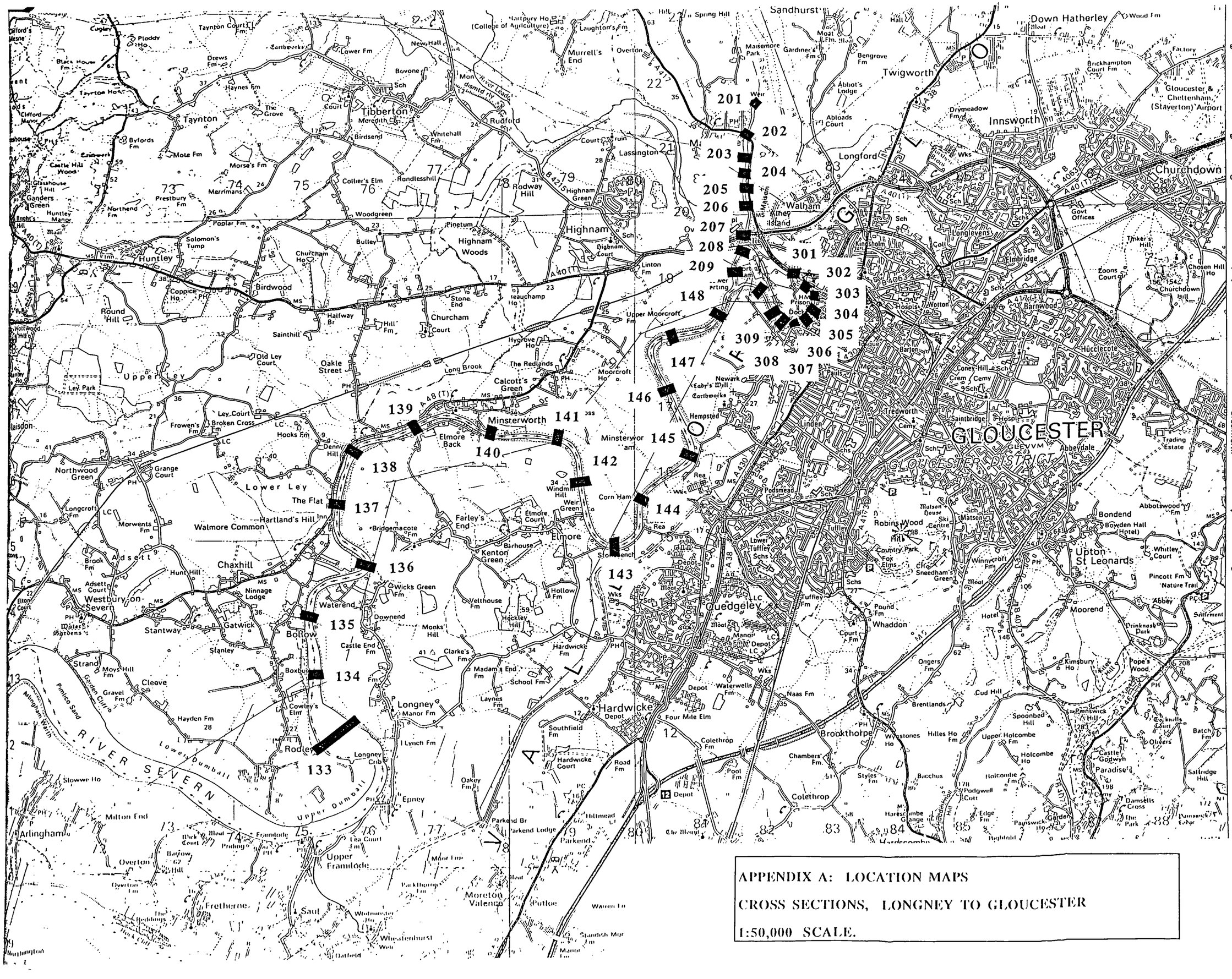
Longney
Hardwicke
Quedgeley
GLOUCESTER
Twigworth
Innsworth
Down Hatherley
Churchdown
Brockworth
Upton St Leonards
Abbeydale
Tuffley
Matson
Podsmead
Barnwood
Hucclecote
Brookthorpe
Colethrop
Whaddon
Moorend
Longford
Walham
Highnham
Tibberton
Taynton
Huntley
Birdwood
Minsterworth
Elmore
Chaxhill
Westbury-on-Severn
Stantway
Bollow
Rodley
Arlingham
Upper Framilode
Saul
Fretherne
Moreton Valence
Epney
Lower Ley
Upper Ley
Northwood Green
Adsett
Walmore Common
Hartland's Hill
Sandhurst
Maisemore
Abbots Lodge
Longlevens
Kingsholm
Wotton
Tredworth
Linden
Robins Wood
Upton St Leonards
Cheltenham 6 km or 4 miles A40 (T)
Cheltenham 6 km or 4 miles B 4075
Cheltenham 10 km or 6 miles A46
Tewkesbury 18 km or 11 miles A38
CHELTENHAM
Cotswold Way
RIVER SEVERN
Lower Dumbell
Upper Dumbell
Pmlico Sand
Gravel
Mingham Warth
Garden Cliff
Hock Cliff
Oldbury Ho (College of Agriculture)
Laughton's Fm
Murrell's End
Overton
Spring Hill
Mon & Brec Canal
River Leadon
dismtd rly
Gloucester & Cheltenham (Staverton) Airport
Brickhampton Court Fm
Drymeadow Fm
Abloads Court
Bengrove Fm
Gardiner's Fm
Moat Fm
Factory
Wood Fm
Govt Offices
Tinker's Hill
Chosen Hill Ho
Churchdown Hill
Zoons Court
Longlevens
Imbridge
Kingsholm
Wotton
Hospl
Barton
Mosque
Coney Hill
Crem
Cemy
Fabr's Well
Newark
Cartworks
Saintbridge
Trading Estate
Abbeydale
GLEVUM
GLOUCESTER DISTRICT
Matson House
Ski Centre
Robins Wood Hill
Country Park
Fox Elms
Winnycroft Fm
Bowden Hall (Hotel)
Bondend
Whitley Court
Pincott Fm
Nature Trail
Abbey
Settlement
Prinknash Park
Pope's Wood
Kimsbury Ho
Kites Hill
Cud Hill
Brentlands
Pennswick
Spoonbed Hill
Batch Fm
Daisells Cross
Castle Godwyn
Paradise
Holcombe Ho
Holcombe Fm
Upper Holcombe Fm
Hilles Ho Fm
Wainstones Ho
Podgwell Cott
Bacchus
Styles Fm
Chambers' Fm
Pool Fm
Road Fm
Hardwicke Court
Southfield Fm
Four Mile Elm
Naas Fm
Waterwells Fm
Depot
Manor Fm
Court Fm
Pound Fm
Ongers Fm
Hotel
Sch
Govt Offices
Hospl
Cemy
Crem
Wks
Ruin
Mill
Ch
Meeting House
Factory
Depot
Weir
Ferry
Ford
Footbridge
Pier
Lock
Sluice
Tunnel
Cutting
Embankment
Level Crossing
Station
Bridge
Viaduct
Aqueduct

APPENDIX B

NOMENCLATURE USED

Appendix B: Terminology Used.

Nomenclature used in main body of text;

A	Cross-sectional area (m^2)
a (k , i , z)	Tabulated value of cross-sectional area at section i on branch k, for given height z, at metre intervals (in programme).
area (k , i , t)	Value of cross-sectional area at section i on branch k at time t (in programme).
{A,B,C,D}	Set of four points in the Preissman scheme
(A,B,C)	Reaches about a river branch
B	Breadth (m).
B_W	Breadth of weir (m).
b (k , i , z)	Tabulated value of breadth at cross section j on branch k, for given height z, at metre intervals (in programme).
b_i	Breadth of slice i
breadth (i,j,t)	Value of breadth at section j, on branch k at time t (in programme).
c1-c7	Coefficients used to simplify frequantly used calculations.
CR	Courant number
C	Resistance constant
c	Wave speed or celerity
E	Central point in the Preissman scheme
F(1)t	Known value of a function (at a position and time)
F_H	Total hydrostatic pressure force.
F_B	Force due to breadth change.
F_G	Total force due to gravity.
F_F	Friction resistance force.
G	Value of an equation
G_d	Value of the discrete form of an equation
g	Acceleration due to gravity (m/s^2)
HAT	Highest Astronomical Tide

h	Water depth (maximum) (m).
I	Integral term.
I	End (I th) section of channel reach, an external boundary section.
i	Sectional position definer.
J	Final (J th) time level of calculation (end of simulation period).
j	Time level definer.
K	Conveyance factor
L	Lateral inflow / outflow per unit length of reach.
LAT	Lowest Astronomical Tide
M	Momentum flux at a section.
M_F	Net momentum flux.
MHWS	Mean High Water Spring
MLWS	Mean Low Water Spring
MHWN	Mean High Water Neap
MLWN	Mean Low Water Neap
ML	Mean Level
MSL	Mean Sea Level
MTL	Mean Tidal Level
m	Mass.
mAOD	Metres above Ordnance Datum
n	Manning roughness value
O	Truncation error
PF_H	Hydrostatic pressure force.
Q	Quantity of flow ($m^3 s^{-1}$).
q	Coefficient in compatibility equations.
qq	Coefficient in compatibility equations.
R	Hydrualic radius.
R_n	Residual terms not covered by Taylor series expansion.
S	Channel slope.
S_f	Friction slope.

S_o	Channel slope.
t	Time (s).
T	Period
u or U	Depth averaged velocity of flow (m/s)
U_L	Velocity of lateral inflow or outflow per unit length.
V	Velocity of flow (m/s)
W	Wetted perimeter
wp	Tabulated value of wetted perimeter at cross section j, for given height z, at metre intervals (in programme).
Wetp	Value of wetted perimeter at section j , branch k at time t (in programme).
x	Distance point.
xdist	Distance between sections in metres (in programme).
Z	Elevation of water surface (m).
$Z_{ds\ or\ us}$	Elevation of water surfece upstream or downstream of a point
α	Coefficient in linearisation of recurrence relations
β	Coefficient in linearisation of recurrence relations
ß	Coefficient of non linear velocity (Boussinesq Coefficient)
γ	Coefficient in linearisation of recurrence relations
δ	Coefficient in linearisation of recurrence relations
ε	Coefficient in linearisation of recurrence relations
alpha	Coefficient in linearisation of recurrence relations (in programme)
beta	Coefficient in linearisation of recurrence relations (in programme)
delta	Coefficient in linearisation of recurrence relations (in programme)
gamma	Coefficient in linearisation of recurrence relations (in programme)
epsilon	Coefficient in linearisation of recurrence relations (in programme)
branchα	Coefficient in branched river calculations
branchβ	Coefficient in branched river calculations
branchγ	Coefficient in branched river calculations
Δx	Distance between sections (m).
ΔM	Change in momentum.

f	Function of
f'	First derivative of a function
ρ	Density.
μ	Weir flow coefficient

APPENDIX C

FRICTION VALUES

Appendix C, *Friction Values,* Main Channel

SECTION	SECTION NUMBER	UPSTREAM DISTANCE (m)	BASIC MANNING'S n	VEGETATION (+)	SIZE CHANGE (+)	n'	MEANDERS (+)	FINAL n
AVONMOUTH	100	0	0.022	0.000	0.002	0.024	0.000	0.024
SHOOTS	101	4588	0.022	0.000	0.002	0.024	0.000	0.024
SUDBROOK	102	6963	0.024	0.000	0.002	0.026	0.000	0.026
NORTHWICK	103	8963	0.022	0.000	0.002	0.024	0.000	0.024
AUSTWHARF	104	10538	0.022	0.000	0.004	0.026	0.000	0.026
BEACHLEY	105	11913	0.024	0.000	0.005	0.029	0.000	0.029
LITTLETON	106	13463	0.022	0.000	0.004	0.026	0.000	0.026
INWARD ROCK	107	16726	0.022	0.000	0.004	0.026	0.000	0.026
NARLWOOD	108	18813	0.020	0.000	0.005	0.025	0.000	0.025
WHITE HOUSE	109	21088	0.022	0.000	0.000	0.022	0.000	0.022
LYDNEY	110	23563	0.022	0.000	0.000	0.022	0.000	0.022
BERKELEY	111	25900	0.022	0.000	0.000	0.022	0.000	0.022
FAIRTIDE ROCKS	112	27550	0.022	0.000	0.000	0.022	0.000	0.022
SHARPNESS	113	29313	0.022	0.000	0.000	0.022	0.000	0.022
WELLHOUSE ROCK	114	30313	0.022	0.000	0.000	0.022	0.000	0.022
PURTON	115	30809	0.022	0.000	0.000	0.022	0.000	0.022
GATCOMBE	116	31833	0.020	0.000	0.000	0.020	0.000	0.020

SECTION	SECTION NUMBER	UPSTREAM DISTANCE	BASIC MANNING'S n	VEGETATION (+)	SIZE CHANGE (+)	n'	MEANDERS (+)	FINAL n
SLIMBRIDGE	117	35291	0.020	0.000	0.000	0.020	0.000	0.020
FRAMPTON	118	37509	0.020	0.000	0.000	0.020	X0.15n	0.023
FRETHERN	119	38913	0.020	0.000	0.004	0.024	X0.15n	0.028
NORTHINGTON	120	40745	0.020	0.000	0.000	0.020	X0.15n	0.023
BOXGROVE	121	41812	0.020	0.000	0.000	0.020	X0.15n	0.023
BULLOPILL	122	42889	0.020	0.000	0.000	0.020	X0.15n	0.023
NEWNHAM	123	43882	0.020	0.000	0.000	0.020	X0.15n	0.023
HAWKING PILL	124	44843	0.020	0.000	0.000	0.020	X0.15n	0.023
ARLINGHAM WHARF	125	45855	0.020	0.000	0.000	0.020	X0.15n	0.023
PIMLICO SANDS	126	46995	0.020	0.000	0.000	0.020	X0.15n	0.023
ARLINGTON	127	47945	0.020	0.000	0.000	0.020	X0.15n	0.023
LOWER DUMBALL	128	49133	0.020	0.000	0.000	0.020	X0.15n	0.023
PRIDING	129	50031	0.020	0.000	0.000	0.020	X0.15n	0.023
FRAMILODE	130	50944	0.020	0.000	0.000	0.020	X0.15n	0.023
UPPER DUMBAL	131	51968	0.020	0.000	0.000	0.020	X0.15n	0.023
NEW INN (EPNEY)	132	53035	0.020	0.000	0.000	0.020	X0.15n	0.023
LONGNEY	133	53758	0.020	0.000	0.030	0.023	X0.15n	0.026
BOLLOPOOL	134	54920	0.020	0.000	0.000	0.020	X0.15n	0.023
CONSTANCE FARM	135	55892	0.020	0.000	0.000	0.020	X0.15n	0.023

SECTION	SECTION NUMBER	UPSTREAM DISTANCE	BASIC MANNING'S n	VEGETATION (+)	SIZE CHANGE (+)	n'	MEANDERS (+)	FINAL n
HILL FARM	136	57022	0.020	0.000	0.000	0.020	X0.15n	0.023
THE FLAT	137	58120	0.020	0.000	0.000	0.020	X0.15n	0.023
DENNY HILL	138	59239	0.020	0.000	0.000	0.020	X0.15n	0.023
WEST MINSTERWORTH	139	60242	0.020	0.000	0.000	0.020	0.000	0.020
MIDDLE MINSTERWORTH	140	61319	0.020	0.000	0.000	0.020	0.000	0.020
EAST MINSTERWORTH	141	62407	0.020	0.000	0.000	0.020	0.000	0.020
WINDMILL HILL	142	63326	0.020	0.000	0.000	0.020	0.000	0.020
ELMORE	143	64361	0.020	0.000	0.000	0.020	0.000	0.020
CORNHAM	144	65501	0.020	0.000	0.000	0.020	0.000	0.020
UPPER REA	145	66504	0.020	0.000	0.000	0.020	0.000	0.020
MINSTERWORTH HAM	146	67560	0.020	0.000	0.000	0.020	0.000	0.020
MOOR FARM	147	68674	0.020	0.000	0.000	0.020	0.000	0.020
SUMEADOW	148	69693	0.020	0.000	0.000	0.020	0.000	0.020

Calculation of Manning friction values, *SCS method (1963), main channel.*

Appendix C, Friction Values, Main Channel

SECTION	SECTION NUMBER	UPSTREAM DISTANCE (m)	CHOW
AVONMOUTH	100	0	0.025
SHOOTS	101	4588	0.025
SUDBROOK	102	6963	0.025
NORTHWICK	103	8963	0.025
AUSTWHARF	104	10538	0.025
BEACHLEY	105	11913	0.025
LITTLETON	106	13463	0.025
INWARD ROCK	107	16726	0.025
NARLWOOD	108	18813	0.025
WHITE HOUSE	109	21088	0.025
LYDNEY	110	23563	0.025
BERKELEY	111	25900	0.025
FAIRTIDE ROCKS	112	27550	0.025
SHARPNESS	113	29313	0.025
WELLHOUSE ROCK	114	30313	0.025
PURTON	115	30809	0.025
GATCOMBE	116	31833	0.025
SLIMBRIDGE	117	35291	0.025
FRAMPTON	118	37509	0.025
FRETHERN	119	38913	0.025
NORTHINGTON	120	40745	0.025
BOXGROVE	121	41812	0.025
BULLOPILL	122	42889	0.025
NEWNHAM	123	43882	0.025
HAWKING PILL	124	44843	0.025
ARLINGHAM WHARF	125	45855	0.025
PIMLICO SANDS	126	46995	0.025
ARLINGTON	127	47945	0.025

SECTION	SECTION NUMBER	UPSTREAM DISTANCE	CHOW
LOWER DUMBALL	128	49133	0.025
PRIDING	129	50031	0.025
FRAMILODE	130	50944	0.025
UPPER DUMBAL	131	51968	0.025
NEW INN (EPNEY)	132	53035	0.025
LONGNEY	133	53758	0.025
BOLLOPOOL	134	54920	0.025
CONSTANCE FARM	135	55892	0.025
HILL FARM	136	57022	0.025
THE FLAT	137	58120	0.025
DENNY HILL	138	59239	0.025
WEST MINSTERWORTH	139	60242	0.025
MIDDLE MINSTERWORTH	140	61319	0.025
EAST MINSTERWORTH	141	62407	0.025
WINDMILL HILL	142	63326	0.025
ELMORE	143	64361	0.025
CORNHAM	144	65501	0.025
UPPER REA	145	66504	0.025
MINSTERWORTH HAM	146	67560	0.025
MOOR FARM	147	68674	0.025
SUMEADOW	148	69693	0.025

Manning friction values, after Chow (1959), main channel.

Appendix C, Friction Values, West Channel

SECTION	SECTION NUMBER	UPSTREAM DISTANCE (m)	BASIC MANNING'S n	VEGETATION (+)	SIZE CHANGE (+)	n'	MEANDERS (+)	FINAL n
PORT HAM	209	70504	0.023	0.000	0.000	0.023	0.000	0.023
PORT HAM NORTH	208	70764	0.023	0.000	0.000	0.023	0.000	0.023
OVER	207	71020	0.023	0.000	0.000	0.023	0.000	0.023
ALNEY ISLAND	206	71353	0.023	0.000	0.000	0.023	0.000	0.023
MAISEMORE HAM SOUTH	205	71670	0.023	0.000	0.000	0.023	0.000	0.023
MAISEMORE HAM MIDDLE	204	71966	0.023	0.000	0.000	0.023	0.000	0.023
MAISEMORE HAM NORTH	203	72278	0.023	0.000	0.000	0.023	0.000	0.023
MAISEMORE	202	72610	0.023	0.000	0.000	0.023	0.000	0.023
MAISEMORE WEIR	201	72911	0.023	0.000	0.000	0.023	0.000	0.023

Calculation of Manning friction values, SCS method (1963), West channel.

Appendix C, Friction Values, West Channel

SECTION	SECTION NUMBER	UPSTREAM DISTANCE (m)	CHOW
PORT HAM	209	70504	0.025
PORT HAM NORTH	208	70764	0.025
OVER	207	71020	0.025
ALNEY ISLAND	206	71353	0.025
MAISEMORE HAM SOUTH	205	71670	0.025
MAISEMORE HAM MIDDLE	204	71966	0.025
MAISEMORE HAM NORTH	203	72278	0.025
MAISEMORE	202	72610	0.025
MAISEMORE WEIR	201	72911	0.025

Manning friction values, after Chow (1959), West channel.

Appendix C, Friction Values, East Channel

SECTION	SECTION NUMBER	UPSTREAM DISTANCE (m)	BASIC MANNING'S n	VEGETATION (+)	SIZE CHANGE (+)	n'	MEANDERS (+)	FINAL n
SOUTH SUD MEADOW	309	70503	0.023	0.000	0.000	0.023	0.000	0.023
SUD MEADOW NORTH	308	70957	0.023	0.000	0.000	0.023	0.000	0.023
LLANTHONY MILL	307	71603	0.023	0.000	0.002	0.025	0.000	0.025
LLANTHONY	306	71221	0.023	0.000	0.000	0.023	0.000	0.023
CASTLEMEADS SOUTH	305	71490	0.023	0.000	0.000	0.023	0.000	0.023
GLOUCESTER DOCKS	304	71733	0.023	0.000	0.000	0.023	0.000	0.023
GLOUCESTER PRISON	303	71897	0.023	0.000	0.000	0.023	0.000	0.023
CASTLEMEADS NORTH	302	72272	0.023	0.000	0.000	0.023	0.000	0.023
WESTGATE BRIDGE	301	72541	0.023	0.000	0.000	0.023	0.000	0.023

Calculation of Manning friction values, SCS method (1963), East channel.

Appendix C, Friction Values, East Channel

SECTION	SECTION NUMBER	UPSTREAM DISTANCE (m)	CHOW
SOUTH SUD MEADOW	309	70503	0.025
SUD MEADOW NORTH	308	70957	0.025
LLANTHONY MILL	307	71603	0.025
LLANTHONY	306	71221	0.025
CASTLEMEADS SOUTH	305	71490	0.025
GLOUCESTER DOCKS	304	71733	0.025
GLOUCESTER PRISON	303	71897	0.025
CASTLEMEADS NORTH	302	72272	0.025
WESTGATE BRIDGE	301	72541	0.025

Manning friction values, after Chow (1959), East Channel.

APPENDIX D

COMPUTER PROGRAM

University of Bristol
Dept.of Geology
Damian Taylor 1991

Arguments

nosects	- number of sections
xdist	- distance between section n and n+1
friction	- friction between section n and n+1
snames	- section names
mn,mx	- minimum and maximum tabulated elevations for each section
a	- area of section at given position and tidal elevation
b	- breadth of section at given position and tidal elevation
wp	- wetted perimeter of section at given position and tidal elevation
weirht	- height of weir at end section
weirb	- breadth of weir at end section
weirprob	- =true if weir problem is required
z	- tidal elevation at given position and time
Q	- quantity of flow at given position and time
l	- lateral inflow at a given position (may be set for position and time)
ul	- velocity of flow of lateral inflow at a given position
area	- area of section at given position and time
breadth	- breadth of section at given position and time
wetp	- wetted perimeter of section at given postion and time
sect	- section number used in loops
t	- time step
n,m	- section,time parameters used in loops
iter	- iteration number for each time step
convey	- conveyance of section at given postion and time
g	- acceleration due to gravity
c1-c7	- variables used in first sweep
alpha -epsilon	- variables used in first sweep calculated from c1-c5
p-t	- variables used in first sweep calculated from alpha - epsilon at a given position
z/Qresid	- residuals used in calculation of convergence
z/Qdummy	- dummy variables used in calculation of convergence
z/Qtol	- tolerance allowed for convergence
ht1-3	- ht at section used in interpolation routine
theta	- time weighting factor
tinc	- time step in seconds
tj	- number of time steps in tidal cycle

```
declare variables
integer nosects(3),weirprob
real xdist(3,0:50),friction(3,50),zmax(3,50),zmin(3,50)
character*8 snames(3,50)
integer branch
```

```
      integer mn(3,50),mx(3,50),stats(3,10),zt,noweirs,weirpos(3,50)
      real a(3,50,-10:15),b(3,50,-10:15),wp(3,50,-10:15)
      real area(3,50,0:2000),breadth(3,50,0:2000),wetp(3,50,0:2000)
      real z(3,50,0:2000),Q(3,50,0:2000),convey(3,50,0:2000)
      real l(3,50,0:2000),ul(3,50,0:2000),least(3,50),lmax(3,50)
      real tinc,theta,ztol,Qtol,xd,lh(3,50),rh(3,50)
      integer tmax(3,50),tmin(3,50)
      integer sect,t,iter,tj,i,cyc,j,k,tcycle
      real g,p(3,50),qq(3,50),r(3,50),s(3,50),tt(3,50)
      real branchalpha,branchbeta,branchgamma
      real weirht(3,50),weirb(3,50),fr
      parameter (g=9.81)
      character*8 savename
c
c     ----------------------------------------------------------------
c
c     declare common blocks
c
      common /hthydro/a,b,wp
      common /thydro/area,breadth,wetp,convey,friction
      common /weight/tinc,theta
      common /inf/l,ul,lh,rh
      common /weirdo/weirpos,weirht,weirb
      common /dependants/z,Q
      common /coeffs/p,qq,r,s,tt
c
c
c      ----------------------------------------------------------------
c
c     read breath and height of weir from file 'weir'
c     read weir problem value (=1) if weir problem is required
c
      open(unit=11,file='weirbranch2',status='old',form='formatted')
      rewind(11)
      read(11,*) weirprob,noweirs
      if (noweirs.ne.0.and.weirprob.ne.0) then
      do 89 i=1,noweirs
      read(11,*) branch,sect
      weirpos(branch,sect)=1
      read(11,*) weirht(branch,sect),weirb(branch,sect)
89    continue
      endif
      close(11)

c     ----------------------------------------------------------------
c
c     read values of time increment, time weighting and tolerance for
c     convergence
c
      open (unit=15,file='xtras3',status='old',form='formatted')
      rewind(15)
      read(15,*) tinc,theta,ztol,Qtol,cyc,savename,fr
      close(15)
c
c     ----------------------------------------------------------------
c
c     open and read data from general file including
c     number of sections, distances between sections, friction and
c     file names of sections.
c
c     friction may be adjusted so that it is time dependant as well
c     as by position
c
      if (weirprob.eq.0) then
      open(unit=9,file='severn1wall',status='old',form 'formatted')
      else
```

```
      open(unit=9,file='severn1weirwall',status='old',form='formatted')
      endif
      rewind(9)
      read(9,*) nosects(1)
      do 110 i=nosects(1),2,-1
        if (weirpos(1,i).eq.1.and.weirprob.eq.1) then
         i=i-1
        endif
        read(9,*) snames(1,i),xdist(1,i-1),friction(1,i-1),lh(1,i-1)
     *    ,rh(1,i-1)
      if (fr.ne.0) then
       friction(1,i-1)=fr
       friction(1,nosects(1))=fr
      endif
110   continue
        read(9,*) snames(1,1),xdist(1,0)
        read(9,*) xdist(1,nosects(1)),friction(1,nosects(1))
     *             ,lh(1,nosects(1)),rh(1,nosects(1))
      close(9)
      if (weirprob.eq.0) then
      open(unit=9,file='severn2wall',status='old',form='formatted')
      else
      open(unit=9,file='severn2weirwall',status='old',form='formatted')
      endif
      rewind(9)
      read(9,*) nosects(2)
      do 111 i=nosects(2),1,-1
        if (weirpos(2,i).eq.1.and.weirprob.eq.1) then
         i=i-1
        endif
        read(9,*) snames(2,i),xdist(2,i),friction(2,i),lh(2,i)
     *    ,rh(2,i)
      if (fr.ne.0) then
        friction(2,i)=fr
      endif
111   continue
      close(9)
      if (weirprob.eq.0) then
      open(unit=9,file='severn3wall',status='old',form='formatted')
      else
      open(unit=9,file='severn3weirwall',status='old',form='formatted')
      endif
      rewind(9)
      read(9,*) nosects(3)
      do 112 i=nosects(3),1,-1
        if (weirpos(3,i).eq.1.and.weirprob.eq.1) then
         i=i-1
        endif
        read(9,*) snames(3,i),xdist(3,i),friction(3,i),lh(3,i)
     *    ,rh(3,i)
      if (fr.ne.0) then
        friction(3,i)=fr
      endif
112   continue
      close(9)

c
c     ------------------------------------------------------------
c
c     open and read from individual section files the
c     values of area, breadth, wetted perimeter between mn and mx
c     values.
c
      do 113 j=1,3
      do 99 i=1,nosects(j)
        if (weirpos(j,i).ne.1) then
```

```
          open(unit=10,file=snames(j,i),status='old',form='formatted')
          rewind(10)
          read(10,*) least(j,i),mx(j,i),dummy,dummy
          mn(j,i)=int(least(j,i))
          read(10,*) (a(j,i,k),k=mn(j,i),mx(j,i))
          read(10,*) (b(j,i,k),k=mn(j,i),mx(j,i))
          read(10,*) (wp(j,i,k),k=mn(j,i),mx(j,i))
        close(10,*)
        endif
99      continue
113     continue
c
c
c       ---------------------------------------------------------------
c
c       read boundary conditions at section 1 (tidal altitudes)
c       and end section (N) (quantity of flow)
c
c
        open(unit=12,file='zbound',status='old',form='formatted')
        rewind(12)
        tj=0
        read(12,*) z(1,nosects(1),0)
        do 115 while (z(1,nosects(1),tj).lt.999)
          tj=tj+5
          read(12,*) z(1,nosects(1),tj)
          z(1,nosects(1),tj-4)=(z(1,nosects(1),tj)
     *     -z(1,nosects(1),tj-5))/5+z(1,nosects(1),tj-5)
          z(1,nosects(1),tj-3)=(z(1,nosects(1),tj)
     *     -z(1,nosects(1),tj-5))*2/5+z(1,nosects(1),tj-5)
          z(1,nosects(1),tj-2)=(z(1,nosects(1),tj)
     *     -z(1,nosects(1),tj-5))*3/5+z(1,nosects(1),tj-5)
          z(1,nosects(1),tj-1)=(z(1,nosects(1),tj)
     *     -z(1,nosects(1),tj-5))*4/5+z(1,nosects(1),tj-5)
115     continue
        close(12)
        z(1,nosects(1),tj)=z(1,nosects(1),0)
        tj=tj-10
        z(1,nosects(1),tj+1)=z(1,nosects(1),0)
        open(unit=18,file='qbound',status='old',form='formatted')
        open(unit=23,file='qboundc',status='old',form='formatted')
        rewind(18)
        rewind(23)
        read(18,*) (Q(2,1,j),j=0,tj,5)
        read(23,*) (Q(3,1,j),j=0,tj,5)
        close(18)
        close(23)
        do 40 j=1,tj,5
          Q(3,1,j)=Q(3,1,j-1)
          Q(3,1,j+1)=Q(3,1,j-1)
          Q(3,1,j+2)=Q(3,1,j-1)
          Q(3,1,j+3)=Q(3,1,j-1)
          Q(2,1,j)=Q(2,1,j-1)
          Q(2,1,j+1)=Q(2,1,j-1)
          Q(2,1,j+2)=Q(2,1,j-1)
          Q(2,1,j+3)=Q(2,1,j-1)
40      continue
c
c       ---------------------------------------------------------------
c
c       read initial conditions for points at time = 0
c       from file initial
c
        open(unit=13,file='zinitial',status='old',form='formatted')
        rewind(13)
        read(13,*) (z(1,i,0),i=1,nosects(1)-1)
```

```
      read(13,*) (z(2,i,0),i=1,nosects(2))
      read(13,*) (z(3,i,0),i=1,nosects(3))
      close(13)
      open(unit=19,file='qinitial',status='old',form='formatted')
      rewind(19)
      read(19,*) (Q(1,i,0),i=1,nosects(1))
      read(19,*) (Q(2,i,0),i=2,nosects(2))
      read(19,*) (Q(3,i,0),i=2,nosects(3))
      close(19)
      do 190 j=1,3
        do 191 i=1,nosects(j)
          if (j.eq.1) then
            Q(1,i,0)=Q(3,1,0)+Q(2,1,0)
          elseif (j.eq.2) then
            Q(2,i,0)=Q(2,1,0)
          elseif (j.eq.3) then
            Q(3,i,0)=Q(3,1,0)
          endif
191       continue
190     continue

c
c       Q at all points except end point (N) will usually be set to
c       zero, assumng tide is on the turn.
c       the effect of initial values is quickly diminished with this
c       form of solution
c
c       ---------------------------------------------------------------
c
c       read lateral inflow quantities and velocities for each point
c       These can be adjusted to be time dependant,
c       especially in an estuary of small tidal range.
c       SET TO ZERO IN THIS EXAMPLE
c       open (unit=14,file='lateral',status='old',form='formatted')
c       rewind(14)
        do 117 j=1,3
        do 231 i=1,nosects(j)
        l(j,i,0)=0
c       read(14,*) (l(j,i,0),i=1,nosects(j))
c       read(14,*) (ul(j,i),i=1,nosects(j))
231     continue
117     continue
c       close(14)
c
c
c       ---------------------------------------------------------------
c
        open(unit=20,file='stationsbranch',status='old'
     *           ,form='formatted')
        rewind(20)
        read(20,*) (stats(1,i),i=1,10)
        read(20,*) (stats(2,i),i=1,5)
        read(20,*) (stats(3,i),i=1,5)
        close(20)
c
c       ---------------------------------------------------------------
c
c       run main program for three three tidal cycles (tcycle)
c       each cycle is for tj time steps (10 mnutes each over tidal period )

        do 180 i=1,3
          do 181 j=1,nosects(i)
            if (weirpos(i,j).eq.1) then
                Q(i,j,0)=Q(i,1,0)
            endif
181       continue
```

```
180     continue
c
c
        do 100 tcycle=1,cyc
         do 101 t=0,tj
c
            iter=1
c           m=t+1
c
c           check to see if this is the first iteration at this position
c           and time, and set future values accordingly. With z and q being
c           set at the same value on previous time step for the first
c           iteration and as the best estimate for future iterations
c
200         if (iter.eq.1) then
              do 104 sect=1,nosects(1)-1
                z(1,sect,t+1)=z(1,sect,t)
                Q(1,sect+1,t+1)=Q(1,sect+1,t)
104           continue
              do 145 sect=1,nosects(2)-1
                z(2,sect,t+1)=z(2,sect,t)
                Q(2,sect+1,t+1)=Q(2,sect+1,t)
145           continue
              do 146 sect=1,nosects(3)-1
                z(3,sect,t+1)=z(3,sect,t)
                Q(3,sect+1,t+1)=Q(3,sect+1,t)
146           continue
                Q(1,1,t+1)=Q(1,1,t)
                z(3,nosects(3),t+1)=z(3,nosects(3),t)
                z(2,nosects(2),t+1)=z(2,nosects(2),t)
            endif
c
c           calculate hydraulic constants at all positions  and at
c           present time step using interpol subroutine
c
            do 121 i=1,3
            do 150 sect=1,nosects(i)
            call interpol(t,sect,least,i)
            call interpol(t+1,sect,least,i)
150         continue
121         continue
            do 120 i=1,3
            do 133 sect=1,nosects(i)-1
            if (amax1(z(i,sect,t),z(i,sect+1,t)).gt.
     *         amin1(lh(i,sect),lh(i,sect+1)
     *         ,rh(i,sect),rh(i,sect+1))) then
            call inflow(t,sect,i,xdist)
            call inflow(t+1,sect,i,xdist)
            endif
133         continue
120         continue
c
c           calculate conveyance for present and next time step
c           using con subroutine
c
          do 122 i=1,3
              do  167 j=1,nosects(i)
                if (z(i,j,t).lt.least(i,j)+1.0.or.z(i,j,t+1)
     *             .lt.least(i,j)+1.0) then
                   friction(i,j)=friction(i,j)+0.02
                endif
167           continue
            call con(t,nosects,g,i)
            call con(t+1,nosects,g,i)
               do 168 j=1,nosects(i)
                 if (z(i,j,t).lt.least(i,j)+1.0.or.z(i,j,t+1)
```

```
     *              .lt.least(i,j)+1.0) then
                   friction(i,j)=friction(i,j)-0.02
                 endif
168           continue
122           continue
c
c             check to see if weir problem is required and that the weir
c             is overtopped, correcting q at this boundary point as required
c
c             If the boundary conditions are corrected for overtopping the
c             a greater number of tidal cycles will be required to reach a
c             convergent solution
c
c             first sweep
c
              do 123 i=3,1,-1
              do 102 sect=1,nosects(i)-1
                if (weirprob.eq.1.and.weirpos(i,sect+1).eq.1) then
c               call sweep1weir(i,sect+1,t)
                call sweep1weir(i,sect+1,t+1)
                sect=sect+2
                endif
                call sweep1(t,nosects,sect,xdist,g,i
     *               ,branchalpha,branchbeta,branchgamma)
102           continue
123           continue
c
c              second sweep
c
              zresid=0
              Qresid=0
              do 124 i=1,3
              do 103 sect=nosects(i)-1,1,-1
                   n=sect+1
                if (weirprob.eq.1.and.weirpos(i,sect).eq.1.and.
     *               sect.ne.1) then
c               call sweep2weir(i,sect,t,area)
                call sweep2weir(i,sect,t+1,area)
                sect=sect-2
               endif
               zdummy=z(i,sect+1,t+1)
               Qdummy=Q(i,sect,t+1)
               call sweep2(t,sect,nosects,least,breadth,area,
     *            friction,xdist,zt,tcycle,i,branchalpha,branchbeta
     *            ,branchgamma)
              zresid=zresid+abs(zdummy-z(i,sect+1,t+1))
              Qresid=Qresid+abs(Qdummy-Q(i,sect,t+1))
             if (i.eq.2.or.i.eq.3.and.sect.eq.1.and.tcycle.gt.3) then
c              Q(i,sect,t+1)=Q(i,sect+1,t+1)
             endif
103           continue
124           continue
c
c             check for convergence, if outside of tolerance then reiterate
c             at this time level to a maximum of 60 iterations
c

              if (iter.ge.60) then
                 iter=1
                 goto 101
              endif
              if (zresid.gt.ztol.or.Qresid.gt.Qtol) then
                iter=iter+1
                goto 200
              endif
```

```
c             Allow upstream boundaries to vary in this example.

          if (tcycle.gt.3) then
            Q(2,1,t)=Q(2,2,t)
            Q(3,1,t)=Q(3,2,t)
          endif

101       continue
          if (tcycle.le.cyc) then
          do 142 sect=1,nosects(1)-1
            z(1,sect,0)=z(1,sect,tj+1)
            Q(1,sect+1,0)=Q(1,sect+1,tj+1)
142       continue
          do 143 sect=2,nosects(3)
            z(3,sect-1,0)=z(3,sect-1,tj+1)
            Q(3,sect,0)=Q(3,sect,tj+1)
143       continue
          do 144 sect=2,nosects(2)
            z(2,sect-1,0)=z(2,sect-1,tj+1)
            Q(2,sect,0)=Q(2,sect,tj+1)
144       continue
            Q(1,1,0)=Q(1,1,tj+1)
            z(3,nosects(3),0)=z(3,nosects(3),tj+1)
            z(2,nosects(2),0)=z(2,nosects(2),tj+1)
            Q(2,1,0)=Q(2,1,tj+1)
            Q(3,1,0)=Q(3,1,tj+1)
          endif
100     continue
c
c       Save data to file
c
        do 172 j=1,3
        if (j.eq.1) then
          il=10
        elseif (j.ne.1) then
          il=5
        endif
        do 106 i=1,il
        open(unit=16,file=' tmp1 damian/''//snames(j,stats(j,i))
     *          //savename  '.dat'
     *      ,status='new',form='formatted')
        rewind(16)
        do 169 t=0,tj,10
          write(16,210) t,z(j,stats(j,i),t),
     *                  Q(j,stats(j,i),t),Q(j,stats(j,i),t)/area
     *                      (j,stats(j,i),t),l(j,stats(j,i),t)
     *      ,area(j,i,t),breadth(j,i,t)
169     continue
        close(16)
106     continue
172     continue
        open(unit 21,file='/tmp1/damian/''//savename//'se.dat'
     *      ,status='new'
     *      ,form='formatted')
        open(unit=22,file='/tmp1/damian/''//savename//''
     *  sw.dat',status='new'
     *      ,form 'formatted')
        rewind(21)
        rewind(22)
        xd=0
        do 173 j=1,3
        sectinit=(nosects(j))
        do 175 i=nosects(j),1,-1
        zmax(j,i)=z(j,i,10)
        zmin(j,i)=z(j,i,10)
        tmax(j,i)=10
```

```
      tmin(j,i)=10
      do 171 k=10,tj
      if (z(j,i,k).gt.zmax(j,i)) then
        zmax(j,i)=z(j,i,k)
        tmax(j,i)=k
      endif
      if (z(j,i,k).lt.zmin(j,i)) then
        zmin(j,i)=z(j,i,k)
        tmin(j,i)=k
      endif
      if (l(j,i,k).lt.lmax(j,i)) then
        lmax(j,i)=l(j,i,k)
      endif
171   continue
      if (j.eq.2.and.i.eq.nosects(2)) then
      xd=xi
      elseif (j.eq.3.and.i.eq.nosects(3)) then
      xd=xi
      endif
      xd=xd+xdist(j,i)
      if (j.eq.1.and.i.eq.1) then
      xi=xd+xdist(1,0)
      endif
      if (j.eq.1) then
      write(21,211) xd,zmax(j,i),zmin(j,i),tmax(j,i),tmin(j,i),
     *     lmax(j,i),snames(j,i),area(j,i,tmin(j,i)),
     *     breadth(j,i,tmin(j,i))
      write(22,211) xd,zmax(j,i),zmin(j,i),tmax(j,i),tmin(j,i),
     *     lmax(j,i),snames(j,i),area(j,i,tmin(j,i)),
     *     breadth(j,i,tmin(j,i))
      elseif (j.eq.2) then
      write(22,211) xd,zmax(j,i),zmin(j,i),tmax(j,i),tmin(j,i),
     *     lmax(j,i),snames(j,i),area(j,i,tmin(j,i)),
     *     breadth(j,i,tmin(j,i))
      elseif (j.eq.3) then
      write(21,211) xd,zmax(j,i),zmin(j,i),tmax(j,i),tmin(j,i),
     *     lmax(j,i),snames(j,i),area(j,i,tmin(j,i))
     *     ,breadth(j,i,tmin(j,i))
      endif
175   continue
173   continue
      close(21)
      close(22)
210   format(i8,",",f12.2,",",f12.2,",",f12.2,",",f12.8,",",f12.8,","
     *          ,f12.8)
211   format(f8.1,",",f8.2,",",f8.2,",",i8,",",i8,",",
     *  3x,",",f10.7,",",6x,",",a8,",",f8.2,",",f8.2)

      end
c
c
c     ------------------------------------------------------------
c
      subroutine interpol(t,sect,least,i)
      common /hthydro/a,b,wp
      common /dependants/z,Q
      common /thydro/area,breadth,wetp,convey,friction
      real z(3,50,0:2000),a(3,50,-10:15),b(3,50,-10:15),wp(3,50,-10:15)
      real area(3,50,0:2000),breadth(3,50,0:2000),wetp(3,50,0:2000)
      real Q(3,50,0:2000),convey(3,50,0:2000),friction(3,50)
      integer sect,t,ht1,ht2,i
      real ht3,least(3,50),dummy
c
c     subroutine calculates values of area, breadth and wetp
c     from tabulated values a,b,wp at set heights
c
```

```
      ht1=1
        if (z(i,sect,t).ge.1) then
          ht1=int(z(i,sect,t))
        elseif (z(i,sect,t).lt.-1) then
         ht1=nint(z(i,sect,t)-0.5)
        elseif (z(i,sect,t).lt.1.and.z(i,sect,t).ge.0) then
          ht1=0
        elseif (z(i,sect,t).lt.0.and.z(i,sect,t).ge.-1) then
          ht1=-1
        endif
        ht2=ht1+1
        ht3=z(i,sect,t)-real(ht1)
        if (a(i,sect,ht1).eq.0.0) then
          dummy=((z(i,sect,t)-least(i,sect))/(ht2-least(i,sect)))
          area(i,sect,t)=dummy*a(i,sect,ht2)
          breadth(i,sect,t)=dummy*b(i,sect,ht2)
          wetp(i,sect,t)=dummy*wp(i,sect,ht2)
        else
        area(i,sect,t)=a(i,sect,ht1)
     *                 +((a(i,sect,ht2)-a(i,sect,ht1))*ht3)
        breadth(i,sect,t)=b(i,sect,ht1)
     *                 +((b(i,sect,ht2)-b(i,sect,ht1))*ht3)
        wetp(i,sect,t)=wp(i,sect,ht1)
     *                 +((wp(i,sect,ht2)-wp(i,sect,ht1))*ht3)
        endif
      return
      end
c
c     ---------------------------------------------------------------
c
      subroutine con(t,nosects,g,i)
      common /thydro/area,breadth,wetp,convey,friction
      real area(3,50,0:2000),friction(3,50),wetp(3,50,0:2000)
      real breadth(3,50,0:2000),convey(3,50,0:2000)
      real g,hydrad
      integer sect,t,nosects(3),i
      sect=1
c
c     subroutine calculates conveyance (K*K) using Dechezy coefficient
c
      do 151 sect=1,nosects(i)
        hydrad=area(i,sect,t)/wetp(i,sect,t)
        convey(i,sect,t)=((hydrad**0.66666667)*area(i,sect,t)
     *   /friction(i,sect))**2
151   continue
      return
      end
c
c     ---------------------------------------------------------------
c
      subroutine sweep1(t,nosects,sect,xdist,g,i
     *            ,branchalpha,branchbeta,branchgamma)
      common /thydro/area,breadth,wetp,convey,friction
      common /weight/tinc,theta
      common /hthydro/a,b,wp
      common /dependants/z,Q
      common /inf/l,ul,lh,rh
      common /coeffs/p,qq,r,s,tt
      integer t,sect,nosects(3),m,n,i
      real area(3,50,0:2000),breadth(3,50,0:2000),wetp(3,50,0:2000)
      real convey(3,50,0:2000),friction(3,50)
      real z(3,50,0:2000),a(3,50,-10:15),b(3,50,-10:15),wp(3,50,-10:15)
      real Q(3,50,0:2000),l(3,50,0:2000),ul(3,50,0:2000)
      real tinc,theta,lh(3,50),rh(3,50)
      real c1(3,50),c2(3,50),c3(3,50),c4(3,50),c5(3,50)
      real alpha(3,50),beta(3,50),gamma(3,50),delta(3,50),epsilon(3,50)
```

```
      real p(3,50),qq(3,50),r(3,50),s(3,50),tt(3,50),c6(3,50)
      real xdist(3,0:50),g,bp,dqdp,c7(3,50)
      real branchalpha,branchbeta,branchgamma
c
c     subroutine calculates first sweep parameters used to
c     calculate future values in second sweep
c
c     calculate c1(sect)-c7(sect) coefficients
c
      m=t+1
      n=sect+1
      c1(i,sect)=g*(theta*(area(i,n,m)+area(i,sect,m))
     *    +(1-theta)*(area(i,sect,t)+area(i,n,t)))
      c2(i,sect)=xdist(i,sect)/(theta*tinc)
      c3(i,sect)=(1-theta)/theta
      c4(i,sect)=(theta*(convey(i,n,m)+convey(i,sect,m))
     *    +(1-theta)*(convey(i,n,t)+convey(i,sect,t)))/xdist(i,sect)
      c5(i,sect)=theta*(breadth(i,n,m)+breadth(i,sect,m))
     *    +(1-theta)*(breadth(i,n,t)+breadth(i,sect,t))
      c6(i,sect)=(xdist(i,sect)/(2*theta))*
     *             (theta*(l(i,n,m)+l(i,sect,m))
     *            +(1-theta)*(l(i,n,t)+l(i,sect,t)))
      c7(i,sect)=((theta*(ul(i,n,m)+ul(i,sect,m)))+(
     *             (1-theta)*(ul(i,n,t)+ul(i,sect,t))))/2
c
c     calculate alpha(sect) to epsilon(sect) using c1(sect)-c7(sect) values
c
      alpha(i,sect)=(c2(i,sect)/c1(i,sect))
     *      +(2*Q(i,n,m)/area(i,n,m)/c1(i,sect))
     *      +(abs(Q(i,n,m))/c4(i,sect))
     *      +(theta*c6(i,sect)/(c1(i,sect)*area(i,n,m)))
      beta(i,sect)=(c2(i,sect)/c1(i,sect))
     *      -(2*Q(i,sect,m)/(area(i,sect,m)*c1(i,sect)))
     *      +(abs(Q(i,sect,m))/c4(i,sect))
     *      +(theta*c6(i,sect)/(c1(i,sect)*area(i,sect,m)))
      gamma(i,sect)=(c3(i,sect)*(z(i,sect,t)-z(i,n,t)))
     *      +(c2(i,sect)*(Q(i,n,t)+Q(i,sect,t))/c1(i,sect))
     *      -(c3(i,sect)*((Q(i,n,t)*abs(Q(i,n,t)))+(Q(i,sect,t)*
     *       abs(Q(i,sect,t))))/c4(i,sect))
     *      +(2*c6(i,sect)*c7(i,sect)/c1(i,sect))
     *      -(2*c3(i,sect)*(((Q(i,n,t)**2)/area(i,n,t))-
     *       ((Q(i,sect,t)**2)/area(i,sect,t)))/c1(i,sect))
     *      -(theta*c6(i,sect)*c3(i,sect)*((Q(i,n,t)/area(i,n,t))+
     *       (Q(i,sect,t)/area(i,sect,t)))/c1(i,sect))
      delta(i,sect)=c2(i,sect)*c5(i,sect)/4
      epsilon(i,sect)=(z(i,n,t)+z(i,sect,t))*delta(i,sect)
     *      +c3(i,sect)*(Q(i,sect,t)-Q(i,n,t))
     *      +c6(i,sect)
c
c     calculate values of p-t
c
      if (sect.eq.1.and.i.eq.3) then
        p(3,sect)=0
        r(3,sect)=Q(3,sect,m)
      endif
      if (sect.eq.1.and.i.eq.2) then
        p(2,sect)=0
        r(2,sect)=Q(2,sect,m)
      endif
      if (sect.eq.1.and.i.eq.1) then
        branchalpha=Q(1,1,t+1)/(19.6*(area(1,1,t+1)**2))
        branchgamma=Q(3,nosects(3),t+1)
     *          /(19.6*(area(3,nosects(3),t+1)**2))
        branchbeta=Q(2,nosects(2),t+1)
     *          /(19.6*(area(2,nosects(2),t+1)**2))
        branchdiv=1+((branchalpha*p(2,nosects(2)))/
```

```
*                    (1-(branchbeta*p(2,nosects(2)))))
*                +((branchalpha*p(3,nosects(3)))/
*                  (1-(branchgamma*p(3,nosects(3)))))
      p(1,1)=((p(2,nosects(2))/(1-(branchbeta*p(2,nosects(2)))))
*              +(p(3,nosects(3))/(1-(branchgamma*p(3,nosects(3))))))
*               /branchdiv
      r(1,1)=(r(2,nosects(2))+r(3,nosects(3))+
*              ((p(2,nosects(2))*branchbeta*r(2,nosects(2)))
*                /(1-(branchbeta*p(2,nosects(2)))))
*             +((p(3,nosects(3))*branchgamma*r(3,nosects(3)))
*                /(1-(branchgamma*p(3,nosects(3))))))
*              /branchdiv
      endif
      bp=beta(i,sect)+p(i,sect)
      dqdp=delta(i,sect)+(qq(i,sect)*(1+(delta(i,sect)*p(i,sect))))
      tt(i,sect)=1/(delta(i,sect)+p(i,sect))
      qq(i,sect)=delta(i,sect)/(delta(i,sect)+p(i,sect))
      s(i,sect)=(epsilon(i,sect)+r(i,sect))/
*               (delta(i,sect)+p(i,sect))
      p(i,n)=(1+(qq(i,sect)*(1+(beta(i,sect)*p(i,sect)))))
*           /(alpha(i,sect)+(tt(i,sect)*(1+(beta(i,sect)*
*              p(i,sect)))))
      r(i,n)=(gamma(i,sect)+(s(i,sect)*(1+(p(i,sect)*beta(i,sect))))-
*               (beta(i,sect)*r(i,sect)))
*           /(alpha(i,sect)+(tt(i,sect)*(1+(beta(i,sect)*
*              p(i,sect)))))
      return
      end
c
c     ----------------------------------------------------------------
c
c
      subroutine sweep2(t,sect,nosects,least,breadth,area,
*                       friction,xdist,zt,
*                       tcycle,i,branchalpha,branchbeta,branchgamma)
      common /weirdo/weirpos,weirht,weirb
      common /dependants/z,Q
      common /coeffs/p,qq,r,s,tt
      integer t,sect,nosects(3),m,n,zt,tcycle
*     ,weirpos(3,50),i
      real p(3,50),qq(3,50),r(3,50),s(3,50),tt(3,50)
      real z(3,50,0:2000),Q(3,50,0:2000)
      real least(3,50)
      real breadth(3,50,0:2000),area(3,50,0:2000)
      real friction(3,50),xdist(3,0:50),weirht(3,50),weirb(3,50)
      real branchalpha,branchbeta,branchgamma
c
c     subroutine calculates future values of z and Q
c     using values calculated in first sweep
c
      m=t+1
      n=sect+1
      if (i.eq.2) then
        if (n.eq.nosects(2)) then
          z(2,n,m)=((z(1,1,m)*(1-(branchalpha*p(1,1))))+(branchalpha
*         *r(1,1))-(branchbeta*r(2,nosects(2))))/
*           (1-(branchbeta*p(2,nosects(2))))
        endif
        if (weirpos(i,n+1).ne.1) then
        Q(i,n,m)=r(i,n)-(p(i,n)*z(i,n,m))
        endif
        z(i,sect,m)=s(i,sect)-(qq(i,sect)*z(i,n,m))-(tt(i,sect)
*       *Q(i,n,m))
      elseif (i.eq.3) then
        if (n.eq.nosects(3)) then
          z(3,n,m)=((z(1,1,m)*(1-(branchalpha*p(1,1))))+(branchalpha
```

```
*       *r(1,1))-(branchgamma*r(3,nosects(3))))/
*         (1-(branchgamma*p(3,nosects(3))))
        endif
        if (weirpos(i,n+1).ne.1) then
        Q(i,n,m)=r(i,n)-(p(i,n)*z(i,n,m))
        endif
        z(i,sect,m)=s(i,sect)-(qq(i,sect)*z(i,n,m))-(tt(i,sect)
*             *Q(i,n,m))
      elseif (i.eq.1) then
        if (weirpos(i,n+1).ne.1) then
        Q(i,n,m)=r(i,n)-(p(i,n)*z(i,n,m))
        endif
        z(i,sect,m)=s(i,sect)-(qq(i,sect)*z(i,n,m))
*           -(tt(i,sect)*Q(i,n,m))
        if (n.eq.2) then
          Q(1,1,m)=r(1,1)-(p(1,1)*z(1,1,m))
      endif
      endif

c       low flow problem
c
      if (z(i,n,m).le.least(i,n)+.4.and.weirpos(i,n).ne.1
*             .and.n.ne.nosects(i)) then
        if (z(i,n,m).lt.least(i,n)+0.2) then
          z(i,n,m)=least(i,n)+.2
        call interpol(t,sect,least,i)
       endif
        if (z(i,sect,m).le.z(i,n+1,m)) then
         if (z(i,n,m).lt.z(i,n+1,m)) then
           Q(i,n,m)=-0.544*0.5*((9.81*area(i,n,m)/breadth(i,n,m))**0.5)
         elseif (z(i,n+1,m).le.z(i,n,m)) then
           Q(i,n,m)=Q(i,n+1,m)
         endif
        elseif (z(i,sect,m).gt.z(i,n,m)) then
         if (z(i,sect,m).gt.z(i,n,m)) then
           Q(i,n,m)=0.544*0.5*((9.81*area(i,n,m)/breadth(i,n,m))**0.5)
         elseif (z(i,sect,m).lt.z(i,n,m)) then
          Q(i,n,m)=Q(i,sect,m)
         endif
         endif
              Q(i,n,m)=0.8*Q(i,n,m)+
*             +0.15*Q(i,n,t)
*             +0.05*Q(i,n,t-1)
      endif
      return
      end
c
c     ------------------------------------------------------------
      subroutine inflow(t,sect,i,xdist)
      common /inf/l,ul,lh,rh
      common /dependants/z,Q
      real  Q(3,50,0:2000)
      real  z(3,50,0:2000),lh(3,50),rh(3,50)
      real  xdist(3,0:50)
      real  muwall,lhout,rhout,ulhout,urhout
      real zstage(0:6),rwallstage(0:6),lwallstage(0:6)
      real l(3,50,0:2000),ul(3,50,0:2000)
      integer t,i,sect,j
      muwall=0.65
      l(i,sect,t)=0
      do 235 j=0,6
        if (rh(i,sect+1).eq.0) then
          rh(i,sect+1)=rh(i,sect)
        elseif (lh(i,sect+1).eq.0) then
         lh(i,sect+1)=lh(i,sect)
        endif
```

```
          zstage(j)=z(i,sect,t)-(j*((z(i,sect,t)-z(i,sect+1,t))/6))
          rwallstage(j)=rh(i,sect)-(j*((rh(i,sect)-rh(i,sect+1))/6))
          lwallstage(j)=lh(i,sect)-(j*((lh(i,sect)-lh(i,sect+1))/6))
235     continue
        do 236 j=1,5,2
          if (zstage(j).gt.rwallstage(j)) then
            lhout=
     *                muwall*4.43*(xdist(i,sect)/3)
     *                *((zstage(j)-lwallstage(j))**1.5)
            ulhout= lhout/(zstage(j)-lwallstage(j))
          endif
          if (zstage(j).gt.lwallstage(j)) then
            rhout=
     *                muwall*4.43*(xdist(i,sect)/3)
     *                *((zstage(j)-rwallstage(j))**1.5)
            urhout= rhout/(zstage(j)-rwallstage(j))
          endif
          if (zstage(j).le.lwallstage(j)) then
            lhout=0
            ulhout=0
          endif
          if (zstage(j).le.rwallstage(j)) then
            rhout=0
            urhout=0
          endif
          l(i,sect,t)=l(i,sect,t)-lhout
     *      -rhout
          ul(i,sect,t)=ul(i,sect,t)-ulhout-urhout
236     continue
          l(i,sect,t)=l(i,sect,t)/xdist(i,sect)
          ul(i,sect,t)=ul(i,sect,t)/xdist(i,sect)
          if (t.gt.3) then
          l(i,sect,t)=(0.34*l(i,sect,t))
     *                +(0.33*l(i,sect,t-1))
     *                +(0.33*l(i,sect,t-2))
          ul(i,sect,t)=(0.34*ul(i,sect,t))
     *                +(0.33*ul(i,sect,t-1))
     *                +(0.33*ul(i,sect,t-2))
          endif
          if (l(i,sect,t).le.-0.3) then
            l(i,sect,t)=-.3
          endif
          if (l(i,sect,t).ge.-0.0000001) then
            l(i,sect,t)=0.0
          endif
        return
        end
c
c       ----------------------------------------------------------------------
c
        subroutine sweep1weir(i,weir,t)
        common /dependants/z,Q
        common /coeffs/p,qq,r,s,tt
        integer i,t,weir
        real Q(3,50,0:2000),z(3,50,0:2000)
        real qq(3,50),s(3,50),tt(3,50)
        real p(3,50),r(3,50)
        p(i,weir+1)=0
        r(i,weir+1)=Q(i,weir-1,t)
        return
        end

c       ----------------------------------------------------------------------
c
        subroutine sweep2weir(i,weir,t,area)
        common /weirdo/weirpos,weirht,weirb
```

```
      common /dependants/z,Q
      common /coeffs/p,qq,r,s,tt
      integer i,weir,t,weirpos(3,50)
      real muweir1,muweir2,muweir3
      real fz,ffz,area(3,50,0:2000)
      real Q(3,50,0:2000),z(3,50,0:2000)
      real p(3,50),r(3,50),qq(3,50),s(3,50),tt(3,50)
      real weirht(3,50),weirb(3,50)
      muweir1=weirb(i,weir)*4.43*1
      muweir2=weirb(i,weir)*4.43*1
      muweir3=weirb(i,weir)*4.43*1
c
c     solve by iteration
c
      if (Q(i,weir+2,t).lt.0) then
        Q(i,weir+1,t)=Q(i,weir+2,t)
        Q(i,weir-1,t)=Q(i,weir+1,t)
      else
        Q(i,weir+1,t)=Q(i,weir-1,t)
      endif
      do 189 k=1,4
      if (Q(i,weir+1,t).gt.0.0.and.z(i,weir-1,t).lt.z(i,weir+1,t)) then
        z(i,weir-1,t)=z(i,weir+1,t)+0.05
      elseif (Q(i,weir+1,t).lt.0.and
     *          .z(i,weir-1,t).ge.z(i,weir+1,t)) then
        z(i,weir-1,t)=z(i,weir+1,t)-0.05
      endif
      if (z(i,weir+1,t).lt.weirht(i,weir).and.Q(i,weir+1,t).gt.0) then
        fz=muweir1*((z(i,weir-1,t)-weirht(i,weir))**1.5)
     *     -r(i,weir-1)
     *     +(p(i,weir-1)*z(i,weir-1,t))
        ffz=(1.5*muweir1*((z(i,weir-1,t)-weirht(i,weir))**0.5))
     *          +p(i,weir-1)
      endif
      if (z(i,weir 1,t).gt.weirht(i,weir).and.
     *       z(i,weir+1,t).le.z(i,weir-1,t).
     *       and.Q(i,weir+1,t).gt.0) then
        fz=(muweir2*(z(i,weir+1,t)-weirht(i,weir))*
     *          ((z(i,weir-1,t)-z(i,weir+1,t))**0.5))
     *          -r(i,weir-1)+(p(i,weir-1)*z(i,weir-1,t))
        ffz=(0.5*muweir2*(z(i,weir+1,t)-weirht(i,weir))*
     *          ((z(i,weir-1,t)-z(i,weir+1,t))**-0.5))
     *          +(muweir2*((z(i,weir-1,t)-z(i,weir+1,t))**0.5))
     *          +p(i,weir-1)
      endif
      if (Q(i,weir+1,t).lt.0) then
        fz=(muweir3*(z(i,weir-1,t)-weirht(i,weir))*
     *          ((z(i,weir+1,t)-z(i,weir-1,t))**0.5))
     *           -abs(-r(i,weir-1)+(p(i,weir-1)*z(i,weir-1,t)))
        ffz=(-0.5*muweir3*(z(i,weir-1,t)-weirht(i,weir))*
     *           ((z(i,weir+1,t)-z(i,weir-1,t))**-0.5))
     *         +(muweir3*((z(i,weir+1,t)-z(i,weir-1,t))**0.5))
     *         +p(i,weir-1)
      endif
      z(i,weir-1,t)=z(i,weir-1,t)-(fz/ffz)
      Q(i,weir-1,t)=r(i,weir-1)-(p(i,weir-1)*z(i,weir-1,t))

189   continue
      return
      end
```

APPENDIX E

CROSS SECTIONS

Appendix E, Main Channel Sections.

SECTION	SECTION NUMBER	LENGTH OF SECTION	UPSTREAM DISTANCE (m)	FRICTION MANNING n	LEFT BANK HEIGHT (HRS) (m)	RIGHT BANK HEIGHT (HRS) (m)	BED LEVEL (m)	LEFT BANK HEIGHT LEVELLED (m)	RIGHT BANK HEIGHT LEVELLED (m)
AVONMOUTH	100	4588	0	0.026	9.3	9.3		9	9.2
SHOOTS	101	2375	4588	0.026	9.32	9.3		9.6	9.4
SUDBROOK	102	2000	6963	0.026	10.15	9		9.7	9.7
NORTHWICK	103	1575	8963	0.026	8.63	9		10	10
AUSTWHARF	104	1375	10538	0.026	8.63	9		10	10
BEACHLEY	105	1550	11913	0.026	8.63	9		10	30
LITTLETON	106	3263	13463	0.026	8.74	9		20	10.1
INWARD ROCK	107	2087	16726	0.026	8.67	9		10.5	9.7
NARLWOOD	108	2275	18813	0.026	8.78	9	-7.97	10.1	10.1
WHITE HOUSE	109	2475	21088	0.024	9.89	9.3	-3.65	10	11
LYDNEY	110	2337	23563	0.02	9.46	8.99	-4.6	9.7	9.7
BERKELEY	111	1650	25900	0.02	9.86	9.08	-4.13	9.7	9.7
FAIRTIDE ROCKS	112	1763	27550	0.018	10.45	10	-4.23	24	10
SHARPNESS	113	1000	29313	0.018	10.45	10	-4.83	24	15
WELLHOUSE ROCK	114	496	30313	0.017	10	10	-8.82	10	25
PURTON	115	1024	30809	0.016	10	10	-6.48	10.76	11
GATCOMBE	116	3458	31833	0.015	10.3	10	-1.02	11.82	12
SLIMBRIDGE	117	2218	35291	0.014	10.3	9.86	0.39	10.2	9.7

SECTION	SECTION NUMBER	LENGTH OF SECTION	UPSTREAM DISTANCE (m)	FRICTION MANNING n	LEFT BANK HEIGHT (HRS) (m)	RIGHT BANK HEIGHT (HRS) (m)	BED LEVEL (m)	LEFT BANK HEIGHT LEVELLED (m)	RIGHT BANK HEIGHT LEVELLED (m)
FRAMPTON	118	1404	37509	0.014	10.4	9.78	0.32	9.9	9.8
FRETHERN	119	1832	38913	0.014	10.6	9.53	0.69	9.8	10.2
NORTHINGTON	120	1067	40745	0.014	10.09	9.51	0.91	9.9	9.87
BOXGROVE	121	1077	41812	0.014	10.21	9.56	0.2	10	9.85
BULLOPILL	122	993	42889	0.014	10.4	10	0.71	13	9.9
NEWNHAM	123	961	43882	0.014	10.4	10	2.85	13.71	9.8
HAWKING PILL	124	1012	44843	0.014	10.4	10	1.79	10.1	9.75
ARLINGHAM WHARF	125	1140	45855	0.016	10.4	10	1.82	10.1	9.76
PIMLICO SANDS	126	950	46995	0.016	10.4	10	2.6	15	9.75
ARLINGTON	127	1188	47945	0.016	10.4	9.89	3.91	10	9.8
LOWER DUMBALL	128	898	49133	0.016	10.4	9.71	3.91	10	9.7
PRIDING	129	913	50031	0.016	9.61	9.8	3.13	10	9.75
FRAMILODE	130	1024	50944	0.016	9.73	9.73	2.74	9.99	10.08
UPPER DUMBAL	131	1067	51968	0.023	9.86	9.86	3.5	10.3	10.1
NEW INN (EPNEY)	132	723	53035	0.023	9.97	9.97	-0.2	10.3	10.2
LONGNEY	133	1162	53758	0.023	10.18	10.18	2.67	10.2	10.3
BOLLOPOOL	134	972	54920	0.023	10.27	9.91	4.28	20	10.27
CONSTANCE FARM	135	1130	55892	0.023	10	10	3.83	10.1	10.6
HILL FARM	136	1098	57022	0.023	10.06	10.2	0.17	10.13	10
THE FLAT	137	1119	58120	0.023	10.1	10.2	1.98	10	10.2

SECTION	SECTION NUMBER	LENGTH OF SECTION	UPSTREAM DISTANCE (m)	FRICTION MANNING n	LEFT BANK HEIGHT (HRS) (m)	RIGHT BANK HEIGHT (HRS) (m)	BED LEVEL (m)	LEFT BANK HEIGHT LEVELLED (m)	RIGHT BANK HEIGHT LEVELLED (m)
DENNY HILL	138	1003	59239	0.023	9.96	10.35	-1.21	10.31	10.31
WEST MINSTERWORTH	139	1077	60242	0.023	10.13	10.09	0	10.3	10.01
MIDDLE MINSTERWORTH	140	1088	61319	0.023	10.04	10.09	2.16	10.18	10.12
EAST MINSTERWORTH	141	919	62407	0.023	10.14	10.08	2.6	10	10.1
WINDMILL HILL	142	1035	63326	0.023	10.16	9.78	2.54	9.75	11.93
ELMORE	143	1140	64361	0.023	9.31	9.7	2	9.78	10
CORNHAM	144	1003	65501	0.023	9.22	9.66	3	9.74	9.7
UPPER REA	145	1056	66504	0.023	9.07	9.92	2.75	10.02	9.9
MINSTERWORTH HAM	146	1114	67560	0.023	9.8	9.77	3.67	9.85	9.7
MOOR FARM	147	1019	68674	0.023	10.2	9.95	3.82	10.02	9.86
SUD MEADOW	148	420	69693	0.023	10.2	10.1	3.7	10.1	10.1

Cross section information, Sections, modelled friction and seawall heights, Main Channel

Appendix *E*, *West Channel Sections.*

SECTION	SECTION NUMBER	LENGTH OF SECTION	UPSTREAM DISTANCE (m)	FRICTION MANNING n	LEFT BANK HEIGHT (HRS) (m)	RIGHT BANK HEIGHT (HRS) (m)	BED LEVEL (m)	LEFT BANK HEIGHT LEVELLED (m)	RIGHT BANK HEIGHT LEVELLED (m)
PORT HAM	209	391	70504	0.02	9.14	9.83	3.73	9.8	9.6
PORT HAM NORTH	208	260	70764	0.02	10	10	4.11	10.06	9.6
OVER	207	256	71020	0.02	10	10	3.14	9.7	10
ALNEY ISLAND	206	333	71353	0.02	9.34	9.57	4.08	9.64	9.6
MAISEMORE HAM SOUTH	205	317	71670	0.02	9.45	9.93	4.25	10	9.7
MAISEMORE HAM MIDDLE	204	296	71966	0.02	9.75	10.17	4.42	10.24	10
MAISEMORE HAM NORTH	203	312	72278	0.02	10.11	10.08	4.56	10	10
MAISEMORE	202	332	72610	0.02	9.79	10.25	2.71	10	10
MAISEMORE WEIR	201	301	72911	0.02	9.72	10.35	4.57	9.74	10

Cross section information, Sections, modelled friction and seawall heights, West Channel

Appendix E, East Channel Sections

SECTION	SECTION NUMBER	LENGTH OF SECTION	UPSTREAM DISTANCE (m)	FRICTION MANNING n	LEFT BANK HEIGHT (HRS) (m)	RIGHT BANK HEIGHT (HRS) (m)	BED LEVEL (m)	LEFT BANK HEIGHT LEVELLED (m)	RIGHT BANK HEIGHT LEVELLED (m)
SOUTH SUD MEADOW	309	390	70503	0.02	9.98	10	2.91	10.18	9.9
SUD MEADOW NORTH	308	454	70957	0.02	9.97	9.8	2.91	10.18	9.9
LLANTHONY MILL	307	106	71603	0.02	10.14	10.97	4.18	10.46	10.65
LLANTHONY	306	158	71221	0.02	10.4	11	4.56	11.65	10.77
CASTLEMEADS SOUTH	305	269	71490	0.02	11.3	11	3.8	9.5	11.18
GLOUCESTER DOCKS	304	243	71733	0.02	11.3	10.14	3.94	10.8	10.4
GLOUCESTER PRISON	303	164	71897	0.02	11.3	10	3.86	11.03	10.37
CASTLEMEADS NORTH	302	375	72272	0.02	11.3	9.57	4.09	10	10
WESTGATE BRIDGE	301	269	72541	0.02	11.3	10.58	4.19	10.78	10.66

Cross section information, Sections, modelled friction and seawall heights, East Channel.